

**Small molecule inhibitors of the WDR5-MYC interaction**

By

Selena Chacón Simon

Dissertation

Submitted to the Faculty of the  
Graduate School of Vanderbilt University  
in partial fulfillment of the requirements  
for the degree of

DOCTOR OF PHILOSOPHY

in

Chemical & Physical Biology

May 8<sup>th</sup>, 2020

Nashville, Tennessee

Approved:

Stephen W. Fesik, Ph.D.

Gary Sulikowski, Ph.D.

Steve Townsend, Ph.D.

Vivian Gama, Ph.D.

Oliver G. McDonald, Ph.D., M.D.

Copyright © 2020 by Selena Chacón Simon  
All Rights Reserved



A mi papá, mamá y hermanos por el apoyo durante estos años

A Diego del Alamo, por apoyarme y hacerme sentir amada estando lejos de casa

## Acknowledgments

I would first like to thank Dr. Steve Fesik for the advice, mentorship, and financial support he provided to me during the last years. I will always be grateful for opening your Lab to me. Steve's deep knowledge in the field and desire to improve health encourages me to be a better scientist and never stop learning.

The Fesik Lab is a unique environment to learn drug discovery, it is an interdisciplinary group composed of medicinal chemist, structural biologist, biochemists, and cell biologists. The work presented in this dissertation is the result of team work. I had a lot of help in many aspects of my work. Therefore, I would like to thank Drs. Shaun Stauffer and Alex Waterson for the guidance provided in this project, the chemistry advice, and for always taking a look to my documents. I also want to thank to Dr. Jonathan Macdonald for the synthesis of many of the sulfonamide compounds shown in this work. Also, thanks for guiding me throughout the project, for teaching me to set up scary reactions, and for making me feel welcome to the Lab when I joined. Also, thanks to Dr. Changho Han for synthesizing several of the sulfonamide compounds shown in this dissertation and giving me advice. In addition, I would like to thank the structural biology team: Dr. Bin Zhao, Dr. Feng Weng, Dr. Jason Phan, Dr. Edward Olejniczak, Demarco Camper, and William Payne. They produced protein, conducted the NMR-based fragment screening, and produced the X-ray co-crystal structures shown in here. Moreover, I want to thank the cell biology team: Joannes Yuh, Grace Shaw, and Caden Schlund for running and rerunning these compounds in the FPA. Finally, I want to thank Dr. William Tansey and his Lab for the support provided to this project. Thanks Drs. Jiqing Sai and Lance Thomas for conducting the different biological assays (thermal shift, Co-IPs, ChIPs, and proliferation assays). Also, thanks Natalia Smothers for always helping me organizing meetings and for encouraging words. This work was financially

supported by the Robert J. Kleberg, Jr. and Helen C. Kleberg Foundation, the TJ Martell Foundation, and the NCI/NIH CA236733.

I also appreciate the guidance, time and support provided by my committee members Drs. Gary Sulikowski, Vivian Gama, Steve Townsend, and Oliver McDonald.

Joseph (José!)! You were a great bench neighbor! Your critical thinking and chemistry knowledge are inspiring. Thanks for the friendly critics and for giving me advice with those reactions that did not work. I enjoyed talking and gossiping with you. Also, thanks for the burritos! I miss them.

I would also like to thank Jason Abbott, you are a really smart and talented chemist. I appreciate the advice and guidance provided when I needed to troubleshoot reactions. Thanks for all the moral support and the dark humor.

I also want to express infinite thanks to everyone in the Medicinal Chemistry team (Alexey, Chris, Kyuok, Jim, Rocco, Rush, Sameer, Tim, Dhruba, Naga, Taekyu, Jianwen and Subrata). You guys helped me with advice and ideas at some point of this journey. In general, thanks to Fesik Lab for being so welcoming and for making the Lab a great place to work and learn.

I would also like to acknowledge, what it was at the time, the Vanderbilt International Scholar Program (VISP). Thanks for giving me the opportunity to join this incredible and supportive community. Thanks to the QCB and CPB program, especially Dr. Hassane Mchaourab, Dr. Bruce Damon, and Patricia Mueller.

I also want to thank my friends in Nashville, especially Oscar Ortega, Andrea Cuentas, and Flor Pezzimenti. Graduate school without you all wouldn't have been the same.

Thanks to my family for supporting me from the distance. Thanks Dali y Harvey for pushing me to come when the opportunity arose and for facetimeing with me so I didn't feel lonely. Thanks brothers (Geoffrey, Gabriel, and Emanuel) for also being supportive during the last years.

Thanks to Diego, you have been my constant during almost all graduate school. Thanks for the support, patience, and love. You have taught me to be more spontaneous and caring. Thanks for sharing and celebrating each achievement of this journey.

Finally, I want to thank Sr. Mechas, he was there to welcome me with love and a wagging tail every day I got back from lab. No matter if that day nothing worked, he made me forget about it.

## Table of Contents

	<b>Page</b>
<b>Acknowledgments</b> .....	<b>iv</b>
<b>List of Figures</b> .....	<b>vii</b>
<b>List of Tables</b> .....	<b>xiv</b>
<b>List of Schemes</b> .....	<b>xvi</b>
<b>Chapter</b>	
<b>I. Introduction</b> .....	<b>1</b>
<i>1.1 Cancer and treatment</i> .....	<i>1</i>
<i>1.2 MYC proteins: Structure, Function, and Deregulation</i> .....	<i>3</i>
<i>1.2.1 Structure of MYC proteins</i> .....	<i>4</i>
<i>1.2.2 MYC boxes: six well conserved sequences</i> .....	<i>5</i>
<i>1.2.3 The MAX-MYC interaction</i> .....	<i>7</i>
<i>1.2.4 Transcriptional function of MYC</i> .....	<i>7</i>
<i>1.2.5 MYC regulation</i> .....	<i>11</i>
<i>1.3 MYC in cancer</i> .....	<i>11</i>
<i>1.3.1 MYC in cell cycle</i> .....	<i>12</i>
<i>1.3.2 Apoptosis by MYC</i> .....	<i>13</i>
<i>1.3.3 Cell Growth and Metabolism</i> .....	<i>14</i>
<i>1.3.4 Genomic Instability</i> .....	<i>15</i>
<i>1.3.5 Angiogenesis and metastasis</i> .....	<i>16</i>
<i>1.4 MYC as a therapeutic target</i> .....	<i>17</i>
<i>1.5 Targeting MYC: A Direct Approach</i> .....	<i>18</i>
<i>1.5.1 G-quadruplex stabilizers</i> .....	<i>18</i>
<i>1.5.2 Antisense Oligonucleotides (ASOs)</i> .....	<i>22</i>
<i>1.5.3 siRNA</i> .....	<i>23</i>
<i>1.5.4 Small molecules inhibitors of the MYC-MAX interaction</i> .....	<i>24</i>
<i>1.5.5 Small molecule inhibitors of MYC-MAX binding to DNA</i> .....	<i>29</i>
<i>1.5.6. Small proteins or protein domains</i> .....	<i>31</i>
<i>1.6 Targeting MYC: An Indirect Approach</i> .....	<i>32</i>
<i>1.6.1 Blocking myc transcription</i> .....	<i>32</i>
<i>1.6.2 Blocking myc mRNA translation</i> .....	<i>35</i>
<i>1.6.3 Targeting Regulators of MYC Stability</i> .....	<i>38</i>
<i>1.7 WDR5: Structure, Function and Cancer incidence</i> .....	<i>39</i>

1.7.1 WDR5 protein structure.....	40
1.7.2 Discovery of WDR5.....	41
1.7.3 Interaction partners outside the nucleus.....	42
1.7.4 Role of WDR5 as a Member of Histone H3 Lysine 4 Methyltransferases Complexes.....	42
1.7.5 WDR5 forms part of the NSL Complex.....	43
1.7.6 WDR5 in the NuRD complex.....	44
1.7.7 Other WDR5 interaction partners in the nucleus.....	44
1.7.8 Discovery and characterization of the interaction between WDR5 and MYC.....	45
1.7.9 The WDR5-MYC link to cancer.....	47
1.7.10 Druggability of WDR5 at the WBM site.....	48
1.8 Scope of this thesis.....	49
<b>II. Structure Activity Relationship (SAR) of Sulfonamides.....</b>	<b>50</b>
2.1 Introduction.....	50
2.1.1 Hit identification and validation.....	50
2.1.2 X-ray co-crystal structure of VU0618016 bound to WDR5.....	52
2.1.3 Early SAR.....	54
2.1.4 Pharmaceutical properties.....	59
2.2 SAR of methyl sulfone analogs.....	60
2.2.1 Structure-based design and synthesis of phenolic methyl sulfone analogs.....	60
2.2.2 Physicochemical properties optimization in the methyl sulfone subseries.....	65
2.2.3 Pharmaceutical Properties.....	77
2.3 Biochemical and biological assessment of target engagement.....	78
2.3.1 Thermal shift assay.....	79
2.3.2 Confirmation of target engagement in cell lysates.....	80
2.4 Conclusions.....	82
<b>III. Sulfonamide linker replacements.....</b>	<b>84</b>
3.1 Introduction.....	84
3.2 Benzyl amine linker.....	85
3.3 Amino acetic acid linker.....	86
3.4 Propionic acid linker.....	87
3.3 Conclusions.....	99
<b>IV. Discovery of WDR5-MYC inhibitors using fragment-based methods and structure-based design.....</b>	<b>101</b>
4.1 Introduction.....	101
4.2 Hit Identification from NMR-based fragment screening.....	102
4.3 Structure determination of the fragment complexes.....	104
4.3. Compound design.....	106
4.3.1 N-substituted imidazolyl analogues.....	107

4.3.2	<i>Analogs with alternative heterocycles</i>	112
4.3.3	<i>Growing towards the S<sub>5</sub> pocket</i>	116
4.4	<i>Determination of target engagement</i>	122
4.4.1	<i>Confirmation of target engagement in cell lysates and whole cells</i>	122
4.4.2	<i>Chromatin Immunoprecipitation (ChIP)</i>	124
4.4.3	<i>Histone Methyltransferase activity</i>	127
4.5	<i>Conclusions</i>	127
<b>V.</b>	<b>General Conclusions</b>	<b>Error! Bookmark not defined.</b>
<b>VI.</b>	<b>Experimental</b>	<b>134</b>
6.1	<i>General Chemistry</i>	134
6.2	<i>General Experimental Procedures</i>	135
6.2	<i>Synthesis biaryl sulfonamide analogs</i>	144
6.2.1	<i>Synthesis of sulfonyl chlorides</i>	144
6.2.2	<i>Synthesis of salicylic acid analogs</i>	145
6.2.3	<i>Synthesis of methyl amide analogs</i>	152
6.2.4	<i>Synthesis of methyl sulfone analogs</i>	155
6.3	<i>Synthesis of analogs with sulfonamide replacements</i>	207
6.3.1	<i>Benzyl amine linker</i>	207
6.3.2	<i>Amino acetic acid linker</i>	210
6.3.3	<i>Propionic acid linker</i>	212
6.4	<i>Synthesis of fragment-based heterocyclic benzenesulfonamide analogs</i>	271
6.4.1	<i>N-Substituted imidazolyl analogs</i>	271
6.4.2	<i>Heterocyclic analogs</i>	289
6.4.3	<i>C-2 substituted imidazolyl analogs</i>	296
6.5	<i>Protein expression and purification</i>	307
6.6	<i>HTS screening</i>	308
6.7	<i>Hit validation by NMR</i>	308
6.8	<i>NMR experiments: fragment screening K<sub>d</sub> determination</i>	309
6.9	<i>Protein crystallization, data collection, and structure refinement</i>	309
6.10	<i>Cloning and plasmids</i>	310
6.9	<i>Cell culture</i>	311
6.11	<i>WDR5 immunoprecipitation</i>	311
6.12	<i>Antibodies</i>	311
6.13	<i>Chromatin Immunoprecipitation (ChIP) Experiments</i>	312
6.14	<i>Pharmaceutical property determinations</i>	312
<b>Appendix A</b>		<b>313</b>
<b>References</b>		<b>315</b>

List of Figures

<b>Figure</b>	<b>Page</b>
<b>Figure 1.</b> General architecture of MYC proteins. The image at the top shows a representation of a mammalian MYC protein. Image adapted from Tansey, 2014.....	4
<b>Figure 2.</b> Crystal structure of the MYC/MAX heterodimer bound to a canonical E-box. (PDB: 1NKP).....	5
<b>Figure 3.</b> Transcriptional repression mediated by MIZ1. MYC blocks the transcription of MIZ1-dependent gene expression. Whereas free MIZ1 that is bound to the core promoter in the promoter region of its target genes activates transcription via recruitment of coactivators, including p300 and nucleophosmin (NPM), MYC represses MIZ1-dependent transcriptional activation through disruption of the interaction between MIZ1 and these cofactors. Furthermore, MYC recruits the histone acetylase HDAC3 as well as the DNA methylase Dnmt3a. Adapted from Herkert, B. & Eilers, M., 2010,.....	10
<b>Figure 4.</b> MYC induced tumor suppressive pathways. Adapted from Campaner & Amati, 2012. ....	14
<b>Figure 5.</b> A) G-quadruplex structure shown in pink and B) a schematic diagram of human myc gene structure, the NHE III1 is located upstream of the P1 promoter. Adapted from Chen, B., Wu, Y., Tanaka, Y., and Zhang, W., 2014.....	19
<b>Figure 6.</b> Examples of developed MYC G-quadruplexes stabilizers. Adapted from Chen, B., Wu, Y., Tanaka, Y., and Zhang, W., 2014.....	20
<b>Figure 7.</b> Structures of Quarfloxin and CX-5461. ....	21
<b>Figure 8.</b> Small molecules that disrupt MYC-MAX dimerization. ....	28
<b>Figure 9.</b> Structures of small molecules inhibitors of MYC-MAX binding to DNA. ....	30
<b>Figure 10.</b> Mechanism of action of BRD4 inhibitors as anti-MYC drugs. Adapted from Cortiguera, M., López-Batlle, A., Albajar, M., Delgado, M. and León, J., 2015,.....	33
<b>Figure 11.</b> Structures of some BETi.....	35
<b>Figure 12.</b> The eIF4F complex binds RNA and promotes translation initiation in response of extracellular stimuli. Adapted from Sonenberg, N., Pause, A., 2006. ....	36
<b>Figure 13.</b> Chemical structures of BEZ235 and Silvestrol inhibitors. ....	37
<b>Figure 14.</b> Inhibitors of MYC's stability regulators. ....	39



<b>Figure 15.</b> WDR5 crystal structure (PDB:2H14). A) WDR5 is formed by a seven-bladed $\beta$ -propeller with a doughnut shape. B) Most common binding regions of WD40 proteins. ....	40
<b>Figure 16.</b> Co-crystal structure of WDR5 and MBIIIb. The hydrogen bonds between WDR5 and MYC are highlighted in green. A) Shows electrostatic potential of WDR5 and B) shows close-up of the WDR5-MYC peptide interaction. PDB: 4Y7R.....	46
<b>Figure 17.</b> Example $^1\text{H}$ - $^{15}\text{N}$ HSQC spectra showing the observable effects of compounds that A) induce peak shift and B) induce peak broadening. Apo-WDR5 (Blue), Hit-WDR5 (Red). C) Representative hits that bind WDR5 at the WBM site. $K_d$ values were obtained by FPA. ....	51
<b>Figure 18.</b> A) An overlay of <b>VU0618016</b> with the structure of bound MBIIIb peptide (PDB: 4Y7R), the frame shift of the loop enabling retainment of the H-bond interaction with the N225 is represented by the movement of N225; <b>VU0618016</b> (yellow), WDR5:MBIIIb complex (grey) and B) X-ray co-crystal structure of <b>VU0618016</b> bound to WDR5 (PDB:6U6W). Shown as dashes are the halogen bonding interaction with the bromine atom and W273 and the hydrogen bond between the sulfonamide oxygen and N225.....	53
<b>Figure 19.</b> Chemical structure of FITC-labeled probe for FPA.....	54
<b>Figure 20.</b> X-ray co-crystal structure of <b>VU0660590</b> bound to WDR5 (PDB:6U5Y). The salicylic acid forms a hydrogen bonding interaction with Q289. ....	57
<b>Figure 21.</b> Calculated pKa for compounds representative of each subseries. The salicylic acid subseries was not further evaluated since the pKa of the carboxylic acid negatively affects permeability. The calculated pKa values were obtained using MarvinSketch.....	66
<b>Figure 22.</b> X-ray co-crystal structure of A) <b>VU0814341</b> , the amide group of Q289 side chain was not resolved, and B) <b>VU0826049</b> (PDB:6U5M). ....	71
<b>Figure 23.</b> Chemical structure of negative control compound. ....	79
<b>Figure 24.</b> $\alpha$ -FLAG immunoprecipitation from lysates treated with different compounds. Levels of C-MYC protein in association with WDR5 was assessed after treatment with compound in lysates from WDR5-FLAG and C-MYC-HA co-overexpressing HEK293 cells. An $\alpha$ -FLAG immunoprecipitation was used to isolate WDR5, which is not detectable in the input due to the excess of WDR5 in the IP fraction. Lysates were treated with 50 $\mu\text{M}$ compound, data are representative of two independent biological repeats. ....	81
<b>Figure 25.</b> A) <b>VU0817326</b> chemical structure and B) X-ray co-crystal structure of WDR5 with <b>VU0817326</b> .....	90
<b>Figure 26.</b> X-ray co-crystal structure of <b>VU0817326</b> (orange) bound to WDR5 and overlaid with <b>VU0826049</b> (purple). ....	93

<b>Figure 27.</b> Conformational energy difference for <b>VU0817326</b> . Calculated with MOE using MMFF.....	96
<b>Figure 28.</b> Macrocyclic analogs and their binding affinity data.....	99
<b>Figure 29.</b> A) Overlay of the HMQC spectra of apo-WDR5 (black) and WDR5 with unlabeled MYC peptide (red). B) Overlay of HMQC spectra of apo-WDR5 (black) and WDR5 with MYC site fragment hit <b>F2</b> (red). The shifts upon ligand (peptide or hit) binding are indicated.....	103
<b>Figure 30.</b> Representative MYC site fragment hits. Those with the largest chemical shift perturbations are marked as ‘top hits’ .....	104
<b>Figure 31.</b> X-ray structures of WDR5 in complex with the c-MYC peptide and fragment hits. A) MYC peptide, PDB: 4Y7R; B) <b>F1</b> (PDB:6UJJ); C) <b>F2</b> (PDB: 6UHY); D) <b>F5</b> (PDB: 6UJH); E) <b>F6</b> (PDB: 6UHZ); F) <b>F7</b> (PDB: 6UJL). WDR5 is displayed as the surface model, with the WBM site centered. ....	105
<b>Figure 32.</b> Merging strategy. A) Merging the previously reported HTS hit <b>VU0618016</b> with <b>F2</b> results in a new class of compounds. B) X-ray co-crystal structure of <b>F2</b> bound to WDR5 (blue) and overlaid with <b>VU0618016</b> (yellow). C) Atoms from <b>F2</b> and <b>VU0618016</b> to be merged are colored in green.....	107
<b>Figure 33.</b> X-ray co-crystal structure of compound <b>VU0829217</b> .....	112
<b>Figure 34.</b> A) X-ray co-crystal structure of <b>VU0830052</b> bound to WDR5, B) Overlay of the X-ray crystal structure of <b>VU829217</b> and <b>VU0830052</b> . ....	115
<b>Figure 35.</b> A) X-ray co-crystal structure of <b>VU0848182</b> (green) bound to WDR5. B) Overlay of compound <b>VU0848182</b> and <b>VU0829711</b> (yellow). C) X-ray co-crystal structure of <b>VU0850264</b> (magenta) bound to WDR5. D) X-ray co-crystal structure of <b>VU0830838</b> (salmon) bound to WDR5.....	120
<b>Figure 36.</b> Fragment-inspired compounds without phenols. ....	122
<b>Figure 37.</b> Lysates were prepared from HEK cells over expressing HA-tagged c-MYC and Flag-tagged WDR5. Immunoprecipitations were performed using anti-Flag in the presence of 50 $\mu$ M compound and disruption of c-MYC/WDR5 complexes was measured by immunoblotting for C-MYC. Data is representative of two independent biological repeats. ....	123
<b>Figure 38.</b> HEK293 cells over expressing HA-tagged c-MYC and Flag-tagged WDR5 were treated with 5 $\mu$ M compound for 24 hours. WDR5 complexes were immunoprecipitated using an anti-Flag antibody followed by immunoblotting for C-MYC. Data is representative of two independent biological repeats.....	125

**Figure 39.** (A) Binding of MYC to target genes. Chromatin Immunoprecipitation (ChIP) in c-MYC-HA overexpressing HEK293 cells treated with 20  $\mu$ M compound for 10 h was performed using an  $\alpha$ -HA antibody. Percent recovery was monitored by qPCR at genes dependent on WDR5 for MYC recruitment or two genes independent of WDR5 (ZFPM1 and ZNF771). (B) WDR5 binding to chromatin at MYC target genes. The p values were calculated using a one-tailed student t-test. Data are representative of minimum three independent biological repeats..... 126

**Figure 40.** Physicochemical properties of best-in-class compounds ..... 131

List of Tables

<b>Table</b>	<b>Page</b>
<b>Table 1.</b> Summary of the different MYC Boxes functions or interactions.....	6
<b>Table 2.</b> Early SAR FPA data.....	55
<b>Table 3.</b> Optimization of salicylic acid derived WDR5 WBM-site inhibitors.....	58
<b>Table 4.</b> Structures and biochemical data for salicylamide derived WDR5-WBM site inhibitors. .....	59
<b>Table 5.</b> DMPK profile of select compounds. <sup>a</sup> .....	60
<b>Table 6.</b> Binding affinities of methyl sulfone analogs measured by FPA.....	63
<b>Table 7.</b> Analogs with different alkyl groups alpha to the sulfone.....	64
<b>Table 8.</b> Binding data for methyl sulfone and methyl amide analogs lacking a phenol in the aniline ring. Data determined by FPA.....	70
<b>Table 9.</b> FPA data for compounds lacking the right-hand side phenol.....	73
<b>Table 10.</b> FPA binding data for sulfones with tethered amine.....	75
<b>Table 11.</b> FPA binding data for O-tethered amines.....	77
<b>Table 12.</b> Tier 1 DMPK profile of selected compounds. <sup>a</sup> .....	78
<b>Table 13.</b> Measured $\Delta T_m$ values for different biaryl sulfonamide analogs.....	80
<b>Table 14.</b> FPA data for analogs with basic amine linker.....	86
<b>Table 15.</b> Minimum pharmacophore study. Binding affinity obtained by FPA.....	92
<b>Table 16.</b> Binding affinity data for analogs with different groups sitting in the S <sub>5</sub> pocket.....	94
<b>Table 17.</b> Binding affinity data for analogs with different hydrophobic groups sitting in the S <sub>1</sub> pocket.....	96
<b>Table 18.</b> SAR of substituents at N-1 of the imidazole ring.....	111
<b>Table 19.</b> FPA binding data for different heterocyclic analogs.....	114
<b>Table 20.</b> FPA binding data for compounds substituted in the C-2 of the imidazole ring.....	119

**Table 21.** Pharmaceutical property profile of selected compounds.<sup>a</sup> ..... 121

**Table 22.** Disruption of the WRAD complex as measured by activity in a commercial HMT.. 127

## List of Schemes

<b>Scheme</b>	<b>Page</b>
<b>Scheme 1.</b> Installation of methyl sulfones ortho to the phenol. ....	61
<b>Scheme 2.</b> a) S <sub>2</sub> (CH <sub>3</sub> ) <sub>2</sub> , Cu, pyridine, 90 °C, overnight; b) NaCH <sub>3</sub> SO <sub>2</sub> , L-proline, CuI, NaOH, DMSO, 85 °C, overnight; c) BBr <sub>3</sub> , DCM, -78 °C, 96%; d) NaSCH <sub>3</sub> , Pd <sub>2</sub> (dba) <sub>3</sub> , Xantphos, Et <sub>3</sub> N, THF, 76 C, 18 h, 99%; e) Oxone, EtOH:H <sub>2</sub> O, r.t., 1 h, 95%; f) HNO <sub>3</sub> , H <sub>2</sub> SO <sub>4</sub> , DCM, 0 °C, 4 h, 72%; g) H <sub>2</sub> , Pd/C, EtOH, 2 h, 94%; h) Sulfonyl chloride, pyridine, DCM, 0 °C, overnight, 27%. ....	62
<b>Scheme 3.</b> Synthesis of different analogs lacking the aniline phenol. ....	67
<b>Scheme 4.</b> Synthetic route for <b>VU0850756</b> and <b>VU0850757</b> . ....	68
<b>Scheme 5.</b> Synthesis of sulfonyl chlorides. ....	69
<b>Scheme 6.</b> Synthesis of analogs containing basic amines. ....	74
<b>Scheme 7.</b> Synthetic route for O-tethered amines. ....	76
<b>Scheme 8.</b> Proposed compound design with deleted sulfone from sulfonamide linker. ....	85
<b>Scheme 9.</b> Synthesis of compounds with basic amine linker. ....	85
<b>Scheme 10.</b> Amino acetic acid linker design. ....	87
<b>Scheme 11.</b> Synthetic scheme for the synthesis of amino acetic acid linker. ....	87
<b>Scheme 12.</b> Propionic acid linker. ....	88
<b>Scheme 13.</b> General synthetic route for analogs containing the propionic acid linker. ....	89
<b>Scheme 14.</b> Synthesis of analogs with groups sitting in the S <sub>5</sub> pocket. ....	91
<b>Scheme 15.</b> Synthetic route fo macrocyclic compounds. ....	98
<b>Scheme 16.</b> Synthesis of N-substituted fragment-based compounds. ....	109
<b>Scheme 17.</b> Synthetic routes for the different heterocyclic analogs. ....	113
<b>Scheme 18.</b> Synthesis of compounds with substitutions in C-2 of the imidazole ring. ....	117

## Chapter I

### Introduction

#### 1.1 Cancer and treatment

Cancer causes one of every six worldwide deaths, making it the second cause of death.<sup>1</sup> In 2018 there were 17 millions new cases worldwide and 1,735,350 of them were in the United States.<sup>2,3</sup> The international Agency for Research on Cancer expects an increase of ~26 millions new cases by 2035, this is assuming that national rates, as estimated in 2018, do not change and that the national projections are correct for these years.<sup>4</sup>

The Egyptians and Greeks have been reported to be the first civilizations to attempt treating cancer, they often performed radical surgery and cautery with very little success.<sup>5</sup> Major discoveries through the centuries allowed the identification of some of the pathological and biological qualities of tumors. In the late 1800s, the X-rays were discovered and started to be used for the diagnosis and treatment of some tumors. One of the major revolutions in the field took place after the Second World War, cytotoxic antitumor drugs were discovered which gave birth to chemotherapy.<sup>6,5</sup>

At the present time, chemotherapy is still widely used. Traditional agents act by blocking cell division or DNA replication, while some of them target the mitotic spindle. Examples of these drugs are platinum derivatives, nucleoside analogues, topoisomerase inhibitors, taxanes and vinca alkaloids.<sup>7</sup> In cancers like testicular carcinoma or childhood leukemias, chemotherapy can prolong patient survival; nonetheless, it is not effective for all cancer types and alternative treatments options are often desired.<sup>7</sup>

Patients who have undergone chemotherapy suffer from multiple secondary effects such as nausea, vomiting, oral and gastrointestinal mucositis (which can lead to anorexia, malabsorption, weight loss, and anemia), constipation, diarrhea, increase in cardiovascular disease, and/or others.<sup>8</sup> These effects are caused by the lack of selectivity of the chemotherapeutic agents for tumor cells over normal cells; therefore, there is a constant search for alternative and effective treatment options with fewer or non-secondary effects.<sup>9</sup>

In the late 80's, there was another major breakthrough, the development of drugs for specific molecular targets involved in tumorigenic pathways.<sup>5</sup> The progress made in understanding the different cellular pathways that regulate cell proliferation and survival has allowed the identification of altered or faulty signaling networks in malignant cells. The attempt to “fix” these specific molecular defects has given rise to what we call targeted therapy.<sup>10,11</sup> This approach looks to deliver drugs to particular genes or proteins that are specific to cancerous cells or the tissue environment that promotes cancer growth.<sup>9</sup> The increased selectivity minimizes the off-target side effects that are normally seen after chemotherapy treatment.<sup>9</sup> Some of the first targets approached with targeted therapy were growth factors, signaling molecules, cell-cycle proteins, modulators of apoptosis, and molecules that promoted apoptosis.<sup>11</sup> Nowadays, the target spectra is wider and a significant goal for the field is to find anticancer agents with improved absorption distribution metabolism and excretion (ADME) properties. Ideally, such compounds should be well-absorbed, have a long half-life, a slow rate of metabolism, be metabolically stable, and orally bioavailable with a favorable toxicity profile at biologically effective doses.<sup>11</sup>

Small molecules and monoclonal antibodies are the main types of targeted therapies that have been pursued.<sup>12</sup> Monoclonal antibodies tend to be more specific than small molecules, but the target protein must be in the extracellular space, as antibodies can't cross the cell membrane; therefore,



they have limited use.<sup>10</sup> Small molecules are, by definition, smaller than antibodies which allow them to be more permeable and reach targets in the extra- and intracellular space. Multiple small molecules and monoclonal antibodies have been marketed (imatinib, gefitinib, sorafenib, abiraterone, trastuzumab, bevacizumab) and shown success in the treatment of patients.<sup>10,12</sup>

Despite the progress made with targeted therapies, many patients still have limited options.<sup>13</sup> The main reasons being that the available agents do not treat a wide spectra of cancers (due to the heterogenic nature of tumors) and tumors can develop resistance for drugs.<sup>9,13</sup> In addition, after a therapeutic target is identified, scientific and technical hurdles can prolong the discovery of a drug.<sup>13</sup> Thus, there is a strong need for the identification of new targets and/or the development of alternative therapeutic treatments.

## 1.2 MYC proteins: Structure, Function, and Deregulation

Human *myc* gene is found at locus 8q24.21 on chromosome 8.<sup>14</sup> It encodes transcription factors that can regulate cell growth, proliferation, differentiation, and apoptosis in response to intercellular and environmental cues.<sup>15</sup> *Myc* is one of the most studied oncogenes as it is responsible for an estimated 100,000 cancer-related deaths in the United States every year.<sup>16</sup> MYC's oncogenic nature comes from its recurrent deregulation and increased expression through multiple mechanisms in tumor cells.<sup>16,17</sup>

In mammalian cells, the MYC protein can arise from three different genes: *c-myc*, *l-myc* and *n-myc*, (**Figure 1**). While *c-myc* is nearly ubiquitous expressed in proliferating tissues; *l-myc* and *n-myc* show a more restricted expression pattern.<sup>18</sup> All three proteins function similarly and the distinct expression patterns reflect different spatial and temporal requirements of MYC's activity.<sup>16,19</sup>

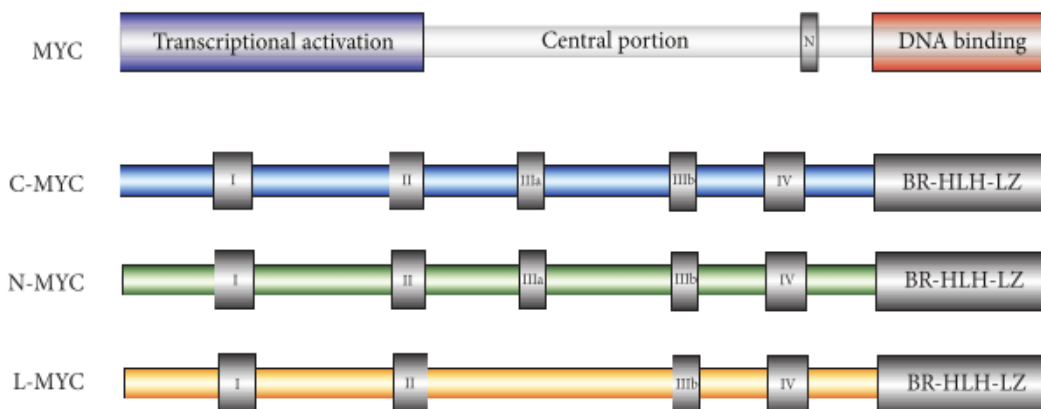


*Figure 1. General architecture of MYC proteins. The image at the top shows a representation of a mammalian MYC protein. Image adapted from Tansey, 2014.*

### 1.2.1 Structure of MYC proteins

*Myc* genes encode nuclear proteins of slightly different sizes: C-MYC has 439 amino acids, N-MYC has 464 amino acids and L-MYC has only 364 amino acids. These proteins contain a transcriptional activation domain (TAD) that is accepted to be the primary element that contacts RNA polymerase-II associated proteins to stimulate gene induction.<sup>16</sup> MYC proteins also contain several conserved regions that are organized in a similar way, they are designated as MYC Boxes (MB numbered 0, I, II, IIIa, IIIb, and IV) and they interact with different effector proteins.<sup>20,21</sup> The carboxy-terminal basic-helix-loop-helix-leucine zipper (bHLH-LZ) domain is also conserved.<sup>20</sup> The HLH-LZ portion (**Figure 2**) mediates the heterodimerization with MAX, a DNA binding domain (DBD). The basic region mediates the binding of MYC-MAX to DNA at the consensus sequence “CACGTG” or “Enhancer Box” (E-box); although, it has been reported to bind other noncanonical DNA sequences.<sup>20–22</sup>

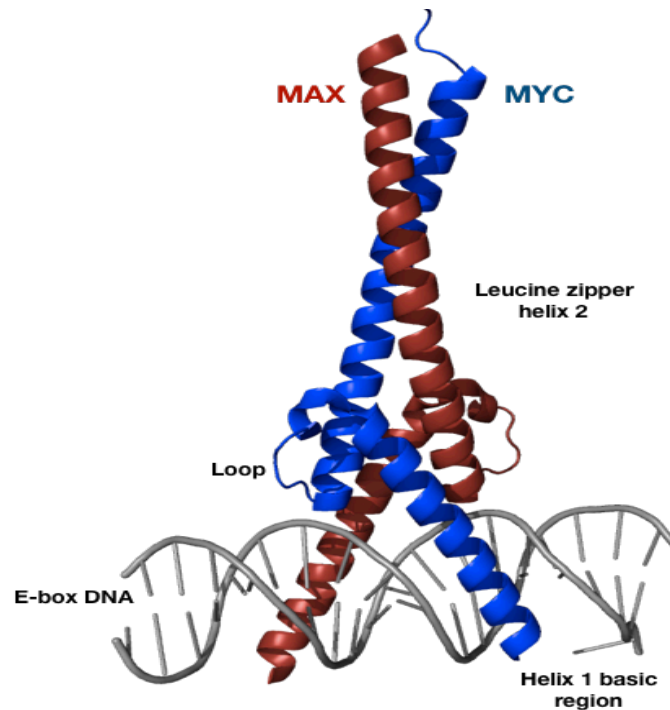



*Figure 2. Crystal structure of the MYC/MAX heterodimer bound to a canonical E-box. (PDB: 1NKP)*

### 1.2.2 MYC boxes: six well conserved sequences

The conservation of the MB elements suggests that they are involved in critical functions. MBI and MBII are the best characterized regions and it was not until recent years that roles to the MBIIIb and MB0 were identified.<sup>23,24</sup> A summary of the MYCBoxes' functions can be found in **Table 1**. Research of the central portion of MYC is ongoing, the conservation of these regions implies a common role and suggests that they might be involved in additional interactions (e.g. protein-protein or DNA-protein interactions) which are critical for MYC function. Moreover, very little is known beyond MYC boxes as these other segments are not conserved within individual members of the MYC family.<sup>16</sup>

**Table 1.** Summary of the different MYC Boxes functions or interactions.



<p>MBIV 317-337 aa</p>	<ul style="list-style-type: none"> <li>• Required for full apoptotic functions<sup>24</sup></li> <li>• Contributes to transcriptional activation and repression of genes<sup>24</sup></li> <li>• Increases DNA binding affinity<sup>24</sup></li> </ul>
<p>MBIIIb 258-267 aa</p>	<ul style="list-style-type: none"> <li>• Interacts with WDR5 and allows target genes recognition<sup>23</sup></li> <li>• Important for driving tumorigenesis<sup>23</sup></li> </ul>
<p>MBIIIa 187-199 aa</p>	<ul style="list-style-type: none"> <li>• Required for transformation <i>in vitro</i> and <i>in vivo</i><sup>25</sup></li> <li>• Important for transcriptional repression by MYC<sup>25</sup></li> <li>• Regulates and directs MYC proteolysis<sup>26</sup></li> <li>• Recruits HDAC3 to Id2 and Gadd153 promoters<sup>27</sup></li> </ul>
<p>MBII 128-143 aa</p>	<ul style="list-style-type: none"> <li>• Ubiquitylation and degradation of C-MYC via proteasome<sup>28</sup></li> <li>• Promotes cellular transformation <i>in vitro</i><sup>29</sup></li> <li>• Promotes tumorigenesis <i>in vivo</i><sup>30</sup></li> <li>• Activates and represses most of its target genes<sup>31,32</sup></li> <li>• Interacts with TRAAP<sup>33</sup></li> </ul>
<p>MBI 45-63 aa</p>	<ul style="list-style-type: none"> <li>• Mediates transcriptional functions.</li> <li>• Important for cellular transformation<sup>29</sup></li> <li>• Interacts with kinase P-TEFb<sup>34</sup>.</li> <li>• Involved in the ubiquitylation and degradation of C-MYC via proteasome<sup>28,35</sup></li> </ul>
<p>MB0 10-32 aa</p>	<ul style="list-style-type: none"> <li>• Mediates transactivation, induces canonical MYC target genes.<sup>21</sup></li> <li>• Induces p53-independent apoptosis.<sup>21</sup></li> </ul>

Findings in mice using a gene-targeting approach have shown that the three MYC proteins perform similar activities. Malynn and coworkers have shown that *n-myc* can replace *c-myc* in mice and support most *c-myc* functions in regulating murine growth and development, which demonstrates a major degree of functional redundancy between these two proteins.<sup>36</sup>

### 1.2.3 The MAX-MYC interaction

In 1991, MAX was discovered as a dimerization partner of MYC proteins.<sup>37</sup> The heterodimerization between MYC and MAX, combined with the specific DNA binding to E-boxes, is critical for all known MYC functions.<sup>37,38</sup> This heterodimer can activate or repress a large number of genes transcribed by RNA polymerase II (RNAPII) that encode proteins involved in ribosome biogenesis, metabolism, differentiation, apoptosis, proliferation, growth, and others.<sup>20</sup> Mice that lack *max* die at day 5-6 of gestation, demonstrating that *max* has an important role in embryonic development.<sup>39</sup> In the same way, mice that lack *c-myc* die before embryonic day 10.5 and show defects in the placenta and in their vascular and hemotopoeitic systems.<sup>40</sup> *N-myc* deficient embryos die between embryonic day 10.5 and 12.5; they show neuroectodermal and heart defects. On the other hand, studies with *l-myc* deficient mice have shown that this gene is non-essential, as no obvious phenotype has been identified.<sup>40,41</sup>

MAX can also heterodimerize with other DNA binding proteins (DBP) like MNT or MAD1-4 and antagonize MYC activities.<sup>19</sup> Ayer and colleagues reported that the MYC-MAX dimer is usually found in proliferating cells, while the MAD-MAX dimer is more commonly found in resting or differentiated cells.<sup>42,43</sup>

### 1.2.4 Transcriptional function of MYC

The identification of MYC-regulated genes has been complicated and it has generally relied on experimental activation of MYC followed by close monitoring of changes in mRNA levels.<sup>44,45</sup> Studies have reported that MYC binds around 25,000 sites in the human genome, although this number changes depending on the experimental conditions and the method(s) used.<sup>46</sup>

MYC proteins levels are low at normal physiological conditions; therefore, the promoter regions where they bind are considered to be high-affinity sites. The reported number of MYC molecules in proliferating cells is less than the number of binding sites, which means that each site is bound temporarily.<sup>47</sup>

The mechanism by which MYC regulates transcription has been coined as the ‘hit and run’ mechanism, meaning that MYC binding is brief but triggers long-lasting changes in the chromatin.<sup>47</sup> When cells express high levels of MYC, there are additional E-boxes and non-sequence-specific sites that are bound by MYC. These sites reflect inefficient binding and are commonly referred as low affinity binding sites.<sup>45,48</sup>

Guccione and coworkers showed that MYC recognizes its binding sites based on epigenetic features.<sup>48</sup> Euchromatic islands, defined as “clusters of specific methyl- and acetyl-histone marks at the 5’ end of active or poised genes”, are essential for *in vivo* binding of MYC to DNA; therefore, the commonly observed association of MYC to binding sites near CpG islands is a consequence of this chromatin structure.<sup>45,48</sup> Less often is seen that MYC binds E-boxes outside of the euchromatic island, but about half of euchromatic islands without E-boxes are bound by MYC.<sup>48</sup>

The direct binding of MYC to the promoter sites to activate or repress genes is not the only way these proteins influence the cell environment. MYC can interact with other proteins or transcription factors to activate genes. Uribealgo *et al* reported that the dimer MYC-MAX is recruited by the retinoic acid receptor- $\alpha$  (RAR $\alpha$ ) to a set of the latter’s target genes, which lack E-boxes.<sup>16,49</sup> Here, MYC works with RAR $\alpha$  to incorporate signals that control the balance between proliferation and differentiation in HL60 cells (leukemic cells).<sup>16,49</sup>

As mentioned above, MYC can also repress genes. The first MYC-repressed gene identified was *c-myc* itself.<sup>50,51</sup> The suppression of endogenous *c-myc* gene was described to occur at the level of

transcriptional initiation and the degree of this suppression is relative to the amount of physiological C-MYC.<sup>51</sup> MYC proteins can additionally repress genes with antiproliferative or anticancer properties, some of the reported genes are related to cell cycle inhibitors (*p21<sup>Cip1</sup>*, *cdkn2c*, *cdkn2b*, *cdkn1b*, *cdkn1c*), tumor-suppressive miRNAs (miR-29, miR-26a), cell proliferation (*ndrg*), and cell adhesion molecules (*galectin-1*, *clusterin*, *integrin $\alpha$ 6*, *integrin $\beta$ 1*, *integrin $\beta$ 4*, *fibronectin*, *tenascin C*, *catenin  $\alpha$ 1*, *adductin*, *procollagen I $\alpha$ 2*, *procollagen V $\alpha$ 2*).<sup>16,52–56</sup> The MYC-MAX dimer can interact with Sp1 and MIZ1, two zinc finger transcription factors that bind to core promoters.<sup>55,57,58</sup> Both proteins are present at the promoter of many MYC-repressed genes.<sup>55</sup> When MIZ1 is not bound to MYC, it stimulates the expression of multiple genes by binding initiator elements surrounding the transcription start site of specific genes.<sup>16,55</sup> Once MYC interacts with MIZ1 it reprograms the transcriptional properties of MIZ1 by inhibiting the interaction with activating cofactors like p300 and also by inducing the formation of inhibitory marks (methylation by engaging Dnmt3a or deacetylation by interacting with HDAC3, **Figure 3**.<sup>27,55,59</sup> Furthermore, the interaction of MYC with SP1 recruits HDAC1, a histone deacetylase, to the chromatin and reduces HIV promoter expression.<sup>60</sup>

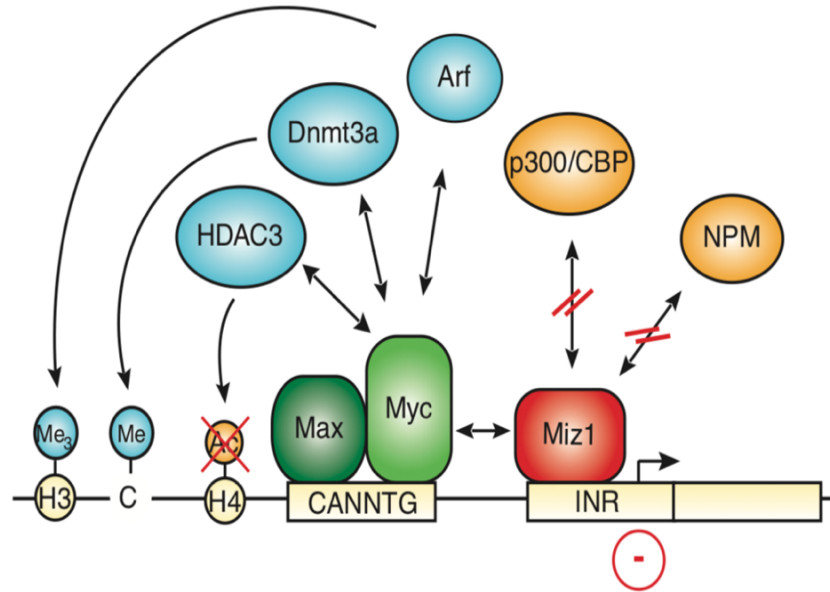


**Figure 3.** Transcriptional repression mediated by MIZ1. MYC blocks the transcription of MIZ1-dependent gene expression. Whereas free MIZ1 that is bound to the core promoter in the promoter region of its target genes activates transcription via recruitment of coactivators, including p300 and nucleophosmin (NPM), MYC represses MIZ1-dependent transcriptional activation through disruption of the interaction between MIZ1 and these cofactors. Furthermore, MYC recruits the histone acetylase HDAC3 as well as the DNA methylase Dnmt3a. Adapted from Herkert, B. & Eilers, M., 2010,

More recently, a new model that explains MYC transcriptional behavior has been proposed. Coined as the “Amplifier Model”, it states that MYC doesn’t regulate a set of specific genes but it rather works by binding to and “amplifying” the expression of every active gene in a given cell type.<sup>16,17,61</sup> The model was derived from the observations made by studying cells containing a tetracycline (Tet)-repressible *myc* transgene, which allowed to control the concentration of MYC in the cells. One of the major criticisms of the model is that it fails to account for the actions of MYC in repressing transcription.<sup>16</sup>



### 1.2.5 MYC regulation

MYC proteins are under stringent control at every step of their life; the half-life of the proteins is between 15 and 30 min.<sup>16,42</sup> MYC's regulation starts at the level of transcription, where mitogens like lipopolysaccharide, concanavalin, epithelial growth factor (EGF), thrombin, and platelet-derived growth factor (PDGF) induce C-MYC mRNA.<sup>62,63</sup> Regulation of transcription has been described to occur at the initiation and of release of paused RNA polymerase II.<sup>16,64,65</sup> After transcription, the MYC mRNA is transported to the cytoplasm by eIF4E, a translation initiation factor that is regulated by mitogenic signals.<sup>16,66</sup> eIF4E reduces the chances of errant MYC mRNA escaping by binding it early during transcription.<sup>16</sup> Translation of mRNA MYC can be suppressed by TIAR which mediates productive ribosome engagement.<sup>16,67</sup> Once MYC mRNA is translated, it is subject of posttranslational modifications. CBP (cAMP-response-element-binding protein) acetylates MYC and decreases ubiquitination by stabilization of the protein.<sup>68</sup>

MYC can also be phosphorylated by CK2 at the basic and acidic regions, the phosphorylation affects the stability and DNA binding of the MYC-MAX dimer.<sup>69</sup> Thr-58 and Ser-62 (both within MBI) can be phosphorylated by GSK3 and proline directed kinases, respectively. Phosphorylation of Ser-62 stabilizes MYC while phosphorylation of Thr-58 can induce MYC degradation.<sup>69</sup> Phosphorylation at these two sites seems to affect MYC stability at the G<sub>0</sub> to G<sub>1</sub> transition.<sup>69</sup> Additional phosphorylation sites have been reported and include Ser-71, Ser-82, Ser-162, and Ser-293.<sup>69</sup> Likewise, Thr-58 has been identified as a site of glycosylation.<sup>70</sup>

### 1.3 MYC in cancer

The study of fulminant chicken tumors caused by oncogenic retroviruses led to the discovery of *v-myc* oncogene, which was shown to produce myelocytomatosis (leukemia and sarcoma).<sup>71</sup> This

led to the search for comparable human retroviruses; although, the search wasn't successful, it led to the discovery that human MYC is frequently altered by chromosomal translocation in Burkitt's lymphoma (BL).<sup>71,72</sup> All these efforts guided the identification of MYC as a bona fide oncogene. It has been shown that *myc* is usually translocated in multiple myeloma (MM) tumors and amplified (increase in number of copies of a gene) in many different cancers.<sup>73,74</sup> In T-cell leukemia, C-MYC can be deregulated by a defective NOTCH1 as it is a direct target gene.<sup>75</sup> MYC is very likely to act by regulating the expression of genes that promote transformation; nonetheless, there is controversy over which genes are important for tumorigenesis, the role of transcriptional activation versus repression and how impactful a modest transcriptional output can be in cell behavior.<sup>16</sup>

### 1.3.1 MYC in cell cycle

MYC proteins influence cells to enter to the cell cycle and can accelerate the rate of key stages.<sup>16</sup> *Myc* is induced after quiescent cells are exposed to mitogenic signals and is required for a robust cell cycle response.<sup>16,62</sup> However, there are reports that show that expression of MYC is sufficient to induce quiescent cells to re-enter the cell cycle.<sup>16,76,77</sup>

The activation of E2F and CDK4 by MYC enables the inactivation of the tumor suppressor gene *Rb* (retinoblastoma) to allow the transcription factors E2F to activate genes involved in DNA replication.<sup>78,79</sup> E2F and MYC and bind numerous genes involved in DNA replication (*MCM3*, *MCM4*, *CDC6*), this suggests that they might work together.<sup>79,80</sup>

### 1.3.2 Apoptosis by MYC

MYC's forced expression in normal cells lacking survival factors can promote apoptosis.<sup>16,81</sup> In order for cells overexpressing MYC to become cancerous, they must circumvent apoptosis. Cells overexpressing MYC usually require a second mutation to inhibit the apoptosis machinery, so that tumor growth can progress. One example of this synergy is the overexpression of BCL-2 (an antiapoptotic protein) and MYC, which promotes the development of lymphomas.<sup>82</sup>

Another common process through which MYC induces apoptosis is via the ARF-MDM2-p53 axis, **Figure 4.**<sup>16,83</sup> This mechanism arises as an intracellular response to stressful situations induced by MYC.<sup>83</sup> In this case, MYC increases the expression of ARF, which destabilizes and inactivates the Ub-ligase MDM2, and leads to induction of the tumor suppressor p53.<sup>16,83</sup> Therefore, loss of p53 is commonly observed in tumors that also up-regulate MYC.

Alternatively, MYC can induce the DNA damage response (DDR) by increasing reactive oxygen species (ROS) and replication stress. Furthermore, oncogenic MYC activation has been associated with ATM inactivation in several tumors.<sup>83</sup> In the presence of accumulated DNA double strand breaks (DSBs), the kinase ATM is responsible for the activation of DDR as it activates multiple substrates upon DNA damage; CHK2 and p53 among them. Once p53 is phosphorylated, it can escape from MDM2 and ensure prolonged G2 arrest and induction of DNA repair or stimulation of apoptosis.<sup>83</sup>

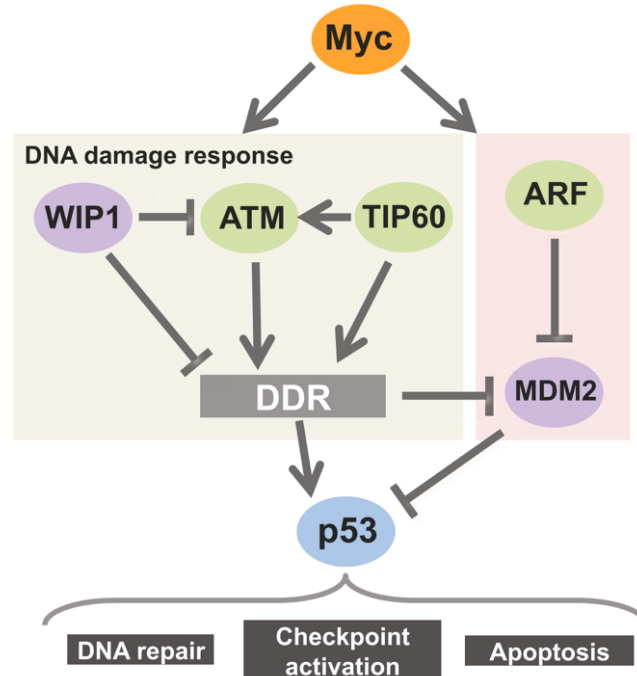


*Figure 4. MYC induced tumor suppressive pathways. Adapted from Campaner & Amati, 2012.*

### 1.3.3 Cell Growth and Metabolism

MYC promotes proliferation and cell cycle progression. Cells that divide rapidly require a constant supply of nutrients, energy, and proteins to sustain their growth.<sup>16</sup> Overexpression of MYC proteins results in an increase of cell size and protein synthesis, it also causes cells to carry twice the total RNA content.<sup>17,84</sup> MYC proteins are capable of sustaining the cell growth by up-regulating ribosome-biogenesis and protein translation genes.<sup>16,85,86</sup> Likewise, MYC can activate transcription by RNA polymerases I and III and increase the translational capacities of cells.<sup>16</sup> The role of MYC in protein synthesis is key in tumor development as it was demonstrated that by reducing the number of ribosomes in precancerous cells overexpressing MYC, it suppresses the transition to a tumorigenic state.<sup>16,87</sup>

The metabolism of cancerous cells is also affected and reprogrammed by overexpression of MYC. MYC proteins enhance the expression of genes involved in glucose uptake and glycolysis.<sup>16,88</sup> MYC also drives transcription of the plasma membrane nutrient transporters that supply the metabolic pathways.<sup>89</sup>

The conversion of pyruvate to alanine has been observed in precancerous tissues prior to observable morphological or histological changes, this could provide a new metabolic marker of cancer progression and regression.<sup>88</sup>

More recently, Carroll *et al* showed that oncogenic MYC requires MondoA, a transcription factor capable of sensing nutrients in the cell, for tumorigenesis.<sup>90</sup> The knockdown of *MondoA* and induction of N-MYC in neuroblastoma cells (Tet21N) impaired proliferation and increased apoptosis.<sup>90</sup> Moreover, they found that there is a gene expression signature consisting of MYC/MondoA-regulated metabolic genes; high expression of these genes correlates with poor prognosis in cancers like neuroblastoma, lung squamous cell carcinoma, liver hepatocellular carcinoma, and colon adenocarcinoma.<sup>90</sup>

#### 1.3.4 Genomic Instability

MYC is capable of inducing replication stress in cells, a systematic state that leads to collapsed DNA replication forks.<sup>91</sup> The specific chromosomal loci where replication stress occurs are called common fragile sites.<sup>91</sup> Replication stress is often associated with oncogene induced DDR.<sup>83</sup> In the case of MYC, DDR accounts for genomic and chromosomal instability, chromosomal translocations, dicentric chromosomes (those containing two centromeres), and tetraploidy.<sup>16,83</sup> Additionally, MYC can cause early origin firing and disrupt the symmetry of the DNA replication

fork, these lead to fork collapse and impacts DNA integrity.<sup>16,92</sup> Finally, MYC can also increase origin density and lead to asymmetrical fork progression.<sup>92</sup>

### 1.3.5 Angiogenesis and metastasis

Malignant tumors are characterized by the development of an ample blood supply. This allows the delivery of oxygen, nutrients, and growth factors; therefore, the development of blood vessels is required for tumor progression and maintenance.<sup>93</sup>

Two steps are involved, 1) Vasculogenesis, which is the establishment of a primitive vascular network from endothelial cells that assemble into vascular tubes. It is regulated by vascular endothelial growth factor (VEGF) and the receptors Flk-1 and Flt-1; and 2) Angiogenesis, which is the sprouting and remodeling of the preexisting vessels.<sup>93</sup> Angiogenesis is provoked early during tumor progression in response to environmental cues such as hypoxia, which regulates the expression of angiogenic factors important for vasculogenesis and angiogenesis.<sup>93</sup> MYC increases the expression of VEGF and decreases the expression of thrombospondin-1, an inhibitor of neovascularization.<sup>16,94</sup> MYC also regulates the expression of angiopoietin-1 (ANG-1) and angiopoietin-2 (ANG-2), two regulators of angiogenesis.<sup>93</sup>

Expression of MYC can activate *galectin-1*, a gene whose protein facilitates metastasis by promoting cell migration, invasion, angiogenesis, and evasion of immune response in various tumors.<sup>95</sup> MYC activation also reduces cell adhesion and components of the extracellular matrix (ECM).<sup>96</sup> Moreover, MYC overexpression has been associated with induction of epithelial mesenchymal transition (EMT), a process that is important in embryonic development and cancer progression.<sup>97,98</sup> In EMT, cells undergo a developmental switch from polarized epithelial phenotype to a motile mesenchymal phenotype.<sup>97</sup>

### 1.3 MYC as a therapeutic target

MYC proteins play multiple roles in regulating pro-tumorigenic functions and they are often found to be deregulated in human cancers; therefore, inhibiting MYC is reasonable and attractive.<sup>99</sup> Some arguments that favor the targeting of MYC have been discussed by Prochownik and Vogt:<sup>99</sup>

1. A study using more than 20 human cancer lines showed that depletion of MYC by short hairpin RNA (shRNA) led to a permanent proliferative arrest in every case.<sup>100</sup> In addition, animal models have shown that a continuous expression of MYC is required in order to sustain tumor proliferation.<sup>101,102</sup> Based on these observations, it is very likely that MYC inhibition will stop tumor progression.
2. Targeting MYC might show low toxicity; its expression in normal quiescent cells is very little, if any. The predicted toxicities would be similar to those shown in non-targeted therapies and would include hematopoietic and gastrointestinal effects.<sup>99</sup>
3. Disruption of protein-protein interactions (PPI) has shown promising results. Substitution of a single amino acid in the bHLH-ZIP domain of MYC affects dimerization with MAX and has been shown to abolish transactivation and biological functions.<sup>99,103,104</sup>

One of the arguments against targeting of MYC is that developing a MYC inhibitor will be difficult, as the most obvious approach would be targeting the MYC-MAX interaction or other essential cofactor, such as TRRAP.<sup>99</sup> This requires the disruption of PPIs, which involves large, flat and featureless surfaces. In the case of MYC and MAX, they are both intrinsically disordered proteins, which means that they are highly difficult to target.<sup>14</sup> Moreover, the disruption of PPIs should take into account the energy of association that is resultant from the interacting proteins.<sup>99</sup>

## 1.4 Targeting MYC: A Direct Approach

Multiple different approaches to directly target MYC have been employed. Several inhibitors of *myc* transcription have been assessed, as well as many small molecules to inhibit the direct interaction between MYC and MAX or MYC-MAX and DNA. Others have tried using small proteins or protein domains to block MYC from associating with different interacting partners.

### 1.5.1 G-quadruplex stabilizers

G-quadruplexes or G-quartets are ternary structures formed in nucleic acids by sequences that are rich in guanine. They are “derived from intramolecular or intermolecular folding of DNA single strands”, **Figure 5a**.<sup>105,106</sup>

In *myc* gene, the promoter nuclease hypersensitive element III1 (NHE III1, also known as Pu27) (**Figure 5b**) controls 80-90% of *myc* transcriptional activity.<sup>107</sup> This is a guanine rich area and the formation of G-quadruplex can silence the *myc* gene.<sup>106,107</sup>

Multiple small ligands have shown to stabilize *myc* G-quadruplexes and successfully repress its transcription. The list includes derivatives of quindoline<sup>108</sup>, perylene<sup>109,110</sup>, cationic porphyrines<sup>111,112</sup>, alkaloids<sup>113,114</sup>, platinum complexes<sup>115</sup>, ellipticine<sup>116</sup>, and carbamide<sup>117</sup>; some examples are shown in **Figure 6**.



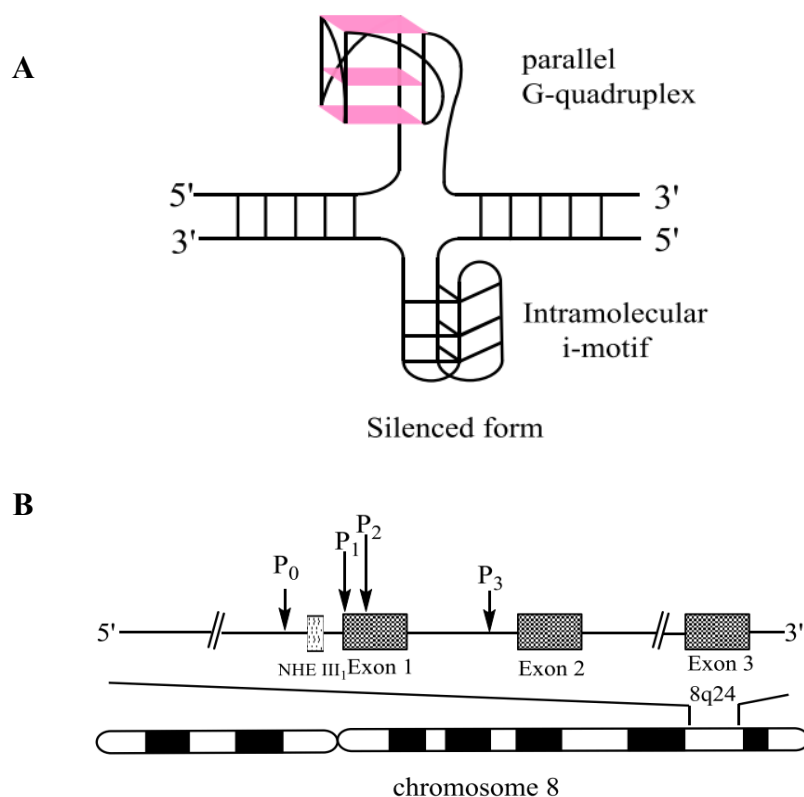


**Figure 5.** A) G-quadruplex structure shown in pink and B) a schematic diagram of human myc gene structure, the NHE III is located upstream of the P1 promoter. Adapted from Chen, B., Wu, Y., Tanaka, Y., and Zhang, W., 2014

The most studied G-quadruplex inhibitor is a fluoroquinolone-based antitumor agent known as Quarfloxin or CX-3543 (**Figure 7**). In 2008, it started phase II clinical trials for neuroendocrine tumors.<sup>14</sup> Quarfloxin was optimized from QQ58, a topoisomerase II intercalator and a G-quadruplex interactor, to be significantly more selective towards G-quadruplexes.<sup>14</sup> Further studies with Quarfloxin showed that its mechanism of action consist of the disruption of nucleolin binding to G-quadruplexes in the nucleolus. This results in the inhibition of Pol I transcription and rRNA biogenesis which induces apoptosis in cancer cells.<sup>14,118</sup>

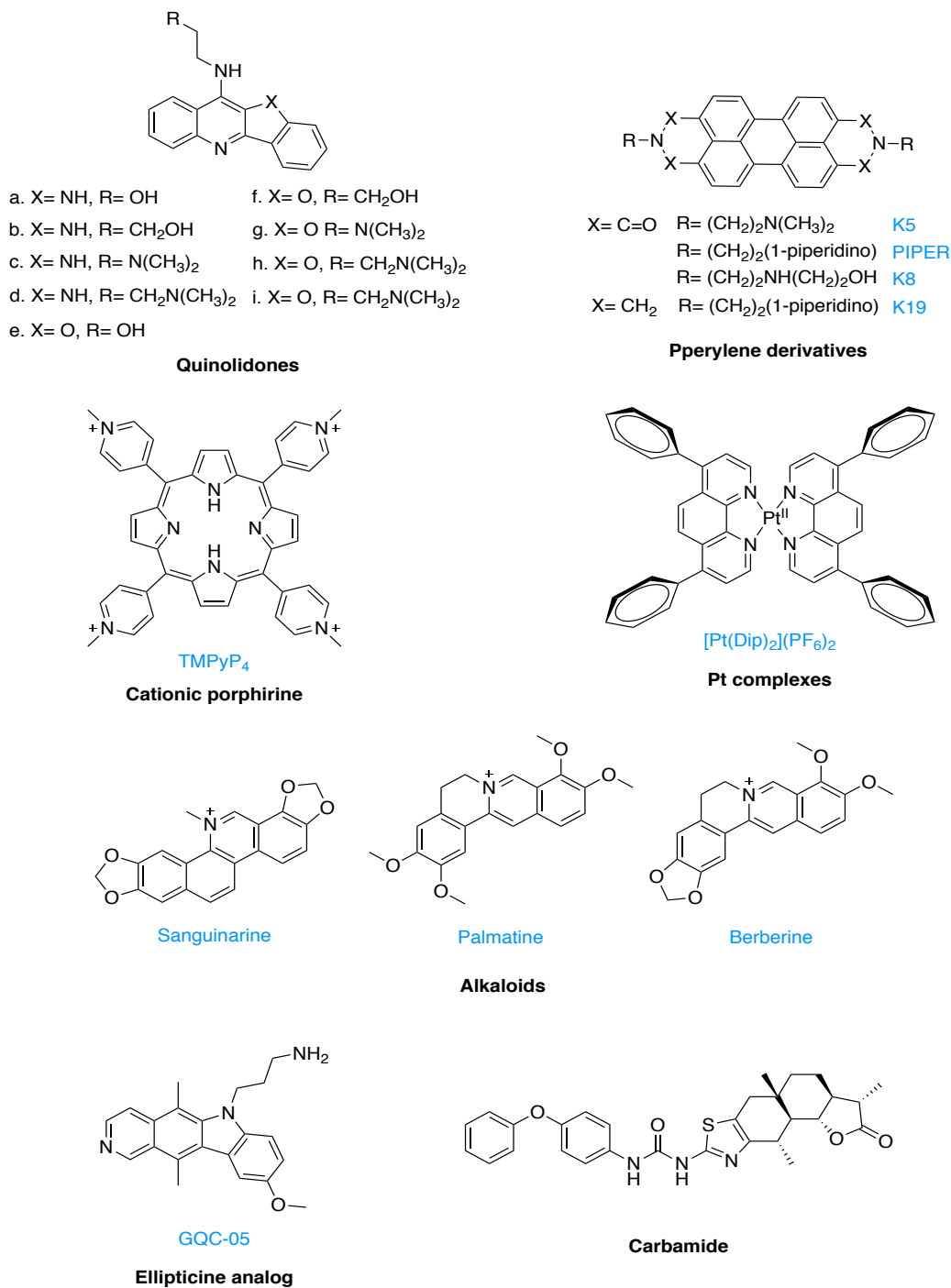


**Figure 6.** Examples of developed MYC G-quadruplexes stabilizers. Adapted from Chen, B., Wu, Y., Tanaka, Y., and Zhang, W., 2014.

Quarfloxin was withdrawn from clinical trials due to problems with bioavailability, but further medicinal chemistry efforts allowed the development of CX-5461 (**Figure 7**Figure 7. Structures of Quarfloxin and CX-5461.).<sup>14</sup> It has been reported that CX-5461 is a selective inhibitor of Pol I-mediated rRNA synthesis and it can also induce DNA damage in DNA-repair deficient cell lines.<sup>14,119,120</sup> Moreover, a FRET-melting assay using DNA oligonucleotides comprising three G-quadruplexes-forming sequences (x-MYC, ckit1 and h-Telo) showed that CX-5461 is a strong binder and stabilizer of G-quadruplexes. This is supported by immunofluorescence experiments which showed *in vivo* stabilization of G-quadruplexes.<sup>120</sup>

More recently, other small molecules capable of stabilizing the *myc* G-quadruplex have been reported. The findings include IZCZ-3<sup>121</sup>, 13-[(dimethylamino)methyl]-12-hydroxy-8*H*-benzo[*c*]indolo[3,2,1-*ij*][1,5]naphthyridine-8-one<sup>122</sup>, and TPP (a carbamoylpiperidinium-containing compound)<sup>123</sup>.

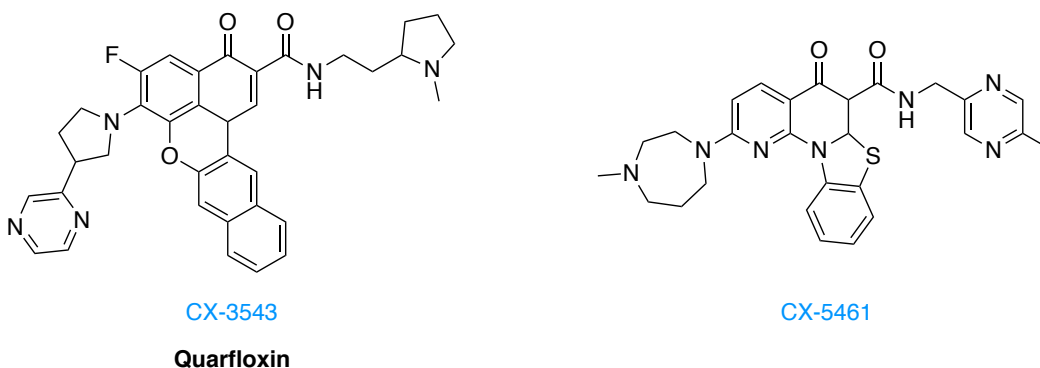


**Figure 7.** Structures of Quarfloxin and CX-5461.

In general, targeting G-quadruplexes appears promising; however, *myc* is not the only gene promoter region to possess this structural motif, thus compound selectivity is a concern. Another

drawback is the existence of only a few G-quadruplexes in the *myc* promoter region under physiological conditions.<sup>124,107</sup>

### 1.5.2 Antisense Oligonucleotides (ASOs)

ASOs are short (8-50 nucleotides) synthetic single stranded oligodeoxynucleotides.<sup>125</sup> ASOs bind to target mRNA by complementary base pairing, this leads to endonuclease-mediated transcript knockdown; therefore, a reduction of the levels of a specific protein is observed.

Targeting *myc* with ASOs was first achieved in F-MEL (Friend murine erythroleukemia), HL-60, CML-BC (chronic myelogenous leukemia blast cells), and *ras* oncogene-transformed NIH 3T3 cells.<sup>126–129</sup> Later on, the phosphorothioate INX-3280 was able to move into Phase I and II clinical trials for treatment of lymphoma and solid tumors.<sup>105</sup> Unfortunately, INX-3280 was withdrawn in 2002 by Inex for unknown reasons.<sup>105</sup> Later on, AVI BioPharma developed AVI-4126, a phosphorodiamidate morpholino oligomer (PMO).<sup>130</sup> They showed that a single intraperitoneal (i.p.) dose (0.5 mg/kg) of AVI-4126 in rats was able to reduce liver C-MYC protein in a sequence-specific and dose dependent manner.<sup>130</sup>

The ASO strategy also has a considerable challenge: targeted delivery. Because the ASOs are have a short chain size, they display a very low charge density and have exposed aromatic bases, which confers a hydrophobic character to the molecule. Progress in this field has been slow also because ASOs show poor stability against intra and extracellular degradation. Some studies have shown activity using “naked” ASOs *in vivo*; however, they accumulate predominantly in the liver and kidney.<sup>131</sup> An additional concern relates to hybridization-dependent toxicity or off-target hybridization.<sup>99,131</sup> In consequence, none of the *myc* ASOs have been further developed to reach the market and actually, very few other ASOs have done so.<sup>105</sup>

### 1.5.3 siRNA

Small interfering RNAs (siRNAs) are double-stranded RNA molecules that bind to complementary sequences in mRNA and degrade them.<sup>132</sup> Wang and coworkers used a lentiviral-based short hairpin RNA (shRNA) expression vector to reduce C-MYC expression in 22 human tumor cell lines and three normal human cell lines. In all cases, cell proliferation was successfully inhibited.<sup>100</sup>

Moreover, Dicerna Pharmaceuticals developed DCR-MYC for the treatment of various cancers. Preclinical studies of this molecule showed strong anti-tumor effects in animal models of human cancers.<sup>133</sup> In 2014, DCR-MYC entered Phase I clinical trials to assess the safety and tolerability in patients with solid tumors, multiple myeloma, or lymphoma. While data from Phase I was promising, Dicerna decided to halt the development of DCR-MYC in 2016 as it did not meet the company's expectations for further development.<sup>134</sup>

In general, siRNAs exhibit poor pharmacokinetic properties which slows down their development. The main issue with siRNAs is that they are prone to rapid enzymatic degradation.<sup>105</sup> One example to overcome this is the use of gold nanoparticles modified by branched polyethyleneimine. They were developed as an efficient and safe intracellular delivery carriers for siRNA.<sup>135</sup> Shaat *et al* reported that when HuH7 cells are treated with *c-myc* siRNA and gold nanoparticles, there is a greater reduction of C-MYC protein translation in comparison to those cells treated with naked *c-myc* siRNA.<sup>135</sup> Zhu *et al* developed a carrier made of liposomes and folate, a compound vital for tumor cells, capable of transporting *n-myc* siRNA.<sup>136</sup> Because many cancer cells overexpress folate receptors, they were able to induce apoptosis in an *in vivo* neuroblastoma model.<sup>105,136</sup>

Additionally, the oncolytic adenovirus ZD55-shMYCN has been used *in vivo* to deliver *n-myc* siRNA and it inhibited xenograft neuroblastoma tumor growth.<sup>105,137</sup>

The different *myc* siRNAs that have been developed are useful tools and have allowed the study of different scenarios in which MYC is overexpressed. However, the use of siRNAs as an approach to treat MYC-driven tumors has proven to be challenging due to stability issues, which has drifted the efforts towards other approaches.

#### 1.5.4 Small molecules inhibitors of the MYC-MAX interaction

The first reported small molecule inhibitor of the MYC-MAX interaction was the peptide mimetic IIA6B17, **Figure 8**.<sup>138</sup> This peptide is capable of disrupting the MYC-MAX interaction in fluorescence resonance energy transfer (FRET) assay, enzyme linked immunosorbent assay (ELISA), and electrophoretic mobility-shift assay (EMSA). IIA6B17 can reduce cell growth in chicken embryo fibroblasts (CEF) but it is not entirely specific to MYC, as it also inhibits Jun (a component of the AP-1 transcription factor complex).<sup>105,138</sup>

Several other compounds were identified using a “credit card” approach, such as NY2280 and NY2276 (**Figure 8**). They showed disruption of the MYC-MAX interaction in biochemical assays (such as FRET and EMSA); however, *in vitro* assays using CEF showed that they interfere with Jun.<sup>139</sup> It is speculated that the compounds’ lack of selectivity for MYC could be due to similar structural features that MYC and Jun proteins share in their leucine zipper domain.<sup>139</sup>

Different compound libraries, containing as many as ~17,000 compounds, have been screened with the goal of identifying more MYC-MAX inhibitors. The compound 10058-F4 (**Figure 8**) was identified in one of these campaigns and showed activity *in vitro* and *in vivo*.<sup>140</sup> The small molecule 10058-F4 has been studied by multiple groups, which have found, collectively, that it can induce cell-cycle arrest, apoptosis, myeloid differentiation in acute myeloid leukemia (AML), and inhibit human telomerase reverse transcriptase.<sup>141,142</sup> While 10058-F4 showed promise for further

development, pharmacokinetic studies showed that it was unstable, had high clearance (its half-life was approximately 1 h), and no significant antitumor activity was observed in tumor-bearing mice.<sup>143</sup> A second and third generation of 10058-F4 analogues were made, they proved to be more stable and active than their parent compound.<sup>38,144</sup>

From the same screening that revealed 10058-F4, compounds 10074-G5 and 10074-A4 (**Figure 8**) were also identified as specific MYC-MAX inhibitors.<sup>145,146</sup> These compounds were used in follow-up work to map their binding sites on MYC.<sup>147,148</sup> Experiments such as point mutations, circular dichroism, fluorescence polarization, and nuclear magnetic resonance (NMR) allowed the identification of three different binding sites on MYC.<sup>147,148</sup> The knowledge derived from the identification of the binding sites allowed the development of further structure activity relationships (SAR); therefore, allowing the improvement of the compounds affinity for MYC. One example is compound JY-3-094 (**Figure 8**), which emerged from several rounds of optimization around 10074-G5. Compound JY-3-094 was shown to be more potent than 10074-G5 in the EMSA assay; though, it was inactive on HL-60 cells due to a permeability issue.<sup>149</sup> Esterification of JY-3-094 yielded compound SF-4-017 (**Figure 8**), which was able to inhibit the dimerization of MYC-MAX in cells.<sup>149</sup> Compound SF-4-017 is a good tool compound as it shows activity in cells; however, it needs to be optimized to increase its potency and drug-like character. Mycro1 and Mycro2 are two tool compounds that have been reported to inhibit MYC-MAX dimerization and the DNA binding of C-MYC.<sup>150</sup> They showed higher selectivity than some of the previously described compounds as they do not disrupt the binding of other dimers (MAX-MAX, Jun-Jun, and C/EBP $\alpha$ -C/EBP $\alpha$ ) to DNA.<sup>150</sup> Mycro1 and Mycro2's activity was confirmed by EMSA and they showed selectivity for MYC-MAX over Jun-Fos.<sup>150</sup> Moreover, both compounds inhibit cell proliferation, gene transcription, and oncogenic transformation.<sup>150</sup>

Another interesting small molecule was found by screening the Kröhnke pyridine library.<sup>151</sup> KJ-Pyr-9 (**Figure 8**) showed inhibition of MYC-MAX dimerization in a FP assay and showed antioncogenic properties in experiments using CEF with MYC-induced oncogenic transformation. Due to its low solubility in water (12.5  $\mu\text{M}$ ) the binding affinity was determined by back scattering interferometry (BSO). It showed a  $K_d = 6.5$  nM for MYC and a  $K_d = 13.4$  nM for the MYC-MAX heterodimer, suggesting that KJ-Pyr-9 can dissociate the intact MYC-MAX complex.<sup>151</sup> In addition, this compound inhibited cell growth in *myc*-amplified human cancer xenografts.<sup>151</sup> The activity of KJ-Pyr-9 has been questioned, the Larsson's group tested this compound in their SPR assays and it was not able to inhibit the MYC-MAX interaction. They also assessed its ability to bind MYC by SPR, but unfortunately no binding was observed up to 8  $\mu\text{M}$ .<sup>152</sup> Larsson's group discovered a small molecule, MYCMI-6 ( $K_d = 1.6$   $\mu\text{M}$ , **Figure 8**), that inhibits the MYC-MAX interaction *in vitro* at single-digit micromolar concentrations and the cell growth in tumor cells. MYCMI-6 has been postulated as an attractive tool to study the disruption of MYC-MAX dimer as it does not affect the expression levels of MYC.<sup>152</sup> However, further studies must be conducted as the precise mechanism of action is unknown.

Several other small molecules have been identified using computational techniques to virtually screen binding to intrinsically disordered proteins and disruption of the MYC-MAX dimer. Some of the identified compounds include PKUMDL-YC-1201<sup>153</sup>, PKUMDL-YC-1203<sup>153</sup>, PKUMDL-YC-1204<sup>153</sup>, and NSC13728<sup>154</sup>.

More recently, Abdulkadir's group has published two MYC inhibitors, MYCi361 and MYCi975, (**Figure 8**) capable of engaging MYC inside cells, disrupting the MYC-MAX interaction, and impairing MYC-driven gene expression.<sup>155</sup> Treatment of cells with MYCi361 triggers MYC-T58 phosphorylation which results in a reduction of the protein. MYCi361 can also inhibit the viability



of MYC-dependent cancer cells (e.g. MYC-Cap, LNCaP, MV4-11, HL-60, SK-N-B2) with low micromolar IC<sub>50</sub> values. Furthermore, animal studies with MYCi361 suggested that this compound might not be tolerated for a prolonged period. An optimization campaign to generate better and more tolerated analogs identified compound MYCi975, which showed similar activity as MYCi361 but with increased tolerability. In conclusion, these compounds are promising starting points for the development of direct MYC inhibitors; nonetheless, further studies are required as both compounds were reported to interact with multiple proteins in addition to MYC.<sup>155</sup>

Finally, the strategy of inhibiting the MYC-MAX interface is challenging because both are intrinsically disordered proteins (IDPs) and the protein-protein interface between them is flat and dynamic.<sup>124</sup> In addition, the low similarity among the MYC-MAX inhibitors suggested the possibility of multiple binding sites, which was later confirmed.<sup>107</sup> Circular dichroism and Nuclear Magnetic Resonance (NMR) experiments identified three different binding sites for 10074-A4<sup>99</sup>, suggesting that selectivity might be hard to attain.

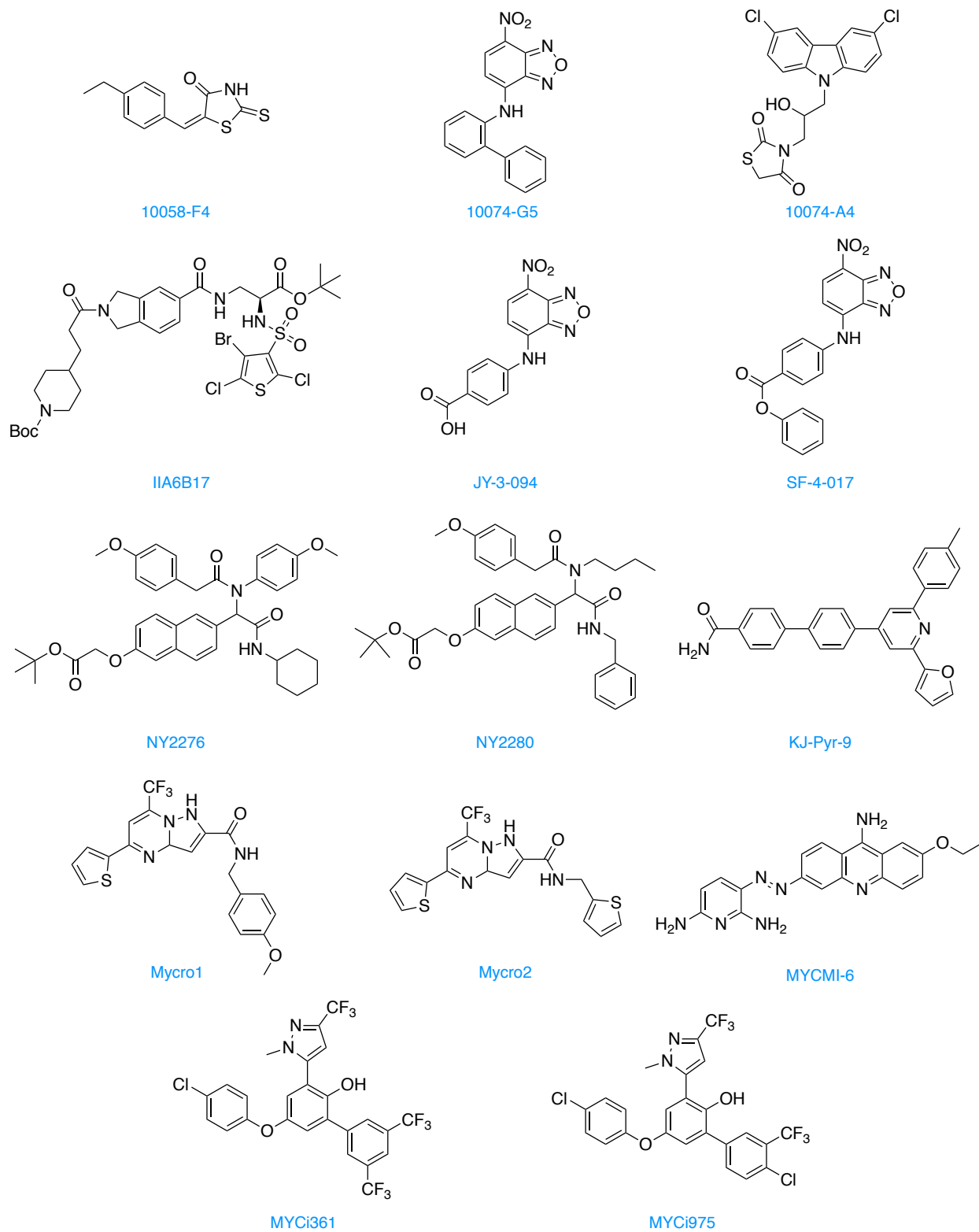


**Figure 8.** Small molecules that disrupt MYC-MAX dimerization.

### 1.5.5 Small molecule inhibitors of MYC-MAX binding to DNA

Screening of compound libraries allowed the identification of several inhibitors of MYC-MAX binding to DNA. One of these studies revealed the compound MYRA-A (**Figure 9**). It inhibits MYC transactivation and the DNA-binding activity of MYC.<sup>156</sup>

Natural product-inspired compounds have also been studied. Celastrol (**Figure 9**) and several Celastrol-inspired triterpenoids were able to disrupt binding of MYC-MAX to DNA, as seen in EMSA.<sup>157</sup> Further experimentation showed that they can reduce the abundance of MYC protein and provoke a global energy crisis characterized by ATP depletion, neutral lipid accumulation, cell cycle arrest and apoptosis.<sup>157</sup>

The small molecule KSI-3716 (**Figure 9**) can inhibit the binding of MYC-MAX to DNA and suppress proliferation of HL-60 cells.<sup>158</sup> Further studies with this compound revealed a reduction in expression of the genes *cyclin*, *D2*, *CDK4*, and *hTERT*, all targets of C-MYC.<sup>159</sup> In addition, KSI-3716 suppressed tumor growth after local instillation in mice bladders.<sup>159</sup>

The compounds mentioned above have shown activity in *in vitro* assays but have not shown selectivity in cells or in *in vivo* experiments.<sup>105</sup> In order to overcome this issue, Jung and coworkers developed  $\alpha$ -helix mimetics that recognize C-MYC when it is bound to MAX.<sup>160</sup> They are capable of inhibiting the binding of the heterodimer to its canonical E-box DNA sequence without disrupting the MYC-MAX interaction.<sup>160</sup> Six analogs were identified to be active in EMSA and demonstrated a dose-dependent inhibition with IC<sub>50</sub> values < 50  $\mu$ M. EMSA using MAX homodimers showed that all compounds are at least 2-fold more selective for C-MYC-MAX-DNA complexes over MAX-MAX-DNA complexes.<sup>160</sup> The six  $\alpha$ -helix mimetics were tested in HL60 and Daudi Burkitt lymphoma cells and five of the six compounds inhibited proliferation of both cell lines; although, one of them (JKY-2-169, **Figure 9**) showed to be superior.<sup>160</sup> Additional cell

experiments with JKY-2-169 revealed that it promotes cell cycle arrest and accumulation of neutral lipids.<sup>160</sup> Unfortunately, JKY-2-169 showed inhibition of proliferation in cells lines that do not express C-MYC.<sup>160</sup>

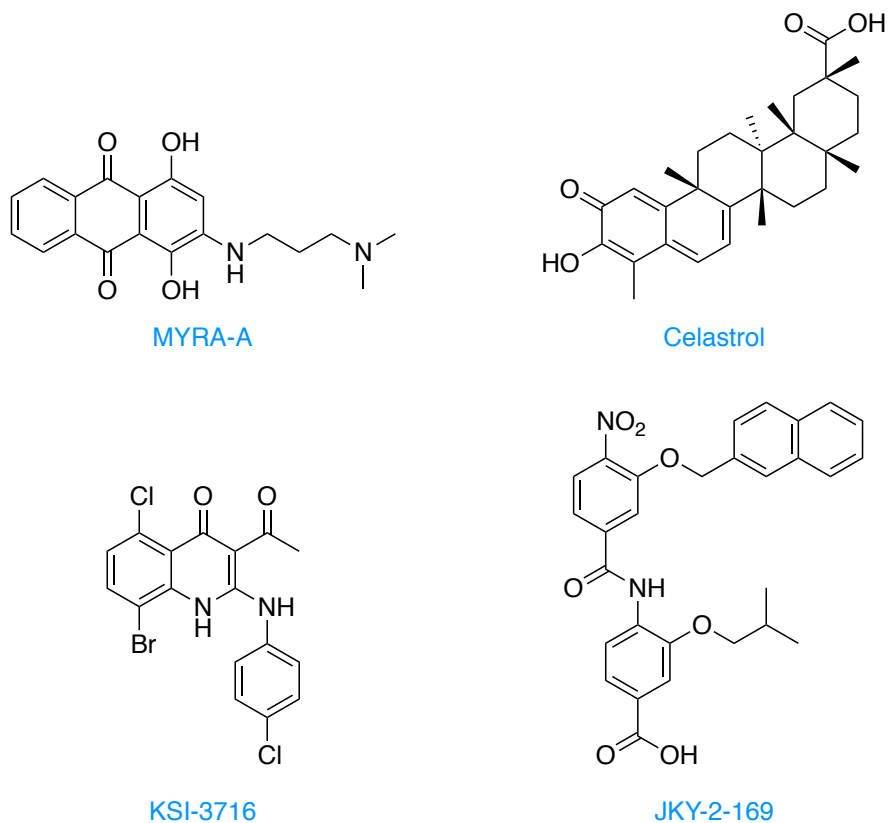


*Figure 9. Structures of small molecules inhibitors of MYC-MAX binding to DNA.*

The development of small molecules that inhibit the MYC-MAX binding to DNA have proved to be a challenging approach as the different identified compounds lack potency and selectivity for the MYC-MAX dimer. Therefore, alternative approaches to target MYC-driven cancers are being investigated.

#### 1.5.6. Small proteins or protein domains

This group of inhibitors consists of structurally-related molecules based on domains from MYC or MAX proteins.<sup>105</sup> The most known and well characterized small protein is Omomyc, which was developed by Soucek *et al* using molecular modeling and mutagenesis studies.<sup>161</sup> Omomyc possesses four mutated amino acids in the leucine zipper region that allows it to heterodimerize with wild type MYC and MAX.<sup>161</sup> As a result, Omomyc is able to repress MYC's transcriptional activity in modified BOSC23 cells and it produces proliferation arrest in NIH3T3 cells.<sup>161</sup> *In vivo* studies using different mouse models of cancer have shown that Omomyc itself is capable of inhibiting tumorigenesis independently of the driving mutation or tissue of origin.<sup>105,162-165</sup> More importantly, these studies showed that MYC is a valid therapeutic target as there were minimal side effects when Omomyc was used. In addition, the animals were able to recover after withdrawing it.<sup>105</sup>

The peptide Int-H1-S6A, F8A is derived from the helix 1 (H1) carboxylic region of C-MYC and contains the *Antennapedia* fragment that allows the internalization of the peptide into cells.<sup>166</sup> This peptide is capable of preventing MYC-MAX dimerization *in vitro* and it inhibits cell growth of MCF-7.<sup>166</sup> Moreover, Int-H1-S6A, F8A also inhibited the transcription of two genes, *ODC* and *p53*.<sup>166</sup>

The peptide derived from helix 1 (H1) of the helix-loop-helix domain of C-MYC, has been mixed with a carrier based on elastin-like polypeptide (ELP) which is thermally stable and responsive.<sup>167</sup> At a specific temperature the biopolymer forms aggregates; hence, its accumulation can be directed *in vivo* to the desired site by external application of heat.<sup>167</sup> This approach showed promising effects in rats with intracerebral gliomas as the administration of the peptide followed by a heat stimuli resulted in tumor volume reduction by 80%.<sup>167</sup>

Studies with the different peptides (or protein domains) have demonstrated that this approach has potential applicability to patients; however, there are some issues regarding their physicochemical properties (e.g. poor permeability and low stability).<sup>167</sup> Therefore, some of the efforts have focused on finding delivery mechanisms that could allow more control over the cargo while providing protection. More studies must be conducted to determine the feasibility of this approach as a therapy.

## 1.6 Targeting MYC: An Indirect Approach

The lack of success in the direct approaches to target MYC has shifted the focus of many groups towards different indirect approaches. Most of the current efforts are focused on finding pathways and target proteins that allow the transcriptional regulation of *myc* and the modulation of MYC's stability and activity.<sup>105</sup>

### 1.6.1 Blocking *myc* transcription

Inhibition of the Bromodomains and Extra Terminal (BET) subfamily of human bromodomains (BRD2, BRD3, and BRD4) has become an attractive approach to treat cancer as they directly regulate the expression of cancer-related genes, including *c-myc*.<sup>168,169</sup> Bromodomains are a family of conserved motifs that bind the acetylated lysine in histone tails.<sup>168</sup> Recognition of this histone mark allows the recruitment of other chromatin factors and transcriptional machinery, ultimately regulating gene transcription.<sup>168</sup> It has been reported that BRD4 enhances mitotic progression by staying bound to the transcriptional start sites of genes expressed during the M/G1 transition.<sup>170</sup> BRD4 also mediates transcriptional elongation by interacting and recruiting the positive transcription elongation factor complex (P-TEFb, composed of cyclin T1 and CDK9) to the core

promoter of the active genes.<sup>170,171</sup> P-TEFb phosphorylates the C-terminal region of RNA Pol II to allow transcriptional elongation (**Figure 10**).<sup>172</sup> C-MYC regulates promoter-proximal pause release of Pol II through recruitment of P-TEFb, causing enhanced transcriptional activity for those cells overexpressing C-MYC.<sup>169,173</sup> These findings have established the rationale to target BET bromodomains to inhibit C-MYC-dependent transcription.<sup>169,170</sup>

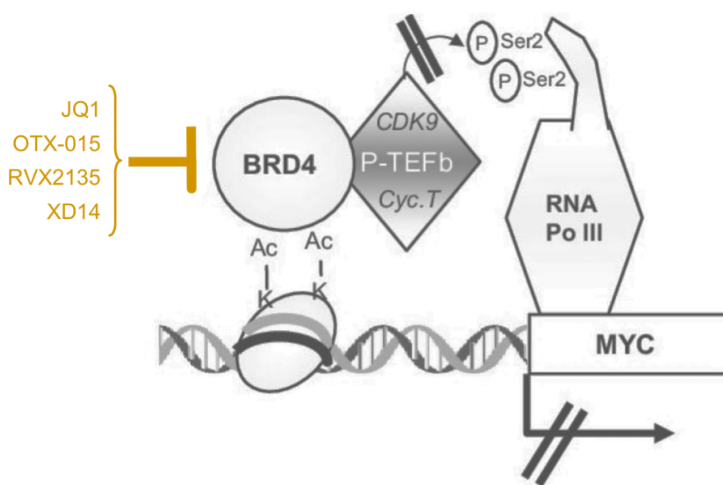


**Figure 10.** Mechanism of action of BRD4 inhibitors as anti-MYC drugs. Adapted from Cortiguera, M., López-Batlle, A., Albajar, M., Delgado, M. and León, J., 2015,

The first small molecule inhibitor of BET bromodomain (BETi) identified was (+)-JQ1 (hereafter JQ1, **Figure 11**).<sup>170</sup> Isothermal titration calorimetry (ITC) was used to assess its binding affinity, JQ1 showed a  $K_d = 50$  nM and 90 nM for the first and second domain of BRD4.<sup>170</sup> Moreover, the crystal structure of JQ1 bound to BRD4 confirmed binding to the acetyl-lysine site.<sup>170</sup> Initial studies showed that it can displace the BRD4 fusion oncoprotein from chromatin in human squamous carcinoma, consequently promoting squamous differentiation and antiproliferation effects in BRD4-dependent cell lines and patient-derived xenograft models.<sup>170</sup> Further studies with

JQ1 showed a robust inhibition of MYC expression in MM cell lines caused by downregulation of *myc* transcription itself.<sup>169</sup> JQ1 proved to be able to cause proliferation arrest, cell-cycle arrest, and cellular senescence in MM cells.<sup>169</sup> *In vivo* evaluation of JQ1 using mice models of MM, as well xenograft models of BL and AML, showed anti-tumor activity.<sup>105,169,174</sup> Multiple groups have studied JQ1 and have found that this small molecule may function by inhibiting additional oncogenic factors, most likely due to its lack of selectivity for BRD4.<sup>105,175–178</sup> It also seems that the mechanism and effectiveness of the inhibitor on MYC expression depends on the cell type.<sup>179</sup> JQ1 proved to be a good chemical probe but it has a short half-life (1 hour) and the required dose concentrations to mediate activity are above physiologic safety levels *in vivo*.<sup>146,175,179</sup> This led to the development of other small molecule BETi; several of them are currently in Phase I and/or II of clinical studies. One example is OTX015 (**Figure 11**), an inhibitor of BRD2 and 4. Preclinical studies showed antiproliferative effects in lymphoma models by affecting MYC, NFkB, JAK/STAT pathways and chromatin structure.<sup>179</sup> ABBV-075 (**Figure 11**) is another BETi that also targets BRD2 and BRD4.<sup>179,180</sup> It entered Phase I clinical trials for advanced hematological and solid tumors. GSK developed I-BET762 (GSK525762A, **Figure 11**); it shows reduction of MYC expression in prostate cancer cells and triggers apoptosis in neuroblastoma models by inhibiting *n-myc* and *bcl-2*.<sup>179,181</sup> CPI203, TEN-010, and BAY1238097 are also BETi that have entered clinical trials.<sup>179</sup>

Alternatively, strategies to target CDK7 and CDK9 have emerged. These two CDKs have roles in transcription initiation and elongation.<sup>182</sup> Both of them phosphorylate specific serine residues of RNA Pol II, allowing them to regulate transcriptional initiation, pause release, and elongation.<sup>182,183</sup> A covalent inhibitor of CDK7, THZ1, was shown to disrupt the transcription of amplified *n-myc* in neuroblastoma cells.<sup>184</sup> Mice bearing *n-myc*-amplified neuroblastoma tumors



were treated with THZ1 and a significant reduction of tumor volume was observed in comparison to those mice treated with vehicle.<sup>184</sup> Mice models of small cell lung carcinoma (SCLC) treated with THZ1 also displayed increased survival compared to the control group.<sup>185</sup> Additional studies showed that the stability of THZ1 *in vivo* limits its utility; hence, THZ2 (a regioisomer of THZ1) was synthesized and it shows increased stability and similar antitumor properties.<sup>186</sup>

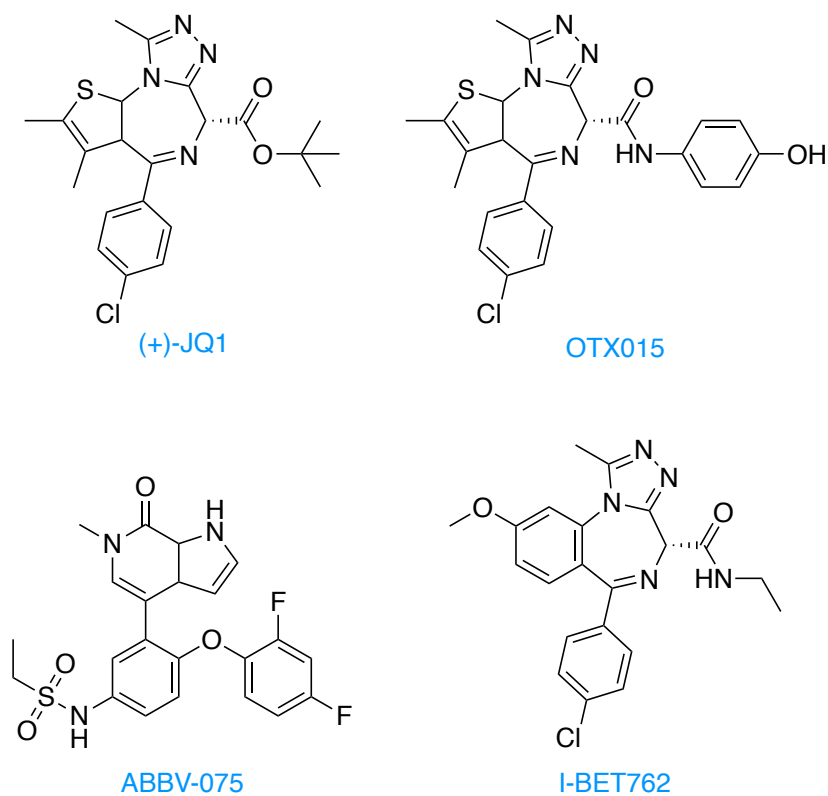


*Figure 11. Structures of some BETi.*

### 1.6.2 Blocking *myc* mRNA translation

Inhibition of the mTOR (mammalian target of rapamycin) pathway has been shown to be a plausible way to inhibit *myc* translation. The mTOR complex 1 (mTORC1) can phosphorylate and inactivate 4E-BP1 and PDCD4 (**Figure 12**); both are negative regulators of translation that bind

and sequester two eukaryotic initiation factors (eIF), eIF4E (cap-binding protein) and eIF4A (RNA helicase).<sup>187,188</sup> These eIF (eIF4E and eIF4A), together with eIF4G (a scaffolding protein), target *myc* genes and all together form the eIF4F complex that recruits ribosomes to the 5'-cap of mRNA. The translation of some mRNAs can be initiated by an internal ribosomal entry site (IRES) localized at the 5' untranslated region (5'-UTR) of the mRNAs. The 5'-UTR of *myc*'s mRNA allows for both cap- and IRES-mediated translation, the latter one being dependent on eIF4A.<sup>187</sup>

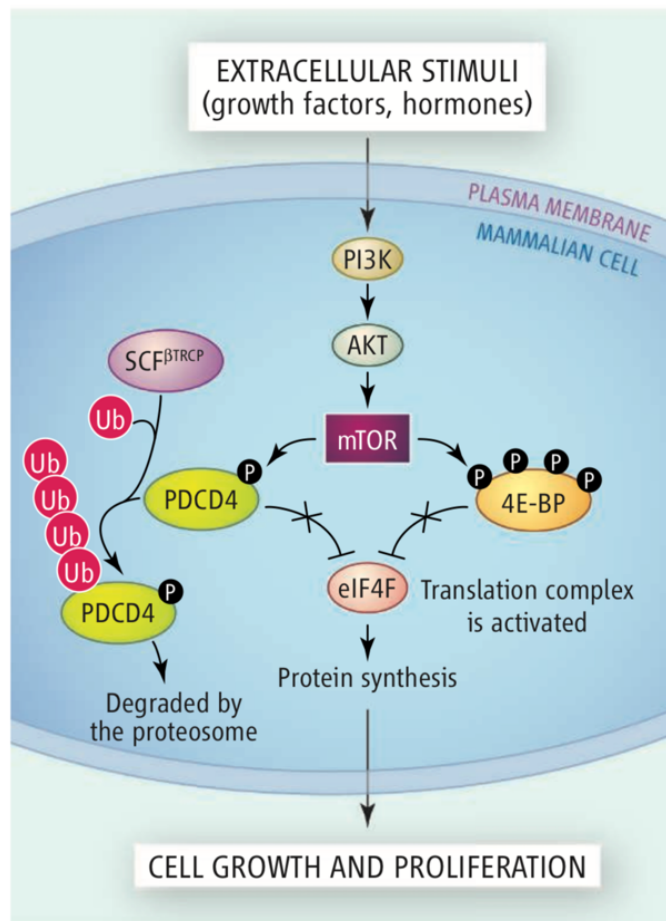


**Figure 12.** The eIF4F complex binds RNA and promotes translation initiation in response of extracellular stimuli. Adapted from Sonenberg, N., Pause, A., 2006.

Therefore, there have been attempts to target different components in this pathway as well as some upstream controllers of its activity.

Inhibition of mTOR has been attempted using BEZ235 (**Figure 13**). This inhibitor of mTOR and PI3K showed that when used to treat colon cancer cells, it can cause reversible cell cycle arrest but does not induce apoptosis.<sup>189</sup> Further analysis showed that BEZ235 increased MYC levels in SW480, CACO2, Ls174T, and HCT116 cells.<sup>189</sup> Treatment with BEZ235 did not affect the expression of eIF4A or eIF4E but did show dephosphorylation of 4EBP1. Additionally, cell treatment with this inhibitor does not interfere with eIF4E, but reduces cap binding of eIF4A and eIF4G.<sup>189</sup> Later findings, show that mTOR inhibition using BEZ235 fails because a) the levels of 4EBPs are insufficient to fully sequester eIF4E and b) the IRES of *myc*'s mRNA allows translation independent of eIF4E.<sup>189</sup>

Other inhibitors of mTOR have been developed and continue to be tested; these include MLN0128/INK128, AZD805, AZD2014, PP242 and OSI-027.<sup>190</sup> However, it is expected that these inhibitors affect other proteins or processes besides *myc* translation.<sup>105</sup>

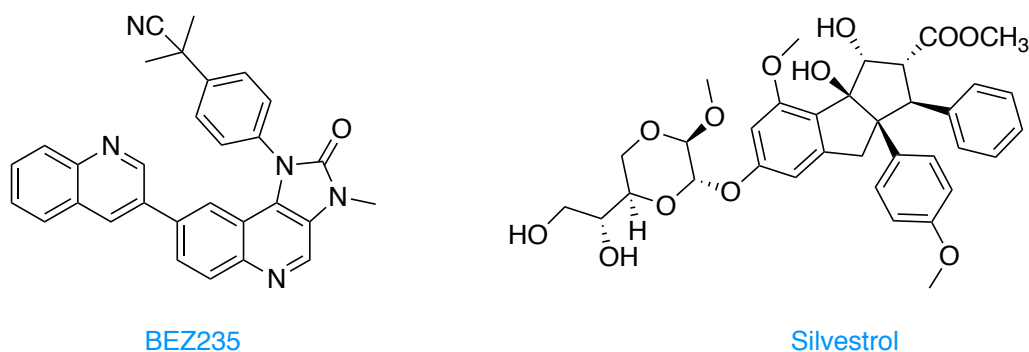


**Figure 13.** Chemical structures of BEZ235 and Silvestrol inhibitors.

Silvestrol (**Figure 13**) is another inhibitor of the mTOR pathway, that more specifically inhibits eIF4A. It was studied in mouse models of colorectal cancer and it showed reduction of *myc* translation and inhibition of tumor growth.<sup>189</sup>

### 1.6.3 Targeting Regulators of MYC Stability

The targeting of ubiquitinases or phosphatases for the degradation of MYC has been proposed; however, it is not clear whether these are specific for MYC or if the side effects will be minimal.<sup>105</sup> MYC stability can be either positively or negatively regulated depending on the E3 (ubiquitin ligase). E3s like SCF<sup>Fbw7</sup>, CHIP, TRIM32, SCF<sup>Skp2</sup>, HUWE1, FBXO28, and others can ubiquitinate MYC.<sup>191</sup> SCF<sup>Fbw7</sup> negatively regulates MYC and it has been shown that Oridonin (**Figure 14**), a natural diterpenoid, can promote FBW7-mediated ubiquitination and MYC breakdown.<sup>192</sup> An Oridonin derivative, HAO472, entered to clinical trials in China for leukemia treatment.<sup>193</sup> Moreover, BI8622 and BI8626 (**Figure 14**) were discovered in a High Throughput Screen (HTS) as inhibitors of HUWE1.<sup>194</sup> HUWE1 is required for growth in colorectal cancer cells and treatment with these compounds showed inhibition of MYC-dependent transactivation but not in stem and normal colon epithelial cells.<sup>194</sup>

MYC can also be deubiquitinated and stabilized by DUBs. USP28, USP37 and USP36 are Ubiquitin-Specific Proteases (USPs), a subfamily of DUBs, they all enhance MYC's activity and their inhibition has been proposed as a means of MYC inhibition.<sup>191</sup>

Furthermore, N-MYC can form a complex with Aurora A (kinase) and be “saved” from proteasomal degradation by SCF<sup>Fbw7</sup>.<sup>195</sup> Therefore, inhibitors of this interaction have been pursued, two examples are MLN8054 and MLN8237 (**Figure 14**).<sup>196</sup> Both inhibitors promote N-MYC degradation mediated by SCF<sup>Fbw7</sup> in neuroblastoma cells.<sup>196</sup> Also, tumor-bearing mice that are

treated with either MLN8054 or MLN8237 show increased survival and reduction of N-MYC levels *in vivo*.<sup>196</sup> The clinical development of MLN8054 was terminated due to side effects; nonetheless, MLN8237 (Alisertib) is being evaluated in multiple Phase I and II studies.<sup>105</sup>

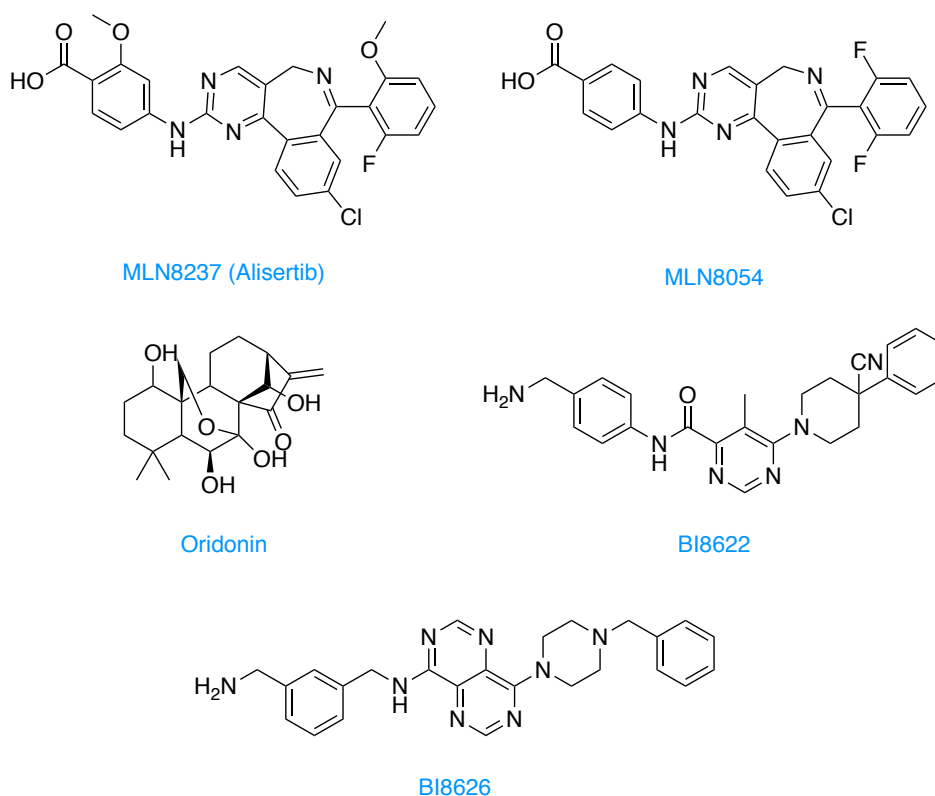


**Figure 14.** Inhibitors of MYC's stability regulators.

### 1.7 WDR5: Structure, Function and Cancer incidence

An alternative and indirect approach to inhibit MYC's function has recently emerged. The discovery of WDR5 as a MYC cofactor and its biological implication during tumorigenesis has raised questions about the possibility to treat MYC-driven tumors by disrupting the interaction between this scaffolding protein and MYC.

### 1.7.1 WDR5 protein structure

WDR5 belongs to the family of WD40 repeat (WDR) proteins. WDR contains a seven-bladed  $\beta$ -propeller domain with an overall doughnut shape (**Figure 15A**) and each blade has a conserved serine-histidine and tryptophan-aspartate (WD) motif.<sup>197</sup>

This domain usually works as a scaffold within large multiprotein complexes and is the fourth most abundant domain in the human proteome.<sup>197</sup> This type of domain is considered to have two main distinct surfaces available for interactions: 1) the top region of the propeller, identified by the area where the loops connecting the strands D and A lay and 2) the bottom (**Figure 15B**).<sup>198</sup> The two regions can simultaneously interact with different binding partners including proteins, peptides, RNA and DNA.<sup>197</sup>

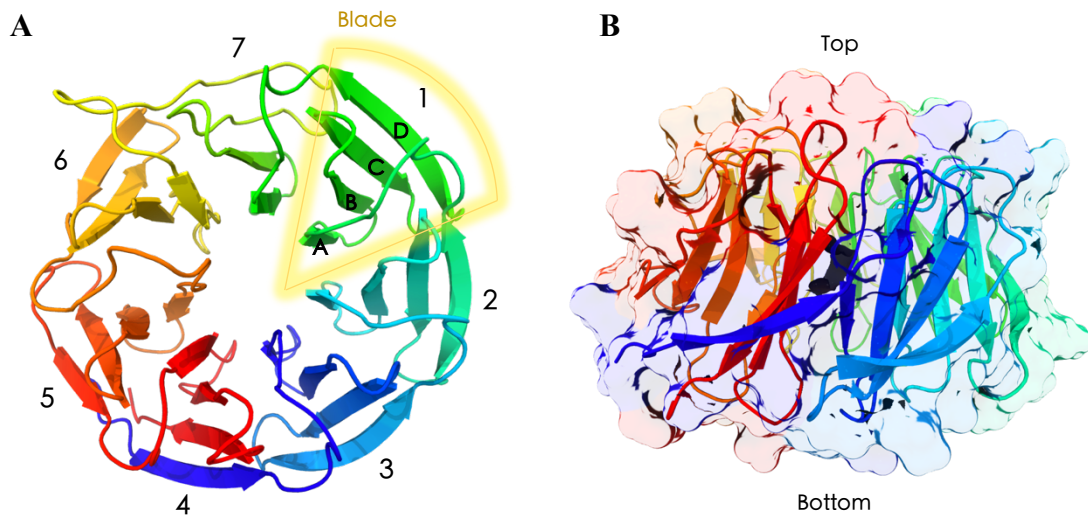


**Figure 15.** WDR5 crystal structure (PDB:2H14). A) WDR5 is formed by a seven-bladed  $\beta$ -propeller with a doughnut shape. B) Most common binding regions of WD40 proteins.

### 1.7.2 Discovery of WDR5

Mammalian WDR5 was identified while studying bone formation.<sup>199</sup> Differential display PCR allowed the identification of the encoding gene, which was initially called *BIG-3* (BMP-2-induced gene 3 Kb) and later renamed *Wdr5*, as this better represents its architecture.<sup>199–201</sup>

WDR5 was found to promote differentiation in cells and to assist with proper bone formation.<sup>199–202</sup> Overexpression of WDR5 in mice was shown to accelerate osteoblast and chondrocyte differentiation and promote the formation of enlarged skeletal structures.<sup>200,203</sup> On the other hand, the silencing of *Wdr5* in the limb of a developing chicken embryo resulted in a shortening of the skeletal elements.<sup>204</sup>

Six months after WDR5 was discovered, it was reported that Swd3, the WDR5 homolog in *Saccharomyces cerevisiae*, is a component of the histone methyltransferase complex COMPASS (Complex of Proteins Associated with SET1).<sup>205</sup> COMPASS is the homolog of the mammalian SET1 and MLL protein complexes that catalyzes histone 3 lysine 4 (H3K4) di- and tri-methylation (H3K4me2 and H3K4me3).<sup>201</sup> This finding provided insights about other possible roles of WDR5. Indeed, WDR5 was confirmed to directly associate with methylated histone H3, allowing connection to the developmental phenotypes previously observed with epigenetic changes.<sup>201,206</sup> The Allis group showed that WDR5 regulates gene expression by acting as a “sensor” protein that participates in the reading and writing of the methylation mark at H3K4.<sup>206</sup> In addition, they observed a decrease in the expression of *HOX* genes, important for development, when WDR5 was knocked down in human cells.<sup>206</sup> In tadpoles, WDR5 knock down produced developmental defects and abnormal spatial *Hox* gene expression.<sup>206</sup> Furthermore, WDR5 expression and H3K4me3 levels are high in an undifferentiated embryonic stem (ES) cell state and decreases as cells differentiate.<sup>201,207</sup> Reduction of WDR5 in ES cells impairs differentiation and induces

repression of the self-renewal transcriptional program. These data supports the relationship of WDR5 with developmental processes.<sup>201</sup>

Currently, more than two dozen direct interaction partners have been reported for WDR5.<sup>201</sup> All interactions identified to date bind one of two sites, a shallow cleft on the bottom surface known as “WDR5-binding motif” (WBM) site or the arginine-binding cavity at the top surface called “WDR5-interacting motif” (WIN) site.<sup>201</sup>

### 1.7.3 Interaction partners outside the nucleus

WDR5 has been found to participate in cytokinesis, the process where the cytoplasm of a parent cell partitions into two daughter cells.<sup>208</sup> More specifically, WDR5 was found in the midbody, a transient structure that connects the two daughter cells at the end of the cytokinesis.<sup>209</sup> Depletion of WDR5 in HeLa and RPE1 cells increases the number of multinucleated cells and may also stabilize the microtubules, affecting the cytokinesis process.<sup>208</sup> Furthermore, mutational experiments showed that an intact WIN site is required for proper performance of the midbody.<sup>208</sup> Interestingly, it has been reported that MLL1 (or SETD1A) and WDR5 are required for chromosome alignment during metaphase; cells that are depleted of either of these two proteins exhibit similar defects.<sup>210</sup> A proteomic screening identified another direct interaction partner of WDR5, KIF2A (a kinesin motor protein), which has a WIN motif that is thought to interact with the WIN site of WDR5.<sup>201,210</sup>

### 1.7.4 Role of WDR5 as a Member of Histone H3 Lysine 4 Methyltransferases Complexes

Regulation of gene expression can be controlled by post-translational modifications on histones.<sup>201</sup>

The combination of marks at a particular region of the genome will dictate the type(s) of protein(s)



that will engage to the chromatin in order to carry processes such as transcriptional activation (or repression) and chromatin remodeling.<sup>201</sup> H3K4me2 and H3K4me3 are hallmarks of transcriptionally active chromatin that are catalyzed by the SET1/MLL family of histone methyltransferases (HMT).<sup>211</sup> MLL1 was first characterized as a gene inducing human leukemia caused by chromosomal translocations.<sup>211</sup> In mammals, there are six COMPASS-like complexes with essential and non-redundant functions that can methylate H3K4.<sup>201,211</sup> SET1A, SET1B, MLL1, MLL2, MLL3, and MLL4 are the catalytic subunits of these complexes; all of them contain a core set of proteins known as “WRAD” (WDR5, RBBP5, ASH2L, and DPY30) which stimulate the basal activity of the HMT.<sup>201</sup> WDR5 engages RBBP5 through its WBM site and SET1/MLL through its WIN site; therefore, it plays a crucial role as a scaffolding protein.<sup>212–214</sup>

#### 1.7.5 WDR5 forms part of the NSL Complex

The Non-Specific-Lethal (NSL) complex possesses histone acetyltransferase (HAT) activity and comprises nine subunits: males absent on the first (MOF), KANSL1, KANSL2, KANSL3, microspherule protein 1 (MCRS1), WDR5, O-linked *N*-acetylglucosamine transferase isoform 1 (OGT1), HCF1, and PHF20.<sup>215</sup> In the NSL complex, MOF is the enzyme responsible for the HAT activity and under this context it can acetylate histone H4 on lysine 5, 8 and 16.<sup>215</sup> WDR5 directly interacts with KANSL1 at the WIN site and with KANSL2 at the WBM site.<sup>216</sup> Studies carried out in *Drosophila* showed that the interaction of WDR5 with KANSL1 is important for proper assembly and efficient recruitment of the NSL complex to target promoters.<sup>216</sup> Moreover, it has been shown that there is a crosstalk between the NSL and SET1/MLL complexes as NSL enhances the methyltransferase activity of SET1/MLL.<sup>201,217</sup>

### 1.7.6 WDR5 in the NuRD complex

The Nucleosome Remodeling and Deacetylase (NuRD) complex is a multipurpose complex widely expressed in both developing and mature tissues.<sup>218</sup> NuRD engages in several different activities; it can act as a gene expression regulator and it has also been reported to participate in DNA repair.<sup>218</sup> The NuRD complex has six proteins, several of them have isoforms that generate different NuRD complexes with cell type- or context-specific activities.<sup>201</sup> WDR5 was identified as one of the NuRD components and it was later discovered that it interacts with MBD3C (an isoform of MBD3) through its WIN site.<sup>201,219</sup> MBD3C is expressed in ES cells and it is thought that the NuRD complex contributes to the maintenance of the stem-like state, as it disappears when the cells differentiate.<sup>201</sup>

### 1.7.7 Other WDR5 interaction partners in the nucleus

Multiple interaction partners continue to be reported for WDR5. Chromatin remodelers associate with WDR5 as it interacts with CHD8<sup>220</sup> and INO80.<sup>201,221</sup> WDR5 forms part of other HAT complexes such as ATAC<sup>222</sup> and more recently it has been reported to form part of the WHHERE coactivator complex which is required to regulate retinoic acid (RA) signaling and to control embryonic symmetry.<sup>223</sup> HOTTIP, a long non-coding RNAs (lncRNAs), has been identified to interact with WDR5.<sup>224</sup> HOTTIP coordinates the expression of *HOXA9* to *HOXA13* genes (important for distal identity) by binding to WDR5 at the WBM site and recruiting the MLL complex to maintain H3K4me3.<sup>225</sup> Furthermore, RNA:protein immunoprecipitation in tandem sequencing (RIPit-seq) found 1434 RNAs that associate with WDR5 in ES cells. This finding included mRNAs, lncRNAs, pri-miRNAs, and snoRNAs.<sup>225</sup>

### 1.7.8 Discovery and characterization of the interaction between WDR5 and MYC

In 2014, Ullius *et al* reported WDR5 as a direct interaction partner of MYC while studying additional transcriptional cofactor complexes that interact with MYC.<sup>226</sup> A year later, the Tansey group in collaboration with our group confirmed the finding and fully characterized the interaction.<sup>23</sup> Analysis of reported ChIP-seq data for WDR5 and MYC guided further experimentation, as it was found that they both share 79% of their chromatin binding sites in HEK293 cells.<sup>23</sup> The identification of the specific region of MYC responsible for the interaction with WDR5 was determined by coimmunoprecipitation (CoIP) analysis; the 10-residue MbIIIb peptide (residues 258-267 of C-MYC) was shown to engage WDR5 with a  $K_d = 9.3 \mu\text{M}$  measured by FPA.<sup>23</sup> A co-crystal structure of this peptide bound to WDR5 was obtained (**Figure 16**) and showed the MbIIIb peptide bound to the WBM site. Analysis of the structure resulted in a series of important observations: 1) The WDR5 structure is barely affected by the binding of the peptide; 2) The cleft where the MYC peptide binds is hydrophobic in nature and surrounded by positive charges; 3) Two hydrophobic pockets mediate key interactions. One such pocket is created by Y228, L240, and L249 of WDR5 (I262 of MYC occupies this site), and the other one is created by F266 and V268 of WDR5 (V264 and V265 of MYC sit here); and 4) The side chains of N225 and Q289 participate in key hydrogen bond interactions that help stabilize the complex.<sup>23</sup> Three MbIIIb peptide mutants (WBM, V264G or I262G) unable to bind WDR5 were made and used to assess the biological role of this interaction *in vivo*.<sup>23</sup> The WBM mutant was used in ChIP-seq experiments, and the data showed that 80% of the WT MYC binding sites were lost, 78% of them were sites where MYC and WDR5 colocalize.<sup>23</sup> Moreover, the biological implication of disrupting the interaction between WDR5 and MYC was evaluated by studying tumor growth in mice that were treated with fibroblast cells expressing either of the MYC peptide mutants (WBM or V264G)

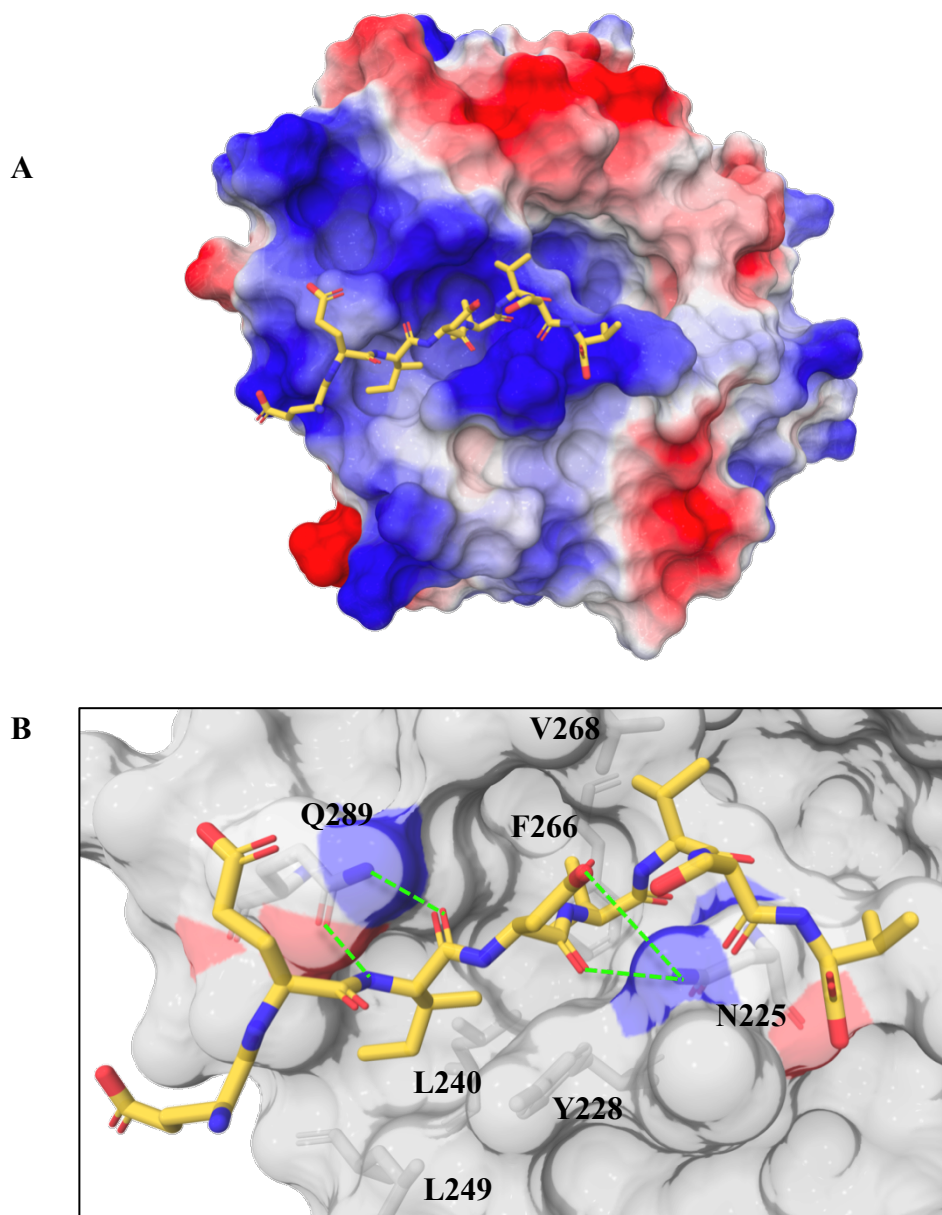


*Figure 16. Co-crystal structure of WDR5 and MBIIIb. The hydrogen bonds between WDR5 and MYC are highlighted in green. A) Shows electrostatic potential of WDR5 and B) shows close-up of the WDR5-MYC peptide interaction. PDB: 4Y7R.*

or WT MYC.<sup>23</sup> Mice treated with fibroblasts containing the MYC mutants were less tumorigenic with tumors that were, on average, 80% smaller than those mice treated with WT MYC-expressing fibroblasts.<sup>23</sup> Together, these data demonstrate that the interaction between WDR5 and MYC is required for MYC to effectively recognize its target genes in the context of chromatin, and that this interaction is required to drive *in vivo* tumorigenesis. Therefore, it was postulated that disruption of the WDR5-MYC interaction may be a viable approach for developing MYC inhibitors.<sup>23</sup>

#### 1.7.9 The WDR5-MYC link to cancer

Sun and coworkers have shown that MYC can upregulate WDR5 expression by binding to E-boxes at the WDR5 gene promoter.<sup>227</sup> WDR5 was also shown to interact with N-MYC in neuroblastoma cells which leads to histone H3K4 trimethylation, transcriptional activation of N-MYC target genes, and reduction of p53 protein.<sup>227</sup> Silencing of WDR5 induced apoptosis in p53 wild-type neuroblastoma cells, this demonstrated that WDR5 is a key cofactor for N-MYC-regulated transcriptional activation and tumorigenesis.<sup>227</sup>

Moreover, microarray data from patient-derived pancreatic ductal adenocarcinoma (PDAC) xenografts revealed that WDR5 is overexpressed and required for tumor maintenance.<sup>228</sup> Consequently, silencing WDR5 in PDAC cells showed a reduction of chromatin-bound MYC.<sup>228</sup> Additionally, inhibition of the WDR5-MYC interaction by mutation of key residues in the WBM site of WDR5 (L240K and V268E) caused accumulation of DNA damage, a similar effect to that observed when WDR5 was knocked down.<sup>228</sup>

Recently, the Tansey Lab engineered a Burkitt's Lymphoma (BL) system that allows the exchange of wild-type (WT) for WDR5-interaction-defective (WBM) MYC when treated with 3-hydroxytamoxifen (OHT).<sup>229</sup> With this system, they were able to show that WDR5 recruits MYC

to chromatin at protein synthesis genes. The disruption of this interaction by switching WT MYC to WBM MYC caused the transcription decrease of 128 genes and the transcription increase of 66 genes.<sup>229</sup> In addition, the ability of the BL system to grow tumor and maintain it was assessed by switching the cells from endogenous MYC to WT or WBM MYC and injecting them into mice. Mice injected with WT MYC developed tumors rapidly; however, mice injected with WBM displayed delayed tumor growth.<sup>229</sup> In the case where the tumor was already established (by injecting unswitched cells into the flanks of mice), the administration of OHT for 3 days to switch the cells into WBM MYC caused rapid regression of the tumor after a week of OHT treatment.<sup>229</sup> The results of this study suggest that the disruption of the WDR5-MYC with small molecules could be a feasible approach to treat MYC-driven cancers.

#### 1.7.10 Druggability of WDR5 at the WBM site

The druggability of WDR5 is unclear. The WBM interface is shallow ( $\sim 1000 \text{ \AA}^2$ ) but it is surrounded by several hydrophobic residues, which might make it a possible site to target with small molecules. Furthermore, the universal conservation of MYC proteins and their relatively weak binding to WDR5 ( $K_d = 9.3 \text{ \mu M}$ ) makes it well suited for drug discovery.<sup>23,230</sup>

Based on studies carried by different groups, a small molecule inhibitor of the WDR5-MYC interaction would be expected to chemically recapitulate the effects observed when mutants of MYC are used. A small molecule inhibitor should prevent MYC association with chromatin at WDR5-directed genes and disable its tumorigenic activities.<sup>230</sup>

Despite being a challenging site to target, we set out to find out if this interface is druggable or not.

## 1.8 Scope of this thesis

In the next chapters, I describe my efforts towards the discovery of small molecule inhibitors of the WDR5-MYC interaction. In Chapter II, I describe the synthesis, structure activity relationship, and physicochemical properties of the main series of compounds, the biaryl sulfonamides. This series was derived from the most potent high-throughput screen hit. In Chapter III, I describe my efforts towards the replacement of the middle portion of these compounds, the sulfonamide linker. In Chapter IV, I show the application of fragment-based methods to design and synthesize a new subseries of compounds. The effects of these compounds in cells are also described. In Chapter V, I summarize the results and discuss possible future directions for targeting the WDR5-MYC interaction. Finally, in Chapter VI I provide the synthesis and characterization of the compounds shown in this dissertation.

## Chapter II

### Structure Activity Relationship (SAR) of Sulfonamides

Sections of this chapter are based on the publication “Discovery and Optimization of Salicylic Acid-derived sulfonamide inhibitors of the WD Repeat-Containing Protein 5-MYC Protein-Protein Interaction”.<sup>231</sup>

#### 2.1 Introduction

To determine if WDR5 is druggable at the WBM-site, we conducted an HTS campaign of two Vanderbilt libraries. We were able to identify several compounds that bind to WDR5 and disrupt the interaction with MYC. In the following chapter, the development of SAR and optimization of compounds derived the leading HTS hit are described.

##### 2.1.1 Hit identification and validation

A HTS was performed using a competition Fluorescence Polarization Anisotropy (FPA, or FP)-based assay to assess the interruption of the binding of WDR5 and a FITC-labeled peptide probe derived from the MYC MbIIIb sequence.<sup>23,232</sup> Compounds from the Vanderbilt Discovery and VICB libraries (~250,000 total) were screened at 50  $\mu$ M; 410 preliminary ‘hit’ compounds demonstrated greater than 15% inhibition of the interaction. After duplicate screening, 110 compounds were confirmed as hits. Each of these was subsequently evaluated using a dose-response protocol to generate an  $IC_{50}$  from which a binding affinity ( $K_d$ ) was calculated.<sup>23,232</sup> In total, 76 compounds afforded a measurable  $K_d$  value and were taken forward as MYC-site hits



(0.03% confirmed hit-rate). These hits were validated in an orthogonal biophysical assay using NMR to further confirm the direct binding of the compounds to WDR5. Validated hits induced either peak shift (**Figure 17A**) or peak broadening (**Figure 17B**). Multiple confirmed hits contain

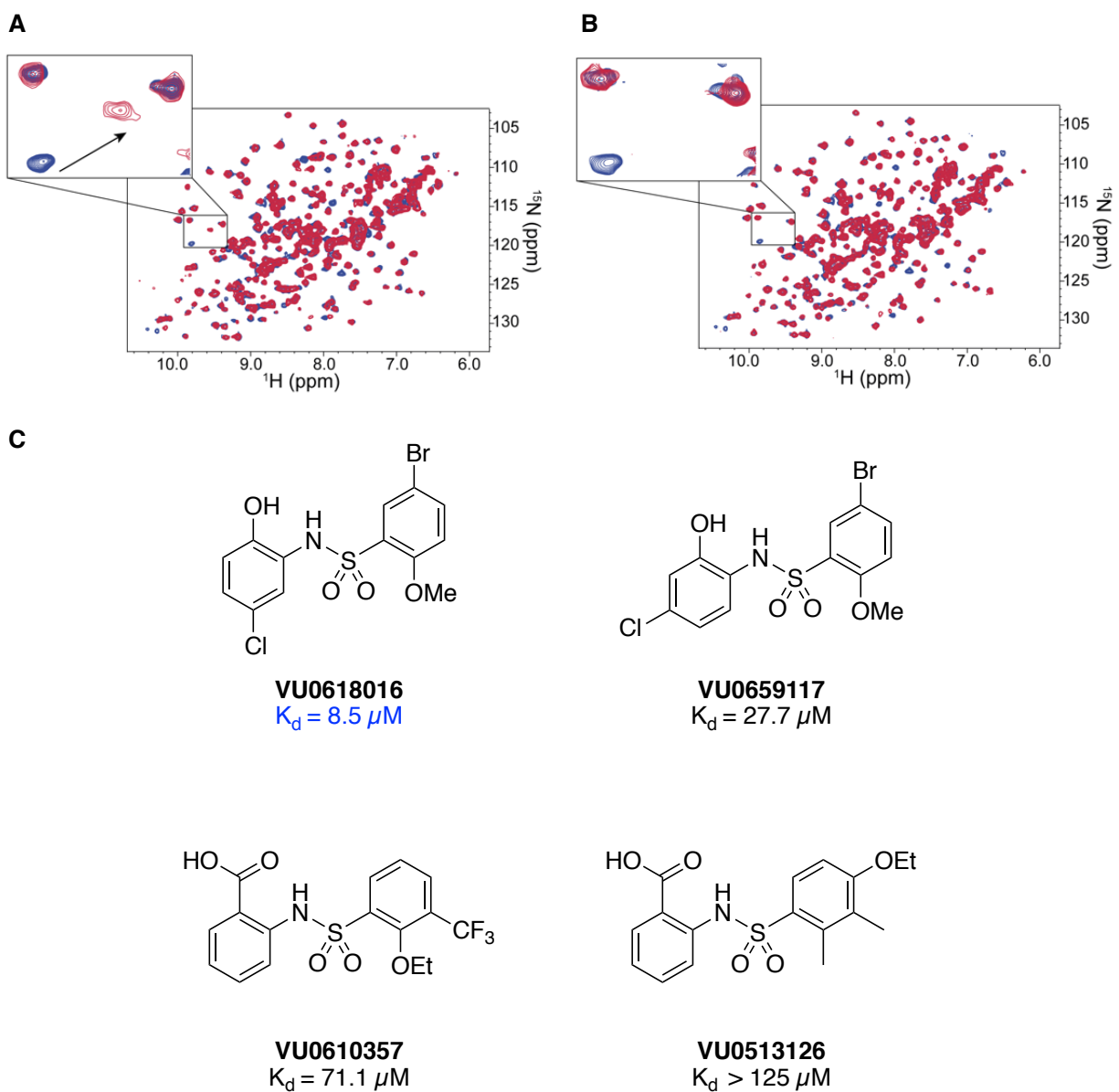


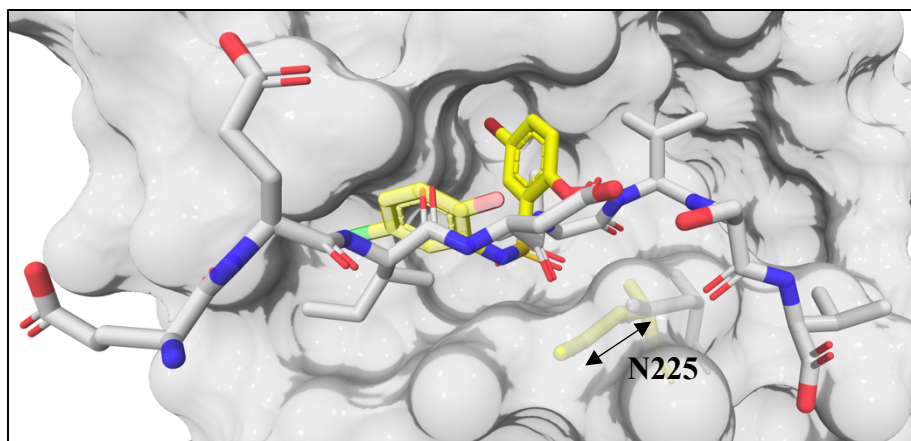
**Figure 17.** Example  $^1\text{H}$ - $^{15}\text{N}$  HSQC spectra showing the observable effects of compounds that A) induce peak shift and B) induce peak broadening. Apo-WDR5 (Blue), Hit-WDR5 (Red). C) Representative hits that bind WDR5 at the WBM site.  $K_d$  values were obtained by FPA.

a bi-aryl sulfonamide motif (exemplar hits shown in **Figure 17C**). As measured by the FP assay, the hits show binding affinities ranging from 8–175  $\mu$ M.

### 2.1.2 X-ray co-crystal structure of **VU0618016** bound to WDR5

We obtained an X-ray co-crystal structure of the leading hit, **VU0618016**, bound to WDR5 by co-crystallization. The overlay of this structure with those of the published peptides confirmed that the small molecule bound into the WBM site that mediates the binding of WDR5 to MYC and RBBP5 (**Figure 18A**). A chlorine atom on the aniline ring mimics the hydrophobic side-chain of the isoleucine of the IDVV motif of the MBIIIb peptide and occupies a hydrophobic pocket (herein described as S<sub>1</sub>). Additional key interactions responsible for compound binding include: 1) a hydrogen bond from one oxygen of the sulfonamide to the backbone NH of ASN225, which causes a significant shift of the protein loop towards the ligand; and a halogen bonding interaction from the aromatic bromine to the carbonyl of TRP273 (**Figure 18A and B**).

A



B

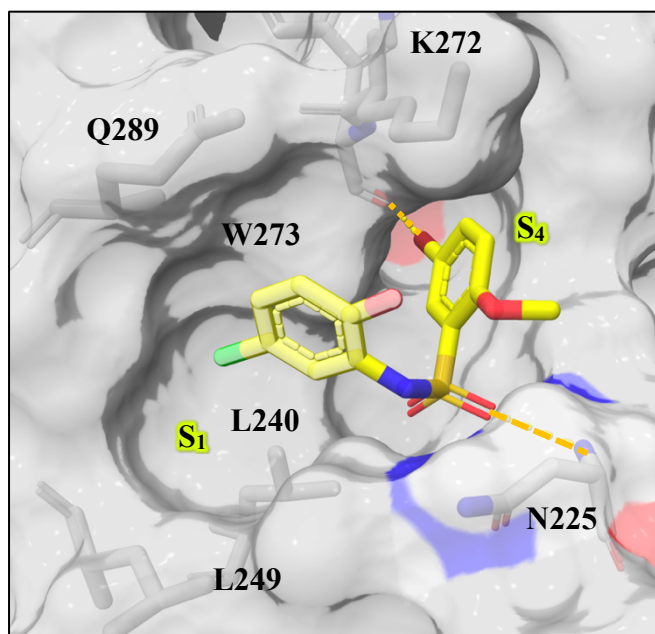
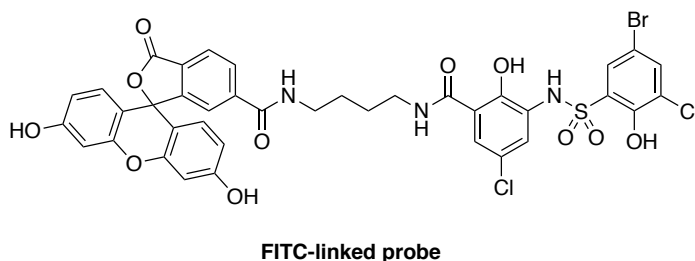


**Figure 18.** A) An overlay of VU0618016 with the structure of bound MBIIIb peptide (PDB: 4Y7R), the frame shift of the loop enabling retainment of the H-bond interaction with the N225 is represented by the movement of N225; VU0618016 (yellow), WDR5:MBIIIb complex (grey) and B) X-ray co-crystal structure of VU0618016 bound to WDR5 (PDB:6U6W). Shown as dashes are the halogen bonding interaction with the bromine atom and W273 and the hydrogen bond between the sulfonamide oxygen and N225.

### 2.1.3 Early SAR

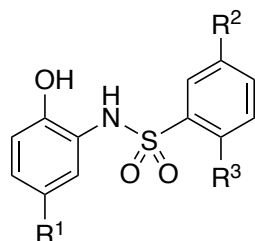
The initial focus in our synthetic efforts was to optimize the two halogen substituents, the aniline ring chlorine, and the sulfonyl ring bromide. The bromine atom forms a key halogen-bonding interaction in the X-ray structure. Indeed, when this bromine atom is removed, all binding affinity for WDR5 is lost, while replacement with either chlorine (**VU0660996**, **Table 2**) or an iodide (**VU0807214**, **Table 2**) both affords a compound with reduced affinity. Interestingly, removing any one of the four-substituents that decorate the hit biaryl sulfonamide substructure proved highly deleterious (**Table 2**) demonstrating that this substitution pattern shows good shape complementarity for this binding surface. Similarly, we observed a consistent, significant improvement in affinity when switching from a methoxy R<sub>3</sub> group to a phenol (**VU0661191**).

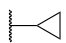
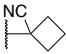
Early in the project, we observed compounds that were able to bind below the threshold ( $K_d < 2.5 \mu\text{M}$ ) of the original HTS FP assay that uses the a FITC-labeled MBIIIb peptide. We later synthesized a fluorescein-labeled small molecule probe with a higher affinity for WDR5 compared to the peptide, thus offering lower limits of detection and improved compound measurements. Over the course of the project, measurements were obtained with multiple generations of such probes. For clarity, further data shown here utilize only a single small molecule fluorescein probe (**Figure 19**).



*Figure 19. Chemical structure of FITC-labeled probe for FPA.*

**Table 2.** Early SAR.



Compounds	R <sup>1</sup>	R <sup>2</sup>	R <sup>3</sup>	FPA K <sub>d</sub> (μM) <sup>a</sup>
VU0618016	Cl	Br	OMe	5 ± 2
VU0660996	Cl	Cl	OMe	8.4 ± 0.6
VU0807214	Cl	I	OMe	8 ± 2
VU0659693	H	Br	OMe	>40
VU0660623	Cl	H	OMe	>40
VU0660009	Cl	Br	H	36 ± 7
VU0661191	Cl	Br	OH	1.2 ± 0.5
VU0659969	Ph	Br	OMe	37 ± 7
VU0661126	<i>t</i> -Bu	Br	OMe	4 ± 2
VU0829278		Br	OH	0.8 ± 0.4
VU0808446	OCF <sub>3</sub>	Br	OH	0.549 ± 0.008
VU0825555	SF <sub>5</sub>	Br	OH	0.11 ± 0.08
VU0814043		Br	OH	0.3 ± 0.2

<sup>a</sup> Data displayed is the average of at least 2 independent replicates ± standard deviation.

On the aniline ring, a chlorine atom occupies the same region as the isoleucine of the native IDVV motif, and as such, this was substituted for a range of hydrophobic groups that were hypothesized to more optimally occupy this region of the protein. Replacement of the halogen with phenyl (VU0659969) was unfavorable and resulted in a loss of binding affinity. The *tert*-butyl analog (VU0661126) proved to be similar to the parent chlorine. X-ray crystallography demonstrated that larger groups tended to occupy in the same space in the binding pocket, but doing so forces the

rest of the molecule to shift upward; smaller aliphatic groups complement this pocket much better (**VU0829278**, **VU0808446**). Pentafluorosulfanyl groups have been reported as metabolically inert *tert*-butyl analogs<sup>233</sup>, and their use herein affords the most potent example of this phenolic class, **VU0825555**.

Cyano-spirocyclic examples were initially designed to act as a handle for further growth of the compounds along the edge of this pocket, with the hydrocarbon chain hypothesized using molecular docking studies to complement the hydrophobic region. Of these, only **VU0814043** is shown in **Table 2**, as it was the best of 3-6 carbon spirocycles synthesized. However, we observed by X-ray crystallography that the cyano moiety of **VU0814043** is instead oriented toward the protein, with no obvious directional interaction.

The X-ray co-crystal structure of **VU0618016** allowed us to employ structure-based design for the development of further optimized compounds. A significant challenge to this effort relates to the shallow nature of this binding interface, which contains few areas that may traditionally be referred to as ‘pockets’.<sup>234</sup> In addition to the early optimization of the hydrophobic moiety in the ‘ILE’ region of the peptide-binding site, a further breakthrough came from the addition of a carboxylic acid directed toward Q289, affording salicylic acid derivative **VU0768593** ( $K_d = 0.4 \pm 0.1 \mu\text{M}$ , **Table 3**). This engagement of Q289 afforded a significant increase in binding affinity compared to **VU0618016**, and the positive interaction was confirmed by X-ray crystallography (**Figure 20**).

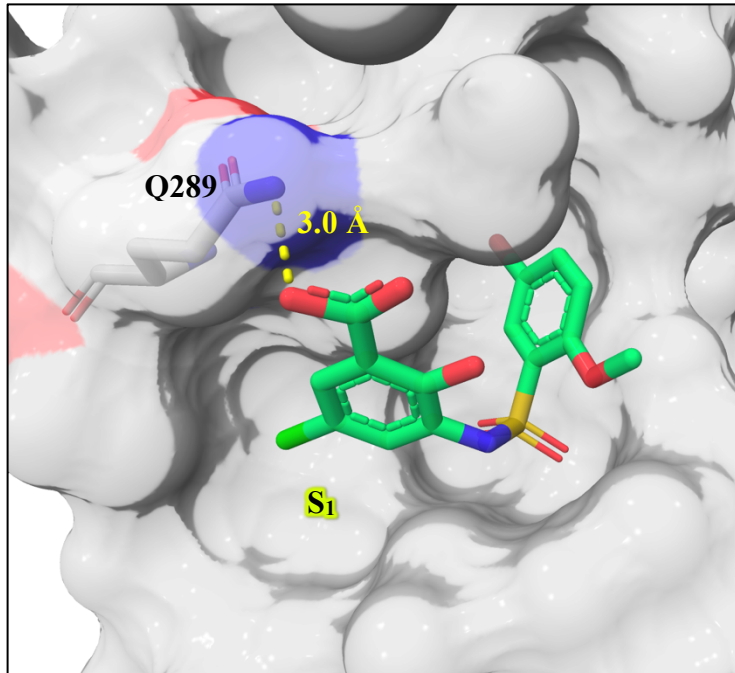
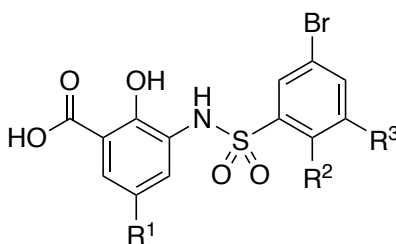


*Figure 20. X-ray co-crystal structure of VU0660590 bound to WDR5 (PDB:6U5Y). The salicylic acid forms a hydrogen bonding interaction with Q289.*

Similarly, a significant potency increase was obtained by the addition of a chlorine *ortho* to the phenol of the sulfonyl ring (**Table 3**); gaining additional hydrophobic contacts with WDR5 in the area occupied by a valine side chain of MYC and RBBP5 (herein denoted as S<sub>4</sub>). The cyclopropyl derivatives (**VU0829706** and **VU0829710**) demonstrated an improvement versus the parent chloro-containing compound, in line with the SAR trends of **Table 2**. The hydrophobic chloro-replacement pentafluorosulfonyl and cyano-spirocycle derivatives afforded low nanomolar potency, with improvements of 5 to 11-fold upon the addition of the acid.

**Table 3.** Optimization of salicylic acid derived WDR5 WBM-site inhibitors.



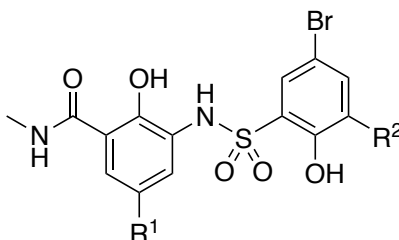
Compounds	R <sup>1</sup>	R <sup>2</sup>	R <sup>3</sup>	FPA K <sub>d</sub> (μM) <sup>a</sup>
VU0768593	-Cl	-OH	-H	0.22 ± 0.03
VU0660590	-Cl	-OMe	-H	0.4 ± 0.1
VU0809065	-Cl	-OH	-Cl	0.16 ± 0.02
VU0808607		-OH	-H	0.2 ± 0.1
VU0810571		-OH	-Cl	0.21 ± 0.06
VU0849832	-SF <sub>5</sub>	-OH	-H	0.05 ± 0.02
VU0849828	-SF <sub>5</sub>	-OH	-Cl	0.03 ± 0.02
VU0829706		-OH	-H	0.07 ± 0.04
VU0829710		-OH	-Cl	0.03 ± 0.02

<sup>a</sup> Data displayed is the average of at least 2 independent replicates ± standard deviation.

While we were able to reach low nanomolar levels of potency with this series of salicylic acid-based compounds, they have inherent issues related to permeability and plasma protein binding, (*vide infra*) limiting their use in whole-cell mechanism of action (MOA) studies. To avoid these problems, we explored the replacement of the carboxylic acid with a methyl amide (**Table 4**). Within this salicylamide series, a reduction in potency compared to the direct acid analogs was observed. However, by combining optimal SAR observations in the I262 region, we were able to retain analogs with binding affinity below 0.10 μM.



**Table 4.** Structures and biochemical data for salicylamide derived WDR5-WBM site inhibitors.



Compounds	R <sup>1</sup>	R <sup>2</sup>	FPA K <sub>d</sub> (μM) <sup>a</sup>
VU0809232	-Cl	-H	0.75 ± 0.03
VU0824673	-Cl	-Cl	0.30 ± 0.09
VU0810523		-H	1.99 ± 0.01
VU0810514		-Cl	0.91 ± 0.06
VU0849833	-SF <sub>5</sub>	-H	0.20 ± 0.03
VU0849820	-SF <sub>5</sub>	-Cl	0.19 ± 0.03
VU0829704		-H	0.57 ± 0.02
VU0829711		-Cl	0.16 ± 0.03

<sup>a</sup> Data displayed is the average of at least 2 independent replicates ± standard deviation.

#### 2.1.4 Pharmaceutical properties

We explored the tier 1 DMPK profile of a number of compounds within this class (**Table 5**). These data demonstrate that all tested analogs have good solubility and the amide series has significantly improved permeability in comparison to the salicylic acid comparators. This data shows that there was no evidence of P-gp mediated efflux with the tested analogs (only one example is shown in **Table 5**). A remaining major limitation of this compound class is that they are limited by severe plasma protein binding; indeed, salicylic acid itself is known to be a substrate for human serum albumin.<sup>235</sup>

Table 5. DMPK profile of select compounds.<sup>a</sup>

Compounds	Solubility ( $\mu\text{M}$ )	MDCK A-B $P_{\text{app}}$ ( $10^6/\text{s}$ )	MDCK B-A $P_{\text{app}}$ ( $10^6/\text{s}$ )	$F_u$ (%)
VU0661191	>100	36.4	n.d.	<0.0026
VU0814043	>100	27.8	n.d.	<0.0005
VU0825564	>100	14.7	n.d.	n.d.
VU0829710	>100	0.33	n.d.	<0.0003
VU0809232	>100	16.7	14.1	<0.0004
VU0829704	>100	45.2	n.d.	<0.0006
VU0829711	>100	14.0	n.d.	<0.0006

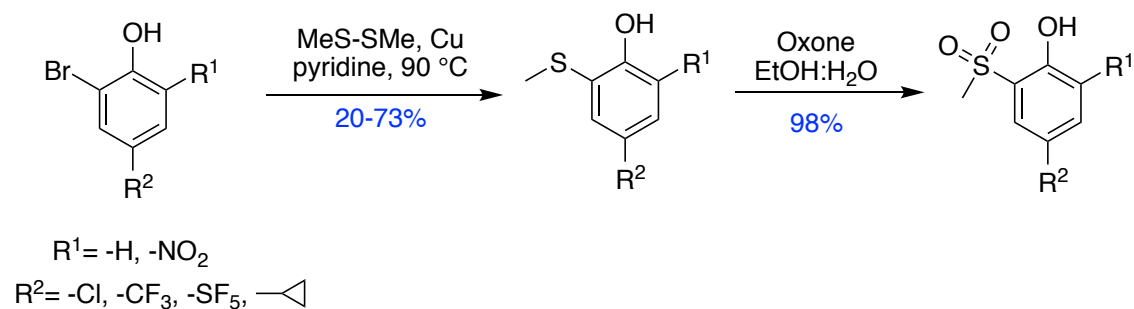
<sup>a</sup> All experiments performed at Q<sup>2</sup> Solutions Ltd.

## 2.2 SAR of methyl sulfone analogs

### 2.2.1 Structure-based design and synthesis of phenolic methyl sulfone analogs

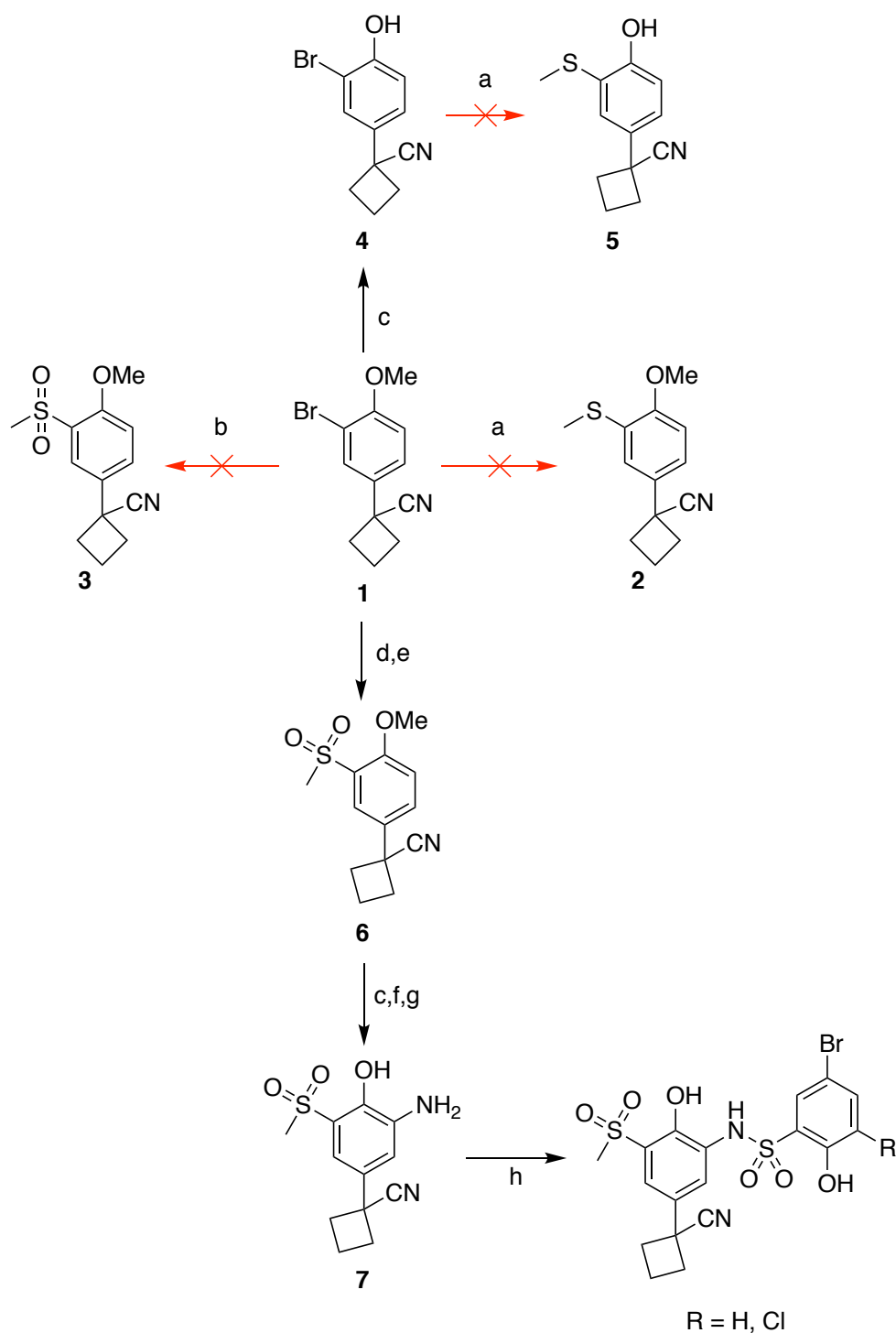
In order to overcome some of the limitations observed in the salicylic acid subseries, we explored a new subseries of compounds based on a methyl sulfone substitution that replaces the carboxylic acid of the main series. The sulfone is a neutral, polar, and tridimensional group that offers opportunities for expandability. These characteristics make sulfones desirable and suitable for our series of compounds. Moreover, we envisioned that the sulfone would be able to interact with Q289 through a hydrogen bond, similar to the carboxylic acid and amide groups.

Ten analogs containing the best-in-class pieces were synthesized (**Table 6**) following the general route shown in **Scheme 1**. The methyl sulfide was installed via an Ullmann coupling<sup>236</sup> and oxidation of this intermediate with Oxone provided the desired methyl sulfone.



*Scheme 1. Installation of methyl sulfones ortho to the phenol.*

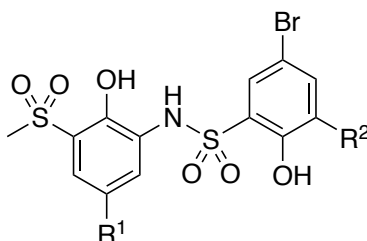
The installation of the methyl sulfide in presence of the cyano-spirocyclic substrate did not proceed under the conditions shown above. An alternative route using sodium methanesulfinate, CuI, *L*-proline, and NaOH in DMSO (conditions developed by Ma *et al*<sup>237</sup>) was attempted with no success (**Scheme 2**), as only starting material was recovered. Moreover, we wanted to eliminate the possibility of the methoxy group generating steric hindrance during the coupling reaction, this prompted us to convert it to the phenol, **4**. Nevertheless, the coupling reaction did not proceed. At this point, it became obvious to us that there was a compatibility issue between the nitrile and the copper. It has been reported that nitrile groups can form complexes with Cu and this may lead to its deactivation<sup>238</sup>, thus we decided to change the catalyst. A Pd-mediated coupling of the aryl bromide and sodium methanthiolate<sup>239,240</sup> was able to provide the desired aryl methyl sulfide in 99% yield. This intermediate was oxidized to generate **6** (**Scheme 2**) which was O-demethylated, nitrated and reduced to the aniline **7**. Reaction of **7** with the respective sulfonyl chloride afforded the desired products (**VU0849710** and **VU0830616**).



**Scheme 2.** a)  $S_2(CH_3)_2$ , Cu, pyridine, 90 °C, overnight; b)  $NaCH_3SO_2$ , L-proline, CuI, NaOH, DMSO, 85 °C, overnight; c)  $BBr_3$ , DCM, -78 °C, 96%; d)  $NaSCH_3$ ,  $Pd_2(dba)_3$ , Xantphos,  $Et_3N$ , THF, 76 °C, 18 h, 99%; e) Oxone, EtOH:H<sub>2</sub>O, r.t., 1 h, 95%; f)  $HNO_3$ ,  $H_2SO_4$ , DCM, 0 °C, 4 h, 72%; g)  $H_2$ , Pd/C, EtOH, 2 h, 94%; h) Sulfonyl chloride, pyridine, DCM, 0 °C, overnight, 27%.

**Table 6** shows the binding affinity data for the analogs described above. As a general trend, it was noticed that the addition of a chlorine *ortho* to the phenol of the sulfonyl ring (S<sub>4</sub> region) improves the binding affinity by several folds in comparison to the acid and amide series. Incorporation of the best-in-class hydrophobic groups in S<sub>1</sub>, such as -SF<sub>5</sub> (**VU0830070**) and -CF<sub>3</sub> (**VU0830459**) resulted in some of the most potent analogs. Incorporation of the cyano-spirocycle group (**VU084970** and **VU0830613**) resulted in compounds with binding affinities similar to those of the amides. Overall, we were able to demonstrate that the methyl sulfone containing analogs are well tolerated and that the acid or amide moiety could be exchanged with this group.

**Table 6.** Binding affinities of methyl sulfone analogs measured by FPA.

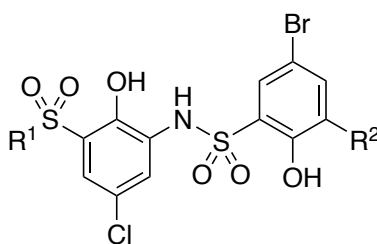


Compound	R <sup>1</sup>	R <sup>2</sup>	K <sub>d</sub> (μM) <sup>a</sup>	Compound	R <sup>1</sup>	R <sup>2</sup>	K <sub>d</sub> (μM) <sup>a</sup>
<b>VU0829548</b>	-Cl	-Cl	0.12 ± 0.05	<b>VU0830460</b>	-CF <sub>3</sub>	-H	0.097 ± 0.005
<b>VU0829581</b>	-Cl	-H	1.1 ± 0.3	<b>VU0832281</b>		-Cl	0.3 ± 0.2
<b>VU0830070</b>	-SF <sub>5</sub>	-Cl	0.04 ± 0.01	<b>VU0832278</b>		-H	0.7 ± 0.4
<b>VU0830056</b>	-SF <sub>5</sub>	-H	0.17 ± 0.05	<b>VU0849710</b>		-Cl	0.11 ± 0.06
<b>VU0830459</b>	-CF <sub>3</sub>	-Cl	0.07 ± 0.02	<b>VU0830613</b>		-H	0.4 ± 0.2

<sup>a</sup>Data displayed is the average of at least 2 independent replicates ± standard deviation.

In addition to optimizing the compounds with different groups that sit in the S<sub>1</sub> pocket, we explored the effect of larger groups alpha to the sulfone. The compounds shown in **Table 7** were synthesized by a route analogous to the one shown in **Scheme 1**, diethyl disulfide or diisopropyl disulfide were used instead of dimethyl disulfide. The three compounds synthesized showed a maximum ~2-fold decrease in K<sub>d</sub> compared to **VU0829548**. This suggested that further modifications might be tolerated in this position. Moreover, two sulfoxide analogs were also synthesized (**VU0830434** and **VU0830423**) and exhibited slightly higher K<sub>d</sub> values in comparison with **VU0830428**.

*Table 7. Analogs with different alkyl groups alpha to the sulfone.*



Compound	R <sup>1</sup>	R <sup>2</sup>	K <sub>d</sub> (μM) <sup>a</sup>
<b>VU0829548</b>	-CH <sub>3</sub>	-Cl	0.12 ± 0.05
<b>VU0830465</b>	-CH <sub>2</sub> CH <sub>3</sub>	-Cl	0.27 ± 0.04
<b>VU0830483</b>	-CH <sub>2</sub> CH <sub>3</sub>	-H	0.253 ± 0.005
<b>VU0830428</b>	-CH(CH <sub>3</sub> ) <sub>2</sub>	-Cl	0.17 ± 0.06
<b>VU0830434*</b>	-CH(CH <sub>3</sub> ) <sub>2</sub>	-Cl	0.34 ± 0.01
<b>VU0830423*</b>	-CH(CH <sub>3</sub> ) <sub>2</sub>	-H	0.37 ± 0.02

<sup>a</sup> Data displayed is the average of at least 2 independent replicates ± standard deviation.

\*Sulfoxide instead of sulfone.

### 2.2.2 Physicochemical properties optimization in the methyl sulfone subseries

Previous studies have demonstrated that small anionic aromatic compounds bind to the 3A domain of Human Serum Albumin (HSA-3A).<sup>241</sup> The very low  $F_u$  of the acids and amides suggested that the acidic character of the compounds should be reduced to improve the protein binding characteristics. Besides finding ways to reduce the acidic nature of the compounds, we were also interested in removing the phenols as they may be prone to glucuronidation or other types of metabolism.<sup>242,243</sup>

The calculated pKa of representative compounds from each subseries is shown in **Figure 21**. Based on these calculations, at physiological pH (~7.4) our compounds are expected to be primarily negatively charged (sulfonamide pKa < 7). One way to increase the pKa of the sulfonamide and reduce the overall acidity is by eliminating the phenol on the aniline ring, the calculated pKa for the sulfonamide is shown to increase to an average of 7.6 for the given examples, **Figure 21**. Furthermore, the deletion or substitution of the phenols has been one of our main goals as they are prone to glucuronidation and other types of metabolism.<sup>243,244</sup> Hence, we decided to synthesize compounds without the phenol in the aniline ring.

The synthesized des-phenol analogs and their binding affinity are shown in **Table 8**. The compounds **VU0814341**, **VU0816974**, **VU0822856**, **VU0816977**, **VU0816987**, **VU0821589**, and **VU0822864** were synthesized following the route shown in **Scheme 3A**. An Ullmann-type coupling was used to install the methyl sulfone (**1**) with yields ranging between 42-55%. The resulting intermediates were reacted with the respective sulfonyl chloride to provide the final compounds. **VU0822864** and **VU0825944** followed a similar synthetic route. First, the methyl sulfone group was installed on 3-bromo-5-iodoaniline. Then, the cyclopropyl group was installed

using a Suzuki coupling. Finally, the intermediate (3-cyclopropyl-5-(methylsulfonyl)aniline) was reacted with the respective sulfonyl chloride.

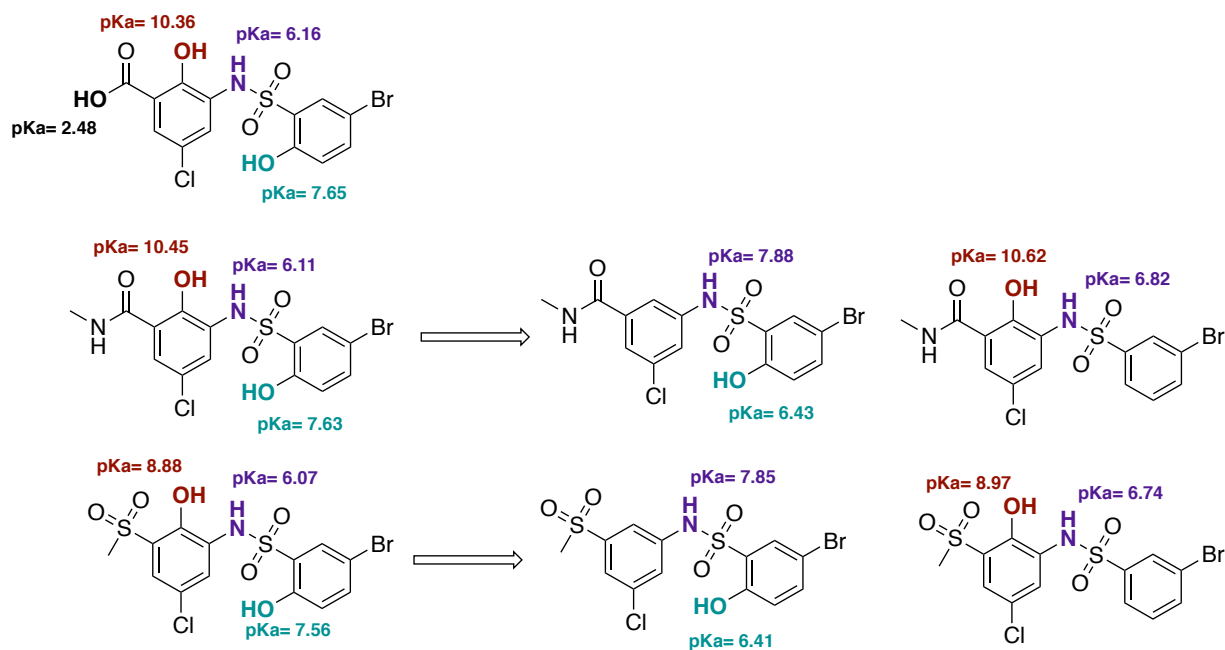
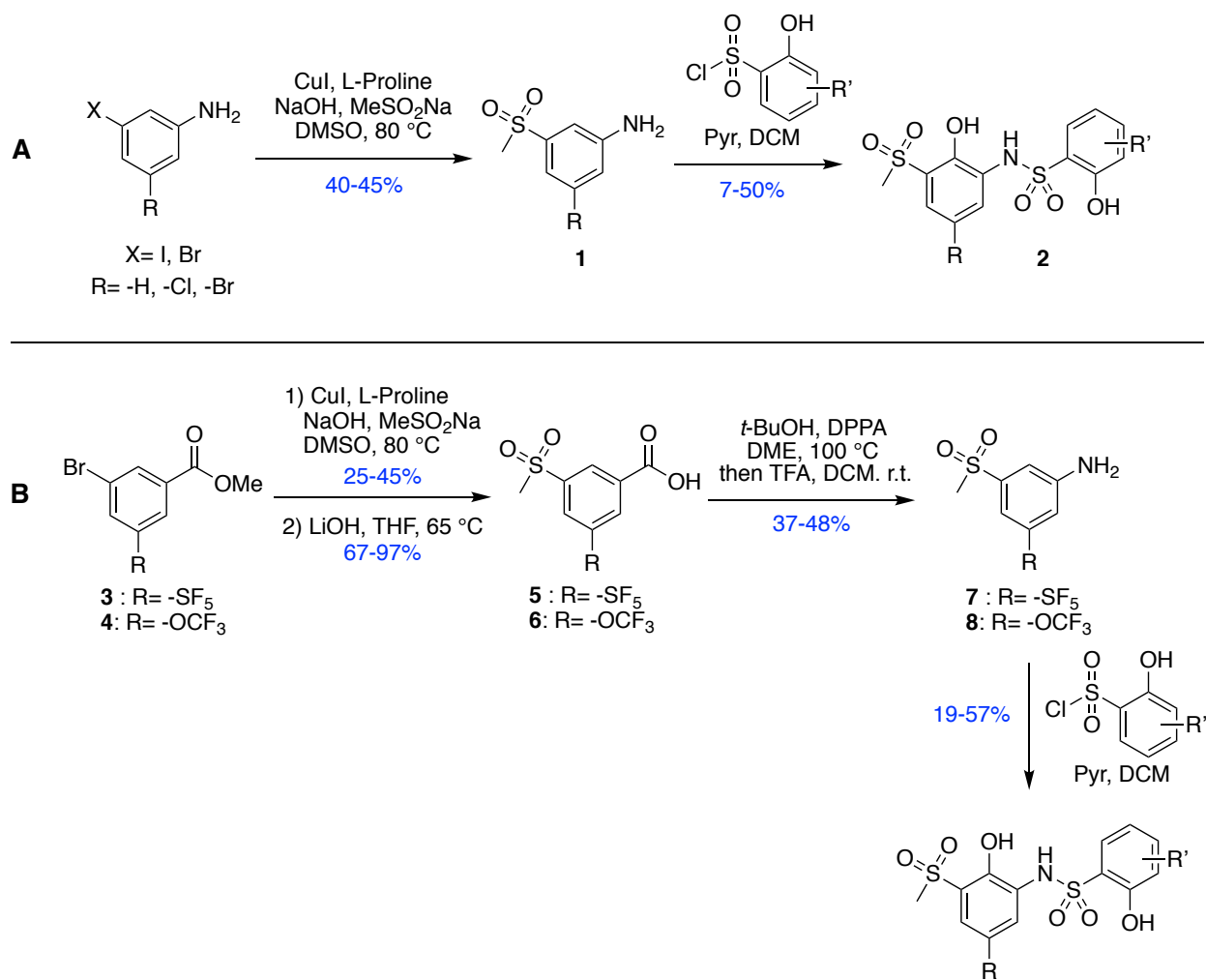


**Figure 21.** Calculated pKa for compounds representative of each subseries. The salicylic acid subseries was not further evaluated since the pKa of the carboxylic acid negatively affects permeability. The calculated pKa values were obtained using MarvinSketch.

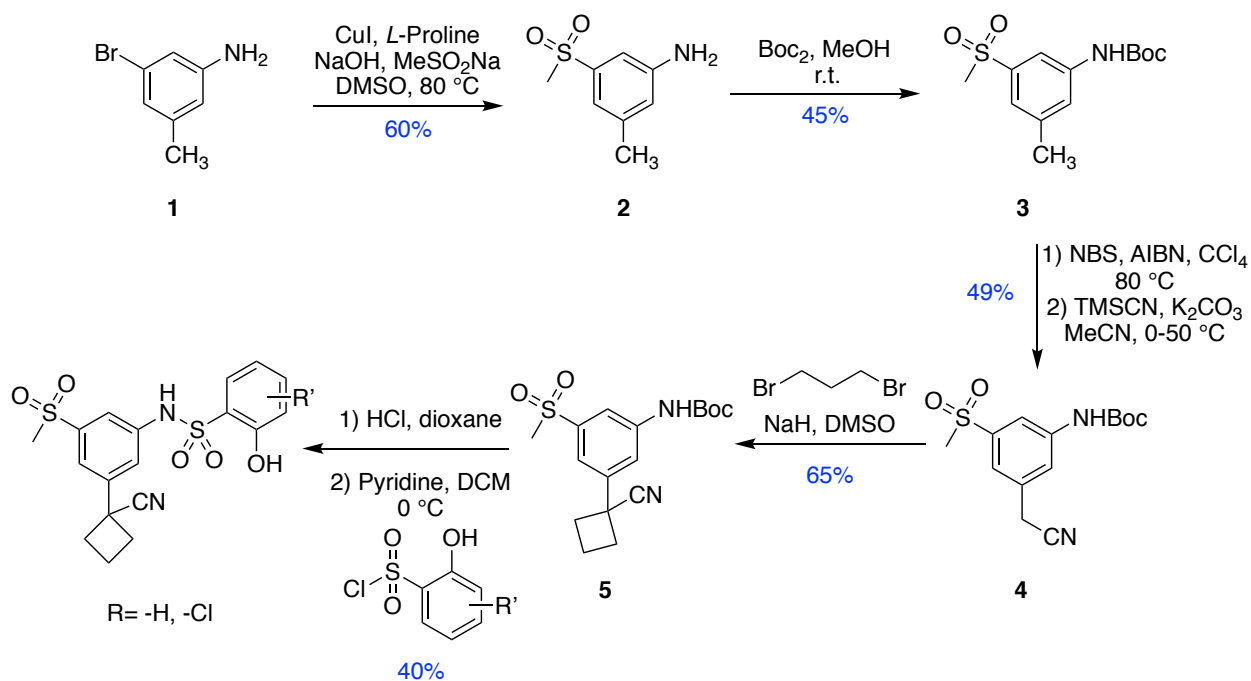
The analogs **VU0826052**, **VU0826067**, **VU0826051**, and **VU0826049** were synthesized following the route shown in **Scheme 3B**. Starting with the aryl bromide, the methyl sulfone was installed and the methyl ester was hydrolyzed (**5** or **6**). Next, a Curtius rearrangement was used to furnish a Boc-protected aniline which was treated with acid to furnish **7** or **8**. Finally, the aniline was reacted with the desired sulfonyl chloride.





*Scheme 3. Synthesis of different analogs lacking the aniline phenol.*

The synthetic route of the analogs **VU0850756** and **VU0850757** is shown in **Scheme 4**. 3-Bromo-5-methylaniline was coupled with sodium sulfinate using Ma's conditions to form **2**. The resulting aniline was Boc-protected (**3**) and submitted to benzylic bromination. The resulting bromide was further converted to the nitrile **4**. Next, treatment of **4** with 1,3-dibromopropane and NaH produced the spirocycle **5**. Finally, **5** was deprotected and reacted with the respective sulfonyl chloride.



*Scheme 4. Synthetic route for VU0850756 and VU0850757.*

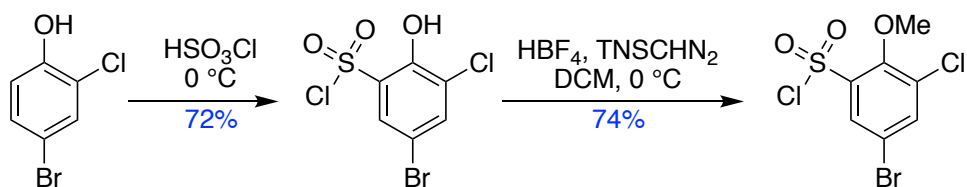
In almost all cases, the elimination of the phenol in the aniline ring resulted in compounds with reduced binding affinity in comparison with their phenol-containing analog. The compound **VU0826051**, with a  $-\text{SF}_5$  group was the best compound in this set as it retained high potency. Similarly, compound **VU0850756** shows only a 2-fold decrease in binding affinity in comparison with its phenol-containing analog, **VU0849710** (Table 6). Nonetheless, compounds with easier synthetic routes, such as **VU0822878**, **VU0826067**, and **VU0822864**, showed better or similar potency in comparison to **VU0850756**. In comparison to the methyl amide analogs, the methyl sulfone compounds displayed better binding affinity in several cases (**VU0816987** vs **VU0850029**, **VU0822864** vs **VU0850031**, and **VU0826049** vs **VU0823786**).

The compounds **VU0814341** and **VU0826049** were co-crystallized with WDR5 (Figure 22). The formation of a hydrogen bond with Q289 appears to be a weak interaction in both cases as a poor

definition of the electron density of the side chain of Q289 was observed in the X-ray co-crystal structures. This weak interaction also caused some uncertainty around the orientation of the methyl sulfone. An advantage of the sulfone not being “fixed” to a position, is that it may offer an avenue for expansion and the possibility to further tune the physicochemical properties in this subseries. Nevertheless, the overall binding pose of both compounds is similar to the previously co-crystallized compounds.

As part of the phenol elimination or substitution effort, the phenol in the aniline ring was replaced with a fluorine atom (**VU0849444**, **Table 8**). Fluorine has been reported as a hydrogen, nitrile, carbinol, and carbonyl bioisostere.<sup>245</sup> The fluorine was also chosen because its electronegativity is closer to that of the oxygen’s and might improve potency. Unfortunately, **VU0849444** was four-fold less potent than its direct H-containing analog (**VU0822864**). Furthermore, we evaluated the effect of moving the methyl sulfone moiety *ortho* to the aniline (**VU0849408**); this change resulted in a drop-off in binding affinity.

The elimination of the phenol in the sulfonyl ring (right-hand side ring) was also evaluated. Most of the sulfonyl chlorides used for the synthesis of these compounds were commercially available. For those that needed to be synthesized, a chlorosulfonation reaction of the starting material allowed the preparation of the desired sulfonyl chloride, **Scheme 5**.



*Scheme 5. Synthesis of sulfonyl chlorides.*

**Table 8.** Binding data for methyl sulfone and methyl amide analogs lacking a phenol in the aniline ring. Data determined by FPA.



Compound	R <sup>1</sup>	R <sup>2</sup>	K <sub>d</sub> (μM) <sup>a</sup>	Compound	R <sup>1</sup>	R <sup>2</sup>	K <sub>d</sub> (μM) <sup>a</sup>
VU0822856	-H	-Cl	4 ± 6	-	-	-	-
VU0816987	-Cl	-H	1.9 ± 0.4	VU0850029	-Cl	-H	3.8 ± 0.6
VU0822864	-Cl	-Cl	0.22 ± 0.03	VU0850031	-Cl	-Cl	1.2 ± 0.3
VU0814341	-Cl	-OCF <sub>3</sub>	0.7 ± 0.5	-	-	-	-
VU0821589	-Br	-OCF <sub>3</sub>	0.7 ± 0.3	-	-	-	-
VU0826052	-OCF <sub>3</sub>	-H	0.9 ± 0.2	VU0823787	-OCF <sub>3</sub>	-H	0.70 ± 0.04
VU0826067	-OCF <sub>3</sub>	-Cl	0.12 ± 0.05	-	-	-	-
VU0825944		-H	1.1 ± 0.1	VU0823793		-H	1.24 ± 0.05
VU0822878		-Cl	0.23 ± 0.07	-	-	-	-
VU0826049	-SF <sub>5</sub>	-H	0.51 ± 0.05	VU0823786	-SF <sub>5</sub>	-H	0.8 ± 0.2
VU0826051	-SF <sub>5</sub>	-Cl	0.093 ± 0.001	-	-	-	-
VU0850757		-H	1.4 ± 0.5	VU0827038		-H	1.1 ± 0.4
VU0850756		-Cl	0.25 ± 0.08	VU0826966		-Cl	0.13 ± 0.02
VU0849444*	-Cl	-Cl	0.9 ± 0.1	-	-	-	-
VU0849408*	-Cl	-Cl	16 ± 5	-	-	-	-

<sup>a</sup> Data displayed is the average of at least 2 independent replicates ± standard deviation.

\* F instead of H

\*Methyl sulfone *ortho* to aniline.

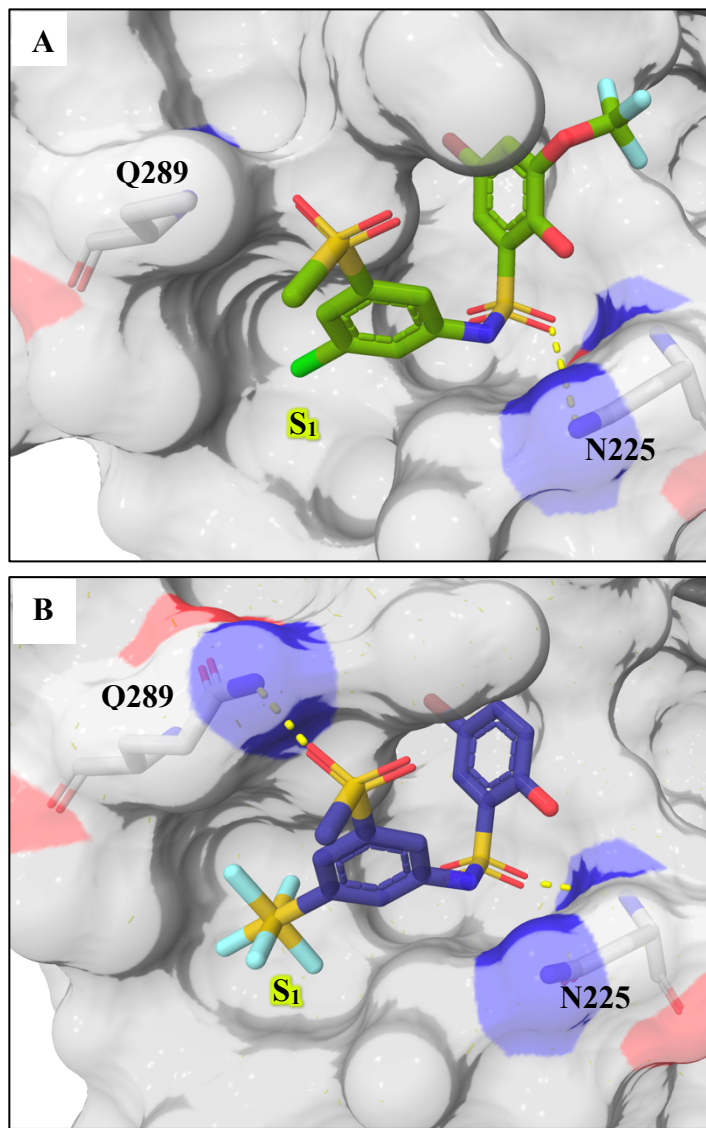


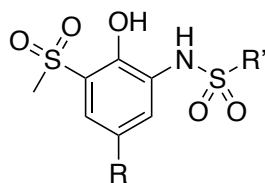
**Figure 22.** X-ray co-crystal structure of A) *VU0814341*, the amide group of Q289 side chain was not resolved, and B) *VU0826049* (PDB:6U5M).

Multiple phenol and bromine replacement strategies (*VU0849713*, *VU0849714*, *VU0849656*, and *VU0849227*) failed to provide potent inhibitors (**Table 9**); however, using optimized aniline-ring groups and “capping” the phenol as a methoxy (e.g. *VU0849229*, *VU0849712*) led to inhibitors with sub-micromolar affinity in selected cases. Further, combining the best-in-class aniline groups

to generate 6-bromoquinoline-8-sulfonamides afforded high nanomolar analogs that do not contain the *para*-bromophenol motif. In this class, we observed that the sulfone derivatives **VU0849547** and **VU0849711** retain promising affinity in comparison to their direct *ortho*-chlorophenol analogs.

The elimination of the phenols represented a general decrease in binding affinity. As mentioned before, negatively charged compounds are known to bind HSA-3A; thus, they will display low free fraction values ( $F_u$ ) and will be less available to interact with the intended target. Attempts to crystallize our compounds with this domain were not successful; nonetheless, the probability of interaction at this site cannot be discarded. A chemometric model for the reduction of compound binding to HSA-3A was reported.<sup>241</sup> This model shows that amines, carbamates sulfones, and amides can help to reduce the binding affinity towards HSA-3A.<sup>241</sup> Similarly, traditional approaches to optimize compounds with high plasma protein binding (PPB) have entailed the incorporation of polar or positively charged groups at various positions of the compound. For example, there are several published cases that show the incorporation of basic amines in solvent-exposed regions of the compound as a way to reduce PPB.<sup>246</sup>

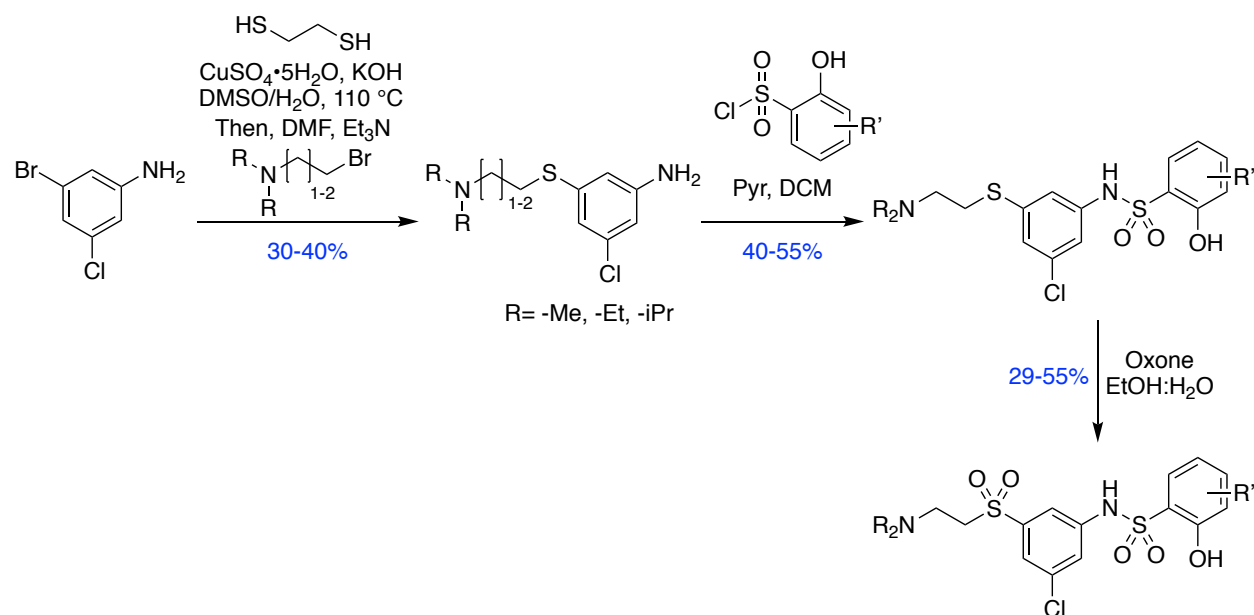
**Table 9.** FPA data for compounds lacking the right-hand side phenol.



Compound	R	R'	K <sub>d</sub> (μM) <sup>a</sup>	Compound	R	R'	K <sub>d</sub> (μM) <sup>a</sup>
VU0849229	-Cl		0.30 ± 0.02	VU0849547	-Cl		0.4 ± 0.1
VU0849712			0.32 ± 0.06	VU0849711			0.27 ± 0.09
VU0849713			> 40	VU0849714	-Cl		0.78 ± 0.05
VU0849227	-Cl		5.9 ± 0.9	VU0849656	-Cl		1.14 ± 0.03

<sup>a</sup> Data displayed is the average of at least 2 independent replicates ± standard deviation.

In light of these reports, we thought that the introduction of basic amines into our compounds could balance the net charge and increase the F<sub>u</sub>. Formerly, we indicated that the methyl sulfone group is not in a “fixed” position and this may allow modifications to optimize the physicochemical properties. Therefore, we hypothesized that the installation of different basic amines that extend from the sulfone can help reduce the PPB. We synthesized six analogs (**Table 10**) to test our hypothesis; their synthetic route is shown in **Scheme 6**. The aryl bromide was reacted with 1,2-dithioethane following conditions reported by Liu, *et al*<sup>247</sup> to form the aryl thiol. The crude was then treated with the desired alkyl amine and base to furnish the alkylated thioaniline. Then, this intermediate was reacted with the desired sulfonyl chloride, and the resulting sulfonamide intermediate was oxidized to form the final product.

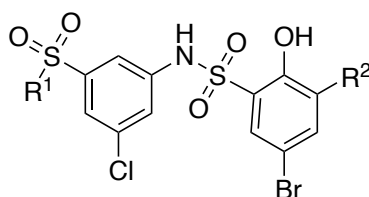


*Scheme 6. Synthesis of analogs containing basic amines.*

The set of compounds containing basic amines and their binding affinities is shown in **Table 10** along with compound **VU0822864** as reference. An unexpected drop-off in binding affinity was noticed when we eliminated the chlorine that sits in the  $S_4$  pocket. On the other hand, compounds **VU0848793**, **VU0822864**, and **VU0849253** displayed similar  $K_d$  values. This may indicate that the alkyl amines point towards the solvent and more diverse groups could be installed while paying a small penalty in potency. Overall, these analogs showed that the location of the basic amines is tolerated and it might be possible to improve the binding affinity by installing some of the best-in-class groups that sit in the  $S_1$  pocket.



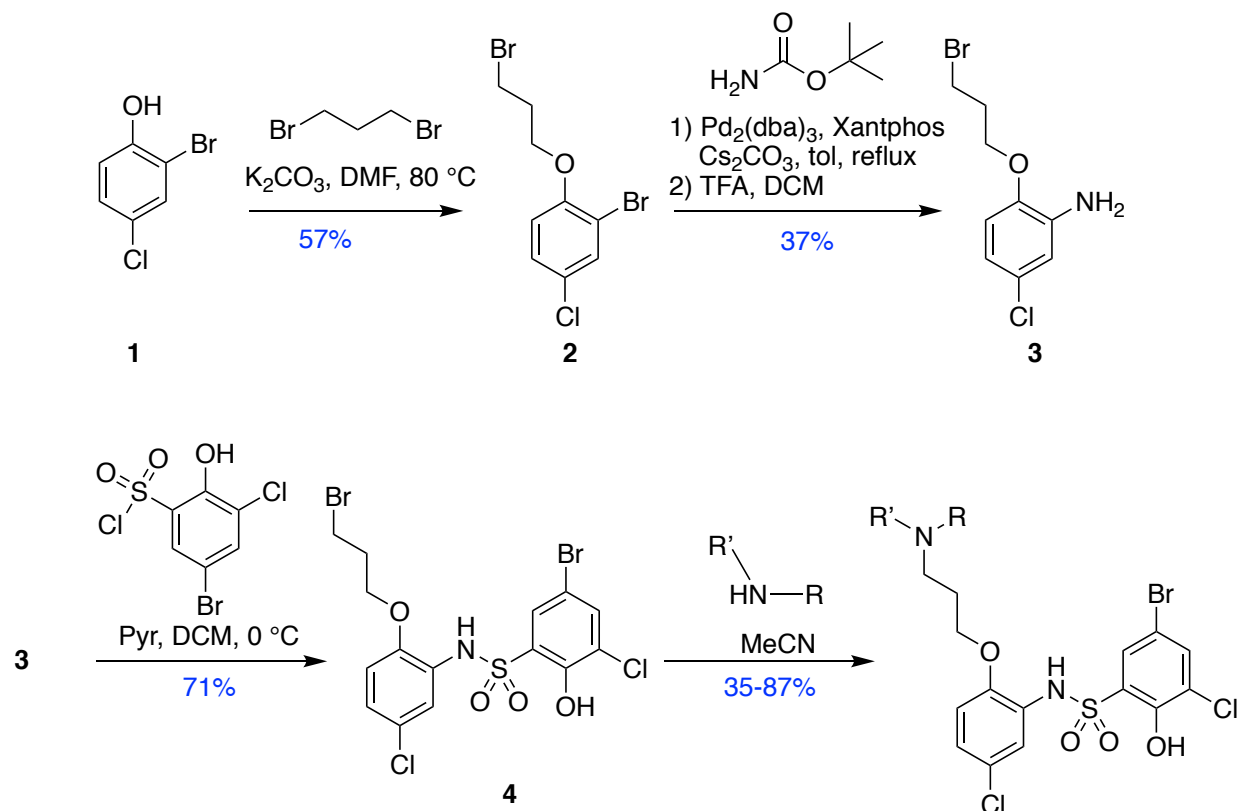
**Table 10.** FPA binding data for sulfones with tethered amine.



Compound	R <sup>1</sup>	R <sup>2</sup>	K <sub>d</sub> (μM) <sup>a</sup>
VU0822864	-CH <sub>3</sub>	-Cl	0.22 ± 0.03
VU0848787		-H	4.0 ± 0.2
VU0848793		-Cl	0.5 ± 0.2
VU0848788		-H	3.53 ± 0.06
VU0848797		-Cl	0.686 ± 0.009
VU0849254		-H	7 ± 2
VU0849253		-Cl	0.59 ± 0.03

<sup>a</sup> Data displayed is the average of at least 2 independent replicates ± standard deviation.

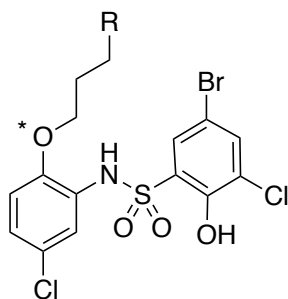
We were also interested in linking basic amines to the phenol of the aniline ring in as an alternative placement option. Unfortunately, the installation of the amines was not straightforward; the different routes that were tried were characterized by very low yields and intermediates or products that were difficult to purify. Nevertheless, in the absence of the sulfone group, the synthesis of these analogs was easier (**Scheme 7**). Starting with the phenol, alkylation with 1,3-dibromopropane generated the intermediate **2**. Then, a Buchwald coupling<sup>248</sup> of *tert*-butylcarbamate with **2** and treatment with TFA in DCM generated **3**. The reaction of **3** with the desired sulfonyl chloride furnished **4**, which upon treatment with the desired amine in acetonitrile, provides the desired product.



*Scheme 7. Synthetic route for O-tethered amines.*

**Table 11** shows the compounds made through this route. The addition of a tethered amine proved to be deleterious for binding affinity compared to the parent analog, **VU0809018**. The incorporation of a methyl amide or methyl sulfone *ortho*- to the ether could improve the binding affinity by 2- to 10-fold based on previous data; therefore, when extrapolating these numbers to this set of compounds, further exploration of these targets became less attractive.

**Table 11.** FPA binding data for *O*-tethered amines.



Compound	R	K <sub>d</sub> (μM) <sup>a</sup>
VU0809018	-OH*	0.5 ± 0.1
VU0848402		2.6 ± 0.6
VU0848421		14 ± 3
VU0848425		>40
VU0848426		2.3 ± 0.1
VU0848429		>40

\*Parent analog: free phenol (5-bromo-3-chloro-*N*-(5-chloro-2-hydroxyphenyl)-2-hydroxybenzenesulfonamide).

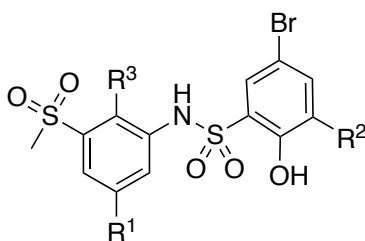
<sup>a</sup>Data displayed is the average of at least 2 independent replicates ± standard deviation.

### 2.2.3 Pharmaceutical Properties

We explored the tier 1 DMPK profile of a number of compounds within this class (**Table 12**). The data for these compounds showed that replacing the carboxylic acid by a methyl sulfone results in an improvement of the permeability while maintaining good kinetic solubility (>100 μM). Interestingly, the permeability of these sulfone analogs increases when a chlorine sits in the S<sub>4</sub> pocket. This is opposite to the trend observed in the direct amide and acid analogs. A remaining major limitation of this subseries is that they also show severe plasma protein binding. The deletion

of a single phenol was not enough to affect the  $F_u$  values. Unfortunately, the analogs with a basic amine tethered to the sulfone and the analogs lacking the phenol in the sulfonyl ring were not tested for tier 1 DMPK. The data collected here suggest that, in order to achieve a reduction of plasma protein binding, a bigger structural change may be required. Indeed, it is known that sulfonamides are also prone to displaying high PPB.<sup>249,250</sup>

*Table 12. Tier 1 DMPK profile of selected compounds.<sup>a</sup>*



Compound	R <sup>1</sup>	R <sup>2</sup>	R <sup>3</sup>	K <sub>d</sub> (μM)	Solubility (μM)	MDCK A-B (10 <sup>6</sup> cm/s)	F <sub>u</sub> (%)
VU0826049	-SF <sub>5</sub>	-H	-H	0.51	>100	18.581	<0.0003
VU0826051	-SF <sub>5</sub>	-Cl	-H	0.093	>100	30.562	<0.0003
VU0816987	-Cl	-H	-H	1.9	>100	N/A	0.0005
VU0822864	-Cl	-Cl	-H	0.22	>100	3.38	<0.0002
VU0829548	-Cl	-Cl	-OH	0.12	>100	16.084	<0.0002
VU0829581	-Cl	-H	-OH	1.1	>100	0.907	<0.0004

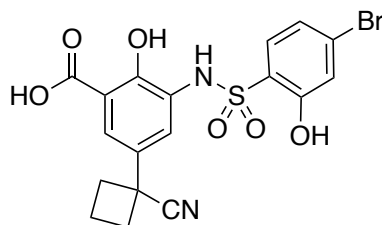
<sup>a</sup>All experiments performed at Q<sup>2</sup> Solutions Ltd.

### 2.3 Biochemical and biological assessment of target engagement

Target engagement was assessed by a thermal shift assay and by Co-IP experiments using lysates of modified HEK293 cells.

### 2.3.1 Thermal shift assay

In order to further demonstrate effective, on-target binding of our inhibitors to WDR5, we used differential scanning fluorimetry (DSF) to examine a subset of compounds (**Table 13**). The salicylic acids **VU0849828** and **VU0829710** are the most potent examples by FPA and also impart the largest  $\Delta T_m$  and thereby stabilization of WDR5. The sulfones **VU0829548** and **VU0849710** and the methyl amide **VU0829711** have similar binding affinity in the FP assay and also stabilize WDR5 to a similar extent. A decrease in binding affinity is also characterized by a smaller  $\Delta T_m$ ; **VU0822864**, **VU0849711**, and **VU0849547** are good examples of this. A negative control compound, **VU0830492** (**Figure 23**. Chemical structure of negative control compound.), contains a regioisomeric bromine designed such that the key halogen bonding bromine atom is moved around the phenyl ring, causing a significant decrease in affinity. This is the direct regioisomer of **VU0829710**, and in this assay, **VU0830492** has minimal effect.



**VU0830492**  
 $K_d > 40 \mu\text{M}$

*Figure 23. Chemical structure of negative control compound.*

*Table 13. Measured  $\Delta T_m$  values for different biaryl sulfonamide analogs*

<b>Compound</b>	<b>K<sub>d</sub> (<math>\mu</math>M)</b>	<b><math>\Delta T_m</math> Avg (<math>^{\circ}</math>C)<sup>a</sup></b>
<b>VU0849828</b>	0.03 $\pm$ 0.02	8.4 $\pm$ 0.4
<b>VU0829710</b>	0.03 $\pm$ 0.02	6.7 $\pm$ 0.4
<b>VU0829548</b>	0.12 $\pm$ 0.05	5.9 $\pm$ 0.3
<b>VU0849710</b>	0.11 $\pm$ 0.06	5.7 $\pm$ 0.3
<b>VU0829711</b>	0.16 $\pm$ 0.03	5.5 $\pm$ 0.3
<b>VU0849820</b>	0.19 $\pm$ 0.03	4.0 $\pm$ 0.3
<b>VU0822864</b>	0.22 $\pm$ 0.03	2.5 $\pm$ 0.3
<b>VU0849711</b>	0.27 $\pm$ 0.09	2.3 $\pm$ 0.3
<b>VU0849547</b>	0.4 $\pm$ 0.1	1.9 $\pm$ 0.3
<b>VU0830492</b>	> 40	0.4 $\pm$ 0.2

<sup>a</sup>Data displayed is the average of at least 2 independent replicates  $\pm$  standard deviation.

### 2.3.2 Confirmation of target engagement in cell lysates

To assess whether compounds disrupt the association between WDR5 and C-MYC at the WBM-site, we immunoprecipitated WDR5 from cell lysates treated with compounds. We chose a representative selection of compounds from the acid, amide, and sulfone subseries with a range of binding affinities to WDR5 as measured by FPA.

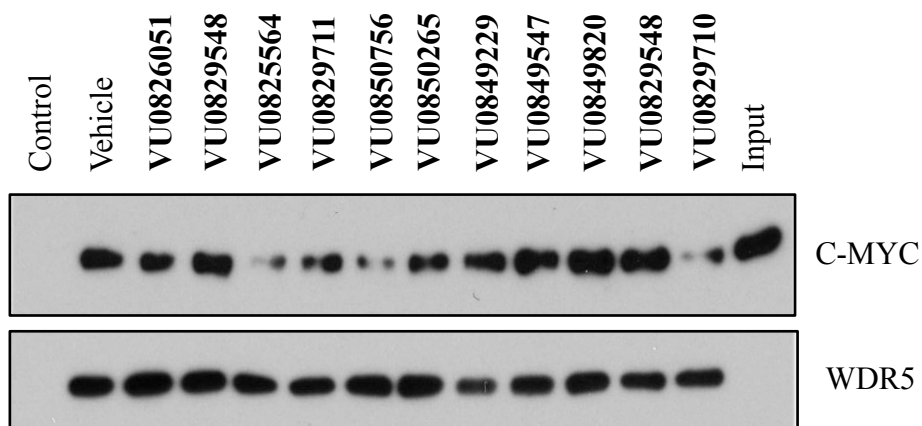


**Figure 24.**  *$\alpha$ -FLAG immunoprecipitation from lysates treated with different compounds. Levels of C-MYC protein in association with WDR5 was assessed after treatment with compound in lysates from WDR5-FLAG and C-MYC-HA co-overexpressing HEK293 cells. An  $\alpha$ -FLAG immunoprecipitation was used to isolate WDR5, which is not detectable in the input due to the excess of WDR5 in the IP fraction. Lysates were treated with 50  $\mu$ M compound, data are representative of two independent biological repeats.*

Cell lysates were treated with 50  $\mu$ M compound and varying degrees of disruption between both WDR5-C-MYC as compared to the vehicle control were observed (**Figure 24**). In most cases, the degree of disruption corresponded to the compound's respective binding affinity to WDR5. Those compounds with higher binding affinity to WDR5 disrupted the WDR5-C-MYC protein interactions to a greater degree (e.g. **VU0829710** and **VU0825564**). The amide **VU0829711** also shows disruption of the WDR5-C-MYC interaction, although less than the acids. Interestingly, the less potent sulfone **VU0850756** is comparable to the acids, as it disrupted the interaction to a similar extent. This may be a consequence of eliminating the phenol from the aniline ring.

Overall, we demonstrated that our compounds bind to WDR5 in two biochemical assays: 1) by displacing a FITC-labeled probe from recombinant, purified WDR5 and 2) by DSF and stabilization of WDR5. We also were able to demonstrate binding to WDR5 in cell lysates when performing co-immunoprecipitation experiments.

## 2.4 Conclusions

The substitution of the carboxylic acid group for a methyl sulfone group allowed the optimization of some of the physicochemical properties of the biaryl sulfonamide series. In combination with some of the best-in-class pieces, the methyl sulfone compounds retained high binding affinity and displayed a more favorable tier 1 DMPK profile. The methyl sulfones were more permeable than the salicylic acid analogs and retained high solubility.

In general, the elimination of the phenol in the aniline ring caused a reduction in the binding affinity of the methyl amide and methyl sulfone analogs. Moreover, the des-phenol methyl sulfone analogs have comparable potency to their equivalent amide. Unfortunately, this small structural modification did not significantly improve the plasma protein binding.

The optimization of the right-hand side piece remains in its early stages. The analog **VU0849656** (**Table 9**) shows a promising future, as the introduction of the quinoline allows the replacement of one of the phenols. Further extensions/modifications on this side of the molecule could help increase the binding affinity and improve the physicochemical properties.

Similarly, the tier 1 DMPK profile of the sulfones tethered to basic amines and the analogs lacking the phenol in the sulfonyl ring should be assessed as availability of these data might enlighten future compound designs.



In addition, target engagement was assessed by Thermal shift assay and Co-IP experiments. All the compounds assessed by DSF were able to stabilize WDR5. Moreover, several of these compounds were used in Co-IP experiments using cell lysates and some showed disruption of the WDR5-MYC interaction. Unfortunately, the low free fraction displayed by most of our compounds limits their utility in whole-cell experiments.

## Chapter III

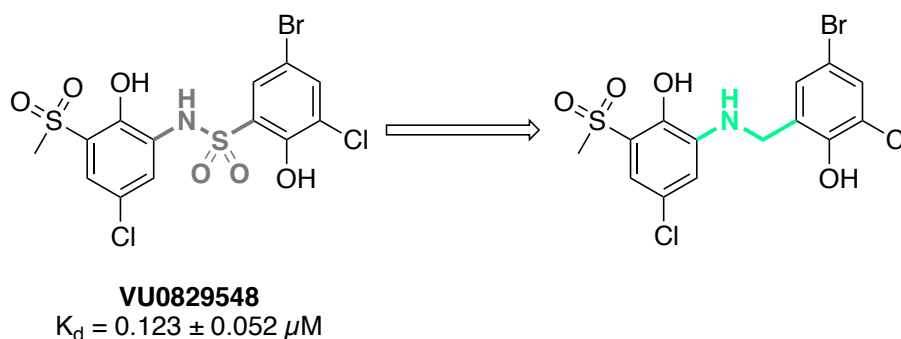
### Sulfonamide linker replacements

#### 3.1 Introduction

The HTS allowed the identification of multiple compounds that bind to WDR5; however, the best hits contain a sulfonamide motif. Consequently, and up to this point, the analogs synthesized have a sulfonamide motif that links two aryl rings. Sulfonamides are, in general, fairly acidic and in some cases they can contribute to high plasma protein binding.<sup>251</sup> In Chapter II, we have shown that our compounds are highly bound to plasma proteins. While it is not fully clear which functional group is the major contributor to the high values observed for PPB, the reported literature and the acquired tier 1 DMPK data suggest that the sulfonamide itself might be the reason why our compounds display such low  $F_u$  values. Therefore, we were interested in finding alternative linkers that could improve our compound's physicochemical properties. In addition to finding a replacement for the sulfonamide linker, this effort would allow the diversification of our chemical matter. This is a common practice in drug discovery, as it can help circumvent toxicity concerns or intellectual property issues.

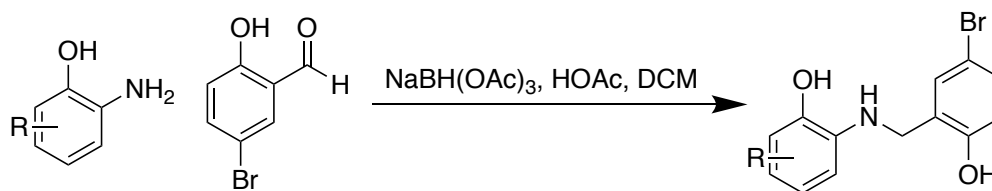
A structure-based approach supported by molecular docking was used during the new linker survey. The main sulfonamide feature that we wanted to preserve and/or mimic with a new linker is its ability to organize the aryl rings in a U-shape, this way the new compounds could capture most of the interactions previously described.

### 3.2 Benzyl amine linker



*Scheme 8. Proposed compound design with deleted sulfone from sulfonamide linker.*

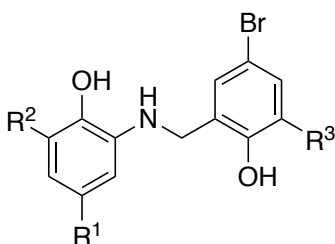
The first design we explored was a benzyl amine linker (**Scheme 8**). Docking studies using Glide Software suggested that compounds with this design could adopt the intended conformation. Although, a concern with this design was the increase in flexibility given by the introduction of the methylene group, as it would allow the compounds to sample more conformations. This event could translate into a decrease in binding affinity if the enthalpic contribution when the compound binds to WDR5 is not large enough to compensate for the reduction in the degrees of freedom.<sup>252</sup> Further, the deletion of the sulfone was expected to reduce the binding affinity as there would not be a hydrogen bond acceptor that could interact with N225.



*Scheme 9. Synthesis of compounds with basic amine linker.*

To test this linker, several compounds were synthesized using a reductive amination reaction between the respective anilines and aldehydes (**Scheme 9**). **Table 14** shows some of the compounds synthesized. Unfortunately, the majority of compounds showed a  $K_d > 40 \mu\text{M}$ . It is likely that both, the increase in flexibility and the loss of the hydrogen bond with N225, affected the binding affinity.

**Table 14.** FPA data for analogs with benzyl amine linker.

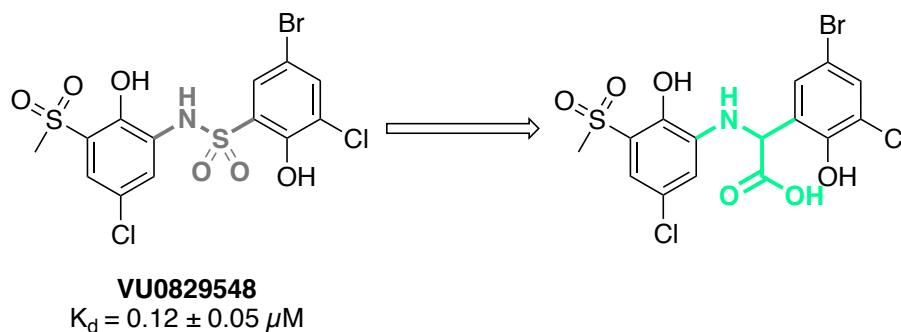


Compound	R <sup>1</sup>	R <sup>2</sup>	R <sup>3</sup>	K <sub>d</sub> (μM) <sup>a</sup>
VU0849826	-Cl	-SO <sub>2</sub> Me	-H	>40
VU0849827		-CONHMe	-H	>40
VU0849831		-COOH	-H	>40
VU0816562	-OCF <sub>3</sub>	-NO <sub>2</sub>	-OCF <sub>3</sub>	35 ± 7
VU0807489	-Cl	-NO <sub>2</sub>	-OCF <sub>3</sub>	16 ± 1

<sup>a</sup> Data displayed is the average of at least 2 independent replicates ± standard deviation.

### 3.3 Amino acetic acid linker

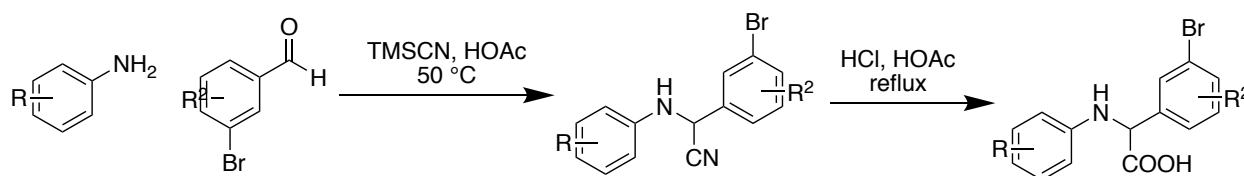
The second design was an attempt to improve the benzyl amine linker by incorporating a carboxylic acid alpha to the amine (**Scheme 10**) with the expectation that it would restore the hydrogen bond with N225 of WDR5.



*Scheme 10. Amino acetic acid linker design.*

A Strecker reaction was used to synthesize this type of compounds. The desired aniline and aldehyde were dissolved in acetic acid and stirred at 50 °C for one hour and then treated with TMSCN to furnish the amino acetonitrile intermediate. This intermediate was treated with acid and heated to reflux to generate the desired analog (**Scheme 11**).

This set of compounds were not tested in the FP assay, since decomposition was observed after one day.

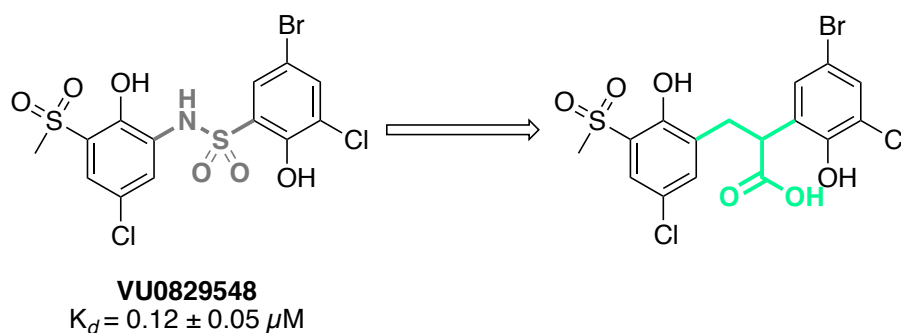


*Scheme 11. Synthetic scheme for the synthesis of amino acetic acid linker.*

### 3.4 Propionic acid linker

For the next type of linker, the amino group of the amino acetic acid linker was removed to create a propionic acid linker, **Scheme 12**. We thought that the deletion of the amine would increase the

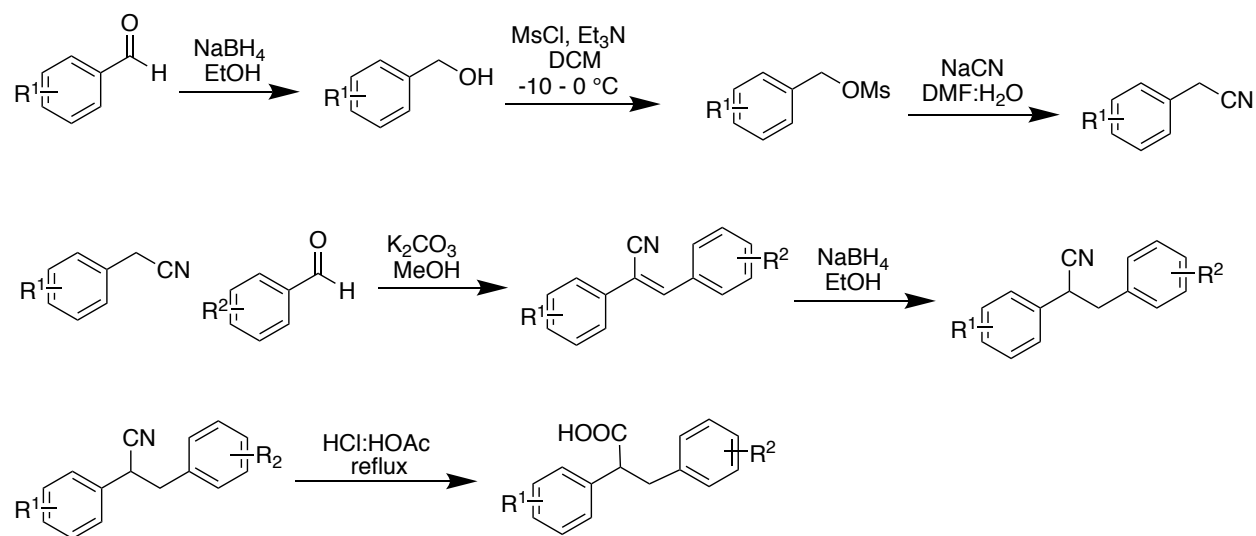
stability of the compounds while maintaining the hydrogen bond between the carboxylic acid and N225.



*Scheme 12. Propionic acid linker.*

The general synthetic route for this type of compounds is shown in **Scheme 12**. The desired aldehyde was reduced to the benzylic alcohol and then treated with base and MsCl. The mesylate intermediate was reacted with NaCN which displaced the mesylate group and formed the acetonitrile intermediate, one of the key pieces. Then, the acetonitrile was treated with base and the desired aldehyde to furnish the acrylonitrile. The reduction of the acrylonitrile with  $\text{NaBH}_4$  formed the substituted diphenylpropanenitrile. Finally, this intermediate was mixed with acid and refluxed to form the final propionic acid linker.

A small number of compounds were synthesized using this route; however, only one compound showed binding affinity in the low micromolar range when tested in the FPA. Compound **VU0817326** (**Figure 25A**) was co-crystalized with WDR5 and surprisingly, the crystal structure (**Figure 25B**) revealed a binding pose that was flipped in comparison to the expected one.



*Scheme 13. General synthetic route for analogs containing the propionic acid linker.*

Analysis of the X-ray co-crystal structure of **VU0817326** revealed that several key interactions with WDR5 were missing. For example, there were no hydrogen bond interactions with N225 or Q289, and there was not a halogen bond with W273. Moreover, the nitro group was seating in a hydrophobic area (S<sub>4</sub>) and the carboxylic acid was pointing towards the solvent. There was also an opening of a new channel that we called S<sub>5</sub> (**Figure 25B**). We postulated that this could be used to improve the compound's binding affinity.

A minimum pharmacophore exploration of **VU0817326** was conducted hoping to find a simplified structure that retains a similar binding affinity for WDR5. **Table 15** shows the K<sub>d</sub> values for the different analogs synthesized. Intriguingly, the deletion of groups that were thought to be “unnecessary”, such as -NO<sub>2</sub>, -OH and -Br, resulted in compounds with complete loss of binding affinity. Substitution of the carboxylic acid for a nitrile or methyl ester also showed to be deleterious to the binding affinity. On the other hand, replacement of the carboxylic acid for tetrazole, a bioisostere, resulted in a ~2-fold increase in the binding affinity.

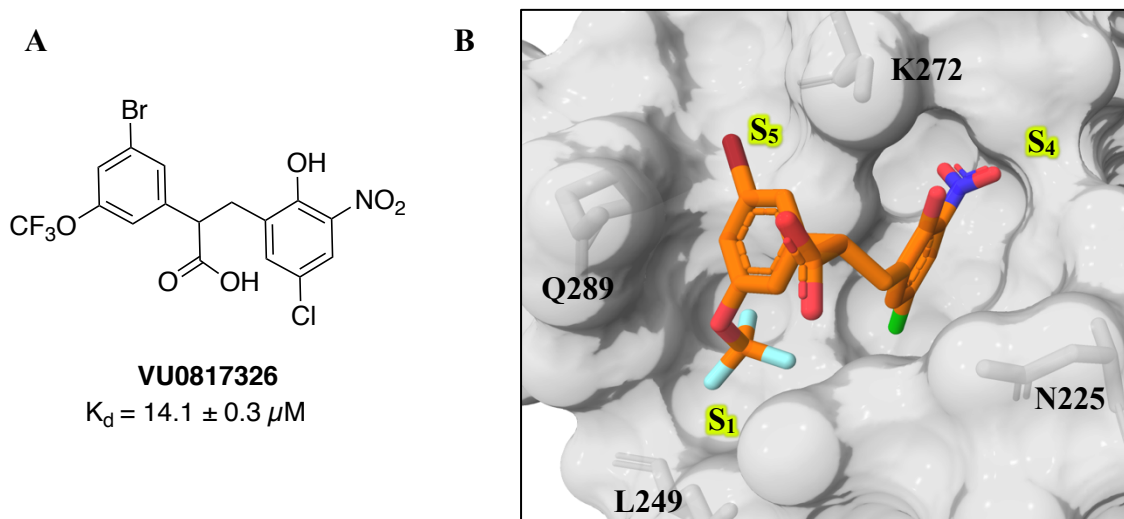


*Figure 25. A) VU0817326 chemical structure and B) X-ray co-crystal structure of WDR5 with VU0817326.*

Based on this data, we decided to explore the SAR around the left side piece, we retained the tetrazole group as it improved the binding affinity. Bromine replacements were evaluated first, several functional groups that could restore the interaction with Q289 and/or grow towards the S<sub>5</sub> channel were installed after confirming the viability of the substitution by docking studies. A general synthetic scheme for the installation of the different groups is shown in **Scheme 14**. Most of the modifications were made using a Suzuki coupling between the desired boronic acid and 2-(3-bromo-5-(trifluoromethoxy)phenyl)acetonitrile (**4**). Installation of the Boc-protected aniline was done early on by reacting 3-bromo-5-(trifluoromethoxy)benzaldehyde (**1**) with *tert*-butyl carbamate using Buchwald's conditions.<sup>248</sup> Next, the resulting intermediate (**2**) was reacted as shown in **Scheme 13** to obtain the propanenitrile intermediate (**3**) which was acylated (or coupled) to the respective acid. Finally, reaction with NaN<sub>3</sub> and NH<sub>4</sub>Cl to form the tetrazole furnished the desired products.





**Table 15.** Minimum pharmacophore study. Binding affinity obtained by FPA.

Structure	Compound	$K_d$ ( $\mu\text{M}$ ) <sup>a</sup>	Structure	Compound	$K_d$ ( $\mu\text{M}$ ) <sup>a</sup>
	<b>VU0817326</b>	$14.1 \pm 0.3$		<b>VU0825987</b>	>40
	<b>VU0825941</b>	>40		<b>VU0817346</b>	>40
	<b>VU0826045</b>	>40		<b>VU0825602</b>	>40
	<b>VU0826458</b>	>40		<b>VU0825970</b>	$8 \pm 4$

<sup>a</sup>Data displayed is the average of at least 2 independent replicates  $\pm$  standard deviation.

These analogs were tested in the FPA and the data is shown in **Table 16**. We started by incorporating smaller groups on the -Br position (which sits in the S<sub>5</sub> channel). Groups like -Cl (**VU0826895**), -F (**VU0827423**), -CH<sub>3</sub> (**VU0826951**), -NH<sub>2</sub>, (**VU0826693**) and -CHCH<sub>2</sub> (**VU0826909**) did not improved the binding affinity. A phenyl ring was also installed (**VU0826911**) with the expectation that it would be tolerated and could offer some expandability opportunities; unfortunately, it was 2-fold less potent than **VU0825970**. A phenyl isostere, thienyl, was also installed to furnish **VU0826483** and **VU0826484**. Both compounds showed similar binding affinities to **VU0826911**. Subsequently, we decided to introduce some polarity in the phenyl ring with **VU082420** and **VU0827421**, but both analogs were inactive. Due to the limited

success, we explored smaller heterocycles (**VU0826691**, **VU0826722**, **VU0826738**, and **VU0826724**), but none of them improved the binding affinity.

In addition to cyclic substituents, we explored some amides with small (**VU0826922** and **VU0826955**), medium (**VU0827042**) and large (**VU0827041**) alkyl/aryl groups. None of these analogs were tolerated. Finally, we tested the alkyne **VU027040**, hoping that an increase in rigidity would help, but it was not tolerated.

Even though we could not find a replacement for the bromine, we thought that we could optimize **VU0825970** by substituting the  $-\text{OCF}_3$  group, which occupies the hydrophobic pocket  $S_1$ . An overlay of **VU0825970** and **VU0826049** (sulfonamide) X-ray crystal structures (**Figure 26**) shows a good overlap of the hydrophobic groups that sit in the  $S_1$  pocket ( $-\text{CF}_3$  and  $-\text{SF}_5$ ). This suggested that we could exploring with some of the best groups used in the sulfonamide series.

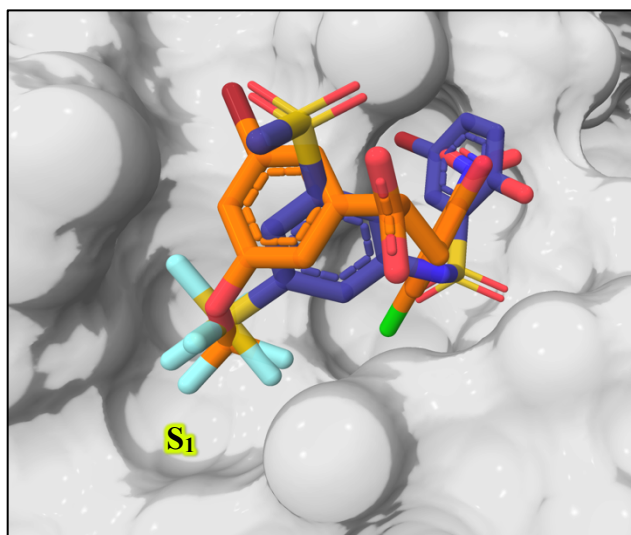
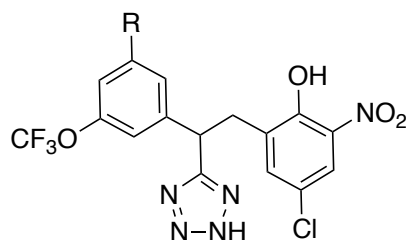


*Figure 26. X-ray co-crystal structure of **VU0817326** (orange) bound to WDR5 and overlaid with **VU0826049** (purple).*

**Table 16.** Binding affinity data for analogs with different groups sitting in the  $S_5$  pocket.



Compound	R	$K_d$ ( $\mu$ M)	Compound	R	$K_d$ ( $\mu$ M)
VU0825970	-Br	$8 \pm 4$	VU0826484		$12 \pm 4$
VU0826895	-Cl	$23 \pm 7$	VU0826691		$>40$
VU0827423	-F	$38 \pm 3$	VU0826722		$>40$
VU0826951	-CH <sub>3</sub>	$>40$	VU0826738		$>40$
VU0826693	-NH <sub>2</sub>	$>40$	VU0826724		$38 \pm 4$
VU0826909		$>40$	VU0826922		$>40$
VU0826694	-NHBoc	$>40$	VU0826955		$>40$
VU0826911		$18 \pm 3$	VU0827041		$>40$
VU0827420		$>40$	VU0827042		$>40$
VU0827421		$>40$	VU0827040		$>40$
VU0826483		$16 \pm 2$			

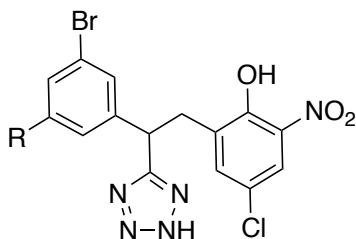
<sup>a</sup>Data displayed is the average of at least 2 independent replicates  $\pm$  standard deviation.

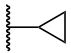
The synthesis of these analogs was simple and followed the route showed **Scheme 13**, since most of the starting aldehydes were commercially available. An exception was compounds **VU0827670** and **VU0827671**. For their synthesis, 3,5-dibromobenzaldehyde was used as the starting material and it was converted to the 2-(3,5-dibromophenyl)acetonitrile, which was then coupled to the respective boronic acid using the conditions shown in **Scheme 14**.

The binding affinity for these analogs is shown in **Table 17**. Groups that were previously identified to be well-tolerated, such as -Cl (**VU0826485**), -SF<sub>5</sub> (**VU0826880**), -cyclopropyl (**VU0827671**), and -*t*-Bu (**VU0826894**) were installed. Unfortunately, none of these groups showed an improvement in binding affinity. Incorporation of a methyl group (**VU0827670**) proved to be a poor binder, per expectation, most likely due to its small size. Replacement of the -OCF<sub>3</sub> with -OCH<sub>3</sub> (**VU0829212**) caused a significant drop in potency; this was not surprising, as the former one is less lipophilic (clogP = 4.33 vs 6.47 respectively). Finally, replacement with a bromine (**VU0827422**) resulted in a compound with a K<sub>d</sub> comparable to that of **VU0825970**.

Further modifications in the right-hand side of **VU0825970** did not show improvement of the binding affinity (data not shown). At this point, we decided to calculate the energies of the bound and unbound conformations of **VU0817326**. We used the software MOE (Molecular Operating Environment) to estimate the difference in energies using the Merck Molecular Force-Field (MMFF94x) parameters. The energy difference found between these two conformations (bound vs unbound, **Figure 27**) was 14.5 Kcal/mol.

**Table 17.** Binding affinity data for analogs with different hydrophobic groups sitting in the  $S_1$  pocket.



Compound	R	$K_d$ ( $\mu\text{M}$ )
VU0825970	-OCF <sub>3</sub>	$8 \pm 4$
VU0826485	-Cl	$12 \pm 2$
VU0826880	-SF <sub>5</sub>	$21 \pm 8$
VU0826894	-C(CH <sub>3</sub> ) <sub>3</sub>	$10 \pm 1$
VU0827671		$10 \pm 1$
VU0827670	-CH <sub>3</sub>	>40
VU0829212	-OCH <sub>3</sub>	$32 \pm 7$
VU0827422	-Br	$8.2 \pm 0.4$

<sup>a</sup> Data displayed is the average of at least 2 independent replicates  $\pm$  standard deviation.

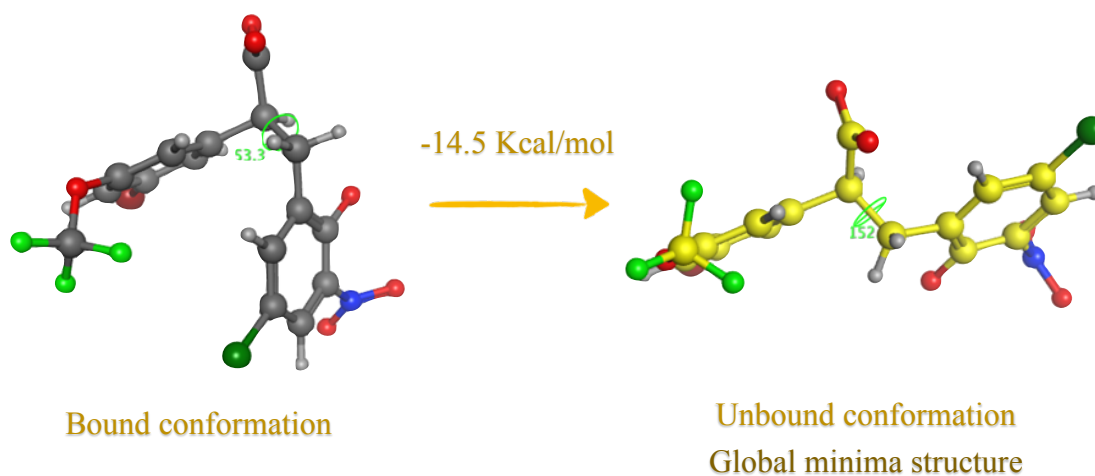
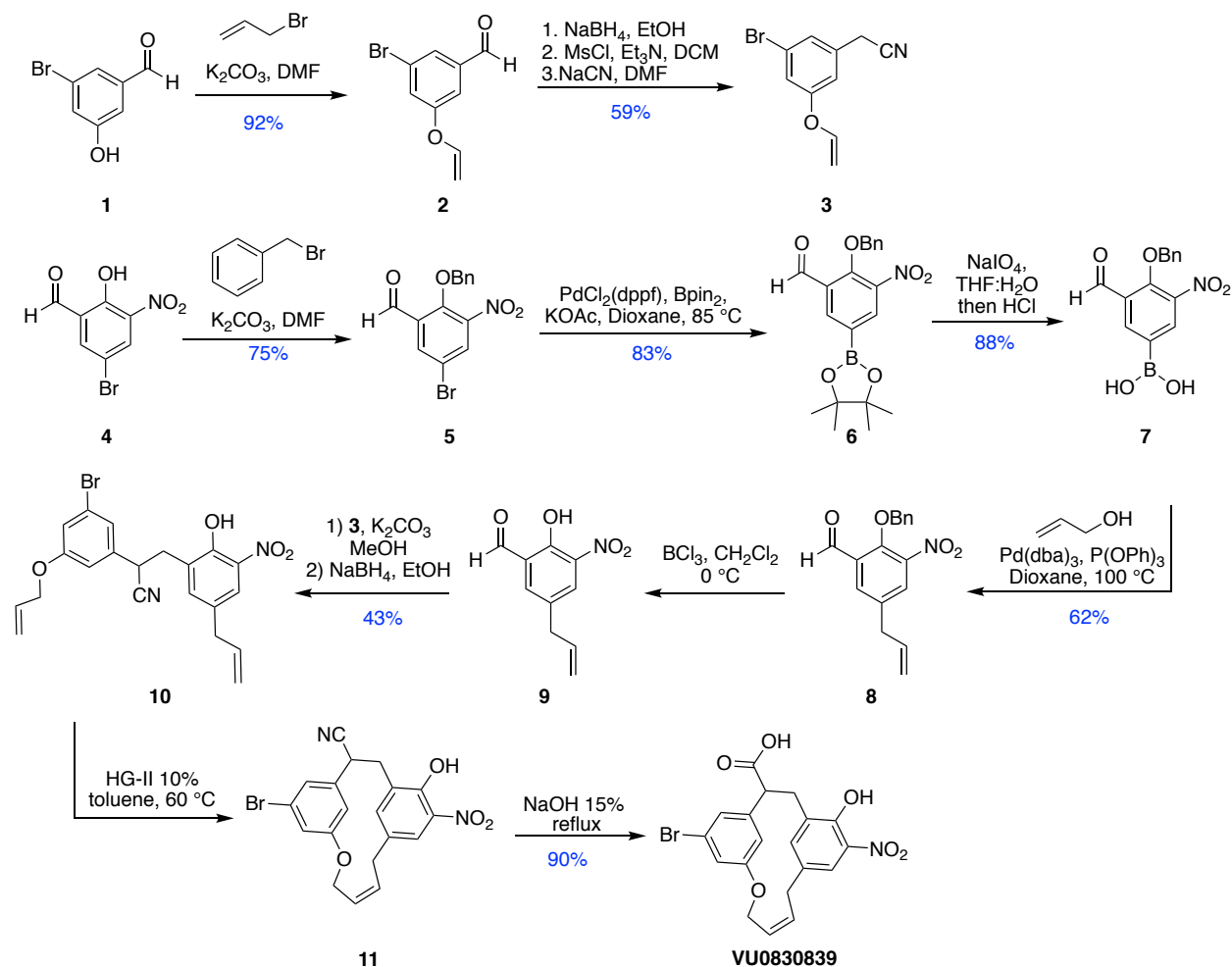


**Figure 27.** Conformational energy difference for VU0817326. Calculated with MOE using MMFF.

In a report, Chen and Foloppe analyzed the conformational energies of 256 drug-like small molecules (publicly available with their X-ray co-crystal structure) using MOE and Catalyst.<sup>253</sup> They reported that for the majority of these compounds there is a  $\leq 3$  Kcal/mol energy difference between the bound state (bioactive conformer) and the unbound state.<sup>253,254</sup> The calculated energy difference between the bound and unbound state for **VU0817326** was  $\sim 5$ -fold higher than the average reported by Chen and Foloppe. Consequently, we decided to “lock” **VU0817326** into its bound and bioactive conformation. Theoretically, an improvement in the binding affinity of a small molecule can be achieved, if the energetic and entropic cost of constraining the molecule is paid at the time of its synthesis. Examples of this strategy have been reported multiple times.<sup>255–258</sup>

We proposed to constrain **VU0817326** by connecting the  $-\text{OCF}_3$  and  $-\text{Cl}$  regions to form a macrocycle. We started by modeling and docking different types of linkers and linker lengths, we found that a 4-carbon unsaturated ether linker was predicted to closely adopt the desired conformation. Thus, we decided to synthesize four compounds with this linker, the synthetic route is shown in **Scheme 15**. The phenol **1** was alkylated with allyl bromide to form **2**, which was then treated as described earlier (**Scheme 13**) to form the acetonitrile intermediate **3**. As a separate piece, the salicylaldehyde **4** was benzyl-protected to form **5**. This intermediate was submitted to a palladium-catalyzed coupling reaction with pinacol ester of diboron ( $\text{Bpin}_2$ ) following the conditions reported by Miyaura *et al*<sup>259</sup> to form **6**. Then, hydrolysis<sup>260</sup> of **6** formed the desired boronic acid **7**, which was subsequently submitted to a Pd-catalyzed cross-coupling with allyl alcohol (as reported by Kayaki *et al*<sup>261</sup>) to furnish **8**. Next, the benzyl protected phenol was treated with  $\text{BCl}_3$  at  $0^\circ\text{C}$  in DCM to produce **9**. The two key pieces, **9** and **3**, were condensed to form the acrylonitrile intermediate. This intermediate was treated with  $\text{NaBH}_4$  to reduce the conjugated double bond (**10**). Afterward, a ring-closing metathesis (RCM) reaction using the 2<sup>nd</sup> Generation

Hoveyda-Grubbs catalyst was used to form **11**. Finally, the nitrile was hydrolyzed to make **VU0830839**, treated with  $\text{NaN}_3$  (same conditions used earlier in this work) to form **VU0830447**, or partially hydrolyzed to form the amide (**VU0830482**).



*Scheme 15. Synthetic route fo macrocyclic compounds.*

The four macrocyclic analogs were tested in the FPA, **Figure 28**. Unfortunately, constraining the compounds with this linker did not improve the binding affinity. Due to the lack of success in the propionic acid series, we decided to no longer pursue this class of compounds.



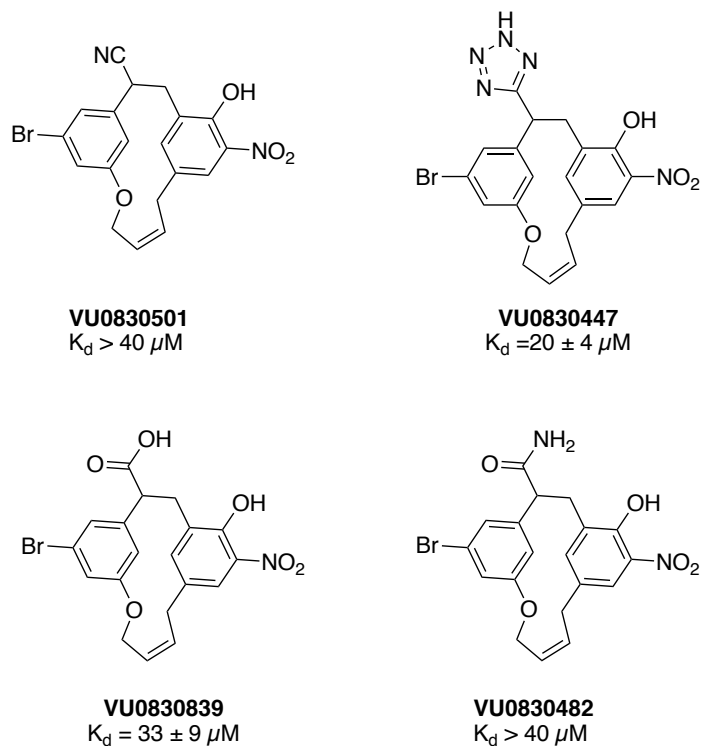


*Figure 28. Macrocyclic analogs and their binding affinity data*

### 3.3 Conclusions

Overall, substitution of the sulfonamide moiety proved to be challenging and deleterious for the binding affinity. Introduction of a benzyl amine linker furnished compounds with binding affinities above the threshold of our FPA ( $> 40 \mu\text{M}$ ). Substitution of the sulfonamide with an amino acetic acid linker introduced chemical instability and discouraged us from pursuing this series. Moreover, the propionic acid series sought to improve the stability of the previous series by removing the amino group. This linker did improve the stability of the compounds and gave rise to a new series of compounds that bind to WDR5 with low micromolar affinities. Optimization of this series was challenging, as most of the modifications worsened the binding affinity. Due to the little success observed during this stage, we calculated the energy difference between the bound and unbound state of **VU0817326**. The high energy difference ( $-14.5 \text{ Kcal/mol}$ ) between the bound and unbound

states suggested that constraining this compound to its bioactive conformation could be beneficial for the binding affinity. However, the synthesis of a macrocyclic version of the propionic acid did not improve the binding affinity to WDR5. It is probable that the linker used to form the macrocycle needs to be optimized in length and chemical character; however, we opted for finding alternative ways to improve the physicochemical properties of the biaryl sulfonamide series.

## Chapter IV

Discovery of WDR5-MYC inhibitors using fragment-based methods and structure-based design

This chapter is based on the paper: “Discovery of WD Repeat-Containing Protein 5 (WDR5)-MYC inhibitors using fragment-based methods and structure-based design”, which has been revised and resubmitted to Journal of Medicinal Chemistry.

### 4.1 Introduction

We have previously reported the first small molecules that bind to the WBM site of WDR5.<sup>231</sup> These salicylic acid-based compounds, discovered from structure-based optimization of a high-throughput screening hit (**VU0618016**), are capable of demonstrating low nanomolar affinity for WDR5 and potent inhibition of histone methyltransferase activity. In addition to inhibiting MYC binding to WDR5 in the biochemical assays, these compounds can inhibit the WDR5-MYC interaction in cellular lysates. However, these bi-aryl sulfonamide series have challenging physicochemical profiles. Multiple subseries of compounds (including acid, amide, and sulfone variants) exhibit very low  $F_u$ , and many of the most potent examples contain multiple phenols that may be prone to glucuronidation or other metabolism.<sup>243,244</sup> To identify additional chemical matter that may aid in the discovery of compounds with improved properties, we conducted an NMR-based fragment screen.<sup>262,263</sup> By merging a fragment hit with the compounds previously reported using structure-guided-design, we have developed a new subseries of compounds that display high nanomolar binding affinity to WDR5. Overall, the compounds in this series showcase improved drug-like properties, and several of them are capable of disrupting the WDR5-MYC interaction in

cell lysates. The best-in-class compound disrupts the WDR5-MYC interaction in whole cells and decreases the amount of MYC at genes requiring WDR5 while leaving MYC levels close to normal at genes where recruitment of MYC is independent of WDR5. Thus, the best-in-class compound can be used as a chemical probe to study the implications of disrupting the interaction between WDR5 and MYC in cells.

#### 4.2 Hit Identification from NMR-based fragment screening

The HMQC spectrum of uniformly  $^{15}\text{N}$ -labeled WDR5 in complex with unlabeled MYC ‘MbIIIb’ peptide was obtained, showing peak shifts in specific regions (**Figure 29A**). Our 13,824-compound fragment library was screened against WDR5 (aa. 23-334) using SOFAST  $^1\text{H}$ - $^{15}\text{N}$  HMQC, collecting the HMQC spectra of  $^{15}\text{N}$ -labeled WDR5 protein in the presence of mixtures of 12 fragments. Fragment mixtures that caused similar peak shifts as the unlabeled MYC peptide were identified as WBM site hits. Deconvolution of the mixtures containing such hits was accomplished by individual assessment of the compounds from each hit pool (**Figure 29B**); thus, identifying 43 hits (0.32% hit rate). Several of the hits that induced large chemical shift perturbations were selected for affinity determination by NMR titration. However, they all showed relatively weak binding, and did not achieve saturable binding at concentrations up to 2 mM, preventing the determination of an accurate  $K_d$ .

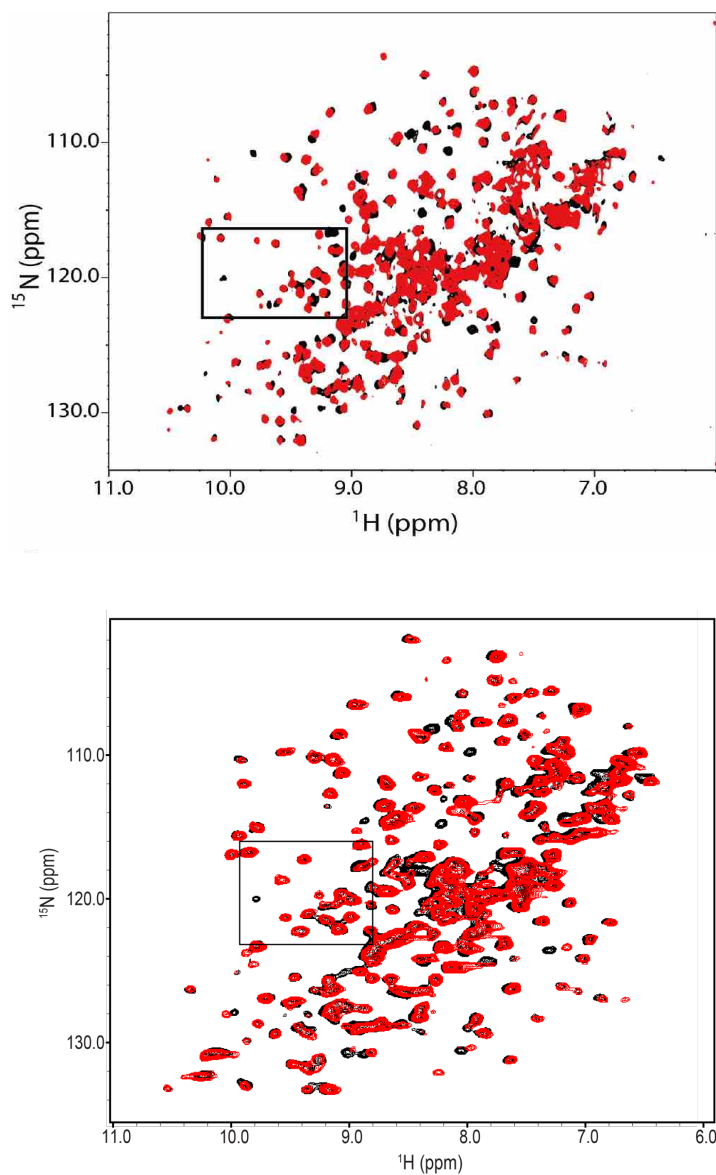


**Figure 29.** A) Overlay of the HMQC spectra of apo-WDR5 (black) and WDR5 with unlabeled MYC peptide (red). B) Overlay of HMQC spectra of apo-WDR5 (black) and WDR5 with MYC site fragment hit F2 (red). The shifts upon ligand (peptide or hit) binding are indicated.

A survey of the chemical structures of the fragment hits reveals some structural diversity; representative fragment hits **F1-8** are shown in **Figure 30**. The 10-mer MYC peptide contains hydrophobic residues flanking multiple acidic amino acids, with Lys and Arg residues around this

hydrophobic cleft. The known native substrate(s) of this site (C-MYC, RBBP5, KANSL2) have previously been shown to have a structurally similar motif (IDVV, VDVT, LDVV respectively).<sup>23</sup> Likewise, we observed that the vast majority of the fragment hits contain an acidic functionality coupled to a hydrophobic motif.

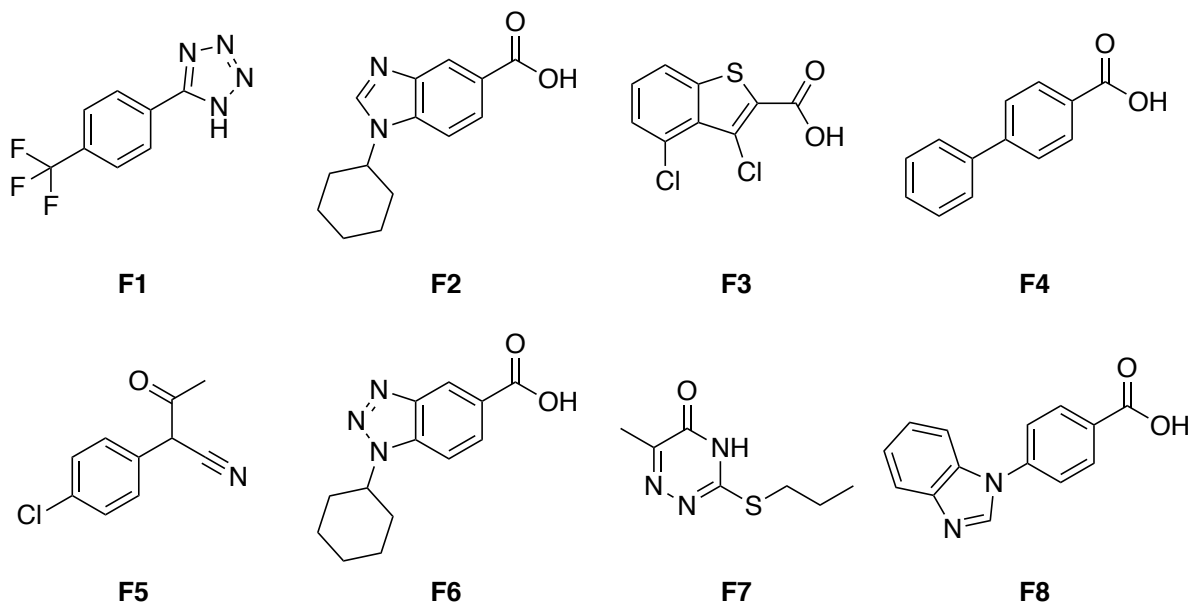


**Figure 30.** Representative MYC site fragment hits. Those with the largest chemical shift perturbations are marked as ‘top hits’

### 4.3 Structure determination of the fragment complexes

Five X-ray co-crystal structures of fragments bound to WDR5 (**F1**, **2**, **5**, **6**, and **7**) were determined using co-crystallization and soaking methods (**Figure 31**). These co-crystal structures confirm the HMQC-indicated binding to the WBM site. However, the fragments are observed to occupy different parts of this cleft. **F1**, **F2**, and **F6** bind to a pocket corresponding to that occupied by the Ile residue (herein designated as  $S_1$ ) of the conserved MYC WBM binding sequence (Figure 31A)

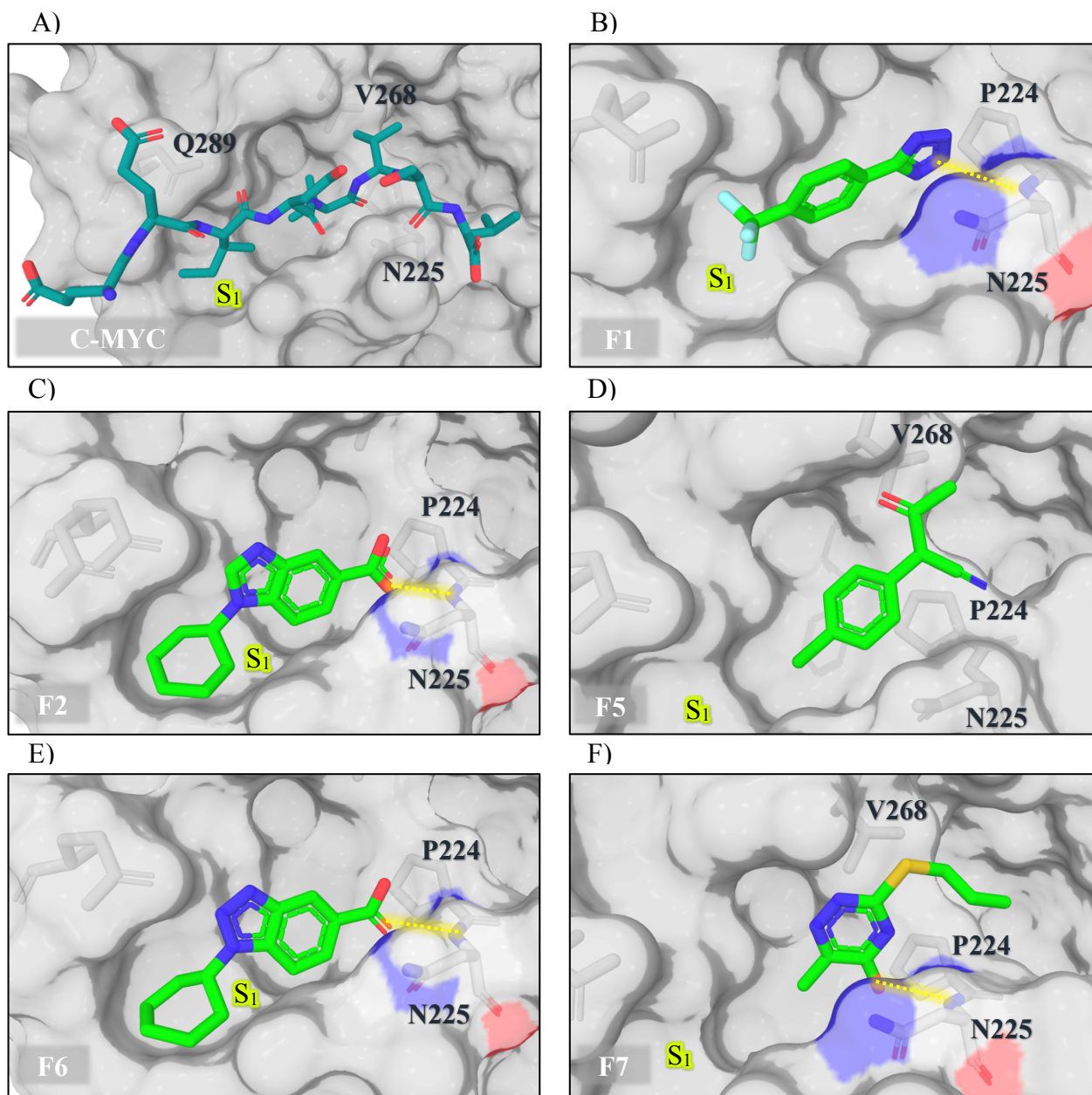


**Figure 31.** X-ray structures of WDR5 in complex with the c-MYC peptide and fragment hits. A) MYC peptide, PDB: 4Y7R; B) F1 (PDB: 6UJJ); C) F2 (PDB: 6UHY); D) F5 (PDB: 6UJH); E) F6 (PDB: 6UHZ); F) F7 (PDB: 6UJL). WDR5 is displayed as the surface model, with the WBM site centered.

and engage the amide group of N225 through an H-bond. The cyclohexyl group of **F2** and **F6** fits into this hydrophobic groove very well, and establishes hydrophobic contacts with a Leu residue of WDR5. The trifluoromethyl group of **F1** occupies the same region (**Figure 31****Figure 31B, C, and E**). In contrast, **F5** and **F7** bind to a different part of the binding cleft. While **F7** retains the hydrogen bond with the amide group of N225, both **F5** and **F7** make hydrophobic contacts with the Val-binding shelf of the pocket (designated as S<sub>4</sub>), mimicking the IDVV conserved sequence. These two fragments make contacts with the loop region of WDR5, directed towards the central core of the protein that has not been demonstrated to be involved in MYC binding (**Figure 31D and F**).

#### 4.3. Compound design

Linking together two fragments bound in close proximity to one another in a protein is a proven strategy that can dramatically improve binding affinity.<sup>264,265</sup> However, analysis of the X-ray co-crystal structures of the different fragment hits did not directly reveal an obvious opportunity to merge or link multiple fragments. Conversely, the overlay of the co-crystal structures of **F2** with WDR5 and the previously reported biaryl sulfonamide, **VU0618016**, which was obtained from our HTS campaign (**Figure 32C and 32B**) showed that merging this chemical matter may represent a viable path forward (**Figure 32C**). The phenyl carboxylic acid of **F2** interacts with Asn225 in a manner highly similar to the sulfonamide of **VU0618016**, and provides a conformation able to the S<sub>4</sub> pocket of the WBM binding site. Retention of the bromide-containing aryl group of **VU0618016** was desired, as it should allow a halogen bond interaction between the bromine and the carbonyl group from Trp273. This was demonstrated to be a key binding interaction in the previously reported series.<sup>231</sup> An additional consideration when designing the merged compound was the location of the *N*-substituent of the imidazole ring. The overlapped atoms (**Figure 32C**) show that



the amine could be placed at the position corresponding to either C-4 or C-5 of the imidazole. We designed the compounds with the amine at C-4, due to anticipation of a better angle to fill the S<sub>1</sub> pocket and easier of synthesis.

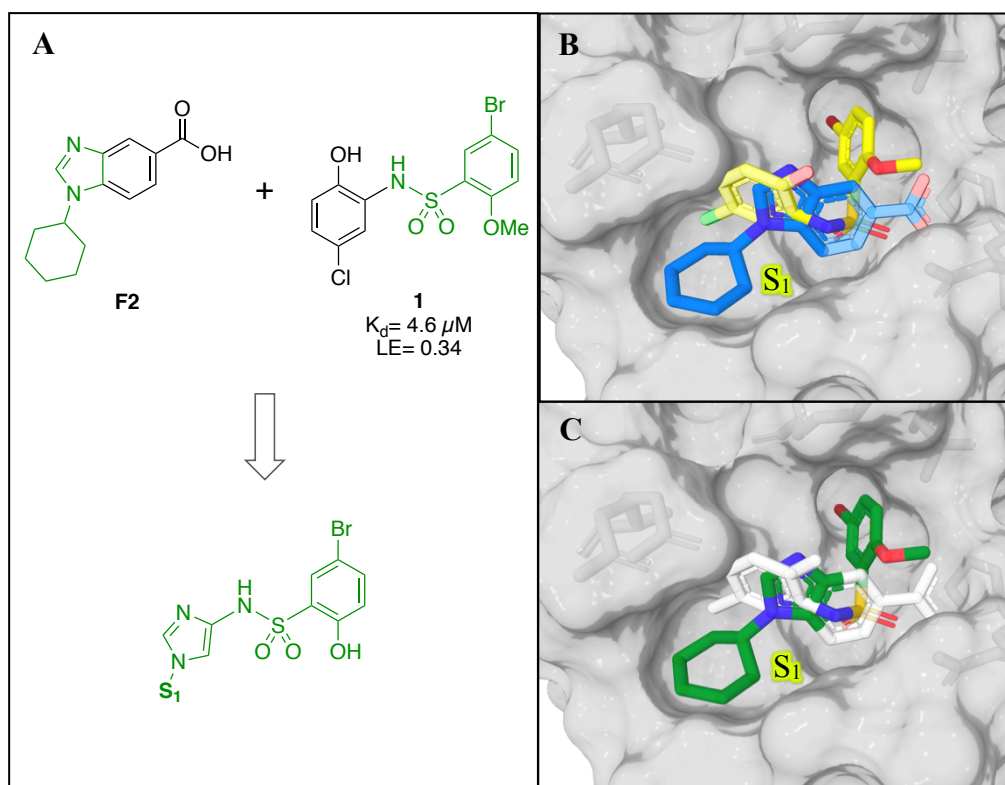


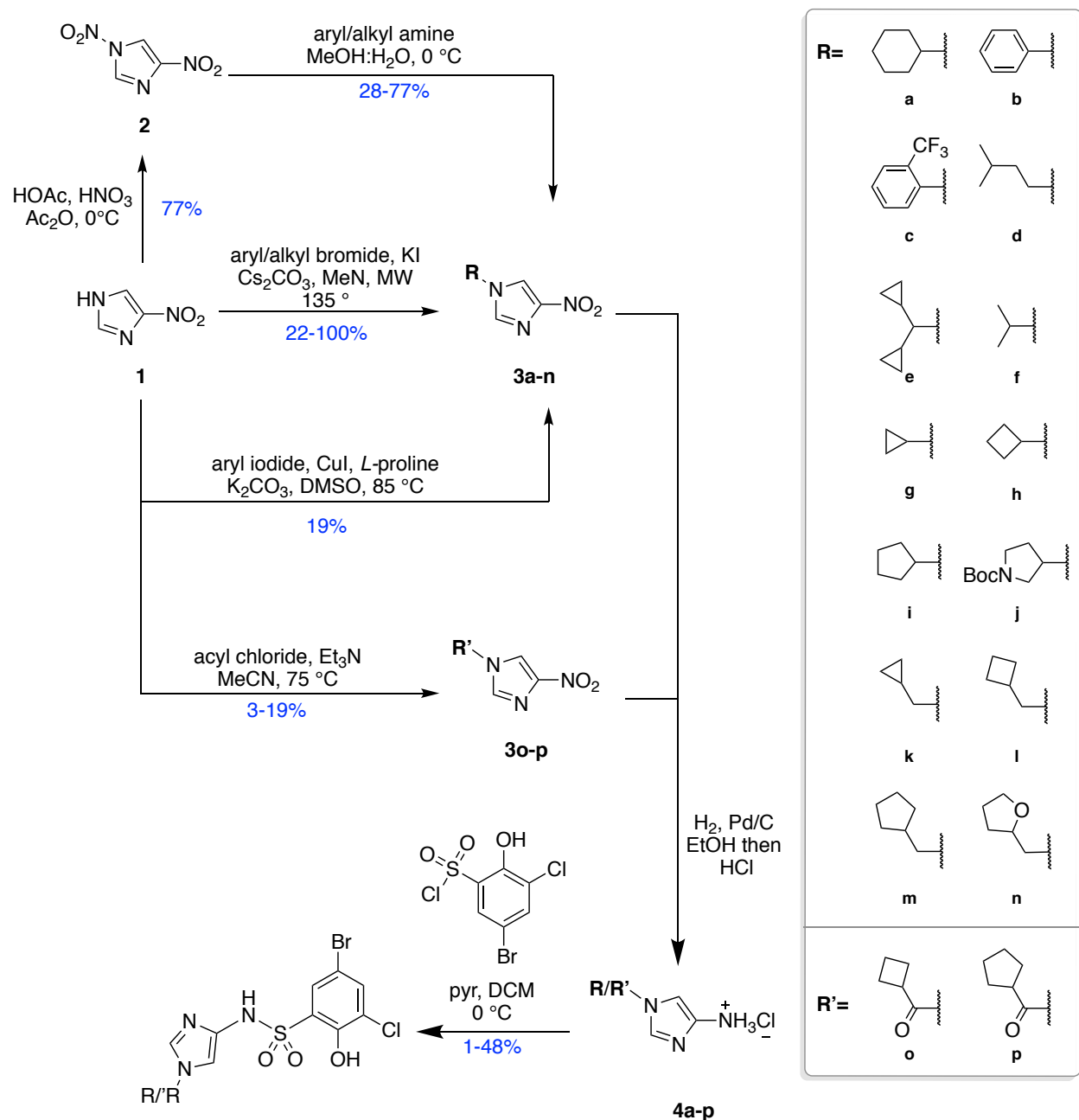
**Figure 32.** Merging strategy. *A)* Merging the previously reported HTS hit **VU0618016** with **F2** results in a new class of compounds. *B)* X-ray co-crystal structure of **F2** bound to WDR5 (blue) and overlaid with **VU0618016** (yellow). *C)* Atoms from **F2** and **VU0618016** to be merged are colored in green.

#### 4.3.1 *N*-substituted imidazolyl analogues.

The synthesis of fragment-merged compounds with different *N*-substituents on the imidazole ring started from the commercially available 4-nitro-1*H*-imidazole, **1** (Scheme 16). Treatment with

base and the desired bromoalkene at 135 °C in a microwave reactor gave the compounds **3a**, **3d**, **3f**, **3h-n**. Bulky haloalkenes exhibited very low yields or did not react using these conditions. Therefore, compounds **3c**, **3e**, **3g** were synthesized using the ANRORC reaction (Addition of Nucleophile, Ring Opening, and Ring Closure).<sup>266</sup> First, 4-nitro-1*H*-imidazole was nitrated to form **2**, and subsequent addition of the desired amine or aniline (**c**, **e**, or **g**) furnished **3c**, **3e**, **3g**. An Ullman-type coupling was used to synthesize **3b**, and acylation of **1** with cyclobutanecarbonyl chloride or cyclopentanecarbonyl chloride allowed the synthesis of **3p** and **3o**, respectively. The *N*-substituted-4-nitroimidazoles were hydrogenated using heterogeneous catalysis (Pd/C); the addition of 3 M aqueous HCl was required to help stabilize the compounds **4a-p**. The crude hydrogenation products were reacted with 5-bromo-3-chloro-2-hydroxybenzenesulfonyl chloride, and the sulfonamides analogues (**Scheme 16**) were isolated with poor yields. Partial hydrogenation of some 4-nitroimidazole intermediates or decomposition of the aminium chlorides contributed to low yields observed within this series.

Evaluation of the initial merged compound **VU0830015** (**Table 18**) in the FPA showed a binding affinity of  $1.00 \pm 0.28 \mu\text{M}$ , representing a several hundred-fold improvement from the fragment **F2** (from which we were unable to ascertain an accurate  $K_d$  via this FPA protocol) and a 5-fold improvement from **VU0618016** ( $K_d = 4.7 \pm 1.6 \mu\text{M}$ ). We were highly encouraged by this initial success of the fragment-merging design strategy. To optimize the binding affinity of the merged compound, a survey of hydrophobic substituents, including different sizes of carbocycles, as well as various alkyl and acyl groups, were installed at the *N*-1 of the imidazole ring (**Table 18**).



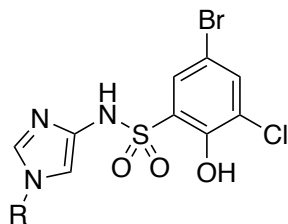
*Scheme 16. Synthesis of N-substituted fragment-based compounds.*

Inspired by other fragment hits (SF-9, see **Appendix A**), a phenyl ring was installed (**VU0831903**), which could potentially generate multiple new vectors for optimization of the compounds. However, **VU0831903** showed reduced affinity, perhaps due to a planar relationship with the imidazole ring. An *ortho*-substituted aryl ring (**VU0848349**) was also explored to induce a twist

in the angle between the rings and to better occupy the pocket. Unfortunately, this was also detrimental to the binding affinity. Previous success was observed with small, cyclic alkyl groups in  $S_1$ .<sup>231</sup> Indeed, flexible, linear chains are not well tolerated in this series (**VU0848258**), and larger groups like dicyclopropylmethane (**VU0848325**) also proved to be deleterious for binding affinity. The better fit of the cyclohexyl group in the  $S_1$  pocket encouraged the study of other acyclic and saturated groups. Smaller substituents, like cyclopropyl (**VU0831899**) and isopropyl (**VU0849775**), appear to not efficiently fill the pocket, as evidenced by the reduced binding affinity to WDR5. Cycloalkanes somewhat smaller than cyclohexane, such as cyclobutane (**VU0829725**) and cyclopentane (**VU0829217**), did show a 2.5-fold improvement in the binding affinity compared to **VU0830015**. We also sought to introduce solvent-facing polarity into the compounds by replacing the lipophilic cyclopentyl ring. However, the pyrrolidine of **VU0850576** was not tolerated. Likewise, the introduction of a methylene spacer between the imidazole and the cycloalkane (**VU0831928**, **VU0848297**, **VU0848300**, and **VU0848319**) was detrimental for binding affinity. We also introduced acyl groups near the  $S_1$  pocket to possibly engage Q289 with a hydrogen bond; however, **VU0831889** and **VU0831900** were very weak binders.

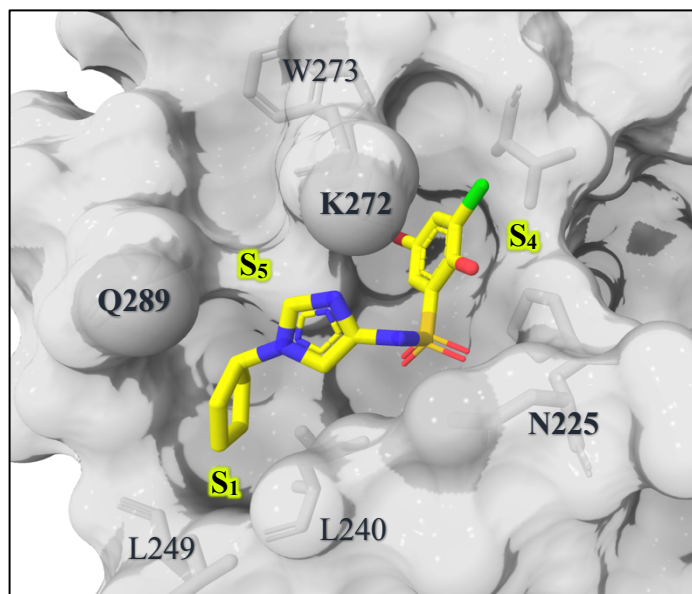
We were able to obtain an X-ray structure of compound **VU0829217** bound to WDR5 (**Figure 33**). As anticipated, the compound forms a hydrogen bond to the NH of Asn225 and a halogen bond to the carbonyl of Trp273. Notably, the X-ray crystal structure also shows a putative interaction between the imidazole nitrogen and the side chain amine of Lys272. The cyclopentyl group sits in the hydrophobic pocket designated as  $S_1$  (**Figure 33**), which is partly formed from the hydrophobic side chains of Leu240, Leu249, and Leu288. In addition, examination of this X-ray co-crystal structure reveals an additional opening ( $S_5$ ) in close proximity to the compound, caused by the side-chain rotation of K272 and Q289.

Table 18. SAR of substituents at N-1 of the imidazole ring



Compound	R	K <sub>d</sub> (μM)	Compound	R	K <sub>d</sub> (μM)
VU0830015		1.0 ± 0.3	VU0829217		0.4 ± 0.1
VU0831903		3.2 ± 0.5	VU0850576		11 ± 3
VU0848349		4.0 ± 0.7	VU0831928		2.1 ± 0.7
VU0848258		5.2 ± 0.9	VU0848297		4.5 ± 0.8
VU0848325		1.2 ± 0.2	VU0848300		3.4 ± 0.7
VU0849775		5.5 ± 0.7	VU0848319		8 ± 2
VU0831899		4.0 ± 0.6	VU0831889		38 ± 3
VU0829725		0.4 ± 0.1	VU0831900		>40

\*Data displayed is the average of at least 3 independent replicates ± standard deviation.



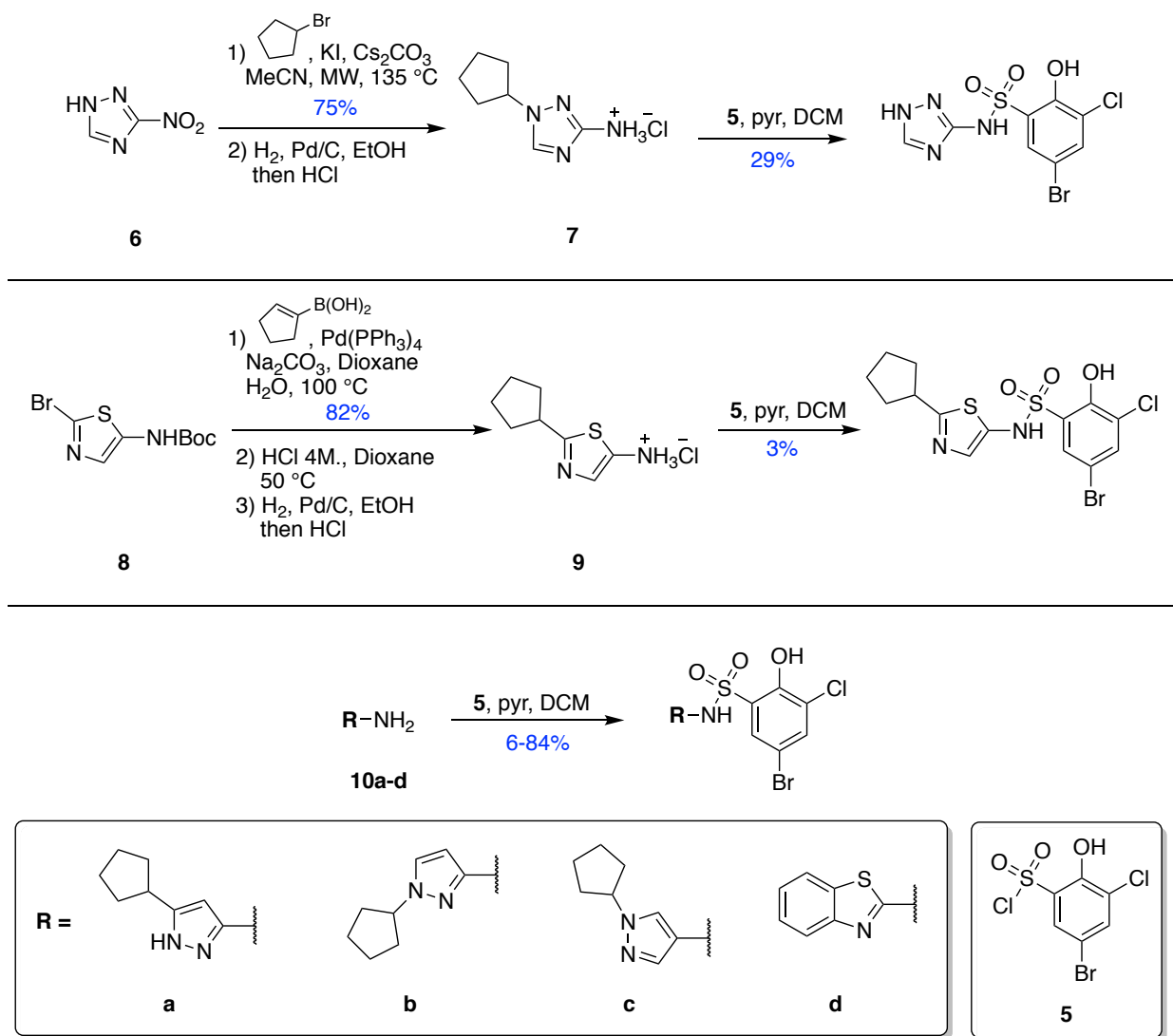
*Figure 33. X-ray co-crystal structure of compound VU0829217.*

#### 4.3.2 Analogs with alternative heterocycles

Having established preferences for the hydrophobic group at S<sub>1</sub>, we transitioned to examining various heterocyclic alternatives to the imidazole ring. The heterocyclic compounds shown in **Table 19** were synthesized by routes analogous to those used for the imidazoles (**Scheme 17**). The 1,2,4,-triazole **6** was first alkylated with bromocyclopentane and the intermediate was submitted to hydrogenation with addition of 3 M aqueous HCl to produce the aminium chloride **7**. Reaction with **5** allowed the synthesis of the sulfonamide **VU0849230**. Compounds **VU0849779**, **VU0849818**, **VU0849822**, and **VU0849477** were synthesized by coupling the commercially available amine or aminium chloride (**10b-e**) with **5**. Analog **VU0849922** required a Suzuki coupling between *tert*-butyl (2-bromothiazol-5-yl)carbamate and cyclopent-1-en-ylboronic acid to produce *tert*-butyl (2-(cyclopent-1-en-1-yl)thiazol-5-yl)carbamate. This intermediate was then deprotected using 4 M HCl in dioxane. The aminium chloride salt was used to avoid poisoning of

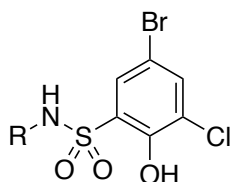
the catalyst in the hydrogenation step. Finally, **9** was reacted with the sulfonyl chloride **5** to give the desired product.

A 1,2,4-triazole ring (**VU0849230**) demonstrated that a third nitrogen atom was disadvantageous in this pocket, as shown by a ~16-fold decrease in binding affinity relative to **VU0829217**. Based on the X-ray crystal structure of **VU0829217**, one of the nitrogen atoms of **VU0849230** is most likely pointing towards the hydrophobic region, explaining this significant loss of affinity.



*Scheme 17. Synthetic routes for the different heterocyclic analogs.*

Table 19. FPA binding data for different heterocyclic analogs



Compound	R	K <sub>d</sub> (μM)	Compound	R	K <sub>d</sub> (μM)
VU0829217		0.4 ± 0.1	VU0830054		0.0983 ± 0.0006
VU0849230		6.5 ± 0.8	VU0830049		0.19 ± 0.06
VU0849779		10 ± 1	VU0830052		1.4 ± 0.3
VU0849819		2.8 ± 0.4	VU0849477		23 ± 18
VU0849822		0.5 ± 0.1	VU0849651		2.2 ± 0.4
VU0849922		0.6 ± 0.1	VU0849648		0.4 ± 0.1

\*Data displayed is the average of at least 3 independent replicates ± standard deviation.

Incorporation of pyrazole rings allowed us to walk the nitrogen atoms around the ring (VU0849779, VU0849819, VU0849822). The regioisomers VU0849779 and VU0849819 did not improve the binding affinity, indicating that the angles and/or the nitrogen distribution were not favorable. On the other hand, analog VU0849822 showed affinity comparable to VU0829217.

Interestingly, analogs of VU0849779 showed higher binding affinity (VU0830054, VU0830049 and VU0830052). Since only three analogs were synthesized, there is not a clear trend; however,



it appears that smaller and more compact hydrophobic groups sitting in the S<sub>1</sub> pocket improve the binding affinity. The X-ray co-crystal structure of **VU0830052** (Figure 34A) shows that it binds to WDR5 with a binding pose similar to of the imidazole **VU0829217** (Figure 34B). It also shows that one of the nitrogens of the pyrazole ring points towards the S<sub>5</sub> pocket. Optimization of the pyrazole subseries has not yet been pursued, we think that incorporation of different groups at the -NH might improve the binding affinity of these analogs.

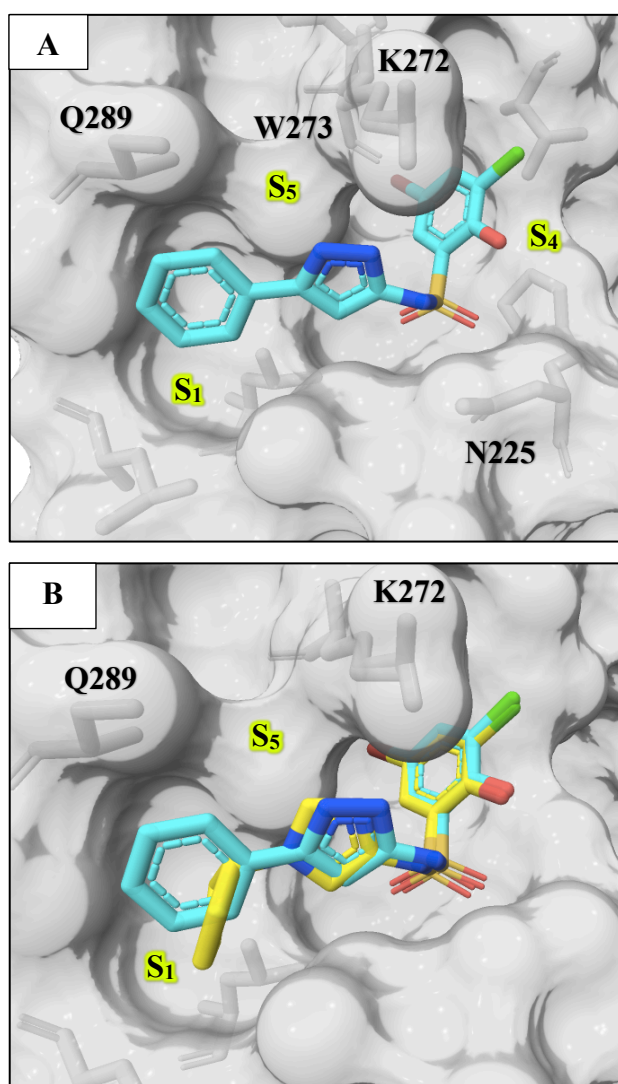


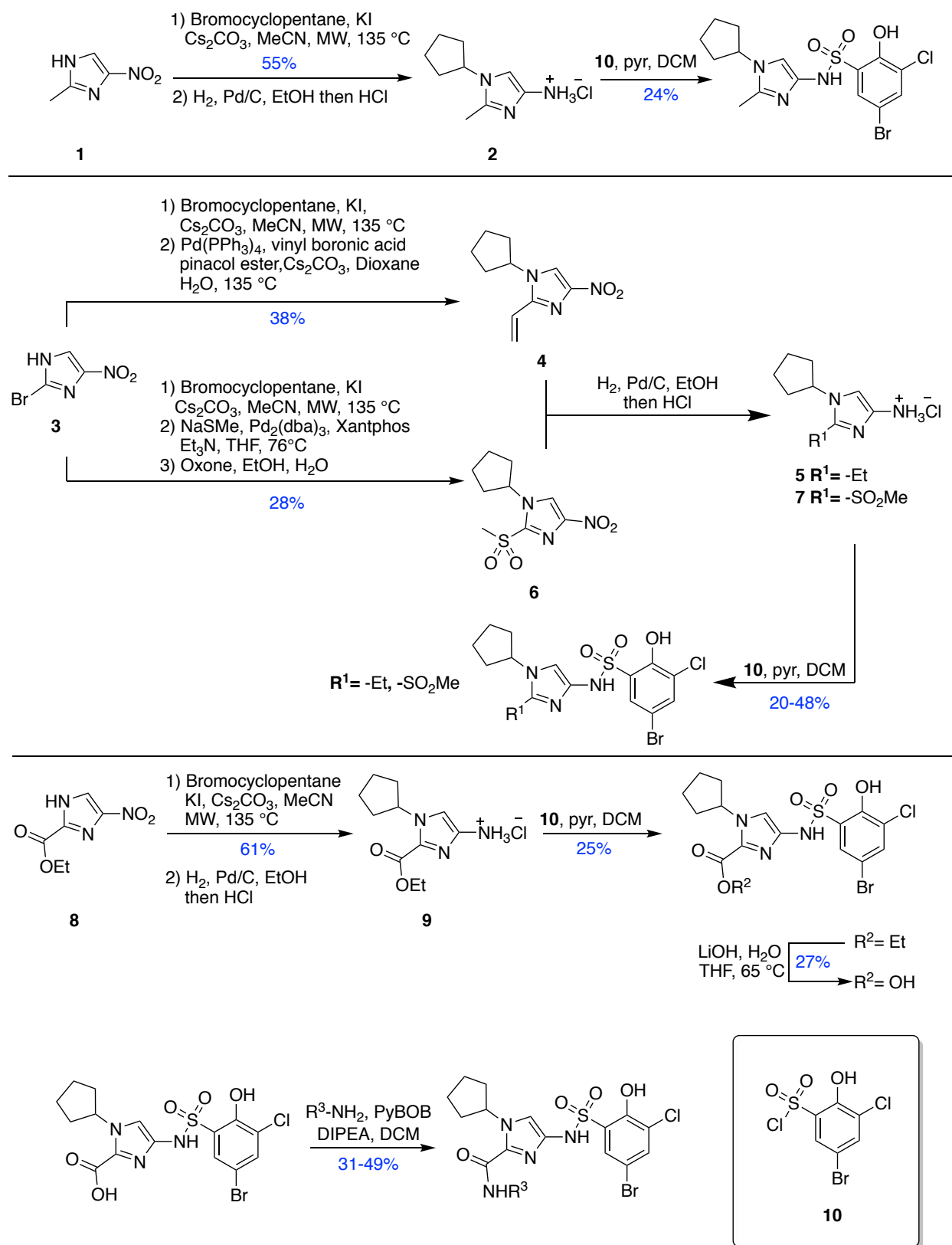
**Figure 34.** A) X-ray co-crystal structure of **VU0830052** bound to WDR5, B) Overlay of the X-ray crystal structure of **VU0829217** and **VU0830052**.

Furthermore, the thiazole **VU0849477** was also tolerated, with only a 1.6-fold decrease in binding affinity relative to **VU0829217**. Finally, the larger and more lipophilic benzothiazole **VU0849477** (AlogP = 4.1, compared to AlogP = 3.5 for **VU0829217**); was not tolerated. A small survey of different substitutions around the benzothiazole (commercially available) generated compounds with  $K_d$  values greater than 3  $\mu$ M. Thiazoles **VU0849651** and **VU0849648** were exceptions, with the last one showing potency similar to **VU0829217**. These benzothiazole analogs were not further studied. Based on this SAR, we decided to retain the imidazole to continue the SAR study as it provides easier and direct access to the  $S_5$  cleft.

#### 4.3.3 Growing towards the $S_5$ pocket

We hypothesized that occupation of the  $S_5$  pocket might lead to further increases in affinity, and C2 of the imidazole ring appears to offer an opportunity to explore this area. Therefore, we synthesized compounds with different groups in the C2 of the imidazole.

The analogs with substituents in the C-2 of the imidazole ring were synthesized using multiple approaches, **Scheme 18**. The synthesis of **VU0848182** started with 5-methyl-4-nitroimidazole **11**, which was *N*-alkylated with bromocyclopentane and then reduced to the aminium chloride **12**. The desired sulfonamide was obtained by reacting **12** with **5**. Compound **VU0848212** was synthesized by *N*-alkylating 2-bromo-4-nitro-1*H*-imidazole (**13**), and coupling it with vinyl boronic pinacol ester using Suzuki conditions (**14**). Hydrogenation of the alkene and nitro groups was achieved in the same step (**15**). Finally, reacting **15** with **5** formed the sulfonamide. Installation of the sulfone group to generate **VU0830838** started with *N*-alkylation of **13**, followed by a palladium-catalyzed cross-coupling of 2-bromo-1-cyclopentyl-4-nitro-1*H*-imidazole with sodium methanethiolate. 1-Cyclopentyl-2-(methylthio)-4-nitro-1*H*-imidazole was oxidized using Oxone in EtOH:H<sub>2</sub>O to give

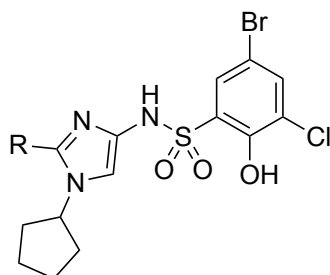


*Scheme 18. Synthesis of compounds with substitutions in C-2 of the imidazole ring.*

**16**. The intermediate **17** was accessible by close monitoring of the hydrogenation step; the reaction was stopped after 10-15 min as longer reaction times generated multiple by-products (not-characterized) and disappearance of the desired aminium chloride. The reaction of **5** with **17** allowed the formation of **VU0830838**. Finally, the synthesis of compounds **VU0850262**, **VU0850263**, **VU0850264**, **VU0857304**, **VU0857305**, and **VU0857306** followed a similar route, in which **18** was *N*-alkylated, reduced (**19**) and reacted with **5** to produce **VU0850262**. Hydrolysis using basic conditions allowed the isolation of **VU0850263**, and PyBOP (or HATU) mediated coupling of the acid with the desired amine furnished **VU0850264**, **VU0857304**, **VU0857305**, and **VU0857306** after Boc-deprotection when required.

Small groups like methyl (**VU0848182**) and ethyl (**VU0848212**) were incorporated onto C-2 of the imidazole (**Table 20**). Assessment by FPA showed that these substitutions are well tolerated. To further guide compound optimization, **VU0848182** was co-crystallized with WDR5 and the X-ray structure (**Figure 35A**) confirmed that the methyl group points towards the S<sub>5</sub> region. and suggested that larger and extended linear groups may also be tolerated. Therefore, we proposed that larger and extended linear groups may also be tolerated. An overlay of the crystal structures of **VU0848182** and **VU0829711** further suggests that incorporation of an amide could allow an additional option to reach to the S<sub>5</sub> pocket. (**Figure 35B**). Compounds **VU0850262**, **VU0850263**, and **VU0850264** were synthesized to test this idea. Interestingly, the ester and the methyl amide bound better than the acid; this is the opposite observations compared to the bi-aryl sulfonamide series. We were encouraged to design and synthesize three amide analogs (**VU0857304**, **VU0857305**, and **VU0857306**) with the intention to occupy the S<sub>5</sub> region. Unfortunately, the FPA data for these three analogs showed a considerable reduction of the binding affinity.

**Table 20.** FPA binding data for compounds substituted in the C-2 of the imidazole ring.



Compound	R	K <sub>d</sub> (μM)	Compound	R	K <sub>d</sub> (μM)
VU0848182	Me	0.17 ± 0.04	VU0857304		5 ± 1
VU0848212	Et	0.22 ± 0.08	VU0857305		1.1 ± 0.1
VU0850262		0.11 ± 0.03	VU0857306		2.3 ± 0.5
VU0850263		0.7 ± 0.2	VU0830838		0.10 ± 0.01
VU0850264		0.17 ± 0.03			

\*Data displayed is the average of at least 3 independent replicates ± standard deviation.

The analog **VU0850264** was co-crystallized with WDR5 to help understand the cause of potency loss upon introduction of larger groups (**Figure 35C**). The crystal structure revealed that the access to S<sub>5</sub> was blocked by the Q289 side chain, which rotates to engage in a hydrogen bond interaction with the carbonyl oxygen of the methyl amide of **VU0850264**, in a similar manner to our previously published compounds. As a consequence of establishing this hydrogen bond, the methyl amide is forced to point towards the solvent rather than along the targeted shelf of the protein. The

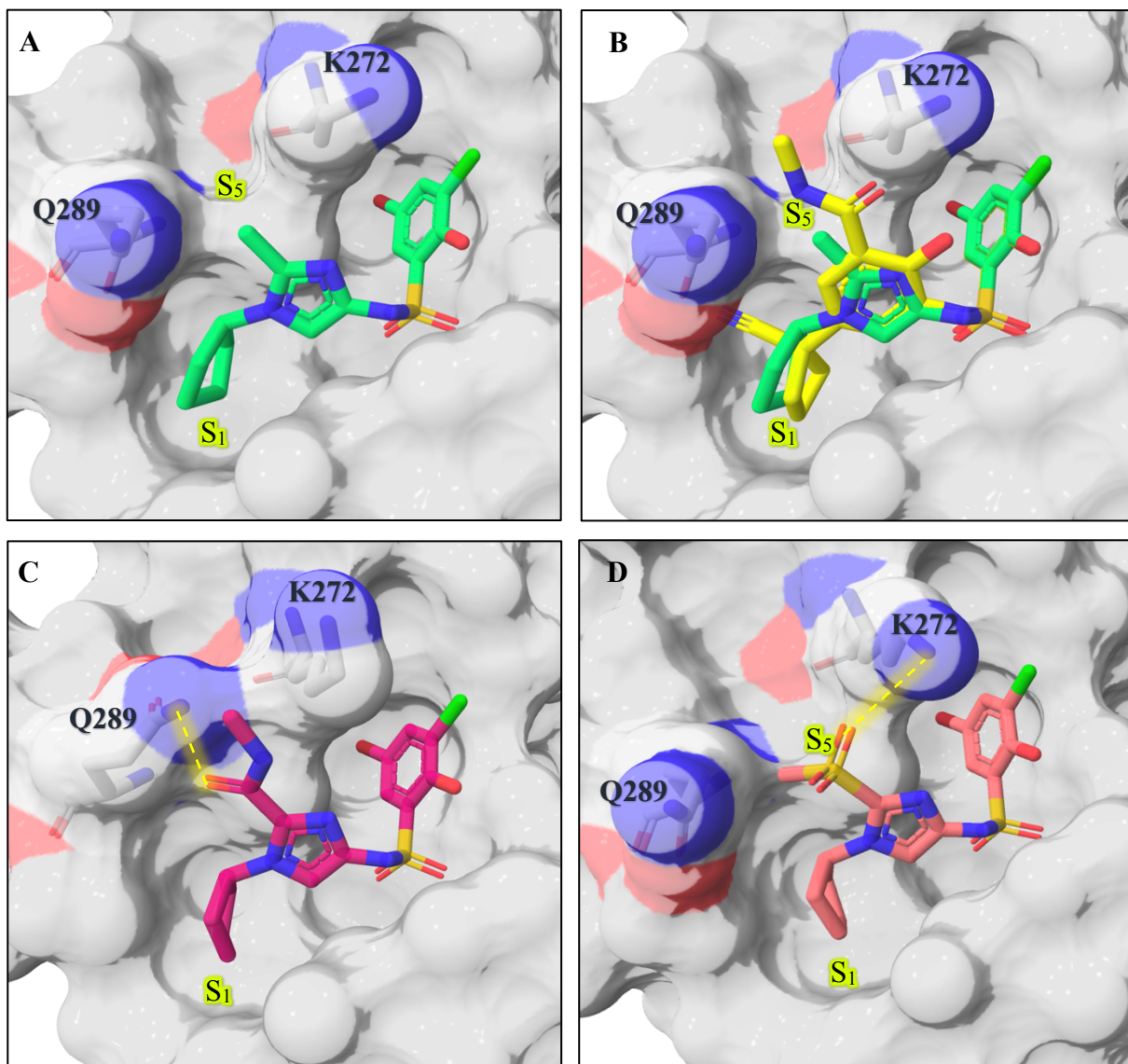


**Figure 35.** A) X-ray co-crystal structure of *VU0848182* (green) bound to *WDR5*. B) Overlay of compound *VU0848182* and *VU0829711* (yellow). C) X-ray co-crystal structure of *VU0850264* (magenta) bound to *WDR5*. D) X-ray co-crystal structure of *VU0830838* (salmon) bound to *WDR5*.

lack of improvement in binding affinity in **VU0857304**, **VU857305**, and **VU0857306** can be explained by a blocked access to the  $S_5$  region, and the loss in binding affinity might be related to

secondary amines not being tolerated lacking a hydrogen that could form an intramolecular H-bond with the imidazole nitrogen.

The fragment screening allowed the identification of new chemical matter that improved the WDR5-MYC inhibitors. The compounds shown here are weaker binders relative to the best biaryl sulfonamide analogs; however, they have the potential to display improved drug-like characteristics. While we did not succeed in significantly improving the  $F_u$  (**Table 21**), we were able to accomplish one of the other goals of the effort, the deletion of one of the phenols, which may represent potential metabolic liabilities.

*Table 21. Pharmaceutical property profile of selected compounds.<sup>a</sup>*

Compound	Solubility ( $\mu\text{M}$ )	MDCK A-B $P_{\text{app}}$ ( $10^6/\text{s}$ )	$F_u$ (%)
<b>VU0849822</b>	>100	57.6	<0.0005
<b>VU0850262</b>	>100	23.9	<0.0002
<b>VU0850264</b>	>100	23.2	< 0.0005
<b>VU0830838</b>	>100	12.0	<0.0005

<sup>a</sup> All experiments performed at Q<sup>2</sup> Solutions Ltd.

Moreover, we removed the phenol in the aryl ring by synthesizing analogs with 6-bromoquinoline-8-sulfonamides (e.g. **VU0849106**, **Figure 36**) or by masking it as a methoxy (e.g. **VU0849117**, **Figure 36**); nonetheless, all of them were shown to be inactive.

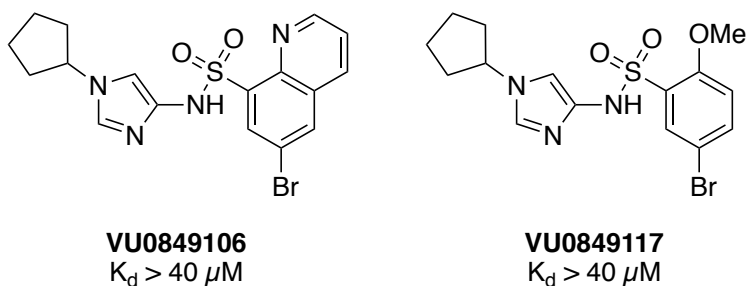


*Figure 36. Fragment-inspired compounds without phenols.*

#### 4.4 Determination of target engagement

##### 4.4.1 Confirmation of target engagement in cell lysates and whole cells

A collection of eight compounds were assayed in cell lysates of HEK293 (engineered to overexpress HA-tagged c-MYC and Flag-tagged WDR5)<sup>231</sup> to determine whether they could disrupt the interaction between WDR5 and MYC at the protein level. Cell lysates were treated with 50  $\mu\text{M}$  of compound and WDR5 was immunoprecipitated (**Figure 37**). Most of the compounds tested disrupt this interaction (**VU0830838**, **VU0850262**, **VU0850264**, **VU0848212**, **VU0829217**, and **VU0849922**), the thiazole **VU0849922** shows no demonstrable effect. The limited disruption shown by the amide was an unexpected result, as its binding affinity is superior ( $K_d = 0.17 \mu\text{M}$ ) to other compounds that did show disruption of the interaction, such as **VU0829217** ( $K_d = 0.39 \mu\text{M}$ ) or **VU0849822** ( $K_d = 0.51 \mu\text{M}$ ). Finally, a structurally related negative control compound, **VU0849117** ( $K_d > 40 \mu\text{M}$ ), was tested and, as expected, it did not disrupt the WDR5-MYC complex, confirming the on-target nature of this disruption.



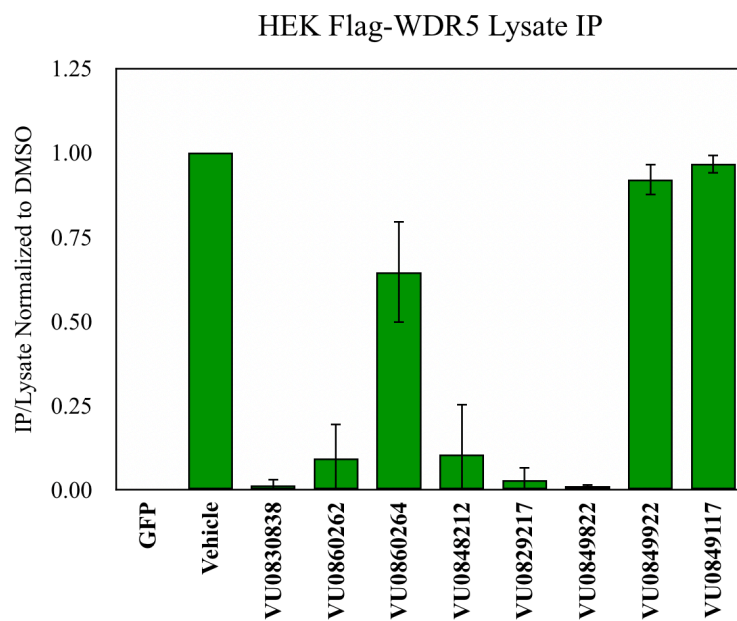
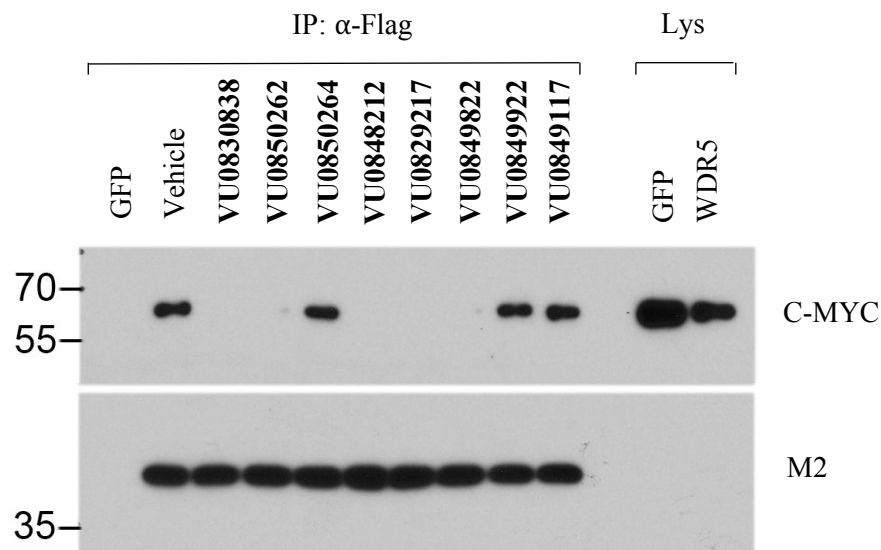


**Figure 37.** Lysates were prepared from HEK cells over expressing HA-tagged c-MYC and Flag-tagged WDR5. Immunoprecipitations were performed using anti-Flag in the presence of 50  $\mu$ M compound and disruption of c-MYC/WDR5 complexes was measured by immunoblotting for C-MYC. Data is representative of two independent biological repeats.

In light of the positive data, we conducted Co-IP experiments in whole cells treated with the same eight compounds, **Figure 38**. Compounds **VU0830838**, **VU0850262**, **VU0850264**, **VU0848212**,

and **VU0849117** decreased complex formation (WDR5-MYC) relative to DMSO. We speculate that the poor performance of **VU0849822** and **VU0849922** is not necessarily due to their physicochemical properties, as the data available for this class of compounds suggest that they all have high solubility and permeability and high binding to serum albumin (**Table 21**). However, the lower binding affinity, in combination with other factors such as other non-specific binding to cellular membrane or proteins, efflux, and/or binding kinetics might decrease their activity in cells. We determined that the results shown here, were not due to altered protein expression after treatment with compound, as the levels of MYC and WDR5 protein were comparable to DMSO treated cells in the lysates used for immunoprecipitation, confirming an on-target effect.

#### 4.4.2 Chromatin Immunoprecipitation (ChIP)

Since **VU0830838** showed the best results at disrupting the MYC-WDR5 interaction in cells, we postulated that it should also break the tether of MYC to chromatin at genomic loci where recruitment of MYC relies on interaction with WDR5. We performed chromatin immunoprecipitation (ChIP) assays and measured MYC binding at known target genes using quantitative PCR. We observed a reduction in the amount of MYC at loci where MYC recruitment is dependent on WDR5 (C7orf40, RNPS1, RPS14, and RPL5)<sup>229</sup> when cells were treated with 20  $\mu$ M of **VU0830838** for 10 h. Importantly, the amount of MYC remained nearly unaffected at ZFPM1 and ZMF771, two sites where MYC binding is independent of WDR5 (**Figure 39A**). Finally, this result was not due to altered expression or binding of WDR5 to these loci because ChIP experiments for WDR5 demonstrated comparable levels between cells treated with **VU0830838** and the negative control, **VU0849117** (**Figure 39B**).

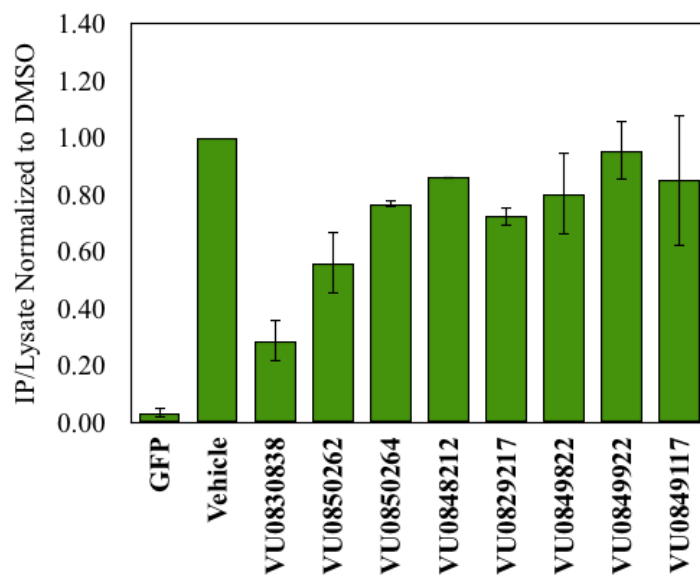
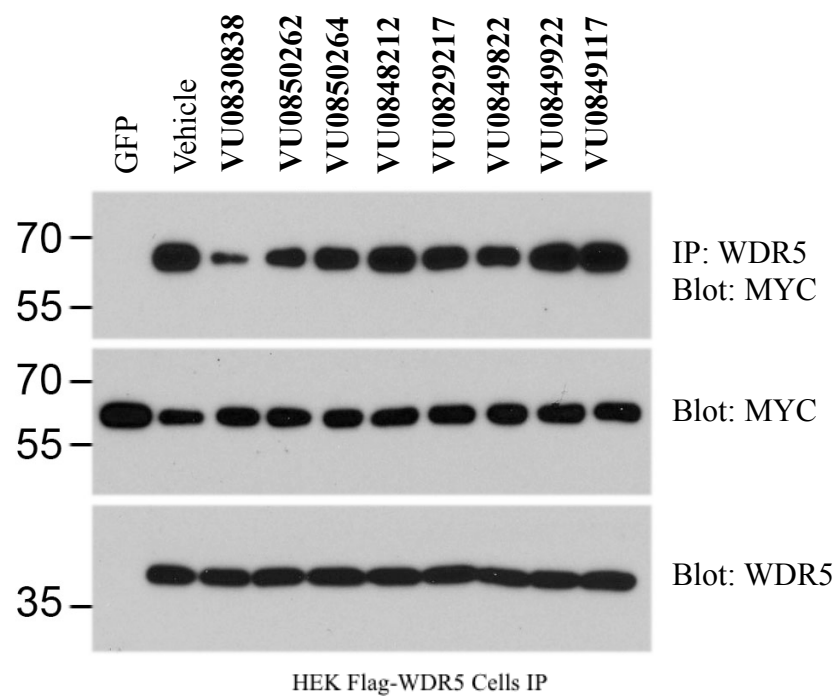


**Figure 38.** HEK293 cells over expressing HA-tagged C-MYC and Flag-tagged WDR5 were treated with 5  $\mu$ M compound for 24 hours. WDR5 complexes were immunoprecipitated using an anti-Flag antibody followed by immunoblotting for C-MYC. Data is representative of two independent biological repeats.

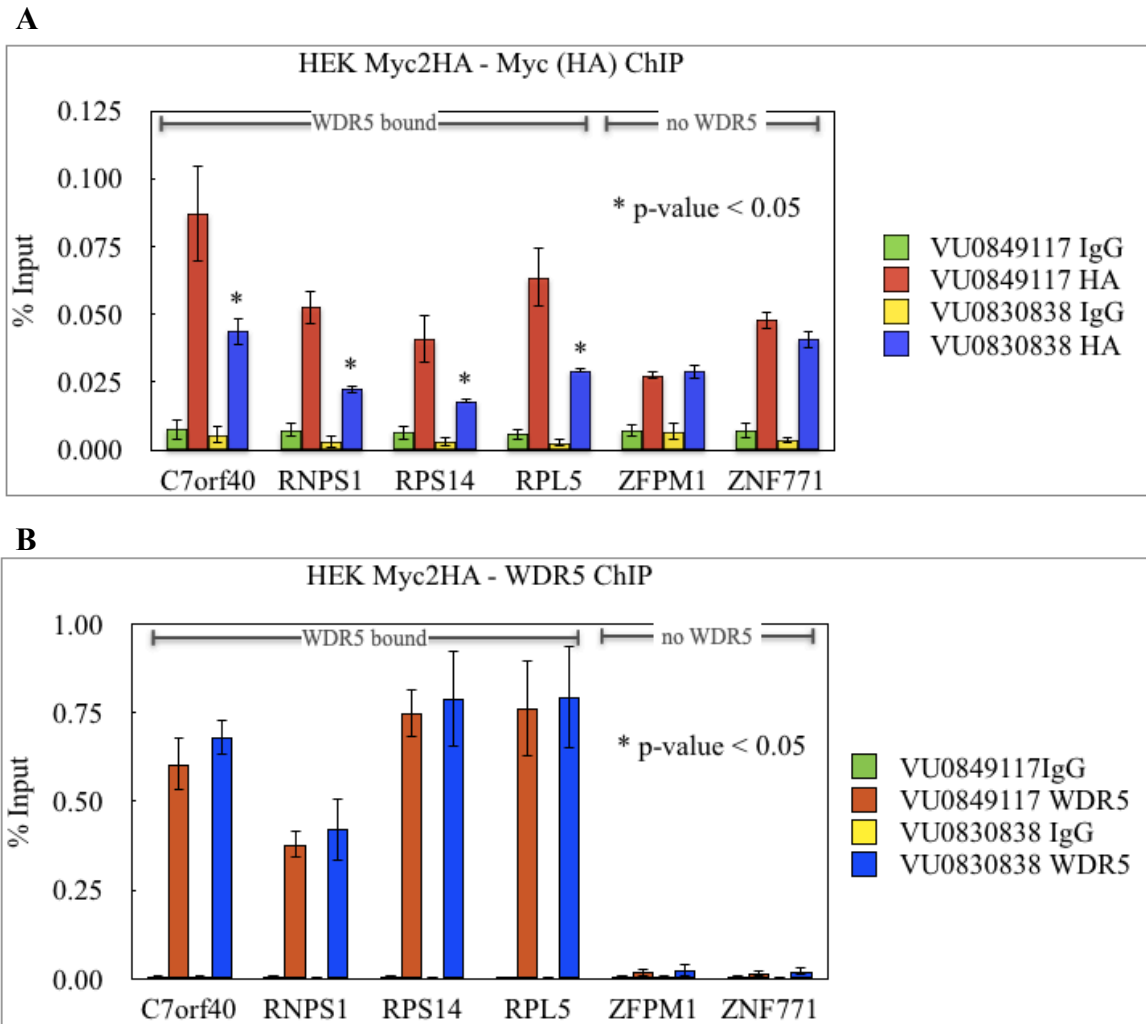


**Figure 39.** (A) Binding of MYC to target genes. Chromatin Immunoprecipitation (ChIP) in *c-MYC-HA* overexpressing HEK293 cells treated with 20  $\mu$ M compound for 10 h was performed using an  $\alpha$ -HA antibody. Percent recovery was monitored by qPCR at genes dependent on WDR5 for MYC recruitment or two genes independent of WDR5 (ZFPM1 and ZNF771). (B) WDR5 binding to chromatin at MYC target genes. The *p* values were calculated using a one-tailed student *t*-test. Data are representative of minimum three independent biological repeats.

#### 4.4.3 Histone Methyltransferase activity

Similar to the effect observed with the previous molecules we demonstrated a functional effect of **VU0849822**, **VU0850262**, **VU0850264**, and **VU0830838** binding to WDR5, as they inhibited the biochemical histone methyltransferase activity of MLL-1 in the full WDR5, RBBP5, ASH2L, and DPY30 (WRAD) complex (**Table 22**). It is known that a functional WRAD MLL complex requires binding of proteins to both the WIN and WBM site of WDR5<sup>216,267,268</sup>. These data confirm that disrupting the interaction at the WBM site can inactivate the transferase activity of the complex, presumably by disrupting the interaction of WDR5-RBBP5, thus preventing the assembly of the WRAD complex.

**Table 22.** Disruption of the WRAD complex as measured by activity in a commercial HMT.

<b>Compound</b>	<b>FPA <math>K_d</math> (<math>\mu</math>M)</b>	<b>HMT <math>IC_{50}</math> (<math>\mu</math>M)<sup>a</sup></b>
<b>VU0849822</b>	0.5 $\pm$ 0.1	2.05
<b>VU0850262</b>	0.11 $\pm$ 0.03	0.581
<b>VU0850264</b>	0.17 $\pm$ 0.03	1.08
<b>VU0830838</b>	0.10 $\pm$ 0.01	0.404

<sup>a</sup> All experiments performed at Reaction Biology.

#### 4.5 Conclusions

In this work, we used structure-based design and new chemical matter identified in an NMR-based fragment screen to discover a new series of compounds with improved physicochemical properties through fragment-merging with our previously established series. Compound **VU0830838** was best-in-class of the new hybrid-series, exhibiting a high binding affinity ( $K_d = 0.10 \mu$ M) in the

FPA and showed robust disruption of the WDR5-MYC interaction in cell lysates. The improvement in drug-like character of this series encouraged studies in a whole cell environment. Co-IP studies showed that **VU0830838** can inhibit the WDR5-MYC complex formation. Further, the compound was shown by ChIP to reduce the amount of MYC bound to chromatin at loci where recruitment of MYC is dependent on WDR5, but did not affect binding of MYC at loci where it binds independently of WDR5. We have confidence that these data replicate prior results observed when switching wild-type MYC to the WDR5-interaction-defective (WBM)<sup>269</sup> and that compound **VU0830838** demonstrates an on-target effect in whole cells.<sup>269</sup> We propose that **VU0830838** can be used to further study the cellular implications of disrupting the WDR5-MYC complex and guide further studies towards the development of therapeutic agents to treat MYC-driven cancers.

## Chapter V

### General Conclusions

Globally, cancer is the second leading cause of death.<sup>1</sup> Over the years, the knowledge acquired through the different scientific discoveries has resulted in a reduction in cancer-related deaths. Currently, there is a global effort to try to walk away from chemotherapeutic agents and develop targeted therapeutic strategies to inhibit oncogenic drivers.<sup>270</sup>

*Myc* is one of the most studied oncogenes and it is upregulated in more than 50% of all human cancers<sup>182</sup>, which makes it responsible for an estimated of 100,000 cancer-related deaths in the United States.

Multiple approaches to target MYC have emerged. Direct approaches have focused primarily on finding inhibitors of: 1) *myc* transcription, 2) MYC-MAX dimerization, and 3) MYC-MAX binding to DNA. Unfortunately, none of these strategies have resulted in a successful therapeutic treatment agent as different challenges emerged in each approach. Nonetheless, many of these inhibitors became useful tools that have expanded the understanding of MYC's role in tumor initiation and progression. Alternative therapeutic opportunities to target MYC are continuously pursued. In the recent years, multiple indirect approaches have emerged and most of them focus on finding pathways that allow the transcriptional regulation of *myc* or the modulation of MYC's stability or activity.

Tansey's group in collaboration with ours confirmed and fully characterized the WDR5-MYC interaction.<sup>23</sup> We determined that WDR5 is as critical co-factor of MYC and their interaction facilitates MYC recruitment to chromatin. Moreover, The *in vivo* disruption of this interaction

within the context of an existing cancer showed rapid and comprehensive tumor regression.<sup>229</sup> This finding together with others, validate WDR5 as a target. Therefore, we proposed that by developing small-molecule inhibitors of the WDR5-MYC interaction, we could determine if a therapeutic window is available for MYC-driven tumors.

In this dissertation, we describe small molecule inhibitors of the WDR5-MYC interaction. First, we conducted an HTS of the Vanderbilt library and obtained a series of biaryl sulfonamide hits that were unambiguously confirmed as inhibitors of this binding site by NMR and X-ray crystallography. Using rational design, we optimized hit compound **VU0618016**, yielding multiple analogs binding at less than 30 nM. Binding to the protein was confirmed by secondary assays, including NMR and DSF. These inhibitors were demonstrated to be highly soluble, and permeability was significantly improved by switching from a salicylic acid to salicylamide or methyl sulfone motif, all of which are able to form a H-bond interaction with GLN289 (**Figure 40**). Compounds from this series are able to disrupt the interaction of WDR5 with C-MYC by co-immunoprecipitation in cellular lysates. However, the low free fraction shown by most analogs limited their utility in whole cells. Due to the significant plasma protein binding exhibited by this series, we set out to find replacements of the sulfonamide linker. Unfortunately, we did not succeed at finding a sulfonamide replacement that improves or retains the binding affinity of the best compounds in the biaryl sulfonamide series.



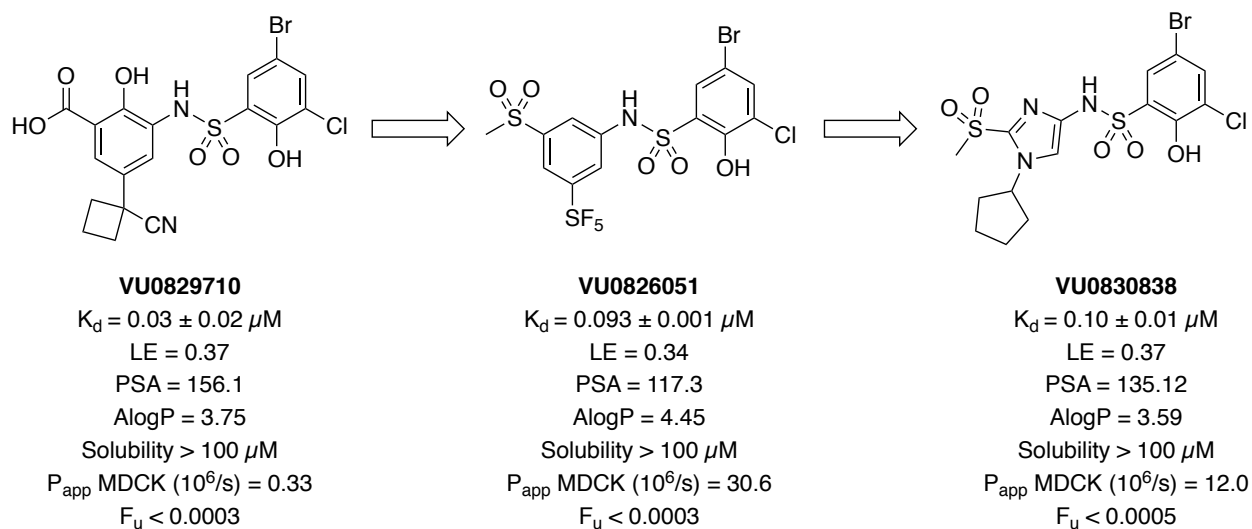


**Figure 40.** Physicochemical properties of best-in-class compounds

In another approach, we identified additional chemical matter to aid the discovery of compounds with improved properties. We conducted an NMR-based fragment screen and using structure-based design and a fragment merging strategy, we discovered a new subseries of compounds. These heterocyclic compounds bind to WDR5 with  $K_d$  values as low as 0.10  $\mu\text{M}$  and show robust disruption of the WDR5-MYC interaction in cell lysates. The substitution of the left-hand side phenyl ring for the imidazole not only allowed the removal of one phenol, but it furnished compounds with reduced polar surface area relative to the biaryl sulfonamides without raising the lipophilicity (**Figure 40**). In addition, most of the compounds shown here were able to maintain good Ligand Efficiencies (LE), which ranged between 0.27 and 0.4, suggesting they remain promising tools for further optimization. The results in the lysates Co-IP experiments and their improved drug-like character encouraged us to conduct whole cell experiments. Co-IP studies showed that the best-in-class compound, **VU0830838**, can reduce the WDR5-MYC complex formation. Furthermore, chromatin immunoprecipitation (ChIP) assays with **VU0830838** showed

a reduction of MYC binding at loci where MYC recruitment is dependent on WDR5 (C7orf40, RNPS1, RPS14, and RPL5). In agreement with previous observations<sup>269</sup>, cells treated with **VU0830838** did not display changes in the amount of MYC at WDR5-independent binding sites (ZFPM1 and ZMF771).

The compounds developed in this work have demonstrated that binding to WDR5 at the WBM site by small molecules is possible. Although, further improvements in binding affinity, cellular activity, and pharmaceutical properties are needed in order to determine if this site is druggable. Exploration on the aniline ring of the biaryl sulfonamide series was extensive; however, the sulfonyl ring was less explored. For the next steps, additional exploration of modifications on the sulfonyl ring and combination of desphenol aryl pieces may help improve the physicochemical properties of the compounds. The fragment-merged subseries can also be further explored. Modifications on the aryl ring may offer a path forward for the improvement of the physicochemical properties and binding affinity. Similarly, the X-ray co-crystal structure of the analog **VU0830838** showed that the S<sub>5</sub> channel is available, which suggests that larger groups coming of the sulfone could be installed as a way to occupy the channel. In order to improve the effectiveness of the compounds, we envision that the unbound fraction (F<sub>u</sub>) must be improved to at least 1-2% while retaining or improving the binding affinity, the permeability, and the solubility. Despite exhibiting sub-optimal physicochemical properties, these compounds are useful tools and will allow to study the effects of inhibiting the interaction between WDR5 and MYC. As future directions, it will be important to also assess if these compounds disrupt the interaction between WDR5 and other proteins that bind to the WBM site (e.g. KANSL2 and RBBP5). In addition, for the next steps of compound development, it will be essential to identify a cell-based assay

(assessment of cell proliferation, viability, or apoptosis) that is predictive of the disease and allow the characterization of the efficacy of the compounds.

A more promising approach to target WDR5 is by inhibiting the interaction with other proteins at the WIN site. Indeed, our group has been actively working on the development of WIN site inhibitors and picomolar compounds have been discovered.<sup>271,272</sup> Further work have demonstrated that the WIN-site links WDR5 to chromatin at a small cohort of loci that includes a subset of genes involved in protein synthesis. Blockade of the WIN-site with our inhibitors causes displacement of WDR5 from chromatin.<sup>273</sup> Moreover, Thomas *et al* reported that WDR5 recruits MYC to chromatin to regulate a set of genes linked to protein synthesis. Consequently, inhibition of the WIN-site could also modulate MYC's activity. In a scenario where WDR5 is not druggable via its WBM-site, we envision that a therapeutic window for the WIN-site inhibitors might be found and could be beneficial for the treatment of MYC-driven cancers.

## Chapter VI

### Experimental

#### 6.1 General Chemistry

All chemical reagents and reaction solvents were purchased from commercial suppliers and used as received. All microwave-assisted reactions were performed using a Biotage Initiator 2.0 microwave reactor. Hydrogenation reactions are performed using an atmospheric balloon, or using a Parr hydrogenation shaker apparatus where stated. Analytical thin-layer chromatography (TLC) was performed on Kieselgel 60 F254 glass plates precoated with a 0.25 mm thick silica gel. TLC plates were visualized with UV light and iodine.

All compounds were obtained at 95% purity or higher, unless otherwise noted, as measured by analytical reversed-phase HPLC. Analytical HPLC was performed on an Agilent 1200 series system with UV detection at 214 and 254 nm, along with evaporative light-scattering detection (ELSD). Low-resolution mass spectra were obtained on an Agilent 6140 mass spectrometer with electrospray ionization (ESI). For LCMS characterization of the compounds in the present work, one of the following methods were used: Method A: A Phenomenex Kinetex 2.6  $\mu\text{m}$  XB-C18 100  $\text{\AA}$  LC column (50  $\text{\AA}$ ~ 2.1 mm) was used with a 2 min gradient of 5–95% MeCN in H<sub>2</sub>O and 0.1% TFA. Method B: A Phenomenex Kinetex 2.6  $\mu\text{m}$  XB-C18 100  $\text{\AA}$  LC column (50  $\text{\AA}$ ~ 2.1 mm) was used with a 1 min gradient of 5–95% MeCN in H<sub>2</sub>O and 0.1% TFA. Normal phase flash silica gel-based column chromatography was performed using ready-to-connect cartridges from ISCO, on irregular silica gel, particle size 15-40  $\mu\text{m}$  using a Teledyne ISCO Combiflash Rf system. Preparative reverse-phase HPLC was performed on a Gilson instrument equipped with a

Phenomenex Kinetex C18 column, using varying concentrations of MeCN in H<sub>2</sub>O and 0.1% TFA, unless otherwise stated and basic method was used (MeCN in H<sub>2</sub>O and 0.05% NH<sub>4</sub>OH).

## 6.2 General Experimental Procedures

### ***General Procedure A (Chlorosulfonation)***

Chlorosulfonic acid (7-10 eq) was cooled to -10 °C in a bath of ice. To this was added the corresponding aromatic species (1 eq), portion-wise, as required; the mixture was stirred for 4–16 h. The mixture was quenched by careful addition to a slurry of ice and CH<sub>2</sub>Cl<sub>2</sub>, extracting with CH<sub>2</sub>Cl<sub>2</sub>. The crude material was purified by ISCO flash chromatography or used directly with no purification.

### ***General Procedure B (Nitration)***

A 0.34 M solution containing the appropriate reactant (1 eq) in CH<sub>2</sub>Cl<sub>2</sub> was cooled to 0 °C in an ice/water bath. To this was added HNO<sub>3</sub> (conc., 2 eq) and H<sub>2</sub>SO<sub>4</sub> (conc., 1.5 eq) drop-wise. The mixture was stirred for 1–4 h, allowing to warm to r.t., then poured over ice and extracted with CH<sub>2</sub>Cl<sub>2</sub>. The crude material was purified by ISCO flash chromatography.

### ***General Procedure B-B (Nitration)***

A solution of the 4-Nitroimidazole (1 eq) in HOAc (35 eq) was cooled to 0 °C in an ice/water bath. HNO<sub>3</sub> (14 eq) and Ac<sub>2</sub>O (14.3 eq) were added and continued stirring at 0 °C for 10 min. Then the mixture was allowed to reach room temperature and stirred for 1 hour. Water was added and extracted with EtOAc. The organic phase was dried over Na<sub>2</sub>SO<sub>4</sub>, filtered and the solvent removed under vacuum. The crude was used without further purification.

### ***General Procedure C (Hydrogenation)***

To a solution containing the appropriate reactant (1 eq) and EtOH (0.4 M), was added Pd/C (10% C by wt., 5 mol%) and the mixture was stirred under a H<sub>2</sub> atmosphere for 10 min-18 h. The mixture was filtered through celite, concentrated, and purified by ISCO flash chromatography if required.

### ***General Procedure D (Sulfonamide Coupling)***

To a solution containing the corresponding aniline (1 eq), pyridine (4 eq), and CH<sub>2</sub>Cl<sub>2</sub>, at 0.2 M at 0 °C, was added sulfonyl chloride (1.5–4 eq). The mixture was allowed to stir for 1–16 h, then concentrated under reduced pressure and purified by ISCO flash chromatography or preparative HPLC, unless otherwise stated.

### ***General Procedure E (Ester Hydrolysis)***

To a 0.2 M solution containing the corresponding ester (1 eq) and THF was added a 2 M aqueous solution of LiOH (5 eq). The reaction mixture was heated at 65 °C for 2–16 h, unless otherwise stated. The mixture was acidified with hydrochloric acid, extracted with EtOAc and washed with brine. The crude material was purified by preparative HPLC.

### ***General Procedure F (Methyl Amide Synthesis)***

To the corresponding salicylate ester (1 eq) was added a 2.0 M solution of methylamine in THF (10 eq) and the mixture was heated at 65 °C for 1–16 h. The mixture was concentrated under reduced pressure and purified by preparative HPLC.

***General Procedure H (HATU Mediated Amide Coupling)***

A 0.3 M solution containing the corresponding carboxylic acid (1 eq) and DIPEA (3 eq) in DMF was cooled to 0 °C in an ice/water bath. HATU (1.2 eq) was added and the reaction mixture was stirred for 30 mins, followed by the addition of amine (1-2 eq). The solution was warmed to r.t. and stirred for 18 h, then diluted with EtOAc and washed with H<sub>2</sub>O. Crude product was purified by ISCO flash chromatography or preparative HPLC.

***General Procedure I (PyBOP Mediated Amide Coupling)***

To a 0.08 M solution containing the corresponding carboxylic acid (1 eq), DIPEA (1.2 eq), and the corresponding amine (2 eq) in CH<sub>2</sub>Cl<sub>2</sub> was added PyBOP (1.5 eq). The reaction mixture was stirred at r.t. for 18 h, then diluted with CH<sub>2</sub>Cl<sub>2</sub> and washed with water and concentrated. Crude product was purified by preparative HPLC.

***General Procedure J (Suzuki-Miyaura Coupling – (Hetero)Aromatic Boronic Acids)***

To a solution containing the corresponding bromide (1 eq), (hetero)aromatic boronic acid or pinacol ester (1.2 eq), and Pd(dppf)Cl<sub>2</sub> (0.05 eq) in de-gassed anhydrous dioxane (0.2 M) was added a 3 M aqueous solution of Cs<sub>2</sub>CO<sub>3</sub> (3 eq). The reaction mixture was heated at 95 °C for 1–16 h. The cooled mixture was filtered through celite, washing with CH<sub>2</sub>Cl<sub>2</sub>, and purified by ISCO flash chromatography.

***General Procedure J-B (Suzuki-Miyaura Coupling – (Hetero)Aromatic Boronic Acids)***

To degassed anhydrous dioxane at 0.24 M was added bromothiazole (1 eq), Pd(PPh<sub>3</sub>)<sub>4</sub> (0.05 eq) and the boronic acid (1.2 eq), and a solution of Na<sub>2</sub>CO<sub>3</sub> (3 eq) at 2.0 M in water. The mixture was

stirred at 100 °C for 18 h. EtOAc was added and washed with a saturated solution of NH<sub>4</sub>Cl. The crude was purified using ISCO flash chromatography.

***General Procedure K (Suzuki Coupling – Cyclopropylboronic Acid)***

A mixture containing the intermediate bromide (1 eq), cyclopropylboronic acid (1.2 eq), Pd(OAc)<sub>2</sub> (0.05 eq), PCy<sub>3</sub>.HBF<sub>4</sub> (0.1 eq), and K<sub>3</sub>PO<sub>4</sub> (2.5 eq) in a mixture of toluene:H<sub>2</sub>O (10:1, 0.2 M final concentration) was heated at 110 °C for 1–16 h. The cooled reaction mixture was filtered through celite, washed with CH<sub>2</sub>Cl<sub>2</sub>, and purified by ISCO flash chromatography.

***General Procedure L (Boron Tribromide Demethylation)***

A 0.4 M solution containing the corresponding intermediate (1 eq) in anhydrous DCM was cooled to -78 °C in an acetone/dry ice bath under an inert atmosphere. To this was added a 1.0 M solution of BBr<sub>3</sub> in DCM (2 eq) drop-wise, and the mixture was stirred for 1 h at -78 °C, then allowed to warm to r.t. The reaction mixture was poured over an ice-water slurry, extracted with EtOAc, washed with water and brine, and purified by ISCO flash chromatography.

***General Procedure M (Sulfone Coupling)***

The corresponding aryl iodide or bromide (1 eq) was combined with sodium methanesulfinate (1.2 eq), CuI (0.10 eq), *L*-proline (0.20 eq) and NaOH (0.2 eq). The reaction vessel was purged with Ar, sufficient DMSO to produce a 0.5 M concentration was added, and the mixture was heated at 57–85 °C for 16–20 h. Upon cooling, the mixture was diluted with water and extracted with CH<sub>2</sub>Cl<sub>2</sub>. The organic phase was dried and concentrated. The crude material was taken forward without purification.



### ***General Procedure N (Sulfide Coupling)***

To a 0.4 M solution containing the corresponding aryl bromide (1 eq) in pyridine was added Cu (2 eq) and dialkyl disulfide (2 eq). The reaction mixture was stirred at 90-115 °C for 16-20 h. The mixture was allowed to reach room temperature and then filtered. The filter cake was washed with CH<sub>2</sub>Cl<sub>2</sub> and the filtrate was concentrated to dryness and then re-suspended in a 3 M aqueous solution of HCl. This mixture was extracted with CH<sub>2</sub>Cl<sub>2</sub> and the organic phase was separated, and concentrated and the residue was purified by ISCO flash chromatography.

### ***General Procedure N-B (Sulfide Coupling)***

The aryl/heteroaryl iodide or bromide (1 eq), sodium methanethiolate (1.05 eq), Pd<sub>2</sub>(dba)<sub>3</sub> (0.025 eq), and Xantphos (0.05 eq) were mixed with de-gassed anhydrous THF at 0.34 M. Then, Et<sub>3</sub>N (1.25 eq) was added and the mixture was heated to 76 °C for 18 h. Upon cooling the mixture was filtered and the solvent was removed under vacuum. The crude was purified using ISCO Flash chromatography.

### ***General Procedure O (Sulfide–Sulfone Oxidation)***

To a 0.32 M solution of the corresponding sulfide in a 1: mixture of H<sub>2</sub>O:EtOH was added Oxone (2 eq). The reaction mixture was stirred at r.t. for 4–20 h. Water was added to the mixture and it was extracted with CH<sub>2</sub>Cl<sub>2</sub>. The organic phase was dried using a phase separator and the solvent was removed under vacuum. If required, the residue was purified by ISCO flash chromatography.

### ***General Procedure P (Curtius rearrangement)***

A 0.2 M mixture containing the corresponding carboxylic acid (1 eq), *t*-BuOH (5 eq), diphenylphosphoryl azide (DPPA, 1.2 eq), and 1,2-dimethoxyethane was heated at 100 °C for 16-20 h. The reaction mixture was allowed to reach room temperature, quenched with a saturated solution of NH<sub>4</sub>Cl, and extracted with EtOAc. The organic phase was washed with a saturated solution of NaHCO<sub>3</sub> and then with water. The organic phase was dried over Na<sub>2</sub>SO<sub>4</sub> and filtered, and the solvent removed under vacuum.

The crude residue was resuspended in CH<sub>2</sub>Cl<sub>2</sub> (at 0.2 M) and Trifluoroacetic Acid (TFA, 0.007 eq) was added. The reaction mixture was stirred at room temperature for 1-16 h, quenched by the addition of a saturated solution of NaHCO<sub>3</sub>, and then extracted with CH<sub>2</sub>Cl<sub>2</sub>. The organic phase was dried over a phase separator and the solvent removed under vacuum. The crude residue was purified using ISCO flash chromatography.

### ***General Procedure Q (Thiol Coupling and alkylation)***

A mixture containing the corresponding aryl bromide (1 eq), CuSO<sub>4</sub>•5H<sub>2</sub>O (0.05 eq), and KOH (5 eq) in DMSO:H<sub>2</sub>O (9:1, [0.45 M] final) was purged by bubbling Argon for 10 min and then 2 eq of 1,2-dithioethane were added. The vial was sealed and was heated at 110 °C for 20 h. To isolate the thiol, the mixture was treated with 3 M HCl and then extracted with EtOAc. The organic phase was dried over a phase separator and the solvent removed under vacuum. The crude material was purified using ISCO flash chromatography. When the alkylated thiol was desired, the reaction mixture was treated with a solution made of the corresponding alkyl bromide (3 eq) in DMF ([3 M]) and Et<sub>3</sub>N (3 eq) and reaction mixture was allowed to stir overnight at room temperature. The reaction mixture was quenched by the addition of water and extracted with EtOAc. The organic

phase was dried over a phase separator and the solvent removed under vacuum. The crude was purified using ISCO flash chromatography.

***General Procedure R (Nitro Reduction)***

To a mixture containing the corresponding nitrobenzene and HOAc, iron powder was added. The reaction mixture is allowed to stir overnight at room temperature, then filtered and concentrated. The crude material was purified by ISCO chromatography or preparative HPLC.

***General Procedure S (Boc deprotection)***

A mixture containing the corresponding carbamate (1 eq) and a 4 M solution of HCl in dioxane was heated at 50 °C for 1-4 h. The solvent was removed under vacuum to obtain the crude, which was purified by ISCO flash chromatography.

***General Procedure T (Aldehyde / Conjugated double bond reduction)***

A 0.2-0.4 M solution of the desired aldehyde (1 eq) in EtOH was cooled to 0 °C in a water/ice bath and NaBH<sub>4</sub> (1.1 eq) was added slowly. The mixture was allowed to reach r.t. and stirred for 1-5 h. The mixture was diluted with water and neutralized with HCl 3 M. CH<sub>2</sub>Cl<sub>2</sub> was used to extract the product and the crude was purified using ISCO flash chromatography.

***General Procedure U (Mesylate formation)***

A 0.2 M solution of the primary alcohol (1 eq) in CH<sub>2</sub>Cl<sub>2</sub> was cooled to 0 °C in a water/ice bath. To this solution Et<sub>3</sub>N (3.5 eq) and mesyl chloride (1.2 eq) were added and stirred for 20 min-1 h.

The solution was diluted with ice-cold water and  $\text{CH}_2\text{Cl}_2$  and then washed with HCl 3M and a sat. solution of  $\text{NaHCO}_3$ . The crude was purified using ISCO flash chromatography.

***General Procedure V (Kolbe nitrile synthesis)***

To a 0.5 M solution of the mesylate (1 eq) in DMF:H<sub>2</sub>O (9:1) was added NaCN (2 eq) and stirred at 40 °C for 30-60 min. Water was added and extracted with EtOAc. The crude was purified using ISCO flash chromatography.

***General Procedure W (Condensation of aldehyde with acetonitrile)***

A mixture of the acetonitrile (1 eq) and the aldehyde (1 eq) was dissolved in MeOH at 0.5 M and  $\text{K}_2\text{CO}_3$  (4 eq) was added. The mixture was stirred at 40 °C for 60-90 min. Water was added and neutralized with HCl 3 M, the product was extracted with  $\text{CH}_2\text{Cl}_2$  and used as a crude when stated, otherwise it was purified using ISCO flash chromatography.

***General Procedure X (N-alkylation)***

A mixture of imidazole (1 eq), aryl/alkyl halide (1.2 eq),  $\text{Cs}_2\text{CO}_3$  (3 eq) and KI (4 eq) were suspended in MeCN at 0.5 M. It was heated under microwave irradiation at 135 °C for 45 min. The mixture was filtered and the solvent was removed under vacuum. The crude was purified by ISCO flash chromatography.

***General Procedure X-B (N-alkylation)***

1,4-dinitro-1H-imidazole (1 eq) was dissolved in MeOH:H<sub>2</sub>O at 0.3 M (1:1) and cooled to 0 °C in a water/ice bath. The amine/aniline (1.1 eq) was added dropwise and the solution was stirred

overnight. Water was added and extracted with EtOAc. The crude was purified using ISCO flash chromatography.

***General Procedure Y (Reductive amination)***

The corresponding aniline (1.2 eq) and aldehyde (1 eq) were dissolved in CH<sub>2</sub>Cl<sub>2</sub> at 0.1 M. and acetic acid (2 eq) was added. The solution was premixed for 5 min and NaBH<sub>3</sub>OAc (2 eq) was added. The solution was stirred at r.t. for 1 h. Acetone was added and the solvent removed under vacuum. The crude was purified by preparative HPLC.

***General Procedure Z (Benzyl Protection)***

The intermediate phenol (1 eq), benzyl bromide (1-2 eq) and potassium carbonate (1.1-2 eq) were combined in acetonitrile and stirred at 25-82 °C for 18 h. Upon cooling the mixture was concentrated *in vacuo*, re-dissolved in EtOAc and washed with water, brine. Crude material was purified by ISCO flash chromatography.

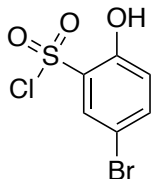
***General Procedure TZ (Tetrazole formation)***

A mixture of propanenitrile (1 eq), NaN<sub>3</sub> (7 eq), and NH<sub>4</sub>Cl (8 eq) was suspended in DMF at 0.13 M. The mixture was heated under microwave irradiation at 130 °C for 30 min. The mixture was washed with HCl 1 M and extracted with CH<sub>2</sub>Cl<sub>2</sub>. The crude was purified by preparative HPLC.

## 6.2 Synthesis biaryl sulfonamide analogs

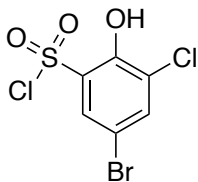
### 6.2.1 Synthesis of sulfonyl chlorides

#### *5-Bromo-2-hydroxybenzenesulfonyl chloride*



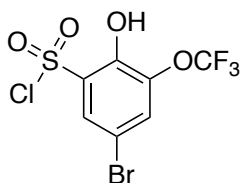
4-Bromophenol (1.73 g, 10 mmol) was reacted with chlorosulfonic acid (4.77 mL, 70 mmol) following General Procedure A. Purification by flash chromatography afforded title compound as a pale brown oily solid (1.50 g, 5.53 mmol, 55%).  $^1\text{H NMR}$  (400 MHz,  $\text{CDCl}_3$ )  $\delta$  7.95 (d,  $J = 2.4$  Hz, 1H), 7.71 (dd,  $J = 8.9, 2.4$  Hz, 1H), 7.04 (d,  $J = 8.9$  Hz, 1H).

#### *5-Bromo-3-chloro-2-hydroxybenzenesulfonyl chloride*



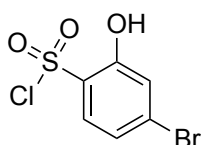
2-Chloro-4-bromophenol (2.08 g, 10 mmol) was reacted with chlorosulfonic acid following General Procedure A. Purification by flash chromatography afforded title compound as a colorless solid (2.19 g, 7.15 mmol, 72%).  $^1\text{H NMR}$  (400 MHz,  $\text{CDCl}_3$ )  $\delta$  7.92 (1H, d,  $J = 2.4$  Hz), 7.86 (1H, d,  $J = 2.4$  Hz).

#### *5-Bromo-2-hydroxy-3-(trifluoromethoxy)benzenesulfonyl chloride*



4-Bromo-2-(trifluoromethoxy)phenol (200 mg, 0.78 mmol) was reacted following General Procedure D. A light-yellow oil was obtained as a crude (180 mg) and it was used without further purification. LCMS (Method A)  $t_R = 1.754$  min,  $m/z =$  does not ionize by ESI.

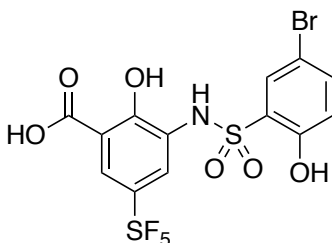
#### *4-Bromo-2-hydroxybenzenesulfonyl chloride*



3-Bromophenol (1095  $\mu$ L, 10 mmol) was added portion-wise to ice-cold chlorosulfonic acid (4.66 mL, 70 mmol). The mixture was stirred for 4 h, then poured into a slurry of ice, DCM and brine, extracting the DCM layer. The crude oil was taken forward (842 mg).  $^1\text{H}$  NMR (400 MHz,  $\text{CDCl}_3$ )  $\delta$  8.10 (d,  $J = 8.9$  Hz, 1H), 7.33 (d,  $J = 2.5$  Hz, 1H), 6.95 (dd,  $J = 8.9, 2.5$  Hz, 1H).

### 6.2.2 Synthesis of salicylic acid analogs

#### *3-((5-Bromo-2-hydroxyphenyl)sulfonamido)-2-hydroxy-5-(pentafluorosulfanyl)benzoic acid (VU0849832)*



#### Step A: Phenyl 2-methoxy-5-(pentafluorosulfanyl)benzoate

(3-Bromo-4-methoxyphenyl)pentafluorosulfane, (939 mg, 3.0 mmol),  $\text{Pd}(\text{OAc})_2$  (34 mg, 0.15 mmol),  $\text{P}(\text{tBu})_3 \cdot \text{HBF}_4$  (174 mg, 0.60 mmol) and phenol (282 mg, 3.0 mmol) were taken in MeCN

(13.7 mL) in a 40 mL reaction vial and phenyl formate (500  $\mu$ L) and Et<sub>3</sub>N (1.25 mL, 9.0 mmol) were added. The reaction was run in 5-parallel reactions. The sealed vials were heated to 90 °C for 18 h, then combined after filtration through celite, concentrated, re-dissolved in EtOAc (100 mL) and washed with H<sub>2</sub>O (100 mL). Purification by flash chromatography afforded a pale brown liquid (4.36 g, 12.3 mmol, 82%). <sup>1</sup>H NMR (400 MHz, CDCl<sub>3</sub>)  $\delta$  8.41 (d,  $J$  = 2.9 Hz, 1H), 7.93 (dd,  $J$  = 9.2, 2.9 Hz, 1H), 7.48 – 7.40 (m, 2H), 7.31 – 7.26 (m, 2H), 7.07 (d,  $J$  = 9.2 Hz, 1H), 6.93 (tt,  $J$  = 7.3, 1.1 Hz, 1H), 4.00 (s, 3H); <sup>19</sup>F NMR (376 MHz, CDCl<sub>3</sub>)  $\delta$  84.52 (d,  $J$  = 150 Hz, 1F), 64.07 (d,  $J$  = 150 Hz, 4F). LCMS (Method B)  $t_R$  = 1.246 min  $m/z$  = 355.2 [M+H]<sup>+</sup>; Purity (AUC)  $\geq$  95%.

Step B: Phenyl 2-hydroxy-5-(pentafluorosulfanyl)benzoate

Phenyl 2-methoxy-5-(pentafluorosulfanyl)benzoate (3.54 g, 10.0 mmol) was reacted following General Procedure L. Purification by flash chromatography afforded a colorless solid (2.93 g, 6.02 mmol, 60%). <sup>1</sup>H NMR (400 MHz, CDCl<sub>3</sub>)  $\delta$  10.88 (s, 1H), 8.50 (d,  $J$  = 2.8 Hz, 1H), 7.92 (dd,  $J$  = 9.2, 2.8 Hz, 1H), 7.53 – 7.45 (m, 2H), 7.40 – 7.31 (m, 1H), 7.29 – 7.20 (m, 3H), 7.11 (d,  $J$  = 9.2 Hz, 1H); <sup>19</sup>F NMR (376 MHz, CDCl<sub>3</sub>)  $\delta$  84.58 (p,  $J$  = 151 Hz, 1F), 63.90 (d,  $J$  = 151 Hz, 4F). LCMS (Method B)  $t_R$  = 1.288 min,  $m/z$  = 341.2 [M+H]<sup>+</sup>; Purity (AUC)  $\geq$  70%.

Step C: 2-Hydroxy-5-(pentafluorosulfanyl)benzoic acid

Phenyl 2-hydroxy-5-(pentafluorosulfanyl)benzoate (1.81 g, 5.32 mmol) was reacted following General Procedure E. Purification by flash chromatography afforded title compound (1.15 g, 4.35 mmol, 82%). <sup>1</sup>H NMR (400 MHz, MeOH-*d*<sub>4</sub>)  $\delta$  8.27 (d,  $J$  = 2.9 Hz, 1H), 7.91 (dd,  $J$  = 9.2, 2.9 Hz, 1H), 7.07 (d,  $J$  = 9.2 Hz, 1H); <sup>19</sup>F NMR (376 MHz, MeOH-*d*<sub>4</sub>)  $\delta$  83.68 (p  $J$  = 149 Hz, 1F), 62.35 (d,  $J$  = 149 Hz, 4F). LCMS (Method B)  $t_R$  = 0.975 min;  $m/z$  = 265.4 [M+H]<sup>+</sup>; Purity (AUC)  $\geq$  95%.



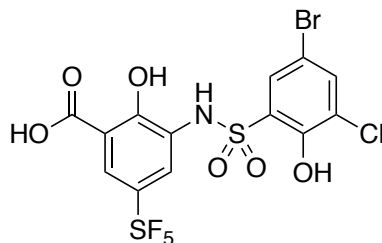
Step D: 2-Hydroxy-3-nitro-5-(pentafluorosulfanyl)benzoic acid

2-Hydroxy-5-(pentafluorosulfanyl)benzoic acid (300 mg, 1.14 mmol) was reacted following General Procedure B. Purification by flash chromatography afforded title compound (159 mg, 0.51 mmol, 45%). <sup>1</sup>H NMR (400 MHz, MeOH-*d*<sub>4</sub>) δ 8.60 (d, *J* = 2.8 Hz, 4H), 8.53 (d, *J* = 2.8 Hz, 4H). <sup>19</sup>F NMR (376 MHz, MeOH-*d*<sub>4</sub>) δ 80.9 (p, *J* = 149 Hz, 1F), 62.4 (d, *J* = 149 Hz, 4F). LCMS (Method B) *t*<sub>R</sub> = 0.807 min, does not ionize by ESI; Purity (AUC) ≥ 95%.

Step E: Methyl 2-hydroxy-3-nitro-5-(pentafluorosulfanyl)benzoate

To a mixture containing 2-hydroxy-3-nitro-5-(pentafluorosulfanyl)benzoic acid (60 mg, 0.19 mmol) in MeOH (1 mL), two drops of H<sub>2</sub>SO<sub>4</sub> were added. The reaction mixture was heated to reflux and stirred overnight. The cooled mixture was concentrated and the residue dissolved in DCM and washed with water. The organic phase was concentrated to afford crude title compound which was used without purification (60 mg, 0.19 mmol, 96%). <sup>1</sup>H NMR (400 MHz, CDCl<sub>3</sub>) δ 8.55 (d, *J* = 2.9 Hz, 1H), 8.51 (d, *J* = 2.9 Hz, 1H), 4.09 (s, 3H). LCMS (Method B) *t*<sub>R</sub> = 1.093 min *m/z* = 324.2 [M+H]<sup>+</sup>; Purity (AUC) ≥ 95%.

3-((5-Bromo-3-chloro-2-hydroxyphenyl)sulfonamido)-2-hydroxy-5-(pentafluoro-λ6-sulfaneyl)benzoic acid (VU0849828)



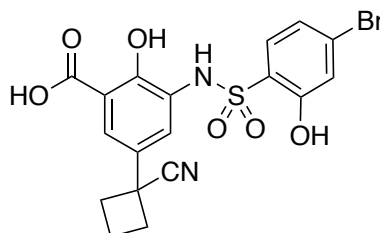
Step A: Methyl 3-((5-bromo-3-chloro-2-hydroxyphenyl)sulfonamido)-2-hydroxy-5-(pentafluorosulfanyl)benzoate

Methyl 3-amino-2-hydroxy-5-(pentafluorosulfanyl)benzoate (50 mg, 0.17 mmol) was reacted with 5-bromo-3-chloro-2-hydroxybenzenesulfonyl chloride following General Procedure D. Purification by flash chromatography afforded the title compound (21 mg, 0.04 mmol, 19%) as a colorless solid. <sup>1</sup>H NMR (400 MHz, CDCl<sub>3</sub>) δ 8.72 – 8.67 (m, 1H), 8.11 (d, *J* = 2.6 Hz, 1H), 8.02 (d, *J* = 2.6 Hz, 1H), 7.74 (d, *J* = 2.4 Hz, 1H), 7.63 (d, *J* = 2.4 Hz, 1H), 3.99 (s, 3H); <sup>19</sup>F NMR (376 MHz, CDCl<sub>3</sub>) δ 83.3 (p, *J* = 151 Hz, 1F), 63.7 (d, *J* = 151 Hz, 4F). LCMS (Method B): t<sub>R</sub> = 1.191 min, *m/z* = 562.1, 564.1 [M+H]<sup>+</sup>; Purity (AUC) ≥ 80%.

Step B: 3-((5-Bromo-3-chloro-2-hydroxyphenyl)sulfonamido)-2-hydroxy-5-(pentafluorosulfanyl)benzoic acid

Methyl 3-((5-bromo-3-chloro-2-hydroxyphenyl)sulfonamido)-2-hydroxy-5-(pentafluorosulfanyl)benzoate (20 mg, 0.032 mmol) was reacted following General Procedure E. Purification by preparative HPLC afforded the title compound (8 mg, 0.015 mmol, 47%) as a colorless solid. <sup>1</sup>H NMR (400 MHz, Acetone-*d*<sub>6</sub>) δ 8.12 (d, *J* = 2.7 Hz, 1H), 8.09 (d, *J* = 2.7 Hz, 1H), 7.86 (d, *J* = 2.4 Hz, 1H), 7.81 (d, *J* = 2.4 Hz, 1H); <sup>19</sup>F NMR (376 MHz, MeOH-*d*<sub>4</sub>) δ 82.94 (p, *J* = 149 Hz, 1F), 62.21 (d, *J* = 149 Hz, 4F). LCMS (Method B) t<sub>R</sub> = 1.111 min, *m/z* = 548.1, 550.1 [M+H]<sup>+</sup>, Purity (AUC) ≥ 95%.

*3-((4-Bromo-2-hydroxyphenyl)sulfonamido)-5-(1-cyanocyclobutyl)-2-hydroxybenzoic acid (VU0830492)*



Step A: 1-(3-Bromo-4-methoxyphenyl)cyclobutane-1-carbonitrile

2-(3-Bromo-4-methoxyphenyl)acetonitrile (4.52 g, 20 mmol) and 1,3-dibromopropane (2.23 mL, 22 mmol) were dissolved in DMSO (100 mL), to this mixture was added NaH (60% dispersion in mineral oil, 2.0 g, 50 mmol) portion-wise. The solution was stirred for 16 h at r.t., then diluted with EtOAc:Et<sub>2</sub>O (200 mL, 1:1) and washed with water. The combined aqueous layers were back-extracted with further EtOAc (200 mL). The combined organics were washed with sat. aq. NaCl, concentrated and purified by ISCO flash column chromatography, which afforded 3.65 g (13.7 mmol, 68%) of title compound as a colorless oil. <sup>1</sup>H NMR (400 MHz, CDCl<sub>3</sub>) δ 7.61 (d, *J* = 2.4 Hz, 1H), 7.34 (dd, *J* = 8.6, 2.4 Hz, 1H), 6.93 (d, *J* = 8.6 Hz, 1H), 3.93 (s, 3H), 2.88 – 2.78 (m, 2H), 2.66 – 2.54 (m, 2H), 2.44 (dt, *J* = 11.6, 8.7 Hz, 1H), 2.16 – 2.04 (m, 1H). LCMS (Method B) *t<sub>R</sub>* = 1.100 min, does not ionize by ESI.

Step B: Phenyl 5-(1-cyanocyclobutyl)-2-methoxybenzoate

1-(3-Bromo-4-methoxyphenyl)cyclobutane-1-carbonitrile (531 μL, 3.43 mmol), Pd(OAc)<sub>2</sub> (39 mg, 0.17 mmol), P(<sup>t</sup>Bu<sub>4</sub>).HBF<sub>4</sub> (199 mg, 0.69 mmol) and phenol (323 mg, 3.43 mmol) were taken up in anhydrous MeCN (13.7 mL) in a sealed tube. Phenyl formate (687 μL, 6.86 mmol) and NEt<sub>3</sub> (1.43 mL, 10.3 mmol) were added and the mixture heated to 90 °C for 18 h. This reaction was performed in quadruplicate. Upon cooling the four reactions were combined, filtered through celite, and concentrated. The residue was dissolved in EtOAc and washed with water. The crude was purified by flash chromatography and afforded 3.72 g (12.1 mmol, 88%) of the title compound as a colorless solid. <sup>1</sup>H NMR (CDCl<sub>3</sub>) δ 8.04 (d, *J* = 2.6 Hz, 1H), 7.61 (dd, *J* = 8.7, 2.6 Hz, 1H), 7.49 – 7.42 (m, 2H), 7.33 – 7.23 (m, 3H), 7.09 (d, *J* = 8.7 Hz, 1H), 3.98 (s, 3H), 2.93 – 2.83 (m, 2H), 2.66 (dt, *J* = 11.8, 9.0 Hz, 2H), 2.55 – 2.41 (m, 1H), 2.19 – 2.06 (m, 1H). LCMS (Method A) *t<sub>R</sub>* = 1.710 min, *m/z* = 308.1 [M+H]<sup>+</sup>.

Step C: Phenyl 5-(1-cyanocyclobutyl)-2-hydroxybenzoate

Phenyl 5-(1-cyanocyclobutyl)-2-methoxybenzoate (3.72 g, 12.1 mmol) was reacted following General Procedure L. Purification by flash chromatography afforded the title compound (3.47 g, 11.84 mmol, 98%) as a colorless oil. <sup>1</sup>H NMR (400 MHz, CDCl<sub>3</sub>) δ 10.55 (s, 1H), 8.09 (d, *J* = 2.5 Hz, 1H), 7.59 (dd, *J* = 8.7, 2.5 Hz, 1H), 7.52 – 7.43 (m, 2H), 7.34 (d, *J* = 7.4 Hz, 1H), 7.25 – 7.20 (m, 2H), 7.09 (d, *J* = 8.7 Hz, 1H), 2.91 – 2.81 (m, 2H), 2.72 – 2.59 (m, 2H), 2.53 – 2.38 (m, 1H), 2.16 – 2.05 (m, 1H). LCMS (Method A): *t<sub>R</sub>* = 1.200 min, *m/z* = 294.1 [M+H]<sup>+</sup>.

Step D: Phenyl 5-(1-cyanocyclobutyl)-2-hydroxy-3-nitrobenzoate

Phenyl 5-(1-cyanocyclobutyl)-2-hydroxybenzoate (2.93 g, 10 mmol) was dissolved in DCE/H<sub>2</sub>O (1:1, 20 mL) and cooled to 0 °C in an ice/water bath. Tetrabutylammonium bromide (161 mg, 0.50 mmol) was added, followed by HNO<sub>3</sub> (conc., 1.3 mL, 20 mmol). The mixture was stirred vigorously at 60 °C for 16 h, then cooled, diluted with CH<sub>2</sub>Cl<sub>2</sub>, and washed with water. The crude was purified by flash chromatography. The title product was obtained (2.71 g, 8.0 mmol, 80%) as a pale-yellow solid. <sup>1</sup>H NMR (400 MHz, CDCl<sub>3</sub>) δ 8.42 (d, *J* = 2.5 Hz, 1H), 8.31 (d, *J* = 2.6 Hz, 1H), 7.55 – 7.48 (m, 2H), 7.43 – 7.35 (m, 1H), 7.32 – 7.24 (m, 3H), 3.00 – 2.89 (m, 2H), 2.76 – 2.63 (m, 2H), 2.61 – 2.49 (m, 1H), 2.25 – 2.11 (m, 1H). LCMS (Method B) *t<sub>R</sub>* = 1.18 min, *m/z* = 339.0 [M+H]<sup>+</sup>.

Step E: Phenyl 3-amino-5-(1-cyanocyclobutyl)-2-hydroxybenzoate

Phenyl 5-(1-cyanocyclobutyl)-2-hydroxy-3-nitrobenzoate (2.71 g, 8.0 mmol) was reacted according to General Procedure C. Purification by flash chromatography afforded the title compound (2.15 g (7.0 mmol, 87%) as a cream solid. <sup>1</sup>H NMR (400 MHz, CDCl<sub>3</sub>) δ 10.70 (d, *J* = 0.7 Hz, 1H), 7.52 – 7.46 (m, 2H), 7.48 (d, *J* = 2.3 Hz, 1H), 7.38 – 7.32 (m, 1H), 7.27 – 7.22 (m,

2H), 6.98 (dd,  $J = 2.3, 0.7$  Hz, 1H), 2.90 – 2.77 (m, 2H), 2.71 – 2.58 (m, 2H), 2.54 – 2.39 (m, 1H), 2.16 – 2.07 (m, 1H). LCMS (Method B)  $t_R = 1.08$  min,  $m/z = 309.2$  [M+H]<sup>+</sup>.

Step F: Phenyl 3-((4-bromo-2-hydroxyphenyl)sulfonamido)-5-(1-cyanocyclobutyl)-2-hydroxybenzoate

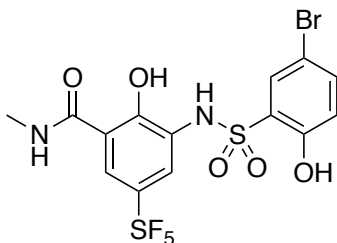
Phenyl 3-amino-5-(1-cyanocyclobutyl)-2-hydroxybenzoate (462 mg, 1.5 mmol) and 4-bromo-2-hydroxybenzenesulfonyl chloride (550 mg, 2.0 mmol) were reacted following General Procedure D. Purification by flash chromatography afforded the title compound (102 mg, 0.19 mmol, 12%) as a colorless solid. <sup>1</sup>H NMR (400 MHz, CDCl<sub>3</sub>)  $\delta$  8.08 (d,  $J = 8.7$  Hz, 1H), 7.79 – 7.72 (m, 2H), 7.52 – 7.44 (m, 3H), 7.35 (t,  $J = 7.5$  Hz, 1H), 7.23 – 7.16 (m, 4H), 6.86 (dd,  $J = 8.7, 2.5$  Hz, 1H), 2.90 – 2.78 (m, 4H), 2.63 – 2.52 (m, 2H), 2.51 – 2.38 (m, 1H), 2.18 – 2.04 (m, 1H).

Step G: 3-((4-Bromo-2-hydroxyphenyl)sulfonamido)-5-(1-cyanocyclobutyl)-2-hydroxybenzoic acid

Phenyl 3-((4-bromo-2-hydroxyphenyl)sulfonamido)-5-(1-cyanocyclobutyl)-2-hydroxybenzoate (27 mg, 0.05 mmol) was reacted following General Procedure E (at r.t.) to afford the title compound (13 mg, 0.028 mmol, 56%) as a colorless solid. <sup>1</sup>H NMR (400 MHz, MeOH-*d*<sub>4</sub>)  $\delta$  7.95 (d,  $J = 8.8$  Hz, 1H), 7.63 (d,  $J = 2.4$  Hz, 1H), 7.56 (d,  $J = 2.4$  Hz, 1H), 7.15 (d,  $J = 2.4$  Hz, 1H), 6.82 (dd,  $J = 8.8, 2.4$  Hz, 1H), 2.82 – 2.70 (m, 2H), 2.58 – 2.48 (m, 2H), 2.44 – 2.30 (m, 1H), 2.13 – 2.01 (m, 1H). LCMS  $t_R = 1.35$  min,  $m/z = 466.8, 468.7$  [M+H]<sup>+</sup>; Purity (AUC)  $\geq 95\%$ ; HRMS (ESI/TOF) [M+H]<sup>+</sup> *calculated* for C<sub>18</sub>H<sub>16</sub>BrN<sub>2</sub>O<sub>6</sub>S 466.9907, *found* 466.9913.

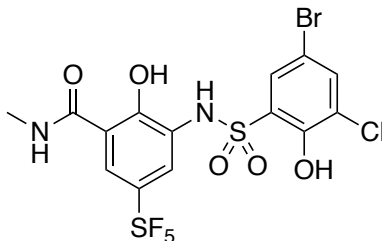
### 6.2.3 Synthesis of methyl amide analogs

#### *3-((5-Bromo-2-hydroxyphenyl)sulfonamido)-2-hydroxy-N-methyl-5-(pentafluorosulfanyl)benzamide (VU0849833)*



Methyl 3-((5-bromo-2-hydroxyphenyl)sulfonamido)-2-hydroxy-5-(pentafluorosulfanyl)benzoate (26 mg, 0.05 mmol) was reacted following General Procedure F. Purification by preparative HPLC afforded the title compound (7 mg, 0.013 mmol, 26%) as a colorless solid. <sup>1</sup>H NMR (400 MHz, CDCl<sub>3</sub>) δ 8.34 (s, 1H), 8.05 (s, 2H), 7.68 (d, *J* = 2.4 Hz, 1H), 7.50 (dd, *J* = 8.8, 2.4 Hz, 1H), 7.28 (s, 1H), 6.87 (d, *J* = 8.8 Hz, 1H), 4.00 (s, 3H). <sup>19</sup>F NMR (376 MHz, CDCl<sub>3</sub>) δ 83.3 (p, *J* = 150 Hz, 1F), 63.7 (d, *J* = 150 Hz, 4F). LCMS (Method A) *t*<sub>R</sub> = 1.890 min, *m/z* = 527.9, 529.9 [M+H]<sup>+</sup>; Purity (AUC) ≥ 95%.

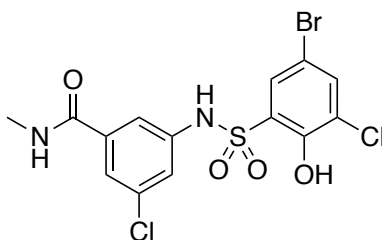
#### *3-((5-Bromo-3-chloro-2-hydroxyphenyl)sulfonamido)-2-hydroxy-N-methyl-5-(pentafluorosulfanyl)benzamide (VU0849820)*



Methyl 3-((5-bromo-3-chloro-2-hydroxyphenyl)sulfonamido)-2-hydroxy-5-(pentafluorosulfanyl)benzoate (18 mg, 0.03 mmol) was reacted following General Procedure F.

Purification by preparative HPLC afforded the title compound (3 mg, 0.005 mmol, 17%) as a colorless solid.  $^1\text{H}$  NMR (400 MHz,  $\text{CDCl}_3$ )  $\delta$  8.04 (d,  $J = 2.4$  Hz, 1H), 7.72 (d,  $J = 2.4$  Hz, 1H), 7.64 (d,  $J = 2.3$  Hz, 1H), 7.53 (d,  $J = 2.3$  Hz, 1H), 6.42 (br s, 1H), 3.04 (d,  $J = 4.9$  Hz, 3H).  $^{19}\text{F}$  NMR (376 MHz,  $\text{CDCl}_3$ )  $\delta$  84.0 (p,  $J = 150$  Hz, 1F), 64.1 (d,  $J = 150$  Hz, 4F). LCMS (Method B)  $t_{\text{R}} = 1.16$  min,  $m/z = 561.1, 563.1$   $[\text{M}+\text{H}]^+$ ; Purity (AUC)  $\geq 95\%$ .

*3-((5-Bromo-3-chloro-2-hydroxyphenyl)sulfonamido)-5-chloro-N-methylbenzamide*  
*(VU0850031)*



*Step A: Methyl 3-((5-bromo-3-chloro-2-hydroxyphenyl)sulfonamido)-5-chlorobenzoate*

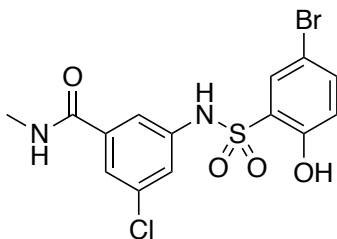
Methyl 3-amino-5-chlorobenzoate (50 mg, 0.27 mmol) was reacted with 5-bromo-3-chloro-2-hydroxy-benzenesulfonyl chloride following General Procedure D. After purification by flash chromatography, the title compound was obtained (64 mg, 0.070 mmol, 26%).  $^1\text{H}$  NMR (400 MHz, Chloroform-*d*)  $\delta$  7.76 (t,  $J = 1.7$  Hz, 1H), 7.73 (d,  $J = 2.4$  Hz, 1H), 7.64 (t,  $J = 1.7$  Hz, 1H), 7.61 (d,  $J = 2.4$  Hz, 1H), 7.43 (t,  $J = 2.4$  Hz, 1H), 3.89 (s, 3H). LCMS (Method B)  $t_{\text{R}} = 1.103$  min,  $m/z = 471.1$   $[\text{M}+\text{NH}_4]^+$ ; Purity (AUC)  $\geq 50\%$ .

*Step B: 3-((5-Bromo-3-chloro-2-hydroxyphenyl)sulfonamido)-5-chloro-N-methylbenzamide*

Methyl 3-((5-bromo-3-chloro-2-hydroxyphenyl)sulfonamido)-5-chlorobenzoate (64 mg, 0.070 mmol) was reacted following General Procedure F. Purification by preparative HPLC afforded the title compound (15 mg, 0.033 mmol, 47%).  $^1\text{H}$  NMR (400 MHz, Chloroform-*d*)  $\delta$  8.62 (br s, 1H),

7.70 (d,  $J = 2.4$  Hz, 1H), 7.61 (d,  $J = 2.4$  Hz, 1H), 7.57 (t,  $J = 1.9$  Hz, 1H), 7.52 (t,  $J = 1.9$  Hz, 1H), 7.40 (t,  $J = 1.9$  Hz, 1H), 6.32 (br d,  $J = 5.0$  Hz, 1H), 3.06 (d,  $J = 5.0$  Hz, 3H). LCMS (Method B)  $t_R = 0.984$  min,  $m/z = 453.1$ ,  $[M+H]^+$ ; Purity (AUC)  $\geq 95\%$ .

*3-((5-Bromo-2-hydroxyphenyl)sulfonamido)-5-chloro-N-methylbenzamide (VU0850029)*



*Step A: Methyl 3-((5-bromo-3-2-hydroxyphenyl)sulfonamido)-5-chlorobenzoate*

Methyl 3-amino-5-chlorobenzoate (50 mg, 0.27 mmol) was reacted with 5-bromo-2-hydroxybenzenesulfonyl chloride following General Procedure D. After purification by flash chromatography, the title compound was obtained (86 mg, 0.15 mmol, 56%). LCMS (Method B)  $t_R = 1.052$  min,  $m/z = 552.2$   $[M+CH_3OH+H]^+$ ; Purity (AUC)  $\geq 74\%$ .

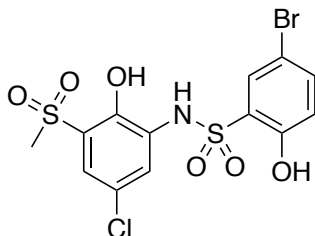
*Step B: 3-((5-Bromo-2-hydroxyphenyl)sulfonamido)-5-chloro-N-methylbenzamide*

3-((5-Bromo-2-hydroxyphenyl)sulfonamido)-5-chlorobenzoate (86 mg, 0.15 mmol) was reacted following General Procedure F. Purification by preparative HPLC afforded the title compound (18 mg, 0.043 mmol, 29%).  $^1H$  NMR (400 MHz, Methanol- $d_4$ )  $\delta$  7.82 (d,  $J = 2.6$  Hz, 1H), 7.52 (t,  $J = 1.8$  Hz, 1H), 7.49 (dd,  $J = 8.8, 2.5$  Hz, 1H), 7.44 (t,  $J = 1.8$  Hz, 1H), 7.34 (t,  $J = 1.8$  Hz, 1H), 6.84 (d,  $J = 8.8$  Hz, 1H), 2.87 (s, 3H). LCMS (Method B)  $t_R = 0.903$  min,  $m/z = 419.2, 422.2$   $[M+H]^+$ ; Purity (AUC)  $\geq 95\%$ .



## 6.2.4 Synthesis of methyl sulfone analogs

### *5-Bromo-N-(3-chloro-5-(methylsulfonyl)phenyl)-2-hydroxybenzenesulfonamide (VU0829581)*



#### Step A: 4-Chloro-2-(methylthio)-6-nitrophenol

2-Bromo-4-chloro-6-nitrophenol (3000 mg, 11.9 mmol) was reacted with dimethyl disulfide General procedure N. Purification by flash chromatography afforded the title compound (1893 mg, 8.6 mmol, 73%). <sup>1</sup>H NMR (400 MHz, Chloroform-d) δ 11.04 (br s, 1H), 7.89 (d, *J* = 2.4 Hz, 1H), 7.32 (d, *J* = 2.4 Hz, 1H), 2.50 (s, 3H). LCMS (Method B): *t*<sub>R</sub> = 1.063 min, does not ionize by ESI; Purity (AUC) ≥ 95%.

#### Step B: 4-Chloro-2-(methylsulfonyl)-6-nitrophenol

4-Chloro-2-(methylthio)-6-nitrophenol (1024 mg, 4.66 mmol) was reacted with Oxone following General Procedure O. A yellow solid was obtained as a crude and it was taken forward without further purification (1155 mg, 4.59 mmol, 98%). <sup>1</sup>H NMR (400 MHz, CDCl<sub>3</sub>) δ 11.40 (s, 1H), 8.39 (d, *J* = 2.7 Hz, 1H), 8.31 (d, *J* = 2.7 Hz, 1H), 7.26 (s, 1H), 3.34 (s, 3H); Purity (H-NMR) ≥ 95%.

#### Step C: 2-Amino-4-chloro-6-(methylsulfonyl)phenol

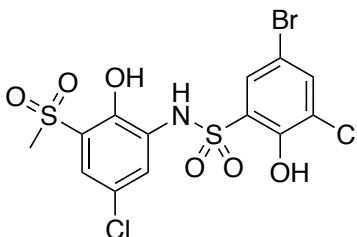
4-Chloro-2-(methylsulfonyl)-6-nitrophenol (600 mg, 2.38 mmol) was reacted following General Procedure C. ISCO flash chromatography afforded the title compound as a brown solid (408 mg, 1.84 mmol, 77%). <sup>1</sup>H NMR (400 MHz, CDCl<sub>3</sub>) δ 7.00 (d, *J* = 2.3 Hz, 1H), 6.86 (d, *J* = 2.4 Hz,

1H), 3.12 (s, 3H). LCMS (Method B):  $t_R = 0.584$  min,  $m/z = 222.1, 224.1$   $[M+H]^+$ ; Purity (AUC)  $\geq 95\%$ .

*Step D: 5-Bromo-N-(5-chloro-2-hydroxy-3-(methylsulfonyl)phenyl)-2-hydroxybenzenesulfonamide*

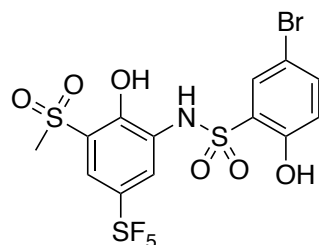
Amino-4-chloro-6-(methylsulfonyl)phenol (21 mg, 0.09 mmol) and 5-bromo-2-hydroxybenzenesulfonyl chloride were reacted following General Procedure D. Purification by preparative HPLC afforded the title compound (11 mg, 0.024 mmol, 26%).  $^1H$  NMR (400 MHz,  $CDCl_3$ )  $\delta$  9.13 (s, 1H), 8.33 (s, 1H), 7.72 (d,  $J = 2.5$  Hz, 1H), 7.63 (d,  $J = 2.4$  Hz, 1H), 7.54 (dd,  $J = 8.9, 2.4$  Hz, 1H), 7.48 (d,  $J = 2.4$  Hz, 1H), 7.18 (s, 1H), 6.91 (d,  $J = 8.9$  Hz, 1H), 3.08 (s, 3H). LCMS (Method B):  $t_R = 1.71$  min,  $m/z = 475.1$   $[M+NH_4]^+$ ; Purity (AUC)  $\geq 95\%$ .

*5-Bromo-3-chloro-N-(5-chloro-2-hydroxy-3-(methylsulfonyl)phenyl)-2-hydroxybenzenesulfonamide (VU0829548)*



Amino-4-chloro-6-(methylsulfonyl)phenol (21 mg, 0.09 mmol) was reacted with 5-bromo-3-chloro-2-hydroxybenzenesulfonyl chloride following General Procedure D. Purification by preparative HPLC afforded the title compound (12.2 mg, 0.024 mmol, 28%) as a colorless solid.  $^1H$  NMR (400 MHz,  $CDCl_3$ )  $\delta$  7.76 (d,  $J = 2.5$  Hz, 1H), 7.74 (d,  $J = 2.4$  Hz, 1H), 7.69 (d,  $J = 2.4$  Hz, 1H), 7.45 (d,  $J = 2.5$  Hz, 1H), 3.11 (s, 3H). LCMS:  $t_R = 1.06$  min,  $m/z = 509.1, 511.1$   $[M+NH_4]^+$ ; Purity (AUC)  $\geq 95\%$ .

*5-Bromo-2-hydroxy-N-(2-hydroxy-3-(methylsulfonyl)-5-(pentafluorosulfanyl)phenyl)benzenesulfonamide (VU0830056)*



*Step A: 2-Bromo-4-(pentafluorosulfanyl)phenol*

To 4-(pentafluorosulfanyl)phenol (800 mg, 3.63 mmol) in acetic acid (4 mL) was added FeCl<sub>3</sub> (59 mg, 0.36 mmol). The mixture was cooled to 0 °C and then Br<sub>2</sub> (812 mg, 5.45 mmol) was added. The mixture was allowed to reach room temperature and stirred for 2 h. Then, the solvent was removed under reduced pressure and the crude material was purified by flash chromatography to afford the title compound (439 mg, 1.47 mmol, 41%). <sup>1</sup>H NMR (400 MHz, CDCl<sub>3</sub>) δ 7.90 (d, *J* = 2.6 Hz, 1H), 7.63 (dd, *J* = 9.0, 2.6 Hz, 1H), 7.06 (d, *J* = 9.0 Hz, 1H); Purity (H-NMR) ≥ 95%.

*Step B: 2-(Methylthio)-4-(pentafluorosulfanyl)phenol*

2-Bromo-4-(pentafluorosulfanyl)phenol (439 mg, 1.47 mmol) was reacted with dimethyl disulfide following General Procedure N. Purification by flash chromatography afforded the title compound (84 mg, 0.29 mmol, 20%). <sup>1</sup>H NMR (400 MHz, CDCl<sub>3</sub>) δ 7.89 (d, *J* = 2.7 Hz, 1H), 7.63 (dd, *J* = 9.0, 2.7 Hz, 1H), 7.05 – 6.97 (m, 2H), 2.37 (s, 3H); <sup>19</sup>F NMR (376 MHz, CDCl<sub>3</sub>) δ 85.5 (p, *J* = 151 Hz, 1F), 64.3 (d, *J* = 151 Hz, 4F). LCMS (Method B): t<sub>R</sub> = 0.156 min, *m/z* = 266.0 [M+H]<sup>+</sup>; Purity (AUC) ≥ 90%.

*Step C: 2-(Methylsulfonyl)-4-(pentafluorosulfanyl)phenol*

2-(Methylthio)-4-(pentafluorosulfanyl)phenol (84 mg, 0.32 mmol) was reacted with Oxone following General Procedure O. The crude was taken forward (74 mg). <sup>1</sup>H NMR (400 MHz,

CDCl<sub>3</sub>)  $\delta$  9.25 (s, 1H), 8.11 (d,  $J$  = 2.7 Hz, 1H), 7.91 (dd,  $J$  = 9.2, 2.7 Hz, 1H), 7.13 (d,  $J$  = 9.2 Hz, 1H), 3.18 (s, 3H); <sup>19</sup>F NMR (376 MHz, CDCl<sub>3</sub>)  $\delta$  83.2 (p,  $J$  = 151 Hz, 1F), 64.0 (d,  $J$  = 151 Hz, 4F). LCMS (Method A):  $t_R$  = 1.318 min, does not ionize by ESI.

Step D: 2-(Methylsulfonyl)-6-nitro-4-(pentafluorosulfanyl)phenol

2-(Methylsulfonyl)-4-(pentafluorosulfanyl)phenol (74 mg, crude) was reacted following General Procedure B. Purification by flash chromatography afforded the title compound (68 mg, 0.20 mmol, 62%) as a yellow solid. <sup>1</sup>H NMR (400 MHz, CDCl<sub>3</sub>)  $\delta$  8.81 (s, 1H), 8.70 (s, 1H), 3.38 (s, 3H); <sup>19</sup>F NMR (376 MHz, CDCl<sub>3</sub>)  $\delta$  80.0 (p,  $J$  = 152 Hz, 1F), 63.9 (d,  $J$  = 152 Hz, 4F). LCMS (Method B):  $t_R$  = 0.762 min, does not ionize by ESI; Purity (AUC)  $\geq$  95%.

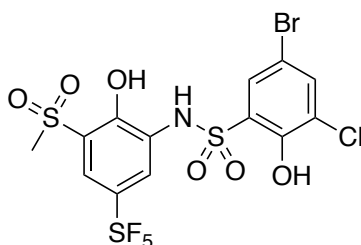
Step E: 2-Amino-6-(Methylsulfonyl)-4-(pentafluorosulfanyl)phenol

2-(Methylsulfonyl)-6-nitro-4-(pentafluorosulfanyl)phenol (235 mg, 0.68 mmol) was reacted following General Procedure C. A light brown solid was obtained as a crude and it was taken forward without further purification (214 mg, 0.68 mmol, quant.). LCMS (Method B):  $t_R$  = 0.118 min,  $m/z$  = 314.1, 315.1 [M+H]<sup>+</sup>; Purity (AUC)  $\geq$  95%.

Step F: 5-Bromo-2-hydroxy-N-(2-hydroxy-3-(methylsulfonyl)-5-(pentafluorosulfanyl)phenyl)benzenesulfonamide

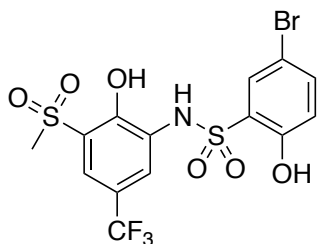
2-Amino-6-(methylsulfonyl)-4-(pentafluorosulfanyl)phenol (40 mg, 0.13 mmol) was reacted with 5-bromo-2-hydroxy-benzenesulfonyl chloride following General Procedure D. Purification by preparative HPLC afforded the title compound (24 mg, 0.044 mmol, 34%). <sup>1</sup>H NMR (400 MHz, CDCl<sub>3</sub>)  $\delta$  8.03 (d,  $J$  = 2.8 Hz, 1H), 7.75 (d,  $J$  = 2.5 Hz, 1H), 7.67 (d,  $J$  = 2.8 Hz, 1H), 7.62 (dd,  $J$  = 8.8, 2.5 Hz, 1H), 6.97 (d,  $J$  = 8.8 Hz, 1H), 3.31 (s, 3H); <sup>19</sup>F NMR (376 MHz, MeOH-*d*<sub>4</sub>)  $\delta$  79.1 (p,  $J$  = 149 Hz, 1F), 59.4 (d,  $J$  = 149 Hz, 4F). LCMS (Method B)  $t_R$  = 1.016 min,  $m/z$  = 547.9, 549.9 [M+H]<sup>+</sup>; Purity (AUC)  $\geq$  95%.

*5-Bromo-3-chloro-2-hydroxy-N-(2-hydroxy-3-(methylsulfonyl)-5-(pentafluorosulfanyl)phenyl)benzenesulfonamide (VU0830070)*



2-Amino-6-(methylsulfonyl)-4-(pentafluorosulfanyl)phenol (21 mg, 0.09 mmol) and 5-bromo-3-chloro-2-hydroxy-benzenesulfonyl chloride was reacted following General Procedure D. Purification by preparative HPLC afforded the title compound (32 mg, 0.055 mmol, 42%). <sup>1</sup>H NMR (400 MHz, CDCl<sub>3</sub>) δ 8.16 (d, *J* = 2.5 Hz, 1H), 7.85 (d, *J* = 2.4 Hz, 1H), 7.78 (d, *J* = 2.4 Hz, 1H), 7.71 (d, *J* = 2.5 Hz, 1H), 3.17 (s, 3H); <sup>19</sup>F NMR (376 MHz, CDCl<sub>3</sub>) δ 79.0 (p, *J* = 151 Hz, 1F), 60.7 (d, *J* = 151 Hz, 4F). LCMS (Method B) *t*<sub>R</sub> = 1.113 min, *m/z* = 566.3, 569.9 [M+H]<sup>+</sup>; Purity (AUC) ≥ 95%.

*5-Bromo-3-chloro-2-hydroxy-N-(2-hydroxy-3-(methylsulfonyl)-5-(trifluoromethyl)phenyl)benzenesulfonamide (VU0830460)*



Step A: 2-(Methylthio)-4-(trifluoromethyl)phenol

2-Bromo-4-(trifluoromethyl)phenol (700 mg, 2.90 mmol) was reacted with dimethyl disulfide following General Procedure N. The crude was taken forward (868 mg). LCMS (Method A):  $t_R = 1.509$  min,  $m/z = 209.1$   $[M+H]^+$ .

Step B: 2-(Methylsulfonyl)-4-(trifluoromethyl)phenol

2-(Methylthio)-4-(trifluoromethyl)phenol (868 mg, crude) was reacted with Oxone following General Procedure O. Purification by flash chromatography afforded the title compound (220 mg, 0.92 mmol, 32%).  $^1H$  NMR (400 MHz, Chloroform-*d*)  $\delta$  9.23 (br s, 1H), 7.98 (d,  $J = 1.9$  Hz, 1H), 7.76 (dd,  $J = 8.7, 1.9$  Hz, 1H), 7.16 (d,  $J = 8.7$  Hz, 1H), 3.17 (s, 3H). LCMS (Method B):  $t_R = 0.967$  min,  $m/z = 266.0$   $[M+H]^+$ ; Purity (AUC)  $\geq 80\%$ .

Step C: 2-(Methylsulfonyl)-6-nitro-4-(trifluoromethyl)phenol

2-(Methylsulfonyl)-4-(trifluoromethyl)phenol (220 mg, 0.92 mmol) was reacted following General Procedure B (Heated to 50 °C and stirred overnight). The crude was taken forward (211 mg).  $^1H$  NMR (400 MHz, Chloroform-*d*)  $\delta$  8.69 (d,  $J = 2.2$  Hz, 1H), 8.59 (d,  $J = 2.2$  Hz, 1H), 3.37 (s, 3H).  $^{19}F$  NMR (376 MHz, Chloroform-*d*)  $\delta$  -62.4 (3F). LCMS (Method B):  $t_R = 0.808$  min, does not ionize by ESI.

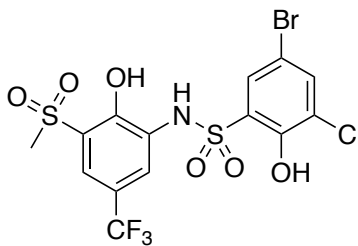
Step D: 2-Amino-6-(methylsulfonyl)-4-(trifluoromethyl)phenol

2-(Methylsulfonyl)-6-nitro-4-(trifluoromethyl)phenol (211 mg, crude) was reacted following General Procedure C. The crude was taken forward (171 mg).  $^1H$  NMR (400 MHz, Chloroform-*d*)  $\delta$  7.31 (dd,  $J = 2.1, 1.0$  Hz, 1H), 7.10 (d,  $J = 2.1$  Hz, 1H), 3.15 (s, 3H).  $^{19}F$  NMR (376 MHz, Chloroform-*d*)  $\delta$  -62.4 (3F). LCMS (Method B):  $t_R = 0.748$  min,  $m/z = 256.1$   $[M+H]^+$ .

Step \_\_\_\_\_ E: 5-Bromo-3-2-hydroxy-N-(2-hydroxy-3-(methylsulfonyl)-5-(trifluoromethyl)phenyl)benzenesulfonamide

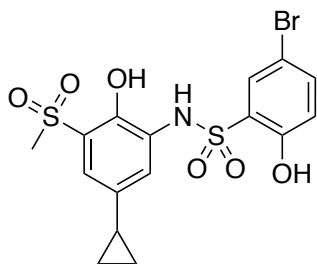
2-Amino-6-(methylsulfonyl)-4-(trifluoromethyl)phenol (30 mg, 0.096 mmol) was reacted with 5-bromo-2-hydroxy-benzenesulfonyl chloride following General Procedure D. Purification by preparative HPLC afforded the title compound (16 mg, 0.032 mmol, 3%). <sup>1</sup>H NMR (400 MHz, Chloroform-*d*) δ 9.61 (br s, 1H), 8.29 (br s, 1H), 7.96 (s, 1H), 7.77 (s, 1H), 7.65 (d, *J* = 2.5 Hz, 1H), 7.55 (dd, *J* = 8.8, 2.5 Hz, 1H), 6.91 (d, *J* = 8.8 Hz, 1H), 3.12 (s, 3H). <sup>19</sup>F NMR (376 MHz, Chloroform-*d*) -65.4. LCMS (Method A): *t*<sub>R</sub> = 1.624 min, *m/z* = 489.7 [M+H]<sup>+</sup>; Purity (AUC) ≥ 95%.

*5-Bromo-3-chloro-2-hydroxy-N-(2-hydroxy-3-(methylsulfonyl)-5-(trifluoromethyl)phenyl)benzenesulfonamide (VU0830459)*



2-Amino-6-(methylsulfonyl)-4-(trifluoromethyl)phenol (30 mg, 0.096 mmol) was reacted with 5-bromo-3-chloro-2-hydroxy-benzenesulfonyl following General Procedure D. Purification by preparative HPLC afforded the title compound (18 mg, 0.034 mmol, 35%). <sup>1</sup>H NMR (400 MHz, Chloroform-*d*) δ 9.67 (br s, 1H), 8.01 (d, *J* = 2.3 Hz, 1H), 7.76 (d, *J* = 2.3 Hz, 1H), 7.75 – 7.73 (m, 1H), 7.70 (d, *J* = 2.3 Hz, 1H), 7.60 (br s, 1H), 7.49 (br s, 1H), 3.15 (s, 3H). <sup>19</sup>F NMR (376 MHz, Chloroform-*d*) δ -65.4; LC-MS (Method B): *t*<sub>R</sub> = 1.062 min, *m/z* = 548.1 [M+Na]<sup>+</sup>; Purity (AUC) ≥ 95%.

*5-Bromo-N-(5-cyclopropyl-2-hydroxy-3-(methylsulfonyl)phenyl)-2-hydroxybenzenesulfonamide*  
(VU0832278)



Step A: 2-(Benzyloxy)-5-chloro-1-(methylsulfonyl)-3-nitrobenzene

Amino-4-chloro-6-(methylsulfonyl)phenol (150 mg, 0.60 mmol) was reacted following General Procedure Z. Purification by flash chromatography afforded the title compound (57 mg, 0.17 mmol, 28%). <sup>1</sup>H NMR (400 MHz, Chloroform-*d*) δ 8.27 (d, *J* = 2.7 Hz, 1H), 8.16 (d, *J* = 2.7 Hz, 1H), 7.63 – 7.53 (m, 2H), 7.49 – 7.36 (m, 3H), 5.24 (s, 2H), 3.22 (s, 3H). LCMS (Method B): *t*<sub>R</sub> = 1.109 min, *m/z* = 359.3, 361.3 [M+H]<sup>+</sup>; Purity (AUC) ≥ 95%.

Step B: 2-(Benzyloxy)-5-cyclopropyl-1-(methylsulfonyl)-3-nitrobenzene

2-(Benzyloxy)-5-chloro-1-(methylsulfonyl)-3-nitrobenzene (57 mg, 0.17 mmol) was reacted following General Procedure K. Purification by flash chromatography afforded the title compound (32 mg, 0.092 mmol, 54%). <sup>1</sup>H NMR (400 MHz, Chloroform-*d*) δ 7.97 (d, *J* = 2.4 Hz, 1H), 7.86 (d, *J* = 2.4 Hz, 1H), 7.63 – 7.56 (m, 2H), 7.47 – 7.37 (m, 3H), 5.21 (s, 2H), 3.21 (s, 3H), 2.03 (m, 1H), 1.14 (td, *J* = 7.0, 5.0 Hz, 2H), 0.82 (dt, *J* = 7.0, 5.0 Hz, 2H).

Step C: 2-Amino-4-cyclopropyl-6-(methylsulfonyl)phenol

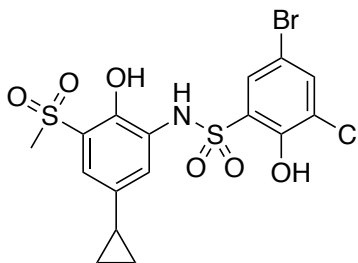
2-(Benzyloxy)-5-cyclopropyl-1-(methylsulfonyl)-3-nitrobenzene (32 mg, 0.092 mmol) was reacted following General Procedure C. The crude was taken forward (19 mg). LCMS (Method B): *t*<sub>R</sub> = 0.482 min, *m/z* = 228.2 [M+H]<sup>+</sup>



Step D: 5-Bromo-N-(5-cyclopropyl-2-hydroxy-3-(methylsulfonyl)phenyl)-2-hydroxybenzenesulfonamide

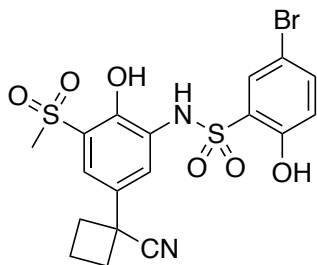
2-Amino-4-cyclopropyl-6-(methylsulfonyl)phenol (9 mg, crude) was reacted with 5-bromo-2-hydroxy-benzenesulfonyl following General Procedure D. Purification by preparative HPLC afforded the title compound (7 mg, 0.015 mmol, 8%). <sup>1</sup>H NMR (400 MHz, Chloroform-*d*) δ 8.86 (br s, 1H), 8.49 (br s, 1H), 7.59 (d, *J* = 2.4 Hz, 1H), 7.50 (dd, *J* = 8.9, 2.2 Hz, 1H), 7.37 (d, *J* = 2.2 Hz, 1H), 7.24 (d, *J* = 2.2 Hz, 1H), 7.13 (br s, 1H), 6.87 (d, *J* = 8.9 Hz, 1H), 3.03 (s, 3H), 1.93 – 1.84 (m, 1H), 1.06 – 0.98 (m, 2H), 0.66 (dt, *J* = 6.5, 4.9 Hz, 2H). LCMS (Method B): *t*<sub>R</sub> = 0.986 min, *m/z* = 480.3 [M+H]<sup>+</sup>; Purity (AUC) ≥ 95%.

*5-Bromo-3-chloro-N-(5-cyclopropyl-2-hydroxy-3-(methylsulfonyl)phenyl)-2-hydroxybenzenesulfonamide (VU0832281)*



2-Amino-4-cyclopropyl-6-(methylsulfonyl)phenol (10 mg, crude) was reacted with 5-bromo-3-chloro-2-hydroxy-benzenesulfonyl chloride following General Procedure D. Purification by preparative HPLC afforded the title compound (9 mg, 0.018 mmol, 10%). <sup>1</sup>H NMR (400 MHz, Chloroform-*d*) δ 7.65 (q, *J* = 2.3 Hz, 2H), 7.40 (d, *J* = 2.3 Hz, 1H), 7.31 (s, 1H), 7.22 (d, *J* = 2.3 Hz, 1H), 3.06 (s, 3H), 1.95 – 1.81 (m, 1H), 1.07 – 0.96 (m, 2H), 0.65 (dt, *J* = 6.6, 4.9 Hz, 2H). LCMS (Method B): *t*<sub>R</sub> = 1.051 min, *m/z* = 498.2 [M+H]<sup>+</sup>; Purity (AUC) ≥ 95%.

*5-Bromo-N-(5-(1-cyanocyclobutyl)-2-hydroxy-3-(methylsulfonyl)phenyl)-2-hydroxybenzenesulfonamide (VU0830613)*



*Step A: 1-(3-Bromo-4-methoxyphenyl)cyclobutane-1-carbonitrile*

2-(3-Bromo-4-methoxyphenyl)acetonitrile (4.52 g, 20 mmol) and 1,3-dibromopropane (2.23 mL, 22 mmol) were dissolved in DMSO (100 mL), to this mixture was added NaH (60% dispersion in mineral oil, 2.0 g, 50 mmol) portion-wise. The solution was stirred for 16 h at r.t., then diluted with EtOAc:Et<sub>2</sub>O (200 mL, 1:1) and washed with water (3 x 400 mL). The combined aqueous layers were back-extracted with further EtOAc (200 mL). The combined organics were washed with sat. aq. NaCl, concentrated. Purification by ISCO flash column afforded 3.65 g (13.7 mmol, 68%) of the title compound as a colorless oil. <sup>1</sup>H NMR (400 MHz, CDCl<sub>3</sub>) δ 7.61 (d, *J* = 2.4 Hz, 1H), 7.34 (dd, *J* = 8.6, 2.4 Hz, 1H), 6.93 (d, *J* = 8.6 Hz, 1H), 3.93 (s, 3H), 2.88 – 2.78 (m, 2H), 2.66 – 2.54 (m, 2H), 2.44 (dt, *J* = 11.6, 8.7 Hz, 1H), 2.16 – 2.04 (m, 1H). LCMS (Method B) t<sub>R</sub> = 1.10 min, does not ionized by ESI; Purity (AUC) ≥ 95%

*Step B: 1-(4-Methoxy-3-(methylthio)phenyl)cyclobutane-1-carbonitrile*

1-(3-Bromo-4-methoxyphenyl)cyclobutane-1-carbonitrile (200 mg, 0.75 mmol) was reacted following General Procedure N-B. Purification by flash chromatography afforded the title compound (174 mg, 0.746 mmol, 99% yield) as a yellow oil. <sup>1</sup>H NMR (400 MHz, CDCl<sub>3</sub>) δ 7.21 – 7.13 (m, 2H), 6.87 – 6.80 (m, 1H), 3.90 (s, 3H), 2.88 – 2.75 (m, 2H), 2.59 (dt, *J* = 9.8, 8.0 Hz,

2H), 2.45 (s, 3H), 2.43 – 2.36 (m, 1H), 2.12 – 2.00 (m, 1H). LCMS (Method B): LCMS (Method B)  $t_R = 1.035$  min  $m/z = 234.2$   $[M+H]^+$ ; Purity (AUC)  $\geq 90\%$ .

Step C: 1-(4-Methoxy-3-(methylsulfonyl)phenyl)cyclobutane-1-carbonitrile

1-(4-Methoxy-3-(methylthio)phenyl)cyclobutane-1-carbonitrile (174 mg, 0.671 mmol) was reacted with Oxone following General Procedure O. A light-yellow solid was obtained as a crude and it was taken forward (188 mg).  $^1H$  NMR (400 MHz,  $CDCl_3$ )  $\delta$  8.03 (d,  $J = 2.5$  Hz, 1H), 7.67 (dd,  $J = 8.6, 2.5$  Hz, 1H), 7.10 (d,  $J = 8.6$  Hz, 1H), 2.91 – 2.81 (m, 1H), 2.68 – 2.58 (m, 2H), 2.53 – 2.40 (m, 1H), 2.17 – 2.07 (m, 1H). LCMS (Method B)  $t_R = 0.756$  min,  $m/z = 283.3$   $[M+NH_4]^+$ .

Step D: 1-(4-Hydroxy-3-(methylsulfonyl)phenyl)cyclobutane-1-carbonitrile

1-(4-Methoxy-3-(methylsulfonyl)phenyl)cyclobutane-1-carbonitrile (188 mg, crude) was reacted following General Procedure L. The crude was taken forward (170 mg).  $^1H$  NMR (400 MHz,  $CDCl_3$ )  $\delta_H$  8.86 (s, 1H), 7.68 (d,  $J = 2.5$  Hz, 1H), 7.58 (dd,  $J = 8.7, 2.5$  Hz, 1H), 7.10 (d,  $J = 8.7$  Hz, 1H), 3.15 (s, 3H), 2.91 – 2.77 (m, 2H), 2.69 – 2.54 (m, 2H), 2.54 – 2.39 (m, 1H), 2.17 – 2.02 (m, 1H). LCMS (Method B)  $t_R = 0.081$  min, does not ionize by ESI.

Step E: 1-(4-Hydroxy-3-(methylsulfonyl)-5-nitrophenyl)cyclobutane-1-carbonitrile

1-(4-Hydroxy-3-(methylsulfonyl)phenyl)cyclobutane-1-carbonitrile (170 mg, 0.68 mmol) was reacted following General Procedure B. Purification by flash chromatography afforded the title compound (145 mg, 0.49 mmol, 73%).  $^1H$  NMR (400 MHz, Chloroform-d)  $\delta$  8.41 (d,  $J = 2.5$  Hz, 1H), 8.33 (dt,  $J = 2.2, 1.0$  Hz, 1H), 3.34 (s, 3H), 2.95 – 2.84 (m, 2H), 2.69 – 2.57 (m, 2H), 2.57 – 2.43 (m, 1H), 2.19 – 2.06 (m, 1H). LCMS (Method B)  $t_R = 0.654$  min,  $m/z = 314.3$   $[M+NH_4]^+$ ; Purity (AUC)  $\geq 95\%$ .

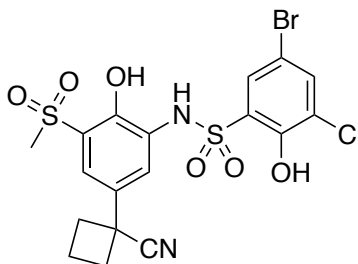
Step F: 1-(3-Amino-4-hydroxy-5-(methylsulfonyl)phenyl)cyclobutane-1-carbonitrile

1-(4-Hydroxy-3-(methylsulfonyl)-5-nitrophenyl)cyclobutane-1-carbonitrile (145 mg, 0.489 mmol) was reacted following General Procedure C. Purification by flash chromatography afforded the title compound (122 mg, 0.458 mmol, 94%). <sup>1</sup>H NMR (400 MHz, Chloroform-d) δ 7.01 (d, *J* = 2.2 Hz, 1H), 6.93 (d, *J* = 2.2 Hz, 1H), 3.13 (s, 3H), 2.83 – 2.72 (m, 2H), 2.62 – 2.50 (m, 2H), 2.41 (dt, *J* = 11.5, 8.8 Hz, 1H), 2.11 – 1.98 (m, 1H). LCMS (Method B) *t<sub>R</sub>* = 0.614 min, *m/z* = 267.2 [M+H]<sup>+</sup>; Purity (AUC) ≥ 95%.

Step G: 5-Bromo-N-(5-(1-cyanocyclobutyl)-2-hydroxy-3-(methylsulfonyl)phenyl)-2-hydroxybenzenesulfonamide

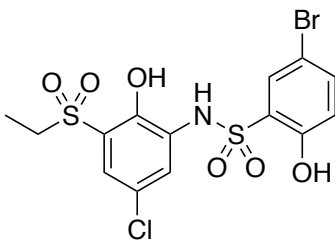
1-(3-Amino-4-hydroxy-5-(methylsulfonyl)phenyl)cyclobutane-1-carbonitrile (11 mg, 0.04 mmol) and 5-bromo-2-hydroxy-benzenesulfonyl chloride were reacted following General Procedure D. Purification by preparative HPLC afforded the title compound (3 mg, 0.006 mmol, 15%). <sup>1</sup>H NMR (400 MHz, CDCl<sub>3</sub>) δ 7.76 (d, *J* = 2.5 Hz, 1H), 7.68 (d, *J* = 2.4 Hz, 1H), 7.60 (dd, *J* = 8.8, 2.5 Hz, 1H), 7.38 (d, *J* = 2.4 Hz, 1H), 6.96 (d, *J* = 8.8 Hz, 1H), 3.27 (s, 3H), 2.80 – 2.65 (m, 2H), 2.56 – 2.24 (m, 3H), 2.15 – 1.94 (m, 1H). LCMS (Method B) *t<sub>R</sub>* = 1.44 min, *m/z* = 501.0, 503.0 [M+H]<sup>+</sup>; Purity (AUC) ≥ 95%.

*5-Bromo-3-chloro-N-(5-(1-cyanocyclobutyl)-2-hydroxy-3-(methylsulfonyl)phenyl)-2-hydroxybenzenesulfonamide (VU0849710)*



1-(3-Amino-4-hydroxy-5-(methylsulfonyl)phenyl)cyclobutane-1-carbonitrile (15 mg, 0.056 mmol) and 5-bromo-3-chloro-2-hydroxy-benzenesulfonyl chloride were reacted following General Procedure D. Purification by preparative HPLC afforded the title compound (8 mg, 0.015 mmol, 27%). <sup>1</sup>H NMR (400 MHz, Acetonitrile-*d*<sub>3</sub>) δ 7.81 (d, *J* = 2.4 Hz, 1H), 7.69 (d, *J* = 2.4 Hz, 1H), 7.61 (d, *J* = 2.4 Hz, 1H), 7.46 (d, *J* = 2.4 Hz, 1H), 3.16 (s, 3H), 2.77 – 2.70 (m, 2H), 2.53 – 2.45 (m, 2H), 2.34 (dq, *J* = 11.5, 8.6 Hz, 1H), 2.06 – 1.97 (m, 1H). LCMS (Method B) *t*<sub>R</sub> = 1.015 min, *m/z* = 552.2, 553.2 [M+NH<sub>4</sub>]<sup>+</sup>; Purity (AUC) ≥ 95%.

*5-Bromo-N-(5-chloro-3-(ethylsulfonyl)-2-hydroxyphenyl)-2-hydroxybenzenesulfonamide*  
(VU0830483)



Step A: 4-Chloro-2-(ethylthio)-6-nitrophenol

2-Bromo-4-Chloro-6-nitrophenol (500 mg, 1.98 mmol) was reacted with diethyl disulfide following General Procedure N to afford the title compound as a crude (463 mg) <sup>1</sup>H NMR (400 MHz, Chloroform-*d*) δ 11.02 (br s, 1H), 7.89 (s, 1H), 7.40 (s, 1H), 2.98 (q, *J* = 7.5 Hz, 2H), 1.37 (t, *J* = 7.5 Hz, 3H). LCMS (Method A): *t*<sub>R</sub> = 1.722 min, does not ionize by ESI.

Step B: 4-Chloro-2-(ethylsulfonyl)-6-nitrophenol

4-Chloro-2-(ethylthio)-6-nitrophenol (463 mg, crude) was reacted with Oxone following General Procedure O. Purification by flash chromatography afforded the title compound (300 mg, 0.77 mmol, 39%). <sup>1</sup>H NMR (400 MHz, Chloroform-*d*) δ<sub>H</sub> 11.35 (br s, 1H), 8.38 (d, *J* = 2.7 Hz, 1H),

8.27 (d,  $J = 2.7$  Hz, 1H), 3.49 (q,  $J = 7.5$  Hz, 2H), 1.33 (t,  $J = 7.5$  Hz, 3H). LCMS (Method B): 0.824 min,  $m/z = 267.1$   $[M+H]^+$ . Purity (AUC)  $\geq 68\%$ .

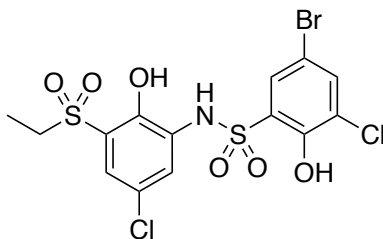
Step C: 2-Amino-4-chloro-6-(ethylsulfonyl)-phenol

4-Chloro-2-(ethylsulfonyl)-6-nitrophenol (300 mg, 0.77 mmol) was reacted following General Procedure C. The crude was taken forward (240 mg).  $^1\text{H}$  NMR (400 MHz, Chloroform- $d$ )  $\delta$  6.91 (d,  $J = 3.3$  Hz, 1H), 6.84 (d,  $J = 3.3$  Hz, 1H), 3.16 (q,  $J = 7.4$  Hz, 2H), 1.30 (t,  $J = 7.4$  Hz, 3H). LCMS (Method B):  $t_R = 0.728$  min,  $m/z = 236.2, 238.2$ .

Step D: 5-Bromo-N-(5-chloro-3-(ethylsulfonyl)-2-hydroxyphenyl)-2-hydroxybenzenesulfonamide

2-Amino-4-chloro-6-(ethylsulfonyl)-phenol (40 mg, crude) was reacted with 5-bromo-2-hydroxybenzenesulfonyl chloride following General Procedure D. Purification by preparative HPLC (basic method) afforded the title compound (5 mg, 0.011 mmol).  $^1\text{H}$  NMR (400 MHz, Chloroform- $d$ )  $\delta$  7.73 (d,  $J = 2.5$  Hz, 1H), 7.65 (d,  $J = 2.4$  Hz, 1H), 7.52 (dd,  $J = 8.8, 2.4$  Hz, 1H), 7.42 (d,  $J = 2.5$  Hz, 1H), 7.20 (s, 1H), 6.88 (d,  $J = 8.8$  Hz, 1H), 3.12 (q,  $J = 7.4$  Hz, 2H), 1.21 (t,  $J = 7.4$  Hz, 3H). LCMS:  $t_R$  (Method B) = 1.020 min,  $m/z = 488.1, 490.1$   $[M+NH_4]^+$ ; Purity (AUC)  $\geq 95\%$ .

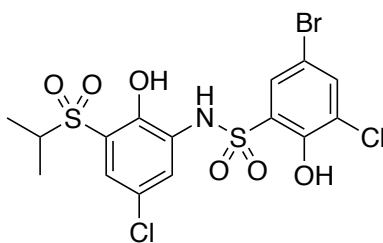
*5-Bromo-3-Chloro-N-(5-chloro-3-(ethylsulfonyl)-2-hydroxyphenyl)-2-hydroxybenzenesulfonamide (VU0830465)*



2-Amino-4-chloro-6-(ethylsulfonyl)-phenol (60 mg, crude) was reacted with 5-bromo-3-chloro-2-hydroxybenzenesulfonyl chloride following General Procedure D. Purification by preparative

HPLC afforded the title compound (18 mg, 0.036 mmol). <sup>1</sup>H NMR (400 MHz, Chloroform-*d*) δ 7.76 (d, *J* = 2.5 Hz, 1H), 7.73 (d, *J* = 2.4 Hz, 1H), 7.68 (d, *J* = 2.4 Hz, 1H), 7.41 (d, *J* = 2.5 Hz, 1H), 3.15 (q, *J* = 7.4 Hz, 3H), 1.24 (t, *J* = 7.4 Hz, 3H). LCMS (Method B): *t*<sub>R</sub> = 1.093 min, *m/z* = 528.1 [M+Na]<sup>+</sup>; Purity (AUC) ≥ 95%.

*5-Bromo-3-chloro-N-(5-chloro-2-hydroxy-3-(isopropylsulfonyl)phenyl)-2-hydroxybenzenesulfonamide (VU0830428)*



*Step A: 4-Chloro-2-(isopropylthio)-6-nitrophenol*

2-Bromo-4-chloro-6-nitrophenol (500 mg, 1.98 mmol) was reacted with diisopropyl disulfide following General Procedure N. The crude was taken forward (661 mg). <sup>1</sup>H NMR (400 MHz, Chloroform-*d*) δ 7.95 (d, *J* = 2.5 Hz, 1H), 7.54 (d, *J* = 2.5 Hz, 1H), 3.57 (hept, *J* = 6.7 Hz, 1H), 1.34 (d, *J* = 6.7 Hz, 6H).

*Step B: 4-Chloro-2-(isopropylsulfonyl)-6-nitrophenol*

4-Chloro-2-(isopropylsulfonyl)-6-nitrophenol (661 mg, crude) was reacted with Oxone following General Procedure O. Purification by flash chromatography afforded the title compound (241 mg) as a mixture with the corresponding sulfoxide. <sup>1</sup>H NMR (400 MHz, Chloroform-*d*) δ 10.84 (br s, 1H), 8.20 (d, *J* = 2.6 Hz, 1H), 7.98 (d, *J* = 2.7 Hz, 1H), 3.29 (hept, *J* = 6.9 Hz, 1H), 1.48 (d, *J* = 7.1 Hz, 3H), 1.04 (d, *J* = 6.8 Hz, 3H). LCMS (Method B): *t*<sub>R</sub> = 0.797 min, *m/z* = 278.8 [M+H]<sup>+</sup>.

Step C: 2-Amino-4-chloro-6-(isopropylsulfonyl)phenol

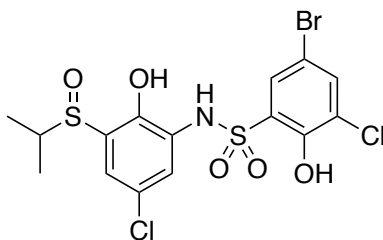
4-Chloro-2-(isopropylsulfonyl)-6-nitrophenol (241 mg, crude mixture) was reacted following General Procedure C. Purification by flash chromatography afforded the title compound as a mixture with the sulfoxide, 3:2 respectively, (81 mg, 0.13 mmol of sulfone, 6%). LCMS (Method B):  $t_{R(\text{sulfoxide})} = 0.132$  min,  $m/z = 234.2, 236.2$   $[\text{M}+\text{H}]^+$ ,  $t_{R(\text{sulfone})} = 0.690$  min,  $m/z = 250.1, 252.0$   $[\text{M}+\text{H}]^+$

Step D: 5-Bromo-3-chloro-N-(5-chloro-2-hydroxy-3-(isopropylsulfonyl)phenyl)-2-hydroxybenzenesulfonamide

2-Amino-4-chloro-6-(isopropylsulfonyl)phenol (38 mg, 0.029 mmol of sulfone), was reacted with 5-bromo-3-chloro-2-hydroxy-benzenesulfonyl following General Procedure D. Purification by preparative HPLC afforded the title compound (7 mg, 0.011 mmol, 40%).  $^1\text{H}$  NMR (400 MHz, Chloroform-*d*)  $\delta$  9.41 (br s, 1H), 7.82 (br s, 1H), 7.77 (d,  $J = 2.4$  Hz, 1H), 7.72 (d,  $J = 2.4$  Hz, 1H), 7.67 (d,  $J = 2.4$  Hz, 1H), 7.37 (d,  $J = 2.4$  Hz, 1H), 7.36 (br s, 1H), 3.19 (hept,  $J = 6.9$  Hz, 1H), 1.26 (d,  $J = 6.9$  Hz, 6H). LCMS (Method B):  $t_R = 1.136$  min,  $m/z = 518.1, 520.1$   $[\text{M}+\text{H}]^+$ ; Purity (AUC)  $\geq 89\%$ .

*5-Bromo-3-chloro-N-(5-chloro-2-hydroxy-3-(isopropylsulfonyl)phenyl)-2-*

*hydroxybenzenesulfonamide (VU0830434)*

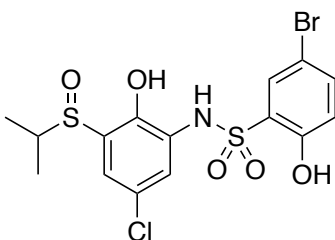


From the procedures in *5-Bromo-3-chloro-N-(5-chloro-2-hydroxy-3-(isopropylsulfonyl)phenyl)-2-hydroxybenzenesulfonamide (VU0830428)*, steps A-B, 5-bromo-3-chloro-*N*-(5-chloro-2-



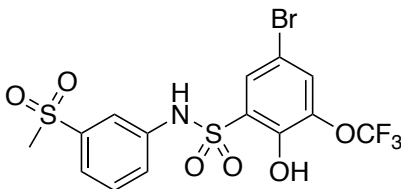
hydroxy-3-(isopropylsulfinyl)phenyl)-2-hydroxybenzenesulfonamide was also obtained (14 mg, 0.028 mmol, 2%). <sup>1</sup>H NMR (400 MHz, Chloroform-*d*) δ 7.70 (d, *J* = 2.4 Hz, 1H), 7.63 (d, *J* = 2.4 Hz, 1H), 7.60 (d, *J* = 2.4 Hz, 1H), 7.54 (br s, 1H), 6.77 (d, *J* = 2.4 Hz, 1H), 3.06 (hept, *J* = 6.9 Hz, 1H), 1.23 (m, 6H). LCMS (Method B): *t*<sub>R</sub> = 1.086 min, *m/z* = 504.1, 506.1 [M+H]<sup>+</sup>; Purity (AUC) ≥ 95%.

*5-Bromo-N-(5-chloro-2-hydroxy-3-(isopropylsulfinyl)phenyl)-2-hydroxybenzenesulfonamide*



2-Amino-4-chloro-6-(isopropylsulfonyl)phenol (43 mg, 0.10 mmol of sulfoxide) was reacted with 5-bromo-2-hydroxy-benzenesulfonyl following General Procedure D. Purification by preparative HPLC afforded the title compound (12 mg, 0.020 mmol, 20%). <sup>1</sup>H NMR (400 MHz, Chloroform-*d*) δ 7.65 (d, *J* = 2.4 Hz, 1H), 7.59 (d, *J* = 2.4 Hz, 1H), 7.48 (dd, *J* = 8.9, 2.4 Hz, 1H), 7.30 (br s, 1H), 6.85 (d, *J* = 8.9 Hz, 1H), 6.78 (d, *J* = 2.4 Hz, 1H), 3.06 (hept, *J* = 6.8 Hz, 1H), 1.22 (d, *J* = 2.1 Hz, 3H), 1.20 (d, *J* = 2.1 Hz, 6H). LCMS (Method B): *t*<sub>R</sub> = 1.022 min, *m/z* = 469.2, 471.1 [M+H]<sup>+</sup>; Purity (AUC) ≥ 83%.

*5-Bromo-2-hydroxy-N-(3-(methylsulfonyl)phenyl)-3-(trifluoromethoxy)benzenesulfonamide (VU0816974)*



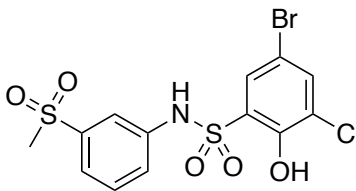
Step A: 3-(Methylsulfonyl)aniline

3-Iodoaniline (300 mg, 1.37 mmol) was reacted with sodium methanesulfinate following General Procedure M. Purification by flash chromatography afforded the title compound (102.9 mg, 0.60 mmol, 44%) as a green oil. <sup>1</sup>H NMR (400 MHz, Methanol-*d*<sub>4</sub>) δ 7.30 (t, *J* = 7.9 Hz, 1H), 7.20 (t, *J* = 2.1 Hz, 1H), 7.17 – 7.12 (m, 1H), 6.99 – 6.93 (m, 1H), 3.06 (s, 3H). LCMS (Method A) *t*<sub>R</sub> = 0.157 min, *m/z* = 172.1 [M+H]<sup>+</sup>; Purity (AUC) ≥ 95%.

Step B: 5-Bromo-2-hydroxy-N-(3-(methylsulfonyl)phenyl)-3-(trifluoromethoxy)benzenesulfonamide

3-(Methylsulfonyl)aniline 14 mg (0.08 mmol) was reacted with 5-Bromo-2-hydroxy-3-(trifluoromethoxy)benzenesulfonyl chloride following General Procedure D. Purification by preparative HPLC afforded the title compound (20 mg, 0.041 mmol, 50%) as a colorless. <sup>1</sup>H NMR (400 MHz, Chloroform-*d*) δ 7.91 (s, 1H), 7.76 (d, *J* = 2.3 Hz, 1H), 7.73 (dt, *J* = 6.7, 1.6 Hz, 1H), 7.65 (d, *J* = 2.3 Hz, 1H), 7.56 – 7.52 (m, 2H), 7.51 (dd, *J* = 2.3, 1.6 Hz, 1H), 7.06 (br s, 1H), 3.07 (s, 3H). <sup>19</sup>F NMR (376 MHz, Chloroform-*d*) δ -61.4 (s, 3F). LCMS (Method A): *t*<sub>R</sub> = 1.652 min, *m/z* = 506.7, 508.7 [M+NH<sub>4</sub>]<sup>+</sup>; Purity (AUC) ≥ 95%.

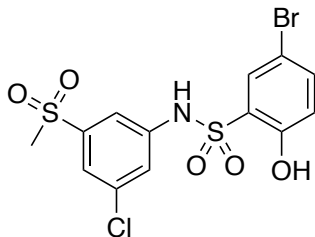
*5-Bromo-3-chloro-2-hydroxy-N-(3-(methylsulfonyl)phenyl)benzenesulfonamide (VU0822856)*



3-(Methylsulfonyl)aniline (20 mg, 0.10 mmol) was reacted with 5-bromo-3-chloro-2-hydroxybenzenesulfonyl chloride following General Procedure D. Purification by preparative HPLC afforded the title compound (25.0 mg, 0.057 mmol, 28%). <sup>1</sup>H NMR (400 MHz, Chloroform-

d)  $\delta$  7.94 (br s, 1H), 7.73 (d,  $J = 2.3$  Hz, 1H), 7.71 (s, 1H), 7.66 (s, 1H), 7.63 (d,  $J = 2.3$  Hz, 1H), 7.57 – 7.49 (m, 2H), 3.07 (s, 3H). LCMS (Method B):  $t_R = 0.996$  min,  $m/z = 458.9$   $[M+NH_4]^+$ ; Purity (AUC)  $\geq 95\%$ .

*5-Bromo-N-(3-chloro-5-(methylsulfonyl)phenyl)-2-hydroxybenzenesulfonamide (VU0816987)*



*Step A: 1-Chloro-3-(methylsulfonyl)-5-nitrobenzene*

1-Chloro-3-iodo-5-nitrobenzene (500 mg, 1.77 mmol) was reacted with sodium methanesulfinate following General Procedure M. Purification by flash chromatography afforded the title compound (189.2 mg, 0.78 mmol, 44%).  $^1H$  NMR (400 MHz, Methanol- $d_4$ )  $\delta$  8.67 (s, 1H), 8.60 (s, 1H), 8.39 (s, 1H), 3.26 (s, 3H). LCMS (Method A):  $t_R = 1.282$  min,  $m/z = 235.8, 237.8$   $[M+H]^+$ ; Purity (AUC)  $\geq 95\%$ .

*Step C: 3-Chloro-5-(methylsulfonyl)aniline*

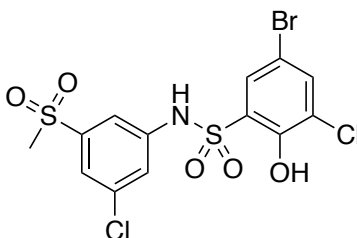
1-Chloro-3-(methylsulfonyl)-5-nitrobenzene (70 mg, 0.30 mmol) was reacted following General Procedure C. Purification by preparative HPLC afforded the title compound (37.8 mg, 0.18 mmol, 61%).  $^1H$  NMR (400 MHz, Methanol- $d_4$ )  $\delta$  7.15 (dd,  $J = 2.2, 1.6$  Hz, 2H), 6.98 (t,  $J = 2.2$  Hz, 1H), 3.09 (s, 3H). LCMS (Method A):  $t_R = 0.176$  min,  $m/z = 206.1, 208.0$   $[M+H]^+$ ; Purity (AUC)  $\geq 95\%$ .

Step D: 5-Bromo-N-(3-chloro-5-(methylsulfonyl)phenyl)-3-ethyl-2-hydroxybenzenesulfonamide

3-Chloro-5-(methylsulfonyl)aniline (20 mg, 0.10 mmol) was reacted with 5-bromo-2-hydroxybenzenesulfonyl chloride following General Procedure D. Purification by preparative HPLC afforded the title compound (20.4 mg, 0.046 mmol, 48%) as a colorless solid. <sup>1</sup>H NMR (400 MHz, Methanol-d<sub>4</sub>) δ 7.88 (d, *J*=2.6, 1H), 7.65 (t, *J* = 1.8 Hz, 1H), 7.58 (t, *J* = 1.8 Hz, 1H), 7.52 (dd, 8.8, 2.6 Hz, 1H), 7.47 (t, 1.8 Hz, 1H), 6.85 (d, *J* = 8.8 Hz, 1H), 3.06 (s, 3H). LCMS (Method A): t<sub>R</sub> = 1.626 min, m/z = 458.7 [M+NH<sub>4</sub>]<sup>+</sup>; Purity (AUC) ≥ 95%.

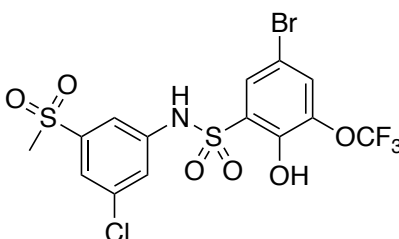
*5-Bromo-3-chloro-N-(3-chloro-5-(methylsulfonyl)phenyl)-2-hydroxybenzenesulfonamide*

**(VU0822864)**



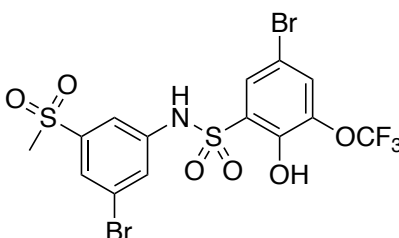
3-Chloro-5-(methylsulfonyl)aniline (50 mg, 0.24 mmol) was reacted with 5-bromo-3-chloro-2-hydroxybenzenesulfonyl following General Procedure D. Purification by preparative HPLC afforded the title compound (37.6 mg, 0.085 mmol, 35%) as a white solid. <sup>1</sup>H NMR (400 MHz, Chloroform-*d*) δ 7.79 (s, 1H), 7.70 (s, 2H), 7.51 (s, 2H), 3.05 (s, 3H). LCMS (Method B): t<sub>R</sub> = 1.072 min, m/z = 492.8 [M+NH<sub>4</sub>]<sup>+</sup>; Purity (AUC) ≥ 95%.

*5-Bromo-N-(3-chloro-5-(methylsulfonyl)phenyl)-2-hydroxy-3-(trifluoromethoxy)benzenesulfonamide (VU0814341)*



3-Chloro-5-(methylsulfonyl)aniline (24 mg, 0.12 mmol) was reacted with 5-bromo-2-hydroxy-3-(trifluoromethoxy)benzenesulfonyl chloride following General Procedure D. Purification by preparative HPLC afforded the title compound (11.9 mg, 0.023 mmol, 20%). <sup>1</sup>H NMR (400 MHz, Chloroform-*d*) δ 7.90 (br s, 1H), 7.78 (d, *J* = 2.4 Hz, 1H), 7.73 (t, *J* = 1.5 Hz, 1H), 7.58 (dd, *J* = 2.4, 1.5 Hz, 1H), 7.51 (d, *J* = 1.9 Hz, 1H), 7.50 (d, *J* = 1.9 Hz, 1H), 7.29 (br s, 1H), 3.04 (s, 3H). <sup>19</sup>F NMR (376 MHz, Chloroform-*d*) δ -61.31 (3F). LCMS (Method B): *t*<sub>R</sub> = 1.126 min, *m/z* = 542.8 [M+NH<sub>4</sub>]<sup>+</sup>; Purity (AUC) ≥ 95%.

*5-Bromo-N-(3-bromo-5-(methylsulfonyl)phenyl)-2-hydroxy-3-(trifluoromethoxy)benzenesulfonamide (VU0821589)*



Step A: 3-Bromo-5-(methylsulfonyl)aniline

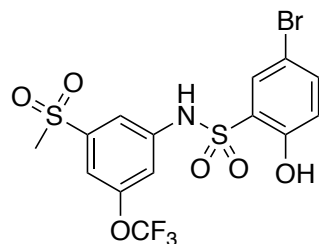
3-Bromo-5-iodoaniline (250 mg, 0.84 mmol) was reacted with sodium methanesulfinate following General Procedure M (reaction temperature was set to 55 °C). Purification by flash

chromatography afforded the title compound (84 mg, 0.34 mmol, 40%). LCMS (Method B)  $t_R = 0.629$  min,  $m/z = 250.0, 251.9$   $[M+H]^+$ ; Purity (AUC)  $\geq 95\%$ .

Step B: 5-Bromo-N-(3-bromo-5-(methylsulfonyl)phenyl)-2-hydroxy-3-(trifluoromethoxy)benzenesulfonamide

3-Bromo-5-(methylsulfonyl)aniline (27 mg, 0.11 mmol) was reacted with 5-bromo-2-hydroxy-3-(trifluoromethoxy)benzenesulfonyl following General Procedure D. Purification by preparative HPLC afforded the title compound (4.2 mg, 0.0074 mmol, 7%) of title compound.  $^1H$  NMR (400 MHz, Chloroform-*d*)  $\delta$  7.87 (t,  $J=1.8$  Hz, 1H), 7.78 (d,  $J= 2.3$  Hz, 1H), 7.64 (t,  $J=1.8$  Hz, 1H), 7.58-7.56 (m, 2H), 3.04 (s, 3H);  $^{19}F$  NMR (376 MHz, Chloroform-*d*)  $\delta$  -58.2 (3F). LCMS (Method A):  $t_R =$  LCMS (Method A):  $t_R = 1.749$  min,  $m/z = 584.5, 586.5$   $[M+NH_4]^+$ ; Purity (AUC)  $\geq 86\%$ .

*5-Bromo-2-hydroxy-N-(3-(methylsulfonyl)-5-(trifluoromethoxy)phenyl)benzenesulfonamide*  
(VU026052)



Step A: Methyl 3-(methylsulfonyl)-5-(trifluoromethoxy)benzoate

Methyl 3-bromo-5-(trifluoromethoxy)benzoate (600 mg, 2.01 mmol) was reacted with sodium methanesulfinate following General Procedure M. Purification by flash chromatography afforded the title compound (270.1 mg, 0.91 mmol, 45%) as a white solid.  $^1H$  NMR (400 MHz, Chloroform-*d*)  $\delta$  8.50 (s, 1H), 8.12 (s, 1H), 7.96 (s, 1H), 3.97 (s, 3H), 3.10 (s, 3H). LCMS (Method B):  $t_R = 0.977$  min, does not ionize by ESI; Purity (AUC)  $\geq 95\%$ .

Step B: 3-(Methylsulfonyl)-5-(trifluoromethoxy)benzoic acid

Methyl 3-(methylsulfonyl)-5-(trifluoromethoxy)benzoate (64 mg, 0.21 mmol) was reacted following General Procedure E. Purification by flash chromatography afforded the title compound (57.7 mg, 0.20 mmol, 97%) as a white solid. <sup>1</sup>H NMR (400 MHz, Chloroform-*d*) δ 8.60 (s, 1H), 8.21 (s, 1H), 8.05 (s, 1H), 3.15 (s, 3H). <sup>19</sup>F NMR (376 MHz, Chloroform-*d*) δ -58.0 (3F). LCMS (Method B): t<sub>R</sub> = 0.824 min, does not ionize by ESI; Purity (AUC) ≥ 95%.

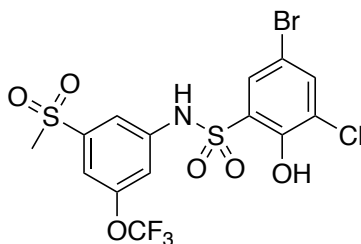
Step C: 3-(Methylsulfonyl)-5-(trifluoromethoxy)aniline

3-(Methylsulfonyl)-5-(trifluoromethoxy)benzoic acid (55 mg, 0.19 mmol) was reacted following General Procedure P. Purification by flash chromatography afforded the title compound (18.2 mg, 0.071 mmol, 37%) as a white solid. <sup>1</sup>H NMR (400 MHz, Chloroform-*d*) δ 7.13 (t, *J* = 1.9 Hz, 1H), 7.09 (s, 1H), 6.71 (s, 1H), 4.22 (br s, 2H), 3.05 (s, 3H). <sup>19</sup>F NMR (376 MHz, Chloroform-*d*) δ<sub>F</sub> -60.8 (3F). LCMS (Method B): t<sub>R</sub> = 0.807 min, m/z = 256.1 [M+H]<sup>+</sup>; Purity (AUC) ≥ 95%.

Step D: 5-bromo-2-hydroxy-N-(3-(methylsulfonyl)-5-(trifluoromethoxy)phenyl)benzenesulfonamide

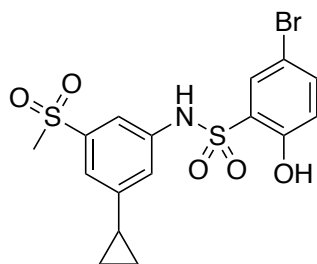
3-(Methylsulfonyl)-5-(trifluoromethoxy)aniline (18 mg, 0.07 mmol) was reacted with 5-bromo-2-hydroxybenzenesulfonyl chloride following General Procedure D. Purification by preparative HPLC afforded the title compound (21 mg, 0.04 mmol, 57%) as a white solid. <sup>1</sup>H NMR (400 MHz, Chloroform-*d*) δ 8.35 (br s, 1H), 7.86 (s, 1H), 7.75 (d, *J* = 2.4 Hz, 1H), 7.56 – 7.50 (m, 3H), 7.43 (s, 1H), 6.89 (d, *J* = 8.8 Hz, 1H), 3.09 (s, 3H). <sup>19</sup>F NMR (376 MHz, Chloroform-*d*) δ -61.0 (3F). LCMS (Method B): t<sub>R</sub> = 1.084 min, m/z = 506.8, 508.8 [M+NH<sub>4</sub>]<sup>+</sup>; Purity (AUC) ≥ 95%.

*5-Bromo-3-chloro-2-hydroxy-N-(3-(methylsulfonyl)-5-(trifluoromethoxy)phenyl)benzenesulfonamide (VU0826067)*



3-(Methylsulfonyl)-5-(trifluoromethoxy)aniline (20 mg, 0.07 mmol) was reacted with 5-bromo-3-chloro-2-hydroxybenzenesulfonyl chloride following General Procedure D. Purification by preparative HPLC afforded the title compound (15.3 mg, 0.027 mmol, 40%) as a white solid. <sup>1</sup>H NMR (400 MHz, Chloroform-*d*) δ 7.80 (d, *J* = 2.4 Hz, 1H), 7.70 (d, *J* = 2.4 Hz, 1H), 7.55 (s, 2H), 7.42 (s, 1H), 3.07 (s, 3H). <sup>19</sup>F NMR (376 MHz, Chloroform-*d*) δ -58.0 (3F). LCMS (Method B): *t*<sub>R</sub> = 1.166 min, *m/z* = 542.8 [M+NH<sub>4</sub>]<sup>+</sup>; Purity (AUC) ≥ 95%.

*5-Bromo-N-(3-cyclopropyl-5-(methylsulfonyl)phenyl)-2-hydroxybenzenesulfonamide (VU0825944)*



*Step A: 3-Cyclopropyl-5-(methylsulfonyl)aniline*

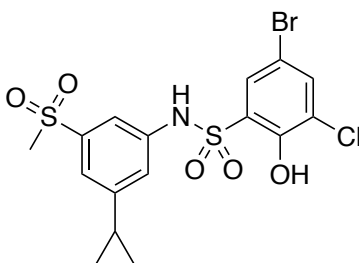
3-Bromo-5-(methylsulfonyl)aniline (149 mg, 0.60 mmol) was reacted according to General Procedure K. Purification by flash chromatography afforded the title compound (101.1 mg, 0.48 mmol, 80%). <sup>1</sup>H NMR (400 MHz, Chloroform-*d*) δ 6.97 (d, *J* = 2.0 Hz, 2H), 6.59 (t, *J* = 2.0 Hz, 1H), 3.92 (br s, 2H), 3.00 (s, 3H), 1.92 – 1.80 (m, 1H), 1.03 – 0.94 (m, 2H), 0.75 – 0.66 (m, 2H). LCMS (Method B): *t*<sub>R</sub> = 0.421 min, *m/z* = 212.2 [M+H]<sup>+</sup>; Purity (AUC) ≥ 89%.



Step B: 5-Bromo-N-(3-cyclopropyl-5-(methylsulfonyl)phenyl)-2-hydroxybenzenesulfonamide

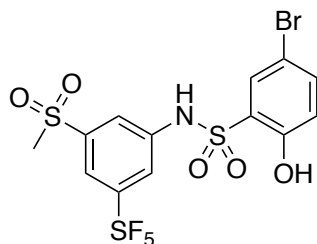
3-Cyclopropyl-5-(methylsulfonyl)aniline (44.5 mg, 0.21 mmol) was reacted with 5-bromo-2-hydroxybenzenesulfonyl chloride following General Procedure D. Purification by preparative HPLC afforded the title compound (56.6 mg, 0.71 mmol, 54%) as a white solid. <sup>1</sup>H NMR (400 MHz, Chloroform-*d*) δ 7.65 (d, *J* = 2.6 Hz, 1H), 7.51 (dd, *J* = 8.8, 2.6 Hz, 1H), 7.45 (s, 1H), 7.32 – 7.28 (m, 1H), 7.17 (s, 1H), 7.14 – 7.09 (m, 1H), 6.88 (d, *J* = 8.8 Hz, 1H), 3.00 (s, 3H), 1.93 (dt, *J* = 8.8, 4.9 Hz, 2H), 1.13 – 1.04 (m, 2H), 0.77 – 0.68 (m, 2H). LCMS (Method B): *t*<sub>R</sub> = 1.036 min, *m/z* = 462.9, 464.9 [M+NH<sub>4</sub>]<sup>+</sup>; Purity (AUC) ≥ 95%.

*5-Bromo-3-chloro-N-(3-cyclopropyl-5-(methylsulfonyl)phenyl)-2-hydroxybenzenesulfonamide (VU0822878)*



3-Cyclopropyl-5-(methylsulfonyl)aniline (23 mg, 0.11 mmol) was reacted with 5-bromo-3-chloro-2-hydroxybenzenesulfonyl chloride following General Procedure D. Purification by preparative HPLC afforded the title compound (22.5 mg, 0.047 mmol, 44%) as a white solid. <sup>1</sup>H NMR (400 MHz, Chloroform-*d*) δ 7.71 (d, *J* = 2.4 Hz, 1H), 7.66 (d, *J* = 2.4 Hz, 1H), 7.42 (d, *J* = 1.8 Hz, 1H), 7.36 (br s, 1H), 7.34 (t, *J* = 1.8 Hz, 1H), 7.15 (t, *J* = 1.8 Hz, 1H), 3.01 (s, 3H), 1.98 – 1.90 (m, 1H), 1.12 – 1.05 (m, 2H), 0.77 – 0.69 (m, 2H). LCMS (Method B): *t*<sub>R</sub> = 1.119 min, *m/z* = 479.8 [M+NH<sub>4</sub>]<sup>+</sup>; Purity (AUC) ≥ 95%.

*5-Bromo-2-hydroxy-N-(3-(methylsulfonyl)-5-(pentafluorosulfaneyl)phenyl)benzenesulfonamide*  
(VU0826049)



Step A: Methyl 3-(methylsulfonyl)-5-(pentafluorosulfaneyl)benzoate

Methyl 3-bromo-5-(pentafluorosulfaneyl)benzoate (600 mg, 1.91 mmol) was reacted with sodium methanesulfinate following General Procedure M. Purification by flash chromatography afforded the title compound (164.1 mg, 0.48 mmol, 25%) as a white solid. <sup>1</sup>H NMR (400 MHz, Chloroform-*d*) δ<sub>H</sub> 8.74 (d, *J* = 1.7 Hz, 1H), 8.68 (t, *J* = 1.7 Hz, 1H), 8.50 (t, *J* = 1.7 Hz, 1H), 4.02 (s, 3H), 3.15 (s, 3H). <sup>19</sup>F NMR (376 MHz, Chloroform-*d*) δ 80.43 (p, *J* = 151 Hz, 1F), 63.01 (d, *J* = 151 Hz, 4F). LCMS (Method B): t<sub>R</sub> = 0.978 min, m/z = 341 [M+H]<sup>+</sup>; Purity (AUC) ≥ 95%.

Step B: 3-(methylsulfonyl)-5-(pentafluorosulfaneyl)benzoic acid

Methyl 3-(methylsulfonyl)-5-(pentafluorosulfaneyl)benzoate (162 mg, 0.54 mmol) was reacted following General Procedure E Purification by flash chromatography afforded the title compound (117.7 mg, 0.36 mmol, 67%) as a white solid. <sup>1</sup>H NMR (400 MHz, Chloroform-*d*) δ 8.79 (s, 1H), 8.73 (s, 1H), 8.56 (d, *J* = 1.9 Hz, 1H), 3.17 (s, 3H). <sup>19</sup>F NMR (376 MHz, Chloroform-*d*) δ 80.24 (p, *J* = 151 Hz, 1 F), 63.03 (d, *J* = 151 Hz, 4F). LCMS (Method B): t<sub>R</sub> = 0.766 min, does not ionize by ESI; Purity (AUC) ≥ 95%.

Step C: 3-(Methylsulfonyl)-5-(pentafluorosulfaneyl)aniline

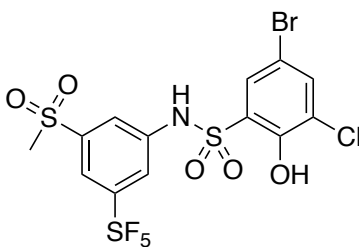
3-(Methylsulfonyl)-5-(pentafluorosulfaneyl)benzoic acid (117 mg, 0.36 mmol) was reacted following General Procedure P. Purification by flash chromatography afforded the title compound

(51.2 mg, 0.17 mmol, 48%) as a white solid.  $^1\text{H}$  NMR (400 MHz, Chloroform-*d*)  $\delta$  7.61 (t,  $J = 1.9$  Hz, 1H), 7.32 (t,  $J = 1.9$  Hz, 1H), 7.25 (t,  $J = 1.9$  Hz, 1H), 4.29 (br s, 2H), 3.07 (s, 3H).  $^{19}\text{F}$  NMR (376 MHz, Chloroform-*d*)  $\delta$  79.62 (p,  $J = 150$  Hz, 1F), 59.53 (d,  $J = 150$  Hz, 4F). LCMS (Method B):  $t_{\text{R}} = 1.184$  min, does not ionize by ESI; Purity (AUC)  $\geq 90\%$ .

Step D: 5-Bromo-2-hydroxy-*N*-(3-(methylsulfonyl)-5-(pentafluorosulfaneyl)phenyl)benzenesulfonamide

3-(Methylsulfonyl)-5-(pentafluorosulfaneyl)aniline (20 mg, 0.07 mmol) was reacted with 5-bromo-2-hydroxybenzenesulfonyl chloride following General Procedure D. Purification by preparative HPLC afforded the title compound (8.4 mg, 0.016 mmol, 23%) as a white solid.  $^1\text{H}$  NMR (400 MHz, Chloroform-*d*)  $\delta$  8.08 (s, 1H), 7.82 (t,  $J = 1.9$  Hz, 1H), 7.77 (s, 1H), 7.73 (d,  $J = 2.5$  Hz, 1H), 7.65 (br s, 1H), 7.54 (dd,  $J = 8.8, 2.5$  Hz, 1H), 6.90 (d,  $J = 8.8$  Hz, 1H), 3.08 (s, 3H).  $^{19}\text{F}$  NMR (376 MHz, Chloroform-*d*)  $\delta$  80.5 (p,  $J = 151$  Hz, 1F), 62.92 (d,  $J = 151$  Hz, 4F). LCMS (Method B):  $t_{\text{R}} = 1.128$  min,  $m/z = 548.8$  [ $\text{M} + \text{NH}_4$ ] $^+$ ; Purity (AUC)  $\geq 95\%$ .

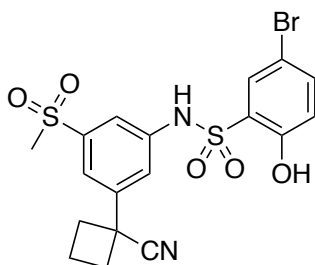
*5-Bromo-3-chloro-2-hydroxy-*N*-(3-(methylsulfonyl)-5-(pentafluorosulfaneyl)phenyl)benzenesulfonamide (VU0826051)*



3-(Methylsulfonyl)-5-(pentafluorosulfaneyl)aniline (20 mg, 0.07 mmol) was reacted with 5-bromo-3-chloro-2-hydroxybenzenesulfonyl chloride following General Procedure D. Purification by preparative HPLC afforded the title compound (7.3 mg, 0.013 mmol, 19%) of title compound

as a white solid.  $^1\text{H}$  NMR (400 MHz, Chloroform-*d*)  $\delta$  8.07 (s, 1H), 7.85 (t,  $J = 2.2$  Hz, 1H), 7.82 (d,  $J = 2.2$  Hz, 2H), 7.72 (d,  $J = 2.2$  Hz, 1H), 7.54 (br s, 1H), 3.09 (s, 3H).  $^{19}\text{F}$  NMR (376 MHz, Chloroform-*d*)  $\delta$  80.5 (p,  $J = 151$  Hz, 1F), 62.93 (d,  $J = 151$  Hz, 4F). LCMS (Method B):  $t_{\text{R}} = 1.201$  min,  $m/z = 584.7$   $[\text{M}+\text{NH}_4]^+$ ; Purity (AUC)  $\geq 95\%$ .

*5-Bromo-3-chloro-N-(3-(1-cyanocyclobutyl)-5-(methylsulfonyl)phenyl)-2-hydroxybenzenesulfonamide (VU0850757)*



Step A: 3-Methyl-5-(methylsulfonyl)aniline

3-Bromo-5-methylaniline (2.000 g, 10.75 mmol) was reacted with sodium methanesulfinate following General Procedure M. Purification by flash chromatography afforded the title compound (1.196 g, 6.46 mmol, 60%) of title compound.  $^{13}\text{C}$  NMR (101 MHz, Chloroform-*d*)  $\delta$  147.4, 141.5, 140.9, 120.5, 117.7, 110.4, 44.6, 21.5.  $^1\text{H}$  NMR (400 MHz,  $\text{CDCl}_3$ )  $\delta$  7.10 (d,  $J = 1.6$  Hz, 1H), 7.01 (d,  $J = 2.1$  Hz, 1H), 6.71 (dd,  $J = 2.1, 1.6$  Hz, 1H), 3.90 (s, 2H), 3.01 (s, 3H), 2.36 – 2.31 (m, 3H). LCMS (Method B)  $t_{\text{R}} = 0.111$  min,  $m/z = 371.4$   $[2\text{M}+\text{H}]^+$ ; Purity (AUC)  $\geq 95\%$ .

Step B: tert-Butyl (3-methyl-5-(methylsulfonyl)phenyl) carbamate

3-Methyl-5-(methylsulfonyl)aniline 1.196 g (6.46 mmol, 1 eq) was mixed with di-*tert*-butyl dicarbonate (1.671 g, 7.66 mmol, 1.2 eq) and dissolved in MeOH at 0.30 M. The solution was stirred overnight at room temperature. Next day, the solvent was removed under vacuum and the crude was purified by ISCO flash chromatography to afford the title compound (826 mg, 2.89

mmol, 45%). <sup>1</sup>H NMR (400 MHz, Chloroform-*d*) δ 7.71 (t, *J* = 1.9 Hz, 1H), 7.56 (s, 1H), 7.39 (d, *J* = 1.9 Hz, 1H), 6.86 (s, 1H), 3.03 (s, 3H), 2.39 (s, 3H), 1.51 (s, 9H). LCMS (Method B) *t*<sub>R</sub> = 0.916 min, *m/z* = 303.2 [M+NH<sub>4</sub>]<sup>+</sup>; Purity (AUC) ≥ 95%.

*Step C: tert-Butyl (3-(bromomethyl-5-(methylsulfonyl)phenyl) carbamate*

*tert*-Butyl (3-methyl-5-(methylsulfonyl)phenyl) carbamate (826 mg, 2.89 mmol, 1 eq) was mixed with NBS (618 mg, 3.47 mmol, 1.2 eq) and dissolved in CCl<sub>4</sub> at 0.13 M. The solution was degassed with Ar for 10 min and AIBN (119 mg, 724 μmol, 0.25 eq) was added. The mixture was heated to 80 °C and stirred for 16 h. The solution was filtered and the filtrate was washed first with HCl [1 M] and then with a saturated solution of NaHCO<sub>3</sub>. The organic phase was dried using a phase separator and the solvent was removed under reduced pressure. The crude was purified using ISCO flash chromatography to afford the title compound (961 mg) as a mixture with the dibrominated byproduct. <sup>1</sup>H NMR (400 MHz, Chloroform-*d*) δ 7.84 (d, *J* = 1.8 Hz, 1H), 7.60 (s, 1H), 6.88 (s, 1H), 4.47 (s, 2H), 3.06 (s, 3H), 1.52 (s, 9H). LCMS (Method B) *t*<sub>R</sub> = 0.952 min, *m/z* = 381.3, 383.2 [M+NH<sub>4</sub>]<sup>+</sup>.

*Step D: tert-Butyl (3-(cyanomethyl-5-(methylsulfonyl)phenyl) carbamate*

*tert*-Butyl (3-(bromomethyl-5-(methylsulfonyl)phenyl) carbamate (961 mg of the mixture) was dissolved in 5.0 mL of MeCN and cooled to 0 °C using an ice/water bath. Then, 438 mg (3.17 mmol, 1.2 eq) of K<sub>2</sub>CO<sub>3</sub> and 0.420 mL (3.17 mmol, 1.2 eq) of TMSCN were added. The mixture was heated to 50 °C and stirred for 16 h. NaOH [3 M] was added and extracted with EtOAc. The organic phase was dried using a phase separator and the solvent was removed under reduced pressure. The crude was purified using ISCO flash chromatography and 441 mg (1.42 mmol, 49%) of the title compound were obtained. <sup>13</sup>C NMR (101 MHz, Chloroform-*d*) δ 152.4, 142.2, 140.9, 132.9, 122.5, 120.4, 117.0, 116.7, 81.8, 44.4, 28.3, 23.6. <sup>1</sup>H NMR (400 MHz, Chloroform-*d*) δ

7.89 (t,  $J = 1.8$  Hz, 1H), 7.77 (s, 1H), 7.55 (t,  $J = 1.8$  Hz, 1H), 6.82 (br s, 1H), 3.81 (s, 2H), 3.07 (s, 3H), 1.53 (s, 9H). LCMS (Method B)  $t_R = 0.849$  min,  $m/z = 328.3$   $[M+NH_4]^+$ ; Purity (AUC)  $\geq 95\%$ .

Step E: *tert*-Butyl (3-(1-cyanocyclobutyl)-5-(methylsulfonyl)phenyl) carbamate

*tert*-Butyl (3-(cyanomethyl-5-(methylsulfonyl)phenyl) carbamate (421 mg, 1.36 mmol, 1 eq) and 1,3-dibromopropane (151  $\mu$ L, 1.49 mmol, 1.1 eq) were dissolved in of DMSO at 0.2 M. Then, NaH (140 mg, 3.39mmol, 2.5 eq) was added in portions. It was stirred overnight at room temperature. Water was added and extracted with EtOAc. The organic phase was dried over a phase separator and the solvent removed under reduced pressure. The crude was purified using ISCO flash chromatography and 311 mg (0.887 mmol, 65%) of the title compound were obtained.  $^{13}C$  NMR (101 MHz, Chloroform-*d*)  $\delta$  152.4, 142.5, 142.1, 140.8, 123.5, 120.6, 118.0, 116.5, 81.6, 44.4, 40.1, 34.6, 28.3, 17.1.  $^1H$  NMR (400 MHz, Chloroform-*d*)  $\delta$  7.94 (s, 1H), 7.80 (s, H), 7.56 (s, 1H), 7.30 (s, 1H), 3.06 (s, 3H), 2.87 – 2.76 (m, 2H), 2.69-2.56 (m, 2H), 2.43 (dt,  $J = 11.9, 8.8$  Hz, 1H), 2.13 – 2.04 (m, 1H), 1.50 (s, 9H). LCMS (Method B)  $t_R = 0.994$  min,  $m/z = 368.3$   $[M+NH_4]^+$ ; Purity (AUC)  $\geq 95\%$ .

Step F: *1*-(3-Amino-5-(methylsulfonyl)phenyl)cyclobutane-1-carbonitrile

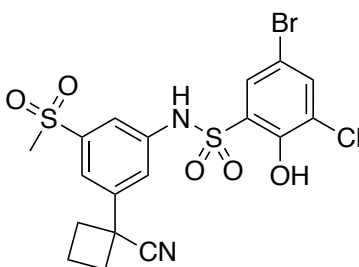
*tert*-Butyl (3-(1-cyanocyclobutyl)-5-(methylsulfonyl)phenyl) carbamate (311 mg, 0.887 mmol) was reacted following General Procedure S. The crude was taken forward (253 mg, 0.84 mmol, 94%). LCMS (Method B)  $t_R = 0.588$  min,  $m/z = 251.0$   $[M+H]^+$ ; Purity (H-NMR)  $\geq 95\%$ .

Step G: *5*-Bromo-3-chloro-*N*-(3-(1-cyanocyclobutyl)-5-(methylsulfonyl)phenyl)-2-hydroxybenzenesulfonamide

1-(3-Amino-5-(methylsulfonyl)phenyl)cyclobutene-1-carbonitrile (82 mg, 0.33 mmol) was reacted with 5-bromo-2-hydroxy-benzenesulfonyl chloride following to General Procedure D.

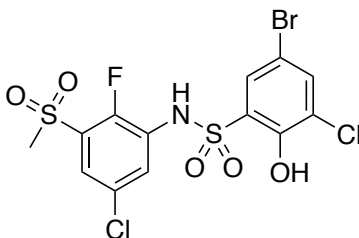
Purification by preparative HPLC afforded the title compound (62 mg, 0.13 mmol, 40%). <sup>1</sup>H NMR (400 MHz, Chloroform-*d*) δ 8.32 (br s, 1H), 7.77 (d, *J* = 2.5 Hz, 1H), 7.71 (t, *J* = 1.7 Hz, 1H), 7.63 (t, *J* = 1.7 Hz, 1H), 7.53 (t, *J* = 1.7 Hz, 1H), 7.47 (dd, *J* = 8.8, 2.5 Hz, 1H), 6.88 (d, *J* = 8.8 Hz, 1H), 3.08 (s, 3H), 2.90 – 2.79 (m, 2H), 2.63 – 2.54 (m, 2H), 2.54 – 2.40 (m, 1H), 2.17 – 2.04 (m, 1H). LCMS (Method A) *t*<sub>R</sub> = 1.715 min, *m/z* = 484.9; Purity (AUC) ≥ 95%.

*5-Bromo-3-chloro-N-(3-(1-cyanocyclobutyl)-5-(methylsulfonyl)phenyl)-2-hydroxybenzenesulfonamide (VU0850756)*



1-(3-Amino-5-(methylsulfonyl)phenyl)cyclobutene-1-carbonitrile (83 mg, 0.33 mmol) was reacted with 5-bromo-3-chloro-2-hydroxy-benzenesulfonyl chloride following to General Procedure D. Purification by preparative HPLC afforded the title compound (55 mg, 0.11 mmol, 33%). <sup>1</sup>H NMR (400 MHz, Chloroform-*d*) δ 7.90 (br s, 1H), 7.78 (d, *J* = 2.4 Hz, 1H), 7.73 (d, *J* = 1.8 Hz, 1H), 7.67 (d, *J* = 2.4 Hz, 1H), 7.62 (d, *J* = 1.8 Hz, 1H), 7.53 (t, *J* = 1.8 Hz, 1H), 3.08 (s, 3H), 2.92-2.81 (m, 2H), 2.64 – 2.52 (m, 2H), 2.52 – 2.42 (m, 1H), 2.16-2.07 (m, 1H). LCMS (Method A) *t*<sub>R</sub> = 1.812 min, *m/z* = 518.9, 521.9 [M+NH<sub>4</sub>]<sup>+</sup>; Purity (AUC) ≥ 95%.

*5-Bromo-3-chloro-N-(5-chloro-2-fluoro-3-(methylsulfonyl)phenyl)-2-hydroxybenzenesulfonamide (VU0849444)*



Step A: 3-Bromo-5-chloro-2-fluoroaniline

3-Bromo-5-chloro-2-fluoronitrobenzene (200 mg, 0.79 mmol, 1 eq) was dissolved in 7.8 mL of HOAc (glacial) and iron powder (2194 mg, 3.93 mmol, 5 eq) was added. It was stirred at room temperature for 16 h. The mixture was filtered and the solvent removed under reduced pressure. The crude was suspended in a saturated solution of Na<sub>2</sub>CO<sub>3</sub> and it was extracted with CH<sub>2</sub>Cl<sub>2</sub>. The organic phase was dried over a phase separator and the solvent removed under reduced pressure. The crude was taken forward without further purification (134 mg, 0.60 mmol, 76%). <sup>1</sup>H NMR (400 MHz, Chloroform-*d*) δ 6.87 (dd, *J* = 6.2, 2.5 Hz, 1H), 6.69 (dd, *J* = 6.2, 2.5 Hz, 1H), 3.89 (br s, 2H). <sup>19</sup>F NMR (376 MHz, Chloroform-*d*) δ -134.9 (1F). LCMS (Method B): t<sub>R</sub> = 1.030 min, m/z = 288.4 [M+ACN+Na]<sup>+</sup>; Purity (AUC) ≥ 95%.

Step B: 5-Chloro-2-fluoro-3-(methylsulfonyl)aniline

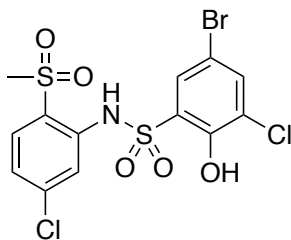
3-Bromo-5-chloro-2-fluoroaniline (134 mg, 0.60 mmol) was reacted with sodium methanesulfinate following General Procedure M. Purification by flash chromatography afforded the title compound (6 mg, 0.045 mmol, 7%). <sup>1</sup>H NMR (400 MHz, Chloroform-*d*) δ 7.23 (dd, *J* = 6.2, 2.6 Hz, 1H), 7.01 (dd, *J* = 6.2, 2.6 Hz, 1H), 4.07 (br s, 2H), 3.21 (s, 3H). <sup>19</sup>F NMR (376 MHz, Chloroform-*d*) δ -136.2 (1F). LCMS (Method B): t<sub>R</sub> = 0.116 min, m/z = 224.2 [M+H]<sup>+</sup>; Purity (AUC) ≥ 95%.



Step C: 5-Bromo-3-chloro-N-(5-chloro-2-fluoro-3-(methylsulfonyl)phenyl)-2-hydroxybenzenesulfonamide

5-Chloro-2-fluoro-3-(methylsulfonyl)aniline (6 mg, 0.045 mmol) was reacted with 5-bromo-3-chloro-2-hydroxybenzenesulfonyl chloride following General Procedure D, CH<sub>2</sub>Cl<sub>2</sub> was substituted with pyridine. Purification by preparative HPLC afforded the title compound (3 mg, 0.0061 mmol, 14% yield). <sup>1</sup>H NMR (400 MHz, Chloroform-*d*) δ 7.85 (dd, *J* = 6.0, 2.6 Hz, 1H), 7.82 (d, *J* = 2.4 Hz, 1H), 7.73 (d, *J* = 2.4 Hz, 1H), 7.70 (dd, *J* = 6.0, 2.6 Hz, 1H), 7.30 (s, 1H), 3.16 (s, 3H). <sup>19</sup>F NMR (376 MHz, Chloroform-*d*) δ -132.7 (1F). LCMS (Method B): t<sub>R</sub> = 1.070 min, m/z = 510.2, 511.1 [M+NH<sub>4</sub>]<sup>+</sup>; Purity (AUC) ≥ 89%.

*5-Bromo-3-chloro-N-(5-chloro-2-(methylsulfonyl)phenyl)-2-hydroxybenzenesulfonamide (VU0849408)*



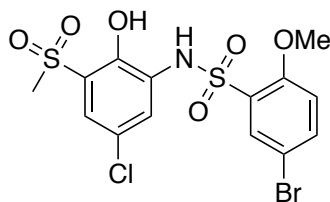
Step A: 5-Chloro-2-(methylsulfonyl)aniline

5-Chloro-2-iodoaniline (150 mg, 0.59 mmol) was reacted with sodium methanesulfinate following General Procedure M. Purification by flash chromatography afforded the title compound (92 mg, 0.45 mmol, 76%). <sup>1</sup>H NMR (400 MHz, Chloroform-*d*) δ 7.65 (d, *J* = 8.4 Hz, 1H), 6.83 – 6.75 (m, 2H), 5.11 (br s, 2H), 3.04 (s, 3H). LCMS (Method B): t<sub>R</sub> = 0.460 min, m/z = 206.2, 208.2 [M+H]<sup>+</sup>; Purity (AUC) ≥ 95%.

Step B: 5-Bromo-3-chloro-N-(5-chloro-2-(methylsulfonyl)phenyl)-2-hydroxybenzenesulfonamide

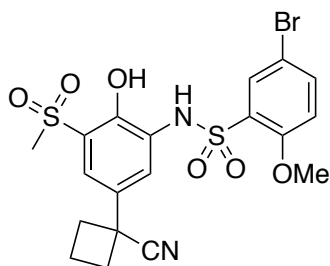
Title compound was prepared by reacting 20 mg (0.10 mmol) of 5-chloro-2-(methylsulfonyl)aniline with 5-bromo-3-chloro-2-hydroxy-benzenesulfonyl chloride following General Procedure D (500  $\mu$ L pyridine was used as solvent). It was obtained 5 mg (0.010 mmol, 10% yield).  $^1\text{H}$  NMR (400 MHz, Chloroform-*d*)  $\delta$  9.54 (br s, 1H), 7.93 (d,  $J = 2.4$  Hz, 1H), 7.82 (d,  $J = 8.4$  Hz, 1H), 7.73 (d,  $J = 2.4$  Hz, 1H), 7.58 (d,  $J = 1.9$  Hz, 1H), 7.24 (dd,  $J = 8.4, 1.9$  Hz, 1H), 3.05 (s, 3H). LCMS:  $t_{\text{R}} = 1.150$  min,  $m/z = 493.1$   $[\text{M}+\text{H}]^+$ ;  $\geq 89\%$  (AUC).

*5-Bromo-N-(5-chloro-2-hydroxy-3-(methylsulfonyl)phenyl)-2-methoxybenzenesulfonamide*  
(VU0849228)



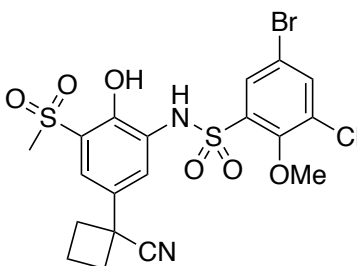
Amino-4-chloro-6-(methylsulfonyl)phenol (50 mg, 0.23 mmol) was reacted with 5-bromo-2-methoxybenzenesulfonyl chloride following General Procedure D. Purification by preparative HPLC afforded the title compound (3 mg, 0.006 mmol, 3%) of title compound.  $^1\text{H}$  NMR (400 MHz, Chloroform-*d*)  $\delta$  9.24 (s, 1H), 8.00 (d,  $J = 2.5$  Hz, 1H), 7.82 (d,  $J = 2.5$  Hz, 1H), 7.68 (s, 1H), 7.63 (dd,  $J = 8.8, 2.5$  Hz, 1H), 7.34 (d,  $J = 2.5$  Hz, 1H), 6.89 (d,  $J = 8.8$  Hz, 1H), 3.96 (s, 3H), 3.11 (s, 3H). LCMS (Method B):  $t_{\text{R}} = 1.055$  min,  $m/z = 489.2$   $[\text{M}+\text{NH}_4]^+$ ; Purity (AUC)  $\geq 95\%$ .

*5-Bromo-N-(5-(1-cyanocyclobutyl)-2-hydroxy-3-(methylsulfonyl)phenyl)-2-methoxybenzenesulfonamide (VU0849712)*



1-(3-Amino-4-hydroxy-5-(methylsulfonyl)phenyl)cyclobutane-1-carbonitrile (20 mg, 0.075 mmol) was reacted with 5-bromo-2-methoxy-benzenesulfonyl chloride following General Procedure D. Purification by preparative HPLC afforded the title compound (8 mg, 0.016 mmol, 21%). <sup>1</sup>H NMR (400 MHz, Chloroform-*d*) δ 9.34 (br s, 1H), 8.00 (d, *J* = 2.5 Hz, 1H), 7.82 (d, *J* = 2.5 Hz, 1H), 7.70 (s, 1H), 7.62 (dd, *J* = 8.9, 2.5 Hz, 1H), 7.37 (d, *J* = 2.3 Hz, 1H), 6.89 (d, *J* = 8.9 Hz, 1H), 3.96 (s, 3H), 3.13 (s, 3H), 2.87 – 2.76 (m, 2H), 2.55 – 2.37 (m, 3H), 2.13 – 2.02 (m, 1H). LCMS (Method B): *t*<sub>R</sub> = 1.008 min, *m/z* = 515.2 [M+H]<sup>+</sup>; Purity (AUC) ≥ 95%.

*5-Bromo-3-chloro-N-(5-(1-cyanocyclobutyl)-2-hydroxy-3-(methylsulfonyl)phenyl)-2-methoxybenzenesulfonamide (VU0849713)*



Step A: 5-bromo-3-chloro-2-methoxybenzenesulfonyl chloride

To a stirred solution of HBF<sub>4</sub> (21 μL, 0.2 mmol, 60%) and CH<sub>2</sub>Cl<sub>2</sub> (2 mL) was added 5-bromo-3-chloro-2-hydroxybenzenesulfonyl chloride (30 mg, 0.09 mmol) at 0 °C. TMSCHN<sub>2</sub> (0.34 mmol,

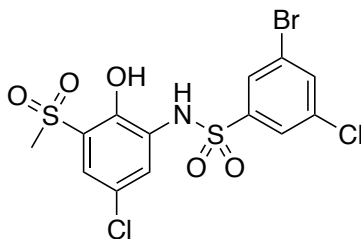
0.2 mL, 2 M hexane solution) was added dropwise in three portions at intervals of 30 min, and the reaction mixture was stirred for further 40 min at the same temperature after the additions were complete. The mixture was diluted with water, extracted with DCM, dried (Na<sub>2</sub>SO<sub>4</sub>), and concentrated. The crude was purified by ISCO flash chromatography and 23 mg (0.07 mmol, 73%) of the title compound were obtained. <sup>1</sup>H NMR (400 MHz, CDCl<sub>3</sub>) δ 8.003 (d, *J* = 2.4 Hz, 1H), 7.88 (d, *J* = 2.4 Hz, 1H), 4.12 (s, 3H).

Step B: 5-Bromo-3-chloro-N-(5-(1-cyanocyclobutyl)-2-hydroxy-3-(methylsulfonyl)phenyl)-2-methoxybenzenesulfonamide

1-(3-Amino-4-hydroxy-5-(methylsulfonyl)phenyl)cyclobutane-1-carbonitrile (20 mg, 0.075 mmol) was reacted with 5-bromo-3-chloro-2-methoxy-benzenesulfonyl chloride following General Procedure D. Purification by preparative HPLC afforded the title compound (2 mg, 0.004 mmol, 5%). <sup>1</sup>H NMR (400 MHz, Chloroform-*d*) δ 7.96 (d, *J* = 2.4 Hz, 1H), 7.86 (d, *J* = 2.4 Hz, 1H), 7.33 (d, *J* = 2.4 Hz, 1H), 7.10 (d, *J* = 2.4 Hz, 1H), 4.13 (s, 3H), 3.01 (s, 3H), 2.85 – 2.77 (m, 2H), 2.65 – 2.56 (m, 2H), 2.48 – 2.39 (m, 1H), 2.13 – 2.04 (m, 1H). LCMS (Method B): t<sub>R</sub> = 1.146 min, m/z = 549.2, 550.2 [M+H]<sup>+</sup>; Purity (AUC) ≥ 95%.

*3-Bromo-5-chloro-N-(5-chloro-2-hydroxy-3-(methylsulfonyl)phenyl)benzenesulfonamide*

*(VU0849227)*

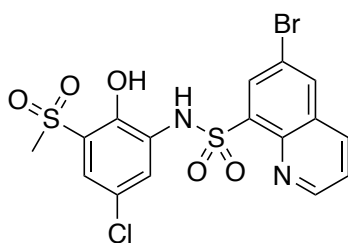


Amino-4-chloro-6-(methylsulfonyl)phenol (50 mg, 0.23 mmol) was reacted with 3-bromo-5-chlorobenzenesulfonyl chloride following General Procedure D. Purification by preparative HPLC

afforded the title compound (15 mg, 0.03 mmol, 14%) of title compound.  $^1\text{H}$  NMR (400 MHz, Methanol- $d_4$ )  $\delta$  7.90 (d,  $J = 1.7$  Hz, 1H), 7.82 (t,  $J = 1.7$  Hz, 1H), 7.74 (t,  $J = 1.7$  Hz, 1H), 7.64 (d,  $J = 2.6$  Hz, 1H), 7.38 (d,  $J = 2.6$  Hz, 1H), 3.20 (s, 3H). LCMS (Method B):  $t_R = 1.104$  min,  $m/z = 558.1$   $[\text{M}+2\text{ACN}+\text{H}]^+$ ; Purity (AUC)  $\geq 95\%$ .

*6-Bromo-N-(5-chloro-2-hydroxy-3-(methylsulfonyl)phenyl)quinoline-8-sulfonamide*

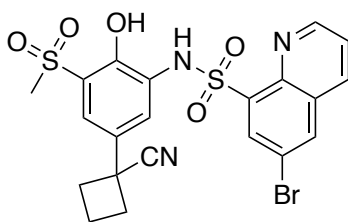
*(VU0849547)*



Amino-4-chloro-6-(methylsulfonyl)phenol (10 mg, 0.045 mmol) was reacted with 3-bromo-5-chlorobenzenesulfonyl chloride following General Procedure D. Purification by preparative HPLC afforded the title compound (4 mg, 0.03 mmol, 18%) of title compound.  $^1\text{H}$  NMR (400 MHz, Methanol- $d_4$ )  $\delta$  9.10 (dd,  $J = 1.7$  Hz, 1H), 8.48 (d,  $J = 2.2$  Hz, 1H), 8.23 (d,  $J = 2.2$  Hz, 1H), 8.20 (dd,  $J = 8.4, 1.7$  Hz, 1H), 7.93 (d,  $J = 2.5$  Hz, 1H), 7.62 (dd,  $J = 8.4, 4.3$  Hz, 1H), 7.32 (d,  $J = 2.5$  Hz, 1H), 3.05 (s, 3H). LCMS (Method B):  $t_R = 1.038$  min,  $m/z = 491.2, 493.2$   $[\text{M}+\text{H}]^+$ ; Purity (AUC)  $\geq 95\%$ .

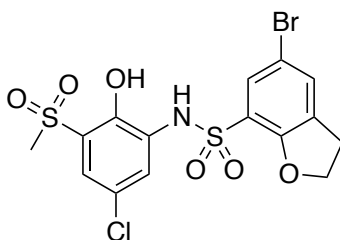
*6-Bromo-N-(5-(1-cyanocyclobutyl)-2-hydroxy-3-(methylsulfonyl)phenyl)quinoline-8-sulfonamide*

*(VU0849711)*



1-(3-Amino-4-hydroxy-5-(methylsulfonyl)phenyl)cyclobutane-1-carbonitrile (21 mg, 0.079 mmol) was reacted with 6-bromoquinoline-8-sulfonyl chloride following General Procedure D. Purification by preparative HPLC afforded the title compound (16 mg, 0.030 mmol, 38%) of title compound. <sup>1</sup>H NMR (400 MHz, Chloroform-*d*) δ 9.11 (d, *J* = 4.0 Hz, 1H), 8.46 (d, *J* = 2.2 Hz, 1H), 8.23 (d, *J* = 2.2 Hz, 1H), 8.21 (d, *J* = 8.6 Hz, 2H), 7.93 (d, *J* = 2.2 Hz, 1H), 7.62 (dd, *J* = 8.6, 4.0 Hz, 1H), 7.37 (d, *J* = 2.2 Hz, 1H), 3.06 (s, 3H), 2.86 – 2.78 (m, 2H), 2.54 (q, *J* = 10.1, 9.5 Hz, 2H), 2.47 – 2.37 (m, 1H), 2.16 – 2.03 (m, 1H). LCMS (Method B): *t*<sub>R</sub> = 1.015 min, *m/z* = 552.2, 553.2 [M+H]<sup>+</sup>; Purity (AUC) ≥ 95%.

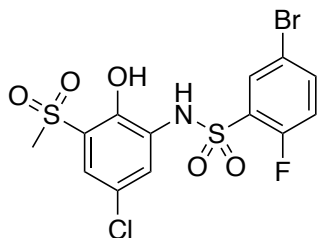
*5-Bromo-N-(5-chloro-2-hydroxy-3-(methylsulfonyl)phenyl)-2,3-dihydrobenzofuran-7-sulfonamide (VU0849714)*



Amino-4-chloro-6-(methylsulfonyl)phenol (20 mg, 0.090 mmol) was reacted with 5-bromo-2,3-dihydrobenzofuran-7-sulfonyl chloride following General Procedure D. Purification by preparative HPLC afforded the title compound (10 mg, 0.021 mmol, 23%) of title compound. <sup>1</sup>H NMR (400 MHz, Chloroform-*d*) δ 9.20 (br s, 1H), 7.79 (d, *J* = 2.2 Hz, 1H), 7.71 (d, *J* = 2.2 Hz, 1H), 7.54 (br s, 1H), 7.48 (d, *J* = 1.8 Hz, 1H), 7.35 (d, *J* = 2.4 Hz, 1H), 4.76 (t, *J* = 8.8 Hz, 2H), 3.27 (t, *J* = 8.8 Hz, 2H), 3.12 (s, 3H). LCMS (Method B): *t*<sub>R</sub> = 1.035 min, *m/z* = 288.4 [M+ACN+Na]<sup>+</sup>; Purity (AUC) ≥ 95%.

*5-Bromo-N-(5-chloro-2-hydroxy-3-(methylsulfonyl)phenyl)-2-fluorobenzenesulfonamide*

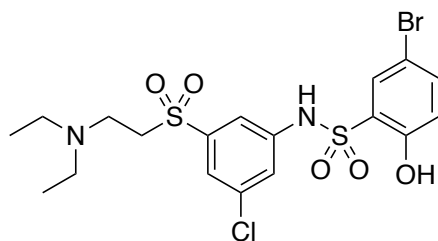
*(VU0849656)*



Amino-4-chloro-6-(methylsulfonyl)phenol (30 mg, 0.14 mmol) was reacted with 5-bromo-2-fluorobenzenesulfonyl chloride following General Procedure D. Purification by preparative HPLC afforded the title compound (6 mg, 0.013 mmol, 10%) of title compound. <sup>1</sup>H NMR (400 MHz, Chloroform-*d*) δ 9.22 (br s, 1H), 8.01 (dd, *J* = 6.2, 2.4 Hz, 1H), 7.78 (d, *J* = 2.4 Hz, 1H), 7.72 – 7.65 (m, 1H), 7.44 (br s, 1H), 7.40 (d, *J* = 2.4 Hz, 1H), 7.11 (t, *J* = 9.1 Hz, 1H), 3.11 (s, 3H). LCMS (Method A): *t*<sub>R</sub> = 1.800 min, *m/z* = 479.8, 480.9 [M+Na]<sup>+</sup>; Purity (AUC) ≥ 95%.

*5-Bromo-N-(3-chloro-5-((2-(diethylamino)ethyl)sulfonyl)phenyl)-2-hydroxybenzenesulfonamide*

*(VU0848787)*



*Step A: 3-Chloro-5-((2-(diethylamino)ethyl)thio)aniline*

3-Bromo-5-chloroaniline (250 mg, 1.21 mmol) was reacted with 2-(diethylamino)ethyl bromide hydrobromide following General Procedure Q. Purification by flash chromatography afforded the title compound (127 mg, 0.49 mmol, 40. LCMS (Method B): *t*<sub>R</sub> = 0.101 min, *m/z* = 259.2 [M+H]<sup>+</sup>; Purity (AUC) ≥ 95%.

Step B: 5-Bromo-N-(3-chloro-5-((2-(diethylamino)ethyl)thio)phenyl)-2-hydroxybenzenesulfonamide

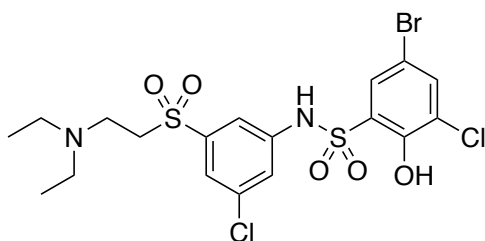
3-Chloro-5-((2-(diethylamino)ethyl)thio)aniline (50 mg, 0.19 mmol) was reacted with 5-bromo-2-hydroxybenzenesulfonyl chloride following General Procedure D. ISCO flash chromatography was used to purify the crude and 51 mg (0.09 mmol, 45%) of the title compound were obtained as a yellow oil. <sup>1</sup>H NMR (400 MHz, Chloroform-*d*) δ 7.81 (d, *J* = 2.6 Hz, 1H), 7.34 (dd, *J* = 8.8, 2.6 Hz, 1H), 7.24 – 7.17 (m, 2H), 6.96 (t, *J* = 1.5 Hz, 1H), 6.82 (d, *J* = 8.8 Hz, 1H), 3.31 – 3.22 (m, 2H), 3.15 – 2.97 (m, 6H), 1.23 (t, *J* = 7.3 Hz, 6H). LCMS (Method B): *t*<sub>R</sub> = 0.888 min, *m/z* = 493.3, 496.3 [M+H]<sup>+</sup>; Purity (AUC) ≥ 95%.

Step C: 5-Bromo-N-(3-chloro-5-((2-(diethylamino)ethyl)sulfonyl)phenyl)-2-hydroxybenzenesulfonamide

5-Bromo-N-(3-chloro-5-((2-(diethylamino)ethyl)thio)phenyl)-2-hydroxybenzenesulfonamide (29 mg, 0.06 mmol) was reacted with Oxone following General Procedure O. Purification by preparative HPLC afforded the title compound as the TFA salt (11 mg, 0.017 mmol, 29%). <sup>1</sup>H NMR (400 MHz, Chloroform-*d*) δ 7.94 (d, *J* = 2.5 Hz, 1H), 7.68 (s, 1H), 7.62 (d, *J* = 1.8 Hz, 1H), 7.57 (s, 1H), 7.41 (dd, *J* = 8.7, 2.5 Hz, 1H), 6.84 (d, *J* = 8.7 Hz, 1H), 3.78 – 3.65 (m, 2H), 3.63 – 3.50 (m, 2H), 3.29 – 3.08 (m, 4H), 1.35 (t, *J* = 7.2 Hz, 6H). LCMS (Method B): *t*<sub>R</sub> = 0.878 min, *m/z* = 525.2 [M+H]<sup>+</sup>; Purity (AUC) ≥ 95%.



*5-Bromo-3-chloro-N-(3-chloro-5-((2-(diethylamino)ethyl)sulfonyl)phenyl)-2-hydroxybenzenesulfonamide (VU0848793)*



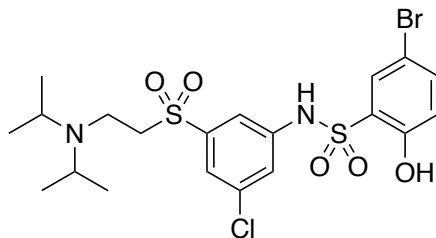
Step A: 5-Bromo-3-chloro-N-(3-chloro-5-((2-(diethylamino)ethyl)thio)phenyl)-2-hydroxybenzenesulfonamide

3-Chloro-5-((2-(diethylamino)ethyl)thio)aniline (50 mg, 0.19 mmol) was reacted with 5-bromo-3-chloro-2-hydroxy-benzenesulfonyl chloride following General Procedure D. ISCO flash chromatography afforded the title compound (62 mg, 0.10 mmol, 53%). <sup>1</sup>H NMR (400 MHz, Chloroform-*d*) δ 7.58 (d, *J* = 2.6 Hz, 1H), 7.44 (d, *J* = 2.6 Hz, 1H), 7.30 (s, 1H), 7.21 (s, 1H), 7.03 (s, 1H), 3.44 – 3.35 (m, 2H), 3.15 – 3.07 (m, 6H), 1.26 (t, *J* = 7.1 Hz, 6H). LCMS (Method B): *t*<sub>R</sub> = 0.955 min, *m/z* = 529.2, 531.2 [M+H]<sup>+</sup>; Purity (AUC) ≥ 90%.

Step B: 5-Bromo-3-chloro-N-(3-chloro-5-((2-(diethylamino)ethyl)sulfonyl)phenyl)-2-hydroxybenzenesulfonamide

5-Bromo-3-chloro-*N*-(3-chloro-5-((2-(diethylamino)ethyl)thio)phenyl)-2-hydroxybenzenesulfonamide (43 mg, 0.08 mmol) was reacted with Oxone following General Procedure O. Purification by preparative HPLC afforded the title compound as the TFA salt (16 mg, 0.024 mmol, 30%). <sup>1</sup>H NMR (400 MHz, Chloroform-*d*) δ 7.88 (s, 1H), 7.68 (s, 1H), 7.65 (s, 1H), 7.60 (d, *J* = 2.4 Hz, 1H), 7.58 (s, 1H), 3.86 – 3.77 (m, 2H), 3.50 – 3.42 (m, 2H), 3.20 – 3.09 (m, 4H), 1.35 (t, *J* = 7.3 Hz, 6H). LCMS (Method B): *t*<sub>R</sub> = 0.927 min, *m/z* = 561.2, 563.1 [M+H]<sup>+</sup>; Purity (AUC) ≥ 95%.

*5-Bromo-N-(3-chloro-5-((2-(diisopropylamino)ethyl)thio)phenyl)-2-hydroxybenzenesulfonamide*  
(VU0848788)



Step A: 3-Chloro-5-((2-(diisopropylamino)ethyl)thio)aniline

3-Bromo-5-chloroaniline (250 mg, 1.21 mmol) was reacted with 2-diisopropylaminoethylchloride hydrochloride according General Procedure Q. Purification by flash chromatography afforded the title compound (100 mg, 0.38 mmol, 32%). LCMS (Method B):  $t_R = 0.112$  min,  $m/z = 287.3$ , 289.4  $[M+H]^+$ ; Purity (AUC)  $\geq 95\%$ .

Step B: 5-Bromo-N-(3-chloro-5-((2-(diisopropylamino)ethyl)thio)phenyl)-2-hydroxybenzenesulfonamide

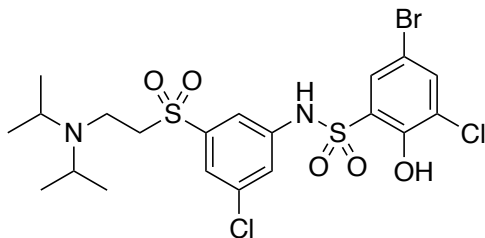
3-Chloro-5-((2-(diisopropylamino)ethyl)thio)aniline (50 mg, 0.19 mmol) was reacted with 5-bromo-2-hydroxy-benzenesulfonyl chloride following General Procedure D. Purification by preparative HPLC afforded the title compound as the TFA salt (51 mg, 0.082 mmol, 48%).  $^1H$  NMR (400 MHz, Chloroform-*d*)  $\delta$  10.07 (br s, 1H), 8.39 (br s, 1H), 7.79 (d,  $J = 2.5$  Hz, 1H), 7.41 (dd,  $J = 8.8, 2.5$  Hz, 1H), 7.34 (s, 1H), 6.99 (s, 1H), 6.95 – 6.90 (m, 2H), 3.70 – 3.58 (m, 2H), 3.40 – 3.32 (m, 2H), 3.14 – 3.05 (m, 2H), 1.37 (dd,  $J = 11.2, 6.6$  Hz, 12H). LCMS (Method B):  $t_R = 0.919$  min,  $m/z = 521.3$   $[M+H]^+$ ; Purity (AUC)  $\geq 95\%$ .

Step C: 5-Bromo-N-(3-chloro-5-((2-(diisopropylamino)ethyl)sulfonyl)phenyl)-2-hydroxybenzenesulfonamide

5-Bromo-N-(3-chloro-5-((2-(diisopropylamino)ethyl)thio)phenyl)-2-hydroxybenzenesulfonamide (31 mg, 0.06 mmol) was reacted with Oxone following General

Procedure O. Purification by preparative HPLC afforded the title compound as the TFA salt (22 mg, 0.034 mmol, 56%). <sup>1</sup>H NMR (400 MHz, Chloroform-*d*) δ 10.51 (br s, 1H), 7.92 (d, *J* = 2.5 Hz, 1H), 7.85 (br s, 1H), 7.72 (s, 1H), 7.61 (s, 1H), 7.53 (s, 1H), 7.40 (dd, *J* = 8.8, 2.5 Hz, 1H), 6.84 (d, *J* = 8.8 Hz, 1H), 3.90 – 3.81 (m, 2H), 3.66 (p, *J* = 6.2 Hz, 2H), 3.56 (dd, *J* = 10.4, 6.2 Hz, 2H), 1.49 – 1.31 (m, 12H). LCMS (Method B): *t*<sub>R</sub> = 0.817 min, *m/z* = 553.3, 556.3 [M+H]<sup>+</sup>; Purity (AUC) ≥ 95%.

*5-Bromo-3-chloro-N-(3-chloro-5-((2-(diisopropylamino)ethyl)sulfonyl)phenyl)-2-hydroxybenzenesulfonamide (VU0848797)*



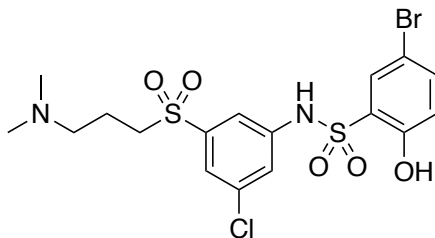
Step A: 5-Bromo-3-chloro-N-(3-chloro-5-((2-(diisopropylamino)ethyl)thio)phenyl)-2-hydroxybenzenesulfonamide

3-Chloro-5-((2-(diisopropylamino)ethyl)thio)aniline (50 mg, 0.17 mmol) was reacted with 5-bromo-3-chloro-2-hydroxy-benzenesulfonyl chloride following General Procedure D. ISCO flash chromatography was used to purify the crude and 49 mg (0.093 mmol, 55%) of the title compound were obtained as a yellow oil. <sup>1</sup>H NMR (400 MHz, Chloroform-*d*) δ 7.60 (d, *J* = 2.6 Hz, 1H), 7.45 (d, *J* = 2.6 Hz, 1H), 7.35 (s, 1H), 7.21 (s, 1H), 7.04 (s, 1H), 3.67 (p, *J* = 6.6 Hz, 2H), 3.57 – 3.51 (m, 2H), 3.06 (dd, *J* = 9.9, 6.6 Hz, 2H), 1.25 (d, *J* = 6.6 Hz, 12H). LCMS (Method B): *t*<sub>R</sub> = 0.997 min, *m/z* = 557.2, 559.2 [M+NH<sub>4</sub>]<sup>+</sup>; Purity (AUC) ≥ 95%.

Step B: 5-Bromo-3-chloro-N-(3-chloro-5-((2-(diisopropylamino)ethyl)sulfonyl)phenyl)-2-hydroxybenzenesulfonamide

5-Bromo-3-chloro-N-(3-chloro-5-((2-(diisopropylamino)ethylthio)phenyl)-2-hydroxybenzenesulfonamide (36 mg, 0.06 mmol) was reacted with Oxone following General Procedure O. Purification by preparative HPLC afforded the title compound as the TFA salt (22 mg, 0.031 mmol, 52%). <sup>1</sup>H NMR (400 MHz, Chloroform-*d*) δ 7.85 (d, *J* = 2.4 Hz, 1H), 7.74 (d, *J* = 1.9 Hz, 1H), 7.64 (t, *J* = 1.7 Hz, 1H), 7.59 (d, *J* = 2.4 Hz, 1H), 7.55 (t, *J* = 1.8 Hz, 1H), 4.03 – 3.90 (m, 2H), 3.66 (p, *J* = 6.6 Hz, 2H), 3.53 – 3.43 (m, 2H), 1.39 (d, *J* = 6.6 Hz, 12H). LCMS (Method B): *t*<sub>R</sub> = 0.961 min, *m/z* = 589.2, 591.2 [M+H]<sup>+</sup>; Purity (AUC) ≥ 95%.

*5-Bromo-N-(3-chloro-5-((3-(dimethylamino)propyl)sulfonyl)phenyl)-2-hydroxybenzenesulfonamide (VU0849254)*



Step A: 3-Chloro-5-((3-(dimethylamino)propyl)thio)aniline

3-Bromo-5-chloroaniline (400 mg, 1.94 mmol) was reacted with 3-bromo-N,N-dimethylpropan-1-amine hydrobromide following General Procedure Q. Purification by ISCO flash chromatography afforded 168 mg (0.69 mmol, 35%) of title compound. LCMS (Method B): *t*<sub>R</sub> = 0.107 min, *m/z* = 245.2, 246.4 [M+H]<sup>+</sup>; Purity (AUC) ≥ 95%.

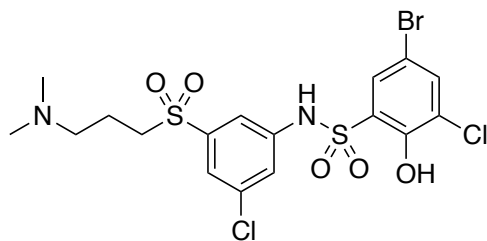
Step B: 5-Bromo-N-(3-chloro-5-((3-(dimethylamino)propyl)thio)phenyl)-2-hydroxybenzenesulfonamide

3-Chloro-5-((3-(dimethylamino)propyl)thio)aniline (50 mg, 0.20 mmol) was reacted with 5-bromo-2-hydroxy-benzenesulfonyl chloride following General Procedure D. The crude was taken forward (35 mg). LCMS (Method B):  $t_R = 0.912$  min,  $m/z = 481.2, 483.2$   $[M+H]^+$ .

Step C: 5-Bromo-N-(3-chloro-5-((3-(dimethylamino)propyl)sulfonyl)phenyl)-2-hydroxybenzenesulfonamide

5-Bromo-N-(3-chloro-5-((3-(dimethylamino)propyl)thio)phenyl)-2-hydroxybenzenesulfonamide (35 mg, crude) was reacted with Oxone following General Procedure O. Purification by preparative HPLC afforded the title compound as the TFA salt (6 mg, 0.0098 mmol, 5%).  $^1H$  NMR (400 MHz, Chloroform-*d*)  $\delta$  8.50 (br s, 1H), 7.86 (d,  $J = 2.5$  Hz, 1H), 7.65 (t,  $J = 1.6$  Hz, 2H), 7.60 (t,  $J = 1.6$  Hz, 1H), 7.46 (dd,  $J = 8.8, 2.5$  Hz, 1H), 6.91 (d,  $J = 8.8$  Hz, 1H), 3.33 (t,  $J = 7.9$  Hz, 2H), 3.23 (t,  $J = 6.8$  Hz, 2H), 2.89 (s, 6H), 2.26 (t,  $J = 7.9, 6.8$  Hz, 2H). LCMS (Method B):  $t_R = 0.867$  min,  $m/z = 513.2$   $[M+H]^+$ ; Purity (AUC)  $\geq 95\%$ .

*5-Bromo-3-chloro-N-(3-chloro-5-((3-(dimethylamino)propyl)sulfonyl)phenyl)-2-hydroxybenzenesulfonamide (VU0849253)*



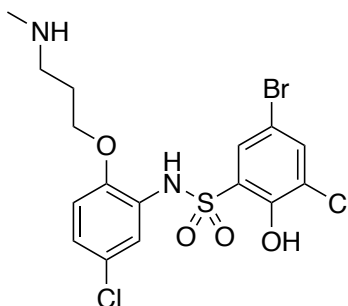
Step A: 5-Bromo-3-chloro-N-(3-chloro-5-((3-(dimethylamino)propyl)thio)phenyl)-2-hydroxybenzenesulfonamide

3-Chloro-5-((3-(dimethylamino)propyl)thio)aniline (50 mg, 0.20 mmol) was reacted with 5-bromo-3-chloro-2-hydroxy-benzenesulfonyl chloride following General Procedure D. The crude was taken forward (57 mg). LCMS (Method B):  $t_R = 0.957$  min,  $m/z = 515.2, 513.2$   $[M+H]^+$ .

Step B: 5-Bromo-3-chloro-N-(3-chloro-5-((3-(dimethylamino)propyl)sulfonyl)phenyl)-2-hydroxybenzenesulfonamide

5-Bromo-3-chloro-N-(3-chloro-5-((3-(dimethylamino)propyl)thio)phenyl)-2-hydroxybenzenesulfonamide (57 mg, crude) was reacted with Oxone following General Procedure O. Purification by preparative HPLC afforded the title compound as the TFA salt (39 mg, 0.059 mmol, 30%).  $^1H$  NMR (400 MHz, Chloroform-*d*)  $\delta$  10.66 (br s, 1H), 7.80 (d,  $J = 2.4$  Hz, 1H), 7.64 (d,  $J = 2.4$  Hz, 1H), 7.63 – 7.58 (m, 3H), 7.19 (br s, 1H), 3.39 – 3.34 (m, 2H), 3.25 (t,  $J = 6.9$  Hz, 2H), 2.92 (s, 6H), 2.34 – 2.25 (m, 2H). LCMS (Method B):  $t_R = 0.895$  min,  $m/z = 547.2, 549.2$   $[M+H]^+$ ; Purity (AUC)  $\geq 95\%$ .

*5-Bromo-3-chloro-N-(5-chloro-2-(3-(methylamino)propoxy)phenyl)-2-hydroxybenzenesulfonamide (VU0848402)*



Step A: 2-Bromo-1-(3-bromopropoxy)-4-chlorobenzene

2-Bromo-5-chlorophenol (1000 mg, 4.82 mmol, 1 eq) was mixed with K<sub>2</sub>CO<sub>3</sub> (732 mg, 5.30 mmol, 1.1 eq) and dissolved in DMF at 0.8 M. The mixture was pre-stirred for 40 min. Then, 1,3-dibromopropane (1.3 mL, 9.64 mmol, 2 eq) was added and heated to 80 °C for 16 h. After cooling it down to r.t. water was added and extracted with CH<sub>2</sub>Cl<sub>2</sub>. The organic phase was concentrated and the crude purified by ISCO flash chromatography to obtain the title compound (662 mg, 2.02 mmol, 42%). <sup>1</sup>H NMR (400 MHz, Chloroform-*d*) δ 7.53 (d, *J* = 2.6 Hz, 1H), 7.23 (dd, *J* = 8.8, 2.6 Hz, 1H), 6.83 (d, *J* = 8.8 Hz, 1H), 4.14 (t, *J* = 6.0 Hz, 2H), 3.66 (t, *J* = 6.0 Hz, 2H), 2.35 (p, *J* = 6.0 Hz, 2H). LCMS (Method B): t<sub>R</sub> = 1.234 min, does not ionize by ESI; Purity (AUC) ≥ 95%.

Step B: tert-Butyl (2-(3-bromopropoxy)-5-chlorophenyl)carbamate

2-Bromo-1-(3-bromopropoxy)-4-chlorobenzene (662 mg, 2.02 mmol, 1 eq), *tert*-butyl carbamate (260 mg, 2.22 mmol, 1.1 eq), Pd<sub>2</sub>(dba)<sub>3</sub> (37 mg, 0.04 mmol, 0.02 eq), Xantphos (70 mg, 0.12 mmol, 0.06 eq) and Cs<sub>2</sub>CO<sub>3</sub> (1970 mg, 6.05 mmol, 3 eq) were suspended in toluene (8.0 mL) and the mixture was purged with Ar. Then, it was stirred at 90 °C for 16 h. The mixture was filter through celite, and the solvent was removed under reduced pressure. The solid was re-dissolved in CH<sub>2</sub>Cl<sub>2</sub> and washed with water. The organic phase was concentrated and the crude was purified by ISCO flash chromatography to obtained the title compound (218 mg, 0.60 mmol, 30%). <sup>1</sup>H NMR (400 MHz, Chloroform-*d*) δ 8.15 (s, 1H), 7.00 (s, 1H), 6.90 (dd, *J* = 8.7, 2.3 Hz, 1H), 6.76 (d, *J* = 8.7 Hz, 1H), 4.14 (t, *J* = 6.1 Hz, 2H), 3.57 (t, *J* = 6.1 Hz, 2H), 2.37 (p, *J* = 6.1 Hz, 2H). LCMS (Method B): t<sub>R</sub> = 1.277 min, m/z = 264.1 [M-Boc]<sup>+</sup>; Purity (AUC) ≥ 95%.

Step C: 2-(3-bromopropoxy)-5-chloroaniline

*tert*-Butyl (2-(3-bromopropoxy)-5-chlorophenyl)carbamate (218 mg, 0.60 mmol) was reacted following General Procedure S. The crude was taken forward without further purification (158

mg, 0.60 mmol, quant.). <sup>1</sup>H NMR (400 MHz, Chloroform-*d*) δ 6.71 – 6.63 (m, 3H), 4.10 (t, *J* = 6.2 Hz, 2H), 3.77 – 3.68 (m, 2H), 3.58 (t, *J* = 6.2 Hz, 2H), 2.33 (p, *J* = 6.2 Hz, 2H). LCMS (Method B): *t*<sub>R</sub> = 0.904 min, *m/z* = 264.2, 266.1 [M+H]<sup>+</sup>; Purity (AUC) ≥ 95%.

Step D: 5-Bromo-*N*-(2-(3-bromopropoxy)-5-chlorophenyl)-3-chloro-2-hydroxybenzenesulfonamide

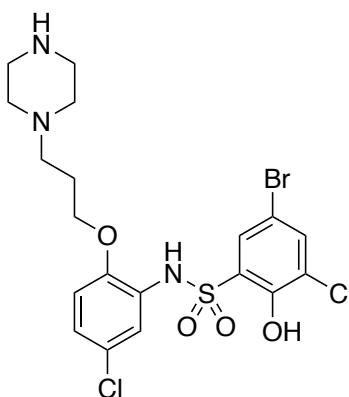
2-(3-Bromopropoxy)-5-chloroaniline (158 mg, 0.60 mmol) was reacted with 5-bromo-3-chloro-2-hydroxy-benzenesulfonyl chloride following General Procedure D. Purification by flash chromatography afforded the title compound (182 mg, 0.34 mmol, 57%). <sup>1</sup>H NMR (400 MHz, Chloroform-*d*) δ 7.65 – 7.58 (m, 2H), 7.50 (d, *J* = 2.5 Hz, 1H), 7.10 (dd, *J* = 8.8, 2.5 Hz, 1H), 6.75 (d, *J* = 8.8 Hz, 1H), 3.99 (t, *J* = 6.1 Hz, 2H), 3.51 (t, *J* = 6.1 Hz, 2H), 2.26 (p, *J* = 6.1 Hz, 2H). LCMS (Method B): *t*<sub>R</sub> = 1.242 min, *m/z* = 534.1, 536.0 [M+H]<sup>+</sup>; Purity (AUC) ≥ 95%.

Step E: 5-bromo-3-chloro-*N*-(5-chloro-2-(3-(methylamino)propoxy)phenyl)-2-hydroxybenzenesulfonamide

5-Bromo-*N*-(2-(3-bromopropoxy)-5-chlorophenyl)-3-chloro-2-hydroxybenzenesulfonamide (20 mg, 0.04 mmol, 1 eq) was dissolved in MeCN at 0.4 M and cooled to 0 °C using an ice/water bath. To this solution, methylamine (5.8 mg, 0.19 mmol, 5 eq) was added and stirred for 2 h. The solvent was removed under reduced pressure and the crude was purified by preparative HPLC, the title compound was obtained as the TFA salt (7 mg, 0.012 mmol, 30%). <sup>1</sup>H NMR (400 MHz, Methanol-*d*<sub>4</sub>) δ 7.47 (d, *J* = 2.7 Hz, 1H), 7.45 (d, *J* = 2.7 Hz, 1H), 7.42 (d, *J* = 2.7 Hz, 1H), 7.04 (dd, *J* = 8.8, 2.6 Hz, 1H), 6.90 (d, *J* = 8.8 Hz, 1H), 4.03 (t, *J* = 5.6 Hz, 2H), 3.26 (t, *J* = 5.6 Hz, 3H), 2.79 (s, 3H), 2.16 – 2.06 (m, 2H). LCMS (Method A): *t*<sub>R</sub> = 1.425 min, *m/z* = 484.8, 486.7 [M+H]<sup>+</sup>; Purity (AUC) ≥ 95%.



*5-Bromo-3-chloro-N-(5-chloro-2-(3-(piperazin-1-yl)propoxy)phenyl)-2-hydroxybenzenesulfonamide (VU0848421)*



Step A: *tert-butyl 4-(3-(2-((5-bromo-3-chloro-2-hydroxyphenyl)sulfonamido)-4-chlorophenoxy)propyl)piperazine-1-carboxylate*

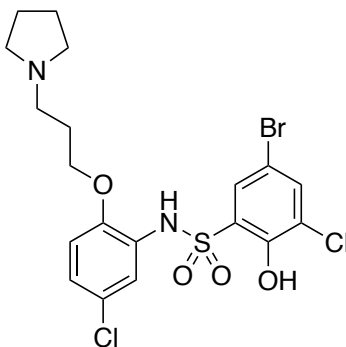
5-Bromo-*N*-(2-(3-bromopropoxy)-5-chlorophenyl)-3-chloro-2-hydroxybenzenesulfonamide (20 mg, 0.04 mmol, 1 eq) was dissolved in MeCN at 0.15 M and cooled to 0 °C using an ice/water bath. To this solution, *tert*-butyl piperazine-1-carboxylate (35 mg, 0.19 mmol, 5 eq) was added and stirred for 2 h. The solvent was removed under reduced pressure and the crude was purified by ISCO flash chromatography, 24 mg (0.04 mmol, quant) of the title compound were obtained. LCMS (Method A):  $t_R = 1.669$  min,  $m/z = 639.7, 641.7$   $[M+H]^+$ ; Purity (AUC)  $\geq 95\%$ .

Step B: *5-Bromo-3-chloro-N-(5-chloro-2-(3-(piperazin-1-yl)propoxy)phenyl)-2-hydroxybenzenesulfonamide*

*tert*-Butyl 4-(3-(2-((5-bromo-3-chloro-2-hydroxyphenyl)sulfonamido)-4-chlorophenoxy)propyl)piperazine-1-carboxylate (24 mg, 0.04 mmol) was reacted following General Procedure S. Purification by preparative HPLC afforded the title compound as the TFA salt (12 mg, 0.02 mmol, 50%).  $^1H$  NMR (600 MHz, DMSO- $d_6$ )  $\delta$  7.38 (d,  $J = 2.8$  Hz, 1H), 7.36 (d,  $J = 2.8$  Hz, 1H), 7.33 (s, 1H), 6.90 (s, 2H), 3.96 (t,  $J = 5.4$  Hz, 2H), 3.07 (br s, 5H), 2.68 (br s,

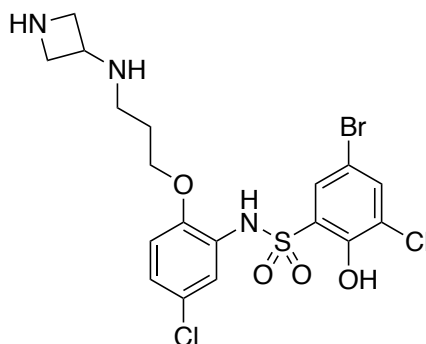
5H), 1.90 (t,  $J = 6.4$  Hz, 2H). LCMS (Method A):  $t_R = 1.308$  min,  $m/z = 539.7, 541.8$   $[M+H]^+$ ; Purity (AUC)  $\geq 95\%$ .

*5-bromo-3-chloro-N-(5-chloro-2-(3-(pyrrolidin-1-yl)propoxy)phenyl)-2-hydroxybenzenesulfonamide (VU0848425)*



5-Bromo-*N*-(2-(3-bromopropoxy)-5-chlorophenyl)-3-chloro-2-hydroxybenzenesulfonamide (20 mg, 0.04 mmol, 1 eq) was dissolved in MeCN at 0.4 M and cooled to 0 °C using an ice/water bath. To this solution, pyrrolidine (13 mg, 0.19 mmol, 5 eq) was added and stirred for 2 h. The solvent was removed under reduced pressure and the crude was purified by ISCO flash chromatography. Purification by preparative HPLC afforded the title compound as the TFA salt (11 mg, 0.021 mmol, 52%).  $^1\text{H}$  NMR (400 MHz, Acetone- $d_6$ )  $\delta$  7.57 (d,  $J = 2.5$  Hz, 1H), 7.51 (d,  $J = 2.7$  Hz, 1H), 7.37 (d,  $J = 2.7$  Hz, 1H), 7.02 (d,  $J = 8.7$  Hz, 1H), 6.95 (dd,  $J = 8.7, 2.5$  Hz, 1H), 4.23 – 4.16 (m, 2H), 3.70 – 3.45 (m, 6H), 2.42 – 2.31 (m, 2H), 2.21 – 2.13 (m, 4H). LCMS (Method A):  $t_R = 1.442$  min,  $m/z = 524.7, 526.8$   $[M+H]^+$ ; Purity (AUC)  $\geq 95\%$ .

*N*-(2-(3-(Azetidin-3-ylamino)propoxy)-5-chlorophenyl)-5-bromo-3-chloro-2-hydroxybenzenesulfonamide (VU0848426)



Step A: *tert*-butyl 3-((3-(2-((5-bromo-3-chloro-2-hydroxyphenyl)sulfonamido)-4-chlorophenoxy)propyl)amino)azetidine-1-carboxylate

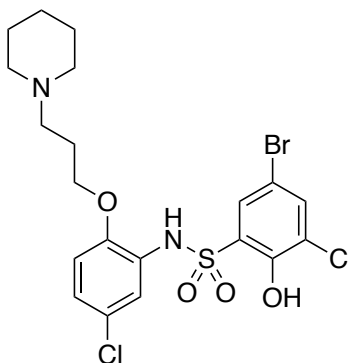
5-Bromo-*N*-(2-(3-bromopropoxy)-5-chlorophenyl)-3-chloro-2-hydroxybenzenesulfonamide (20 mg, 0.04 mmol, 1 eq) was dissolved in MeCN at 0.15 M and cooled to 0 °C using an ice/water bath. To this solution, *tert*-butyl piperazine-1-carboxylate (32 mg, 0.19 mmol, 5 eq) was added and stirred for 2 h. The solvent was removed under reduced pressure and the crude was purified by preparative HPLC, 18 mg (0.025 mmol, 62%) of the title compound were obtained as the TFA salt. LCMS (Method A):  $t_R = 1.697$  min,  $m/z = 625.8, 627.7$   $[M+H]^+$ ; Purity (AUC)  $\geq 95\%$ .

Step B: *N*-(2-(3-(Azetidin-3-ylamino)propoxy)-5-chlorophenyl)-5-bromo-3-chloro-2-hydroxybenzenesulfonamide

*tert*-Butyl 3-((3-(2-((5-bromo-3-chloro-2-hydroxyphenyl)sulfonamido)-4-chlorophenoxy)propyl)amino)azetidine-1-carboxylate (18 mg, 0.025 mmol) was reacted following General Procedure S. Purification by flash chromatography afforded the title compound (13 mg, 0.024 mmol, 99%).  $^1H$  NMR (400 MHz, Methanol- $d_4$ )  $\delta$  7.50 (d,  $J = 2.6$  Hz, 1H), 7.48 (d,  $J = 2.6$  Hz, 1H), 7.46 (d,  $J = 2.6$  Hz, 1H), 7.03 (dd,  $J = 8.8, 2.6$  Hz, 1H), 6.94 (d,  $J = 8.8$  Hz, 1H), 4.64 – 4.56 (m, 2H), 4.47 (dd,  $J = 12.1, 8.0$  Hz, 2H), 4.31 – 4.24 (m, 1H), 4.04 (t,  $J = 5.6$  Hz, 2H), 3.23

(t,  $J = 5.6$  Hz, 2H), 2.19 – 2.11 (m, 2H). LCMS (Method A):  $t_R = 1.284$  min,  $m/z = 525.7, 528.7$   $[M+H]^+$ ; Purity (AUC)  $\geq 95\%$ .

*5-Bromo-3-chloro-N-(5-chloro-2-(3-(piperidin-1-yl)propoxy)phenyl)-2-hydroxybenzenesulfonamide (VU0848429)*

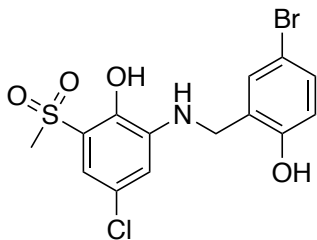


5-Bromo-*N*-(2-(3-bromopropoxy)-5-chlorophenyl)-3-chloro-2-hydroxybenzenesulfonamide (20 mg, 0.04 mmol, 1 eq) was dissolved in MeCN at 0.15 M and cooled to 0 °C using an ice/water bath. To this solution, piperidine (16 mg, 0.19 mmol, 5 eq) was added and stirred for 2 h. The solvent was removed under reduced pressure and the crude was purified by ISCO flash chromatography, 7 mg (0.013 mmol, 33%) of the title compound were obtained.  $^1\text{H}$  NMR (400 MHz, Methanol- $d_4$ )  $\delta$  7.47 (d,  $J = 2.6$  Hz, 1H), 7.45 – 7.40 (m, 2H), 7.02 (dd,  $J = 8.8, 2.6$  Hz, 1H), 6.87 (d,  $J = 8.8$  Hz, 1H), 4.01 (t,  $J = 5.3$  Hz, 2H), 3.43 – 3.30 (m, 8H), 2.23 (p,  $J = 6.1$  Hz, 2H), 1.94 (p,  $J = 6.1$  Hz, 4H). LCMS (Method A):  $t_R = 1.029$  min,  $m/z = 539.2, 541.2$   $[M+H]^+$ ; Purity (AUC)  $\geq 95\%$ .

## 6.3 Synthesis of analogs with sulfonamide replacements

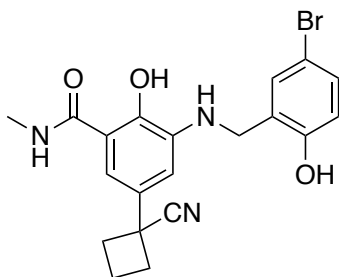
### 6.3.1 Benzyl amine linker

#### *2-((5-Bromo-2-hydroxybenzyl)amino)-4-chloro-6-(methylsulfonyl)phenol (VU0849826)*



2-Amino-4-chloro-6-(methylsulfonyl)phenol (33 mg, 0.15 mmol) was reacted with 5-bromo-2-hydroxybenzaldehyde following General Procedure Y. Purification by preparative HPLC afforded the title compound 40 mg (0.098 mmol, 79%) of title compound.  $^1\text{H NMR}$  (400 MHz, Chloroform-*d*)  $\delta$  7.32 (d,  $J = 8.0$  Hz, 2H), 7.07 (d,  $J = 2.3$  Hz, 1H), 6.84 (d,  $J = 2.3$  Hz, 1H), 6.76 (d,  $J = 8.0$  Hz, 1H), 4.37 (s, 2H), 3.14 (s, 3H). LCMS (Method B):  $t_{\text{R}} = 1.033$  min,  $m/z = 406.1, 408.2$   $[\text{M}+\text{H}]^+$ ; Purity (AUC)  $\geq 95\%$ .

#### *3-((5-Bromo-2-hydroxybenzyl)amino)-5-(1-cyanocyclobutyl)-2-hydroxy-N-methylbenzamide (VU0849831)*



#### Step A: Phenyl 3-((5-bromo-2-hydroxybenzyl)amino)-5-(1-cyanocyclobutyl)-2-hydroxybenzoate

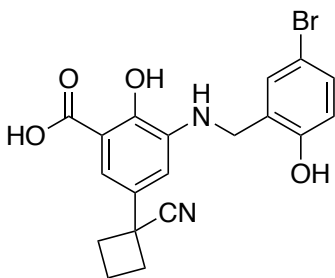
Phenyl 3-amino-5-(1-cyanocyclobutyl)-2-hydroxybenzoate (92 mg, 0.30 mmol) was reacted with 5-bromo-2-hydroxybenzaldehyde (50 mg, 0.25 mmol) following General Procedure Y.

Purification by preparative HPLC afforded the title compound as a yellow oil (127 mg, 0.25 mmol, 83%). LCMS (Method B):  $t_R = 1.264$  min,  $m/z = 493.3, 495.3$   $[M+H]^+$ ; Purity (AUC)  $\geq 95\%$ .

Step B: 3-((5-bromo-2-hydroxybenzyl)amino)-5-(1-cyanocyclobutyl)-2-hydroxy-N-methylbenzamide

Phenyl 3-((5-bromo-2-hydroxybenzyl)amino)-5-(1-cyanocyclobutyl)-2-hydroxybenzoate (63.5 mg, 0.129 mmol) was reacted following General Procedure F. Purification by preparative HPLC afforded the title compound as a yellow solid (31 mg, 0.072 mmol, 56%).  $^1H$  NMR (400 MHz, Chloroform-*d*)  $\delta$  7.32 (d,  $J = 2.4$  Hz, 1H), 7.29 (dd,  $J = 8.5, 2.4$  Hz, 1H), 6.88 (q,  $J = 2.4$  Hz, 2H), 6.76 (d,  $J = 8.5$  Hz, 1H), 6.53 (br d,  $J = 4.9$  Hz, 1H), 4.43 (s, 2H), 3.01 (d,  $J = 4.9$  Hz, 3H), 2.79 – 2.69 (m, 2H), 2.49 – 2.30 (m, 3H), 2.01 – 1.92 (m, 1H). LCMS (Method B):  $t_R = 1.034$  min,  $m/z = 430.3, 432.3$   $[M+H]^+$ ; Purity (AUC)  $\geq 95\%$ .

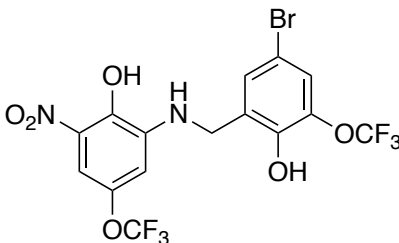
*3-((5-Bromo-2-hydroxybenzyl)amino)-5-(1-cyanocyclobutyl)-2-hydroxybenzoic acid*  
**(VU0849831)**



Phenyl 3-((5-bromo-2-hydroxybenzyl)amino)-5-(1-cyanocyclobutyl)-2-hydroxybenzoate (63 mg, 0.13 mmol) was reacted following General Procedure E. Purification by preparative HPLC afforded the title compound (4 mg, 0.010 mmol, 7%).  $^1H$  NMR (400 MHz, Chloroform-*d*)  $\delta$  7.50 (d,  $J = 2.3$  Hz, 1H), 7.35 – 7.29 (m, 2H), 7.12 (d,  $J = 2.3$  Hz, 1H), 6.78 (d,  $J = 9.2$  Hz, 1H), 4.46

(s, 2H), 2.81 – 2.74 (m, 1H), 2.53 – 2.33 (m, 4H), 2.05 – 1.96 (m, 1H). LCMS (Method B):  $t_R = 1.003$  min,  $m/z = 417.3, 419.2$   $[M+H]^+$ ; Purity (AUC)  $\geq 95\%$ .

*4-Bromo-2-(((2-hydroxy-3-nitro-5-(trifluoromethoxy)phenyl)amino)methyl)-6-(trifluoromethoxy)phenol (VU0816562)*



Step A: 2-Amino-6-nitro-4-(trifluoromethoxy)phenol

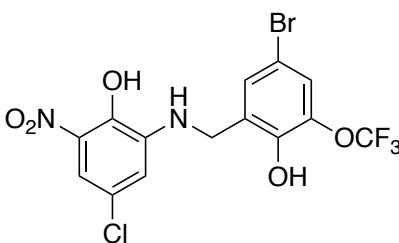
2,6-Dinitro-4-(trifluoromethoxy)phenol (60 mg, 0.22 mmol, 1 eq) was dissolved in EtOAc:H<sub>2</sub>O (10:1) at 0.11 M and SnCl<sub>2</sub>•2H<sub>2</sub>O (335 mg, 1.49 mmol, 5 eq) was added. The reaction mixture stirred at reflux temperature for 70 min. Upon cooling to r.t., a solution of celite and KF in H<sub>2</sub>O was added and stirred for 30 min. The mixture was filtered and the filtrate was extracted with EtOAc. The organic phase was concentrated and the crude was used without further purification (43 mg). LCMS (Method A):  $t_R = 1.572$  min,  $m/z = 239.1$ .

Step B: 4-Bromo-2-(((2-hydroxy-3-nitro-5-(trifluoromethoxy)phenyl)amino)methyl)-6-(trifluoromethoxy)phenol

2-Amino-6-nitro-4-(trifluoromethoxy)phenol (43 mg, crude) was reacted with 5-bromo-2-hydroxy-3-(trifluoromethoxy)benzaldehyde (30 mg, 0.15 mmol) following General Procedure Y. Purification by preparative HPLC afforded the title compound (11 mg, 0.022 mmol, 9%). <sup>1</sup>H NMR (400 MHz, Chloroform-*d*)  $\delta$  10.95 (s, 1H), 7.35 (s, 1H), 7.32 (d,  $J = 2.5$  Hz, 1H), 7.29 (d,  $J = 2.5$

Hz, 1H), 6.60 (d,  $J = 2.5$  Hz, 1H). LCMS (Method A):  $t_R = 2.064$  min,  $m/z = 456.7, 458.8$   $[M+H]^+$ ; Purity (AUC)  $\geq 95\%$ .

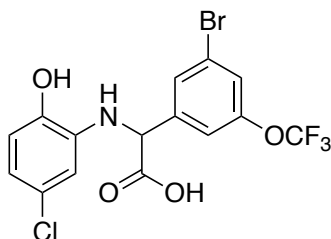
*4-Bromo-2-(((5-chloro-2-hydroxy-3-nitrophenyl)amino)methyl)-6-(trifluoromethoxy)phenol*  
*(VU0807489)*



2-Amino-4-chloro-6-nitrophenol (30 mg, 0.11 mmol) was reacted with 5-bromo-2-hydroxy-3-(trifluoromethoxy)benzaldehyde (24 mg, 0.13 mmol) following General Procedure Y. Purification by preparative HPLC afforded the title compound as an orange solid (11 mg, 0.24 mmol, 23%).  $^1\text{H}$  NMR (400 MHz, Chloroform-*d*)  $\delta$  7.42 (d,  $J = 2.3$  Hz, 1H), 7.35 (s, 1H), 7.32 (d,  $J = 2.3$  Hz, 1H), 6.70 (d,  $J = 2.3$  Hz, 1H), 5.11 (br s, 1H), 4.44 (s, 2H). LCMS (Method A):  $t_R = 2.064$  min,  $m/z = 456.7, 458.8$   $[M+H]^+$ ; Purity (AUC)  $\geq 95\%$ .

### 6.3.2 Amino acetic acid linker

*2-(3-Bromo-5-(trifluoromethoxy)phenyl)-2-((5-chloro-2-methoxyphenyl)amino)acetic acid (SC-1-93)*





Step A: 2-(3-Bromo-5-(trifluoromethoxy)phenyl)-2-((5-chloro-2-methoxyphenyl)amino)acetonitrile

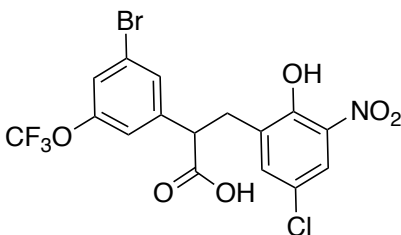
2-Methoxy-3-chloroaniline (44 mg, 0.28 mmol, 1.5 eq) and 5-bromo-3-(trifluoromethoxy)benzaldehyde (50 mg, 0.19 mmol, 1.0 eq) were dissolved in acetic acid (glacial) at 0.09 M. The solution was stirred at 50 °C for 1 h. Then, TMSCN (330 µL, 2.23 mmol, 12 eq) was added and continue stirring at 60 °C for 2 h. The solution was poured over a mixture of ice and NH<sub>4</sub>OH and it was extracted with CH<sub>2</sub>Cl<sub>2</sub>. The organic phase was concentrated and 92.1 mg of the title compound were obtained as a crude. LCMS (Method A): t<sub>R</sub> = 1.969 min, m/z = 453.7, 456.7 [M+NH<sub>4</sub>]<sup>+</sup>.

Step B: 2-(3-Bromo-5-(trifluoromethoxy)phenyl)-2-((5-chloro-2-methoxyphenyl)amino)acetic acid

2-(3-Bromo-5-(trifluoromethoxy)phenyl)-2-((5-chloro-2-methoxyphenyl)amino)acetonitrile (92.1 mg, crude) was dissolved in 2.5 mL of HCl (concentrated) and 0.50 mL of HOAc (glacial). The solution was refluxed until consumption of the starting material. Water was added and it was extracted with EtOAc. The organic phase was concentrated and the crude was purified using preparative HPLC, 22.2 mg (0.049 mmol, 26% yield) of the title compound were obtained. <sup>1</sup>H NMR (400 MHz, Chloroform-*d*) δ 7.62 (t, *J* = 1.9 Hz, 1H), 7.37 (s, 1H), 7.33 (s, 1H), 6.69 – 6.67 (m, 2H), 6.19 (d, *J* = 1.9 Hz, 1H), 5.04 (s, 1H), 3.89 (s, 3H). <sup>19</sup>F NMR (376 MHz, Chloroform-*d*) δ -55.62 (3F). LCMS (Method A): t<sub>R</sub> = 2.041 min, m/z = 453.7, 454.8 [M+H]<sup>+</sup>; Purity (AUC) ≥ 95%.

### 6.3.3 Propionic acid linker

#### *2-(3-Bromo-5-(trifluoromethoxy)phenyl)-3-(5-chloro-2-hydroxy-3-nitrophenyl)propanoic acid (VU0817326)*



##### Step A: (3-Bromo-5-(trifluoromethoxy)phenyl)methanol

3-Bromo-5-(trifluoromethoxy)benzaldehyde (3.000 g, 11.15 mmol) was reacted following General Procedure T. The crude was taken forward (3.020 g, 11.15 mmol, quant).  $^1\text{H}$  NMR (400 MHz, Chloroform-*d*)  $\delta$  7.44 (s, 1H), 7.30 (s, 1H), 7.16 (s, 1H), 4.68 (s, 2H).  $^{19}\text{F}$  NMR (376 MHz, Chloroform-*d*)  $\delta$  -60.94 (3F). LCMS (Method B):  $t_{\text{R}}$  = 0.976 min, does not ionize by ESI; Purity (AUC)  $\geq$  95%.

##### Step B: 3-Bromo-5-(trifluoromethoxy)benzyl methanesulfonate

(3-Bromo-5-(trifluoromethoxy)phenyl)methanol (1.820 g, 6.72 mmol) was reacted following General Procedure U. Purification by flash chromatography afforded the title compound (1.921 g, 5.50 mmol, 92%).  $^1\text{H}$  NMR (400 MHz, Chloroform-*d*)  $\delta$  7.50 (s, 1H), 7.41 (s, 1H), 7.21 (s, 1H), 5.19 (s, 2H), 3.03 (s, 3H).  $^{19}\text{F}$  NMR (376 MHz, Chloroform-*d*)  $\delta$  -57.94 (3F). LCMS (Method B):  $t_{\text{R}}$  = 1.175 min, does not ionize by ESI; Purity (AUC)  $\geq$  95%.

##### Step C: 2-(3-Bromo-5-(trifluoromethoxy)phenyl)acetonitrile

3-Bromo-5-(trifluoromethoxy)benzyl methanesulfonate (1.850 g, 5.30 mmol) was reacted following General Procedure V. Purification by flash chromatography afforded the title compound as a pale-yellow liquid (951 mg, 3.40 mmol, 64%).  $^1\text{H}$  NMR (400 MHz, Chloroform-*d*)  $\delta$  7.45 (s,

1H), 7.37 (s, 1H), 7.15 (s, 1H), 3.77 (s, 2H). <sup>19</sup>F NMR (376 MHz, Chloroform-*d*) δ -61.0 (3F). LCMS (Method B): t<sub>R</sub> = 1.123 min, does not ionize by ESI; Purity (AUC) ≥ 95%.

Step D: 2-(3-Bromo-5-(trifluoromethoxy)phenyl)-3-(5-chloro-2-hydroxy-3-nitrophenyl)acrylonitrile

2-(3-Bromo-5-(trifluoromethoxy)phenyl)acetonitrile (1.000 g, 3.57 mmol) was reacted with 5-chloro-2-hydroxy-3-nitrobenzaldehyde following General Procedure W. Purification by flash chromatography afforded the title compound (984 mg, 2.35 mmol, 66%). <sup>1</sup>H NMR (400 MHz, Chloroform-*d*) δ 11.12 (br s, 1H), 8.40 (d, *J* = 2.5 Hz, 1H), 8.24 (d, *J* = 2.5 Hz, 1H), 7.90 (s, 1H), 7.79 (t, *J* = 1.7 Hz, 1H), 7.48 (s, 2H). <sup>19</sup>F NMR (376 MHz, Chloroform-*d*) δ -60.9. LCMS (Method A): A mixture of *cis* and *trans* was observed t<sub>R</sub> = 2.059 min and 2.184 min m/z = 462.7, 463.8 (same for both peaks) [M+H]<sup>+</sup>.

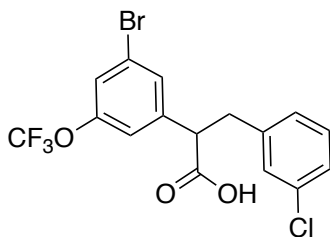
Step E: 2-(3-Bromo-5-(trifluoromethoxy)phenyl)-3-(5-chloro-2-hydroxy-3-nitrophenyl)propanenitrile (VU0817346)

2-(3-Bromo-5-(trifluoromethoxy)phenyl)-3-(5-chloro-2-hydroxy-3-nitrophenyl)acrylonitrile (500 mg, 1.08 mmol) was reacted following General Procedure T. The crude was taken forward without further purification (502 mg, 1.08 mmol, quant). <sup>1</sup>H NMR (400 MHz, Chloroform-*d*) δ 10.94 (br s, 1H), 8.12 (d, *J* = 2.6 Hz, 1H), 7.52 (t, *J* = 1.5 Hz, 1H), 7.48 (d, *J* = 2.6 Hz, 1H), 7.42 (s, 1H), 7.16 (s, 1H), 4.28 (dd, *J* = 9.9, 5.6 Hz, 1H), 3.33 (dd, *J* = 13.6, 5.7 Hz, 1H), 3.14 (dd, *J* = 13.6, 9.9 Hz, 1H). <sup>19</sup>F NMR (376 MHz, Chloroform-*d*) δ -57.9 (3F). LCMS (Method B): t<sub>R</sub> = 1.508 min, does not ionize by ESI; Purity (AUC) ≥ 95%.

Step F: 2-(3-Bromo-5-(trifluoromethoxy)phenyl)-3-(5-chloro-2-hydroxy-3-nitrophenyl)propanoic acid

2-(3-Bromo-5-(trifluoromethoxy)phenyl)-3-(5-chloro-2-hydroxy-3-nitrophenyl)propanenitrile (14 mg, 0.030 mmol) was dissolved in 100  $\mu$ L of HOAc (glacial) and 500  $\mu$ L of HCl (concentrated). The mixture was stirred overnight while heating to reflux. The solvent was removed under reduced pressure and the crude was purified using preparative HPLC. Purification by preparative HPLC afforded the title compound as a yellow solid (13.7 mg, 0.028, 94%).  $^1\text{H}$  NMR (400 MHz, Methanol- $d_4$ )  $\delta$  7.99 (d,  $J$  = 2.6 Hz, 1H), 7.55 – 7.50 (m, 1H), 7.41 (d,  $J$  = 2.6 Hz, 1H), 7.39 (s, 1H), 7.24 (s, 1H), 4.13 (t,  $J$  = 7.8 Hz, 1H), 3.43 (dd,  $J$  = 13.7, 7.8 Hz, 1H), 3.16 (dd,  $J$  = 13.7, 7.8 Hz, 1H).  $^{19}\text{F}$  NMR (376 MHz, Methanol- $d_4$ )  $\delta$  -62.7 (3F). LCMS (Method A):  $t_{\text{R}}$  = 1.992 min, does not ionize by ESI; Purity (AUC)  $\geq$  94%.

2-(3-Bromo-5-(trifluoromethoxy)phenyl)-3-(3-chlorophenyl)propanoic acid (VU0825941)



Step A: 2-(3-Bromo-5-(trifluoromethoxy)phenyl)-3-(3-chlorophenyl)acrylonitrile

2-(3-Bromo-5-(trifluoromethoxy)phenyl)acetonitrile (100 mg, 0.36 mmol) was reacted with 3-chlorobenzaldehyde following General Procedure W. The crude was taken forward (160 mg). LCMS (Method B, 2 min gradient): 1.616 min, does not ionize by ESI.

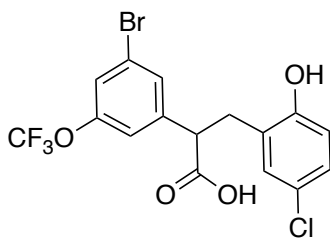
Step B: 2-(3-Bromo-5-(trifluoromethoxy)phenyl)-3-(3-chlorophenyl)propanenitrile

2-(3-Bromo-5-(trifluoromethoxy)phenyl)-3-(5-chloro-2-hydroxy-3-nitrophenyl)acrylonitrile (160 mg, crude) was reacted following General Procedure T. Purification by preparative HPLC afforded the title compound (77.2 mg, 0.19 mmol, 53%). <sup>1</sup>H NMR (400 MHz, Chloroform-*d*) δ 7.41 (d, *J* = 1.8 Hz, 2H), 7.31 – 7.29 (m, 1H), 7.28 (d, *J* = 1.8 Hz, 1H), 7.14 (t, *J* = 1.8 Hz, 1H), 7.07 – 7.01 (m, 2H), 4.02 (dd, *J* = 8.1, 6.5 Hz, 1H), 3.29 – 3.07 (m, 2H). <sup>19</sup>F NMR (376 MHz, Chloroform-*d*) δ -61.0 (3F). LCMS (Method B): *t*<sub>R</sub> = 1.482 min, does not ionize by ESI; Purity (AUC) ≥ 93%.

Step C: 2-(3-Bromo-5-(trifluoromethoxy)phenyl)-3-(3-chlorophenyl)propanoic acid

2-(3-Bromo-5-(trifluoromethoxy)phenyl)-3-(3-chlorophenyl)propanenitrile (77 mg, 0.19 mmol) was dissolved in 200 μL of HOAc (glacial) and 1000 μL of HCl (concentrated). The mixture was stirred overnight while heating to reflux. The solvent was removed under reduced and Purification by preparative HPLC afforded the title compound (34.7 mg, 0.082, 43%). <sup>1</sup>H NMR (400 MHz, Chloroform-*d*) δ 7.40 (t, *J* = 1.7 Hz, 1H), 7.32 (s, 1H), 7.19 – 7.15 (m, 2H), 7.12 – 7.07 (m, 2H), 6.94 (dt, *J* = 6.7, 1.7 Hz, 1H), 3.82 (t, *J* = 7.8 Hz, 1H), 3.36 (dd, *J* = 13.9, 7.8 Hz, 1H), 2.99 (dd, *J* = 13.9, 7.8 Hz, 1H). <sup>19</sup>F NMR (376 MHz, Methanol-*d*<sub>4</sub>) δ -61.0 (3F). LCMS (Method B): *t*<sub>R</sub> = 1.285 min, *m/z* = 439.3 [M+NH<sub>4</sub>]<sup>+</sup>; Purity (AUC) ≥ 95%.

*2-(3-Bromo-5-(trifluoromethoxy)phenyl)-3-(5-chloro-2-hydroxyphenyl)propanoic acid*  
(VU0826045)



Step A: 2-((tert-Butyldimethylsilyl)oxy)-5-chlorobenzaldehyde

5-Chloro-2-hydroxybenzaldehyde (300 mg, 1.92 mmol, 1 eq) was dissolved in CH<sub>2</sub>Cl<sub>2</sub> at 0.30 M. TBDMSCl (433 mg, 2.88 mmol, 1.5 eq) and Et<sub>3</sub>N (1.35 mL, 9.62 mmol, 5 eq) were added and the solution was stirred at room temperature for 3 h. The solvent was removed under reduced pressure and the crude was purified using ISCO flash chromatography. Purification by flash chromatography afforded the title compound as a light-yellow solid (511.7 mg, 1.89 mmol, 98%). LCMS (Method B): t<sub>R</sub> = 1.4805 min, m/z = 271.2, 2732 [M+H]<sup>+</sup>; Purity (AUC) ≥ 95%.

Step B: 2-(3-Bromo-5-(trifluoromethoxy)phenyl)-3-(5-chloro-2-hydroxyphenyl)acrylonitrile

2-(3-Bromo-5-(trifluoromethoxy)phenyl)acetonitrile (92 mg, 0.36 mmol) was reacted with 2-((tert-butyldimethylsilyl)oxy)-5-chlorobenzaldehyde following General Procedure W. The deprotected title compound was obtained as a crude (170 mg) which was taken forward without further purification. LCMS (Method B): 1.010 min, m/z = 418.0, 420.0 [M+H]<sup>+</sup>.

Step C: 2-(3-Bromo-5-(trifluoromethoxy)phenyl)-3-(5-chloro-2-hydroxyphenyl)propanenitrile

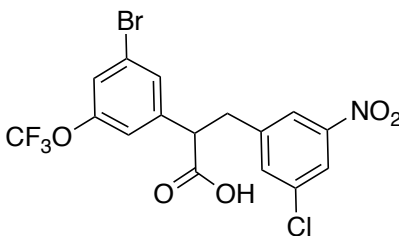
2-(3-Bromo-5-(trifluoromethoxy)phenyl)-3-(5-chloro-2-hydroxyphenyl)acrylonitrile (170 mg, crude) was reacted following General Procedure T. Purification by preparative HPLC afforded the title compound (60.4 mg, 0.14 mmol, 40%). <sup>1</sup>H NMR (400 MHz, Chloroform-*d*) δ 7.47 (t, *J* = 1.6 Hz, 1H), 7.38 (s, 1H), 7.13 (dd, *J* = 8.5, 2.6 Hz, 1H), 7.10 (s, 1H), 7.04 (d, *J* = 2.6 Hz, 1H), 6.71 (d, *J* = 8.5 Hz, 1H), 4.25 (dd, *J* = 8.2, 5.7 Hz, 1H), 3.12 (dd, *J* = 7.2, 5.7 Hz, 2H). <sup>19</sup>F NMR (376 MHz, Chloroform-*d*) δ -61.0 (3F). LCMS (Method B): t<sub>R</sub> = 1.349 min, does not ionize by ESI; Purity (AUC) ≥ 95%.

Step D: 2-(3-Bromo-5-(trifluoromethoxy)phenyl)-3-(5-chloro-2-hydroxyphenyl)propanoic acid

2-(3-Bromo-5-(trifluoromethoxy)phenyl)-3-(5-chloro-2-hydroxyphenyl)propanenitrile (60.4 mg, 0.14 mmol) was dissolved in 120 μL of HOAc (glacial) and 600 μL of HCl (concentrated). The

mixture was stirred overnight while heating to reflux. The solvent was removed under reduced pressure and the crude was purified by preparative HPLC, 18.8 mg (0.043 mmol, 31%) of the title compound were obtained. <sup>1</sup>H NMR (400 MHz, Chloroform-*d*) δ 7.43 (t, *J* = 1.5 Hz, 1H), 7.34 (s, 1H), 7.13 (s, 1H), 7.07 (dd, *J* = 8.5, 2.6 Hz, 1H), 7.00 (d, *J* = 2.6 Hz, 1H), 6.75 (d, *J* = 8.5 Hz, 1H), 4.00 (dd, *J* = 9.8, 5.3 Hz, 1H), 3.33 (dd, *J* = 13.9, 9.8 Hz, 1H), 2.91 (dd, *J* = 13.9, 5.3 Hz, 1H). <sup>19</sup>F NMR (376 MHz, Methanol-*d*<sub>4</sub>) δ -60.9 (3F). LCMS (Method A): *t*<sub>R</sub> = 1.871 min, *m/z* = 439.0, 442.9 [M+H]<sup>+</sup>; Purity (AUC) ≥ 95%.

*2-(3-bromo-5-(trifluoromethoxy)phenyl)-3-(3-chloro-5-nitrophenyl)propanoic acid (VU0826458)*



*Step A: 2-(3-bromo-5-(trifluoromethoxy)phenyl)-3-(3-chloro-5-nitrophenyl)acrylonitrile*

2-(3-Bromo-5-(trifluoromethoxy)phenyl)acetonitrile (20 mg, 0.071 mmol) was reacted with 3-chloro-5-nitrobenzaldehyde following General Procedure W. It was obtained 32.0 mg of title compound as the crude which was taken forward without further purification. LCMS (Method A): 2.258 min, *m/z* = 465.7, 467.7 [M+NH<sub>4</sub>]<sup>+</sup>.

*Step B: 2-(3-Bromo-5-(trifluoromethoxy)phenyl)-3-(3-chloro-5-nitrophenyl)propanenitrile*

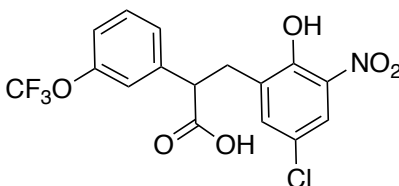
2-(3-Bromo-5-(trifluoromethoxy)phenyl)-3-(3-chloro-5-nitrophenyl)acrylonitrile (32.0 mg, crude) was reacted following General Procedure T. It was obtained 40.0 mg of title compound as the crude which was used without further purification. LCMS (Method A): *t*<sub>R</sub> = 2.064 min, does not ionize by ESI.

Step C: 2-(3-Bromo-5-(trifluoromethoxy)phenyl)-3-(3-chloro-5-nitrophenyl)propanoic acid

2-(3-Bromo-5-(trifluoromethoxy)phenyl)-3-(3-chloro-5-nitrophenyl)propanenitrile (40 mg, crude) was dissolved in 300  $\mu$ L of HOAc (glacial) and 300  $\mu$ L of HCl (concentrated). The mixture was stirred overnight while heating to reflux. The solvent was removed under reduced pressure. The crude was purified using preparative HPLC and 7.6 mg (0.016 mmol, 23%) of the title compound were obtained.  $^1\text{H}$  NMR (400 MHz, Chloroform-*d*)  $\delta$  8.09 (t,  $J = 1.8$  Hz, 1H), 7.90 (t,  $J = 1.8$  Hz, 1H), 7.43 (dt,  $J = 6.0, 1.8$  Hz, 2H), 7.36 (s, 1H), 7.10 (s, 1H), 3.88 (dd,  $J = 8.7, 6.8$  Hz, 1H), 3.47 (dd,  $J = 14.0, 8.7$  Hz, 1H), 3.10 (dd,  $J = 14.0, 6.8$  Hz, 1H). LCMS (Method A):  $t_{\text{R}} = 2.082$  min, does not ionize by ESI; Purity (AUC)  $\geq 95\%$ .

*3-(5-Chloro-2-hydroxy-3-nitrophenyl)-2-(3-(trifluoromethoxy)phenyl)propanenitrile*

*(VU0825987)*



Step A: 2-((tert-Butyldimethylsilyl)oxy)-5-chloro-3-nitrobenzaldehyde

5-Chloro-2-hydroxy-3-nitrobenzaldehyde (500 mg, 2.48 mmol, 1 eq) was dissolved in  $\text{CH}_2\text{Cl}_2$  at 0.30 M. TBDMSCl (744 mg, 4.96 mmol, 2 eq) and  $\text{Et}_3\text{N}$  (1.0 mL, 7.44 mmol, 3 eq) were added and the solution was stirred overnight at room temperature. The solvent was removed under reduced pressure and the crude was purified using ISCO flash chromatography. The title compound was afforded as a yellow solid (570.3 mg, 1.89 mmol, 98%).  $^1\text{H}$  NMR (400 MHz, Chloroform-*d*)  $\delta$  10.30 (s, 1H), 8.04 (d,  $J = 2.8$  Hz, 1H), 8.00 (d,  $J = 2.8$  Hz, 1H), 1.05 (s, 9H), 0.13 (s, 6H). LCMS (Method A):  $t_{\text{R}} = 2.406$  min, does not ionize by ESI; Purity (AUC)  $\geq 95\%$ .



Step B: 3-(Trifluoromethoxy)phenyl)methanol

3-(Trifluoromethoxy)benzaldehyde (800 mg, 4.21 mmol) was reacted following General Procedure T. The crude was taken forward (500 mg). LCMS (Method B):  $t_R = 0.825$  min,  $m/z = 215.2$  [M+Na]<sup>+</sup>.

Step C: 3-(Trifluoromethoxy)benzyl methanesulfonate

(3-(Trifluoromethoxy)phenyl)methanol (500 mg, crude) was reacted following General Procedure U. Purification by ISCO flash chromatography afforded the title compound (189 mg, 0.54 mmol, 22%) of title compound. <sup>1</sup>H NMR (400 MHz, Chloroform-*d*)  $\delta$  7.44 (t,  $J = 7.9$  Hz, 1H), 7.35 (d,  $J = 7.7$  Hz, 1H), 7.27 (s, 1H), 7.25 (d,  $J = 8.0$  Hz, 1H), 5.24 (s, 2H), 2.98 (s, 3H). LCMS (Method B):  $t_R = 1.033$  min, does not ionize by ESI; Purity (AUC)  $\geq 95\%$ .

Step D: 2-(3-(Trifluoromethoxy)phenyl)acetonitrile

3-(Trifluoromethoxy)benzyl methanesulfonate (189 mg, 0.54 mmol) was reacted following General Procedure V. It was obtained 100 mg (0.50 mmol, 93%) of title compound. <sup>1</sup>H NMR (400 MHz, Chloroform-*d*)  $\delta$  7.41 (t,  $J = 8.3$  Hz, 1H), 7.32 – 7.25 (m, 1H), 7.19 (d,  $J = 6.4$  Hz, 2H), 3.77 (s, 2H). LCMS (Method B):  $t_R = 1.021$  min, does not ionize by ESI; Purity (AUC)  $\geq 95\%$ .

Step E: 3-(2-((tert-Butyldimethylsilyl)oxy)-5-chloro-3-nitrophenyl)-2-(3-(trifluoromethoxy)phenyl)acrylonitrile

2-(3-(Trifluoromethoxy)phenyl)acetonitrile (100 mg, 0.50 mmol) was reacted with 2-((tert-butyl)dimethylsilyl)oxy)-5-chloro-3-nitrobenzaldehyde following General Procedure W. The crude was taken forward (250 mg). LCMS (Method B):  $t_R = 1.045$  min,  $m/z = 384.3, 386.0$  [M-Boc]<sup>+</sup>.

Step F: 3-(5-Chloro-2-hydroxy-3-nitrophenyl)-2-(3-(trifluoromethoxy)phenyl)propanenitrile

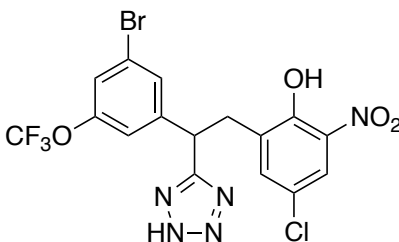
3-(2-((tert-Butyldimethylsilyl)oxy)-5-chloro-3-nitrophenyl)-2-(3-(trifluoromethoxy)phenyl)acrylonitrile (250 mg, crude) was reacted following General Procedure

T. Purification by preparative HPLC afforded the title compound (10.5 mg, 0.027 mmol, 5%). <sup>1</sup>H NMR (400 MHz, Chloroform-d) δ 10.97 (s, 1H), 8.09 (d, *J* = 2.6 Hz, 1H), 7.46 (t, *J* = 8.0 Hz, 1H), 7.42 (d, *J* = 2.6 Hz, 1H), 7.34 (d, *J* = 8.0 Hz, 1H), 7.24 (d, *J* = 8.0 Hz, 1H), 7.20 (s, 1H), 4.30 (dd, *J* = 9.5, 6.0 Hz, 1H), 3.32 (dd, *J* = 13.6, 6.0 Hz, 1H), 3.19 (dd, *J* = 13.6, 9.5 Hz, 1H). <sup>19</sup>F NMR (376 MHz, Chloroform-d) δ -57.9 (3F). LCMS (Method B): *t*<sub>R</sub> = 1.367 min, *m/z* = 404.8 [M+NH<sub>4</sub>]<sup>+</sup>; Purity (AUC) ≥ 90%.

*Step G: 3-(5-Chloro-2-hydroxy-3-nitrophenyl)-2-(3-(trifluoromethoxy)phenyl)propanoic acid*

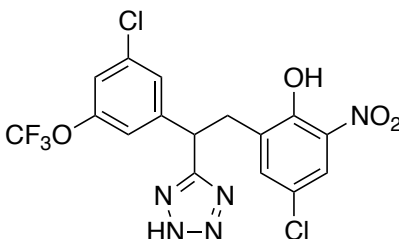
3-(5-Chloro-2-hydroxy-3-nitrophenyl)-2-(3-(trifluoromethoxy)phenyl)propanenitrile (10.5 mg, 0.027 mmol) was dissolved in 120 μL of HOAc (glacial) and 600 μL of HCl (concentrated). The mixture was stirred overnight while heating to reflux. The solvent was removed under reduced pressure and the crude was purified using preparative HPLC to obtain the title compound (9.7 mg, 0.024 mmol, 94%) of title compound as a yellow solid. <sup>1</sup>H NMR (400 MHz, Chloroform-*d*) δ 10.90 (s, 1H), 7.98 (d, *J* = 2.6 Hz, 1H), 7.41 – 7.32 (m, 1H), 7.28 (d, *J* = 2.6 Hz, 1H), 7.24 (d, *J* = 7.6 Hz, 1H), 7.16 (d, *J* = 7.6 Hz, 2H), 4.12 (dd, *J* = 8.4, 7.0 Hz, 1H), 3.43 (dd, *J* = 13.7, 8.4 Hz, 1H), 3.14 (dd, *J* = 13.7, 7.0 Hz, 1H). <sup>19</sup>F NMR (376 MHz, Chloroform-*d*) δ -57.9. LCMS (Method B): *t*<sub>R</sub> = 1.197 min, *m/z* = 423.4 [M+NH<sub>4</sub>]<sup>+</sup>; Purity (AUC) ≥ 95%.

*2-(2-(3-Bromo-5-(trifluoromethoxy)phenyl)-2-(2H-tetrazol-5-yl)ethyl)-4-chloro-6-nitrophenol*  
(VU0825970)



2-(3-Bromo-5-(trifluoromethoxy)phenyl)-3-(5-chloro-2-hydroxy-3-nitrophenyl)propanenitrile (40 mg, 0.07 mmol) was reacted following General Procedure TZ. It was obtained 28.3 mg (0.056, 80%) of title compound. <sup>1</sup>H NMR (400 MHz, Chloroform-*d*) δ 10.94 (br s, 1H), 7.96 (d, *J* = 2.6 Hz, 1H), 7.43 (s, 1H), 7.31 (s, 1H), 7.27 (d, *J* = 2.6 Hz, 1H), 7.15 (s, 1H), 4.91 (t, *J* = 7.8 Hz, 1H), 3.69 (dd, *J* = 13.7, 7.8 Hz, 1H), 3.48 (dd, *J* = 13.7, 7.8 Hz, 1H). <sup>19</sup>F NMR (376 MHz, Methanol-*d*<sub>4</sub>) δ -57.9 (3F). LCMS (Method B): *t*<sub>R</sub> = 1.317 min, *m/z* = 508.0, 510.9 Purity (AUC) ≥ 95%.

*4-Chloro-2-(2-(3-chloro-5-(trifluoromethoxy)phenyl)-2-(2H-tetrazol-5-yl)ethyl)-6-nitrophenol (VU0826895)*



*Step A: (3-Chloro-5-(trifluoromethoxy)phenyl)methanol*

3-Chloro-5-(trifluoromethoxy)benzaldehyde (500 mg, 2.23 mmol) was reacted following General Procedure T. It was obtained 291 mg (1.28 mmol, 58%) of title compound after ISCO flash chromatography. <sup>1</sup>H NMR (400 MHz, Chloroform-*d*) δ 7.29 (s, 1H), 7.15 (s, 1H), 7.12 (s, 1H), 4.69 (s, 2H). <sup>19</sup>F NMR (376 MHz, Chloroform-*d*) δ -57.9 (3F). LCMS (Method B): *t*<sub>R</sub> = 1.011 min, does not ionize by ESI; Purity (AUC) ≥ 95%.

*Step B: 3-Chloro-5-(trifluoromethoxy)benzyl methanesulfonate*

(3-Chloro-5-(trifluoromethoxy)phenyl)methanol (291 mg, 1.28 mmol) was reacted following General Procedure U. It was obtained 164 mg (0.54 mmol, 42%) of title compound. <sup>1</sup>H NMR (400 MHz, Chloroform-*d*) δ 7.37 (d, *J* = 1.9 Hz, 1H), 7.26 (s, 1H), 7.19 (s, 1H), 5.21 (s, 2H), 3.04 (s,

3H). <sup>19</sup>F NMR (376 MHz, Chloroform-*d*) δ -58.0 (3F). LCMS (Method B): t<sub>R</sub> = 1.655 min, does not ionize by ESI; Purity (AUC) ≥ 95%.

Step C: 2-(3-Chloro-5-(trifluoromethoxy)phenyl)acetonitrile

3-Chloro-5-(trifluoromethoxy)benzyl methanesulfonate (164 mg, 0.54 mmol) was reacted following General Procedure V. It was obtained 68 mg (0.29 mmol, 53%) of title compound. <sup>1</sup>H NMR (400 MHz, Chloroform-*d*) δ 7.31 (s, 1H), 7.22 (s, 1H), 7.11 (s, 1H), 3.77 (s, 2H). <sup>19</sup>F NMR (376 MHz, Chloroform-*d*) δ -58.0 (3F). LCMS (Method B): t<sub>R</sub> = 1.171 min, m/z = 236.3; Purity (AUC) ≥ 95%.

Step D: 2-(3-Chloro-5-(trifluoromethoxy)phenyl)-3-(5-chloro-2-hydroxy-3-nitrophenyl)acrylonitrile

2-(3-Chloro-5-(trifluoromethoxy)phenyl)acetonitrile (68 mg, 0.29 mmol) was reacted with 5-chloro-2-hydroxy-3-nitrobenzaldehyde following General Procedure W. The crude was taken forward (121 mg). LCMS (Method B) observed t<sub>R</sub> = 1.577 min, m/z = 419.1, 421.3 [M+H]<sup>+</sup>.

Step E: 2-(3-Chloro-5-(trifluoromethoxy)phenyl)-3-(5-chloro-2-hydroxy-3-nitrophenyl)propanenitrile

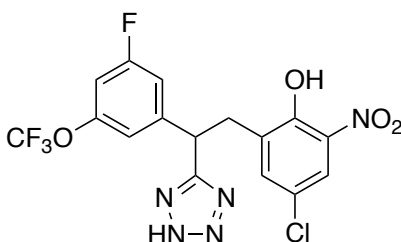
2-(3-Chloro-5-(trifluoromethoxy)phenyl)-3-(5-chloro-2-hydroxy-3-nitrophenyl)acrylonitrile (121 mg, crude) was reacted following General Procedure T. The crude was taken forward (123.9 mg). LCMS (Method B): t<sub>R</sub> = 1.492 min, does not ionize by ESI.

Step F: 4-Chloro-2-(2-(3-chloro-5-(trifluoromethoxy)phenyl)-2-(2H-tetrazol-5-yl)ethyl)-6-nitrophenol

2-(3-Chloro-5-(trifluoromethoxy)phenyl)-3-(5-chloro-2-hydroxy-3-nitrophenyl)propanenitrile (123.9 mg, crude) was reacted following General Procedure TZ. Purification by preparative HPLC afforded the title compound as a yellow solid (48.9 mg, 0.11 mmol, 38%). <sup>1</sup>H NMR (400 MHz,

Chloroform-*d*)  $\delta$  10.93 (br s, 1H), 7.94 (d,  $J = 2.6$  Hz, 1H), 7.29 (t,  $J = 1.7$  Hz, 1H), 7.27 (s, 1H), 7.15 (s, 1H), 7.11 (s, 1H), 4.96 (t,  $J = 7.8$  Hz, 1H), 3.70 (dd,  $J = 13.7, 7.8$  Hz, 1H), 3.50 (dd,  $J = 13.7, 7.8$  Hz, 1H). LCMS (Method B):  $t_R = 1.333$  min,  $m/z = 464.2, 466.3$   $[M+H]^+$ ; Purity (AUC)  $\geq 95\%$ .

*4-Chloro-2-(2-(3-fluoro-5-(trifluoromethoxy)phenyl)-2-(2H-tetrazol-5-yl)ethyl)-6-nitrophenol*  
(VU0827423)



Step A: 2-(3-Fluoro-5-(trifluoromethoxy)phenyl)acetonitrile

3-Fluoro-5-(trifluoromethoxy)benzylbromide (200 mg, 0.73 mmol) was reacted following General Procedure V. It was obtained 44.1 mg (0.20 mmol, 28%) of title compound.  $^1\text{H}$  NMR (400 MHz, Chloroform-*d*)  $\delta$  7.05 (dd,  $J = 8.7, 2.1$  Hz, 1H), 7.02 (s, 1H), 6.96 (d,  $J = 8.7$  Hz, 1H), 3.78 (s, 2H).  $^{19}\text{F}$  NMR (376 MHz, Chloroform-*d*)  $\delta$  -61.1 (3F), -110.8 (1F). LCMS (Method B):  $t_R = 1.013$  min, does not ionize by ESI; Purity (AUC)  $\geq 95\%$ .

Step B: 3-(5-Chloro-2-hydroxy-3-nitrophenyl)-2-(3-fluoro-5-(trifluoromethoxy)phenyl)acrylonitrile

2-(3-Fluoro-5-(trifluoromethoxy)phenyl)acetonitrile (44.1 mg, 0.20 mmol) was reacted with 5-chloro-2-hydroxy-3-nitrobenzaldehyde following General Procedure W. The crude was taken forward (91.7 mg). LCMS (Method B):  $t_R = 1.133$  min,  $m/z = 403.2, 404.2$   $[M+H]^+$ .

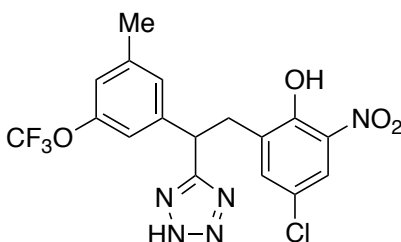
Step C: 3-(5-Chloro-2-hydroxy-3-nitrophenyl)-2-(3-fluoro-5-(trifluoromethoxy)phenyl)propanenitrile

3-(5-Chloro-2-hydroxy-3-nitrophenyl)-2-(3-fluoro-5-(trifluoromethoxy)phenyl)acrylonitrile (91.7 mg, crude) was reacted following General Procedure T. Purification by flash chromatography afforded the title compound as a yellow solid (36.4 mg, 0.077 mmol, 26%). <sup>1</sup>H NMR (400 MHz, Chloroform-*d*) δ 10.99 (br s, 1H), 8.11 (d, *J* = 2.6 Hz, 1H), 7.47 (d, *J* = 2.6 Hz, 1H), 7.15 – 7.09 (m, 1H), 7.03 (s, 1H), 7.01 – 6.94 (m, 2H), 4.31 (dd, *J* = 9.7, 5.8 Hz, 1H), 3.34 (dd, *J* = 13.6, 5.8 Hz, 1H), 3.16 (dd, *J* = 13.6, 9.7 Hz, 1H). <sup>19</sup>F NMR (376 MHz, Chloroform-*d*) δ -58.1 (3F), -107.0 (1F). LCMS (Method B): *t*<sub>R</sub> = 1.301 min, does not ionize by ESI; Purity (AUC) ≥ 87%.

Step D: 4-Chloro-2-(2-(3-fluoro-5-(trifluoromethoxy)phenyl)-2-(2H-tetrazol-5-yl)ethyl)-6-nitrophenol

3-(5-Chloro-2-hydroxy-3-nitrophenyl)-2-(3-fluoro-5-(trifluoromethoxy)phenyl)propanenitrile (36.4 mg, 0.052 mmol) was reacted following General Procedure TZ. Purification by preparative HPLC to afford the title compound as a yellow solid (17.2 mg, 0.038 mmol, 49%). <sup>1</sup>H NMR (400 MHz, Chloroform-*d*) δ 10.96 (s, 1H), 7.96 (d, *J* = 2.7 Hz, 1H), 7.27 (d, *J* = 2.7 Hz, 1H), 7.03 (d, *J* = 8.8 Hz, 1H), 6.98 (s, 1H), 6.89 (d, *J* = 8.8 Hz, 1H), 4.92 (t, *J* = 7.8 Hz, 1H), 3.70 (dd, *J* = 13.7, 7.8 Hz, 1H), 3.48 (dd, *J* = 13.7, 7.8 Hz, 1H). <sup>19</sup>F NMR (376 MHz, Chloroform-*d*) δ -61.1 (3F), -110.7 (1F). LCMS (Method B): *t*<sub>R</sub> = 1.203 min, *m/z* = 448.2, 450.2 [M+H]<sup>+</sup>; Purity (AUC) ≥ 95%.

*4-Chloro-2-(2-(3-methyl-5-(trifluoromethoxy)phenyl)-2-(2H-tetrazol-5-yl)ethyl)-6-nitrophenol*



Step A: 2-(3-Methyl-5-(trifluoromethoxy)phenyl)acetonitrile

2-(3-Bromo-5-(trifluoromethoxy)phenyl)acetonitrile (80 mg, 0.29 mmol) was reacted with methyl boronic acid following General Procedure J. It was obtained 13.7 mg (0.064 mmol, 22%) of title compound (some was lost during the collection of fractions). <sup>1</sup>H NMR (400 MHz, Chloroform-*d*) δ 7.10 (s, 1H), 7.01 (s, 1H), 6.98 (s, 1H), 3.73 (s, 2H), 2.39 (s, 3H). <sup>19</sup>F NMR (376 MHz, Chloroform-*d*) δ -60.8 (3F). LCMS (Method B): t<sub>R</sub> = 1.154 min, does not ionize by ESI; Purity (AUC) ≥ 95%.

Step B: 3-(5-chloro-2-hydroxy-3-nitrophenyl)-2-(3-methyl-5-(trifluoromethoxy)phenyl)acrylonitrile

2-(3-Methyl-5-(trifluoromethoxy)phenyl)acetonitrile (13.8 mg, 0.064 mmol) was reacted with 5-chloro-2-hydroxy-3-nitrobenzaldehyde following General Procedure W. The crude was taken forward (28.0 mg). LCMS (Method B): t<sub>R</sub> = 1.637 min, m/z = 399.6 [M+H]<sup>+</sup>.

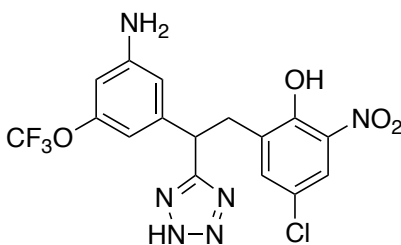
Step C: 3-(5-Chloro-2-hydroxy-3-nitrophenyl)-2-(3-methyl-5-(trifluoromethoxy)phenyl)propanenitrile

3-(5-Chloro-2-hydroxy-3-nitrophenyl)-2-(3-methyl-5-(trifluoromethoxy)phenyl)acrylonitrile (28.0 mg, crude) was reacted following General Procedure T. The crude was taken forward (28.0 mg).

Step D: 4-Chloro-2-(2-(3-methyl-5-(trifluoromethoxy)phenyl)-2-(2H-tetrazol-5-yl)ethyl)-6-nitrophenol

3-(5-Chloro-2-hydroxy-3-nitrophenyl)-2-(3-methyl-5-(trifluoromethoxy)phenyl)propanenitrile (28 mg, crude) was reacted following General Procedure TZ. Purification by preparative HPLC afforded the title compound as a yellow solid (6.7 mg, 0.015 mmol, 23. <sup>1</sup>H NMR (400 MHz, Chloroform-*d*) δ 10.93 (s, 1H), 7.94 (d, *J* = 2.6 Hz, 1H), 7.25 (s, 1H), 7.03 (s, 1H), 6.94 (s, 2H), 4.84 (t, *J* = 7.8 Hz, 1H), 3.74 (dd, *J* = 13.7, 7.8 Hz, 1H), 3.45 (dd, *J* = 13.7, 7.8 Hz, 1H), 2.32 (s, 3H). <sup>19</sup>F NMR (376 MHz, Chloroform-*d*) δ -57.8 (3F). LCMS (Method B): *t*<sub>R</sub> = 1.328 min, *m/z* = 444.3, 446.3 [M+H]<sup>+</sup>; Purity (AUC) ≥ 95%.

*2-(2-(3-Amino-5-(trifluoromethoxy)phenyl)-2-(2H-tetrazol-5-yl)ethyl)-4-chloro-6-nitrophenol (VU0826693)*



Step A: tert-Butyl (3-formyl-5-(trifluoromethoxy)phenyl)carbamate

3-Bromo-5-(trifluoromethoxy)benzaldehyde (3000 mg, 11.15 mmol, 1 eq), *tert*-butyl carbamate (1437 mg, 12.26 mmol, 1.1 eq), Pd<sub>2</sub>(dba)<sub>3</sub>•CHCl<sub>3</sub> (231 mg, 0.22 mmol, 0.02 eq), Xantphos (387 mg, 0.67 mmol, 0.06 eq) and Cs<sub>2</sub>CO<sub>3</sub> (10897 mg, 33.45 mmol, 3 eq) were suspended in toluene (45.0 mL) and the mixture was purged with Ar. Then, it was stirred at 90 °C for 16 h. The mixture was filter through celite, and the solvent was removed under reduced pressure. The solid was re-dissolved in CH<sub>2</sub>Cl<sub>2</sub> and washed with water. The organic phase was concentrated and the crude was purified by ISCO flash chromatography, 2375 mg (7.78 mmol, 70%) of the title compound



were obtained. <sup>1</sup>H NMR (400 MHz, Chloroform-*d*) δ 9.95 (s, 1H), 7.78 (s, 1H), 7.65 (s, 1H), 7.39 (s, 1H), 7.26 (s, 1H), 6.70 (br s, 1H), 1.54 (s, 9H). <sup>19</sup>F NMR (376 MHz, Chloroform-*d*) δ -57.8 (3F). LCMS (Method B): t<sub>R</sub> = 1.010 min, does not ionize; Purity (AUC) ≥ 95%.

Step B: *tert*-Butyl (3-(hydroxymethyl)-5-(trifluoromethoxy)phenyl)carbamate

*tert*-Butyl (3-formyl-5-(trifluoromethoxy)phenyl)carbamate (2375 mg, 7.65 mmol) was reacted following General Procedure T. The crude was taken forward (2560 mg). <sup>1</sup>H NMR (400 MHz, Chloroform-*d*) δ 7.23 (s, 2H), 6.90 (br s, 1H), 6.85 (s, 1H), 4.60 (s, 2H), 1.49 (s, 9H). LCMS (Method B): t<sub>R</sub> = 1.164 min, m/z = 330.0 [M+Na]<sup>+</sup>.

Step C: 3-((*tert*-Butoxycarbonyl)amino)-5-(trifluoromethoxy)benzyl methanesulfonate

*tert*-Butyl (3-(hydroxymethyl)-5-(trifluoromethoxy)phenyl)carbamate (2560 mg, crude) was reacted following General Procedure U. Purification by ISCO flash chromatography afforded the title compound (564 mg, 1.46 mmol, 19%). <sup>1</sup>H NMR (400 MHz, Chloroform-*d*) δ 7.39 (s, 1H), 7.32 (s, 1H), 6.92 (s, 1H), 6.76 (br s, 1H), 5.17 (s, 2H), 2.98 (s, 3H), 1.51 (s, 9H). LCMS (Method B): t<sub>R</sub> = 1.279 min, m/z = 403.3 [M+NH<sub>4</sub>]<sup>+</sup>; Purity (AUC) ≥ 95%.

Step D: *tert*-Butyl (3-(cyanomethyl)-5-(trifluoromethoxy)phenyl)carbamate

3-((*tert*-Butoxycarbonyl)amino)-5-(trifluoromethoxy)benzyl methanesulfonate (564 mg, 1.46 mmol) was reacted following General Procedure V. Purification by ISCO flash chromatography afforded the title compound (339 mg, 1.06 mmol, 73%). <sup>1</sup>H NMR (400 MHz, Chloroform-*d*) δ 7.31 (s, 2H), 6.94 (br s, 1H), 6.83 (s, 1H), 3.71 (s, 2H), 1.50 (s, 9H). <sup>19</sup>F NMR (376 MHz, Chloroform-*d*) δ -60.8 (3F). LCMS (Method B): t<sub>R</sub> = 1.227 min, m/z = 334.4 [M+NH<sub>4</sub>]<sup>+</sup>; Purity (AUC) ≥ 95%.

Step D: tert-Butyl (3-(2-(5-chloro-2-hydroxy-3-nitrophenyl)-1-cyanovinyl)-5-(trifluoromethoxy)phenyl)carbamate

tert-Butyl (3-(cyanomethyl)-5-(trifluoromethoxy)phenyl)carbamate (339 mg, 1.06 mmol) was reacted with 5-chloro-2-hydroxy-3-nitrobenzaldehyde following General Procedure W. The crude was taken forward (545 mg). LCMS (Method B):  $t_R = 1.616$  min,  $m/z = 500.3, 502.4$   $[M+H]^+$ .

Step E: 2-(3-Amino-5-(trifluoromethoxy)phenyl)-3-(5-chloro-2-hydroxy-3-nitrophenyl)propanenitrile

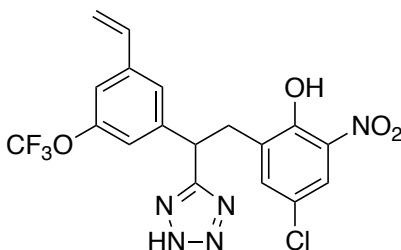
tert-Butyl (3-(2-(5-chloro-2-hydroxy-3-nitrophenyl)-1-cyanovinyl)-5-(trifluoromethoxy)phenyl)carbamate (545 mg, crude) was reacted following General Procedure T. The crude was then dissolved in 3.00 mL of  $CH_2Cl_2$  and 300  $\mu$ L of TFA were added. The solution was stirred overnight at 40 °C. The solvent was removed under reduced pressure and the crude was purified using ISCO flash chromatography, 120 mg (0.30 mmol, 28%) of the title compound were obtained.  $^1H$  NMR (400 MHz, Chloroform-*d*)  $\delta$  10.96 (br s, 1H), 8.08 (d,  $J = 2.6$  Hz, 1H), 7.43 (d,  $J = 2.6$  Hz, 1H), 6.62 (t,  $J = 1.7$  Hz, 1H), 6.51 (s, 1H), 6.50 – 6.47 (m, 1H), 4.16 (dd,  $J = 9.6, 6.0$  Hz, 1H), 3.95 (br s, 2H), 3.30 (dd,  $J = 13.6, 6.0$  Hz, 1H), 3.14 (dd,  $J = 13.6, 9.6$  Hz, 1H).  $^{19}F$  NMR (376 MHz, Chloroform-*d*)  $\delta$  -60.7 (3F). LCMS (Method B):  $t_R = 1.284$  min,  $m/z = 402.4$   $[M+H]^+$ ; Purity (AUC)  $\geq 95\%$ .

Step F: 2-(2-(3-Amino-5-(trifluoromethoxy)phenyl)-2-(2H-tetrazol-5-yl)ethyl)-4-chloro-6-nitrophenol

2-(3-Amino-5-(trifluoromethoxy)phenyl)-3-(5-chloro-2-hydroxy-3-nitrophenyl)propanenitrile (18 mg, 0.04 mmol) was reacted following General Procedure W. Purification by preparative HPLC afforded the title compound as a yellow solid (13.8 mg, 0.03 mmol, 78%).  $^1H$  NMR (400 MHz, Chloroform-*d*)  $\delta$  10.95 (br s, 1H), 7.96 (d,  $J = 2.6$  Hz, 2H), 7.30 (d,  $J = 2.6$  Hz, 2H), 6.46 (s,

3H), 6.42 (s, 2H), 4.68 (t,  $J = 7.7$  Hz, 2H), 3.75 (dd,  $J = 13.7, 7.7$  Hz, 2H), 3.42 (dd,  $J = 13.7, 7.7$  Hz, 2H).  $^{19}\text{F}$  NMR (376 MHz, Chloroform- $d$ )  $\delta$  -57.7 (3F), -110.7 (1F). LCMS (Method B):  $t_{\text{R}} = 1.030$  min,  $m/z = 445.3, 447.2$   $[\text{M}+\text{H}]^+$ ; Purity (AUC)  $\geq 95\%$ .

*2-(2-(2H-Tetrazol-5-yl)-2-(3-(trifluoromethoxy)-5-vinylphenyl)ethyl)-4-chloro-6-nitrophenol*  
(VU0826909)



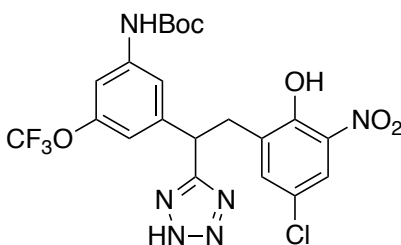
Step A: 3-(5-Chloro-2-hydroxy-3-nitrophenyl)-2-(3-(trifluoromethoxy)-5-vinylphenyl)propanenitrile

2-(3-Bromo-5-(trifluoromethoxy)phenyl)-3-(5-chloro-2-hydroxy-3-nitrophenyl)propanenitrile (30 mg, 0.064 mmol) was reacted with vinylboronic pinacol ester following General Procedure J. Purification by flash chromatography afforded the title compound (10.4 mg, 0.025 mmol, 39%). One peak of the  $^1\text{H}$ -NMR seems to be behind the solvent peak as it looks wider than normal.  $^1\text{H}$  NMR (400 MHz, Chloroform- $d$ )  $\delta$  10.98 (br s, 1H), 8.10 (d,  $J = 2.6$  Hz, 1H), 7.46 (d,  $J = 2.6$  Hz, 1H), 7.35 (s, 1H), 7.08 (s, 1H), 6.70 (dd,  $J = 17.5, 10.9$  Hz, 1H), 5.83 (d,  $J = 17.5$  Hz, 1H), 5.43 (d,  $J = 10.9$  Hz, 1H), 4.29 (dd,  $J = 9.7, 5.8$  Hz, 1H), 3.34 (dd,  $J = 13.6, 5.8$  Hz, 1H), 3.17 (dd,  $J = 13.6, 9.7$  Hz, 1H).  $^{19}\text{F}$  NMR (376 MHz, Chloroform- $d$ )  $\delta$  -57.8 (3F). LCMS (Method B):  $t_{\text{R}} = 1.464$  min,  $m/z = 413.4$   $[\text{M}+\text{H}]^+$ ; Purity (AUC)  $\geq 95\%$ .

Step B: 2-(2-(2H-Tetrazol-5-yl)-2-(3-(trifluoromethoxy)-5-vinylphenyl)ethyl)-4-chloro-6-nitrophenol

3-(5-Chloro-2-hydroxy-3-nitrophenyl)-2-(3-(trifluoromethoxy)-5-vinylphenyl)propanenitrile (10.4 mg, 0.025 mmol) was reacted following General Procedure W. Purification by preparative HPLC afforded the title compound as a yellow solid (3.2 mg, 0.0070 mmol, 28%). <sup>1</sup>H NMR (400 MHz, Chloroform-*d*) δ 10.95 (br s, 1H), 7.95 (d, *J* = 2.6 Hz, 1H), 7.29 (d, *J* = 2.6 Hz, 2H), 7.23 (s, 2H), 7.17 (s, 1H), 7.04 (s, 1H), 6.63 (dd, *J* = 17.6, 10.9 Hz, 1H), 5.75 (d, *J* = 17.6 Hz, 1H), 5.36 (d, *J* = 10.9 Hz, 1H), 4.86 (dd, *J* = 8.5, 7.0 Hz, 1H), 3.74 (dd, *J* = 13.7, 8.5 Hz, 1H), 3.48 (dd, *J* = 13.7, 7.0 Hz, 1H). <sup>19</sup>F NMR (376 MHz, Chloroform-*d*) δ -57.8 (3F). LCMS (Method B): *t*<sub>R</sub> = 1.353 min, *m/z* = 456.2, 457.2 [M+H]<sup>+</sup>; Purity (AUC) ≥ 95%.

*tert*-Butyl (3-(2-(5-chloro-2-hydroxy-3-nitrophenyl)-1-(2H-tetrazol-5-yl)ethyl)-5-(trifluoromethoxy)phenyl)carbamate (VU0826694)



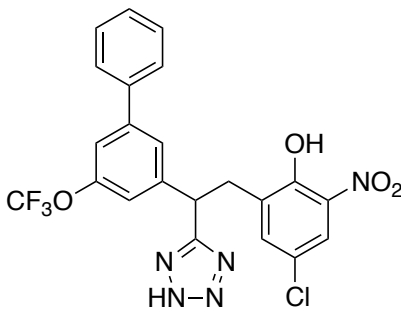
Step A: 2-(3-Amino-5-(trifluoromethoxy)phenyl)-3-(5-chloro-2-hydroxy-3-nitrophenyl)propanenitrile

*tert*-Butyl (3-(2-(5-chloro-2-hydroxy-3-nitrophenyl)-1-cyanovinyl)-5-(trifluoromethoxy)phenyl)carbamate (400 mg, crude) was reacted following General Procedure T. Purification by flash chromatography afforded the title compound (140 mg, 0.28 mmol). LCMS (Method B): *t*<sub>R</sub> = 1.471 min, *m/z* = 519.4, 520.4 [M+NH<sub>4</sub>]<sup>+</sup>; Purity (AUC) ≥ 95%.

Step B: tert-Butyl (3-(2-(5-chloro-2-hydroxy-3-nitrophenyl)-1-(2H-tetrazol-5-yl)ethyl)-5-(trifluoromethoxy)phenyl)carbamate

2-(3-Amino-5-(trifluoromethoxy)phenyl)-3-(5-chloro-2-hydroxy-3-nitrophenyl)propanenitrile (140 mg, 0.28 mmol) was reacted following General Procedure W. Purification by flash chromatography afforded the title compound (118.9 mg, 0.22 mmol, 79%). <sup>1</sup>H NMR (400 MHz, Chloroform-*d*) δ 7.92 (d, *J* = 2.0 Hz, 1H), 7.33 (s, 1H), 7.28 (d, *J* = 2.0 Hz, 1H), 7.16 (s, 1H), 6.90 (br s, 1H), 6.80 (s, 1H), 4.84 (t, *J* = 7.5 Hz, 1H), 3.68 (dd, *J* = 13.7, 7.5 Hz, 1H), 3.46 (dd, *J* = 13.7, 7.5 Hz, 1H). <sup>19</sup>F NMR (376 MHz, Chloroform-*d*) δ -60.8 (3F). LCMS (Method B): *t*<sub>R</sub> = 1.384 min, *m/z* = 545.2, 547.2 [M+H]<sup>+</sup>; Purity (AUC) ≥ 95%.

*2-(2-(2H-Tetrazol-5-yl)-2-(5-(trifluoromethoxy)-[1,1'-biphenyl]-3-yl)ethyl)-4-chloro-6-nitrophenol (VU0826911)*



Step A: 2-(5-(Trifluoromethoxy)-[1,1'-biphenyl]-3-yl)acetonitrile

2-(3-Bromo-5-(trifluoromethoxy)phenyl)acetonitrile (80 mg, 0.29 mmol) was reacted with phenylboronic acid following General Procedure J. Purification by ISCO flash chromatography afforded the title compound (79 mg, 0.28 mmol, 98%). <sup>1</sup>H NMR (400 MHz, Chloroform-*d*) δ 7.58 (s, 1H), 7.56 (s, 1H), 7.53 – 7.45 (m, 3H), 7.43 (d, *J* = 7.5 Hz, 2H), 7.18 (s, 1H), 3.84 (s, 2H). <sup>19</sup>F NMR (376 MHz, Chloroform-*d*) δ -57.7 (3F). LCMS (Method B): *t*<sub>R</sub> = 1.334 min, does not ionize by ESI; Purity (AUC) ≥ 95%.

Step B: 3-(5-Chloro-2-hydroxy-3-nitrophenyl)-2-(5-(trifluoromethoxy)-[1,1'-biphenyl]-3-yl)acrylonitrile

2-(5-(Trifluoromethoxy)-[1,1'-biphenyl]-3-yl)acetonitrile (70 mg, 0.25 mmol) was reacted with 5-chloro-2-hydroxy-3-nitrobenzaldehyde following General Procedure W. The crude was taken forward (147.1 mg). LCMS (Method B, 2 min) both isomers were observed  $t_R = 1.365$  and  $1.740$  min,  $m/z = 461.3, 463.3$   $[M+H]^+$  (same fragmentation for both peaks).

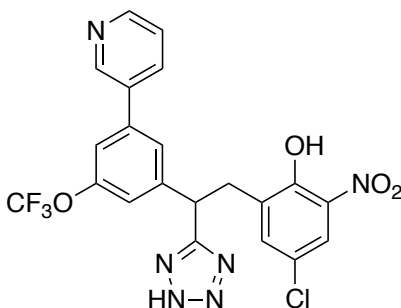
Step C: 3-(5-Chloro-2-hydroxy-3-nitrophenyl)-2-(5-(trifluoromethoxy)-[1,1'-biphenyl]-3-yl)propanenitrile

3-(5-Chloro-2-hydroxy-3-nitrophenyl)-2-(5-(trifluoromethoxy)-[1,1'-biphenyl]-3-yl)acrylonitrile (147.1 mg, crude) was reacted following General Procedure T. Purification by ISCO flash chromatography afforded the title compound (97.7 mg, 0.17 mmol, 68%). LCMS (Method B, 2 min):  $t_R = 1.536$  min,  $m/z = 463.3$ ; Purity (AUC)  $\geq 81\%$ .

Step D: 2-(2-(2H-Tetrazol-5-yl)-2-(5-(trifluoromethoxy)-[1,1'-biphenyl]-3-yl)ethyl)-4-chloro-6-nitrophenol

3-(5-Chloro-2-hydroxy-3-nitrophenyl)-2-(5-(trifluoromethoxy)-[1,1'-biphenyl]-3-yl)propanenitrile (60.3 mg, 0.11 mmol) was reacted following General Procedure TZ. Purification by preparative HPLC afforded the title compound (26.0 mg, 0.051, 47%).  $^1H$  NMR (400 MHz, Chloroform-*d*)  $\delta$  10.90 (br s, 1H), 7.90 (d,  $J = 2.6$  Hz, 1H), 7.47 – 7.42 (m, 3H), 7.41 – 7.34 (m, 3H), 7.31 (s, 1H), 7.24 (d,  $J = 2.6$  Hz, 1H), 7.13 (s, 1H), 5.00 (t,  $J = 7.8$  Hz, 1H), 3.75 (dd,  $J = 13.7, 7.8$  Hz, 1H), 3.51 (dd,  $J = 13.7, 7.8$  Hz, 1H).  $^{19}F$  NMR (376 MHz, Chloroform-*d*)  $\delta$  -60.8 (3F). LCMS (Method B, 2 min):  $t_R = 1.465$  min,  $m/z = 506.4, 507.2$   $[M+H]^+$ ; Purity (AUC)  $\geq 95\%$ .

*4-Chloro-2-nitro-6-(2-(3-(pyridin-3-yl)-5-(trifluoromethoxy)phenyl)-2-(2H-tetrazol-5-yl)ethyl)phenol (VU0827420)*



Step A: 3-(5-Chloro-2-hydroxy-3-nitrophenyl)-2-(3-(pyridin-3-yl)-5-(trifluoromethoxy)phenyl)propanenitrile

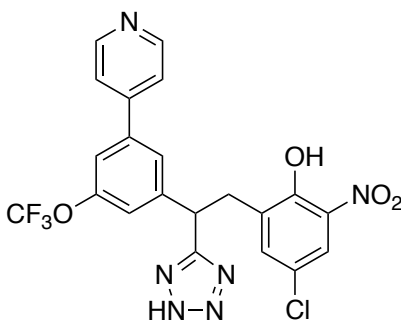
2-(3-Bromo-5-(trifluoromethoxy)phenyl)-3-(5-chloro-2-hydroxy-3-nitrophenyl)propanenitrile (60 mg, 0.128 mmol) was reacted with pyridine-3-ylboronic acid following General Procedure J. Purification by ISCO flash chromatography afforded the title compound (18.2 mg, 0.039 mmol, 31%) of title compound. <sup>1</sup>H NMR (400 MHz, Chloroform-*d*)  $\delta$  10.96 (br s, 1H), 8.83 (s, 1H), 8.74 – 8.61 (m, 1H), 8.11 (d, *J* = 2.5 Hz, 1H), 7.87 (d, *J* = 7.9 Hz, 1H), 7.54 (s, 1H), 7.49 (d, *J* = 2.5 Hz, 1H), 7.44 (s, 2H), 4.39 (dd, *J* = 9.8, 5.7 Hz, 1H), 3.40 (dd, *J* = 13.6, 5.7 Hz, 1H), 3.22 (dd, *J* = 13.6, 9.8 Hz, 1H). <sup>19</sup>F NMR (376 MHz, Chloroform-*d*)  $\delta$  -60.8 (3F). LCMS (Method B): *t*<sub>R</sub> = 1.034 min, *m/z* = 464.2, 465.2 [M+H]<sup>+</sup>; Purity (AUC)  $\geq$  88%.

Step B: 4-Chloro-2-nitro-6-(2-(3-(pyridin-3-yl)-5-(trifluoromethoxy)phenyl)-2-(2H-tetrazol-5-yl)ethyl)phenol

3-(5-Chloro-2-hydroxy-3-nitrophenyl)-2-(3-(pyridin-3-yl)-5-(trifluoromethoxy)phenyl)propanenitrile (18.2 mg, 0.039 mmol) was reacted following General Procedure TZ. Purification by preparative HPLC afforded the title compound as the TFA salt (15.9 mg, 0.0070 mmol, 28%). <sup>1</sup>H NMR (400 MHz, Chloroform-*d*)  $\delta$  9.85 (s, 1H), 8.75 (s, 1H), 8.64

(dd,  $J = 5.2, 1.5$  Hz, 1H), 8.20 – 8.07 (m, 1H), 7.90 (d,  $J = 2.6$  Hz, 1H), 7.68 (dd,  $J = 8.1, 5.2$  Hz, 1H), 7.56 (s, 1H), 7.36 – 7.30 (m, 2H), 5.04 (dd,  $J = 8.5, 7.5$  Hz, 1H), 3.78 (dd,  $J = 13.7, 7.5$  Hz, 1H), 3.55 (dd,  $J = 13.7, 7.5$  Hz, 1H).  $^{19}\text{F}$  NMR (376 MHz, Chloroform- $d$ )  $\delta$  -57.8 (3F), -75.6 (TFA). LCMS (Method B):  $t_{\text{R}} = 0.971$  min,  $m/z = 507.3, 509.3$   $[\text{M}+\text{H}]^+$ ; Purity (AUC)  $\geq 95\%$ .

*4-Chloro-2-nitro-6-(2-(3-(pyridin-4-yl)-5-(trifluoromethoxy)phenyl)-2-(2H-tetrazol-5-yl)ethyl)phenol (VU0827421)*



Step A: 3-(5-Chloro-2-hydroxy-3-nitrophenyl)-2-(3-(pyridin-4-yl)-5-(trifluoromethoxy)phenyl)propanenitrile

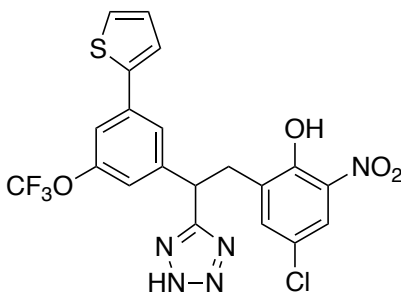
2-(3-Bromo-5-(trifluoromethoxy)phenyl)-3-(5-chloro-2-hydroxy-3-nitrophenyl)propanenitrile (60 mg, 0.128 mmol) was reacted with pyridine-4-ylboronic acid following General Procedure J. Purification by ISCO flash chromatography the title compound (18.9 mg, 0.040 mmol, 32%).  $^1\text{H}$  NMR (400 MHz, Chloroform- $d$ )  $\delta$  11.01 (br s, 1H), 8.75 (br s, 2H), 8.12 (d,  $J = 2.6$  Hz, 1H), 7.59 (t,  $J = 1.6$  Hz, 1H), 7.52 – 7.43 (m, 4H), 7.29 (s, 1H), 4.39 (dd,  $J = 9.8, 5.7$  Hz, 1H), 3.40 (dd,  $J = 13.6, 5.7$  Hz, 1H), 3.21 (dd,  $J = 13.6, 9.8$  Hz, 1H).  $^{19}\text{F}$  NMR (376 MHz, Chloroform- $d$ )  $\delta$  -60.8 (3F). LCMS (Method B):  $t_{\text{R}} = 1.010$  min,  $m/z = 464.2, 466.2$   $[\text{M}+\text{H}]^+$ ; Purity (AUC)  $\geq 95\%$ .



Step B: 4-Chloro-2-nitro-6-(2-(3-(pyridin-4-yl)-5-(trifluoromethoxy)phenyl)-2-(2H-tetrazol-5-yl)ethyl)phenol

3-(5-Chloro-2-hydroxy-3-nitrophenyl)-2-(3-(pyridin-4-yl)-5-(trifluoromethoxy)phenyl)propanenitrile (18.9 mg, 0.040 mmol) was reacted following General Procedure TZ. Purification by preparative HPLC and addition of HCl 3 M afforded the title compound as the HCl salt (16.3 mg, 0.032 mmol, 80%). <sup>1</sup>H NMR (400 MHz, Chloroform-*d*) δ 8.72 (d, *J* = 6.4 Hz, 2H), 7.95 (d, *J* = 2.6 Hz, 1H), 7.77 (d, *J* = 6.2 Hz, 2H), 7.62 (s, 1H), 7.42 (s, 2H), 7.35 (d, *J* = 2.6 Hz, 1H), 5.04 (t, *J* = 8.8, 6.7 Hz, 1H), 3.76 (dd, *J* = 13.7, 8.8 Hz, 1H), 3.59 (dd, *J* = 13.7, 6.7 Hz, 1H). <sup>19</sup>F NMR (376 MHz, Chloroform-*d*) δ -57.8 (3F). LCMS (Method B): *t*<sub>R</sub> = 0.971 min, *m/z* = 507.3, 509.3 [M+H]<sup>+</sup>; Purity (AUC) ≥ 95%.

*2-(2-(2H-Tetrazol-5-yl)-2-(3-(thiophen-2-yl)-5-(trifluoromethoxy)phenyl)ethyl)-4-chloro-6-nitrophenol (VU0826483)*



Step A: 2-(3-(thiophen-2-yl)-5-(trifluoromethoxy)phenyl)acetonitrile

2-(3-Bromo-5-(trifluoromethoxy)phenyl)acetonitrile (100 mg, 0.36 mmol) was reacted with thiophene-2-boronic acid following General Procedure J. Purification by flash chromatography afforded the title compound (97 mg, 0.34 mmol, 95%). <sup>1</sup>H NMR (400 MHz, Chloroform-*d*) δ 7.49 (s, 1H), 7.41 (s, 1H), 7.36 (d, *J* = 4.4 Hz, 2H), 7.11 (s, 2H), 3.80 (s, 2H). <sup>19</sup>F NMR (376 MHz,

Chloroform-*d*)  $\delta$  -57.7 (3F). LCMS (Method B, 2 min):  $t_R$  = 1.230 min, does not ionize by ESI; Purity (AUC)  $\geq$  95%.

Step B: 3-(5-Chloro-2-hydroxy-3-nitrophenyl)-2-(3-(thiophen-2-yl)-5-(trifluoromethoxy)phenyl)acrylonitrile

2-(3-(Thiophen-2-yl)-5-(trifluoromethoxy)phenyl)acetonitrile (40 mg, 0.17 mmol) was reacted with 5-chloro-2-hydroxy-3-nitrobenzaldehyde following General Procedure W. The crude was taken forward (74.9 mg). LCMS (Method B, 2 min):  $t_R$  = 1.252 min,  $m/z$  = 467.0, 469.0 [M+H]<sup>+</sup>.

Step C: 3-(5-Chloro-2-hydroxy-3-nitrophenyl)-2-(3-(thiophen-2-yl)-5-(trifluoromethoxy)phenyl)propanenitrile

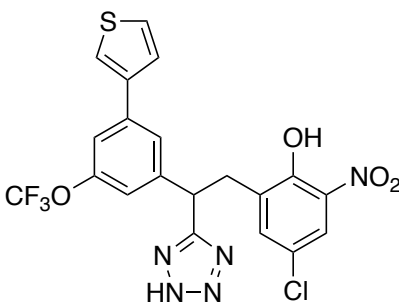
3-(5-Chloro-2-hydroxy-3-nitrophenyl)-2-(3-(thiophen-2-yl)-5-(trifluoromethoxy)phenyl)acrylonitrile (74.9 mg, crude) was reacted following General Procedure T. Purification by flash chromatography afforded 25 mg of a mixture that contained 2-(3-(thiophen-2-yl)-5-(trifluoromethoxy)phenyl)acetonitrile and the title compound. LCMS (Method B, 2 min):  $t_R$  = 1.446 min, does not ionize by ESI.

Step D: 2-(2-(2H-Tetrazol-5-yl)-2-(3-(thiophen-2-yl)-5-(trifluoromethoxy)phenyl)ethyl)-4-chloro-6-nitrophenol

3-(5-chloro-2-hydroxy-3-nitrophenyl)-2-(3-(thiophen-2-yl)-5-(trifluoromethoxy)phenyl)propanenitrile (25 mg, mixture) was reacted following General Procedure TZ. Purification by preparative HPLC afforded the title compound (4 mg, 0.0078 mmol, 5%). <sup>1</sup>H NMR (400 MHz, Chloroform-*d*)  $\delta$  10.97 (br s, 1H), 7.95 (d,  $J$  = 2.8 Hz, 1H), 7.49 – 7.43 (m, 2H), 7.41 (dd,  $J$  = 5.5, 2.8 Hz, 1H), 7.34 (s, 1H), 7.30 (dd,  $J$  = 5.5, 2.1 Hz, 2H), 7.07 (s, 1H), 4.90 (t,  $J$  = 7.8 Hz, 1H), 3.76 (dd,  $J$  = 13.7, 7.8 Hz, 1H), 3.51 (dd,  $J$  = 13.7, 7.8 Hz, 1H). <sup>19</sup>F NMR

(376 MHz, Chloroform-*d*)  $\delta$  -60.8 (3F). LCMS (Method B, 2 min):  $t_R$  = 1.698 min,  $m/z$  = 512.0, 513.0  $[M+H]^+$ ; Purity (AUC)  $\geq$  95%.

*2-(2-(2H-Tetrazol-5-yl)-2-(3-(thiophen-3-yl)-5-(trifluoromethoxy)phenyl)ethyl)-4-chloro-6-nitrophenol (VU0826484)*



*Step A: 2-(3-(thiophen-3-yl)-5-(trifluoromethoxy)phenyl)acetonitrile*

2-(3-Bromo-5-(trifluoromethoxy)phenyl)acetonitrile (100 mg, 0.36 mmol) was reacted with thiophene-3-boronic acid following General Procedure J. Purification by flash chromatography afforded the title compound (84.4 mg, 0.30 mmol, 83%).  $^1H$  NMR (400 MHz, Chloroform-*d*)  $\delta$  7.52 (dd,  $J$  = 2.8, 1.4 Hz, 1H), 7.50 (s, 1H), 7.43 (dt,  $J$  = 5.0, 2.8 Hz, 1H), 7.40 (s, 1H), 7.36 (dd,  $J$  = 5.0, 1.4 Hz, 1H), 7.11 (s, 1H), 3.81 (s, 2H).  $^{19}F$  NMR (376 MHz, Chloroform-*d*)  $\delta$  -60.7 (3F). LCMS (Method B, 2 min):  $t_R$  = 1.190 min, does not ionize well by ESI; Purity (AUC)  $\geq$  95%.

*Step B: 3-(5-Chloro-2-hydroxy-3-nitrophenyl)-2-(3-(thiophen-3-yl)-5-(trifluoromethoxy)phenyl)acrylonitrile*

2-(3-(Thiophen-2-yl)-5-(trifluoromethoxy)phenyl)acetonitrile (60 mg, 0.21 mmol) was reacted with 5-chloro-2-hydroxy-3-nitrobenzaldehyde following General Procedure W. The crude was taken forward (102.3 mg). LCMS (Method B, 2 min): Both geometric isomers were observed  $t_R$  = 1.284 and 1.627 min,  $m/z$  = 467.0, 469.0  $[M+H]^+$  (same fragmentation for both peaks).

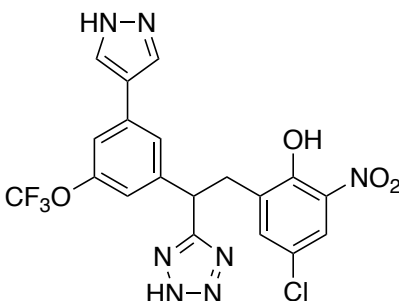
Step C: 3-(5-Chloro-2-hydroxy-3-nitrophenyl)-2-(3-(thiophen-3-yl)-5-(trifluoromethoxy)phenyl)propanenitrile

3-(5-Chloro-2-hydroxy-3-nitrophenyl)-2-(3-(thiophen-3-yl)-5-(trifluoromethoxy)phenyl)acrylonitrile (102.3 mg, crude) was reacted following General Procedure T. Purification by flash chromatography afforded the title compound (27.6 mg, 0.048 mmol, 23%). <sup>1</sup>H NMR (400 MHz, Chloroform-*d*) δ 10.99 (br s, 1H), 8.10 (d, *J* = 2.6 Hz, 1H), 7.56 – 7.53 (m, 2H), 7.49 – 7.44 (m, 2H), 7.44 – 7.42 (m, 1H), 7.37 (dd, *J* = 5.0, 1.4 Hz, 1H), 7.11 (s, 1H), 4.33 (dd, *J* = 9.7, 5.8 Hz, 1H), 3.37 (dd, *J* = 13.6, 5.8 Hz, 1H), 3.20 (dd, *J* = 13.6, 9.7 Hz, 1H). LCMS (Method B, 2 min): *t*<sub>R</sub> = 1.204 min, does not ionize by ESI; Purity (AUC) ≥ 81%.

Step D: 2-(2-(2H-Tetrazol-5-yl)-2-(3-(thiophen-3-yl)-5-(trifluoromethoxy)phenyl)ethyl)-4-chloro-6-nitrophenol

3-(5-Chloro-2-hydroxy-3-nitrophenyl)-2-(3-(thiophen-3-yl)-5-(trifluoromethoxy)phenyl)propanenitrile (27.6 mg, 0.048 mmol) was reacted following General Procedure TZ. Purification by preparative HPLC afforded the title compound (3.9 mg, 0.0076 mmol, 16%). <sup>1</sup>H NMR (400 MHz, Chloroform-*d*) δ 10.97 (s, 1H), 7.96 (d, *J* = 2.6 Hz, 1H), 7.43 (s, 1H), 7.35 (d, *J* = 1.2 Hz, 1H), 7.34 – 7.28 (m, 3H), 7.09 (dd, *J* = 5.1, 3.7 Hz, 1H), 7.06 (s, 1H), 4.89 (dd, *J* = 8.5, 7.1 Hz, 1H), 3.76 (dd, *J* = 13.7, 8.5 Hz, 1H), 3.51 (dd, *J* = 13.7, 7.1 Hz, 1H). <sup>19</sup>F NMR (376 MHz, Chloroform-*d*) δ -60.8 (3F). LCMS (Method B, 2 min): *t*<sub>R</sub> = 1.686 min, *m/z* = 512.0, 513.0 [M+H]<sup>+</sup>; Purity (AUC) ≥ 95%.

*2-(2-(3-(1H-Pyrazol-4-yl)-5-(trifluoromethoxy)phenyl)-2-(2H-tetrazol-5-yl)ethyl)-4-chloro-6-nitrophenol (VU026691)*



Step A: 2-(3-(1H-pyrazol-4-yl)-5-(trifluoromethoxy)phenyl)acetonitrile

2-(3-Bromo-5-(trifluoromethoxy)phenyl)acetonitrile (100 mg, 0.36 mmol) was reacted with (1-(*tert*-butoxycarbonyl)-1H-pyrazol-4-yl)boronic acid pinacol ester following General Procedure J. Purification by flash chromatography afforded the title compound (62.1 mg, 0.17 mmol, 47%). <sup>1</sup>H NMR (400 MHz, Chloroform-*d*)  $\delta$  7.90 (s, 2H), 7.42 (s, 1H), 7.31 (s, 1H), 7.06 (s, 1H), 3.81 (s, 2H). <sup>19</sup>F NMR (376 MHz, Chloroform-*d*)  $\delta$  -57.7 (3F). LCMS (Method B, 2 min):  $t_R$  = 0.957 min,  $m/z$  = 268.5 [M+H]<sup>+</sup>; Purity (AUC)  $\geq$  95%.

Step B: 2-(3-(1H-pyrazol-4-yl)-5-(trifluoromethoxy)phenyl)-3-(5-chloro-2-hydroxy-3-nitrophenyl)acrylonitrile

2-(3-(1H-Pyrazol-4-yl)-5-(trifluoromethoxy)phenyl)acetonitrile (50 mg, 0.19 mmol) was reacted with 5-chloro-2-hydroxy-3-nitrobenzaldehyde following General Procedure W. The crude was taken forward (85.9 mg). LCMS (Method B, 2 min):  $t_R$  = 1.361 min,  $m/z$  = 451.5, 453.6 [M+H]<sup>+</sup>.

Step C: 2-(3-(1H-Pyrazol-4-yl)-5-(trifluoromethoxy)phenyl)-3-(5-chloro-2-hydroxy-3-nitrophenyl)propanenitrile

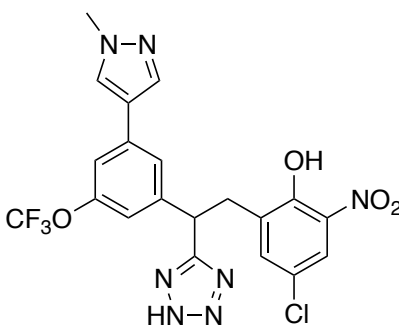
2-(3-(1H-Pyrazol-4-yl)-5-(trifluoromethoxy)phenyl)-3-(5-chloro-2-hydroxy-3-nitrophenyl)acrylonitrile (85.9 mg, crude) was reacted following General Procedure T. Purification by flash chromatography afforded the title compound (54.3 mg, 0.12 mmol, 63%). <sup>1</sup>H NMR (400

MHz, Chloroform-*d*)  $\delta$  8.09 (d,  $J = 2.5$  Hz, 1H), 7.91 (s, 2H), 7.47 (s, 2H), 7.34 (s, 1H), 7.05 (s, 1H), 4.32 (dd,  $J = 9.7, 5.8$  Hz, 1H), 3.37 (dd,  $J = 13.6, 5.8$  Hz, 1H), 3.20 (dd,  $J = 13.6, 9.7$  Hz, 1H).  $^{19}\text{F}$  NMR (376 MHz, Chloroform-*d*)  $\delta$  -57.7 (3F). LCMS (Method B, 2 min):  $t_{\text{R}} = 1.266$  min,  $m/z = 453.2, 455.4$   $[\text{M}+\text{H}]^+$ ; Purity (AUC)  $\geq 95\%$ .

Step D: 2-(2-(3-(1H-Pyrazol-4-yl)-5-(trifluoromethoxy)phenyl)-2-(2H-tetrazol-5-yl)ethyl)-4-chloro-6-nitrophenol

2-(3-(1H-Pyrazol-4-yl)-5-(trifluoromethoxy)phenyl)-3-(5-chloro-2-hydroxy-3-nitrophenyl)propanenitrile (54.3 mg, 0.12 mmol) was reacted following General Procedure TZ. Purification by preparative HPLC afforded the title compound (44.1 mg, 0.089 mmol, 74).  $^1\text{H}$  NMR (400 MHz, Methanol-*d*<sub>4</sub>)  $\delta$  8.02 (s, 2H), 7.99 (d,  $J = 2.6$  Hz, 1H), 7.53 (d,  $J = 1.9$  Hz, 1H), 7.42 (s, 1H), 7.36 (d,  $J = 2.6$  Hz, 1H), 7.06 (s, 1H), 4.97 (t,  $J = 8.0$  Hz, 1H), 3.75 (dd,  $J = 13.6, 8.0$  Hz, 1H), 3.57 (dd,  $J = 13.6, 8.0$  Hz, 1H).  $^{19}\text{F}$  NMR (376 MHz, Chloroform-*d*)  $\delta$  -60.8 (3F). LCMS (Method B, 2 min):  $t_{\text{R}} = 1.136$  min,  $m/z = 496.4, 498.4$   $[\text{M}+\text{H}]^+$ ; Purity (AUC)  $\geq 95\%$ .

*4-Chloro-2-(2-(3-(1-methyl-1H-pyrazol-4-yl)-5-(trifluoromethoxy)phenyl)-2-(2H-tetrazol-5-yl)ethyl)-6-nitrophenol (VU0826722)*



Step A: 2-(3-(1-Methyl-1H-pyrazol-4-yl)-5-(trifluoromethoxy)phenyl)acetonitrile

2-(3-Bromo-5-(trifluoromethoxy)phenyl)acetonitrile (80 mg, 0.29 mmol) was reacted with (1-methyl-1H-pyrazol-4-yl)boronic acid following General Procedure J. Purification by flash chromatography afforded the title compound (52.5 mg, 0.19 mmol, 64%). <sup>1</sup>H NMR (400 MHz, Chloroform-*d*) δ 7.76 (s, 1H), 7.67 (s, 1H), 7.37 (s, 1H), 7.26 (s, 1H), 7.02 (s, 1H), 3.96 (s, 3H), 3.79 (s, 2H). <sup>19</sup>F NMR (376 MHz, Chloroform-*d*) δ -57.7 (3F). LCMS (Method B, 2 min): t<sub>R</sub> = 1.038 min, m/z = 282.4 [M+H]<sup>+</sup>; Purity (AUC) ≥ 95%.

Step B: 3-(5-Chloro-2-hydroxy-3-nitrophenyl)-2-(3-(1-methyl-1H-pyrazol-4-yl)-5-(trifluoromethoxy)phenyl)acrylonitrile

2-(3-(1-Methyl-1H-pyrazol-4-yl)-5-(trifluoromethoxy)phenyl)acetonitrile (52.5 mg, 0.19 mmol) was reacted with 5-chloro-2-hydroxy-3-nitrobenzaldehyde following General Procedure W. The crude was taken forward (91.3 mg).

Step C: 3-(5-Chloro-2-hydroxy-3-nitrophenyl)-2-(3-(1-methyl-1H-pyrazol-4-yl)-5-(trifluoromethoxy)phenyl)propanenitrile

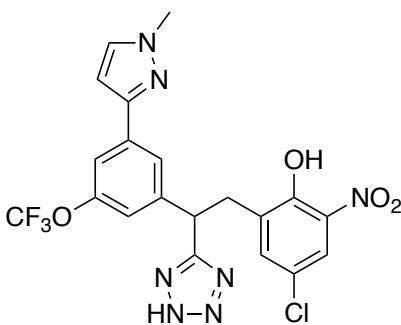
3-(5-Chloro-2-hydroxy-3-nitrophenyl)-2-(3-(1-methyl-1H-pyrazol-4-yl)-5-(trifluoromethoxy)phenyl)acrylonitrile (91.3 mg, crude) was reacted following General Procedure T. The crude was taken forward (52.5 mg). LCMS (Method B, 2 min): t<sub>R</sub> = 1.330 min, m/z = 467.3, 468.4 [M+H].

Step D: 4-Chloro-2-(2-(3-(1-methyl-1H-pyrazol-4-yl)-5-(trifluoromethoxy)phenyl)-2-(2H-tetrazol-5-yl)ethyl)-6-nitrophenol

3-(5-Chloro-2-hydroxy-3-nitrophenyl)-2-(3-(1-methyl-1H-pyrazol-4-yl)-5-(trifluoromethoxy)phenyl)propanenitrile (52.5 mg, crude) was reacted following General Procedure TZ. Purification by preparative HPLC afforded the title compound (12.6 mg, 0.025

mmol, 13%). <sup>1</sup>H NMR (400 MHz, Chloroform-*d*) δ 10.94 (br s, 1H), 7.94 (s, 1H), 7.59 (s, 1H), 7.55 (s, 1H), 7.35 (s, 1H), 7.21 (s, 1H), 7.14 (s, 1H), 7.00 (s, 1H), 4.85 (t, *J* = 7.7 Hz, 1H), 3.88 (s, 3H), 3.81 (dd, *J* = 13.7, 7.7 Hz, 1H), 3.50 (dd, *J* = 13.7, 7.7 Hz, 1H). <sup>19</sup>F NMR (376 MHz, Chloroform-*d*) δ -57.8 (3F). LCMS (Method B, 2 min): *t<sub>R</sub>* = 1.197 min, *m/z* = 510.4, 512.4 [M+H]<sup>+</sup>; Purity (AUC) ≥ 95%.

*4-Chloro-2-(2-(3-(1-methyl-1H-pyrazol-3-yl)-5-(trifluoromethoxy)phenyl)-2-(2H-tetrazol-5-yl)ethyl)-6-nitrophenol (VU0826738)*



*Step A: 2-(3-(1-Methyl-1H-pyrazol-3-yl)-5-(trifluoromethoxy)phenyl)acetonitrile*

2-(3-Bromo-5-(trifluoromethoxy)phenyl)acetonitrile (80 mg, 0.29 mmol) was reacted with (1-methyl-1H-pyrazol-4-yl)boronic acid following General Procedure J. Purification by flash chromatography afforded the title compound (7.5 mg, 0.027 mmol, 9%). <sup>1</sup>H NMR (400 MHz, Chloroform-*d*) δ 7.54 (s, 1H), 7.36 (s, 1H), 7.27 (s, 1H), 7.25 (s, 1H), 6.36 (s, 1H), 3.91 (s, 3H), 3.85 (s, 2H). <sup>19</sup>F NMR (376 MHz, Chloroform-*d*) δ -57.8 (3F). LCMS (Method B, 2 min): *t<sub>R</sub>* = 1.047 min, *m/z* = 282.4 [M+H]<sup>+</sup>; Purity (AUC) ≥ 95%.



Step B: 3-(5-Chloro-2-hydroxy-3-nitrophenyl)-2-(3-(1-methyl-1H-pyrazol-3-yl)-5-(trifluoromethoxy)phenyl)acrylonitrile

2-(3-(1-Methyl-1H-pyrazol-4-yl)-5-(trifluoromethoxy)phenyl)acetonitrile (7.5 mg, 0.027 mmol) was reacted with 5-chloro-2-hydroxy-3-nitrobenzaldehyde following General Procedure W. The crude was taken forward (12.9 mg). LCMS (Method B, 2 min):  $t_R = 1.413$  min,  $m/z = 464.8, 466.3$  [M+H]<sup>+</sup>.

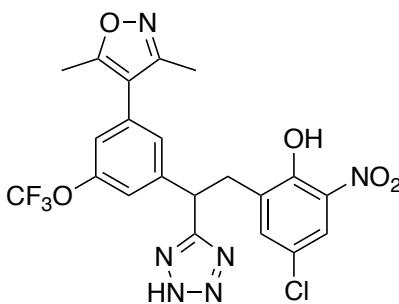
Step C: 3-(5-Chloro-2-hydroxy-3-nitrophenyl)-2-(3-(1-methyl-1H-pyrazol-3-yl)-5-(trifluoromethoxy)phenyl)propanenitrile

3-(5-Chloro-2-hydroxy-3-nitrophenyl)-2-(3-(1-methyl-1H-pyrazol-3-yl)-5-(trifluoromethoxy)phenyl)acrylonitrile (12.6 mg, crude) was reacted following General Procedure T. The crude was taken forward (13 mg). LCMS (Method B, 2 min):  $t_R = 1.342$  min,  $m/z = 467.4, 468.4$  [M+H].

Step D: 4-Chloro-2-(2-(3-(1-methyl-1H-pyrazol-3-yl)-5-(trifluoromethoxy)phenyl)-2-(2H-tetrazol-5-yl)ethyl)-6-nitrophenol

3-(5-Chloro-2-hydroxy-3-nitrophenyl)-2-(3-(1-methyl-1H-pyrazol-3-yl)-5-(trifluoromethoxy)phenyl)propanenitrile (13 mg, crude) was reacted following General Procedure TZ. The title compound was obtained after purification by preparative HPLC (2.8 mg, 0.0055 mmol, 20%). <sup>1</sup>H NMR (400 MHz, Chloroform-*d*)  $\delta$  7.97 (d,  $J = 2.6$  Hz, 1H), 7.55 (d,  $J = 2.0$  Hz, 1H), 7.31 (s, 1H), 7.29 – 7.27 (m, 2H), 7.19 (s, 1H), 6.33 (d,  $J = 2.0$  Hz, 1H), 4.95 (dd,  $J = 8.8, 6.8$  Hz, 1H), 3.81 (s, 3H), 3.73 (dd,  $J = 13.7, 8.8$  Hz, 1H), 3.53 (dd,  $J = 13.7, 6.8$  Hz, 1H). <sup>19</sup>F NMR (376 MHz, Chloroform-*d*)  $\delta$  -57.8 (3F). LCMS (Method B, 2 min):  $t_R = 1.201$  min,  $m/z = 510.4, 512.4$  [M+H]<sup>+</sup>; Purity (AUC)  $\geq 95\%$ .

*4-Chloro-2-(2-(3-(3,5-dimethylisoxazol-4-yl)-5-(trifluoromethoxy)phenyl)-2-(2H-tetrazol-5-yl)ethyl)-6-nitrophenol (VU0826724)*



Step A: 2-(3-(3,5-Dimethylisoxazol-4-yl)-5-(trifluoromethoxy)phenyl)acetonitrile

2-(3-Bromo-5-(trifluoromethoxy)phenyl)acetonitrile (80 mg, 0.29 mmol) was reacted with (3,5-dimethylisoxazol-4-yl)boronic acid following General Procedure J. Purification by flash chromatography afforded the title compound (45.6 mg, 0.12 mmol, 43%). <sup>1</sup>H NMR (400 MHz, Chloroform-*d*) δ 7.20 (s, 2H), 7.10 (s, 1H), 3.84 (s, 2H), 2.43 (s, 3H), 2.28 (s, 3H). <sup>19</sup>F NMR (376 MHz, Chloroform-*d*) δ -57.8 (3F). LCMS (Method B, 2 min): t<sub>R</sub> = 1.131 min, m/z = 297.5 [M+H]<sup>+</sup>; Purity (AUC) ≥ 83%.

Step B: 3-(5-chloro-2-hydroxy-3-nitrophenyl)-2-(3-(3,5-dimethylisoxazol-4-yl)-5-(trifluoromethoxy)phenyl)acrylonitrile

2-(3-(1-Methyl-1*H*-pyrazol-4-yl)-5-(trifluoromethoxy)phenyl)acetonitrile (45.6 mg, 0.12 mmol) was reacted with 5-chloro-2-hydroxy-3-nitrobenzaldehyde following General Procedure W. The crude was taken forward (82.9 mg).

Step C: 3-(5-Chloro-2-hydroxy-3-nitrophenyl)-2-(3-(3,5-dimethylisoxazol-4-yl)-5-(trifluoromethoxy)phenyl)propanenitrile

3-(5-Chloro-2-hydroxy-3-nitrophenyl)-2-(3-(1-methyl-1*H*-pyrazol-3-yl)-5-(trifluoromethoxy)phenyl)acrylonitrile (82.9 mg, crude) was reacted following General Procedure

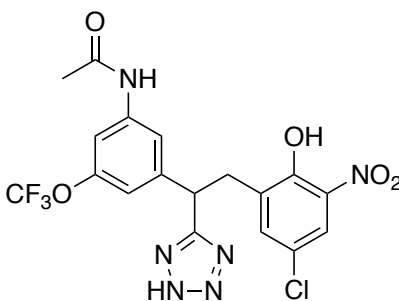
T. The crude was taken forward (84 mg). LCMS (Method B, 2 min):  $t_R = 1.439$  min,  $m/z = 482.0$ , 484.4 [M+H].

Step D: 4-Chloro-2-(2-(3-(3,5-dimethylisoxazol-4-yl)-5-(trifluoromethoxy)phenyl)-2-(2H-tetrazol-5-yl)ethyl)-6-nitrophenol

3-(5-Chloro-2-hydroxy-3-nitrophenyl)-2-(3-(3,5-dimethylisoxazol-4-yl)-5-

(trifluoromethoxy)phenyl)propanenitrile (84.0 mg, crude) was reacted following General Procedure TZ. Purification by preparative HPLC afforded the title compound (35.0 mg, 0.067 mmol, 56%).  $^1\text{H}$  NMR (400 MHz, Chloroform-*d*)  $\delta$  10.95 (br s, 1H), 7.95 (d,  $J = 2.8$  Hz, 1H), 7.27 (d,  $J = 2.8$  Hz, 2H), 7.23 (s, 1H), 7.04 (s, 1H), 5.03 (t,  $J = 7.8$  Hz, 1H), 3.75 (dd,  $J = 13.6, 7.8$  Hz, 1H), 3.57 (dd,  $J = 13.6, 7.8$  Hz, 1H), 2.37 (s, 3H), 2.20 (s, 3H).  $^{19}\text{F}$  NMR (376 MHz, Chloroform-*d*)  $\delta$  -57.9 (3F). LCMS (Method B, 2 min):  $t_R = 1.302$  min,  $m/z = 525.2, 527.2$  [M+H] $^+$ ; Purity (AUC)  $\geq 95\%$ .

*N*-(3-(2-(5-Chloro-2-hydroxy-3-nitrophenyl)-1-(2H-tetrazol-5-yl)ethyl)-5-(trifluoromethoxy)phenyl)acetamide (**VU026922**)



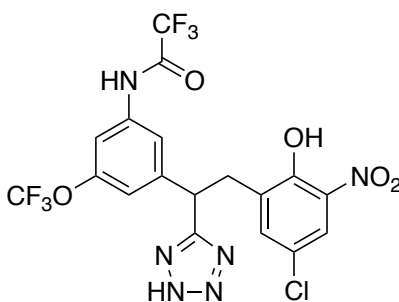
Step A: *N*-(3-(2-(5-Chloro-2-hydroxy-3-nitrophenyl)-1-cyanoethyl)-5-(trifluoromethoxy)phenyl)acetamide

2-(3-Amino-5-(trifluoromethoxy)phenyl)-3-(5-chloro-2-hydroxy-3-nitrophenyl)propanenitrile (20 mg, 0.050 mmol, 1 eq) was dissolved in THF at 0.20 M and acetic anhydride (250  $\mu$ L, 0.050 mmol, 1 eq) was added. It was stirred at room temperature for 6 hours. The solvent was removed under reduced pressure. The crude was taken forward (22 mg). Used without further purification. LCMS (Method B, 2 min):  $t_R = 1.267$  min,  $m/z = 444.4, 446.3$   $[M+H]^+$ .

Step B: *N*-(3-(2-(5-Chloro-2-hydroxy-3-nitrophenyl)-1-(2H-tetrazol-5-yl)ethyl)-5-(trifluoromethoxy)phenyl)acetamide

*N*-(3-(2-(5-Chloro-2-hydroxy-3-nitrophenyl)-1-cyanoethyl)-5-(trifluoromethoxy)phenyl)acetamide (22 mg, crude) was reacted following General Procedure TZ. Purification by preparative HPLC afforded the title compound (16.7 mg, 0.034 mmol, 69%).  $^1H$  NMR (400 MHz, Chloroform-*d*)  $\delta$  10.96 (br s, 1H), 7.98 (d,  $J = 2.6$  Hz, 1H), 7.51 (s, 1H), 7.45 (br s, 1H), 7.33 (d,  $J = 2.6$  Hz, 1H), 7.23 (s, 1H), 6.94 (s, 1H), 4.87 (t,  $J = 7.8$  Hz, 1H), 3.77 (dd,  $J = 13.8, 7.8$  Hz, 1H), 3.50 (dd,  $J = 13.8, 7.8$  Hz, 1H), 2.22 (s, 3H).  $^{19}F$  NMR (376 MHz, Chloroform-*d*)  $\delta$  -60.9 (3F). LCMS (Method B, 2 min):  $t_R = 1.153$  min,  $m/z = 487.4, 489.4$   $[M+H]^+$ ; Purity (AUC)  $\geq 95\%$ .

*N*-(3-(2-(5-Chloro-2-hydroxy-3-nitrophenyl)-1-(2H-tetrazol-5-yl)ethyl)-5-(trifluoromethoxy)phenyl)-2,2,2-trifluoroacetamide (**VU0826955**)



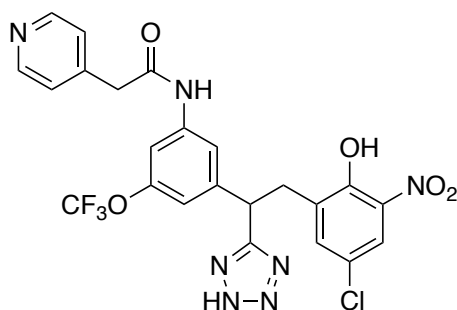
Step A: *N*-(3-(2-(5-Chloro-2-hydroxy-3-nitrophenyl)-1-cyanoethyl)-5-(trifluoromethoxy)phenyl)-2,2,2-trifluoroacetamide

2-(3-Amino-5-(trifluoromethoxy)phenyl)-3-(5-chloro-2-hydroxy-3-nitrophenyl)propanenitrile (20 mg, 0.050 mmol, 1 eq) was dissolved in THF at 0.20 M and trifluoroacetic anhydride (10.5 mg, 0.050 mmol, 1 eq) was added. It was stirred at room temperature for 6 hours. The solvent was removed under reduced pressure. The crude was taken forward (24.0 mg).

Step B: *N*-(3-(2-(5-Chloro-2-hydroxy-3-nitrophenyl)-1-(2H-tetrazol-5-yl)ethyl)-5-(trifluoromethoxy)phenyl)acetamide

*N*-(3-(2-(5-Chloro-2-hydroxy-3-nitrophenyl)-1-cyanoethyl)-5-(trifluoromethoxy)phenyl)acetamide (24.0 mg, crude) was reacted following General Procedure TZ. Purification by preparative HPLC afforded the title compound (16.7 mg, 0.031 mmol, 62%). <sup>1</sup>H NMR (400 MHz, Methanol-*d*<sub>4</sub>) δ 7.98 (d, *J* = 2.6 Hz, 1H), 7.63 (s, 1H), 7.57 (s, 1H), 7.32 (d, *J* = 2.6 Hz, 1H), 7.07 (s, 1H), 4.95 (t, *J* = 8.0 Hz, 1H), 3.71 (dd, *J* = 13.6, 8.0 Hz, 1H), 3.51 (dd, *J* = 13.6, 8.0 Hz, 1H). <sup>19</sup>F NMR (376 MHz, Chloroform-*d*) δ -59.5 (3F), -80.3 (TFA). LCMS (Method B, 2 min): *t*<sub>R</sub> = 1.280 min, *m/z* = 541.4, 543.3 [M+H]<sup>+</sup>; Purity (AUC) ≥ 95%.

*N*-(3-(2-(5-chloro-2-hydroxy-3-nitrophenyl)-1-(2H-tetrazol-5-yl)ethyl)-5-(trifluoromethoxy)phenyl)-2-(pyridin-4-yl)acetamide (**VU0827041**)



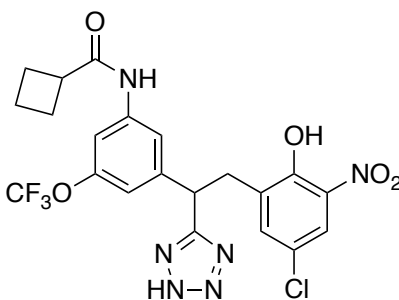
Step A: *N*-(3-(2-(5-Chloro-2-hydroxy-3-nitrophenyl)-1-cyanoethyl)-5-(trifluoromethoxy)phenyl)-2-(pyridin-4-yl)acetamide

2-(3-Amino-5-(trifluoromethoxy)phenyl)-3-(5-chloro-2-hydroxy-3-nitrophenyl)propanenitrile (32.5 mg, 0.081 mmol) was reacted with 4-pyridilacetic acid hydrochloride following General Procedure H. The crude was taken forward (50 mg). Used without further purification. LCMS (Method B):  $t_R = 1.008$  min,  $m/z = 521.2, 523.1$   $[M+H]^+$ .

Step B: *N*-(3-(2-(5-chloro-2-hydroxy-3-nitrophenyl)-1-(2H-tetrazol-5-yl)ethyl)-5-(trifluoromethoxy)phenyl)-2-(pyridin-4-yl)acetamide

*N*-(3-(2-(5-Chloro-2-hydroxy-3-nitrophenyl)-1-cyanoethyl)-5-(trifluoromethoxy)phenyl)-2-(pyridin-4-yl)acetamide (50 mg, crude) was reacted following General Procedure TZ. Purification by preparative HPLC afforded the title compound (21.9 mg, 0.039 mmol, 48%).  $^1H$  NMR (400 MHz, Methanol- $d_4$ )  $\delta$  8.83 – 8.77 (m, 2H), 8.08 – 8.02 (m, 2H), 7.96 (d,  $J = 2.7$  Hz, 1H), 7.57 (s, 1H), 7.43 (t,  $J = 1.7$  Hz, 1H), 7.28 (d,  $J = 2.7$  Hz, 1H), 6.93 (s, 1H), 4.95 – 4.88 (m, 3H), 3.69 (dd,  $J = 13.5, 8.0$  Hz, 1H), 3.48 (dd,  $J = 13.5, 8.0$  Hz, 1H).  $^{19}F$  NMR (376 MHz, Chloroform- $d$ )  $\delta$  -62.5 (3F). LCMS (Method B):  $t_R = 0.941$  min,  $m/z = 564.2, 565.2$   $[M+H]^+$ ; Purity (AUC)  $\geq 95\%$ .

*N*-(3-(2-(5-Chloro-2-hydroxy-3-nitrophenyl)-1-(2H-tetrazol-5-yl)ethyl)-5-(trifluoromethoxy)phenyl)cyclobutanecarboxamide (**VU0827042**)



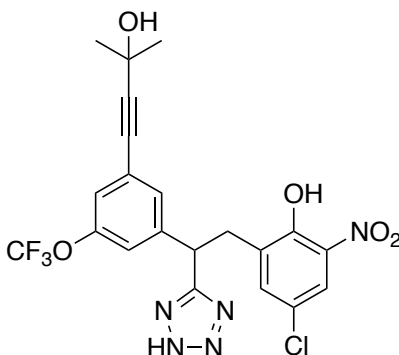
Step A: *N*-(3-(2-(5-Chloro-2-hydroxy-3-nitrophenyl)-1-cyanoethyl)-5-(trifluoromethoxy)phenyl)cyclobutanecarboxamide

2-(3-Amino-5-(trifluoromethoxy)phenyl)-3-(5-chloro-2-hydroxy-3-nitrophenyl)propanenitrile (40.0 mg, 0.10 mmol) was reacted with 4-pyridilacetic acid hydrochloride following General Procedure H. The crude was taken forward (48 mg). LCMS (Method B):  $t_R = 1.329$  min,  $m/z = 484.2, 486.0$   $[M+H]^+$ .

Step B: *N*-(3-(2-(5-Chloro-2-hydroxy-3-nitrophenyl)-1-(2H-tetrazol-5-yl)ethyl)-5-(trifluoromethoxy)phenyl)cyclobutanecarboxamide

*N*-(3-(2-(5-Chloro-2-hydroxy-3-nitrophenyl)-1-cyanoethyl)-5-(trifluoromethoxy)phenyl)cyclobutanecarboxamide (48 mg, crude) was reacted following General Procedure TZ. Purification by preparative HPLC afforded the title compound (2.7 mg, 0.0051 mmol, 5%).  $^1H$  NMR (400 MHz, Chloroform-*d*)  $\delta$  10.91 (br s, 1H), 7.95 (d,  $J = 2.6$  Hz, 1H), 7.52 (s, 1H), 7.31 (d,  $J = 2.4$  Hz, 2H), 7.21 (br s, 1H), 6.89 (s, 1H), 4.84 (t,  $J = 7.8$  Hz, 1H), 3.74 (dd,  $J = 13.8, 7.8$  Hz, 1H), 3.47 (dd,  $J = 13.8, 7.8$  Hz, 1H), 3.21 – 3.12 (m, 1H), 2.42 – 2.32 (m, 2H), 2.30 – 2.19 (m, 2H), 2.08 – 2.00 (m, 1H).  $^{19}F$  NMR (376 MHz, Chloroform-*d*)  $\delta$  -57.8 (3F). LCMS (Method B):  $t_R = 1.206$  min,  $m/z = 527.2, 529.2$   $[M+H]^+$ ; Purity (AUC)  $\geq 95\%$ .

*4-Chloro-2-(2-(3-(3-hydroxy-3-methylbut-1-yn-1-yl)-5-(trifluoromethoxy)phenyl)-2H-tetrazol-5-yl)ethyl)-6-nitrophenol (VU0827040)*



*Step A: 2-(3-(3-Hydroxy-3-methylbut-1-yn-1-yl)-5-(trifluoromethoxy)phenyl)acetonitrile*

2-(3-Bromo-5-(trifluoromethoxy)phenyl)acetonitrile (100 mg, 0.36 mmol) was mixed with CuI (3.4 mg, 0.02 mmol, 0.05 eq) and purged with Ar. THF (0.357 mL), Et<sub>3</sub>N (0.715 mL) and PdCl<sub>2</sub>(PPh<sub>3</sub>)<sub>2</sub> were added in that order and the solution was stirred for 16 h at 60 °C. The mixture was filtered through celite and the solvent of the filtrate was removed under reduced pressure. The crude was purified using ISCO flash chromatography to obtain the title compound as a dark-yellow liquid (85 mg, 0.30 mmol, 83%). <sup>1</sup>H NMR (400 MHz, Chloroform-*d*) δ 7.32 (s, 1H), 7.22 (s, 1H), 7.10 (s, 1H), 3.73 (s, 2H), 2.51 (br s, 1H), 1.60 (d, *J* = 3.0 Hz, 6H). <sup>19</sup>F NMR (376 MHz, Chloroform-*d*) δ -57.8 (3F). LCMS (Method B, 2 min): *t<sub>R</sub>* = 1.105 min, *m/z* = 266.4 [M-OH]<sup>+</sup>; Purity (AUC) ≥ 95%.

*Step B: 3-(5-chloro-2-hydroxy-3-nitrophenyl)-2-(3-(3-hydroxy-3-methylbut-1-yn-1-yl)-5-(trifluoromethoxy)phenyl)acrylonitrile*

2-(3-(3-Hydroxy-3-methylbut-1-yn-1-yl)-5-(trifluoromethoxy)phenyl)acetonitrile (40 mg, 0.14 mmol) was reacted with 5-chloro-2-hydroxy-3-nitrobenzaldehyde following General Procedure W. The crude was taken forward (62.6 mg). LCMS (Method B, 2 min): *t<sub>R</sub>* = 1.491 min, *m/z* = 467.2, 469.4 [M+H]<sup>+</sup>.



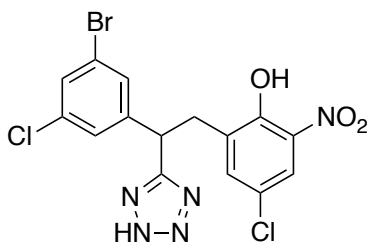
Step C: 3-(5-Chloro-2-hydroxy-3-nitrophenyl)-2-(3-(3-hydroxy-3-methylbut-1-yn-1-yl)-5-(trifluoromethoxy)phenyl)propanenitrile

3-(5-Chloro-2-hydroxy-3-nitrophenyl)-2-(3-(3-hydroxy-3-methylbut-1-yn-1-yl)-5-(trifluoromethoxy)phenyl)acrylonitrile (62.6 mg, crude) was reacted following General Procedure T. The crude was taken forward (62.2 mg). LCMS (Method B, 2 min):  $t_R = 1.414$  min,  $m/z = 485.3$ , 487.4  $[M+NH_4]$ .

Step D: 4-Chloro-2-(2-(3-(3-hydroxy-3-methylbut-1-yn-1-yl)-5-(trifluoromethoxy)phenyl)-2-(2H-tetrazol-5-yl)ethyl)-6-nitrophenol

3-(5-Chloro-2-hydroxy-3-nitrophenyl)-2-(3-(3-hydroxy-3-methylbut-1-yn-1-yl)-5-(trifluoromethoxy)phenyl)propanenitrile (62.2 mg, crude) was reacted following General Procedure TZ. Purification by preparative HPLC afforded the title compound (35 mg, 0.067 mmol, 56%).  $^1H$  NMR (400 MHz, Chloroform-*d*)  $\delta$  10.91 (br s, 1H), 7.93 (d,  $J = 2.6$  Hz, 1H), 7.25 (s, 1H), 7.17 (s, 1H), 7.09 (s, 2H), 4.85 (t,  $J = 7.8$  Hz, 1H), 3.68 (dd,  $J = 13.7, 7.8$  Hz, 1H), 3.44 (dd,  $J = 13.7, 7.8$  Hz, 1H), 1.62 (s, 6H).  $^{19}F$  NMR (376 MHz, Chloroform-*d*)  $\delta$  -57.9 (3F). LCMS (Method B, 2 min):  $t_R = 1.278$  min,  $m/z = 512.6$   $[M+NH_4]^+$ ; Purity (AUC)  $\geq 95\%$ .

*2-(2-(3-Bromo-5-chlorophenyl)-2-(2H-tetrazol-5-yl)ethyl)-4-chloro-6-nitrophenol (VU0826485)*



Step A: (3-Bromo-5-chlorophenyl)methanol

3-Bromo-5-chlorobenzaldehyde (250 mg, 1.14 mmol) was reacted following General Procedure T. The crude was taken forward (195 mg, 0.88 mmol, 77%). LCMS (Method B, 2 min):  $t_R = 0.904$  min, does not ionize by ESI; Purity (AUC)  $\geq 95\%$ .

Step B: 3-Bromo-5-chlorobenzyl methanesulfonate

(3-Bromo-5-chlorophenyl)methanol (195 mg, 0.88 mmol) was reacted following General Procedure U. Purification by flash chromatography afforded the title compound as a clear liquid (149.8 mg, 0.50 mmol, 57%).  $^1\text{H NMR}$  (400 MHz, Chloroform-*d*)  $\delta$  7.50 (s, 1H), 7.43 (s, 1H), 7.32 (s, 1H), 5.13 (s, 2H), 3.02 (s, 3H). LCMS (Method B, 2 min):  $t_R = 1.052$  min, does not ionize by ESI; Purity (AUC)  $\geq 95\%$ .

Step C: 2-(3-Bromo-5-chlorophenyl)acetonitrile

3-Bromo-5-chlorobenzyl methanesulfonate (149.8 mg, 0.50 mmol) was reacted following General Procedure V. Purification by flash chromatography afforded the title compound (55 mg, 0.24 mmol, 48%).  $^1\text{H NMR}$  (400 MHz, Chloroform-*d*)  $\delta$  7.48 (s, 1H), 7.38 (s, 1H), 7.28 (s, 1H), 3.72 (s, 2H). LCMS (Method B, 2 min):  $t_R = 1.045$  min, does not ionize by ESI; Purity (AUC)  $\geq 95\%$ .

Step D: 2-(3-Bromo-5-chlorophenyl)-3-(5-chloro-2-hydroxy-3-nitrophenyl)acrylonitrile

2-(3-Bromo-5-chlorophenyl)acetonitrile (55 mg, 0.24 mmol) was reacted with 5-chloro-2-hydroxy-3-nitrobenzaldehyde following General Procedure W. The crude was taken forward (100 mg). LCMS (Method B, 2 min):  $t_R = 1.530$  min  $m/z = 414.8$   $[\text{M}+\text{H}]^+$ .

Step E: 2-(3-Bromo-5-chlorophenyl)-3-(5-chloro-2-hydroxy-3-nitrophenyl)propanenitrile

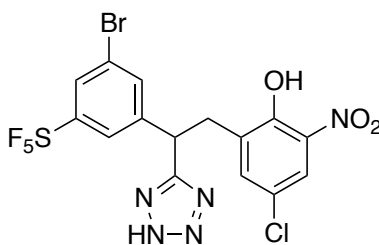
2-(3-Bromo-5-chlorophenyl)-3-(5-chloro-2-hydroxy-3-nitrophenyl)acrylonitrile (100 mg, crude) was reacted following General Procedure T. The crude was taken forward without further purification (70 mg, 0.17 mmol, 70%).  $^1\text{H NMR}$  (400 MHz, Chloroform-*d*)  $\delta$  11.00 (br s, 1H),

8.12 (d,  $J = 2.6$  Hz, 1H), 7.54 (t,  $J = 1.8$  Hz, 1H), 7.49 (d,  $J = 2.6$  Hz, 1H), 7.45 (t,  $J = 1.8$  Hz, 1H), 7.35 (t,  $J = 1.8$  Hz, 1H), 4.24 (dd,  $J = 10.2, 5.4$  Hz, 1H), 3.33 (dd,  $J = 13.6, 5.4$  Hz, 1H), 3.10 (dd,  $J = 13.6, 10.2$  Hz, 1H). LCMS (Method B, 2 min):  $t_R = 1.362$  min, does not ionize by ESI; Purity (AUC)  $\geq 95\%$ .

Step F: 2-(2-(3-Bromo-5-chlorophenyl)-2-(2H-tetrazol-5-yl)ethyl)-4-chloro-6-nitrophenol

2-(3-Bromo-5-chlorophenyl)-3-(5-chloro-2-hydroxy-3-nitrophenyl)propanenitrile (30 mg, 0.072 mmol) was reacted following General Procedure TZ. Purification by preparative afforded the title compound as a yellow solid (12.5 mg, 0.027, 38%).  $^1\text{H NMR}$  (400 MHz, Chloroform- $d$ )  $\delta$  7.97 (d,  $J = 2.6$  Hz, 1H), 7.45 (t,  $J = 1.8$  Hz, 1H), 7.37 (t,  $J = 1.8$  Hz, 1H), 7.33 (d,  $J = 2.6$  Hz, 1H), 7.27 (d,  $J = 1.8$  Hz, 1H), 4.80 (dd,  $J = 9.2, 6.2$  Hz, 1H), 3.68 (dd,  $J = 13.7, 9.2$  Hz, 1H), 3.46 (dd,  $J = 13.7, 6.2$  Hz, 1H). LCMS (Method A):  $t_R = 1.836$  min,  $m/z = 459.7, 461.7$   $[\text{M}+\text{H}]^+$ ; Purity (AUC)  $\geq 95\%$ .

*4-Chloro-2-(2-(3-bromo-5-(pentafluorosulfaneyl)phenyl)-2-(2H-tetrazol-5-yl)ethyl)-6-nitrophenol (VU0826880)*



Step A: (3-Bromo-5-(pentafluorosulfaneyl)phenyl)methanol

$\text{LiAlH}_4$  (93 mg, 2.45 mmol, 2 eq) was dissolved in THF at 0.24 M and cooled to 0 °C in an ice/water bath. A solution of 3-Bromo-5-(pentafluorosulfaneyl)benzoic acid (400 mg, 1.22 mmol) in THF at 1.5 M was added to the reducing solution and stirred for 2 h. To quench the  $\text{LiAlH}_4$ , 92

$\mu\text{L}$  of water were added, then 92  $\mu\text{L}$  of a solution of NaOH at 15% in water and finally 276  $\mu\text{L}$  of water. A white precipitate was formed and the mixture was extracted with  $\text{CH}_2\text{Cl}_2$ . The solvent was removed from the organic phase and the crude was purified using ISCO flash chromatography to obtain the title compound (188.0 mg, 0.60 mmol, 49%).  $^1\text{H}$  NMR (400 MHz, Chloroform-*d*)  $\delta$  7.79 (s, 1H), 7.66 (s, 1H), 7.63 (s, 1H), 4.72 (s, 2H).  $^{19}\text{F}$  NMR (376 MHz, Chloroform-*d*)  $\delta$  82.8 (p,  $J = 150.2$  Hz, 1F), 62.9 (d,  $J = 150.2$  Hz, 4F). LCMS (Method B, 2 min):  $t_{\text{R}} = 1.133$  min, does not ionize by ESI; Purity (AUC)  $\geq 95\%$ .

Step B: 3-Bromo-5-(pentafluorosulfaneyl)benzyl methanesulfonate

(3-Bromo-5-(pentafluorosulfaneyl)phenyl)methanol (185.0 mg, 0.59 mmol) was reacted following General Procedure U. Purification by flash chromatography afforded the title compound (178.9 mg, 0.46 mmol, 78%).  $^1\text{H}$  NMR (400 MHz, Chloroform-*d*)  $\delta$  7.90 (s, 1H), 7.72 (s, 2H), 5.23 (s, 2H), 3.06 (s, 3H).  $^{19}\text{F}$  NMR (376 MHz, Chloroform-*d*)  $\delta$  78.9 (p,  $J = 150$ , 1F), 59.9 (d,  $J = 150$  Hz, 4F). LCMS (Method B, 2 min):  $t_{\text{R}} = 1.225$  min, does not ionize by ESI; Purity (AUC)  $\geq 95\%$ .

Step C: 2-(3-Bromo-5-(pentafluorosulfaneyl)phenyl)acetonitrile

3-Bromo-5-(pentafluorosulfaneyl)benzyl methanesulfonate (178.9 mg, 0.46 mmol) was reacted following General Procedure V. Purification by flash chromatography afforded the title compound (84 mg, 0.24 mmol, 57%).  $^1\text{H}$  NMR (400 MHz, Chloroform-*d*)  $\delta$  7.89 (s, 1H), 7.70 (s, 1H), 7.67 (s, 1H), 3.83 (s, 2H).  $^{19}\text{F}$  NMR (376 MHz, Chloroform-*d*)  $\delta$  81.7 (p,  $J = 151$ , 1F), 62.9 (d,  $J = 151$  Hz, 4F). LCMS (Method B, 2 min):  $t_{\text{R}} = 1.238$  min,  $m/z = 341.5$   $[\text{M}+\text{NH}_4]^+$ ; Purity (AUC)  $\geq 95\%$ .

Step D: 2-(3-Bromo-5-(pentafluorosulfaneyl)phenyl)-3-(5-chloro-2-hydroxy-3-nitrophenyl)acrylonitrile

2-(3-Bromo-5-(pentafluorosulfaneyl)phenyl)acetonitrile (84 mg, 0.24 mmol) was reacted with 5-chloro-2-hydroxy-3-nitrobenzaldehyde following General Procedure W. The crude was taken forward (133.7 mg). LCMS (Method B, 2 min):  $t_R = 1.595$  min,  $m/z = 505.0$   $[M+H]^+$ .

Step E: 2-(3-Bromo-5-(pentafluorosulfaneyl)phenyl)-3-(5-chloro-2-hydroxy-3-nitrophenyl)propanenitrile

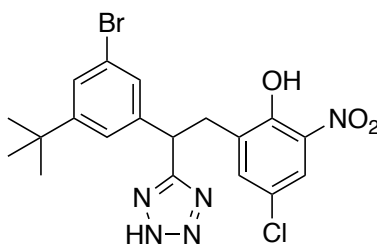
2-(3-Bromo-5-(pentafluorosulfaneyl)phenyl)-3-(5-chloro-2-hydroxy-3-nitrophenyl)acrylonitrile (133.7 mg, crude) was reacted following General Procedure T. The crude was taken forward (131.8 mg). LCMS (Method B, 2 min):  $t_R = 1.509$  min,  $m/z = 524.2$   $[M+NH_4]^+$ .

Step F: 4-Chloro-2-(2-(3-bromo-5-(pentafluorosulfaneyl)phenyl)-2-(2H-tetrazol-5-yl)ethyl)-6-nitrophenol

2-(3-Bromo-5-(pentafluorosulfaneyl)phenyl)-3-(5-chloro-2-hydroxy-3-nitrophenyl)propanenitrile (131.8 mg, crude) was reacted following General Procedure TZ. Purification by preparative HPLC afforded the title compound (55.6 mg, 0.10 mmol, 42%).  $^1H$  NMR (400 MHz, Chloroform-*d*)  $\delta$  10.94 (br s, 1H), 7.96 (d,  $J = 2.6$  Hz, 1H), 7.81 (t,  $J = 1.8$  Hz, 1H), 7.69 (s, 1H), 7.66 (d,  $J = 1.8$  Hz, 1H), 7.28 (d,  $J = 2.6$  Hz, 1H), 4.97 (dd,  $J = 8.9, 6.7$  Hz, 1H), 3.69 (dd,  $J = 13.7, 8.9$  Hz, 1H), 3.51 (dd,  $J = 13.7, 6.7$  Hz, 1H).  $^{19}F$  NMR (376 MHz, Chloroform-*d*)  $\delta$  82.3 (p,  $J = 150$  Hz, 1F), 62.93 (d,  $J = 150$  Hz, 4F). LCMS (Method A):  $t_R = 1.375$  min,  $m/z = 550.2, 552.2$   $[M+H]^+$ ; Purity (AUC)  $\geq 94\%$ .

*2-(2-(3-Bromo-5-(tert-butyl)phenyl)-2-(2H-tetrazol-5-yl)ethyl)-4-chloro-6-nitrophenol*

*(VU0826894)*



*Step A: (3-Bromo-5-(tert-butyl)phenyl)methanol*

LiAlH<sub>4</sub> (147 mg, 3.89 mmol, 2.5 eq) was dissolved in THF at 0.24 M and cooled to 0 °C in an ice/water bath. A solution of 3-Bromo-5-*tert*-butylbenzoic acid (400 mg, 1.56 mmol) in THF at 1.5 M was added to the reducing solution and stirred for 2 h. To quench the LiAlH<sub>4</sub>, 147 μL of water were added, then 147 μL of a solution of NaOH at 15% in water and finally 441 μL of water. A white precipitate was formed and the mixture was extracted with CH<sub>2</sub>Cl<sub>2</sub>. The solvent was removed from the organic phase. Purification by ISCO flash chromatography afforded the title compound (172 mg, 0.71 mmol, 45%). <sup>1</sup>H NMR (400 MHz, Chloroform-*d*) δ 7.43 (s, 1H), 7.33 (s, 1H), 7.29 (s, 1H), 4.64 (s, 2H), 3.11 (br s, 1H), 1.30 (s, 9H). LCMS (Method B, 2 min): t<sub>R</sub> = 1.155 min, m/z = 266.5, 268.4 [M+NH<sub>4</sub>]<sup>+</sup>; Purity (AUC) ≥ 95%.

*Step B: 3-Bromo-5-(tert-butyl)benzyl methanesulfonate*

(3-Bromo-5-(*tert*-butyl)phenyl)methanol (172 mg, 0.71 mmol) was reacted following General Procedure U. Purification by flash chromatography afforded the title compound (114.9 mg, 0.36 mmol, 50%). <sup>1</sup>H NMR (400 MHz, Chloroform-*d*) δ 7.53 (s, 1H), 7.38 (s, 1H), 7.33 (s, 1H), 5.17 (s, 2H), 2.96 (s, 3H), 1.31 (s, 9H). LCMS (Method B, 2 min): t<sub>R</sub> = 1.275 min, m/z = 339.5, 341.0 [M+NH<sub>4</sub>]<sup>+</sup>; Purity (AUC) ≥ 95%.

Step C: 2-(3-Bromo-5-(tert-butyl)phenyl)acetonitrile

3-Bromo-5-(tert-butyl)benzyl methanesulfonate (114.9 mg, 0.36 mmol) was reacted following General Procedure V. Purification by flash chromatography afforded the title compound (68 mg, 0.27 mmol, 75%) of title compound. <sup>1</sup>H NMR (400 MHz, Chloroform-*d*) δ 7.89 (s, 1H), 7.70 (s, 1H), 7.67 (s, 1H), 3.83 (s, 2H). <sup>19</sup>F NMR (376 MHz, Chloroform-*d*) δ 81.7 (p, *J* = 150.6, 1F), 62.9 (d, *J* = 150.6 Hz, 4F). LCMS (Method B, 2 min): *t*<sub>R</sub> = 1.304 min, does not ionize by ESI<sup>+</sup>; Purity (AUC) ≥ 95%.

Step D: 2-(3-Bromo-5-(tert-butyl)phenyl)-3-(5-chloro-2-hydroxy-3-nitrophenyl)acrylonitrile

2-(3-Bromo-5-(tert-butyl)phenyl)acetonitrile (68 mg, 0.27 mmol) was reacted with 5-chloro-2-hydroxy-3-nitrobenzaldehyde following General Procedure W. The crude was taken forward (137.7 mg). LCMS (Method B, 2 min): *t*<sub>R</sub> = 1.719 min, *m/z* = 435.3, 437.3 [M+H]<sup>+</sup>.

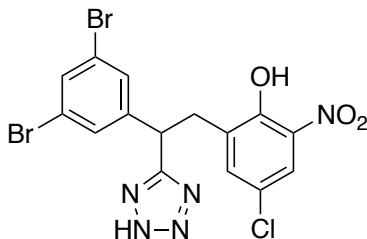
Step E: 2-(3-Bromo-5-(tert-butyl)phenyl)-3-(5-chloro-2-hydroxy-3-nitrophenyl)propanenitrile

2-(3-Bromo-5-(tert-butyl)phenyl)-3-(5-chloro-2-hydroxy-3-nitrophenyl)acrylonitrile (137.7 mg, crude) was reacted following General Procedure T. The crude was taken forward (126.2 mg). LCMS (Method B, 2 min): *t*<sub>R</sub> = 1.601 min, does not ionize by ESI.

Step F: 4-Chloro-2-(2-(3-bromo-5-(tert-butyl)phenyl)-2-(2H-tetrazol-5-yl)ethyl)-6-nitrophenol

2-(3-Bromo-5-(tert-butyl)phenyl)-3-(5-chloro-2-hydroxy-3-nitrophenyl)propanenitrile (123.9 mg, crude) was reacted following General Procedure TZ. Purification by preparative HPLC afforded the title compound (33.5 mg, 0.070 mmol, 26%). <sup>1</sup>H NMR (400 MHz, Chloroform-*d*) δ 10.90 (br s, 1H), 7.92 (d, *J* = 2.6 Hz, 1H), 7.39 (t, *J* = 1.7 Hz, 1H), 7.24 (t, *J* = 1.7 Hz, 1H), 7.21 (d, *J* = 2.6 Hz, 1H), 7.17 (t, *J* = 1.7 Hz, 1H), 4.85 (t, *J* = 7.8 Hz, 1H), 3.77 (dd, *J* = 13.7, 7.8 Hz, 1H), 3.45 (dd, *J* = 13.7, 7.8 Hz, 1H), 1.20 (s, 9H). LCMS (Method B, 2 min): *t*<sub>R</sub> = 1.425 min, *m/z* = 480.3, 482.2 [M+H]<sup>+</sup>; Purity (AUC) ≥ 95%.

*4-Chloro-2-(2-(3,5-dibromophenyl)-2-(2H-tetrazol-5-yl)ethyl)-6-nitrophenol (VU0827422)*



*Step A: (3,5-Dibromophenyl)methanol*

LiAlH<sub>4</sub> (97 mg, 2.55 mmol, 1.5 eq) was dissolved in THF at 0.20 M and cooled to 0 °C in an ice/water bath. A solution of methyl 3,5-dibromobenzoate (500 mg, 1.70 mmol) in THF at 0.6 M was added to the reducing solution and stirred for 1.5 h. To quench the LiAlH<sub>4</sub>, 97 μL of water were added, then 97 μL of a solution of NaOH at 15% in water and finally 291 μL of water. A white precipitate was formed and the mixture was extracted with CH<sub>2</sub>Cl<sub>2</sub>. The solvent was removed from the organic phase. The crude purified using ISCO flash chromatography to afford the title compound (345 mg, 1.30 mmol, 86%). <sup>1</sup>H NMR (400 MHz, Chloroform-*d*) δ 7.58 (t, *J* = 1.7 Hz, 1H), 7.49 – 7.42 (m, 2H), 4.65 (d, *J* = 5.4 Hz, 2H). LCMS (Method B, 2 min): t<sub>R</sub> = 0.957 min, does not ionize by ESI; Purity (AUC) ≥ 95%.

*Step B: 3,5-Dibromobenzyl methanesulfonate*

(3,5-Dibromophenyl)methanol (345 mg, 1.30 mmol) was reacted following General Procedure U. Purification by flash chromatography afforded the title compound (255 mg, 0.74 mmol, 57%). <sup>1</sup>H NMR (400 MHz, Chloroform-*d*) δ 7.67 (t, *J* = 1.8 Hz, 1H), 7.48 (d, *J* = 1.8 Hz, 2H), 5.14 (s, 2H), 3.02 (s, 3H). LCMS (Method B, 2 min): t<sub>R</sub> = 1.064 min, m/z = 367.0, 367.5 [M+Na]<sup>+</sup>; Purity (AUC) ≥ 95%.



Step C: 2-(3,5-Dibromophenyl)acetonitrile

3,5-Dibromobenzyl methanesulfonate (255 mg, 0.74 mmol) was reacted following General Procedure V. Purification by flash chromatography afforded the title compound (131.3 mg, 0.48 mmol, 64%). <sup>1</sup>H NMR (400 MHz, Chloroform-*d*) δ 7.65 (t, *J* = 1.7 Hz, 1H), 7.46 – 7.41 (m, 2H), 3.72 (s, 2H). LCMS (Method B, 2 min): *t*<sub>R</sub> = 1.049 min, does not ionize by ESI; Purity (AUC) ≥ 95%.

Step D: 2-(3,5-Dibromophenyl)-3-(5-chloro-2-hydroxy-3-nitrophenyl)acrylonitrile

2-(3,5-Dibromophenyl)acetonitrile (131.3 mg, 0.48 mmol) was reacted with 5-chloro-2-hydroxy-3-nitrobenzaldehyde following General Procedure W. The crude was taken forward (227 mg). LCMS (Method B): *t*<sub>R</sub> = 1.477 min *m/z* = 459.0, 460.9 [M+H]<sup>+</sup>.

Step E: 2-(3,5-dibromophenyl)-3-(5-chloro-2-hydroxy-3-nitrophenyl)propanenitrile

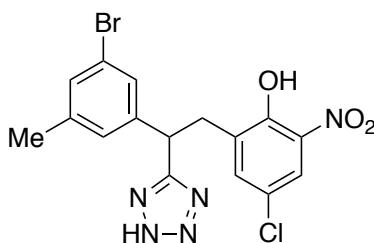
2-(3,5-Dibromophenyl)-3-(5-chloro-2-hydroxy-3-nitrophenyl)acrylonitrile (227 mg, crude) was reacted following General Procedure T. Purification by flash chromatography afforded the title compound (155.9 mg, 0.34 mmol, 71%). <sup>1</sup>H NMR (400 MHz, Chloroform-*d*) δ 10.98 (br s, 1H), 8.11 (d, *J* = 2.6 Hz, 3H), 7.69 (t, *J* = 1.7 Hz, 3H), 7.65 (s, 1H), 7.49 (d, *J* = 1.7 Hz, 6H), 7.44 (s, 2H), 4.23 (dd, *J* = 10.2, 5.4 Hz, 3H), 3.33 (dd, *J* = 13.6, 5.4 Hz, 3H), 3.09 (dd, *J* = 13.6, 10.2 Hz, 3H). LCMS (Method B): *t*<sub>R</sub> = 1.334 min, *m/z* = 459.0, 461.2 [M+H]<sup>+</sup>; Purity (AUC) ≥ 95%.

Step F: 2-(2-(3,5-Dibromophenyl)-2-(2H-tetrazol-5-yl)ethyl)-4-chloro-6-nitrophenol

2-(3,5-Dibromophenyl)-3-(5-chloro-2-hydroxy-3-nitrophenyl)propanenitrile (15 mg, 0.030 mmol) was reacted following General Procedure TZ. Purification by preparative HPLC afforded the title compound (13.7 mg, 0.027, 91%). <sup>1</sup>H NMR (400 MHz, Chloroform-*d*) δ 10.99 (br s, 1H), 7.98 (d, *J* = 2.6 Hz, 1H), 7.61 (s, 1H), 7.42 (s, 2H), 7.33 (s, 1H), 4.78 (dd, *J* = 9.3, 6.1 Hz, 1H),

3.74 – 3.60 (m, 1H), 3.46 (dd,  $J = 13.7, 6.1$  Hz, 1H). LCMS (Method B):  $t_R = 1.234$  min,  $m/z = 504.0, 506.0$   $[M+H]^+$ ; Purity (AUC)  $\geq 95\%$ .

*2-(2-(3-Bromo-5-methylphenyl)-2-(2H-tetrazol-5-yl)ethyl)-4-chloro-6-nitrophenol (VU0827670)*



Step A: 2-(3-Bromo-5-methylphenyl)acetonitrile

2-(3,5-Dibromophenyl)acetonitrile (70 mg, 0.25 mmol) was reacted with methylboronic acid following General Procedure J. The crude was taken forward (26 mg).

Step B: 2-(3-Bromo-5-methylphenyl)-3-(5-chloro-2-hydroxy-3-nitrophenyl)acrylonitrile

2-(3-Bromo-5-methylphenyl)acetonitrile (26 mg, crude) was reacted with 5-chloro-2-hydroxy-3-nitrobenzaldehyde following General Procedure W. The crude was taken forward (53 mg). LCMS (Method B): two peaks with the desired mass were observed  $t_R = 0.997$  min  $m/z = 393.3, 395.0$   $[M+H]^+$  and  $t_R = 1.438$  min  $m/z = 393.0, 395.1$   $[M+H]^+$ .

Step C: 2-(3-Bromo-5-methylphenyl)-3-(5-chloro-2-hydroxy-3-nitrophenyl)propanenitrile

2-(3-Bromo-5-methylphenyl)-3-(5-chloro-2-hydroxy-3-nitrophenyl)acrylonitrile (53 mg, crude) was reacted following General Procedure T. The crude was taken forward (56 mg). LCMS (Method B):  $t_R = 1.347$  min,  $m/z = 395.0$   $[M+H]^+$ .

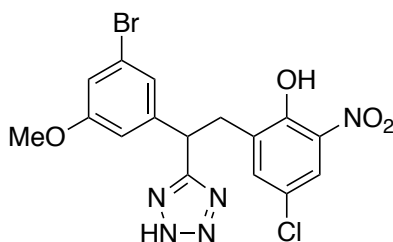
Step D: 2-(2-(3-Bromo-5-methylphenyl)-2-(2H-tetrazol-5-yl)ethyl)-4-chloro-6-nitrophenol

2-(3-Bromo-5-methylphenyl)-3-(5-chloro-2-hydroxy-3-nitrophenyl)propanenitrile (56 mg, crude) was reacted following General Procedure TZ. Purification by preparative HPLC afforded the title

compound (9.9 mg, 0.023 mmol, 9%) of title compound.  $^1\text{H}$  NMR (400 MHz, Chloroform-*d*)  $\delta$  10.93 (br s, 1H), 7.94 (d,  $J = 2.6$  Hz, 1H), 7.30 (d,  $J = 2.6$  Hz, 1H), 7.23 (s, 2H), 7.02 (s, 1H), 4.79 (dd,  $J = 8.7, 6.7$  Hz, 1H), 3.72 (dd,  $J = 13.7, 8.7$  Hz, 1H), 3.44 (dd,  $J = 13.7, 6.7$  Hz, 1H), 2.27 (s, 3H). LCMS (Method B):  $t_{\text{R}} = 1.185$  min,  $m/z = 438.2, 440.2$   $[\text{M}+\text{H}]^+$ ; Purity (AUC)  $\geq 95\%$ .

*2-(2-(3-Bromo-5-methoxyphenyl)-2-(2H-tetrazol-5-yl)ethyl)-4-chloro-6-nitrophenol*

*(VU0829212)*



*Step A: (3-Bromo-5-methoxy)methanol*

3-Bromo-5-methoxybenzaldehyde (600 mg, 2.79 mmol) was reacted following General Procedure T. The crude was taken forward without further purification (605 mg (0.88 mmol, quant.)).  $^1\text{H}$  NMR (400 MHz, Chloroform-*d*)  $\delta$  7.06 (d,  $J = 1.6$  Hz, 1H), 6.95 (t,  $J = 2.1$  Hz, 1H), 6.84 – 6.78 (m, 1H), 4.60 (s, 2H), 3.78 (s, 3H). LCMS (Method B):  $t_{\text{R}} = 0.840$  min, does not ionize by ESI; Purity (AUC)  $\geq 95\%$ .

*Step B: 3-Bromo-5-methoxybenzyl methanesulfonate*

(3-Bromo-5-methoxyphenyl)methanol (605 mg, 2.79 mmol) was reacted following General Procedure U. Purification by flash chromatography afforded the title compound as a clear liquid (531 mg, 1.80 mmol, 64%).  $^1\text{H}$  NMR (400 MHz, Chloroform-*d*)  $\delta$  7.11 (s, 1H), 7.04 (s, 1H), 6.85 (s, 1H), 5.13 (s, 2H), 3.79 (s, 3H), 2.97 (s, 3H). LCMS (Method B):  $t_{\text{R}} = 0.993$  min,  $m/z = 295.4$   $[\text{M}+\text{H}]^+$  (AUC)  $\geq 95\%$ .

Step C: 2-(3-Bromo-5-methoxyphenyl)acetonitrile

3-Bromo-5-methoxybenzyl methanesulfonate (531 mg, 1.80 mmol) was reacted following General Procedure V. Purification by flash chromatography afforded the title compound (338 mg, 1.50 mmol, 83%). <sup>1</sup>H NMR (400 MHz, Chloroform-*d*) δ 7.02 (s, 1H), 6.98 (s, 1H), 6.77 (s, 1H), 3.77 (s, 3H), 3.67 (s, 2H). LCMS (Method B): t<sub>R</sub> = 0.983 min, does not ionize by ESI; Purity (AUC) ≥ 95%.

Step D: 2-(3-Bromo-5-methoxyphenyl)-3-(5-chloro-2-hydroxy-3-nitrophenyl)acrylonitrile

2-(3-Bromo-5-methoxyphenyl)acetonitrile (338 mg, 1.50 mmol) was reacted with 5-chloro-2-hydroxy-3-nitrobenzaldehyde following General Procedure W. The crude was taken forward (631 mg). LCMS (Method B): t<sub>R</sub> = 1.380 min m/z = 409.1, 411.2 [M+H]<sup>+</sup>.

Step E: 2-(3-Bromo-5-methoxyphenyl)-3-(5-chloro-2-hydroxy-3-nitrophenyl)propanenitrile

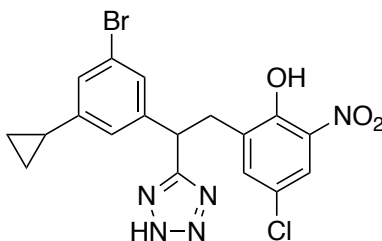
2-(3-Bromo-5-methoxyphenyl)-3-(5-chloro-2-hydroxy-3-nitrophenyl)acrylonitrile (631 mg, crude) was reacted following General Procedure T. Purification by flash chromatography afforded the title compound (357.6 mg, 0.69 mmol, 46%). <sup>1</sup>H NMR (400 MHz, Chloroform-*d*) δ 10.98 (br s, 1H), 8.09 (d, *J* = 2.6 Hz, 1H), 7.46 (d, *J* = 2.6 Hz, 1H), 7.11 (d, *J* = 2.6 Hz, 1H), 7.04 (t, *J* = 2.0 Hz, 1H), 6.85 (t, *J* = 2.0 Hz, 1H), 4.20 (dd, *J* = 10.0, 5.6 Hz, 1H), 3.82 (s, 3H), 3.32 (dd, *J* = 13.6, 5.6 Hz, 1H), 3.11 (dd, *J* = 13.6, 10.0 Hz, 1H). LCMS (Method B): t<sub>R</sub> = 1.270 min, 411.2, 413.2 [M+H]<sup>+</sup>; Purity (AUC) ≥ 80%.

Step F: 2-(2-(3-Bromo-5-methoxyphenyl)-2-(2H-tetrazol-5-yl)ethyl)-4-chloro-6-nitrophenol

2-(3-Bromo-5-methoxyphenyl)-3-(5-chloro-2-hydroxy-3-nitrophenyl)propanenitrile (30 mg, 0.070 mmol) was reacted following General Procedure TZ. Purification by preparative HPLC afforded the title compound 24.4 mg (0.054 mmol, 77%) of title compound. <sup>1</sup>H NMR (400 MHz, Chloroform-*d*) δ 10.94 (br s, 1H), 7.95 (d, *J* = 2.6 Hz, 1H), 7.31 (d, *J* = 2.6 Hz, 1H), 7.01 (t, *J* =

1.8 Hz, 1H), 6.95 (d,  $J = 2.6$  Hz, 1H), 6.76 (t,  $J = 1.8$  Hz, 1H), 4.80 (t,  $J = 7.6$ , 1H) 3.79 – 3.67 (m, 4H), 3.45 (dd,  $J = 13.7, 7.6$  Hz, 1H). LCMS (Method B):  $t_R = 1.144$  min,  $m/z = 454.0, 457.4$   $[M+H]^+$ ; Purity (AUC)  $\geq 95\%$ .

*2-(2-(3-Bromo-5-cyclopropylphenyl)-2-(2H-tetrazol-5-yl)ethyl)-4-chloro-6-nitrophenol*  
(VU0827671)



Step A: 2-(3-Bromo-5-cyclopropylphenyl)acetonitrile

2-(3,5-Dibromophenyl)acetonitrile (70 mg, 0.25 mmol) was reacted with cyclopropylboronic acid following General Procedure J. The crude was taken forward (34.5 mg).

Step B: 2-(3-Bromo-5-cyclopropylphenyl)-3-(5-chloro-2-hydroxy-3-nitrophenyl)acrylonitrile

2-(3-Bromo-5-cyclopropylphenyl)acetonitrile (34.5 mg, crude) was reacted with 5-chloro-2-hydroxy-3-nitrobenzaldehyde following General Procedure W. The crude was taken forward (53.2 mg). LCMS (Method B):  $t_R = 1.151$  min  $m/z = 459.1, 461.1$   $[M+K]^+$ .

Step C: 2-(3-Bromo-5-cyclopropylphenyl)-3-(5-chloro-2-hydroxy-3-nitrophenyl)propanenitrile

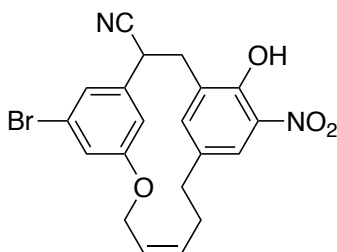
2-(3-Bromo-5-cyclopropylphenyl)-3-(5-chloro-2-hydroxy-3-nitrophenyl)acrylonitrile (53.2 mg, crude) was reacted following General Procedure T. The crude was taken forward (77 mg). LCMS (Method B):  $t_R = 1.401$  min,  $m/z = 420.2, 422.2$   $[M+H]^+$ .

Step D: 2-(2-(3-Bromo-5-cyclopropylphenyl)-2-(2H-tetrazol-5-yl)ethyl)-4-chloro-6-nitrophenol

2-(3-Bromo-5-cyclopropylphenyl)-3-(5-chloro-2-hydroxy-3-nitrophenyl)propanenitrile (77 mg, crude) was reacted following General Procedure TZ. Purification by preparative HPLC afforded

the title compound (7.0 mg, 0.015 mmol, 6%). <sup>1</sup>H NMR (400 MHz, Chloroform-*d*) δ 8.20 (br s, 1H), 7.89 (d, *J* = 2.7 Hz, 1H), 7.23 (d, *J* = 2.7 Hz, 1H), 7.17 (s, 1H), 7.03 (s, 1H), 6.90 (s, 1H), 4.73 (t, *J* = 7.7 Hz, 1H), 3.68 (dd, *J* = 13.7, 7.7 Hz, 1H), 3.39 (dd, *J* = 13.7, 7.7 Hz, 1H), 1.87 – 1.67 (m, 1H), 1.07 – 0.84 (m, 2H), 0.70 – 0.48 (m, 2H). LCMS (Method A): *t*<sub>R</sub> = 1.849 min, *m/z* = 463.8, 464.8 [M+H]<sup>+</sup>; Purity (AUC) ≥ 95%.

*(Z)*-4<sup>5</sup>-bromo-1<sup>6</sup>-hydroxy-15-nitro-5-oxa-1,4(1,3)-dibenzenacyclononaphan-7-ene-3-carbonitrile  
(VU0830501)



Step A: 3-(Allyloxy)-5-bromobenzaldehyde

3-Bromo-5-hydroxybenzaldehyde (1000 mg, 4.96 mmol, 1 eq) was dissolved in DMF at 0.5 M. K<sub>2</sub>CO<sub>3</sub> (531 mg, 9.92 mmol, 2 eq) and allyl bromide (645 mg, 9.92 mmol, 2 eq) were added and the mixture was stirred at 40 °C for 16 h. Water was added and extracted with EtOAc, the organic phase was dried using a phase separator and the solvent was removed under reduced pressure. The crude was taken forward without further purification (1.195 mg, 4.96 mmol, quant.). <sup>1</sup>H NMR (400 MHz, Chloroform-*d*) δ 9.86 (s, 1H), 7.63 – 7.50 (m, 1H), 7.29 (d, *J* = 3.2 Hz, 2H), 6.10 – 5.87 (m, 1H), 5.40 (d, *J* = 17.2 Hz, 1H), 5.30 (d, *J* = 10.5 Hz, 1H), 4.55 (d, *J* = 3.5 Hz, 2H). LCMS (Method B): *t*<sub>R</sub> = 1.122 min, *m/z* = 241.1.8, 243.2 [M+H]<sup>+</sup>; Purity (AUC) ≥ 95%.

Step B: (3-(Allyloxy)-5-bromophenyl)methanol

3-(Allyloxy)-5-bromobenzaldehyde (1195 mg, 4.96 mmol) was reacted following General Procedure T. Purification by flash chromatography afforded the title compound as a yellow oil (995 mg, 4.09 mmol, 83%). <sup>1</sup>H NMR (400 MHz, Chloroform-*d*) δ 7.07 (s, 1H), 6.97 (t, *J* = 2.1 Hz, 1H), 6.83 (s, 1H), 6.09 – 5.95 (m, 1H), 5.45 – 5.35 (m, 1H), 5.33 – 5.25 (m, 1H), 4.60 (s, 2H), 4.51 (dt, *J* = 5.3, 1.5 Hz, 2H). LCMS (Method B): *t*<sub>R</sub> = 0.964 min, does not ionize by ESI; Purity (AUC) ≥ 95%.

Step C: 3-(Allyloxy)-5-bromobenzyl methanesulfonate

(3-(Allyloxy)-5-bromophenyl)methanol (995 mg, 4.09 mmol) was reacted following General Procedure U. Purification by flash chromatography afforded the title compound as a light-orange liquid (1.105 g, 3.44 mmol, 84%). <sup>1</sup>H NMR (400 MHz, Chloroform-*d*) δ 7.12 (s, 1H), 7.06 (t, *J* = 2.0 Hz, 1H), 6.88 (s, 1H), 6.06 – 5.94 (m, 1H), 5.45 – 5.35 (m, 1H), 5.34 – 5.26 (m, 1H), 5.12 (s, 2H), 4.51 (dt, *J* = 5.2, 1.3 Hz, 2H), 2.97 (s, 3H). LCMS (Method B): *t*<sub>R</sub> = 1.099 min, *m/z* = 338.3, 340.3 [M+NH<sub>4</sub>]<sup>+</sup> (AUC) ≥ 95%.

Step D: 2-(3-(Allyloxy)-5-bromophenyl)acetonitrile

3-(Allyloxy)-5-bromobenzyl methanesulfonate (1.105 g, 3.44 mmol) was reacted following General Procedure V. Purification by flash chromatography afforded the title compound (752.4 mg, 2.98 mmol, 87%). <sup>1</sup>H NMR (400 MHz, Chloroform-*d*) δ 7.03 (s, 1H), 7.01 (s, 1H), 6.80 (s, 1H), 6.07 – 5.93 (m, 1H), 5.44 – 5.35 (m, 1H), 5.30 (d, *J* = 10.4 Hz, 1H), 4.54 – 4.45 (m, 2H), 3.66 (d, *J* = 6.8 Hz, 2H). LCMS (Method B): *t*<sub>R</sub> = 1.089 min, does not ionize by ESI; Purity (AUC) ≥ 95%.

Step E: 2-(Benzyloxy)-5-bromo-3-nitrobenzaldehyde

4-Bromo-2-hydroxy-3-nitrobenzaldehyde (2500 mg, 10.16 mmol) was reacted with benzyl bromide following General Procedure Z. Purification by flash chromatography afforded the title

compound as a white solid (2.578 g, 7.67 mmol, 75%). <sup>1</sup>H NMR (400 MHz, Chloroform-*d*) δ 10.04 (s, 1H), 8.25 (d, *J* = 2.5 Hz, 1H), 8.15 (d, *J* = 2.6 Hz, 1H), 7.44 – 7.33 (m, 5H), 5.17 (s, 2H).

Step F: 2-(Benzyloxy)-3-nitro-5-(4,4,5,5-tetramethyl-1,3,2-dioxaborolan-2-yl)benzaldehyde

2-(Benzyloxy)-5-bromo-3-nitrobenzaldehyde (2.578 g, 7.67 mmol, 1 eq), Pd(dppf)Cl<sub>2</sub>•CH<sub>2</sub>Cl<sub>2</sub> (626 mg, 0.77 mmol, 0.10 eq) and KOAc (7497 mg, 23.01 mmol, 3 eq) were dissolved in 51 mL of anhydrous 1,4-dioxane. The solution was degassed for 20 min and then Bis(pinacolato)diboron (367 mg, 1.45 mmol, 1.1 eq) was added and stirred at 85 °C for 16 h. The mixture was cooled to room temperature and filtered. The solvent was removed under reduced pressure and the crude was purified using ISCO flash chromatography, 2.440 g (5.79 mmol, 76%) of the title compound were obtained. <sup>1</sup>H-NMR showed highly pure compound. <sup>1</sup>H NMR (400 MHz, Chloroform-*d*) δ 10.17 (s, 1H), 8.48 (d, *J* = 1.7 Hz, 1H), 8.46 (d, *J* = 1.7 Hz, 1H), 5.18 (s, 2H), 1.35 (s, 12H). LCMS (Method B): *t<sub>R</sub>* = 0.933 min, *m/z* = 319.3 [M+H]<sup>+</sup> for the hydrolyzed compound; Purity (AUC) ≥ 91%.

Step G: (4-(Benzyloxy)-3-formyl-5-nitrophenyl)boronic acid

2-(Benzyloxy)-3-nitro-5-(4,4,5,5-tetramethyl-1,3,2-dioxaborolan-2-yl)benzaldehyde (2.440 g, 5.79 mmol, 1 eq) was dissolved in 42 mL of THF and 11 mL of H<sub>2</sub>O and NaIO<sub>4</sub> (4086 mg, 19.10 mmol, 3 eq) was added. The mixture was stirred for 35 min at room temperature and 4.5 mL of 1 M HCl were added. The mixture was stirred for 18 h at room temperature. Water was added and extracted with EtOAc. The organic phase was dried over a phase separator and the solvent removed under vacuum. The crude was taken forward without further purification (1.740 g, 7.03 mmol, quant). <sup>1</sup>H NMR (400 MHz, Chloroform-*d*) δ 10.18 (s, 1H), 8.53 (d, *J* = 1.8 Hz, 1H), 8.41 (d, *J* = 1.8 Hz, 1H), 7.43 - 7.35 (m, 5H), 5.30 (s, 2H), 5.21 (s, 2H). LCMS (Method A): *t<sub>R</sub>* = 0.973 min, *m/z* = 602.5 [2M]<sup>+</sup>; Purity (AUC) ≥ 95%.



Step H: 5-Allyl-2-(benzyloxy)-3-nitrobenzaldehyde

(4-(Benzyloxy)-3-formyl-5-nitrophenyl)boronic acid (678 mg, 2.25 mmol, 1 eq), Pd<sub>2</sub>(dba)<sub>3</sub> (43 mg, 0.05 mmol, 0.03 eq), and triphenylphosphite (6 mg, 0.02 mmol, 0.01 eq) were dissolved in 1.9 mL of degassed and anhydrous 1,4-dioxane. The solution was stirred at 100 °C for 4 h. Upon cooling to room temperature, water was added and it was extracted with EtOAc. The organic phase was dried over a phase separator and the solvent was removed under reduced pressure. The crude was purified using ISCO flash chromatography, 418 mg (1.24 mmol, 55%) of the title compound were obtained as a green solid. <sup>1</sup>H NMR (400 MHz, Chloroform-*d*) δ 10.15 (s, 1H), 7.96 (d, *J* = 2.4 Hz, 1H), 7.89 (d, *J* = 2.4 Hz, 1H), 7.39 (s, 5H), 6.00 – 5.86 (m, 1H), 5.23 – 5.11 (m, 4H), 3.47 (dt, *J* = 6.7, 0.7 Hz, 2H). LCMS (Method A): t<sub>R</sub> = 2.169 min, m/z = 315.2 [M+NH<sub>4</sub>]<sup>+</sup>; Purity (AUC) ≥ 88%.

Step I: 5-Allyl-2-hydroxy-3-nitrobenzaldehyde

5-Allyl-2-(benzyloxy)-3-nitrobenzaldehyde (375.0 mg, 1.11 mmol, 1 eq) was dissolved in CH<sub>2</sub>Cl<sub>2</sub> at 0.07 M and cooled to 0 °C. BCl<sub>3</sub> (3.8 mL, 3.78 mmol, 3.4 eq) was added and stirred for 2 h. Water was added and extracted with CH<sub>2</sub>Cl<sub>2</sub>. The organic phase was dried over a phase separator and the solvent removed under reduced pressure. The crude was purified using ISCO flash chromatography, 133 mg (0.55 mmol, 50%) of the title compound were obtained as a yellow oil. <sup>1</sup>H NMR (400 MHz, Chloroform-*d*) δ 11.27 (br s, 1H), 10.39 (s, 1H), 8.16 (d, *J* = 2.2 Hz, 1H), 7.94 (d, *J* = 2.2 Hz, 1H), 5.99 – 5.84 (m, 1H), 5.19 (dd, *J* = 14.0, 1.5 Hz, 1H), 5.14 (dd, *J* = 14.0, 1.5 Hz, 1H), 3.43 (d, *J* = 6.6 Hz, 2H). LCMS (Method B): t<sub>R</sub> = 0.895 min, does not ionize by ESI; Purity (AUC) ≥ 86%.

Step J: 3-(5-Allyl-2-hydroxy-3-nitrophenyl)-2-(3-(allyloxy)-5-bromophenyl)acrylonitrile

2-(3-(Allyloxy)-5-bromophenyl)acetonitrile (160 mg, 0.63 mmol) was reacted with 5-allyl-2-hydroxy-3-nitrobenzaldehyde following General Procedure W. The crude was taken forward (292 mg). LCMS (Method B):  $t_R = 1.063$  min,  $m/z = 441.3, 443.3$   $[M+H]^+$ .

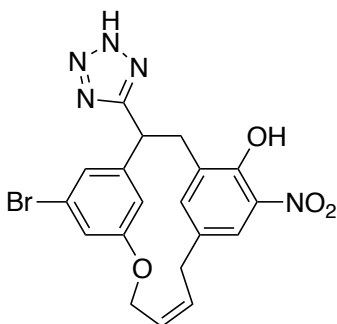
Step K: 3-(5-Allyl-2-hydroxy-3-nitrophenyl)-2-(3-(allyloxy)-5-bromophenyl)propanenitrile

3-(5-Allyl-2-hydroxy-3-nitrophenyl)-2-(3-(allyloxy)-5-bromophenyl)acrylonitrile (292 mg, crude) was reacted following General Procedure T. The crude was taken forward (125 mg, 0.28 mmol, 45%).  $^1H$  NMR (400 MHz, Chloroform-*d*)  $\delta$  10.95 (s, 1H), 7.89 (d,  $J = 2.0$  Hz, 1H), 7.28 (d,  $J = 2.0$  Hz, 1H), 7.09 (s, 1H), 7.04 (s, 1H), 6.86 (s, 1H), 6.08 – 5.96 (m, 1H), 5.93 – 5.82 (m, 1H), 5.42 (dd,  $J = 17.2, 1.7$  Hz, 1H), 5.32 (dd,  $J = 10.3, 1.5$  Hz, 1H), 5.14 (dd,  $J = 10.3, 1.5$  Hz, 1H), 5.07 (dd,  $J = 17.2, 1.7$  Hz, 1H), 4.53 (d,  $J = 5.2$  Hz, 2H), 4.18 (dd,  $J = 9.7, 5.9$  Hz, 1H), 3.34 (d,  $J = 6.7$  Hz, 2H), 3.30 (dd,  $J = 13.5, 5.9$  Hz, 1H), 3.12 (dd,  $J = 13.5, 9.7$  Hz, 1H).

Step L: (Z)-4<sup>5</sup>-Bromo-1<sup>6</sup>-hydroxy-1<sup>5</sup>-nitro-5-oxa-1,4(1,3)-dibenzenacyclononaphan-7-ene-3-carbonitrile

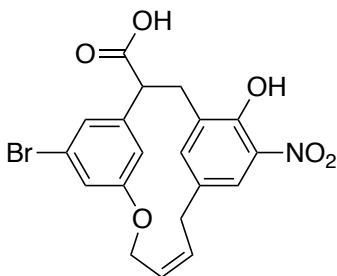
3-(5-Allyl-2-hydroxy-3-nitrophenyl)-2-(3-(allyloxy)-5-bromophenyl)propanenitrile (125 mg, 0.28 mmol, 1 eq) was dissolved in dry toluene at 0.004 M. The solution was degassed with Ar and the Hoveyda-Grubbs catalyst-II (18 mg, 0.030 mmol, 0.10 eq) was added. The mixture was stirred at 60 °C for 24 h. The mixture was filtered and the solvent removed under reduced pressure. The crude was purified using ISCO flash chromatography, 38 mg (0.092 mmol, 33%) of the title compound were obtained.  $^1H$  NMR (400 MHz, Chloroform-*d*)  $\delta$  11.02 (br s, 1H), 7.82 (d,  $J = 2.2$  Hz, 1H), 7.21 (t,  $J = 1.9$  Hz, 1H), 7.17 (t,  $J = 1.9$  Hz, 1H), 6.55 (d,  $J = 2.2$  Hz, 1H), 6.29 (t,  $J = 1.9$  Hz, 1H), 5.79 – 5.67 (m, 1H), 5.39 – 5.27 (m, 1H), 4.60 – 4.55 (m, 2H), 3.95 (dd,  $J = 9.3, 3.1$  Hz, 1H), 3.45 (dd,  $J = 13.8, 3.1$  Hz, 1H), 3.27 (dd,  $J = 13.8, 9.3$  Hz, 1H), 3.20 – 3.14 (m, 2H). LCMS (Method A):  $t_R = 1.871$  min,  $m/z = 414.9$   $[M+H]^+$ ; Purity (AUC)  $\geq 95\%$ .

*(Z)*-4<sup>5</sup>-Bromo-1<sup>5</sup>-nitro-3-(2H-tetrazol-5-yl)-5-oxa-1,4(1,3)-dibenzenacyclononaphan-7-en-1<sup>6</sup>-ol  
(VU0830447)



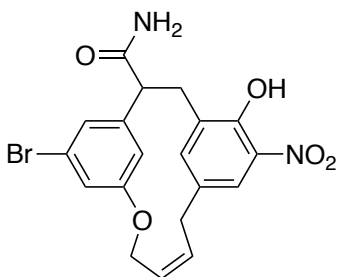
*(Z)*-4<sup>5</sup>-Bromo-1<sup>6</sup>-hydroxy-1<sup>5</sup>-nitro-5-oxa-1,4(1,3)-dibenzenacyclononaphan-7-ene-3-carbonitrile (18 mg, 0.050 mmol) was reacted following General Procedure TZ, it was used 4 eq of NaN<sub>3</sub> and 2 eq of NH<sub>4</sub>Cl. Purification by preparative HPLC afforded the title compound (3 mg, 0.0065 mmol, 13%). <sup>1</sup>H NMR (400 MHz, Chloroform-*d*) δ 11.00 (br s, 1H), 7.74 (d, *J* = 2.2 Hz, 1H), 7.07 (t, *J* = 1.8 Hz, 1H), 6.96 (t, *J* = 1.8 Hz, 1H), 6.77 (d, *J* = 2.2 Hz, 1H), 6.49 (t, *J* = 1.8 Hz, 1H), 5.67 – 5.55 (m, 1H), 5.48 – 5.36 (m, 1H), 4.55 – 4.45 (m, 3H), 3.95 (dd, *J* = 14.2, 3.8 Hz, 1H), 3.32 – 3.16 (m, 2H), 3.10 (dd, *J* = 14.2, 5.3 Hz, 1H). LCMS (Method B): t<sub>R</sub> = 1.069 min, m/z = 458.3, 460.3 [M+H]<sup>+</sup>; Purity (AUC) ≥ 95%.

*(Z)*-4<sup>5</sup>-Bromo-1<sup>6</sup>-hydroxy-1<sup>5</sup>-nitro-5-oxa-1,4(1,3)-dibenzenacyclononaphan-7-ene-3-carboxylic acid (VU0830839)



(Z)-4<sup>5</sup>-Bromo-1<sup>6</sup>-hydroxy-1<sup>5</sup>-nitro-5-oxa-1,4(1,3)-dibenzacyclononaphan-7-ene-3-carbonitrile (16 mg, 0.043 mmol, 1 eq) was dissolved in 2.0 mL of a NaOH solution at 15% in water and 300  $\mu$ L of THF were added. The solution was heated to reflux and stirred for 16 h. Water (2mL) was added and it was extracted with EtOAc. The organic phase was discarded and the aqueous phase was then acidified to pH= 3 with HCl 3 M and extracted again with EtOAc. The organic phase was dried using a phase separator and the solvent removed under reduced pressure. Purification by preparative HPLC afforded the title compound 15 mg (0.34 mmol, 79%). <sup>1</sup>H NMR (400 MHz, Chloroform-*d*)  $\delta$  10.95 (br s, 1H), 7.70 (d, *J* = 2.2 Hz, 1H), 7.08 (t, *J* = 1.8 Hz, 1H), 7.06 (t, *J* = 1.8 Hz, 2H), 6.78 (d, *J* = 2.2 Hz, 1H), 6.54 (s, 1H), 5.60 – 5.42 (m, 2H), 4.53 (dd, *J* = 6.5, 3.9 Hz, 2H), 3.78 (dd, *J* = 12.0, 3.7 Hz, 1H), 3.69 (dd, *J* = 14.1, 3.7 Hz, 1H), 3.19 (dd, *J* = 14.4, 8.0 Hz, 1H), 3.08 (dd, *J* = 14.4, 4.9 Hz, 1H), 2.96 (dd, *J* = 14.1, 12.0 Hz, 1H). LCMS (Method B):  $t_R$  = 1.099 min,  $m/z$  = 515.4 [M+2ACN+H]<sup>+</sup>; Purity (AUC)  $\geq$  95%.

*(Z)-4<sup>5</sup>-Bromo-1<sup>6</sup>-hydroxy-1<sup>5</sup>-nitro-5-oxa-1,4(1,3)-dibenzacyclononaphan-7-ene-3-carboxamide*



(Z)-4<sup>5</sup>-Bromo-1<sup>6</sup>-hydroxy-1<sup>5</sup>-nitro-5-oxa-1,4(1,3)-dibenzacyclononaphan-7-ene-3-carbonitrile (19 mg, 0.046 mmol, 1 eq) was dissolved in 1.8 mL of a 1:1 mixture of EtOH and H<sub>2</sub>O. KOH (19 mg, 0.34 mmol, 7 eq) was added and the solution was heated to 90 °C and stirred for 2 h. The solvent was removed under reduced pressure then water was added and the pH adjusted to 1-2. The mixture was extracted with CH<sub>2</sub>Cl<sub>2</sub> and the organic phase was dried and the solvent removed

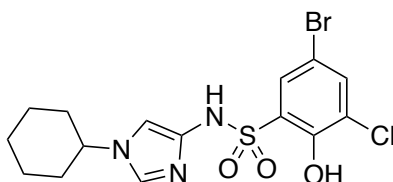
under reduced pressure. The crude was purified using preparative HPLC, 6 mg (0.014 mmol, 30%) of the title compound were obtained.  $^{13}\text{C}$  NMR (101 MHz, Chloroform-*d*)  $\delta$  177.7, 152.3, 141.9, 137.3, 131.4, 128.6, 128.53, 126.3, 124.2, 123.8, 122.5, 73.8, 49.7, 36.5, 32.9.  $^1\text{H}$  NMR (400 MHz, Chloroform-*d*)  $\delta$  10.95 (br s, 1H), 7.68 (d,  $J = 2.3$  Hz, 1H), 7.08 (t,  $J = 1.8$  Hz, 1H), 7.07 (d,  $J = 1.8$  Hz, 1H), 6.74 (d,  $J = 2.3$  Hz, 1H), 6.50 (t,  $J = 1.8$  Hz, 1H), 5.65 – 5.50 (m, 2H), 5.50 – 5.40 (m, 2H), 4.58 – 4.45 (m, 2H), 3.76 (dd,  $J = 14.0, 3.9$  Hz, 1H), 3.60 (dd,  $J = 11.8, 3.9$  Hz, 1H), 3.19 (dd,  $J = 14.4, 8.4$  Hz, 1H), 3.06 (dd,  $J = 14.4, 4.8$  Hz, 1H), 2.92 (dd,  $J = 14.0, 11.8$  Hz, 1H). LCMS (Method B):  $t_{\text{R}} = 1.042$  min,  $m/z = 433.2, 435.2$   $[\text{M}+\text{H}]^+$ ; Purity (AUC)  $\geq 95\%$ .

## 6.4 Synthesis of fragment-based heterocyclic benzenesulfonamide analogs

### 6.4.1 *N*-Substituted imidazolyl analogs

#### *5-Bromo-3-chloro-N-(1-cyclohexyl-1H-imidazol-4-yl)-2-hydroxybenzenesulfonamide*

**(VU0830015)**



#### *Cyclohexyl-4-nitro-1H-imidazole*

4-Nitroimidazole (100 mg, 0.88 mmol) was dissolved in 2.2 mL of DMF and  $\text{K}_2\text{CO}_3$  (183 mg, 1.33 mmol, 1.5 eq) and TBAB (3 mg, 0.01 mmol, 0.01 eq) were added. The mixture was pre-stirred for ~30 min and bromocyclohexane (180 mg, 1.11 mmol, 1.25 eq) was added. The mixture was stirred at 80 °C for 3 days. Upon cooling of the mixture, water was added and DCM was used

to extract the product. Then, the organic phase was dried over a phase separator and the solvent was removed under reduced pressure. The crude was taken forward (175 mg). LCMS (Method B):  $t_R = 1.214$  min,  $m/z = 196.2$   $[M+H]^+$ .

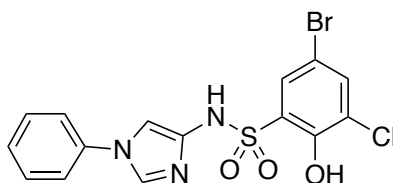
Step B: 1-Cyclohexyl-1H-imidazol-4-aminium chloride

1-Cyclohexyl-4-nitro-1H-imidazole (175 mg, crude) was reacted following General Procedure C. The crude was taken forward (24 mg). LCMS (Method B):  $t_R = 0.565$  min,  $m/z = 166.2$   $[M+H]^+$ .

Step C: 5-Bromo-3-chloro-N-(1-cyclohexyl-1H-imidazol-4-yl)-2-hydroxybenzenesulfonamide

1-Cyclohexyl-1H-imidazol-4-aminium chloride (24 mg, crude) was reacted with 5-bromo-3-chloro-2-hydroxybenzenesulfonyl chloride following General Procedure D. Purification by preparative HPLC afforded the title compound (4 mg, 0.0092 mmol, 1%).  $^1H$  NMR (400 MHz, Chloroform-*d*)  $\delta$  7.61 (d,  $J = 2.4$  Hz, 1H), 7.57 (d,  $J = 2.4$  Hz, 1H), 7.52 (d,  $J = 1.5$  Hz, 1H), 6.76 (d,  $J = 1.6$  Hz, 1H), 3.93 – 3.81 (m, 1H), 2.12 (d,  $J = 12.3$  Hz, 2H), 1.93 (d,  $J = 13.5$  Hz, 2H), 1.76 (d,  $J = 13.2$  Hz, 1H), 1.68 – 1.53 (m, 2H), 1.49 – 1.35 (m, 2H), 1.32 – 1.21 (m, 1H). LCMS (Method B):  $t_R = 0.951$  min,  $m/z = 434.2, 435.3$   $[M+H]^+$ ; Purity (AUC)  $\geq 95\%$ .

*5-Bromo-3-chloro-N-(1-phenyl-1H-imidazol-4-yl)-2-hydroxybenzenesulfonamide (VU0831903)*



Step A: 1-Phenyl-4-nitro-1H-imidazole

4-Nitroimidazole (200 mg, 1.77 mmol) was mixed with iodobenzene (1.77 mmol, 1 eq), CuI (0.27 mmol, 0.15 eq), *L*-proline (0.27 mmol, 0.15 eq) and  $K_2CO_3$  (3.54 mmol, 2 eq). The vial was purged with argon and DMSO [1.4 M] was added. It was capped and stirred overnight at 85 °C. Next day,

it was diluted with EtOAc and then filtered. The filtrate was washed with brine and the organic phase was dried over Na<sub>2</sub>SO<sub>4</sub>. The solvent was then removed under vacuum. The crude was purified using ISCO flash chromatography, 62 mg (0.33 mmol, 19% yield) of the title compound were obtained as a colorless solid. <sup>1</sup>H NMR (400 MHz, Chloroform-*d*) δ 8.11 (s, 1H), 7.84 – 7.75 (m, 1H), 7.62 – 7.54 (m, 2H), 7.54 – 7.49 (m, 1H), 7.45 (dd, *J* = 7.2, 1.9 Hz, 2H). LCMS (Method B): *t*<sub>R</sub> = 0.127 min, *m/z* = 190.2 [M+H]<sup>+</sup>.

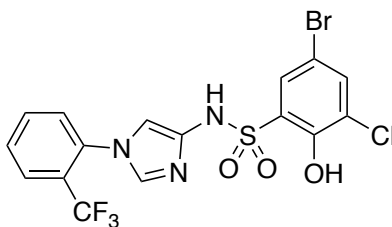
Step B: 1-Phenyl-1H-imidazol-4-aminium chloride

1-Phenyl-4-nitro-1H-imidazole (62 mg, 0.33 mmol) was reacted following General Procedure C. The crude was taken forward (64 mg). LCMS (Method B) *t*<sub>R</sub> = 0.097 min, *m/z* = 160.2 [M+H]<sup>+</sup>.

Step C: 5-Bromo-3-chloro-N-(1-phenyl-1H-imidazol-4-yl)-2-hydroxybenzenesulfonamide

Phenyl-1H-imidazol-4-aminium chloride (64 mg, crude) was reacted with 5-bromo-3-chloro-2-hydroxybenzenesulfonyl chloride following General Procedure D. Purification by preparative HPLC afforded the title compound (50 mg, 0.12 mmol, 35%). <sup>1</sup>H NMR (400 MHz, Chloroform-*d*) δ 9.83 (s, 2H), 8.06 (d, *J* = 1.7 Hz, 1H), 7.74 (d, *J* = 2.4 Hz, 1H), 7.63 (d, *J* = 2.4 Hz, 1H), 7.59 – 7.48 (m, 3H), 7.46 – 7.38 (m, 2H), 7.31 (d, *J* = 1.7 Hz, 1H). LCMS (Method B): *t*<sub>R</sub> = 1.570 min, *m/z* = 427.8, 428.8 [M+H]<sup>+</sup>; Purity (AUC) ≥ 95%.

*5-Bromo-3-chloro-2-hydroxy-N-(1-(2-(trifluoromethyl)phenyl)-1H-imidazol-4-yl)benzenesulfonamide (VU0848349)*



Step A: 1,4-Dinitro-1H-imidazole

4-Nitroimidazole (500 mg, 4.42 mmol) was reacted following General Procedure B-B. Purification by flash chromatography afforded the title compound (538 mg, 3.40 mmol, 77%). <sup>1</sup>H NMR (400 MHz, Chloroform-*d*) δ 8.51 (d, *J* = 1.7 Hz, 1H), 8.38 (d, *J* = 1.7 Hz, 1H). LCMS (Method B): *t*<sub>R</sub> = 0.081 min, *m/z* = 158.3 [M+H]<sup>+</sup>.

Step B: 4-Nitro-1-(2-(trifluoromethyl)phenyl)-1H-imidazole

1,4-Dinitro-1H-imidazole (100 mg, 0.63 mmol) was reacted with 2-(trifluoromethyl)aniline (1.10 mmol) according to General Procedure X-B. Purification by flash chromatography afforded the title compound as a yellow solid (20 mg, 0.08 mmol, 12%). <sup>1</sup>H NMR (400 MHz, Chloroform-*d*) δ 7.96 – 7.87 (m, 2H), 7.87 – 7.70 (m, 2H), 7.58 (dd, *J* = 1.6, 0.8 Hz, 1H), 7.52 – 7.45 (m, 1H). LCMS (Method B): *t*<sub>R</sub> = 0.777 min, *m/z* = 258.2 [M+H]<sup>+</sup>.

Step C: 1-(2-(Trifluoromethyl)phenyl)-1H-imidazole-4-aminium chloride

4-Nitro-1-(2-(trifluoromethyl)phenyl)-1H-imidazole (20 mg, 0.08 mmol) was reacted following General Procedure C. The crude was taken forward (22 mg). LCMS (Method B): *t*<sub>R</sub> = 0.254 min, *m/z* = 228.3 [M+H]<sup>+</sup>.

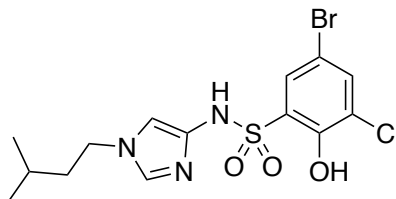
Step D: 5-Bromo-3-chloro-2-hydroxy-N-(1-(2-(trifluoromethyl)phenyl)-1H-imidazol-4-yl)benzenesulfonamide

1-(2-(Trifluoromethyl)phenyl)-1H-imidazole-4-aminium chloride (22 mg, crude) was reacted with 5-bromo-3-chloro-2-hydroxybenzenesulfonyl chloride following General Procedure D. Purification by preparative HPLC afforded the title compound (18 mg, 0.036 mmol, 45%). <sup>1</sup>H NMR (400 MHz, Chloroform-*d*) δ 7.86 (d, *J* = 7.7 Hz, 1H), 7.74 (t, *J* = 7.7 Hz, 1H), 7.71 – 7.63 (m, 3H), 7.50 (s, 1H), 7.45 (d, *J* = 7.7 Hz, 1H), 7.13 (s, 1H). <sup>19</sup>F NMR (376 MHz, Chloroform-*d*)



$\delta$  -59.42 (3F). LCMS (Method B):  $t_R$  = 1.138 min,  $m/z$  = 496.2, 497.2  $[M+H]^+$ , Purity (AUC)  $\geq$  95%.

*5-Bromo-3-chloro-2-hydroxy-N-(1-isopentyl-1H-imidazol-4-yl)benzenesulfonamide*  
(VU0848258)



Step A: 1-Isopentyl-4-nitro-1H-imidazole

4-Nitro-1H-imidazole (200 mg, 1.57 mmol) was reacted with 1-bromo-3-methylbutane (2.05 mmol) following General Procedure X. Purification by flash chromatography afforded the title compound 182 mg (0.99 mmol, 63%).  $^1H$  NMR (400 MHz, Chloroform-*d*)  $\delta$  7.76 (d,  $J$  = 1.6 Hz, 1H), 7.41 (d,  $J$  = 1.6 Hz, 1H), 4.04 – 3.97 (m, 2H), 1.73 – 1.64 (m, 2H), 1.54 (dt,  $J$  = 13.3, 6.7 Hz, 1H), 0.90 (dd,  $J$  = 6.7, 0.9 Hz, 6H). LCMS (Method B):  $t_R$  = 1.303 min,  $m/z$  = 184.2  $[M+H]^+$ .

Step B: 1-Isopentyl-1H-imidazol-4-aminium chloride

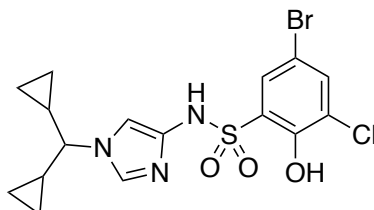
1-Isopentyl-4-nitro-1H-imidazol (100 mg, 0.54 mmol) was reacted following General Procedure C. The crude was taken forward (103 mg). LCMS (Method B):  $t_R$  = 0.192 min,  $m/z$  = 154.3  $[M+H]^+$ .

Step C: 5-Bromo-3-chloro-2-hydroxy-N-(1-isopentyl-1H-imidazol-4-yl)benzenesulfonamide

1-Isopentyl-1H-imidazol-4-aminium chloride (103 mg, crude) was reacted with 5-bromo-3-chloro-2-hydroxybenzenesulfonyl following General Procedure D. Purification by preparative HPLC afforded the title compound (6 mg, 0.014 mmol, 3).  $^1H$  NMR (400 MHz, Chloroform-*d*)  $\delta$  8.07 (s, 1H), 7.73 (d,  $J$  = 2.4 Hz, 1H), 7.65 (d,  $J$  = 2.4 Hz, 1H), 7.01 (s, 1H), 4.07 (t,  $J$  = 7.6 Hz,

2H), 1.75 (dt,  $J = 8.7, 6.7$  Hz, 2H), 1.63 – 1.52 (m, 1H), 0.97 (d,  $J = 6.7$  Hz, 6H). LCMS (Method B):  $t_R = 0.923$  min,  $m/z = 422.2, 423.3$   $[M+H]^+$ ; Purity (AUC)  $\geq 95\%$ .

*5-Bromo-3-chloro-N-(1-(dicyclopropylmethyl)-1-imidazol-4-yl)-2-hydroxybenzenesulfonamide*  
(VU0848258)



Step A: 1-(Dicyclopropylmethyl)-4-nitro-1H-imidazole

1,4-Dinitro-1H-imidazole (100 mg, 0.63 mmol) was reacted with dicyclopropylmethanamine (1.10 mmol) according to General Procedure X-B. Purification by flash chromatography afforded the title compound as a yellow solid (37 mg, 0.18 mmol, 28% yield).  $^1H$  NMR (400 MHz, Chloroform- $d$ )  $\delta$  7.97 (d,  $J = 1.6$  Hz, 1H), 7.60 (d,  $J = 1.6$  Hz, 1H), 2.85 (t,  $J = 8.9$  Hz, 1H), 1.30 – 1.17 (m, 2H), 0.87 – 0.75 (m, 2H), 0.73 – 0.62 (m, 2H), 0.56 – 0.45 (m, 2H), 0.43 – 0.32 (m, 2H).

Step B: 1-(Dicyclopropylmethyl)-1H-imidazol-4-aminium chloride

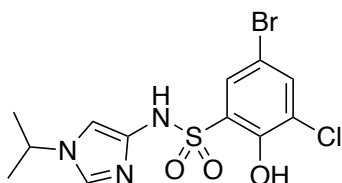
1-(Dicyclopropylmethyl)-4-nitro-1H-imidazole (37 mg, 0.18 mol) was reacted following General Procedure C. The crude was taken forward (44 mg). LCMS (Method B):  $t_R = 0.232$  min,  $m/z = 178.3$   $[M+H]^+$ .

Step C: 5-Bromo-3-chloro-N-(1-dicyclopropylmethyl-1-imidazol-4-yl)-2-hydroxybenzenesulfonamide

1-(Dicyclopropylmethyl)-1H-imidazol-4-aminium chloride (44 mg, crude) was reacted with 5-bromo-3-chloro-2-hydroxybenzenesulfonyl chloride following General Procedure D. Purification

by preparative HPLC afforded the title compound (8 mg, 0.018 mmol, 10%). <sup>1</sup>H NMR (400 MHz, Methanol-*d*<sub>4</sub>) δ 8.66 (d, *J* = 1.7 Hz, 1H), 7.82 (d, *J* = 2.5 Hz, 1H), 7.73 (d, *J* = 2.5 Hz, 1H), 7.30 (d, *J* = 1.7 Hz, 1H), 3.01 (t, *J* = 9.3 Hz, 1H), 1.39 – 1.26 (m, 2H), 0.82 – 0.72 (m, 2H), 0.62 – 0.48 (m, 4H), 0.37 – 0.25 (m, 2H). LCMS (Method B): *t*<sub>R</sub> = 1.615 min, *m/z* = 445.8, 446.8 [M+H]<sup>+</sup>, Purity (AUC) ≥ 95%.

*5-Bromo-3-chloro-2-hydroxy-N-(1-isopropyl-1H-imidazol-4-yl)benzenesulfonamide*  
(VU0849775)



Step A: Isopropyl-4-nitro-1H-imidazole

4-Nitroimidazole (200 mg, 1.77 mmol) was reacted with 2-bromopropane (2.12 mmol) following General Procedure X. Purification by flash chromatography afforded the title compound (225 mg, 1.45 mmol, 82%). <sup>1</sup>H NMR (400 MHz, Chloroform-*d*) δ 7.82 (d, *J* = 1.6 Hz, 1H), 7.49 (d, *J* = 1.6 Hz, 1H), 4.43 (p, *J* = 6.7 Hz, 1H), 1.55 (d, *J* = 6.7 Hz, 6H). LCMS (Method B): *t*<sub>R</sub> = 0.125 min, *m/z* = 156.3 [M+H]<sup>+</sup>; Purity (AUC) ≥ 95%.

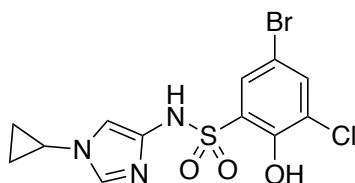
Step B: 1-Isopropyl-1H-imidazol-4-aminium chloride

1-Isopropyl-4-nitro-1H-imidazole (225 mg, 1.45 mmol) was reacted following General Procedure C. The crude was taken forward (295 mg). LCMS (Method B): *t*<sub>R</sub> = 0.086 min, *m/z* = 126.3 [M+H]<sup>+</sup>.

Step C: 5-Bromo-3-chloro-2-hydroxy-N-(1-isopropyl-1H-imidazol-4-yl)benzenesulfonamide

1-Isopropyl-1*H*-imidazol-4-aminium chloride (50 mg, crude) was reacted with 5-bromo-3-chloro-2-hydroxybenzenesulfonyl chloride following General Procedure D. Purification by preparative HPLC afforded the title compound (21 mg, 0.053mmol, 4% yield). <sup>1</sup>H NMR (400 MHz, Chloroform-*d*) δ 9.77 (s, 1H), 8.08 (d, *J* = 1.8 Hz, 1H), 7.73 (d, *J* = 2.4 Hz, 1H), 7.64 (d, *J* = 2.4 Hz, 1H), 7.05 (d, *J* = 1.8 Hz, 1H), 4.46 (p, *J* = 6.7 Hz, 1H), 1.57 (d, *J* = 6.7 Hz, 6H). LCMS (Method B): *t*<sub>R</sub> = 0.809 min, *m/z* = 394.1, 396.2 [M+H]<sup>+</sup>, Purity (AUC) ≥ 95%.

*5-Bromo-3-chloro-N-(1-cyclopropyl-1H-imidazol-4-yl)-2-hydroxybenzenesulfonamide*  
(VU0831899)



Step A: 1-Cyclopropyl-4-nitro-1H-imidazole

1,4-Dinitro-1*H*-imidazole (150 mg, 0.39 mmol) was reacted with cyclopropaneamine (1.04 mmol) according to General Procedure X-B. Purification by flash chromatography afforded the title compound as a yellow solid (105 mg, 0.69 mmol, 72% yield). <sup>1</sup>H NMR (400 MHz, Chloroform-*d*) δ 7.78 (d, *J* = 1.2 Hz, 1H), 7.48 (s, 1H), 3.50 – 3.40 (m, 1H), 1.15 – 1.07 (m, 2H), 1.03 (dt, *J* = 6.0, 4.1 Hz, 2H). LCMS (Method B): *t*<sub>R</sub> = 0.109 min, *m/z* = 154.2 [M+H]<sup>+</sup>.

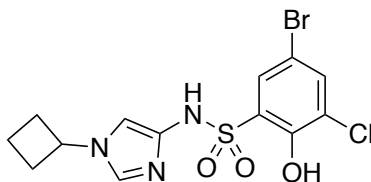
Step B: 1-(Cyclopropyl)-1H-imidazol-4-aminium chloride

1-Cyclopropyl-4-nitro-1*H*-imidazole (50 mg, 0.33 mmol) was reacted following General Procedure C. The crude was taken forward (29 mg). LCMS (Method B): *t*<sub>R</sub> = 0.086 min, *m/z* = 124.2 [M+H]<sup>+</sup>.

Step C: 5-Bromo-3-chloro-N-(1-(cyclopentanecarbonyl)-1H-imidazol-4-yl)-2-hydroxybenzenesulfonamide

1-Cyclopropyl-1*H*-imidazol-4-aminium chloride (29 mg, crude) was reacted with 5-bromo-3-chloro-2-hydroxybenzenesulfonyl chloride following General Procedure D. Purification by preparative HPLC afforded the title compound (13 mg, 0.033 mmol, 10%). <sup>1</sup>H NMR (400 MHz, Chloroform-*d*) δ 7.93 (s, 1H), 7.73 (d, *J* = 2.4 Hz, 1H), 7.65 (d, *J* = 2.4 Hz, 1H), 7.07 (d, *J* = 1.5 Hz, 1H), 3.57 – 3.47 (m, 1H), 1.26 – 1.14 (m, 2H), 1.14 – 1.06 (m, 2H). LCMS (Method B): *t*<sub>R</sub> = 0.808 min, *m/z* = 392.2, 393.4 [M+H]<sup>+</sup>, Purity (AUC) ≥ 95%.

*5-Bromo-3-chloro-N-(1-cyclobutyl-1*H*-imidazol-4-yl)-2-hydroxybenzenesulfonamide*  
(VU0829725)



Step A: 1-Cyclobutyl-4-nitro-1*H*-imidazole

4-Nitroimidazole (100 mg, 0.88 mmol) was reacted with bromocyclobutane following General Procedure X. Purification by flash chromatography afforded the title compound (100 mg, 0.59 mmol, 67%). LCMS (Method B): *t*<sub>R</sub> = 0.097 min, *m/z* = 168.2 [M+H]<sup>+</sup>.

Step B: 1-Cyclobutyl-1*H*-imidazol-4-aminium chloride

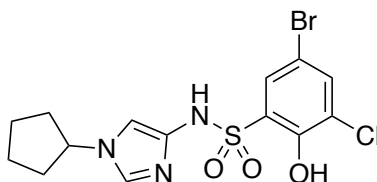
1-Cyclobutyl-4-nitro-1*H*-imidazole (100 mg, 0.59 mmol) was reacted following General Procedure C. The crude was taken forward (50 mg). LCMS (Method B): *t*<sub>R</sub> = 0.090 min, *m/z* = 138.1 [M+H]<sup>+</sup>.

Step C: 5-Bromo-3-chloro-N-(1-cyclobutyl-1*H*-imidazol-4-yl)-2-hydroxybenzenesulfonamide

1-Cyclobutyl-1*H*-imidazol-4-aminium chloride (50 mg, crude) was reacted with 5-bromo-3-chloro-2-hydroxybenzenesulfonyl chloride following General Procedure D. Purification by preparative HPLC afforded the title compound (14 mg, 0.033 mmol, 6%). <sup>1</sup>H NMR (400 MHz,

Chloroform-*d*)  $\delta$  7.62 (s, 1H), 7.54 (s, 1H), 7.39 (s, 1H), 6.81 (s, 1H), 4.56 – 4.47 (m, 1H), 2.50 (s, 2H), 2.37 – 2.28 (m, 2H), 1.89 (dt,  $J = 18.7, 9.5$  Hz, 2H). LCMS (Method B):  $t_R = 1.385$  min,  $m/z = 405.7, 406.8$   $[M+H]^+$ ;  $\geq$  Purity (AUC)  $\geq 95\%$ .

*5-Bromo-3-chloro-N-(1-cyclopentyl-1H-imidazol-4-yl)-2-hydroxybenzenesulfonamide*  
(VU0829217)



Step A: 1-Cyclopentyl-4-nitro-1H-imidazole

4-Nitroimidazole (900 mg, 7.96 mmol) was reacted with bromocyclopentane (10.35 mmol) following General Procedure X. Purification by flash chromatography afforded the title compound as a light-yellow oil (1.277 g, 7.05 mmol, 71%).  $^1H$  NMR (400 MHz, Chloroform-*d*)  $\delta$  7.77 (s, 1H), 7.45 (s, 1H), 4.54 – 4.47 (m, 1H), 2.24 (q,  $J = 8.0$  Hz, 2H), 1.89 – 1.68 (m, 6H). LCMS (Method B):  $t_R = 0.591$  min,  $m/z = 182.3$   $[M+H]^+$ .

Step B: 1-Cyclopentyl-1H-imidazol-4-aminium chloride

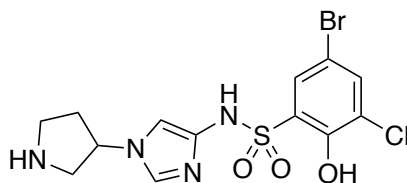
1-Cyclopentyl-4-nitro-1H-imidazole (50 mg, 0.28 mmol) was reacted according to General Procedure C. The crude was taken forward (51 mg). LCMS (Method B):  $t_R = 0.114$  min,  $m/z = 152.3$   $[M+H]^+$ .

Step C: 5-Bromo-3-chloro-N-(1-cyclopentyl-1H-imidazol-4-yl)-2-hydroxybenzenesulfonamide

1-Cyclopentyl-1H-imidazol-4-aminium chloride (51 mg, crude) was reacted with 5-bromo-3-chloro-2-hydroxybenzenesulfonyl chloride following General Procedure D. Purification by preparative HPLC afforded the title compound (13.8 mg, 0.033 mmol, 12%).  $^1H$  NMR (400 MHz,

Chloroform-*d*)  $\delta$  7.61 (d,  $J = 2.4$  Hz, 1H), 7.57 (d,  $J = 2.4$  Hz, 1H), 7.51 (d,  $J = 1.6$  Hz, 1H), 6.75 (d,  $J = 1.6$  Hz, 1H), 4.41 (p,  $J = 6.7$  Hz, 1H), 2.25 – 2.15 (m, 2H), 1.91 – 1.71 (m, 6H). LCMS (Method B):  $t_R = 0.874$  min,  $m/z = 420.1, 422.1$   $[M+H]^+$ ; Purity (AUC)  $\geq 95\%$ .

*5-Bromo-3-chloro-2-hydroxy-N-(1-(pyrrolidin-3-yl)-1H-imidazol-4-yl)benzenesulfonamide*  
(VU0850576)



Step A: tert-Butyl 3-(4-nitro-1H-imidazole-1-yl)pyrrolidine-1-carboxylate

4-Nitroimidazole (150 mg, 1.33 mmol) was reacted with tert-butyl 3-bromopyrrolidine-1-carboxylate following General Procedure X. Purification by flash chromatography afforded the title compound (185 mg, 1.17 mmol, 88%). LCMS (Method B):  $t_R = 0.800$  min,  $m/z = 283.3$   $[M+H]^+$ .

Step B: 1-(Pyrrolidin-3-yl)-1H-imidazol-4-aminium chloride (4j)

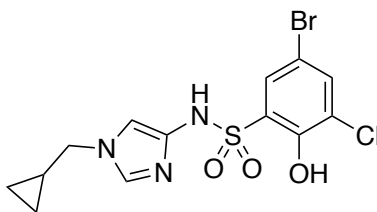
tert-Butyl 3-(4-nitro-1H-imidazole-1-yl)pyrrolidine-1-carboxylate (185 mg, 1.17 mmol) was reacted following General Procedure C. The crude was moved forward (183 mg), the Boc group came off during synthesis. LCMS (Method B):  $t_R = 0.084$  min,  $m/z = 153.3$   $[M+H]^+$ .

Step C: 5-Bromo-3-chloro-2-hydroxy-N-(1-(pyrrolidin-3-yl)-1H-imidazol-4-yl)benzenesulfonamide

1-(Pyrrolidin-3-yl)-1H-imidazol-4-aminium chloride (183 mg, crude) was reacted with 5-bromo-3-chloro-2-hydroxybenzenesulfonyl chloride following General Procedure D. Purification by preparative HPLC afforded the title compound (8 mg, 0.019 mmol, 2%) of title compound.  $^{13}C$

NMR (151 MHz, Chloroform-*d*)  $\delta$  150.23, 148.22, 138.12, 134.96, 129.75, 125.10, 122.99, 117.44, 111.90, 56.85, 53.37, 45.83, 32.24.  $^1\text{H}$  NMR (600 MHz, Chloroform-*d*)  $\delta$  7.81 (d,  $J = 1.6$  Hz, 1H), 7.73 (d,  $J = 2.4$  Hz, 1H), 7.71 (d,  $J = 2.4$  Hz, 1H), 7.58 (d,  $J = 1.6$  Hz, 1H), 4.93 – 4.87 (m, 1H), 3.80 (dd,  $J = 11.1, 6.3$  Hz, 1H), 3.74 – 3.66 (m, 2H), 3.53 – 3.45 (m, 1H), 2.65 – 2.56 (m, 1H), 2.37 – 2.29 (m, 1H), 1.44 (s, 1H). LCMS  $t_{\text{R}} = 0.918$  min,  $m/z = 453.2, 455.2$   $[\text{M} + \text{CH}_3\text{OH} + \text{H}]^+$ ; Purity (AUC)  $\geq 95\%$ .

*5-Bromo-3-chloro-N-(1-(cyclopropylmethyl)-1H-imidazol-4-yl)-2-hydroxybenzenesulfonamide (VU0831928)*



*Step A: 1-(Cyclopropylmethyl)-4-nitro-1H-imidazole*

4-Nitroimidazole (200 mg, 1.77 mmol) was reacted with 1-bromo-1-cyclopropylmethane) following General Procedure X. Purification by preparative flash chromatography afforded the title compound (226 mg, 1.35 mmol, 76%). LCMS (Method B):  $t_{\text{R}} = 0.485$  min,  $m/z = 168.4$   $[\text{M} + \text{H}]^+$ .

*Step B: 1-(Cyclopropylmethyl)-1H-imidazol-4-aminium chloride*

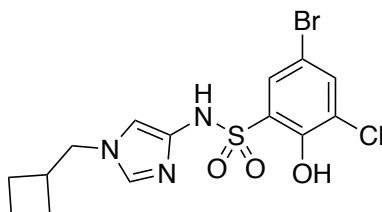
1-Cyclopropylmethyl-4-nitro-1H-imidazole (66 mg, 0.39 mmol) was reacted following General Procedure C. The crude was taken forward (60 mg). LCMS (Method B):  $t_{\text{R}} = 0.089$  min,  $m/z = 138.2$   $[\text{M} + \text{H}]^+$ .

*Step C: 5-Bromo-3-chloro-N-(1-(cyclopropylmethyl)-1H-imidazol-4-yl)-2-hydroxybenzenesulfonamide*



1-(Cyclopropylmethyl)-1*H*-imidazol-4-aminium chloride (60 mg, crude) was reacted with 5-bromo-3-chloro-2-hydroxybenzenesulfonyl chloride following General Procedure D. Purification by preparative HPLC afforded the title compound (8 mg, 0.020 mmol, 5%). <sup>1</sup>H NMR (400 MHz, Chloroform-*d*) δ 8.18 (s, 1H), 7.73 (d, *J* = 2.4 Hz, 1H), 7.65 (d, *J* = 2.4 Hz, 1H), 7.11 (d, *J* = 1.7 Hz, 1H), 3.92 (d, *J* = 7.4 Hz, 2H), 1.30 – 1.19 (m, 1H), 0.87 – 0.81 (m, 2H), 0.46 (q, *J* = 5.4 Hz, 2H). LCMS *t*<sub>R</sub> = 0.758 min, *m/z* = 406.2 [M+H]<sup>+</sup>; Purity (AUC) ≥ 95%.

*5-Bromo-3-chloro-N-(1-(cyclobutylmethyl)-1*H*-imidazol-4-yl)-2-hydroxybenzenesulfonamide (VU0848297)*



*Step A: 1-(Cyclobutylmethyl)-4-nitro-1*H*-imidazole*

4-Nitro-1*H*-imidazole (200 mg, 1.77 mmol) was reacted with (bromomethyl)cyclobutane following General Procedure X. Purification by flash chromatography afforded the title compound (320 mg, 1.77 mmol, quant.). <sup>1</sup>H NMR (400 MHz, Methanol-*d*<sub>4</sub>) δ 8.13 (s, 1H), 7.74 (s, 1H), 4.13 (d, *J* = 7.6 Hz, 2H), 2.79 (p, *J* = 7.7 Hz, 1H), 2.11 – 2.00 (m, 2H), 1.97 – 1.75 (m, 4H). LCMS (Method B) *t*<sub>R</sub> = 0.223 min, *m/z* = 182.3 [M+H]<sup>+</sup>.

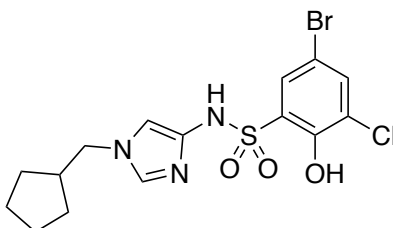
*Step B: 1-(Cyclobutylmethyl)-1*H*-imidazol-4-aminium chloride*

1-(Cyclobutylmethyl)-4-nitro-1*H*-imidazol (320 mg, 1.77 mmol) was reacted following General Procedure C. The crude was taken forward (500 mg). LCMS (Method B): *t*<sub>R</sub> = 0.090 min, *m/z* = 152.3 [M+H]<sup>+</sup>.

Step C: 5-Bromo-3-chloro-N-(1-(cyclobutylmethyl)-1H-imidazol-4-yl)-2-hydroxybenzenesulfonamide

1-(Cyclobutylmethyl)-1H-imidazol-4-aminium chloride (100 mg, crude) with 5-bromo-3-chloro-2-hydroxybenzenesulfonyl chloride following General Procedure D. Purification by preparative HPLC afforded the title compound (26 mg, 0.062 mmol). <sup>1</sup>H NMR (400 MHz, Chloroform-*d*) δ 7.88 (d, *J* = 2.4 Hz, 1H), 7.77 (d, *J* = 2.4 Hz, 1H), 7.32 (d, *J* = 1.7 Hz, 1H), 6.76 (s, 1H), 6.72 (d, *J* = 1.7 Hz, 1H), 3.92 (d, *J* = 7.6 Hz, 2H), 2.70 (p, *J* = 7.6 Hz, 1H), 2.18 – 2.05 (m, 2H), 2.04 – 1.86 (m, 2H), 1.81 – 1.70 (m, 2H). LCMS (Method B): *t*<sub>R</sub> = 1.111 min, *m/z* = 421.2, 422.3 [M+H]<sup>+</sup>; Purity (AUC) ≥ 95%.

*5-Bromo-3-chloro-N-(1-(cyclopentylmethyl)-1H-imidazol-4-yl)-2-hydroxybenzenesulfonamide*  
(VU0848300)



Step A: 1-(Cyclopentylmethyl)-4-nitro-1H-imidazole

4-Nitro-1H-imidazole (200 mg, 1.77 mmol) was reacted with (bromomethyl)cyclopentane following General Procedure X. Purification by flash chromatography afforded the title compound (305 mg, 1.56 mmol, 88%). <sup>1</sup>H NMR (400 MHz, Methanol-*d*<sub>4</sub>) δ 8.18 (d, *J* = 1.5 Hz, 1H), 7.76 (d, *J* = 1.5 Hz, 1H), 4.05 (d, *J* = 7.7 Hz, 2H), 2.37 (p, *J* = 7.7 Hz, 1H), 1.80 – 1.54 (m, 6H), 1.33 – 1.20 (m, 2H). LCMS (Method B): *t*<sub>R</sub> = 0.722 min, *m/z* = 196.3 [M+H]<sup>+</sup>.

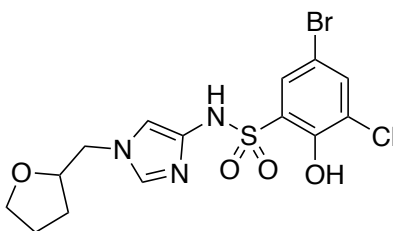
Step B: 1-(Cyclopentylmethyl)-1H-imidazol-4-aminium chloride

1-(Cyclopentylmethyl)-4-nitro-1*H*-imidazole 305 mg (1.56 mmol) was reacted following General Procedure C. The crude was taken forward (204 mg). LCMS (Method B):  $t_R = 0.095$  min,  $m/z = 166.3$  [M+H]<sup>+</sup>.

Step C: 5-Bromo-3-chloro-*N*-(1-(cyclopentylmethyl)-1*H*-imidazol-4-yl)-2-hydroxybenzenesulfonamide

1-(Cyclopentylmethyl)-1*H*-imidazol-4-aminium chloride (102 mg, crude) was reacted with 5-bromo-3-chloro-2-hydroxybenzenesulfonyl chloride following General Procedure D. Purification by preparative HPLC afforded the title compound (18 mg, 0.041 mmol, 13%). <sup>1</sup>H NMR (400 MHz, Chloroform-*d*)  $\delta$  7.92 (d,  $J = 2.4$  Hz, 1H), 7.77 (d,  $J = 2.4$  Hz, 1H), 7.29 (d,  $J = 1.7$  Hz, 1H), 6.74 (d,  $J = 1.7$  Hz, 1H), 3.83 (d,  $J = 7.7$  Hz, 2H), 2.26 (p,  $J = 7.7$  Hz, 1H), 1.83 – 1.71 (m, 2H), 1.71 – 1.55 (m, 4H), 1.26 – 1.13 (m, 2H). LCMS (Method B):  $t_R = 1.151$  min,  $m/z = 435.2, 436.2$  [M+H]<sup>+</sup>; Purity (AUC)  $\geq 95\%$ .

*5-Bromo-3-chloro-2-hydroxy-*N*-(1-((tetrahydrofuran-2-yl)methyl)-1*H*-imidazol-4-yl)benzenesulfonamide (VU0848319)*



Step A: 4-Nitro-1-((tetrahydrofuran-2-yl)methyl)-1*H*-imidazole

4-Nitro-1*H*-imidazole (200 mg, 1.77 mmol) was reacted with 2-(bromomethyl)tetrahydrofuran (2.30 mmol) following General Procedure X. Purification by flash chromatography afforded the title compound as a 3:1 mixture with the regioisomer (280 mg, 0.39 mmol, 22%). LCMS (Method B):  $t_R = 0.098$  min,  $m/z = 198.3$  [M+H]<sup>+</sup>.

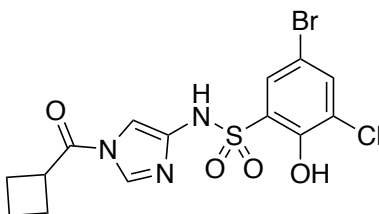
Step B: 1-((Tetrahydrofuran-2-yl)methyl)-1H-imidazol-4-aminium chloride

4-Nitro-1-((tetrahydrofuran-2-yl)methyl)-1H-imidazole (280 mg, 0.39 mmol) was reacted following General Procedure C. The crude was taken forward (205 mg). LCMS (Method B):  $t_R = 0.088$  min,  $m/z = 168.2$   $[M+H]^+$ .

Step C: 5-Bromo-3-chloro-2-hydroxy-N-(1-((tetrahydrofuran-2-yl)methyl)-1H-imidazol-4-yl)benzenesulfonamide

1-((Tetrahydrofuran-2-yl)methyl)-1H-imidazol-4-aminium chloride (100 mg, crude) was reacted with 5-bromo-3-chloro-2-hydroxybenzenesulfonyl chloride following General Procedure D. Purification by preparative HPLC afforded the title compound (13 mg, 0.030 mmol, 8%).  $^1H$  NMR (400 MHz, Methanol- $d_4$ )  $\delta$  7.67 (d,  $J = 2.5$  Hz, 1H), 7.64 (d,  $J = 2.5$  Hz, 1H), 7.53 (d,  $J = 1.6$  Hz, 1H), 6.83 (d,  $J = 1.6$  Hz, 1H), 4.12 – 4.05 (m, 2H), 3.98 – 3.90 (m, 1H), 3.78 – 3.66 (m, 2H), 2.01 – 1.92 (m, 1H), 1.87 – 1.76 (m, 1H), 1.66 – 1.55 (m, 1H), 1.49 – 1.39 (m, 1H). LCMS  $t_R = 0.824$  min,  $m/z = 436.2, 437.3$   $[M+H]^+$ ; Purity (AUC)  $\geq 95\%$ .

*5-Bromo-3-chloro-N-(1-(cyclobutanecarbonyl)-1H-imidazol-4-yl)-2-hydroxybenzenesulfonamide (VU0831889)*



Step A: 1-(Cyclobutanecarbonyl)-4-nitro-1H-imidazole

In a vial, cyclobutanecarbonyl chloride (210 mg, 1.77 mmol, 1 eq) was dissolved in MeCN at 5 M. Then, 4-nitroimidazole (200 mg, 1.77 mmol, 1 eq) and  $Et_3N$  (250  $\mu$ L, 1.77 mmol, 1 eq) were added. It was stirred overnight at 75  $^{\circ}C$ . Next day, it was filtered and washed with EtOAc. The

solvent was dried over a phase separator and the solvent removed under vacuum. The crude was purified using ISCO flash chromatography, 125 mg (0.34 mmol, 19%) of the title compound were obtained. LCMS (Method B):  $t_R = 0.987$  min,  $m/z =$  does not ionize by ESI.

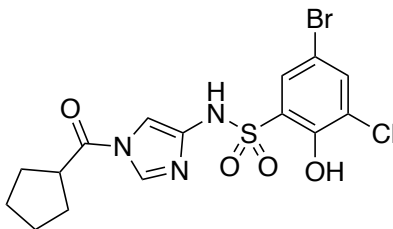
Step B: 1-(1-(Cyclobutanecarbonyl)-1H-imidazol-4-aminium chloride

1-Cyclobutanecarbonyl-4-nitro-1H-imidazole (125 mg, 0.34 mmol) was reacted following General Procedure C. The crude was taken forward (70 mg). LCMS (Method B):  $t_R = 0.347$  min,  $m/z = 166.3$   $[M+H]^+$ .

Step C: 5-Bromo-3-chloro-N-(1-(cyclobutanecarbonyl)-1H-imidazol-4-yl)-2-hydroxybenzenesulfonamide

1-(Cyclobutanecarbonyl)-1H-imidazol-4-aminium chloride (70 mg, crude) was reacted with 5-bromo-3-chloro-2-hydroxybenzenesulfonyl chloride following *General Procedure D*. Purification by preparative HPLC afforded the title compound (3 mg, 0.007 mmol, 2%).  $^1H$  NMR (400 MHz, Chloroform-*d*)  $\delta$  7.94 (d,  $J = 2.4$  Hz, 1H), 7.90 (d,  $J = 1.5$  Hz, 1H), 7.76 (d,  $J = 2.4$  Hz,  $J = 1.5$  Hz, 1H), 7.69 (s, 1H), 7.55 (s, 1H), 3.14 (t,  $J = 8.4$  Hz, 1H), 2.39 – 2.30 (m, 2H), 2.27 – 2.17 (m, 2H), 2.02 (s, 1H), 1.96 – 1.88 (m, 1H). LCMS  $t_R = 1.020$  min,  $m/z = 434.1, 435.2$   $[M+H]^+$ ; Purity (AUC)  $\geq 95\%$ .

*5-Bromo-3-chloro-N-(1-(cyclopentanecarbonyl)-1H-imidazol-4-yl)-2-hydroxybenzenesulfonamide (VU0831900)*



Step A: 1-(Cyclopentanecarbonyl)-4-nitro-1H-imidazole

Cyclopentanecarbonyl chloride (210 mg, 1.77 mmol, 1 eq) was dissolved in MeCN at 5 M. Then, 4-nitroimidazole (200 mg, 1.77 mmol, 1 eq) and Et<sub>3</sub>N (250 μL, 1.77 mmol, 1 eq) were added. It was stirred overnight at 75 °C. Next day, it was filtered and washed with EtOAc. The solvent was dried over a phase separator and the solvent removed under vacuum. The crude was purified using ISCO flash chromatography, 41 mg (0.055 mmol, 3%) of the title compound were obtained. <sup>1</sup>H NMR (400 MHz, Chloroform-*d*) δ 8.26 (d, *J* = 1.7 Hz, 1H), 8.14 (d, *J* = 1.7 Hz, 1H), 3.46 – 3.34 (m, 1H), 2.13 – 1.98 (m, 4H), 1.86 – 1.71 (m, 5H).

Step B: 1-(1-(Cyclopentanecarbonyl)-1H-imidazol-4-aminium chloride

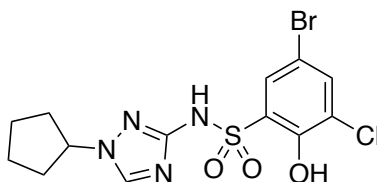
1-Cyclopentanecarbonyl-4-nitro-1H-imidazole (41 mg, 0.55 mmol) following General Procedure C. The crude was taken forward (48 mg). LCMS (Method B): *t*<sub>R</sub> = 0.279 min, *m/z* = 198.4 [M+NH<sub>4</sub>]<sup>+</sup>.

Step C: 5-Bromo-3-chloro-N-(1-(cyclopentanecarbonyl)-1H-imidazol-4-yl)-2-hydroxybenzenesulfonamide

1-(Cyclopentanecarbonyl)-1H-imidazol-4-aminium chloride (48 mg, crude) was reacted with 5-bromo-3-chloro-2-hydroxybenzenesulfonyl chloride following General Procedure D. Purification by preparative HPLC afforded the title compound (4 mg, 0.009 mmol, 33%). <sup>1</sup>H NMR (400 MHz, Chloroform-*d*) δ 8.02 (br s, 1H), 7.95 (t, *J* = 2.4 Hz, 2H), 7.76 (d, *J* = 2.4 Hz, 1H), 7.69 (d, *J* = 1.6 Hz, 1H), 2.74 – 2.68 (m, 1H), 1.93 (d, *J* = 8.2 Hz, 2H), 1.88 – 1.69 (m, 4H), 1.66 – 1.56 (m, 2H). LCMS (Method B): *t*<sub>R</sub> = 1.068 min, *m/z* = 448.1, 449.3 [M+H]<sup>+</sup>; Purity (AUC) ≥ 95%.

## 6.4.2 Heterocyclic analogs

### *5-Bromo-3-chloro-N-(1-cyclopentyl-1H-1,2,4-triazol-3-yl)-2-hydroxybenzenesulfonamide (VU0849230)*



#### Step A: 1-Cyclopentyl-3-nitro-1H-1,2,4-triazole

3-Nitro-1,2,4-triazole (100 mg, 0.88 mmol) was reacted with bromocyclopentane (1.14 mmol) following General Procedure X. Purification by preparative HPLC afforded the title compound (120 mg, 0.66 mmol, 75%). LCMS (Method B):  $t_R = 0.800$  min,  $m/z = 283.3$   $[M+H]^+$ .

#### Step B: 1-Cyclopentyl-1H-1,2,4-triazole-3-aminium chloride

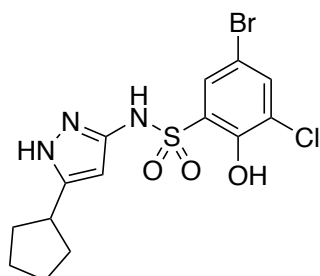
1-Cyclopentyl-3-nitro-1H-1,2,4-triazole (120 mg, 0.66 mmol) was reacted following General Procedure C. The crude was taken forward (124 mg). LCMS (Method B):  $t_R = 0.089$  min,  $m/z = 153.3$   $[M+H]^+$ .

#### Step C: 5-Bromo-3-chloro-N-(1-cyclopentyl-1H-1,2,4-triazol-3-yl)-2-hydroxybenzenesulfonamide

1-Cyclopentyl-1H-1,2,4-triazole-3-aminium chloride (50 mg, 0.27 mmol) was reacted with 5-bromo-3-chloro-2-hydroxybenzenesulfonyl chloride following General Procedure D. Purification by preparative HPLC afforded the title compound (33 mg, 0.030 mmol, 20%) of title compound.  $^1H$  NMR (400 MHz, Chloroform-*d*)  $\delta$  7.95 (s, 1H), 7.87 (d,  $J = 2.4$  Hz, 1H), 7.68 (d,  $J = 2.4$  Hz, 1H), 4.60 (t,  $J = 6.2$  Hz, 1H), 2.19 – 2.12 (m, 2H), 2.00 – 1.85 (m, 4H), 1.77 – 1.69 (m, 2H). LCMS (Method B):  $t_R = 1.038$  min,  $m/z = 421.2, 423.1$   $[M+H]^+$ ; Purity (AUC)  $\geq 95\%$ .

*5-Bromo-3-chloro-N-(5-cyclopentyl-1H-pyrazol-3-yl)-2-hydroxybenzenesulfonamide*

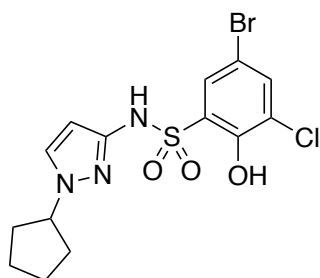
**(VU0849779)**



5-Cyclopentyl-1H-pyrazol-3-amine (50 mg, 0.33 mmol) was reacted with bromo-3-chloro-2-hydroxybenzenesulfonyl chloride following General Procedure D. Purification by preparative HPLC afforded the title compound (25 mg, 0.059 mmol, 18%) of title compound. <sup>13</sup>C NMR (101 MHz, Chloroform-*d*) δ 164.24, 151.42, 149.78, 139.14, 129.16, 127.28, 127.03, 110.52, 88.89, 39.16, 32.23, 25.38. <sup>1</sup>H NMR (400 MHz, Chloroform-*d*) δ 7.84 (d, *J* = 2.4 Hz, 1H), 7.73 (d, *J* = 2.4 Hz, 1H), 5.32 (s, 1H), 2.95 (p, *J* = 8.0 Hz, 1H), 2.05 – 1.94 (m, 2H), 1.77 – 1.57 (m, 6H). LCMS (Method B): *t*<sub>R</sub> = 1.232 min, *m/z* = 420.2, 422.2 [M+H]<sup>+</sup>; Purity (AUC) ≥ 95%.

*5-Bromo-3-chloro-N-(1-cyclopentyl-1H-pyrazol-3-yl)-2-hydroxybenzenesulfonamide*

**(VU0849819)**

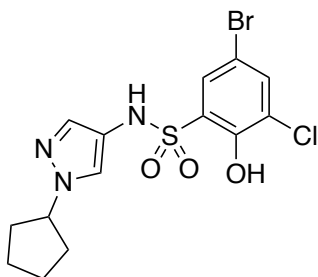


1-Cyclopentyl-1H-pyrazol-3-amine (30 mg, 0.20 mmol) was reacted with bromo-3-chloro-2-hydroxybenzenesulfonyl chloride following General Procedure D. Purification by preparative HPLC afforded the title compound (71 mg, 0.17 mmol, 84%) of title compound. <sup>13</sup>C NMR (101



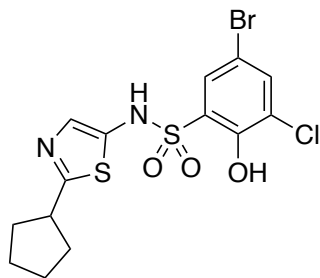
MHz, Chloroform-*d*)  $\delta$  150.50, 143.65, 137.57, 129.94, 129.36, 125.81, 124.57, 111.23, 99.09, 63.42, 32.93, 24.05.  $^1\text{H}$  NMR (400 MHz, Chloroform-*d*)  $\delta$  7.61 (d,  $J = 2.4$  Hz, 1H), 7.57 (d,  $J = 2.4$  Hz, 1H), 7.32 (d,  $J = 2.4$  Hz, 1H), 6.15 (d,  $J = 2.4$  Hz, 1H), 4.63 – 4.52 (m, 1H), 2.16 – 2.04 (m, 2H), 1.90 – 1.61 (m, 6H). LCMS (Method B):  $t_R = 1.118$  min,  $m/z = 420.1, 422.2$   $[\text{M}+\text{H}]^+$ ; Purity (AUC)  $\geq 95\%$ .

*5-Bromo-3-chloro-N-(1-cyclopentyl-1H-pyrazol-4-yl)-2-hydroxybenzenesulfonamide*  
(VU0849822)



1-Cyclopentyl-1H-pyrazol-4-aminium chloride (30 mg, 0.15 mmol) was reacted with bromo-3-chloro-2-hydroxybenzenesulfonyl chloride following General Procedure D. Purification by preparative HPLC afforded the title compound (38 mg, 0.090 mmol, 59%) of title compound.  $^1\text{H}$  NMR (400 MHz, Chloroform-*d*)  $\delta$  7.68 (d,  $J = 2.3$  Hz, 1H), 7.60 (d,  $J = 2.3$  Hz, 1H), 7.37 (d,  $J = 0.8$  Hz, 1H), 7.22 (d,  $J = 0.8$  Hz, 1H), 6.45 (s, 1H), 4.65 – 4.54 (m, 1H), 2.19 – 2.08 (m, 2H), 1.97 – 1.86 (m, 2H), 1.86 – 1.65 (m, 4H). LCMS (Method B):  $t_R = 1.056$  min,  $m/z = 420.2, 422.2$   $[\text{M}+\text{H}]^+$ ; Purity (AUC)  $\geq 95\%$ .

*5-Bromo-3-chloro-N-(2-cyclopentylthiazol-5-yl)-2-hydroxybenzenesulfonamide (VU0849922)*



*Step A: tert-Butyl (2-(cyclopent-1-en-1-yl)thiazol-5-yl)carbamate*

*tert*-Butyl (2-bromothiazol-5-yl)carbamate (200 mg, 0.716 mmol) was reacted with cyclopent-1-en-ylboronic acid (0.860 mmol) following General Procedure J-B. Purification by flash chromatography afforded the title compound (157 mg, 0.589 mmol, 82%). <sup>1</sup>H NMR (400 MHz, Chloroform-*d*) δ 7.46 (br s, 1H), 7.25 (s, 1H), 6.33 (t, *J* = 2.3 Hz, 1H), 2.83 – 2.73 (m, 2H), 2.58 – 2.48 (m, 2H), 2.00 (p, *J* = 7.5 Hz, 2H). LCMS (Method B): *t*<sub>R</sub> = 0.956 min, *m/z* = 267.3 [M+ H]<sup>+</sup>.

*Step B: 2-(Cyclopent-1-en-1-yl)thiazol-5-aminium chloride*

*tert*-Butyl (2-(cyclopent-1-en-1-yl)thiazol-5-yl)carbamate (30 mg, 0.11 mmol) was reacted following General Procedure S. The crude was taken forward (75 mg). <sup>1</sup>H NMR (400 MHz, Methanol-*d*<sub>4</sub>) δ 6.78 (s, 1H), 3.76 – 3.55 (m, 1H), 2.78 (d, *J* = 6.5 Hz, 2H), 2.69 – 2.61 (m, 2H), 2.11 (p, *J* = 7.6 Hz, 2H).

*Step C: 2-Cyclopentylthiazol-5-aminium chloride*

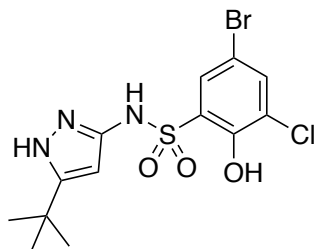
2-(Cyclopent-1-en-1-yl)thiazol-5-aminium chloride (75 mg, crude) was reacted following General Procedure C. The crude was taken forward (50 mg). LCMS (Method B): *t*<sub>R</sub> = 0.214 min, *m/z* = 169.3 [M+H]<sup>+</sup>.

*Step D: 5-Bromo-3-chloro-N-(2-cyclopentylthiazol-5-yl)-2-hydroxybenzenesulfonamide*

2-Cyclopentylthiazol-5-aminium chloride (50 mg, crude) was reacted with 5-bromo-3-chloro-2-hydroxybenzenesulfonyl chloride following General Procedure D. Purification by preparative

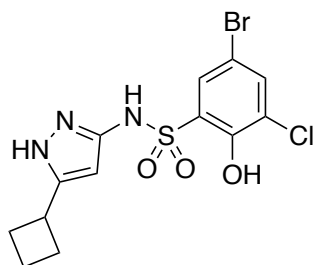
HPLC afforded the title compound (3 mg, 0.007 mmol, 1%) of title compound.  $^{13}\text{C}$  NMR (101 MHz, Chloroform-*d*)  $\delta$  176.86, 149.80, 138.00, 137.78, 130.72, 130.46, 124.92, 124.44, 112.06, 44.51, 34.17, 25.50.  $^1\text{H}$  NMR (400 MHz, Chloroform-*d*)  $\delta$  7.71 (d,  $J = 2.4$  Hz, 1H), 7.68 (d,  $J = 2.4$  Hz, 1H), 7.33 (s, 1H), 3.41 – 3.29 (m, 1H), 2.20 – 2.12 (m, 2H), 1.83 – 1.76 (m, 2H), 1.76 – 1.71 (m, 2H), 1.71 – 1.65 (m, 2H). LCMS (Method B):  $t_{\text{R}} = 1.088$  min,  $m/z = 437.1, 439.2$   $[\text{M}+\text{H}]^+$ ; Purity (AUC)  $\geq 95\%$ .

*5-Bromo-N-(5-(tert-butyl)-1H-pyrazol-3-yl)-3-chloro-2-hydroxybenzenesulfonamide*  
(VU0830054)



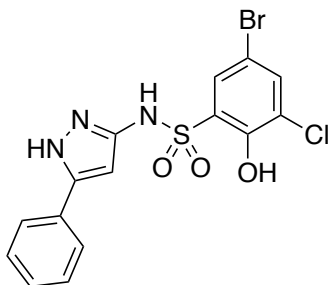
5-*tert*-Butyl-3-aminopyrazole (20 mg, 0.14 mmol) was reacted with 5-bromo-3-chloro-2-hydroxybenzenesulfonyl chloride following General Procedure D. Purification by preparative HPLC afforded the title compound (25 mg, 0.061 mmol, 44%).  $^1\text{H}$  NMR (400 MHz, Chloroform-*d*)  $\delta$  7.66 (d,  $J = 2.4$  Hz, 1H), 7.62 (d,  $J = 2.4$  Hz, 1H), 6.55 (br s, 1H), 6.10 (s, 1H), 1.32 (s, 9H). LCMS (Method B)  $t_{\text{R}} = 1.070$  min,  $m/z = 408.2, 410.2$   $[\text{M}+\text{H}]^+$ , Purity (AUC)  $\geq 95\%$ .

*5-Bromo-3-chloro-2-hydroxy-N-(5-cyclobutyl-1H-pyrazol-3-yl)benzenesulfonamide*  
(VU0830049)



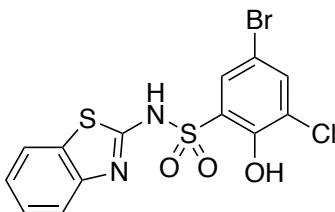
5-Cyclobutyl-3-aminopyrazole (20 mg, 0.15 mmol) was reacted with 5-bromo-3-chloro-2-hydroxybenzenesulfonyl chloride following General Procedure D. Purification by preparative HPLC afforded the title compound (11 mg, 0.027 mmol, 18%). <sup>1</sup>H NMR (400 MHz, Chloroform-*d*) δ 7.67 (d, *J* = 2.3 Hz, 1H), 7.62 (d, *J* = 2.3 Hz, 1H), 6.08 (s, 1H), 3.48 (p, *J* = 8.7, 8.1 Hz, 1H), 2.44 – 2.32 (m, 2H), 2.16 – 1.91 (m, 4H). LCMS (Method B) *t*<sub>R</sub> = 1.044 min, *m/z* = 406.1, 408.2 [M+ H]<sup>+</sup>, Purity (AUC) ≥ 95%.

*5-Bromo-3-chloro-2-hydroxy-N-(5-phenyl-1H-pyrazol-3-yl)benzenesulfonamide (VU0830052)*



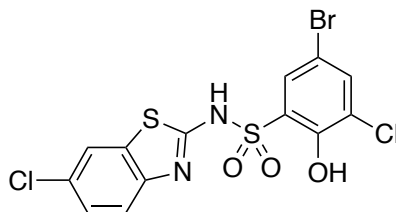
5-Phenyl-3-aminopyrazole (20 mg, 0.15 mmol) was reacted with 5-bromo-3-chloro-2-hydroxybenzenesulfonyl chloride following General Procedure D. Purification by preparative HPLC afforded the title compound (13 mg, 0.030 mmol, 20%). <sup>1</sup>H NMR (400 MHz, DMSO-*d*<sub>6</sub>) δ 7.91 (d, *J* = 2.5 Hz, 1H), 7.78 (d, *J* = 2.5 Hz, 1H), 7.71 – 7.64 (m, 2H), 7.43 (dd, *J* = 8.3, 6.9 Hz, 2H), 7.39 – 7.30 (m, 1H), 6.37 (s, 1H). LCMS (Method B) *t*<sub>R</sub> = 1.055 min, *m/z* = 428.1, 429.2 [M+ H]<sup>+</sup>, Purity (AUC) ≥ 95%.

*N-(Benzo[d]thiazol-2-yl)-5-bromo-3-chloro-2-hydroxybenzenesulfonamide (VU0849477)*



Benzothiazol-2-amine (50 mg, 0.33 mmol) was reacted with bromo-3-chloro-2-hydroxybenzenesulfonyl chloride following General Procedure D. Purification by preparative HPLC afforded the title compound (9.0 mg, 0.021 mmol, 6%). <sup>1</sup>H NMR (400 MHz, Chloroform-*d*) δ 7.82 (d, *J* = 2.4 Hz, 1H), 7.64 (d, *J* = 2.4 Hz, 1H), 7.61 (d, *J* = 7.9 Hz, 1H), 7.49 – 7.42 (m, 2H), 7.37 – 7.31 (m, 1H). LCMS *t*<sub>R</sub> = 1.099 min, *m/z* = 419.1, 422.2 [M+ H]<sup>+</sup>; Purity (AUC) ≥ 95%.

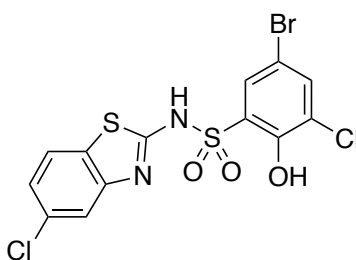
*5-Bromo-3-chloro-N-(6-chlorobenzo[d]thiazol-2-yl)-2-hydroxybenzenesulfonamide*  
(VU0849651)



6-Chlorobenzo[d]thiazol-2-amine (20 mg, 0.11 mmol) was reacted with 5-bromo-3-chloro-2-hydroxybenzenesulfonyl chloride following General Procedure D. Purification by preparative HPLC afforded the title compound (4 mg, 0.0088 mmol, 8%). <sup>1</sup>H NMR (400 MHz, Chloroform-*d*) δ 7.80 (d, *J* = 2.3 Hz, 1H), 7.65 (d, *J* = 2.3 Hz, 1H), 7.59 (d, *J* = 2.3 Hz, 1H), 7.51 (d, *J* = 2.3 Hz, 1H), 7.00 (s, 1H). LCMS (Method B) *t*<sub>R</sub> = 1.161 min, *m/z* = 453.0, 455.0 [M+H]<sup>+</sup>, Purity (AUC) ≥ 95%.

*5-Bromo-3-chloro-N-(5-chlorobenzo[d]thiazol-2-yl)-2-hydroxybenzenesulfonamide*

*(VU0849648)*

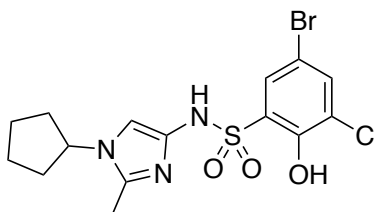


5-Chlorobenzo[d]thiazol-2-amine (20 mg, 0.11 mmol) was reacted with 5-bromo-3-chloro-2-hydroxybenzenesulfonyl chloride following General Procedure D. Purification by preparative HPLC afforded the title compound (18 mg, 0.040 mmol, 36%). <sup>1</sup>H NMR (400 MHz, Chloroform-*d*) δ 7.77 (d, *J* = 2.4 Hz, 1H), 7.71 (d, *J* = 2.4 Hz, 1H), 7.61 (d, *J* = 8.6 Hz, 1H), 7.30 (d, *J* = 2.4 Hz, 1H), 7.11 (dd, *J* = 8.6, 2.4 Hz, 1H). LCMS (Method B): *t*<sub>R</sub> = 1.149 min, *m/z* = 475.0, 477.0 [M+Na]<sup>+</sup>; Purity (AUC) ≥ 95%.

6.4.3 C-2 substituted imidazolyl analogs

*5-Bromo-3-chloro-N-(1-cyclopentyl-2-methyl-1H-imidazol-4-yl)-2-hydroxybenzenesulfonamide*

*(VU0848182)*



Step A: 1-Cyclopentyl-2-methyl-4-nitro-1H-imidazole

2-Methyl-4-nitro-1H-imidazole (800 mg, 6.29 mmol) was reacted with bromocyclopentane (8.18 mmol) following General Procedure X. Purification by flash chromatography afforded the title compound (675 mg, 3.46 mmol, 55%). <sup>1</sup>H NMR (400 MHz, Chloroform-*d*) δ 7.72 (s, 1H), 4.46

(p,  $J = 7.1$  Hz, 1H), 2.46 (s, 3H), 2.30 – 2.18 (m, 2H), 1.99 – 1.86 (m, 2H), 1.85 – 1.73 (m, 4H).

LCMS (Method B):  $t_R = 0.695$  min,  $m/z = 196.3$  [M+H]<sup>+</sup>.

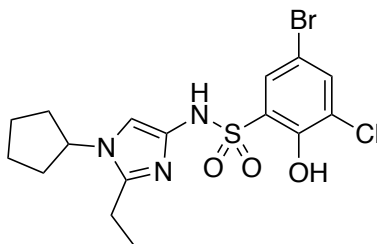
Step B: 1-Cyclopentyl-2-methyl-1H-imidazol-4-aminium chloride

Cyclopentyl-2-methyl-4-nitro-1H-imidazole (21.0 mg, 0.057 mmol) was reacted following General Procedure C. The crude was taken forward (30 mg). LCMS (Method B):  $t_R = 0.280$  min,  $m/z = 166.4$  [M+H]<sup>+</sup>.

Step C: 5-Bromo-3-chloro-N-(1-Cyclopentyl-2-methyl-1H-imidazol-4-yl)-2-hydroxybenzenesulfonamide

1-Cyclopentyl-2-methyl-1H-imidazol-4-aminium chloride (30 mg, crude) was reacted with 5-bromo-3-chloro-2-hydroxybenzenesulfonyl chloride following General Procedure D. Purification by preparative HPLC afforded the title compound (6 mg, 0.014 mmol, 24%). <sup>1</sup>H NMR (400 MHz, Chloroform-*d*)  $\delta$  7.72 (d,  $J = 2.4$  Hz, 1H), 7.65 (d,  $J = 2.4$  Hz, 1H), 6.93 (s, 1H), 4.47 (p,  $J = 7.2$  Hz, 1H), 2.55 (s, 3H), 2.27 – 2.20 (m, 6H), 1.99 – 1.89 (m, 6H), 1.87 – 1.78 (m, 7H). LCMS (Method B):  $t_R = 0.843$  min,  $m/z = 434.2, 435.2$  [M+H]<sup>+</sup>; Purity (AUC)  $\geq 95\%$ .

*5-Bromo-3-chloro-N-(1-cyclopentyl-2-ethyl-1H-imidazol-4-yl)-2-hydroxybenzenesulfonamide (VU0848212)*



Step A: 2-Bromo-1-cyclopentyl-4-nitro-1H-imidazole

2-Bromo-4-nitro-1H-imidazole (700 mg, 3.65 mmol) was reacted with bromocyclopentane (4.74 mmol) following General Procedure X. Purification by flash chromatography afforded the title

compound (691 mg, 2.65 mmol, 72%). <sup>1</sup>H NMR (400 MHz, Methanol-*d*<sub>4</sub>) δ 8.30 (s, 1H), 4.79 – 4.67 (m, 1H), 2.34 – 2.21 (m, 2H), 1.97 – 1.85 (m, 4H), 1.85 – 1.77 (m, 1H), 1.77 – 1.73 (m, 1H). LCMS (Method B): t<sub>R</sub> = 0.837 min, m/z = 260.1, 262.1 [M+H]<sup>+</sup>.

Step B: 1-Cyclopentyl-4-nitro-2-vinyl-1H-imidazole

In a vial, 100 mg (0.38 mmol, 1 eq) of 2-bromo-1-cyclopentyl-4-nitro-1H-imidazole was added with 3.1 mL of 1,4-dioxane and 0.700 mL of H<sub>2</sub>O. The solution was degassed with Ar for 10 min. Then, 44 mg (0.04 mmol, 0.10 eq) of Pd(PPh<sub>3</sub>)<sub>4</sub>, 65 mg (0.42 mmol, 1.1 eq) of vinyl boronic pinacol ester, and 376 mg (1.15 mmol, 3 eq) of Cs<sub>2</sub>CO<sub>3</sub> were added. It was stirred at 135 °C for 36 hours. Water was added and extracted with DCM. The organic phase was dried over a phase separator and the solvent was removed under vacuum. The crude was purified using ISCO flash chromatograph, 60 mg (0.20 mmol, 53%) of the title compound were obtained. <sup>1</sup>H NMR (400 MHz, Chloroform-*d*) δ 7.74 (s, 1H), 6.59 (dd, *J* = 17.1, 11.1 Hz, 1H), 6.36 (dd, *J* = 17.1, 1.4 Hz, 1H), 5.58 (dd, *J* = 11.0, 1.4 Hz, 1H), 4.65 – 4.54 (m, 1H), 2.24 – 2.17 (m, 2H), 1.89 – 1.73 (m, 6H). LCMS (Method B): t<sub>R</sub> = 0.748 min, m/z = 208.3 [M+H]<sup>+</sup>.

Step C: 1-Cyclopentyl-2-ethyl-1H-imidazol-4-aminium chloride

1-Cyclopentyl-4-nitro-2-vinyl-1H-imidazole (50 mg, 0.21 mmol) was reacted following General Procedure C. The crude was taken forward (52 mg). LCMS (Method B): t<sub>R</sub> = 0.092 min, m/z = 180.3 [M+H]<sup>+</sup>.

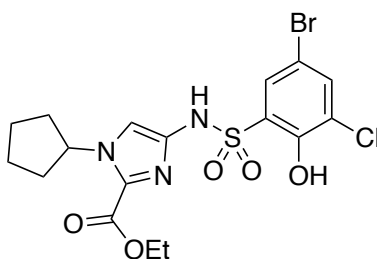
Step D: 5-Bromo-3-chloro-N-(1-cyclopentyl-2-ethyl-1H-imidazol-4-yl)-2-hydroxybenzenesulfonamide

1-Cyclopentyl-2-methyl-1H-imidazol-4-aminium chloride (52 mg, crude) was reacted with 5-bromo-3-chloro-2-hydroxybenzenesulfonyl chloride following General Procedure D. Purification by preparative HPLC afforded the title compound (23 mg, 0.096 mmol, 48%). <sup>1</sup>H NMR (400



MHz, Chloroform-*d*)  $\delta$  7.68 (d,  $J = 2.3$  Hz, 1H), 7.54 (d,  $J = 2.3$  Hz, 1H), 6.42 (s, 1H), 4.43 (p,  $J = 7.2$  Hz, 1H), 2.96 (q,  $J = 7.3$  Hz, 2H), 2.21 – 2.10 (m, 2H), 1.91 (s, 2H), 1.84 – 1.70 (m, 4H), 1.30 (t,  $J = 7.3$  Hz, 3H). LCMS (Method B):  $t_R = 0.901$  min,  $m/z = 448.2, 450.2$   $[M+H]^+$ ; Purity (AUC)  $\geq 95\%$ .

*Ethyl 4-((5-bromo-3-chloro-2-hydroxyphenyl)sulfonamido)-1-cyclopentyl-1H-imidazole-2-carboxylate (VU0850262)*



Step A: Ethyl 1-cyclopentyl-4-nitro-1H-imidazole-2-carboxylate

Ethyl 4-nitro-1H-imidazole-2-carboxylate (300 mg, 1.62 mmol) was reacted with bromocyclopentane following General Procedure X. Purification by flash chromatography afforded the title compound (252 mg, 0.995 mmol, 61%).  $^1H$  NMR (400 MHz, Chloroform-*d*)  $\delta$  7.93 (s, 1H), 5.49 (p,  $J = 7.1$  Hz, 2H), 4.41 – 4.30 (m, 2H), 2.32 – 2.18 (m, 2H), 1.86 – 1.69 (m, 6H), 1.38 – 1.29 (m, 3H). LCMS (Method B):  $t_R = 0.873$  min,  $m/z = 254.2$   $[M+H]^+$ .

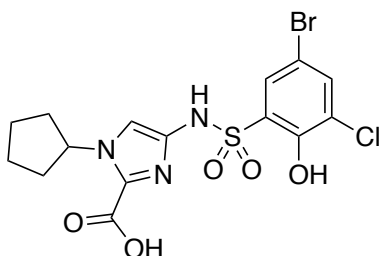
Step B: Ethyl 1-cyclopentyl-1H-imidazole-4-aminium chloride-2-carboxylate

Ethyl 1-cyclopentyl-4-nitro-1H-imidazole-2-carboxylate (150 mg, 0.592 mmol) was reacted following General Procedure C. The crude was taken forward (159 mg). LCMS (Method B):  $t_R = 0.625$  min,  $m/z = 224.3$   $[M+H]^+$ .

Step C: Ethyl 4-((5-bromo-3-chloro-2-hydroxyphenyl)sulfonamido)-1-cyclopentyl-1H-imidazole-2-carboxylate

Ethyl 1-cyclopentyl-1H-imidazole-4-aminium chloride-2-carboxylate (159 mg, crude) was reacted with 5-bromo-3-chloro-2-hydroxybenzenesulfonyl following General Procedure D. Purification by preparative HPLC afforded the title compound (76.5 mg, 0.155 mmol, 25%) of title compound. <sup>13</sup>C NMR (101 MHz, Chloroform-*d*) δ 158.06, 150.81, 137.30, 134.62, 132.77, 130.20, 127.61, 124.45, 112.35, 110.73, 62.02, 59.29, 33.97, 24.15, 13.85. <sup>1</sup>H NMR (400 MHz, Chloroform-*d*) δ 7.70 (d, *J* = 2.4 Hz, 1H), 7.56 (d, *J* = 2.4 Hz, 1H), 7.14 (s, 1H), 5.61 – 5.51 (m, 1H), 4.23 (q, *J* = 7.1 Hz, 2H), 2.30 – 2.19 (m, 2H), 1.90 – 1.71 (m, 6H), 1.15 (t, *J* = 7.1 Hz, 3H). LCMS (Method B): t<sub>R</sub> = 1.128 min, m/z = 492.2, 493.3 [M+H]<sup>+</sup>; Purity (AUC) ≥ 95%.

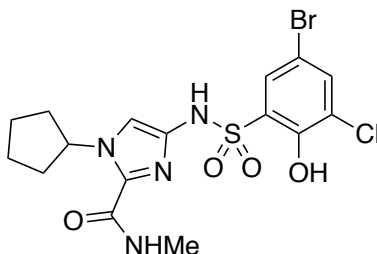
*4-((5-Bromo-3-chloro-2-hydroxyphenyl)sulfonamido)-1-cyclopentyl-1H-imidazole-2-carboxylic acid (VU0850263)*



Ethyl 4-((5-bromo-3-chloro-2-hydroxyphenyl)sulfonamido)-1-cyclopentyl-1H-imidazole-2-carboxylate (27 mg, 0.047 mmol) was reacted following General Procedure E. Purification by preparative HPLC afforded the title compound (6 mg, 0.013 mmol, 27%). <sup>13</sup>C NMR (101 MHz, Chloroform-*d*) δ 158.06, 150.81, 137.30, 134.62, 132.77, 130.20, 127.61, 124.45, 112.35, 110.73, 62.02, 59.29, 33.97, 24.15, 13.85. <sup>1</sup>H NMR (400 MHz, Methanol-*d*<sub>4</sub>) δ 7.76 (d, *J* = 2.4 Hz, 1H), 7.74 (d, *J* = 2.4 Hz, 1H), 7.14 (s, 1H), 5.59 (p, *J* = 6.7 Hz, 1H), 2.25 – 2.15 (m, 2H), 1.87 – 1.80

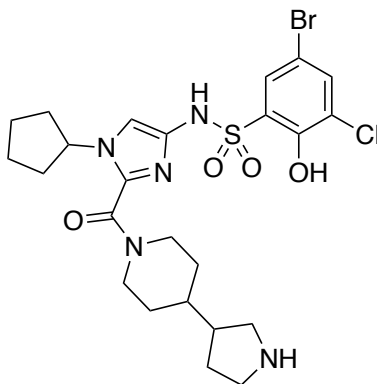
(m, 2H), 1.80 – 1.69 (m, 4H). LCMS (Method B):  $t_R = 1.552$  min,  $m/z = 463.8, 464.8$   $[M+H]^+$ ; Purity (AUC)  $\geq 95\%$ .

*4-((5-Bromo-3-chloro-2-hydroxyphenyl)sulfonamido)-1-cyclopentyl-1H-imidazole-2-carboxylic acid (VU0850264)*



4-((5-Bromo-3-chloro-2-hydroxyphenyl)sulfonamido)-1-cyclopentyl-1H-imidazole-2-carboxylic acid (20 mg, (0.047 mmol) was reacted with methylamine following General Procedure F. Purification by preparative HPLC afforded the title compound (11 mg, 0.023 mmol, 49%).  $^{13}\text{C}$  NMR (151 MHz, Methanol- $d_4$ )  $\delta$  161.27, 152.28, 137.88, 137.21, 135.76, 131.93, 129.35, 125.49, 112.65, 111.04, 59.69, 34.69, 25.97, 24.98.  $^1\text{H}$  NMR (600 MHz, Methanol- $d_4$ )  $\delta$  7.74 (d,  $J = 2.4$  Hz, 1H), 7.71 (d,  $J = 2.4$  Hz, 1H), 6.99 (s, 1H), 5.65 (p,  $J = 7.3$  Hz, 1H), 2.83 (s, 3H), 2.18 – 2.11 (m, 2H), 1.85 – 1.76 (m, 2H), 1.76 – 1.65 (m, 4H). LCMS (Method B):  $t_R = 1.027$  min,  $m/z = 477.2, 478.3$   $[M+H]^+$ , Purity (AUC)  $\geq 95\%$ .

*5-Bromo-3-chloro-N-(1-cyclopentyl-2-(4-(pyrrolidin-3-yl)piperidine-1-carbonyl)-1H-imidazol-4-yl)-2-hydroxybenzenesulfonamide (VU0857304)*



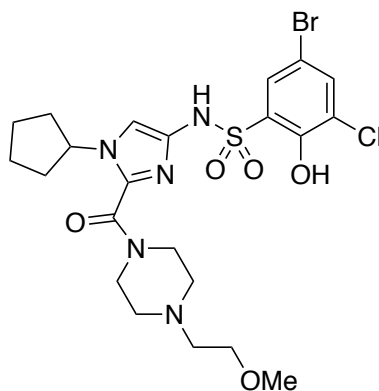
*Step A: tert-Butyl 3-(1-(4-((5-bromo-3-chloro-2-hydroxyphenyl)sulfonamido)-1-cyclopentyl-1H-imidazole-2-carbonyl)piperidin-4-yl)pyrrolidine-1-carboxylate*

4-((5-Bromo-3-chloro-2-hydroxyphenyl)sulfonamido)-1-cyclopentyl-1H-imidazole-2-carboxylic (33 mg, 0.071 mmol, 1 eq) was reacted with *tert*-butyl 3-(piperazin-1-yl)pyrrolidine-1-carboxylate following General Procedure H. The crude material was taken forward (97 mg). LCMS (Method B)  $t_R = 0.975$  min,  $m/z = 701.5, 702.5$  min  $[M+H]^+$ .

*Step B: 5-Bromo-3-chloro-N-(1-cyclopentyl-2-(4-(pyrrolidin-3-yl)piperidine-1-carbonyl)-1H-imidazol-4-yl)-2-hydroxybenzenesulfonamide*

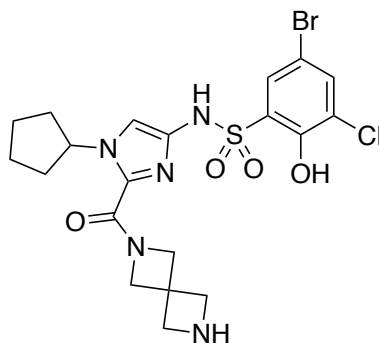
Crude *tert*-butyl 3-(1-(4-((5-bromo-3-chloro-2-hydroxyphenyl)sulfonamido)-1-cyclopentyl-1H-imidazole-2-carbonyl)piperidin-4-yl)pyrrolidine-1-carboxylate (50 mg) was reacted following General Procedure S. Purification by preparative HPLC afforded the title compound (7.0 mg, 0.87 mmol, 15%).  $^1H$  NMR (400 MHz, DMSO- $d_6$ )  $\delta$  8.88 (br s, 1H), 7.40 (d,  $J = 2.7$  Hz, 1H), 7.21 (d,  $J = 2.7$  Hz, 1H), 6.98 (s, 1H), 4.78 (p,  $J = 7.3$  Hz, 1H), 3.54 (br s, 2H), 3.43 (br s, 2H), 3.37 – 3.24 (m, 3H), 3.20 – 3.09 (m, 1H), 3.05 – 2.88 (m, 2H), 2.46 – 2.20 (m, 4H), 2.12 – 1.97 (m, 3H), 1.86 – 1.52 (m, 7H). LCMS (Method B)  $t_R = 0.765$  min,  $m/z = 601.3, 602.4$   $[M+H]^+$ ; Purity (AUC)  $\geq 95\%$ .

*5-Bromo-3-chloro-N-(1-cyclopentyl-2-(4-(2-methoxyethyl)piperazine-1-carbonyl)-1H-imidazol-4-yl)-2-hydroxybenzenesulfonamide (VU0857305)*



4-((5-Bromo-3-chloro-2-hydroxyphenyl)sulfonamido)-1-cyclopentyl-1H-imidazole-2-carboxylic acid (40 mg, 0.086 mmol, 1 eq) was reacted with 1-(2-methoxyethyl)piperazine following General Procedure H. Purification by preparative HPLC afforded the title compound (16 mg, 0.086 mmol, 31%). <sup>1</sup>H NMR (400 MHz, Methanol-*d*<sub>4</sub>) δ 7.80 (d, *J* = 2.4 Hz, 1H), 7.74 (d, *J* = 2.4 Hz, 1H), 7.14 (s, 1H), 4.98 (p, *J* = 7.3 Hz, 1H), 3.76 (t, *J* = 4.9 Hz, 2H), 3.44 (s, 3H), 3.47-3.20 (br s, 10H), 2.24 – 2.15 (m, 2H), 1.91 – 1.80 (m, 2H), 1.73 (s, 4H). LCMS (Method B) *t*<sub>R</sub> = 0.879 min, *m/z* = 590.3, 592.3 [M+H]<sup>+</sup>; Purity (AUC) ≥ 95%.

*5-Bromo-3-chloro-N-(1-cyclopentyl-2-(2,6-diazaspiro[3.3]heptane-2-carbonyl)-1H-imidazol-4-yl)-2-hydroxybenzenesulfonamide (VU0857306)*



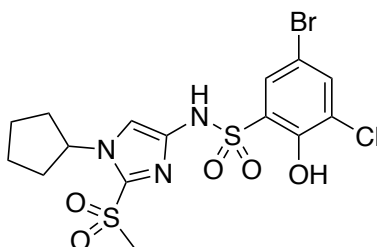
Step A: tert-Butyl 6-(4-((5-bromo-3-chloro-2-hydroxyphenyl)sulfonamido)-1-cyclopentyl-1H-imidazole-2-carbonyl)-2,6-diazaspiro[3.3]heptane-2-carboxylate

4-((5-Bromo-3-chloro-2-hydroxyphenyl)sulfonamido)-1-cyclopentyl-1H-imidazole-2-carboxylic acid (40 mg, 0.086 mmol) was reacted with *tert*-butyl 2,6-diazaspiro[3.3]heptane-2-carboxylate following General Procedure H. The crude material was taken forward (98 mg). LCMS (Method B)  $t_R = 1.130$  min,  $m/z = 544.3, 546.3 [M+H]^+$ .

Step B: 5-Bromo-3-chloro-N-(1-cyclopentyl-2-(2,6-diazaspiro[3.3]heptane-2-carbonyl)-1H-imidazol-4-yl)-2-hydroxybenzenesulfonamide

*tert*-Butyl 6-(4-((5-bromo-3-chloro-2-hydroxyphenyl)sulfonamido)-1-cyclopentyl-1H-imidazole-2-carbonyl)-2,6-diazaspiro[3.3]heptane-2-carboxylate (98 mg, crude) was reacted following General Procedure S. Purification by preparative HPLC afforded the title compound (7.0 mg, 0.87 mmol, 15%).  $^{13}C$  NMR (151 MHz, DMSO- $d_6$ )  $\delta$  159.2, 136.3, 136.0, 134.6, 128.7, 127.7, 126.5, 110.9, 63.2, 57.9, 52.0, 51.3, 47.8, 46.7, 44.5, 41.8, 40.5, 33.7, 28.1, 24.0.  $^1H$  NMR (600 MHz, DMSO- $d_6$ )  $\delta$  8.88 (s, 2H), 7.42 (s, 1H), 7.23 (s, 1H), 6.99 (s, 1H), 4.78 (p,  $J = 7.5$  Hz, 1H), 3.54 (d,  $J = 5.2$  Hz, 2H), 3.43 (s, 2H), 3.36 – 3.26 (m, 3H), 3.18 – 3.12 (m, 1H), 3.00 (dd,  $J = 11.4, 7.6$  Hz, 1H), 2.97 – 2.89 (m, 1H), 2.47 – 2.37 (m, 2H), 2.37 – 2.30 (m, 1H), 2.26 (dt,  $J = 11.0, 5.0$  Hz, 1H), 2.11 – 1.99 (m, 3H), 1.82 – 1.70 (m, 3H), 1.67 – 1.54 (m, 4H). LCMS (Method B)  $t_R = 0.851$  min,  $m/z = 544.3, 546.3 [M+H]^+$ ; Purity (AUC)  $\geq 95\%$ .

*5-Bromo-3-chloro-N-(1-cyclopentyl-2-(methylsulfonyl)-1H-imidazol-4-yl)-2-hydroxybenzenesulfonamide (VU0830838)*



*Step A: 1-Cyclopentyl-2-(methylthio)-4-nitro-1H-imidazole*

2-Bromo-1-cyclopentyl-4-nitro-1H-imidazole (500 mg, 1.92 mmol) was reacted with sodium methanethiolate following General Procedure N-B. Purification by flash chromatography afforded the title compound (124 mg, 0.55 mmol, 29%). <sup>1</sup>H NMR (400 MHz, Chloroform-*d*) δ 7.76 (s, 1H), 4.50 – 4.40 (m, 1H), 2.66 (s, 3H), 2.28 – 2.08 (m, 2H), 1.90 – 1.67 (m, 6H). LCMS (Method B): *t*<sub>R</sub> = 0.881 min, *m/z* = 228.3 [M+H]<sup>+</sup>.

*Step B: 1-Cyclopentyl-2-(methylsulfonyl)-4-nitro-1H-imidazole*

1-Cyclopentyl-2-(methylthio)-4-nitro-1H-imidazole (124 mg, 0.55 mmol) was reacted following General Procedure O. Purification by flash chromatography afforded the title compound (142 mg, 0.54 mmol, 98%). <sup>1</sup>H NMR (400 MHz, Chloroform-*d*) δ 7.92 (s, 1H), 5.33 – 5.22 (m, 1H), 3.47 (s, 3H), 2.41 – 2.30 (m, 2H), 1.93 – 1.74 (m, 6H). LCMS (Method B): *t*<sub>R</sub> = 0.763 min, *m/z* = 260.2 [M+H]<sup>+</sup>.

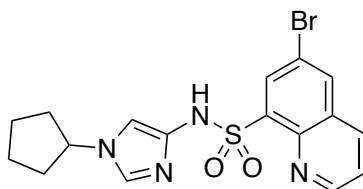
*Step C: 1-Cyclopentyl-2-(methylsulfonyl)-1H-imidazole-4-aminium chloride*

1-Cyclopentyl-2-(methylsulfonyl)-4-nitro-1H-imidazole (30 mg, 0.13 mmol) was reacted following General Procedure C. The crude was taken forward (25 mg). LCMS (Method B): *t*<sub>R</sub> = 0.186 min, *m/z* = 230.3 [M+H]<sup>+</sup>.

Step D: 5-Bromo-3-chloro-N-(1-(cyclobutylmethyl)-2-methyl-1H-imidazol-4-yl)-2-hydroxybenzenesulfonamide

1-Cyclopentyl-2-(methylsulfonyl)-1H-imidazole-4-aminium chloride (25 mg, crude) was reacted with 5-bromo-3-chloro-2-hydroxybenzenesulfonyl chloride following General Procedure D. Purification by preparative HPLC afforded the title compound (13 mg, 0.026 mmol, 20%). <sup>13</sup>C NMR (151 MHz, Chloroform-*d*) δ 149.87, 140.40, 137.65, 133.70, 130.06, 125.71, 124.36, 112.89, 111.50, 59.22, 43.21, 34.21, 24.17. <sup>1</sup>H NMR (400 MHz, Chloroform-*d*) δ 7.88 (d, *J* = 2.3 Hz, 2H), 7.47 (s, 1H), 5.47 (p, *J* = 6.8, 6.4 Hz, 1H), 3.44 (s, 3H), 2.56 – 2.45 (m, 2H), 2.10 – 2.04 (m, 2H), 2.04 – 1.92 (m, 4H). LCMS (Method B): *t*<sub>R</sub> = 1.027 min, *m/z* = 498.2, 499.3 [M+H]<sup>+</sup>; Purity (AUC) ≥ 95%.

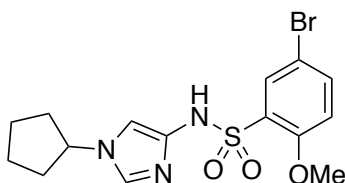
*6-Bromo-N-(1-cyclopentyl-1H-imidazol-4-yl)quinoline-8-sulfonamide (VU0849106)*



Cyclopentyl-1H-imidazol-4-aminium chloride (80 mg, crude) was reacted with 6-bromoquinoline-sulfonyl chloride following General Procedure D. Purification by preparative HPLC afforded the title compound (19 mg, 0.045 mmol). <sup>1</sup>H NMR (400 MHz, Chloroform-*d*) δ 9.04 (dd, *J* = 4.4, 1.8 Hz, 1H), 8.40 (d, *J* = 2.2 Hz, 1H), 8.24 (d, *J* = 2.2 Hz, 1H), 8.19 (dd, *J* = 8.4, 1.8 Hz, 1H), 8.05 (d, *J* = 1.8 Hz, 1H), 7.60 (dd, *J* = 8.4, 4.4 Hz, 1H), 7.14 (d, *J* = 1.8 Hz, 1H), 4.50 (p, *J* = 6.8 Hz, 1H), 2.34 – 2.22 (m, 2H), 1.93 – 1.75 (m, 6H). LCMS (Method B) *t*<sub>R</sub> = 0.800 min, *m/z* = 422.3, 423.3 [M+H]<sup>+</sup>; Purity (AUC) ≥ 95%.



*5-Bromo-N-(1-cyclopentyl-1H-imidazol-4-yl)-2-methoxybenzenesulfonamide (VU0849117)*



Cyclopentyl-1*H*-imidazol-4-aminium chloride (80 mg, crude) was reacted 5-bromo-2-methoxybenzenesulfonyl chloride following General Procedure D. Purification by preparative HPLC afforded the title compound (44 mg, 0.11 mmol). <sup>1</sup>H NMR (400 MHz, Chloroform-*d*) δ 7.79 (d, *J* = 2.7 Hz, 1H), 7.55 (s, 1H), 7.45 (dd, *J* = 8.8, 2.7 Hz, 1H), 6.97 – 6.91 (m, 2H), 4.43 (p, *J* = 6.7 Hz, 1H), 3.94 (s, 3H), 2.27 – 2.17 (m, 2H), 1.90 – 1.71 (m, 6H). LCMS (Method B) *t*<sub>R</sub> = 0.823 min, *m/z* = 400.0 [M+H]<sup>+</sup>; Purity (AUC) ≥ 95%.

### 6.5. Protein expression and purification

Truncated WDR5 (a.a. 22-334) was cloned into a pET vector with a 6xHis-SUMO tag fused at the N-terminus. The plasmids WDR5 was transformed into *E. coli* BL21 (DE3) cells. The overnight culture was used to start a 10 L fermentation (BioFlo 415, New Brunswick Scientific) grown at 37 °C. For NMR samples, uniformly <sup>15</sup>N-labeled protein was produced in minimal M9 medium, where <sup>15</sup>NH<sub>4</sub>Cl (Cambridge Isotope Laboratories) and D-glucose were used as sole nitrogen and carbon sources. When the cell density reached OD<sub>600</sub> = 2.5, the temperature was lowered to 30 °C. The protein was expressed overnight with 1mM isopropyl-β-D-thiogalactoside (IPTG). M peptide (DEEEIDVVSVE) was ordered (Genscript) as HPLC purified synthetic polypeptide. It was dissolved in DMSO for further use.

Cell pellets were dissolved in lysis buffer (1XPBS plus 300 mM NaCl, 20 mM imidazole, 5 mM BME, and 10% glycerol), and broken by homogenization (APV-2000, APV). The lysate was

cleared by centrifugation and filtering, and then applied to an affinity column (140 mL, ProBond, Invitrogen). Bound protein was eluted by an imidazole gradient. The His-SUMO-tag was removed by SUMO protease cleavage during dialysis and the subsequent subtractive second nickel-column. WDR5 protein was then purified by size-exclusion chromatography (HiLoad 26/60, Superdex 75, GE Healthcare) using NMR or crystallization buffer.

## 6.6 HTS screening

The previously described Myc peptide,<sup>23</sup> was labelled with FITC and used as the probe for FPA assays. The probe was ordered from Genscript. 5  $\mu$ M WDR5 protein and 5  $\mu$ M probe were used in the HTS, and the buffer condition was 1XPBS plus 300 mM NaCl, pH 6.0, 0.5mM TCEP, 0.1% CHAP, and 5% DMSO. Vanderbilt Discovery Collection (VDC) and VICB collection compounds (~250,000) were tested at 50  $\mu$ M concentration, and the compounds were put into 781 386-well plates with necessary positive and negative controls in each plate. After adding all reagents, the plates were shaken for ~2 minutes, and incubated for 60 minutes before first plate to be read on plate reader (Biotek). The reading settings of the plate reader were 50 flashes, low lamp energy, and 7.75 read height. All the plates were screened, and those plates (totaling 17) with Z' less than 0.3 were repeated. Compounds, which showed >15% inhibition, were selected for the confirmation screen. Confirmed compounds then were used for a 10-point dose response study.

## 6.7 Hit validation by NMR

NMR samples contained 2 mg/mL (~67  $\mu$ M) <sup>15</sup>N-labeled WDR5 in 25 mM phosphate buffer, pH=6.0, 100 mM NaCl, and 1 mM DTT. HTS hits were used at 100  $\mu$ M. Nuclear magnetic resonance screening was conducted using a Bruker Avance III 600 MHz NMR spectrometer

equipped with a 5mm single-axis z-gradient cryoprobe and a Bruker Sample Jet sample changer. Two-dimensional, gradient-enhanced  $^1\text{H}$ - $^{15}\text{N}$  heteronuclear multiple-quantum coherence (SOFAST-HMQC)<sup>274</sup> spectra were collected at 25 °C and used to track chemical shift perturbation upon compound binding. Spectra were processed and visualized using Topspin (Bruker BioSpin).

#### 6.8. NMR experiments: fragment screening $K_d$ determination

NMR samples contained 2 mg/mL (~67  $\mu\text{M}$ )  $^{15}\text{N}$ -labeled WDR5 in 25 mM phosphate buffer, pH = 6.0, 100 mM NaCl, and 1 mM DTT. Fragment library was screened in the format of 12-mixture, and the mixture hits were then deconvoluted.

Nuclear magnetic resonance (NMR) screening was conducted using a Bruker Avance III 600 MHz NMR spectrometer equipped with a 5mm single-axis z-gradient cryoprobe and a Bruker Sample Jet sample changer. Two dimensional, gradient-enhanced  $^1\text{H}$ - $^{15}\text{N}$  heteronuclear multiple-quantum coherence (SOFAST-HMQC)<sup>275</sup> spectra were collected at 25 °C and used to track chemical shift perturbation upon fragment binding. Spectra were processed and visualized using Topspin (Bruker BioSpin).

NMR titration of WDR5 fragment hits were performed using SOFAST-HMQC to monitor the chemical shift changes (CSC), and the  $K_d$  was calculated using the equation  $CSC =$

$$CSC_{max} \left( \frac{(1)T + (1)T + K_d - \sqrt{\{( (1)T + (1)T + K_d \}^2 - 4(1)T(1)T\}}}{2(1)T(2)} \right)$$

#### 6.9 Protein crystallization, data collection, and structure refinement

WDR5 was concentrated to 10 mg/mL (~300  $\mu\text{M}$ ) in the buffer of 20 mM HEPES, pH 7.0, 250 mM NaCl, and 5 mM DTT. Apo- and co-crystals were obtained at 18 °C using the hanging drop method. The crystallization condition was 0.1 M Bis-Tris pH 6.0, 0.2 M ammonium acetate, 28%

to 32% PEG3350. Soaking was also applied to some compounds using the apo-crystals. Crystals were flash frozen in liquid nitrogen directly.

Diffraction data were collected on the Life Sciences Collaborative Access Team (LS-CAT) 21-ID-D and G beamlines at the Advanced Photon Source (APS), Argonne National Laboratory. Data were indexed, integrated, and scaled with HKL2000.<sup>276</sup> Molecular replacement was achieved with Phaser44 as implemented in CCP4.45<sup>277</sup> using a previously determined WDR5 structure (PDB code 3EG6). Refinement of the structural models was conducted with PHENIX<sup>278</sup> and included rounds of manual model building in COOT.<sup>279</sup> All structure images were prepared with PyMOL.<sup>280</sup>

#### 6.10 Cloning and plasmids

Full length human WDR5 with an N-terminal FLAG tag was cloned into the NgoMIV and Sall sites as a NgoMIV/XhoI fragment. pBabe-GFP was constructed by PCR amplifying the GFP fragment from pEGFP-C2 (Clontech) and cloning the product into the EcoRI and BamHI sites of pBabe Puro. Full length human c-MYC with a C-terminal double HA tag was cloned into the BamHI and EcoRI sites of pBabe-IGH.<sup>23</sup> HEK293 cells stably expressing MYC2HA were made by retroviral transduction followed by selection in Hygromycin (50 µg/ mL). The mixed population was then infected with pBabe-Puro expressing GFP or WDR5 with selection in puromycin (1 µg/ mL). For retroviral transductions, HEK293T cells were transfected with the appropriate pBabe vector, the pCL10A packaging vector, and pMax-GFP to estimate transfection efficiency. Viral supernatant was collected and used to infect HEK293 class over three days.

## 6.9 Cell culture

HEK293 cells expressing HA-tagged MYC with either Flag-tagged WDR5 or GFP by retroviral transduction have been described.<sup>231</sup> Cells were maintained in DMEM supplemented with 10% FBS, Hygromycin B (50  $\mu\text{g}/\text{mL}$ ), and puromycin (100  $\text{ng}/\text{mL}$ ) to maintain transgene expression. Both cell lines were tested and confirmed negative of mycoplasma using the VenorGem PCR test kit (Sigma Aldrich). After thawing from liquid nitrogen, cells were passaged at least twice before use in experiments, and passaged for a maximum of 25 times.

## 6.10 WDR5 immunoprecipitation

HEK293 cells were harvested and lysates were prepared on ice in lysis buffer (50 mM Tris-HCl pH 8.0, 150 mM NaCl, 5 mM EDTA, 1% Triton X100 and supplemented with protease and phosphatase inhibitors). Equal amounts of protein lysate were subject to immunoprecipitation with M2 agarose overnight at 4 °C and immune complexes were recovered, washed in lysis buffer, and resolved by SDS-PAGE. Immunoblotting was performed using the indicated primary antibodies. For experiments in which cells were treated with compound, HEK293 cells were grown to approximately 70% confluence, washed once with PBS then treated for 24 h with compound in OptiMEM media before harvesting.

## 6.11 Antibodies

The following primary antibodies were used for this study:  $\alpha$ -c-MYC (#5605),  $\alpha$ -WDR5 (#13105),  $\alpha$ -HA (#3724) all purchased from Cell Signaling Technology.  $\alpha$ -FLAG-HRP (#A8592) and  $\alpha$ -FLAG M2 Affinity Gel (#A2220) were from Millipore-Sigma.

## 6.12 Chromatin Immunoprecipitation (ChIP) Experiments

HEK293 cells expressing HA-tagged MYC and GFP were plated in growth media. Upon reaching approximately 70% confluence, cells were washed once with PBS then treated for 10 h with compound in OptiMEM media. Cells were cross linked at room temperature in PBS containing 1% Formaldehyde for 10 minutes, then cells were scraped into 1.5 ml PBS supplemented with 125 mM Glycine. Cells were collected by centrifugation, washed once with PBS + 125 mM Glycine, and pellets stored frozen. Chromatin was prepared by lysing cells at  $80 \times 10^6$  per ml in ChIP Lysis Buffer (50 mM Tris pH 8.0, 140 mM NaCl, 1mM EDTA, 1% Triton, 1% SDS and supplemented with protease inhibitor cocktail), Samples were sonicated (BioRuptor) for 30 minutes and cleared by centrifugation. Precipitation was performed essentially as described [Thomas LR 2015 Mol Cell] by diluting chromatin 1:9 in ChIP buffer without SDS. Decrosslinked DNA was diluted to 500  $\mu$ L with water and 7.5  $\mu$ L was used for each qPCR reaction. Percent input was calculated by comparison to a 30-fold dilution of decrosslinked chromatin. Primers used for ChIP have been described<sup>269</sup>.

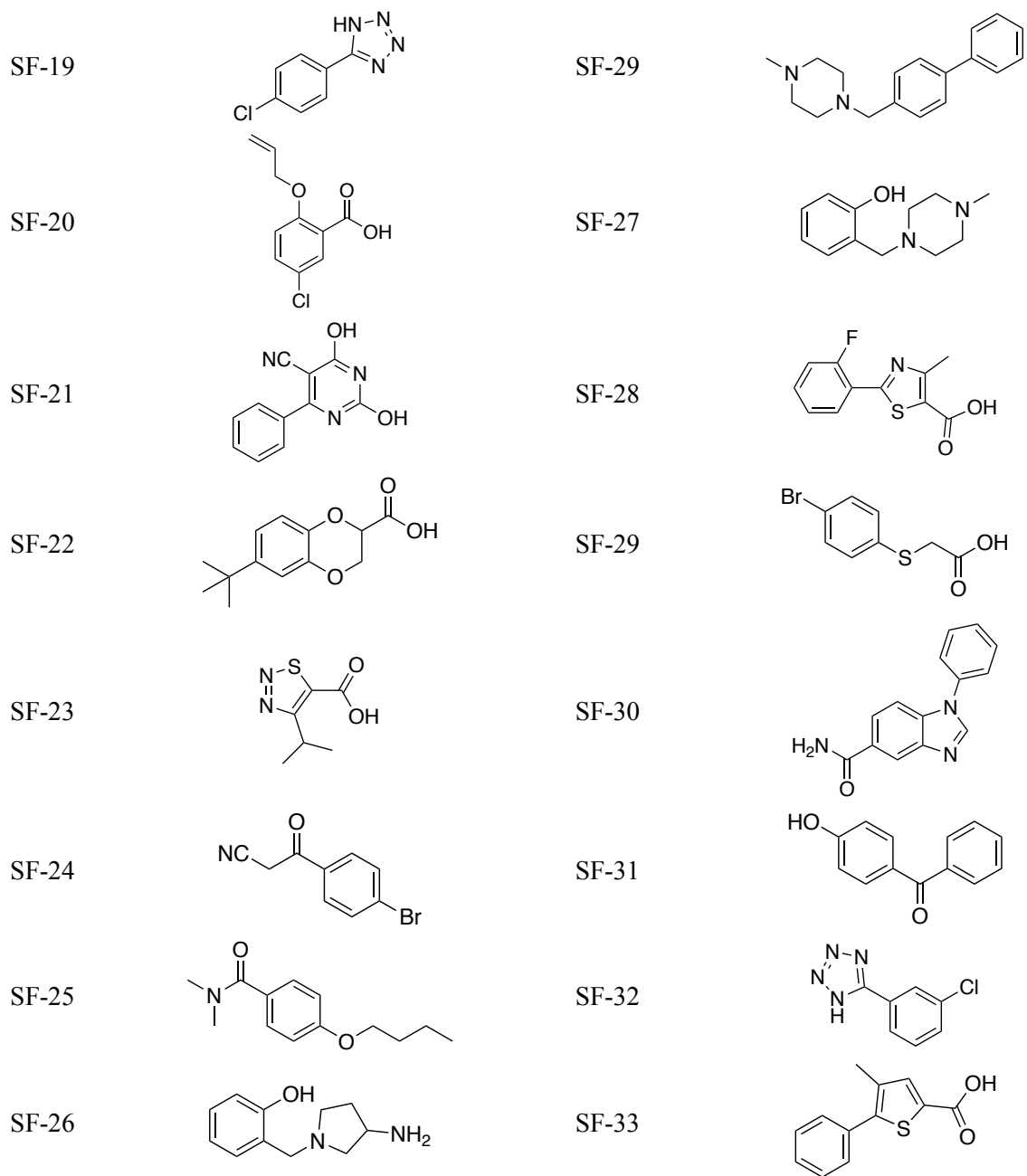
## 6.13 Pharmaceutical property determinations

All experiments performed at Q<sup>2</sup> Solutions Ltd. (<https://www.q2labsolutions.com>) using commercially available, standard assay formats. Kinetic solubility determinations: Method QUI-SOL-001. MDCK permeability determinations: Method QUI-PERM-003. Protein binding assessment: Method QUI-PERM-002.

Appendix A

Hits from the fragments screen of WDR5 at the WBM-site.

Fragment	Structure	Fragment	Structure
SF-1		SF-10	
SF-2		SF-11	
SF-3		SF-12	
SF-4		SF-13	
SF-5		SF-14	
SF-6		SF-15	
SF-7		SF-16	
SF-8		SF-17	
SF-9		SF-18	





## References

- (1) American Cancer Association. *Global Cancer Facts & Figures 4th Edition*; Atlanta, 2018. [https://doi.org/10.1787/health\\_glance\\_eur-2018-graph47-en](https://doi.org/10.1787/health_glance_eur-2018-graph47-en).
- (2) UK, C. R. Worldwide cancer statistics <https://www.cancerresearchuk.org/health-professional/cancer-statistics/worldwide-cancer#heading-Zero> (accessed Nov 6, 2019).
- (3) NCI. Cancer Statistics <https://www.cancer.gov/about-cancer/understanding/statistics> (accessed Nov 6, 2019).
- (4) Ferlay, J.; Ervik, M.; Lam, F.; Colombet, M.; Mery, L.; Piñeros, M.; Znaor, A.; Soerjomataram, I.; Bray, F. Cancer Tomorrow <http://gco.iarc.fr/tomorrow/home> (accessed Nov 6, 2019).
- (5) Falzone, L.; Salomone, S.; Libra, M. Evolution of Cancer Pharmacological Treatments at the Turn of the Third Millennium. *Front. Pharmacol.* **2018**, *9* (NOV). <https://doi.org/10.3389/fphar.2018.01300>.
- (6) Arruebo, M.; Vilaboa, N.; Sáez-Gutierrez, B.; Lambea, J.; Tres, A.; Valladares, M.; González-Fernández, Á. Assessment of the Evolution of Cancer Treatment Therapies. *Cancers (Basel)*. **2011**, *3* (3), 3279–3330. <https://doi.org/10.3390/cancers3033279>.
- (7) Ke, X.; Shen, L. Molecular Targeted Therapy of Cancer: The Progress and Future Prospect. *Front. Lab. Med.* **2017**, *1* (2), 69–75. <https://doi.org/10.1016/j.flm.2017.06.001>.
- (8) Nurgali, K.; Jagoe, R. T.; Abalo, R. Editorial: Adverse Effects of Cancer Chemotherapy: Anything New to Improve Tolerance and Reduce Sequelae? *Front. Pharmacol.* **2018**, *9* (March), 1–3. <https://doi.org/10.3389/fphar.2018.00245>.
- (9) Padama, V. An Overview of Targeted Cancer Therapy. *BioMedicine* **2015**, *5* (4), 1–6. <https://doi.org/10.7603/s40>.
- (10) Baudino, T. A. Targeted Cancer Therapy: The Next Generation of Cancer Treatment. *Curr. Drug Discov. Technol.* **2015**, *12* (1), 3–20.
- (11) BA, C.; TG, R. Chemotherapy and the War on Cancer. *Nat. Rev. Cancer* **2005**, *5* (1), 65–72. <https://doi.org/10/cnv36x>.
- (12) David, G. Targeted Therapies: A New Generation of Cancer Treatments. *Am. Fam. Physician* **2008**, *77* (3), 311–319.
- (13) Hoelder, S.; Clarke, P. A.; Workman, P. Discovery of Small Molecule Cancer Drugs:

- Successes, Challenges and Opportunities. *Mol. Oncol.* **2012**, *6* (2), 155–176. <https://doi.org/10.1016/j.molonc.2012.02.004>.
- (14) Carabet, L. A.; Rennie, P. S.; Cherkasov, A. Therapeutic Inhibition of Myc in Cancer. Structural Bases and Computer-Aided Drug Discovery Approaches. *Int. J. Mol. Sci.* **2019**, *20* (1). <https://doi.org/10.3390/ijms20010120>.
- (15) Young, S. L.; Diolaiti, D.; Conacci-Sorrell, M.; Ruiz-Trillo, I.; Eisenman, R. N.; King, N. Premetazoan Ancestry of the Myc-Max Network. *Mol. Biol. Evol.* **2011**, *28* (10), 2961–2971. <https://doi.org/10.1093/molbev/msr132>.
- (16) Tansey, W. P. Mammalian MYC Proteins and Cancer. *New J. Sci.* **2014**, 1–27. <https://doi.org/10.1155/2014/757534>.
- (17) Lin, C. Y.; Lovén, J.; Rahl, P. B.; Paranal, R. M.; Burge, C. B.; Bradner, J. E.; Lee, T. I.; Young, R. A. Transcriptional Amplification in Tumor Cells with Elevated C-Myc. *Cell* **2012**, *151* (1), 56–67. <https://doi.org/10.1016/j.cell.2012.08.026>.
- (18) Nesbit, C. E.; Grove, L. E.; Yin, X.; Prochownik, E. V. Differential Apoptotic Behaviors of C-Myc, N-Myc, and L-Myc Oncoproteins. *Cell Growth Differentiation* **1998**, *9* (9), 731–742.
- (19) Grandori, C.; Cowley, S. M.; James, L. P.; Eisenman, R. N. The MYC /MAX/Mad Network and the Transcriptional Control of Cell Behavior. *Annu. Rev. Cell Dev. Biol.* **2000**, *16* (1), 653–699. <https://doi.org/10.1146/annurev.cellbio.16.1.653>.
- (20) Rickman, D. S.; Schulte, J. H.; Eilers, M. The Expanding World of N-MYC-Driven Tumors. *Cancer Discov.* **2018**, *8* (2), 150–164. <https://doi.org/10.1158/2159-8290.CD-17-0273>.
- (21) Zhang, Q.; West-Osterfield, K.; Spears, E.; Li, Z.; Panaccione, A.; Hann, S. R. MB0 and MBI Are Independent and Distinct Transactivation Domains in MYC That Are Essential for Transformation. *Genes (Basel)*. **2017**, *8* (5). <https://doi.org/10.3390/genes8050134>.
- (22) Blackwell, T. K.; Huang, J.; Ma, A.; Kretzner, L.; Alt, F. W.; Eisenman, R. N.; Weintraub, H. Binding of Myc Proteins to Canonical and Noncanonical DNA Sequences. *Mol. Cell. Biol.* **1993**, *13* (9), 5216–5224.
- (23) Thomas, L. R.; Wang, Q.; Grieb, B. C.; Phan, J.; Foshage, A. M.; Sun, Q.; Olejniczak, E. T.; Clark, T.; Dey, S.; Lorey, S.; et al. Interaction with WDR5 Promotes Target Gene Recognition and Tumorigenesis by MYC. *Mol. Cell* **2015**, *58* (3), 440–452. <https://doi.org/10.1016/j.molcel.2015.02.028>.

- (24) Cowling, V. H.; Chandriani, S.; Whitfield, M. L.; Cole, M. D. A Conserved Myc Protein Domain, MBIV, Regulates DNA Binding, Apoptosis, Transformation, and G2 Arrest. *Mol. Cell. Biol.* **2006**, *26* (11), 4226–4239. <https://doi.org/10.1128/MCB.01959-05>.
- (25) Herbst, A.; Hemann, M. T.; Tworkowski, K. A.; Salghetti, S. E.; Lowe, S. W.; Tansey, W. P. A Conserved Element in Myc That Negatively Regulates Its Proapoptotic Activity. *EMBO Rep.* **2005**, *6* (2), 177–183. <https://doi.org/10.1038/sj.embor.7400333>.
- (26) Herbst, A.; Salghetti, S. E.; Kim, S. Y.; Tansey, W. P. Multiple Cell-Type-Specific Elements Regulate Myc Protein Stability. *Oncogene* **2004**, *23* (21), 3863–3871. <https://doi.org/10.1038/sj.onc.1207492>.
- (27) Kurland, J. F.; Tansey, W. P. Myc-Mediated Transcriptional Repression by Recruitment of Histone Deacetylases. *Cancer Res.* **2008**, *10* (2), 3624–3629. <https://doi.org/10.1007/s10059-012-2268-3>.
- (28) Flinn, E. M.; Busch, C. M. C.; Wright, A. P. H. Myc Boxes, Which Are Conserved in Myc Family Proteins, Are Signals for Protein Degradation via the Proteasome. *Mol. Cell. Biol.* **1998**, *18* (10), 5961–5969. <https://doi.org/10.1128/mcb.18.10.5961>.
- (29) Stone, J.; de Lange, T.; Ramsay, G.; Jakobovits, E.; Bishop, J. M.; Varmus, H.; Lee, W. Definition of Regions in Human C-Myc That Are Involved in Transformation and Nuclear Localization. *Mol. Cell. Biol.* **1987**, *7* (5), 1697–1709. <https://doi.org/10.1128/mcb.7.5.1697>.
- (30) Hemann, M. T.; Bric, A.; Teruya-Feldstein, J.; Herbst, A.; Nilsson, J. A.; Cordon-Cardo, C.; Cleveland, J. L.; Tansey, W. P.; Lowe, S. W. Evasion of the P53 Tumour Surveillance Network by Tumour-Derived MYC Mutants. *Nature* **2005**, *436* (7052), 807–811. <https://doi.org/10.1038/nature03845>.
- (31) Li, L. H.; Nerlov, C.; Prendergast, G.; MacGregor, D.; Ziff, E. B. C-Myc Represses Transcription in Vivo by a Novel Mechanism Dependent on the Initiator Element and Myc Box II. *EMBO J.* **1994**, *13* (17), 4070–4079. <https://doi.org/10.1002/j.1460-2075.1994.tb06724.x>.
- (32) Zhang, X. Y.; DeSalle, L. M.; McMahon, S. B. Identification of Novel Targets of MYC Whose Transcription Requires the Essential MbII Domain. *Cell Cycle* **2006**, *5* (3), 238–241. <https://doi.org/10.4161/cc.5.3.2409>.
- (33) McMahon, S. B.; Wood, M. A.; Cole, M. D. The Essential Cofactor TRRAP Recruits the

- Histone Acetyltransferase HGCN5 to C-Myc. *Mol. Cell. Biol.* **2000**, *20* (2), 556–562.
- (34) Eberhardy, S. R.; Farnham, P. J. C-Myc Mediates Activation of the Cad Promoter via a Post-RNA Polymerase II Recruitment Mechanism. *J. Biol. Chem.* **2001**, *276* (51), 48562–48571. <https://doi.org/10.1074/jbc.M109014200>.
- (35) Welcker, M.; Orian, A.; Jin, J.; Grim, J. E.; Harper, J. W.; Eisenman, R. N.; Clurman, B. E. The Fbw7 Tumor Suppressor Regulates Glycogen Synthase Kinase 3 Phosphorylation-Dependent c-Myc Protein Degradation. *PNAS* **2004**, *101* (24), 9085–9090.
- (36) Malynn, B. A.; De Alboran, I. M.; O’Hagan, R. C.; Bronson, R.; Davidson, L.; DePinho, R. A.; Alt, F. W. N-Myc Can Functionally Replace c-Myc in Murine Development, Cellular Growth, and Differentiation. *Genes Dev.* **2000**, *14* (11), 1390–1399.
- (37) Blackwood, E. M.; Eisenman, R. N. Max: A Helix-Loop-Helix Zipper Protein That Forms a Sequence-Specific DNA-Binding Complex with Myc. *Science* **1991**, *251* (4998), 1211–1217. <https://doi.org/10.1126/science.2006410>.
- (38) Albiñ, A.; Johnsen, J. I.; Arsenian, M. MYC in Oncogenesis and as a Target for Cancer Therapies. *Adv. Cancer Research* **2010**, No. 10, 163–224. [https://doi.org/10.1016/S0065-230X\(10\)07006-5](https://doi.org/10.1016/S0065-230X(10)07006-5).
- (39) Shen-Li, H.; O’Hagan, R.; Hou, H.; II, J. J. W. H.; Lee, H.-W.; DePinho, R. Essential Role for Max in Early Embryonic Growth and Development Essential Role for Max in Early Embryonic Growth and Development. *Genes Dev.* **1999**, *14*, 17–22.
- (40) Murphy, M. J.; Wilson, A.; Trumpp, A. More than Just Proliferation: Myc Function in Stem Cells. *Trends Cell Biol.* **2005**, *15* (3), 128–137. <https://doi.org/10.1016/j.tcb.2005.01.008>.
- (41) Charron, J.; Malynn, B. A.; Fisher, P.; Stewart, V.; Jeannotte, L.; Goff, S. P.; Robertson, E. J.; Alt, F. W. Embryonic Lethality in Mice Homozygous for a Targeted Disruption of the N-Myc Gene. *Genes Dev.* **1992**, *6* (12 A), 2248–2257. <https://doi.org/10.1101/gad.6.12a.2248>.
- (42) Ayer, D. E.; Eisenman, R. N. Switch from Myc:Max to Mad:Max Heterocomplexes Accompanies Monocyte/Macrophage Differentiation. *Genes Dev.* **1993**, *7*, 2110–2119. <https://doi.org/10.1101/gad.7.11.2110>.
- (43) Su, Y. Function and Regulation of Myc-Family BHLHZip Transcription Factors during the Animal and Plant Cell Cycle, Swedish University of Agricultural Sciences, 2008.
- (44) Patel, J. H.; Loboda, A. P.; Showe, M. K.; Showe, L. C.; McMahon, S. B. Analysis of

- Genomic Targets Reveals Complex Functions of MYC. *Nat. Rev. Cancer* **2004**, *4* (7), 562–568. <https://doi.org/10.1038/nrc1393>.
- (45) Fernandez, P. C.; Frank, S. R.; Wang, L.; Schroeder, M.; Liu, S.; Greene, J.; Cocito, A.; Amati, B. Genomic Targets of the Human C-Myc Protein. *Genes Dev.* **2003**, *17* (9), 1115–1129. <https://doi.org/10.1101/gad.1067003>.
- (46) Ong, S.-E.; Schenone, M.; Margolin, A. a; Li, X.; Do, K.; Doud, M. K.; Mani, D. R.; Kuai, L.; Wang, X.; Wood, J. L.; et al. Identifying the Proteins to Which Small-Molecule Probes and Drugs Bind in Cells. *Proc. Natl. Acad. Sci. U. S. A.* **2009**, *106* (12), 4617–4622. <https://doi.org/10.1073/pnas.0900191106>.
- (47) Adhikary, S.; Eilers, M. Transcriptional Regulation and Transformation by Myc Proteins. *Nat. Rev. Mol. Cell Biol.* **2005**, *6* (8), 635–645. <https://doi.org/10.1038/nrm1703>.
- (48) Guccione, E.; Martinato, F.; Finocchiaro, G.; Luzi, L.; Tizzoni, L.; Dall’Olio, V.; Zardo, G.; Nervi, C.; Bernard, L.; Amati, B. Myc-Binding-Site Recognition in the Human Genome Is Determined by Chromatin Context. *Nat. Cell Biol.* **2006**, *8* (7), 764–770. <https://doi.org/10.1038/ncb1434>.
- (49) Uribealago, I.; Buschbeck, M.; Gutiérrez, A.; Teichmann, S.; Demajo, S.; Kuebler, B.; Nomdedéu, J. F.; Martí-N-Caballero, J.; Roma, G.; Benitah, S. A.; et al. E-Box-Independent Regulation of Transcription and Differentiation by MYC. *Nat. Cell Biol.* **2011**, *13* (12), 1443–1449. <https://doi.org/10.1038/ncb2355>.
- (50) Cleveland, J. L.; Huleihel, M.; Bressler, P.; Siebenlist, U.; Akiyama, L.; Eisenman, R. N.; Rapp, U. R. Negative Regulation of C-Myc Transcription Involves Myc Family Proteins. *Oncogene Res.* **1988**, *3* (4), 357–375.
- (51) Penn, L. J.; Brooks, M. W.; Laufer, E. M.; Land, H. Negative Autoregulation of C-Myc Transcription. *EMBO J.* **1990**, *9* (4), 1113–1121. <https://doi.org/10.1002/j.1460-2075.1990.tb08217.x>.
- (52) SeonaneHong-Van, J. Cell Culture Myc Suppression of the P21 Cip1 Cdk Inhibitor Influences the Outcome of the P53 Response to DNA Damage. *Lett. to Nat.* **2016**, *419* (October), 729–734. <https://doi.org/10.1038/nature01056.1>.
- (53) Zhang, Y.; Chan, J. C.; Fu, K.; Marquez, V. E.; Chen-kiang, S. Coordinated Silencing of Myc-Mediated MiR-29 by HDAC3 and EZH2 As a Therapeutic Target of Histone Modification in Aggressive B-Cell Lymphomas. **2014**, *22* (4), 506–523.

<https://doi.org/10.1016/j.ccr.2012.09.003>.Coordinated.

- (54) Gebhardt, A.; Frye, M.; Herold, S.; Benitah, S. A.; Braun, K.; Samans, B.; Watt, F. M.; Elsässer, H.; Eilers, M. Myc Regulates Keratinocyte Adhesion and Differentiation via Complex Formation with Miz1. **2006**, 139–149. <https://doi.org/10.1083/jcb.200506057>.
- (55) Herkert, B.; Eilers, M. Transcriptional Repression: The Dark Side of Myc. *Genes and Cancer* **2010**, *1* (6), 580–586. <https://doi.org/10.1177/1947601910379012>.
- (56) Shimono, A.; Okuda, T.; Kondoh, H. N-Myc-Dependent Repression of Ndr1, a Gene Identified by Direct Subtraction of Whole Mouse Embryo CDNAs between Wild Type and N-Myc Mutant. *Mech Dev.* **1999**, *83* (1–2), 39–52.
- (57) Gartel, A.; Ye, X.; Goufman, E.; Shianov, P.; Hay, N.; Najmabadi, F.; Tyner, A. MYC Represses the P21(WAF1/CIP1) Promoter and Interacts with Sp1/Sp3. *PNAS* **2001**, *98* (8), 4510–4515. <https://doi.org/10.1089/nat.2015.0537>.
- (58) Peukert, K.; Staller, P.; Schneider, A.; Carmichael, G.; Hänel, F.; Eilers, M. An Alternative Pathway for Gene Regulation by Myc. *EMBO J.* **1997**, *16* (18), 5672–5686. <https://doi.org/10.1093/emboj/16.18.5672>.
- (59) Brenner, C.; Deplus, R.; Didelot, C.; Lorient, A.; Viré, E.; De Smet, C.; Gutierrez, A.; Danovi, D.; Bernard, D.; Boon, T.; et al. Myc Represses Transcription through Recruitment of DNA Methyltransferase Corepressor. *EMBO J.* **2005**, *24* (2), 336–346. <https://doi.org/10.1038/sj.emboj.7600509>.
- (60) Jiang, G.; Espeseth, A.; Hazuda, D. J.; Margolis, D. M. C-Myc and Sp1 Contribute to Proviral Latency by Recruiting Histone Deacetylase 1 to the Human Immunodeficiency Virus Type 1 Promoter. *J. Virol.* **2007**, *81* (20), 10914–10923. <https://doi.org/10.1128/jvi.01208-07>.
- (61) Nie, Z.; Hu, G.; Wei, G.; Cui, K.; Yamane, A.; Resch, W.; Wang, R.; Green, D. R.; Tessarollo, L.; Casellas, R.; et al. C-Myc Is a Universal Amplifier of Expressed Genes in Lymphocytes and Embryonic Stem Cells Zuqin. *Cell* **2012**, *151* (1), 68–79. <https://doi.org/10.1016/j.cell.2012.08.033>.c-Myc.
- (62) Kelly, K.; Cochran, B. H.; Stiles, C. D.; Leder, P. Cell-Specific Regulation of the c-Myc Gene by Lymphocyte Mitogens and Platelet-Derived Growth Factor. **1983**, *35* (December), 603–610.
- (63) Marcu, K. B. Regulation of Expression of the C-Myc. **1986**, *6* (1), 28–32.

- (64) Bentley, D. L.; Groudine, M. A Block to Elongation Is Largely Responsible for Decreased Transcription of C-Myc in Differentiated HL60 Cells. *Nature* **1986**, *321* (12), 702–706.
- (65) Dirk, E.; Bornkamm, G. W. Transcriptional Arrest within the First Exon Is a Fast Control Mechanism in C-Myc Gene Expression. *Nucleic Acids Res.* **1986**, *14* (21), 8331–8346.
- (66) Culjkovic, B.; Topisirovic, I.; Skrabanek, L.; Ruiz-gutierrez, M.; Borden, K. L. B. EIF4E Is a Central Node of an RNA Regulon That Governs Cellular Proliferation. **2006**, *175* (3), 415–426. <https://doi.org/10.1083/jcb.200607020>.
- (67) Mazan-mamczarz, K.; Lal, A.; Martindale, J. L.; Kawai, T.; Gorospe, M. Translational Repression by RNA-Binding Protein TIAR. *Mol. Cell. Biol.* **2006**, *26* (7), 2716–2727. <https://doi.org/10.1128/MCB.26.7.2716>.
- (68) Vervoorts, J.; Lüscher-firzlaff, J. M.; Rottmann, S.; Lilischkis, R.; Walsemann, G.; Dohmann, K.; Austen, M.; Lüscher, B. Stimulation of C-MYC Transcriptional Activity and Acetylation by Recruitment of the Cofactor CBP. *EMBO Rep.* **2003**, *4* (5), 484–490. <https://doi.org/10.1038/sj.embor.embor821>.
- (69) Vervoorts, J.; Lüscher-Firzlaff, J.; Lüscher, B. The Ins and Outs of MYC Regulation by Posttranslational Mechanisms. *J. Biol. Chem.* **2006**, *281* (46), 34725–34729. <https://doi.org/10.1074/jbc.R600017200>.
- (70) Chou, T.-Y.; Hart, G. W.; Dang, C. V. C-MYC Is Glycosylated at Threonine 58, a Known Phosphorylation Site and a Mutation Hot Spot in Lymphomas. *J. Biol. Chem.* **1995**, *270* (32), 18961–18965.
- (71) Dang, C. V. Review MYC on the Path to Cancer. *Cell* **2012**, *149* (1), 22–35. <https://doi.org/10.1016/j.cell.2012.03.003>.
- (72) Dalla-Favera, R.; Bregni, M.; Erikson, J.; Patterson, D.; Gallo, R. C.; Croce, C. M. Human C-Myc Onc Gene Is Located on the Region of Chromosome 8 That Is Translocated in Burkitt Lymphoma Cells. *Proc. Natl. Acad. Sci.* **1982**, *79* (December), 7824–7827. <https://doi.org/10.1073/pnas.79.24.7824>.
- (73) Shou, Y.; Martelli, M. L.; Gabrea, A.; Qi, Y.; Brents, L. A.; Roschke, A.; Dewald, G.; Kirsch, I. R.; Bergsagel, P. L.; Kuehl, W. M. Diverse Karyotypic Abnormalities of the C-Myc Locus Associated with c-Myc Dysregulation and Tumor Progression in Multiple Myeloma. *PNAS* **2000**, *97* (1), 228–233.
- (74) Beroukhi, R.; Mermel, C. H.; Porter, D.; Wei, G.; Raychaudhuri, S.; Donovan, J.;

- Barretina, J.; Boehm, J. S.; Dobson, J.; Urashima, M.; et al. The Landscape of Somatic Copy-Number Alteration across Human Cancers. *Nature* **2010**, *463* (February), 899–905. <https://doi.org/10.1038/nature08822>.
- (75) Amthor, H.; Macharia, R.; Navarrete, R.; Brown, S. C.; Otto, A.; Voit, T.; Muntoni, F.; Vrbo, G.; Partridge, T.; Lim, K.; et al. NOTCH1 Directly Regulates C-MYC and Activates a Feed-Forward-Loop Transcriptional Network Promoting Leukemic Cell Growth. *PNAS* **2007**, *104* (10), 18261–18266.
- (76) Kaczmarek, L.; Hyland, J. K.; Watt, R.; Rosenberg, M.; Baserga, R. Microinjected C-Myc as a Competence Factor. *Science* **1985**, *228* (4705), 1313–1315. <https://doi.org/10.1126/science.4001943>.
- (77) Eilers, M.; Picardt, D.; Yamamoto, K. R.; Bishop, J. M. Chimeras of Myc Oncoprotein Transformation of Cells. *Lett. to Nat.* **1989**, *1276* (1987), 1987–1989.
- (78) Rempel, R. E.; Mori, S.; Gasparetto, M.; Glozak, M. A.; Andrechek, E. R.; Steven, B.; Laakso, N. M.; Lagoo, A. S.; Storms, R.; Smith, C.; et al. A Role for E2F Activities in Determining the Fate of Myc- Induced Lymphomagenesis. **2009**, *5* (9). <https://doi.org/10.1371/journal.pgen.1000640>.
- (79) Dang, C. V. MYC, Metabolism, Cell Growth, and Tumorigenesis. *Cold Spring Harb Perspect Med* **2013**, *3*, 1–15.
- (80) Zeller, K. I.; Zhao, X.; Lee, C. W. H.; Chiu, K. P.; Yao, F.; Yustein, J. T.; Ooi, H. S.; Orlov, Y. L.; Shahab, A.; Yong, H. C.; et al. Global Mapping of C-Myc Binding Sites and Target Gene Networks in Human B Cells. **2006**.
- (81) Evan, G. I.; Wyllie, A. H.; Gilbert, S.; Littlewood, T. D.; Land, H.; Brooks, M.; Waters, C. M.; Penn, L.; Hancock, D. C. Induction of Apoptosis by C-Myc Protein in Fibroblasts. *Cell* **1992**, *69*, 119–128.
- (82) Youle, R. J.; Strasser, A. The BCL-2 Protein Family : Opposing Activities That Mediate Cell Death. *Nat. Rev.* **2008**, *9* (january), 47–59. <https://doi.org/10.1038/nrm2308>.
- (83) Campaner, S.; Amati, B. Two Sides of the Myc-Induced DNA Damage Response: From Tumor Suppression to Tumor Maintenance. *Cell Div.* **2012**, *7* (1), 1–10. <https://doi.org/10.1186/1747-1028-7-6>.
- (84) Iritani, B. M.; Eisenman, R. N. C-Myc Enhances Protein Synthesis and Cell Size during B Lymphocyte Development. *PNAS* **1999**, *96* (23), 13180–13185.



- (85) Boon, K.; Caron, H. N.; Asperen, R. Van; Valentijn, L.; Hermus, M.; Sluis, P. Van; Roobeek, I.; Weis, I.; Vou, P. A. N-Myc Enhances the Expression of a Large Set of Genes Functioning in Ribosome Biogenesis and Protein Synthesis. **2001**, *20* (6), 1383–1393.
- (86) Schlosser, I.; Ho, M.; Hoffmann, R.; Burtscher, H.; Kohlhuber, F.; Schuhmacher, M.; Chapman, R.; Weidle, U. H.; Eick, D. Dissection of Transcriptional Programmes in Response to Serum and C-Myc in a Human B-Cell Line. **2005**, 520–524. <https://doi.org/10.1038/sj.onc.1208198>.
- (87) Barna, M.; Pusic, A.; Zollo, O.; Costa, M.; Kondrashov, N.; Rego, E.; Rao, P. H.; Ruggero, D. Suppression of Myc Oncogenic Activity by Ribosomal Protein Haploinsufficiency. *Nature* **2008**, *456* (7224), 971–975. <https://doi.org/10.1038/nature07449>.
- (88) Hu, S.; Balakrishnan, A.; Bok, R. A.; Anderton, B.; Larson, P. E. Z.; Nelson, S. J.; Kurhanewicz, J.; Vigneron, D. B.; Goga, A. <sup>13</sup>C-Pyruvate Imaging Reveals Alterations in Glycolysis That Precede c-Myc- Induced Tumor Formation and Regression. *Cell Metab. Resour.* **2011**, *14* (1), 131–142. <https://doi.org/10.1016/j.cmet.2011.04.012>.
- (89) Stine, Z. E.; Walton, Z. E.; Altman, B. J.; Hsieh, A. L.; Dang, C. V. MYC, Metabolism, and Cancer. *Cancer Discov.* **2015**, *5* (October), 1024–1039. <https://doi.org/10.1158/2159-8290.CD-15-0507>.
- (90) Carroll, P. A.; Diolaiti, D.; Ayer, D. E.; Eisenman, R. N.; Carroll, P. A.; Diolaiti, D.; McFerrin, L.; Gu, H.; Djukovic, D.; Du, J.; et al. Deregulated Myc Requires MondoA / Mlx for Metabolic Reprogramming and Tumorigenesis. *Cancer Cell* **2015**, *27* (2), 271–285. <https://doi.org/10.1016/j.ccell.2014.11.024>.
- (91) Halazonetis, T. D.; Gorgoulis, V. G.; Bartek, J. An Oncogene-Induced DNA Damage Model for Cancer Development. *Science* **2008**, *319* (March), 1352–1356.
- (92) Srinivasan, S. V.; Dominguez-sola, D.; Wang, L. C.; Hyrien, O.; Gautier, J. Cdc45 Is a Critical Effector of Myc-Dependent DNA Replication Stress. *Cell Rep.* **2013**, *3* (5), 1629–1639. <https://doi.org/10.1016/j.celrep.2013.04.002>.
- (93) Baudino, T. A.; Mckay, C.; Pendeville-samain, H.; Nilsson, J. A.; Maclean, K. H.; White, E. L.; Davis, A. C.; Ihle, J. N.; Cleveland, J. L. C-Myc Is Essential for Vasculogenesis and Angiogenesis during Development and Tumor Progression. *Genes Dev.* **2002**, *16*, 2530–2543. <https://doi.org/10.1101/gad.1024602.formed>.
- (94) Dews, M.; Homayouni, A.; Yu, D.; Murphy, D.; Sevigani, C.; Wentzel, E.; Furth, E. E.;

- Lee, W. M.; Enders, G. H.; Mendell, J. T.; et al. Augmentation of Tumor Angiogenesis by a Myc-Activated MicroRNA Cluster. *Nat. Genet.* **2006**, *38* (9), 1060–1066. <https://doi.org/10.1038/ng1855>.
- (95) Yan, S.; Zhou, C.; Lou, X.; Xiao, Z.; Zhu, H.; Wang, Q.; Wang, Y.; Lu, N.; He, S.; Zhan, Q.; et al. PTTG Overexpression Promotes Lymph Node Metastasis in Human Esophageal Squamous Cell Carcinoma. *Cancer Res.* **2009**, *69* (8), 3283–3290. <https://doi.org/10.1158/0008-5472.CAN-08-0367>.
- (96) Frye, M.; Gardner, C.; Li, E. R.; Arnold, I.; Watt, F. M. Evidence That Myc Activation Depletes the Epidermal Stem Cell Compartment by Modulating Adhesive Interactions with the Local Microenvironment. *Development* **2003**, *130* (12), 2793–2808. <https://doi.org/10.1242/dev.00462>.
- (97) Cho, K. Bin; Cho, M. K.; Lee, W. Y.; Kang, K. W. Overexpression of C-Myc Induces Epithelial Mesenchymal Transition in Mammary Epithelial Cells. *Cancer Lett.* **2010**, *293* (2), 230–239. <https://doi.org/10.1016/j.canlet.2010.01.013>.
- (98) Ma, L.; Young, J.; Prabhala, H.; Pan, E.; Mestdagh, P.; Muth, D.; Teruya-Feldstein, J.; Reinhardt, F.; Onder, T. T.; Valastyan, S.; et al. MiR-9, a MYC/MYCN-Activated MicroRNA, Regulates E-Cadherin and Cancer Metastasis. *Nat. Cell Biol.* **2010**, *12* (3), 247–256. <https://doi.org/10.1038/ncb2024>.
- (99) Prochownik, E. V.; Vogt, P. K. Therapeutic Targeting of Myc. *Genes Cancer* **2010**, *1* (6), 650–659. <https://doi.org/10.1177/1947601910377494>.
- (100) Wang, H.; Mannava, S.; Grachtchouk, V.; Zhuang, D.; Soengas, M.; Gudkov, A.; Prochownik, E.; Nikiforov, M. C-Myc Depletion Inhibits Proliferation of Human Tumor Cells at Various Stages of the Cell Cycle. *Oncogene* **2008**, *27* (13), 1905–1915. <https://doi.org/10.1038/mp.2011.182.doi>.
- (101) Felsher, D. W.; Bishop, J. M. Reversible Tumorigenesis by MYC in Hematopoietic Lineages. *Mol. Cell* **1999**, *4* (2), 199–207. [https://doi.org/10.1016/S1097-2765\(00\)80367-6](https://doi.org/10.1016/S1097-2765(00)80367-6).
- (102) Jain, M.; Arvanitis, C.; Chu, K.; Dewey, W.; Leonhardt, E.; Trinh, M.; Sundberg, C. D.; Bishop, J. M.; Felsher, D. W. Sustained Loss of a Neoplastic Phenotype by Brief Inactivation of MYC. *Science* **2002**, *297* (5578), 102–104. <https://doi.org/10.1126/science.1071489>.

- (103) Bello-Fernandez, C.; Packham, G.; Cleveland, J. L. The Ornithine Decarboxylase Gene Is a Transcriptional Target of C-Myc. *Proc. Natl. Acad. Sci. U. S. A.* **1993**, *90* (16), 7804–7808.
- (104) Smith, M. J.; Charron-Prochownik, D. C.; Prochownik, E. V. The Leucine Zipper of C-Myc Is Required for Full Inhibition of Erythroleukemia Differentiation. *Mol. Cell. Biol.* **1990**, *10* (10), 5333–5339. <https://doi.org/10.1128/mcb.10.10.5333>.
- (105) Whitfield, J. R.; Beaulieu, M.-E.; Soucek, L. Strategies to Inhibit Myc and Their Clinical Applicability. *Front. Cell Dev. Biol.* **2017**, *5* (February), 1–13. <https://doi.org/10.3389/fcell.2017.00010>.
- (106) Brooks, T. a; Hurley, L. H. Targeting MYC Expression through G-Quadruplexes. *Genes Cancer* **2010**, *1* (6), 641–649. <https://doi.org/10.1177/1947601910377493>.
- (107) Chen, B.; Wu, Y.; Tanaka, Y.; Zhang, W. Small Molecules Targeting C-Myc Oncogene : Promising Anti-Cancer Therapeutics. *Int. J. Biol. Sci.* **2008**, *10*, 1084–1096. <https://doi.org/10.7150/ijbs.10190>.
- (108) Ou, T. M.; Lu, Y. J.; Zhang, C.; Huang, Z. S.; Wang, X. D.; Tan, J. H.; Chen, Y.; Ma, D. L.; Wong, K. Y.; Tang, J. C. O.; et al. Stabilization of G-Quadruplex DNA and down-Regulation of Oncogene c-Myc by Quindoline Derivatives. *J. Med. Chem.* **2007**, *50* (7), 1465–1474. <https://doi.org/10.1021/jm0610088>.
- (109) Pivetta, C.; Lucatello, L.; Paul Krapcho, A.; Gatto, B.; Palumbo, M.; Sissi, C. Perylene Side Chains Modulate G-Quadruplex Conformation in Biologically Relevant DNA Sequences. *Bioorganic Med. Chem.* **2008**, *16* (20), 9331–9339. <https://doi.org/10.1016/j.bmc.2008.08.068>.
- (110) Kerwin, S. M.; Chen, G.; Kern, J. T.; Thomas, P. W. Perylene Diimide G-Quadruplex DNA Binding Selectivity Is Mediated by Ligand Aggregation. *Bioorganic Med. Chem. Lett.* **2002**, *12* (3), 447–450. [https://doi.org/10.1016/S0960-894X\(01\)00775-2](https://doi.org/10.1016/S0960-894X(01)00775-2).
- (111) Grand, C. L.; Han, H.; Muñoz, R. M.; Weitman, S.; Von Hoff, D. D.; Hurley, L. H.; Bearss, D. J. The Cationic Porphyrin TMPyP4 Down-Regulates c-MYC and Human Telomerase Reverse Transcriptase Expression and Inhibits Tumor Growth in Vivo. *Mol. Cancer Ther.* **2002**, *1* (8), 565–573.
- (112) Seenisamy, J.; Bashyam, S.; Gokhale, V.; Vankayalapati, H.; Sun, D.; Siddiqui-Jain, A.; Streiner, N.; Shin-ya, K.; White, E.; Wilson, W. D.; et al. Design and Synthesis of an

- Expanded Porphyrin That Has Selectivity for the C-MYC G-Quadruplex Structure. *J. Am. Chem. Soc.* **2005**, *127* (9), 2944–2959. <https://doi.org/10.1021/ja0444482>.
- (113) Ji, X.; Sun, H.; Zhou, H.; Xiang, J.; Tang, Y.; Zhao, C. The Interaction of Telomeric DNA and C-Myc22 G-Quadruplex with 11 Natural Alkaloids. *Nucleic Acid Ther.* **2012**, *22* (2), 127–136. <https://doi.org/10.1089/nat.2012.0342>.
- (114) Lee, H. M.; Chan, D. S. H.; Yang, F.; Lam, H. Y.; Yan, S. C.; Che, C. M.; Ma, D. L.; Leung, C. H. Identification of Natural Product Fonsecain B as a Stabilizing Ligand of C-Myc G-Quadruplex DNA by High-Throughput Virtual Screening. *Chem. Commun.* **2010**, *46* (26), 4680–4682. <https://doi.org/10.1039/b926359d>.
- (115) Wu, P.; Ma, D. L.; Leung, C. H.; Yan, S. C.; Zhu, N.; Abagyan, R.; Che, C. M. Stabilization of G-Quadruplex DNA with Platinum(II) Schiff Base Complexes: Luminescent Probe and down-Regulation of c-Myc Oncogene Expression. *Chem. - A Eur. J.* **2009**, *15* (47), 13008–13021. <https://doi.org/10.1002/chem.200901943>.
- (116) Brown, R. V.; Danford, F. L.; Gokhale, V.; Hurley, L. H.; Brooks, T. A. Demonstration That Drug-Targeted down-Regulation of MYC in Non-Hodgkins Lymphoma Is Directly Mediated through the Promoter G-Quadruplex. *J. Biol. Chem.* **2011**, *286* (47), 41018–41027. <https://doi.org/10.1074/jbc.M111.274720>.
- (117) Mustata, G.; Follis, A. V.; Hammoudeh, D. I.; Metallo, S. J.; Wang, H.; Prochownik, E. V.; Lazo, J. S.; Bahar, I. Discovery of Novel Myc-Max Heterodimer Disruptors with a Three-Dimensional Pharmacophore Model. *J. Med. Chem.* **2009**, *52* (5), 1247–1250. <https://doi.org/10.1021/jm801278g>.
- (118) Drygin, D.; Siddiqui-Jain, A.; O'Brien, S.; Schwaebe, M.; Lin, A.; Bliesath, J.; Ho, C. B.; Proffitt, C.; Trent, K.; Whitten, J. P.; et al. Anticancer Activity of CX-3543: A Direct Inhibitor of RRNA Biogenesis. *Cancer Res.* **2009**, *69* (19), 7653–7661. <https://doi.org/10.1158/0008-5472.CAN-09-1304>.
- (119) Drygin, D.; Lin, A.; Bliesath, J.; Ho, C. B.; O'Brien, S. E.; Proffitt, C.; Omori, M.; Haddach, M.; Schwaebe, M. K.; Siddiqui-Jain, A.; et al. Targeting RNA Polymerase I with an Oral Small Molecule CX-5461 Inhibits Ribosomal RNA Synthesis and Solid Tumor Growth. *Cancer Res.* **2011**, *71* (4), 1418–1430. <https://doi.org/10.1158/0008-5472.CAN-10-1728>.
- (120) Xu, H.; Di Antonio, M.; McKinney, S.; Mathew, V.; Ho, B.; O'Neil, N. J.; Santos, N. Dos; Silvester, J.; Wei, V.; Garcia, J.; et al. CX-5461 Is a DNA G-Quadruplex Stabilizer with

- Selective Lethality in BRCA1/2 Deficient Tumours. *Nat. Commun.* **2017**, *8* (205). <https://doi.org/10.1038/ncomms14432>.
- (121) Hu, M. H.; Wang, Y. Q.; Yu, Z. Y.; Hu, L. N.; Ou, T. M.; Chen, S. Bin; Huang, Z. S.; Tan, J. H. Discovery of a New Four-Leaf Clover-Like Ligand as a Potent c-MYC Transcription Inhibitor Specifically Targeting the Promoter G-Quadruplex. *J. Med. Chem.* **2018**, *61* (6), 2447–2459. <https://doi.org/10.1021/acs.jmedchem.7b01697>.
- (122) Rocca, R.; Costa, G.; Artese, A.; Parrotta, L.; Ortuso, F.; Maccioni, E.; Pinato, O.; Greco, M. L.; Sissi, C.; Alcaro, S.; et al. Hit Identification of a Novel Dual Binder for H-Telo/c-Myc G-Quadruplex by a Combination of Pharmacophore Structure-Based Virtual Screening and Docking Refinement. *ChemMedChem* **2016**, 1721–1733. <https://doi.org/10.1002/cmdc.201600053>.
- (123) Bhat, J.; Mondal, S.; Sengupta, P.; Chatterjee, S. In Silico Screening and Binding Characterization of Small Molecules toward a G-Quadruplex Structure Formed in the Promoter Region of c-MYC Oncogene. *ACS Omega* **2017**, *2* (8), 4382–4397. <https://doi.org/10.1021/acsomega.6b00531>.
- (124) Yu, C.; Niu, X.; Jin, F.; Liu, Z.; Jin, C.; Lai, L. Structure-Based Inhibitor Design for the Intrinsically Disordered Protein c-Myc. *Nat. Publ. Gr.* **2016**, 1–11. <https://doi.org/10.1038/srep22298>.
- (125) Rinaldi, C.; Wood, M. J. A. Antisense Oligonucleotides: The next Frontier for Treatment of Neurological Disorders. *Nat. Rev. Neurol.* **2018**, *14* (1), 9–22. <https://doi.org/10.1038/nrneurol.2017.148>.
- (126) Prochownik, E. V.; Kukowska, J.; Rodgers, C. C-Myc Antisense Transcripts Accelerate Differentiation and Inhibit G1 Progression in Murine Erythroleukemia Cells. *Mol. Cell. Biol.* **1988**, *8* (9), 3683–3695. <https://doi.org/10.1128/mcb.8.9.3683>.
- (127) Sklar, M. D.; Thompson, E.; Welsh, M. J.; Liebert, M.; Harney, J.; Grossman, H. B.; Smith, M.; Prochownik, E. V. Depletion of C-Myc with Specific Antisense Sequences Reverses the Transformed Phenotype in Ras Oncogene-Transformed NIH 3T3 Cells. *Mol. Cell. Biol.* **1991**, *11* (7), 3699–3710. <https://doi.org/10.1128/mcb.11.7.3699>.
- (128) Holt, J. T.; Redner, R. L.; Nienhuis, A. W. An Oligomer Complementary to C-Myc mRNA Inhibits Proliferation of HL-60 Promyelocytic Cells and Induces Differentiation. *Mol. Cell. Biol.* **1988**, *8* (2), 963–973.

- (129) Skorski, B. T.; Nieborowska-skorska, M.; Wlodarski, P.; Zon, G.; Renato, V.; Calabretta, B. Antisense Oligodeoxynucleotide Combination Therapy of Primary Chronic Myelogenous Leukemia Blast Crisis in SCID Mice. *Blood* **1996**, *3*, 1005–1012.
- (130) Arora, V.; Knapp, D. C.; Smith, B. L.; Statfield, M. L.; Stein, D. A.; Reddy, M. T.; Weller, D. D.; Iversen, P. L. C-Myc Antisense Limits Rat Liver Regeneration and Indicates Role for c-Myc in Regulating Cytochrome P-450 3A Activity. *J. Pharmacol. Exp. Ther.* **2000**, *292* (3), 921 LP – 928.
- (131) Moreno, P. M. D.; Pêgo, A. P. Therapeutic Antisense Oligonucleotides against Cancer: Hurdling to the Clinic. *Front. Chem.* **2014**, *2* (October), 87. <https://doi.org/10.3389/fchem.2014.00087>.
- (132) Pierce, B. *Genetics: A Conceptual Approach*, 2nd ed.; W. H. Freeman: New York, 2005.
- (133) Dicerna Pharmaceuticals, I. *2014 Annual Report on Form 10-K*; 2015. <https://doi.org/10.7312/schw92626-018>.
- (134) Solve, S.; Van Rees, A. BioSpace.
- (135) Shaat, H.; Mostafa, A.; Moustafa, M.; Gamal-Eldeen, A.; Emam, A.; El-Hussieny, E.; Elhefnawi, M. Modified Gold Nanoparticles for Intracellular Delivery of Anti-Liver Cancer SiRNA. *Int. J. Pharm.* **2016**, *504* (1–2), 125–133. <https://doi.org/10.1016/j.ijpharm.2016.03.051>.
- (136) Zhu, Q.; Feng, C.; Liao, W.; Zhang, Y.; Tang, S. Target Delivery of MYCN SiRNA by Folate-Nanoliposomes Delivery System in a Metastatic Neuroblastoma Model. *Cancer Cell Int.* **2013**, *13* (1), 1–6. <https://doi.org/10.1186/1475-2867-13-65>.
- (137) Li, Y.; Zhang, B.; Zhang, H.; Zhu, X.; Feng, D.; Zhang, D.; Zhuo, B.; Li, L.; Zheng, J. Oncolytic Adenovirus Armed with ShRNA Targeting MYCN Gene Inhibits Neuroblastoma Cell Proliferation and in Vivo Xenograft Tumor Growth. *J. Cancer Res. Clin. Oncol.* **2013**, *139* (6), 933–941. <https://doi.org/10.1007/s00432-013-1406-4>.
- (138) Berg, T.; Cohen, S. B.; Desharnais, J.; Sonderegger, C.; Maslyar, D. J.; Goldberg, J.; Boger, D. L.; Vogt, P. K. Small-Molecule Antagonists of Myc/Max Dimerization Inhibit Myc-Induced Transformation of Chicken Embryo Fibroblasts. *Proc. Natl. Acad. Sci. U. S. A.* **2002**, *99*, 3830–3835. <https://doi.org/10.1073/pnas.062036999>.
- (139) Xu, Y.; Shi, J.; Yamamoto, N.; Moss, J. A.; Vogt, P. K.; Janda, K. D. A Credit-Card Library Approach for Disrupting Protein-Protein Interactions. *Bioorganic Med. Chem.* **2006**, *14* (8),

- 2660–2673. <https://doi.org/10.1016/j.bmc.2005.11.052>.
- (140) Yin, X.; Giap, C.; Lazo, J. S.; Prochownik, E. V. Low Molecular Weight Inhibitors of Myc-Max Interaction and Function. *Oncogene* **2003**, *22* (40), 6151–6159. <https://doi.org/10.1038/sj.onc.1206641>.
- (141) Huang, M. J.; Cheng, Y. chih; Liu, C. R.; Lin, S.; Liu, H. E. A Small-Molecule c-Myc Inhibitor, 10058-F4, Induces Cell-Cycle Arrest, Apoptosis, and Myeloid Differentiation of Human Acute Myeloid Leukemia. *Exp. Hematol.* **2006**, *34* (11), 1480–1489. <https://doi.org/10.1016/j.exphem.2006.06.019>.
- (142) Lin, C. P.; Liu, J. D.; Chow, J. M.; Liu, C. R.; Eugene Liu, H. Small-Molecule c-Myc Inhibitor, 10058-F4, Inhibits Proliferation, Downregulates Human Telomerase Reverse Transcriptase and Enhances Chemosensitivity in Human Hepatocellular Carcinoma Cells. *Anticancer. Drugs* **2007**, *18* (2), 161–170. <https://doi.org/10.1097/CAD.0b013e3280109424>.
- (143) Guo, J.; Parise, R. A.; Joseph, E.; Egorin, M. J.; Lazo, J. S.; Prochownik, E. V.; Eiseman, J. L. Efficacy, Pharmacokinetics, Tissue Distribution, and Metabolism of the Myc-Max Disruptor, 10058-F4 [Z,E]-5-[4-Ethylbenzylidene]-2-Thioxothiazolidin-4- One, in Mice. *Cancer Chemother. Pharmacol.* **2009**, *63* (4), 615–625. <https://doi.org/10.1007/s00280-008-0774-y>.
- (144) Wang, H.; Hammoudeh, D. I.; Follis, A. V.; Reese, B. E.; Lazo, J. S.; Metallo, S. J.; Prochownik, E. V. Improved Low Molecular Weight Myc-Max Inhibitors. *Mol. Cancer Ther.* **2007**, *6* (9), 2399–2408. <https://doi.org/10.1158/1535-7163.mct-07-0005>.
- (145) Yin, X.; Giap, C.; Lazo, J. S.; Prochownik, E. V. Low Molecular Weight Inhibitors of Myc-Max Interaction and Function. *Oncogene* **2003**, *22* (40), 6151–6159. <https://doi.org/10.1038/sj.onc.1206641>.
- (146) Fletcher, S.; Prochownik, E. V. Small-Molecule Inhibitors of the Myc Oncoprotein. *Biochim. Biophys. Acta* **2015**, *1849* (5), 525–543. <https://doi.org/10.1016/j.bbagr.2014.03.005>.
- (147) Follis, A. V.; Hammoudeh, D. I.; Wang, H.; Prochownik, E. V.; Metallo, S. J. Structural Rationale for the Coupled Binding and Unfolding of the C-Myc Oncoprotein by Small Molecules. *Chem. Biol.* **2008**, *15* (11), 1149–1155. <https://doi.org/10.1016/j.chembiol.2008.09.011>.

- (148) Hammoudeh, D. I.; Follis, A. V.; Prochownik, E. V.; Metallo, S. J. Multiple Independent Binding Sites for Small-Molecule Inhibitors on the Oncoprotein c-Myc. *J. Am. Chem. Soc.* **2009**, *131* (21), 7390–7401. <https://doi.org/10.1021/ja900616b>.
- (149) Wang, H.; Chauhan, J.; Hu, A.; Pendleton, K.; Yap, J. L.; Sabato, P. E.; Jones, J. W.; Perri, M.; Yu, J.; Cione, E.; et al. Disruption of Myc-Max Heterodimerization with Improved Cell-Penetrating Analogs of the Small Molecule 10074-G5. *Oncotarget* **2013**, *9* (80), 936–949. <https://doi.org/10.18632/oncotarget.26241>.
- (150) Kiessling, A.; Sperl, B.; Hollis, A.; Eick, D.; Berg, T. Selective Inhibition of C-Myc/Max Dimerization and DNA Binding by Small Molecules. *Chem. Biol.* **2006**, *13* (7), 745–751. <https://doi.org/10.1016/j.chembiol.2006.05.011>.
- (151) Hart, J. R.; Garner, A. L.; Yu, J.; Ito, Y.; Sun, M.; Ueno, L.; Rhee, J.-K.; Baksh, M. M.; Stefan, E.; Hartl, M.; et al. Inhibitor of MYC Identified in a Krohnke Pyridine Library. *Proc. Natl. Acad. Sci.* **2014**, *111* (34), 12556–12561. <https://doi.org/10.1073/pnas.1319488111>.
- (152) Castell, A.; Yan, Q.; Fawkner, K.; Hydbring, P.; Zhang, F.; Verschut, V.; Franco, M.; Zakaria, S. M.; Bazzar, W.; Goodwin, J.; et al. A Selective High Affinity MYC-Binding Compound Inhibits MYC:MAX Interaction and MYC-Dependent Tumor Cell Proliferation. *Sci. Rep.* **2018**, *8* (1), 1–17. <https://doi.org/10.1038/s41598-018-28107-4>.
- (153) Yu, C.; Niu, X.; Jin, F.; Liu, Z.; Jin, C.; Lai, L. Structure-Based Inhibitor Design for the Intrinsically Disordered Protein c-Myc. *Sci. Rep.* **2016**, *6*, 1–11. <https://doi.org/10.1038/srep22298>.
- (154) Jiang, H.; Bower, K. E.; Beuscher, A. E.; Zhou, B.; Bobkov, A. A.; Olson, A. J.; Vogt, P. K. Stabilizers of the Max Homodimer Identified in Virtual Ligand Screening Inhibit Myc Function. *Mol. Pharmacol.* **2009**, *76* (3), 491–502. <https://doi.org/10.1124/mol.109.054858>.
- (155) Han, H.; Jain, A. D.; Truica, M. I.; Izquierdo-Ferrer, J.; Anker, J. F.; Lysy, B.; Sagar, V.; Luan, Y.; Chalmers, Z. R.; Unno, K.; et al. Small-Molecule MYC Inhibitors Suppress Tumor Growth and Enhance Immunotherapy. *Cancer Cell* **2019**, *36* (5), 483–497.e15. <https://doi.org/10.1016/j.ccell.2019.10.001>.
- (156) Mo, H.; Henriksson, M. Identification of Small Molecules That Induce Apoptosis in a Myc-Dependent Manner and Inhibit Myc-Driven Transformation. *Proc. Natl. Acad. Sci.* **2006**, *103* (16), 6344–6349. <https://doi.org/10.1073/pnas.0601418103>.



- (157) Wang, H.; Teriete, P.; Hu, A.; Raveendra-Panickar, D.; Pendelton, K.; Lazo, J. S.; Eiseman, J.; Holien, T.; Misund, K.; Oliynyk, G.; et al. Direct Inhibition of C-Myc-Max Heterodimers by Celastrol and Celastrol-Inspired Triterpenoids. *Oncotarget* **2015**, *6* (32). <https://doi.org/10.18632/oncotarget.6116>.
- (158) Jeong, K. C.; Ahn, K. O.; Yang, C. H. Small-Molecule Inhibitors of c-Myc Transcriptional Factor Suppress Proliferation and Induce Apoptosis of Promyelocytic Leukemia Cell via Cell Cycle Arrest. *Mol. Biosyst.* **2010**, *6* (8), 1503–1509. <https://doi.org/10.1039/c002534h>.
- (159) Jeong, K. C.; Kim, K. T.; Seo, H. H.; Shin, S. P.; Ahn, K. O.; Ji, M. J.; Park, W. S.; Kim, I. H.; Lee, S. J.; Seo, H. K. Intravesical Instillation of C-MYC Inhibitor KSI-3716 Suppresses Orthotopic Bladder Tumor Growth. *J. Urol.* **2014**, *191* (2), 510–518. <https://doi.org/10.1016/j.juro.2013.07.019>.
- (160) Jung, K. Y.; Wang, H.; Teriete, P.; Yap, J. L.; Chen, L.; Lanning, M. E.; Hu, A.; Lambert, L. J.; Holien, T.; Sundan, A.; et al. Perturbation of the C-Myc-Max Protein-Protein Interaction via Synthetic  $\alpha$ -Helix Mimetics. *J. Med. Chem.* **2015**, *58* (7), 3002–3024. <https://doi.org/10.1021/jm501440q>.
- (161) Soucek, L.; Helmer-Citterich, M.; Sacco, A.; Jucker, R.; Cesareni, G.; Nasi, S. Design and Properties of a Myc Derivative That Efficiently Homodimerizes. *Oncogene* **1998**, *17* (19), 2463–2472. <https://doi.org/10.1038/sj.onc.1202199>.
- (162) Soucek, L.; Nasi, S.; Evan, G. I. Omomyc Expression in Skin Prevents Myc-Induced Papillomatosis. *Cell Death Differ.* **2004**, *11* (9), 1038–1045. <https://doi.org/10.1038/sj.cdd.4401443>.
- (163) Soucek, L.; Whitfield, J.; Martins, C. P.; Finch, A. J.; Murphy, D. J.; Sodik, N. M.; Karnezis, A. N.; Swigart, L. B.; Nasi, S.; Evan, G. I. Modelling Myc Inhibition as a Cancer Therapy. *Nature* **2008**, *455* (7213), 679–683. <https://doi.org/10.1038/nature07260>.
- (164) Soucek, L.; Whitfield, J. R.; Sodik, N. M.; Massó-Vallés, D.; Serrano, E.; Karnezis, A. N.; Swigart, L. B.; Evan, G. I. Inhibition of Myc Family Proteins Eradicates KRas-Driven Lung Cancer in Mice. *Genes Dev.* **2013**, *27* (5), 504–513. <https://doi.org/10.1101/gad.205542.112>.
- (165) Galardi, S.; Savino, M.; Scagnoli, F.; Pellegatta, S.; Pisati, F.; Zambelli, F.; Illi, B.; Annibali, D.; Beji, S.; Orecchini, E.; et al. Resetting Cancer Stem Cell Regulatory Nodes upon MYC Inhibition. *EMBO Rep.* **2016**, *17* (12), 1872–1889.

- <https://doi.org/10.15252/embr.201541489>.
- (166) Giorello, L.; Clerico, L.; Pescarolo, M. P.; Vikhanskaya, F.; Salmona, M.; Colella, G.; Bruno, S.; Mancuso, T.; Bagnasco, L.; Russo, P.; et al. Inhibition of Cancer Cell Growth and C-Myc Transcriptional Activity by a c-Myc Helix 1-Type Peptide Fused to an Internalization Sequence. *Cancer Res.* **1998**, *58* (16), 3654–3659.
- (167) Bidwell, G. L.; Perkins, E.; Hughes, J.; Khan, M.; James, J. R.; Raucher, D. Thermally Targeted Delivery of a C-Myc Inhibitory Polypeptide Inhibits Tumor Progression and Extends Survival in a Rat Glioma Model. *PLoS One* **2013**, *8* (1). <https://doi.org/10.1371/journal.pone.0055104>.
- (168) Pérez-Salvia, M.; Esteller, M. Bromodomain Inhibitors and Cancer Therapy: From Structures to Applications. *Epigenetics* **2017**, *12* (5), 323–339. <https://doi.org/10.1080/15592294.2016.1265710>.
- (169) Delmore, J. E.; Issa, G. C.; Lemieux, M. E.; Rahl, P. B.; Shi, J.; Jacobs, H. M.; Kastiris, E.; Gilpatrick, T.; Paranal, R. M.; Qi, J.; et al. BET Bromodomain Inhibition as a Therapeutic Strategy to Target C-Myc. *Cell* **2011**, *146* (6), 904–917. <https://doi.org/10.1016/j.cell.2011.08.017>.
- (170) Filippakopoulos, P.; Qi, J.; Picaud, S.; Shen, Y.; Smith, W. B.; Fedorov, O.; Morse, E. M.; Keates, T.; Hickman, T. T.; Felletar, I.; et al. Selective Inhibition of BET Bromodomains. *Nature* **2010**, *468* (7327), 1067–1073. <https://doi.org/10.1038/nature09504>.
- (171) Yang, Z.; Yik, J. H. N.; Chen, R.; He, N.; Moon, K. J.; Ozato, K.; Zhou, Q. Recruitment of P-TEFb for Stimulation of Transcriptional Elongation by the Bromodomain Protein Brd4. *Mol. Cell* **2005**, *19* (4), 535–545. <https://doi.org/10.1016/j.molcel.2005.06.029>.
- (172) Cortiguera, M. G.; Batlle-López, A.; Albajar, M.; Delgado, M. D.; Leon, J. MYC as Therapeutic Target in Leukemia and Lymphoma. *Blood Lymphat. Cancer Targets Ther.* **2015**, No. July, 75. <https://doi.org/10.2147/blctt.s60495>.
- (173) Rahl, P. B.; Lin, C. Y.; Seila, A. C.; Flynn, R. A.; McCuine, S.; Burge, C. B.; Sharp, P. A.; Young, R. A. C-Myc Regulates Transcriptional Pause Release. *Cell* **2010**, *141* (3), 432–445. <https://doi.org/10.1016/j.cell.2010.03.030>.
- (174) Mertz, J. A.; Conery, A. R.; Bryant, B. M.; Sandy, P.; Balasubramanian, S.; Mele, D. A.; Bergeron, L.; Sims, R. J. Targeting MYC Dependence in Cancer by Inhibiting BET Bromodomains. *Proc. Natl. Acad. Sci.* **2011**, *108* (40), 16669–16674.

- <https://doi.org/10.1073/pnas.1108190108>.
- (175) Andrieu, G.; Belkina, A. C.; Denis, G. V. Clinical Trials for BET Inhibitors Run Ahead of the Science. *Drug Discov. Today Technol.* **2016**, *19*, 45–50. <https://doi.org/10.1016/j.ddtec.2016.06.004>.
- (176) Liu, S.; Walker, S. R.; Nelson, E. A.; Cerulli, R.; Xiang, M.; Toniolo, P. A.; Qi, J.; Stone, R. M.; Wadleigh, M.; Bradner, J. E.; et al. Targeting STAT5 in Hematologic Malignancies through Inhibition of the Bromodomain and Extra-Terminal (BET) Bromodomain Protein BRD2. *Mol. Cancer Ther.* **2014**, *13* (5), 1194–1205. <https://doi.org/10.1158/1535-7163.mct-13-0341>.
- (177) Hogg, S. J.; Vervoort, S. J.; Deswal, S.; Ott, C. J.; Li, J.; Cluse, L. A.; Beavis, P. A.; Darcy, P. K.; Martin, B. P.; Spencer, A.; et al. BET-Bromodomain Inhibitors Engage the Host Immune System and Regulate Expression of the Immune Checkpoint Ligand PD-L1. *Cell Rep.* **2017**, *18* (9), 2162–2174. <https://doi.org/10.1016/j.celrep.2017.02.011>.
- (178) Feng, Q.; Zhang, Z.; Shea, M. J.; Creighton, C. J.; Coarfa, C.; Hilsenbeck, S. G.; Lanz, R.; He, B.; Wang, L.; Fu, X.; et al. An Epigenomic Approach to Therapy for Tamoxifen-Resistant Breast Cancer. *Cell Res.* **2014**, *24* (7), 809–819. <https://doi.org/10.1038/cr.2014.71>.
- (179) Alqahtani, A.; Choucair, K.; Ashraf, M.; Hammouda, D. M.; Alloghbi, A.; Khan, T.; Senzer, N.; Nemunaitis, J. Bromodomain and Extra-Terminal Motif Inhibitors: A Review of Preclinical and Clinical Advances in Cancer Therapy. *Futur. Sci. OA* **2019**, *5* (3), FSO372. <https://doi.org/10.4155/fsoa-2018-0115>.
- (180) Bui, M. H.; Lin, X.; Albert, D. H.; Li, L.; Lam, L. T.; Faivre, E. J.; Warder, S. E.; Huang, X.; Wilcox, D.; Donawho, C. K.; et al. Preclinical Characterization of BET Family Bromodomain Inhibitor ABBV-075 Suggests Combination Therapeutic Strategies. *Cancer Res.* **2017**, *77* (11), 2976–2989. <https://doi.org/10.1158/0008-5472.CAN-16-1793>.
- (181) Chaidos, A.; Caputo, V.; Gouvedenou, K.; Liu, B.; Marigo, I.; Chaudhry, M. S.; Rotolo, A.; Tough, D. F.; Smithers, N. N.; Bassil, A. K.; et al. Potent Antimyeloma Activity of the Novel Bromodomain Inhibitors. *Blood* **2014**, *123* (5), 697–706. <https://doi.org/10.1182/blood-2013-01-478420>.The.
- (182) Chen, H.; Liu, H.; Qing, G. Targeting Oncogenic Myc as a Strategy for Cancer Treatment. *Signal Transduct. Target. Ther.* **2018**, *3* (1), 1–7. <https://doi.org/10.1038/s41392-018-0008->

7.

- (183) Heidemann, M.; Hintermair, C.; Voß, K.; Eick, D. Dynamic Phosphorylation Patterns of RNA Polymerase II CTD during Transcription. *Biochim. Biophys. Acta - Gene Regul. Mech.* **2013**, *1829* (1), 55–62. <https://doi.org/10.1016/j.bbagr.2012.08.013>.
- (184) Chipumuro, E.; Marco, E.; Christensen, C. L.; Kwiatkowski, N.; Zhang, T.; Hatheway, C. M.; Abraham, B. J.; Sharma, B.; Yeung, C.; Altabef, A.; et al. CDK7 Inhibition Suppresses Super-Enhancer-Linked Oncogenic Transcription in MYCN-Driven Cancer. *Cell* **2014**, *159* (5), 1126–1139. <https://doi.org/10.1016/j.cell.2014.10.024>.
- (185) Christensen, C. L.; Kwiatkowski, N.; Abraham, B. J.; Carretero, J.; Al-Shahrour, F.; Zhang, T.; Chipumuro, E.; Herter-Sprrie, G. S.; Akbay, E. A.; Altabef, A.; et al. Targeting Transcriptional Addictions in Small Cell Lung Cancer with a Covalent CDK7 Inhibitor. *Cancer Cell* **2014**, *26* (6), 909–922. <https://doi.org/10.1016/j.ccell.2014.10.019>.
- (186) Wang, Y.; Zhang, T.; Kwiatkowski, N.; Abraham, B. J.; Lee, T. I.; Xie, S.; Yuzugullu, H.; Von, T.; Li, H.; Lin, Z.; et al. CDK7-Dependent Transcriptional Addiction in Triple-Negative Breast Cancer. *Cell* **2015**, *163* (1), 174–186. <https://doi.org/10.1016/j.cell.2015.08.063>.
- (187) Castell, A.; Larsson, L. G. Targeting MYC Translation in Colorectal Cancer. *Cancer Discov.* **2015**, *5* (7), 701–703. <https://doi.org/10.1158/2159-8290.CD-15-0660>.
- (188) Sonenberg, N.; Pause, A. Protein Synthesis and Oncogenesis Meet Again. *Science* **2006**, *314* (5798), 428–429.
- (189) Wiegering, A.; Uthe, F. W.; Jamieson, T.; Ruoss, Y.; Huttenrauch, M.; Kuspert, M.; Pfann, C.; Nixon, C.; Herold, S.; Walz, S.; et al. Targeting Translation Initiation Bypasses Signaling Crosstalk Mechanisms That Maintain High MYC Levels in Colorectal Cancer. *Cancer Discov.* **2015**, *5* (7), 768–881. <https://doi.org/10.1158/2159-8290.CD-14-1040>.
- (190) Polivka, J.; Janku, F. Molecular Targets for Cancer Therapy in the PI3K/AKT/MTOR Pathway. *Pharmacol. Ther.* **2014**, *142* (2), 164–175. <https://doi.org/10.1016/j.pharmthera.2013.12.004>.
- (191) Sun, X. X.; Sears, R. C.; Dai, M. S. Deubiquitinating C-Myc: USP36 Steps up in the Nucleolus. *Cell Cycle* **2015**, *14* (24), 3786–3793. <https://doi.org/10.1080/15384101.2015.1093713>.
- (192) Huang, H.-L.; Weng, H.-Y.; Wang, L.-Q.; Yu, C.-H.; Huang, Q.-J.; Zhao, P.-P.; Wen, J.-

- Z.; Zhou, H.; Qu, L.-H. Triggering Fbw7-Mediated Proteasomal Degradation of c-Myc by Oridonin Induces Cell Growth Inhibition and Apoptosis. *Mol. Cancer Ther.* **2012**, *11* (5), 1155–1165. <https://doi.org/10.1158/1535-7163.mct-12-0066>.
- (193) Ding, Y.; Ding, C.; Ye, N.; Liu, Z.; Wold, E. A.; Chen, H.; Wild, C.; Shen, Q.; Zhou, J. Discovery and Development of Natural Product Oridonin-Inspired Anticancer Agents. *Eur. J. Med. Chem.* **2016**, *122*, 102–117. <https://doi.org/10.1097/CCM.0b013e31823da96d.Hydrogen>.
- (194) Peter, S.; Bultinck, J.; Myant, K.; Jaenicke, L. A.; Walz, S.; Muller, J.; Gmachl, M.; Treu, M.; Boehmelt, G.; Ade, C. P.; et al. Tumor Cell-Specific Inhibition of MYC Function Using Small Molecule Inhibitors of the HUWE1 Ubiquitin Ligase. *EMBO Mol. Med.* **2014**, *6* (12), 1525–1541. <https://doi.org/10.15252/emmm.201403927>.
- (195) Otto, T.; Horn, S.; Brockmann, M.; Eilers, U.; Schüttrumpf, L.; Popov, N.; Kenney, A. M.; Schulte, J. H.; Beijersbergen, R.; Christiansen, H.; et al. Stabilization of N-Myc Is a Critical Function of Aurora A in Human Neuroblastoma. *Cancer Cell* **2009**, *15* (1), 67–78. <https://doi.org/10.1016/j.ccr.2008.12.005>.
- (196) Brockmann, M.; Poon, E.; Berry, T.; Carstensen, A.; Deubzer, H. E.; Rycak, L.; Jamin, Y.; Thway, K.; Robinson, S. P.; Roels, F.; et al. Small Molecule Inhibitors of Aurora-A Induce Proteasomal Degradation of N-Myc in Childhood Neuroblastoma. *Cancer Cell* **2013**, *24* (1), 75–89. <https://doi.org/10.1016/j.ccr.2013.05.005>.
- (197) Schapira, M.; Tyers, M.; Torrent, M.; Arrowsmith, C. H. WD40 Repeat Domain Proteins: A Novel Target Class? *Nature Reviews Drug Discovery*. 2017, pp 773–786. <https://doi.org/10.1038/nrd.2017.179>.
- (198) Stirnimann, C.; Petsalaki, E.; Russell, R.; Muller, C. WD40 Proteins Propel Cellular Networks. *Trends Biochem. Sci.* **2010**, *35* (10), 565–574. <https://doi.org/10.1016/j.tibs.2010.04.003>.
- (199) Gori, F.; Divieti, P.; Demay, M. B. Cloning and Characterization of a Novel WD-40 Repeat Protein That Dramatically Accelerates Osteoblastic Differentiation. *J. Biol. Chem.* **2001**, *276* (49), 46515–46522. <https://doi.org/10.1074/jbc.M105757200>.
- (200) Gori, F.; Friedman, L. G.; Demay, M. B. Wdr5, a WD-40 Protein, Regulates Osteoblast Differentiation during Embryonic Bone Development. *Dev. Biol.* **2006**, *295* (2), 498–506. <https://doi.org/10.1016/j.ydbio.2006.02.031>.

- (201) Guarnaccia, A.; Tansey, W. Moonlighting with WDR5: A Cellular Multitasker. *J. Clin. Med.* **2018**, *7* (2), 1–17. <https://doi.org/10.3390/jcm7020021>.
- (202) Gori, F.; Demay, M. B. BIG-3, a Novel WD-40 Repeat Protein, Is Expressed in the Developing Growth Plate and Accelerates Chondrocyte Differentiation in Vitro. *Endocrinology* **2004**, *145* (3), 1050–1054. <https://doi.org/10.1210/en.2003-1314>.
- (203) Gori, F.; Zhu, E. D.; Demay, M. B. Perichondrial Expression of Wdr5 Regulates Chondrocyte Proliferation and Differentiation. *Dev. Biol.* **2009**, *329* (1), 36–43. <https://doi.org/10.1016/j.ydbio.2009.02.006>.
- (204) Zhu, S.; Zhu, E. D.; Provot, S.; Gori, F. Wdr5 Is Required for Chick Skeletal Development. *J. Bone Miner. Res.* **2010**, *25* (11), 2504–2514. <https://doi.org/10.1002/jbmr.144>.
- (205) Roguev, A.; Schaft, D.; Shevchenko, A.; Pijnappel, W. W. M. P.; Wilm, M.; Aasland, R.; Stewart, A. F. The Saccharomyces Cerevisiae Set1 Complex Includes an Ash2 Homologue and Methylates Histone 3 Lysine 4. *EMBO J.* **2001**, *20* (24), 7137–7148. <https://doi.org/10.1093/emboj/20.24.7137>.
- (206) Wysocka, J.; Swigut, T.; Milne, T. A.; Dou, Y.; Zhang, X.; Burlingame, A. L.; Roeder, R. G.; Brivanlou, A. H.; Allis, C. D. WDR5 Associates with Histone H3 Methylated at K4 and Is Essential for H3 K4 Methylation and Vertebrate Development. *Cell* **2005**, *121* (6), 859–872. <https://doi.org/10.1016/j.cell.2005.03.036>.
- (207) Ang, Y. S.; Tsai, S. Y.; Lee, D. F.; Monk, J.; Su, J.; Ratnakumar, K.; Ding, J.; Ge, Y.; Darr, H.; Chang, B.; et al. Wdr5 Mediates Self-Renewal and Reprogramming via the Embryonic Stem Cell Core Transcriptional Network. *Cell* **2011**, *145* (2), 183–197. <https://doi.org/10.1016/j.cell.2011.03.003>.
- (208) Bailey, J. K.; Fields, A. T.; Cheng, K.; Lee, A.; Wagenaar, E.; Lagrois, R.; Schmidt, B.; Xia, B.; Ma, D. WD Repeat-Containing Protein 5 (WDR5) Localizes to the Midbody and Regulates Abcission. *J. Biol. Chem.* **2015**, *290* (14), 8987–9001. <https://doi.org/10.1074/jbc.M114.623611>.
- (209) Hu, C.-K.; Coughlin, M.; Mitchison, T. J. Midbody Assembly and Its Regulation during Cytokinesis. *Mol. Biol. Cell* **2012**, *23* (6), 1024–1034. <https://doi.org/10.1091/mbc.e11-08-0721>.
- (210) Ali, A.; Veeranki, S. N.; Chinchole, A.; Tyagi, S. MLL/WDR5 Complex Regulates Kif2A Localization to Ensure Chromosome Congression and Proper Spindle Assembly during

- Mitosis. *Dev. Cell* **2017**, *41* (6), 605-622.e7. <https://doi.org/10.1016/j.devcel.2017.05.023>.
- (211) Schuettengruber, B.; Martinez, A. M.; Iovino, N.; Cavalli, G. Trithorax Group Proteins: Switching Genes on and Keeping Them Active. *Nat. Rev. Mol. Cell Biol.* **2011**, *12* (12), 799–814. <https://doi.org/10.1038/nrm3230>.
- (212) Protein-, L.; Odho, Z.; Southall, S. M.; Jon, R. Characterization of a Novel WDR5-Binding Site That Recruits RbBP5 through a Conserved Motif to Enhance Methylation of Histone H3 Lysine 4 by Mixed Lineage Leukemia Protein-1. *J. Biol. Chem.* **2010**, *285* (43), 32967–32976. <https://doi.org/10.1074/jbc.M110.159921>.
- (213) Patel, A.; Vought, V. E.; Dharmarajan, V.; Cosgrove, M. S. A Conserved Arginine-Containing Motif Crucial for the Assembly and Enzymatic Activity of the Mixed Lineage Leukemia Protein-1 Core Complex. *J. Biol. Chem.* **2008**, *283* (47), 32162–32175. <https://doi.org/10.1074/jbc.M806317200>.
- (214) Patel, A.; Dharmarajan, V.; Cosgrove, M. S. Structure of WDR5 Bound to Mixed Lineage Leukemia Protein-1 Peptide. *J. Biol. Chem.* **2008**, *283* (47), 32158–32161. <https://doi.org/10.1074/jbc.C800164200>.
- (215) Su, J.; Wang, F.; Cai, Y.; Jin, J. The Functional Analysis of Histone Acetyltransferase MOF in Tumorigenesis. *Int. J. Mol. Sci.* **2016**, *17* (1). <https://doi.org/10.3390/ijms17010099>.
- (216) Dias, J.; Van Nguyen, N.; Georgiev, P.; Gaub, A.; Brettschneider, J.; Cusack, S.; Kadlec, J.; Akhtar, A. Structural Analysis of the KANSL1/WDR5/ KANSL2 Complex Reveals That WDR5 Is Required for Efficient Assembly and Chromatin Targeting of the NSL Complex. *Genes Dev.* **2014**, *28* (9), 929–942. <https://doi.org/10.1101/gad.240200.114>.
- (217) Zhao, X.; Su, J.; Wang, F.; Liu, D.; Ding, J.; Yang, Y.; Conaway, J. W.; Conaway, R. C.; Cao, L.; Wu, D.; et al. Crosstalk between NSL Histone Acetyltransferase and MLL/SET Complexes: NSL Complex Functions in Promoting Histone H3K4 Di-Methylation Activity by MLL/SET Complexes. *PLoS Genet.* **2013**, *9* (11). <https://doi.org/10.1371/journal.pgen.1003940>.
- (218) Basta, J.; Rauchman, M. The Nucleosome Remodeling and Deacetylase Complex in Development and Disease. *Transl. Epigenetics to Clin.* **2017**, *165* (1), 37–72. <https://doi.org/10.1016/B978-0-12-800802-7.00003-4>.
- (219) Bode, D.; Yu, L.; Tate, P.; Pardo, M.; Choudhary, J. Characterization of Two Distinct Nucleosome Remodeling and Deacetylase (NuRD) Complex Assemblies in Embryonic

- Stem Cells. *Mol. Cell. Proteomics* **2016**, *15* (3), 878–891. <https://doi.org/10.1074/mcp.m115.053207>.
- (220) Thompson, B. A.; Tremblay, V.; Lin, G.; Bochar, D. A. CHD8 Is an ATP-Dependent Chromatin Remodeling Factor That Regulates  $\beta$ -Catenin Target Genes. *Mol. Cell. Biol.* **2008**, *28* (12), 3894–3904. <https://doi.org/10.1128/mcb.00322-08>.
- (221) Wang, L.; Du, Y.; Ward, J. M.; Shimbo, T.; Lackford, B.; Zheng, X.; Miao, Y. L.; Zhou, B.; Han, L.; Fargo, D. C.; et al. INO80 Facilitates Pluripotency Gene Activation in Embryonic Stem Cell Self-Renewal, Reprogramming, and Blastocyst Development. *Cell Stem Cell* **2014**, *14* (5), 575–591. <https://doi.org/10.1016/j.stem.2014.02.013>.
- (222) Suganuma, T.; Gutiérrez, J. L.; Li, B.; Florens, L.; Swanson, S. K.; Washburn, M. P.; Abmayr, S. M.; Workman, J. L. ATAC Is a Double Histone Acetyltransferase Complex That Stimulates Nucleosome Sliding. *Nat. Struct. Mol. Biol.* **2008**, *15* (4), 364–372. <https://doi.org/10.1038/nsmb.1397>.
- (223) Vilhais-Neto, G. C.; Fournier, M.; Plassat, J. L.; Sardu, M. E.; Saraf, A.; Garnier, J. M.; Maruhashi, M.; Florens, L.; Washburn, M. P.; Pourquié, O. The WHHERE Coactivator Complex Is Required for Retinoic Acid-Dependent Regulation of Embryonic Symmetry. *Nat. Commun.* **2017**, *8* (1). <https://doi.org/10.1038/s41467-017-00593-6>.
- (224) Wang, K. C.; Yang, Y. W.; Liu, B.; Sanyal, A.; Corces-Zimmerman, R.; Chen, Y.; Lajoie, B. R.; Protacio, A.; Flynn, R. A.; Gupta, R. A.; et al. A Long Noncoding RNA Maintains Active Chromatin to Coordinate Homeotic Gene Expression. *Nature* **2011**, *472* (7341), 120–126. <https://doi.org/10.1038/nature09819>.
- (225) Yang, Y. W.; Flynn, R. A.; Chen, Y.; Qu, K.; Wan, B.; Wang, K. C.; Lei, M.; Chang, H. Y. Essential Role of LncRNA Binding for WDR5 Maintenance of Active Chromatin and Embryonic Stem Cell Pluripotency. *Elife* **2014**, *3*. <https://doi.org/10.7554/eLife.02046>.
- (226) Ullius, A.; Lüscher-Firzlaff, J.; Costa, I. G.; Walsemann, G.; Forst, A. H.; Gusmao, E. G.; Kapelle, K.; Kleine, H.; Kremmer, E.; Vervoorts, J.; et al. The Interaction of MYC with the Trithorax Protein ASH2L Promotes Gene Transcription by Regulating H3K27 Modification. *Nucleic Acids Res.* **2014**, *42* (11), 6901–6920. <https://doi.org/10.1093/nar/gku312>.
- (227) Sun, Y.; Bell, J. L.; Carter, D.; Gherardi, S.; Poulos, R. C.; Milazzo, G.; Wong, J. W. H.; Al-Awar, R.; Tee, A. E.; Liu, P. Y.; et al. WDR5 Supports an N-Myc Transcriptional



- Complex That Drives a Protumorigenic Gene Expression Signature in Neuroblastoma. *Cancer Res.* **2015**, *75* (23), 5143–5154. <https://doi.org/10.1158/0008-5472.CAN-15-0423>.
- (228) Carugo, A.; Seth, S.; Heffernan, T. P. In Vivo Functional Platform Targeting Patient-Derived Xenografts Identifies WDR5-Myc Association as a Critical Determinant of Pancreatic Cancer. *Cell Rep.* **2016**, *16*, 133–147. <https://doi.org/10.1016/j.celrep.2016.05.063>.
- (229) Thomas, L. R.; Adams, C. M.; Wang, J.; Weissmiller, A. M.; Creighton, J.; Lorey, S. L.; Liu, Q.; Fesik, S. W.; Eischen, C. M.; Tansey, W. P. Interaction of the Oncoprotein Transcription Factor MYC with Its Chromatin Cofactor WDR5 Is Essential for Tumor Maintenance. *Proc. Natl. Acad. Sci.* **2019**, *116* (50), 25260–25268. <https://doi.org/10.1073/PNAS.1910391116>.
- (230) Thomas, L. R.; Foshage, A. M.; Weissmiller, A. M.; Tansey, W. P. The MYC – WDR5 Nexus and Cancer. **2015**, *75* (19), 4012–4016. <https://doi.org/10.1158/0008-5472.CAN-15-1216>.
- (231) Macdonald, J. D.; Chacón Simon, S.; Han, C.; Wang, F.; Shaw, J. G.; Howes, J. E.; Sai, J.; Yuh, J. P.; Camper, D.; Alicie, B. M.; et al. Discovery and Optimization of Salicylic Acid-Derived Sulfonamide Inhibitors of the WD Repeat-Containing Protein 5–MYC Protein–Protein Interaction. *J. Med. Chem.* **2019**, *62* (24), 11232–11259. <https://doi.org/10.1021/acs.jmedchem.9b01411>.
- (232) Karatas, H.; Townsend, E. C.; Bernard, D.; Dou, Y.; Wang, S. Analysis of the Binding of Mixed Lineage Leukemia 1 (MLL1) and Histone 3 Peptides to WD Repeat Domain 5 (WDR5) for the Design of Inhibitors of the MLL1-WDR5 Interaction. *J. Med. Chem.* **2010**, *53* (14), 5179–5185. <https://doi.org/10.1021/jm100139b>.
- (233) Altomonte, S.; Zanda, M. Synthetic Chemistry and Biological Activity of Pentafluorosulphonyl (SF 5) Organic Molecules. *J. Fluor. Chem.* **2012**, *143*, 57–93. <https://doi.org/10.1016/j.jfluchem.2012.06.030>.
- (234) Nicholls, A.; McGaughey, G. B.; Sheridan, R. P.; Good, A. C.; Warren, G.; Mathieu, M.; Muchmore, S. W.; Brown, S. P.; Grant, J. A.; Haigh, J. A.; et al. Molecular Shape and Medicinal Chemistry: A Perspective. *J. Med. Chem.* **2010**, *53* (10), 3862–3886. <https://doi.org/10.1021/jm900818s>.
- (235) Kramer, S. E.; Routh, J. I. The Binding of Salicylic Acid and Acetylsalicylic Acid to Human

- Serum Albumin. *Clin. Biochem.* **1973**, *6* (C), 98–105. [https://doi.org/10.1016/S0009-9120\(73\)80018-9](https://doi.org/10.1016/S0009-9120(73)80018-9).
- (236) Sun, X.; Qiu, J. Dihydropyrimidin-2(1H)-One Compounds as S-Nitrosoglutathione Reductase Inhibitors. US 9,067,893 B2, 2015.
- (237) Zhu, W.; Ma, D. Synthesis of Aryl Sulfones via L-Proline-Promoted CuI-Catalyzed Coupling Reaction of Aryl Halides with Sulfinic Acid Salts. *J. Org. Chem.* **2005**, *70* (7), 2696–2700. <https://doi.org/10.1021/jo047758b>.
- (238) Wadas, T.; Wong, E.; Weisman, G.; Anderson, C. Copper Chelation Chemistry and Its Role in Copper Radiopharmaceuticals. *Curr. Pharm. Des.* **2006**, *13* (1), 3–16. <https://doi.org/10.2174/138161207779313768>.
- (239) Itoh, T.; Mase, T. A General Palladium-Catalyzed Coupling of Aryl Bromides/Triflates and Thiols. *Org. Lett.* **2004**, *6* (24), 4587–4590. <https://doi.org/10.1021/ol047996t>.
- (240) Eiffe, E.; Heaton, A.; Gunning, P.; Treutlein, H.; Zeng, J.; James, I.; Dixon, I. Functionalised and Substituted Indoles as Anti-Cancer Agents. WO/2016/187667, 2016.
- (241) Hajduk, P. J.; Mendoza, R.; Petros, A. M.; Huth, J. R.; Bures, M.; Fesik, S. W.; Martin, Y. C. Ligand Binding to Domain-3 of Human Serum Albumin: A Chemometric Analysis. *J. Comput. Aided. Mol. Des.* **2003**, *17* (10), 711. <https://doi.org/10.1023/B:JCAM.0000017395.85772.7e>.
- (242) Caira, M. Pathways of Biotransformation — Phase II Reactions. In *Drug Metabolism*; Springer-Verlag: Berlin/Heidelberg, 2006; pp 129–170. [https://doi.org/10.1007/1-4020-4142-X\\_3](https://doi.org/10.1007/1-4020-4142-X_3).
- (243) Rietjens, I. M. C. M.; Besten, C. Den; Hanzlik, R. P.; Van Bladeren, P. J. Cytochrome P450-Catalyzed Oxidation of Halobenzene Derivatives. *Chem. Res. Toxicol.* **1997**, *10* (6), 629–635. <https://doi.org/10.1021/tx9601061>.
- (244) Ionescu, C. Pathways of Biotransformation --- Phase II Reactions. In *Drug Metabolism: Current Concepts*; Caira, M. R., Ed.; Springer: Dordrecht, 2005; pp 129–170. [https://doi.org/10.1007/1-4020-4142-X\\_3](https://doi.org/10.1007/1-4020-4142-X_3).
- (245) Meanwell, N. A. Fluorine and Fluorinated Motifs in the Design and Application of Bioisosteres for Drug Design. *J. Med. Chem.* **2018**, *61* (14), 5822–5880. <https://doi.org/10.1021/acs.jmedchem.7b01788>.
- (246) Bohnert, T.; Gan, L. S. Plasma Protein Binding: From Discovery to Development. *J. Pharm.*

- Sci.* **2013**, *102* (9), 2953–2994. <https://doi.org/10.1002/jps.23614>.
- (247) Liu, Y.; Kim, J.; Seo, H.; Park, S.; Chae, J. Copper(II)-Catalyzed Single-Step Synthesis of Aryl Thiols from Aryl Halides and 1,2-Ethanedithiol. *Adv. Synth. Catal.* **2015**, *357* (10), 2205–2212. <https://doi.org/10.1002/adsc.201400941>.
- (248) Yin, J.; Buchwald, S. L. Pd-Catalyzed Intermolecular Amidation of Aryl Halides: The Discovery That Xantphos Can Be Trans-Chelating in a Palladium Complex. *J. Am. Chem. Soc.* **2002**, *124* (21), 6043–6048. <https://doi.org/10.1021/ja012610k>.
- (249) Belpaire, F.; Marc, B. The Fate of Xenobiotics in Living Organisms. In *The Practice of Medicinal Chemistry*; Wermuth, C., Ed.; Elsevier: San Diego, 2003; pp 501–517.
- (250) Bohnert, T.; Gan, L. Plasma Protein Binding: From Discovery to Development. *J. Pharm. Sci.* **2013**, *102* (9), 2953–2994. <https://doi.org/10.1002/jps.23614>.
- (251) Kadam, S., Bothara, K., Mahadik, K. Sulfonamides and Urinary Tract Antiseptic Agents. In *Principles of Medicinal Chemistry*; Nirali Prakashan: Mumbai, 2007; pp 49–52.
- (252) Du, X.; Li, Y.; Xia, Y. L.; Ai, S. M.; Liang, J.; Sang, P.; Ji, X. L.; Liu, S. Q. Insights into Protein–Ligand Interactions: Mechanisms, Models, and Methods. *Int. J. Mol. Sci.* **2016**, *17* (2), 1–34. <https://doi.org/10.3390/ijms17020144>.
- (253) Chen, I. J.; Foloppe, N. *Thermodynamics in Drug Design. High Affinity and Selectivity*; 2005; Vol. 48. <https://doi.org/10.1021/ci800130k>.
- (254) Peach, M. L.; Cachau, R. E.; Nicklaus, M. C. Conformational Energy Range of Ligands in Protein Crystal Structures: The Difficult Quest for Accurate Understanding. *J. Mol. Recognit.* **2017**, *30* (8), 1–14. <https://doi.org/10.1002/jmr.2618>.
- (255) Gao, C.; Park, M. S.; Stern, H. A. Accounting for Ligand Conformational Restriction in Calculations of Protein-Ligand Binding Affinities. *Biophys. J.* **2010**, *98* (5), 901–910. <https://doi.org/10.1016/j.bpj.2009.11.018>.
- (256) Freire, E. Thermodynamics in Drug Design. High Affinity and Selectivity. In *The chemical theatre of biological systems, Beilstein-Institute*; Bozen, Italy, 2004; pp 1–13.
- (257) Kumar, E. A.; Chen, Q.; Kizhake, S.; Kolar, C.; Kang, M.; Chang, C. E. A.; Borgstahl, G. E. O.; Natarajan, A. The Paradox of Conformational Constraint in the Design of Cbl(TKB)-Binding Peptides. *Sci. Rep.* **2013**, *3*, 1–7. <https://doi.org/10.1038/srep01639>.
- (258) Johannes, J. W.; Bates, S.; Beigie, C.; Belmonte, M. A.; Breen, J.; Cao, S.; Centrella, P. A.; Clark, M. A.; Cuzzo, J. W.; Dumelin, C. E.; et al. Structure Based Design of Non-Natural

- Peptidic Macrocyclic Mel-1 Inhibitors. *ACS Med. Chem. Lett.* **2017**, *8* (2), 239–244. <https://doi.org/10.1021/acsmchemlett.6b00464>.
- (259) Ishiyama, T.; Murata, M.; Miyaura, N. Palladium(0)-Catalyzed Cross-Coupling Reaction of Alkoxydiboron with Haloarenes: A Direct Procedure for Arylboronic Esters. *J. Org. Chem.* **1995**, *60* (23), 7508–7510. <https://doi.org/10.1021/jo00128a024>.
- (260) Ni, W.; Fang, H.; Springsteen, G.; Wang, B. The Design of Boronic Acid Spectroscopic Reporter Compounds by Taking Advantage of the PKa-Lowering Effect of Diol Binding: Nitrophenol-Based Color Reporters for Diols. *J. Org. Chem.* **2004**, *69* (6), 1999–2007. <https://doi.org/10.1021/jo0350357>.
- (261) Kayaki, Y.; Koda, T.; Ikariya, T. A Highly Effective (Triphenyl Phosphite)Palladium Catalyst for a Cross-Coupling Reaction of Allylic Alcohols with Organoboronic Acids. *European J. Org. Chem.* **2004**, No. 24, 4989–4993. <https://doi.org/10.1002/ejoc.200400621>.
- (262) Shuker, S. B.; Hajduk, P. J.; Meadows, R. P.; Fesik, S. W. Discovering High-Affinity Ligands for Proteins: SAR by NMR. *Science* **1996**, *274* (5292), 1531–1534. <https://doi.org/10.1126/science.274.5292.1531>.
- (263) Scott, D. E.; Coyne, A. G.; Hudson, S. A.; Abell, C. Fragment-Based Approaches in Drug Discovery and Chemical Biology. *Biochemistry* **2012**, *51* (25), 4990–5003. <https://doi.org/10.1021/bi3005126>.
- (264) Harner, M. J.; Frank, A. O.; Fesik, S. W. Fragment-Based Drug Discovery Using NMR Spectroscopy. *J. Biomol. NMR* **2013**, *56* (2), 65–75. <https://doi.org/10.1007/s10858-013-9740-z>.
- (265) Ichihara, O.; Barker, J.; Law, R. J.; Whittaker, M. Compound Design by Fragment-Linking. *Mol. Inform.* **2011**, *30* (4), 298–306. <https://doi.org/10.1002/minf.201000174>.
- (266) Hao, C.; Zhao, F.; Song, H.; Guo, J.; Li, X.; Jiang, X.; Huan, R.; Song, S.; Zhang, Q.; Wang, R.; et al. Structure-Based Design of 6-Chloro-4-Aminoquinazoline-2-Carboxamide Derivatives as Potent and Selective P21-Activated Kinase 4 (PAK4) Inhibitors. *J. Med. Chem.* **2018**, *61* (1), 265–285. <https://doi.org/10.1021/acs.jmedchem.7b01342>.
- (267) Southall, S. M.; Wong, P. S.; Odho, Z.; Roe, S. M.; Wilson, J. R. Structural Basis for the Requirement of Additional Factors for MLL1 SET Domain Activity and Recognition of Epigenetic Marks. *Mol. Cell* **2009**, *33* (2), 181–191.

- <https://doi.org/10.1016/j.molcel.2008.12.029>.
- (268) Avdic, V.; Zhang, P.; Lanouette, S.; Groulx, A.; Tremblay, V.; Brunzelle, J.; Couture, J. F. Structural and Biochemical Insights into MLL1 Core Complex Assembly. *Structure* **2011**, *19* (1), 101–108. <https://doi.org/10.1016/j.str.2010.09.022>.
- (269) Thomas, L. R.; Adams, C. M.; Wang, J.; Weissmiller, A. M.; Creighton, J.; Lorey, S. L.; Liu, Q.; Fesik, S. W.; Eischen, C. M.; Tansey, W. P. Interaction of the Oncoprotein Transcription Factor MYC with Its Chromatin Cofactor WDR5 Is Essential for Tumor Maintenance. *Proc. Natl. Acad. Sci. U. S. A.* **2019**, *116* (50), 1–9. <https://doi.org/10.1073/pnas.1910391116>.
- (270) Allen-Petersen, B. L.; Sears, R. C. Mission Possible: Advances in MYC Therapeutic Targeting in Cancer. *BioDrugs* **2019**, *33* (5), 539–553. <https://doi.org/10.1007/s40259-019-00370-5>.
- (271) Tian, J.; Teuscher, K. B.; Aho, E. R.; Alvarado, J. R.; Mills, J. J.; Meyers, K. M.; Gogliotti, R. D.; Han, C.; MacDonald, J. D.; Sai, J.; et al. Discovery and Structure-Based Optimization of Potent and Selective WD Repeat Domain 5 (WDR5) Inhibitors Containing a Dihydroisoquinolinone Bicyclic Core. *J. Med. Chem.* **2020**, *5*. <https://doi.org/10.1021/acs.jmedchem.9b01608>.
- (272) Wang, F.; Jeon, K. O.; Salovich, J. M.; Macdonald, J. D.; Alvarado, J.; Gogliotti, R. D.; Phan, J.; Olejniczak, E. T.; Sun, Q.; Wang, S.; et al. Discovery of Potent 2-Aryl-6,7-Dihydro-5H-Pyrrolo[1,2-a]Imidazoles as WDR5-WIN-Site Inhibitors Using Fragment-Based Methods and Structure-Based Design. *J. Med. Chem.* **2018**, *61* (13), 5623–5642. <https://doi.org/10.1021/acs.jmedchem.8b00375>.
- (273) Aho, E. R.; Wang, J.; Gogliotti, R. D.; Howard, G. C.; Phan, J.; Acharya, P.; Macdonald, J. D.; Cheng, K.; Lorey, S. L.; Lu, B.; et al. Displacement of WDR5 from Chromatin by a WIN Site Inhibitor with Picomolar Affinity. *Cell Rep.* **2019**, *26* (11), 2916-2928.e13. <https://doi.org/10.1016/j.celrep.2019.02.047>.
- (274) Schanda, P.; Kupče, Ě.; Brutscher, B. SOFAST-HMQC Experiments for Recording Two-Dimensional Heteronuclear Correlation Spectra of Proteins within a Few Seconds. *J. Biomol. NMR* **2005**, *33* (4), 199–211. <https://doi.org/10.1007/s10858-005-4425-x>.
- (275) Schanda, P.; Kupce, E.; Brutscher, B. SOFAST-HMQC Experiments for Recording 2D Heteronuclear Correlation Spectra of Proteins within Seconds. *J. Biomol. NMR* **2005**, *33*,

- 199–211. <https://doi.org/10.1007/s10858-005-4425-x>.
- (276) Otwinowski, Z.; Minor, W. Processing of X-Ray Diffraction Data Collected in Oscillation Mode. *Methods Enzymol.* **1997**, *276*, 307–326. [https://doi.org/10.1016/S0076-6879\(97\)76066-X](https://doi.org/10.1016/S0076-6879(97)76066-X).
- (277) Winn, M. D.; Ballard, C. C.; Cowtan, K. D.; Dodson, E. J.; Emsley, P.; Evans, P. R.; Keegan, R. M.; Krissinel, E. B.; Leslie, A. G. W.; McCoy, A.; et al. Overview of the CCP4 Suite and Current Developments. *Acta Crystallogr. Sect. D* **2011**, *67*, 235–242. <https://doi.org/10.1107/S0907444910045749>.
- (278) Adams, P. D.; Grosse-Kunstleve, R. W.; Hung, L. W.; Ioerger, T. R.; McCoy, A. J.; Moriarty, N. W.; Read, R. J.; Sacchettini, J. C.; Sauter, N. K.; Terwilliger, T. C. PHENIX: Building New Software for Automated Crystallographic Structure Determination. In *Acta Crystallographica Section D: Biological Crystallography*; 2002; Vol. 58, pp 1948–1954. <https://doi.org/10.1107/S0907444902016657>.
- (279) Emsley, P.; Cowtan, K. Coot: Model-Building Tools for Molecular Graphics. *Acta Crystallogr. Sect. D* **2004**, *60*, 2126–2132. <https://doi.org/10.1107/S0907444904019158>.
- (280) Schrodinger LLC. The PyMOL Molecular Graphics System, Version 1.8. 2015.